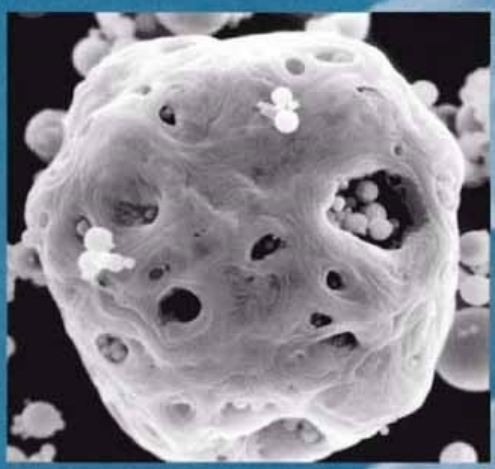
Tracking Environmental Change Using Lake Sediments

Volume 2

Physical and Geochemical Methods

Edited by
William M. Last and John P. Smol



Kluwer Academic Publishers

Tracking Environmental Change Using Lake Sediments.
Volume 2: Physical and Geochemical Methods

Developments in Paleoenvironmental Research

VOLUME 2

Tracking Environmental Change Using Lake Sediments Volume 2: Physical and Geochemical Methods

Edited by

William M. Last

Department of Geological Sciences, University of Manitoba

and

John P. Smol

Department of Biology, Queen's University

KLUWER ACADEMIC PUBLISHERS

NEW YORK, BOSTON, DORDRECHT, LONDON, MOSCOW

eBook ISBN: 0-306-47670-3
Print ISBN: 1-4020-0628-4

©2002 Kluwer Academic Publishers
New York, Boston, Dordrecht, London, Moscow

Print ©2001 Kluwer Academic Publishers
Dordrecht

All rights reserved

No part of this eBook may be reproduced or transmitted in any form or by any means, electronic, mechanical, recording, or otherwise, without written consent from the Publisher

Created in the United States of America

Visit Kluwer Online at: http://kluweronline.com
and Kluwer's eBookstore at: http://ebooks.kluweronline.com

DEDICATION

Dedicated to the memory of Dr. Kerry Kelts, who provided much needed leadership and vision to the science of paleolimnology for the past quarter of a century.

CONTENTS

Preface xiii
The Editors xiv
Aims & Scope of *Developments in Paleoenvironmental Research* Book Series xv
Editors and Board of Advisors of *Developments in Paleoenvironmental Research* Book Series xvi
Contents of Volumes 1 to 4 of the Series xvii
Safety Considerations and Caution xx
List of Contributors xxi

1. An introduction to physical and geochemical methods used in paleolimnology. *William M. Last & John P. Smol* 1

Part I: Physical Lithostratigraphy Techniques

2. Recognition and analysis of bedding and sediment fabric features. *Alan E. S. Kemp, Jean Dean, Richard B. Pearce & Jennifer Pike* 7

Introduction
Approach
Photography and imagery of the core surface
Penetrative imaging of the core
Sampling wet, unconsolidated or semi-consolidated sediment
Sediment drying and resin-embedding
Thin section preparation
SEM analysis of laminated sediment
Summary
Acknowledgements
Appendix 1: Fluid displacive low viscosity resin embedding technique
Method
References

3. Image analysis techniques. *Timo Saarinen & Gunilla Petterson* 23

Introduction
Image analysis in paleolimnology
Material and methods
Future perspectives
Conclusion
Summary
Acknowledgements
References

4. Textural analysis of lake sediments. *William M. Last* 41

Introduction and importance of texture
Size
Form and fabric
Example of application of textural studies
Summary
Acknowledgments
References

Part II: Mineralogical and Geochemical Indicator Techniques

5. Inorganic geochemical methods in paleolimnology. *J. F. Boyle* 83

History & scope
Objectives of inorganic geochemical research
Elemental analysis
Identifying, characterizing, and quantifying sediment components
Areas of contention
Uses of inorganic geochemical data in palaeolimnology
Future developments
Summary
Acknowledgements
References

6. Mineralogical analysis of lake sediments. *William M. Last* 143

Introduction and importance of mineralogy
Mineralogy versus geochemistry
Minerals in lake sediments
A synopsis of methods
X-ray diffraction
Light microscopy
Future developments
Summary
Acknowledgments
References

7. Fluid inclusions in paleolimnological studies of chemical sediments. *Tim Lowenstein & Sean T. Brennan* 189

Introduction
Distinguishing primary from secondary features in chemical sediments
Fluid inclusions in ancient chemical sediments
Fluid inclusion liquid-vapor homogenization temperatures: paleolake temperatures

Fluid inclusion freezing-melting behavior: paleolake chemical compositions
Stable isotopes (δD, $\delta^{18}O$) from fluid inclusion waters
Major element chemistry of fluid inclusions: paleolake water compositions
Summary
Acknowledgements
References

8. Application of mineral magnetic techniques to paleolimnology.
Per Sandgren & Ian Snowball 217

Introduction
A brief history of the application of mineral magnetic measurements to lake sediments
Magnetic properties
Magnetic hysteresis
Anhysteretic remanent magnetisation (ARM)
Sample collection and preparation
Sequence of measurements
Hysteresis curves
Summary
References

9. Sediment organic matter.
Philip A. Meyers & Jane L. Teranes 239

Introduction
Paleolimnological proxies
Summary
Acknowledgments
References

10. Paleolimnological methods and applications for persistent organic pollutants.
Jules M. Blais & Derek C. G. Muir 271

Introduction
Advances in extraction and quantitative analytical techniques for POPs in sediment
Transfer processes in lakes
Summary
Acknowledgments
References

11. Near-Infrared spectrometry (NIRS) in paleolimnology.
Tom Korsman, Ingemar Renberg, Eigil Dåbakk & Mats B. Nilsson 299

Introduction
Theory
Instrumentation
NIR analysis of sediment samples
Uses of NIRS in palaeolimnology
Future perspectives
Summary
References

12. Fly-ash particles. *Neil Rose* 319

Introduction
A brief history
Methods of extraction and enumeration
Temporal distribution
Spatial distribution
Source apportionment
The future
Summary
Acknowledgements
References

Part III: Stable Isotope Techniques

13. Application of stable isotope techniques to inorganic and biogenic carbonates. *Emi Ito* 351

Introduction
Nomenclature and systematics
$\delta^{18}O$ of lake-water
Mg/Ca and Sr/Ca ratios of lake-water
$\delta^{13}C$ of dissolved inorganic carbon (DIC)
Carbonates in lake-sediments
Mollusks
Ostracodes
Charaphytes
Isotope analysis
Preparation of carbonate samples for isotope analysis
Conclusions
Summary
Acknowledgments
References

14. Carbon and oxygen isotope analysis of lake sediment cellulose: methods and applications. *Brent B. Wolfe, Thomas W. D. Edwards, Richard J. Elgood & Kristina R. M. Beuning* 373

Introduction
Stable isotope tracers in lake waters - ^{18}O, ^{2}H, ^{13}C
Historical development
Methods
Key criteria for paleohydrologic reconstruction
Applications
Future research directions
Summary
Acknowledgements
References

15. Nitrogen isotopes in palaeolimnology. *Michael R. Talbot* 401

Introduction
Nitrogen in lakes: forms and distribution
Nitrogen isotopes
Nitrogen isotope studies in palaeolimnology: sampling and measurement
Some examples
Closing remarks
Summary
Acknowledgments
References

Glossary, acronyms and abbreviations 441

Index 493

PREFACE

The explosive growth of paleolimnology over the past two decades has provided impetus for the publication of this series of monographs detailing the numerous advances and new techniques being applied to the interpretation of lake histories. This is the second volume in the series and deals mainly with physical and geochemical analytical techniques. Volume 1 (Last & Smol, 2001) examines the acquisition and archiving of cores, chronological techniques, and large-scale basin analysis methods. Volumes 3 and 4 (Smol et al., 2001 a & b) provide a comprehensive overview of the many biological techniques that are used in paleolimnology. A fifth volume that is currently being prepared (Birks et al., in preparation) examines statistical and data handling methods. It is our hope that these monographs will provide sufficient detail and breadth to be useful handbooks for both seasoned practitioners as well as newcomers to the area of paleolimnology. These books should also be useful to non-paleolimnologists (e.g., limnologists, environmental scientists, archeologists, palynologists, geographers, geologists, etc.) who continue to hear and read about paleolimnology, but have little chance to explore the vast and sometimes difficult to access journal-based reference material for this rapidly expanding field. Although the chapters in these volumes target mainly lacustrine settings, many of the techniques described can also be readily applied to fluvial, glacial, marine, estuarine, and peatland environments.

The 15 chapters in this volume are organized into three major parts. The three chapters in Part I provide an overview of the most common physical lithostratigraphy techniques. Part II discusses geochemical and mineralogical approaches. The third part of this book includes three chapters summarizing oxygen, carbon, and nitrogen isotopic techniques. Following this is a comprehensive glossary and list of acronyms and abbreviations.

Many people have helped with the planning, development, and final production of this volume. In addition to the hard work provided by the authors of these contributions, this publication benefitted from the technical reviews furnished by our scientific colleagues, many of whom remain anonymous. Each chapter was critically examined by two external referees as well as the editors. In order to assure readability for the major target audience, we asked many of our graduate students to also examine selected chapters; their insight and questioning during the reviewing and editorial process are most gratefully acknowledged. The staff of the Environmental, Earth and Aquatic Sciences Division of Kluwer Academic Publishers are commended for their diligence in production of the final presentation. In particular, we would also like to thank Ad Plaizier, Anna Besse-Lototskaya (Publishing Editor, Aquatic Science Division), and Rene Mijs (former Publishing Editor, Biosciences Division) for their long-term support of this new series of monographs and their interest in paleoenvironmental research. Finally, we would like to thank our respective universities and colleagues for support and encouragement during this project.

THE EDITORS

William M. Last is a professor in the Department of Geological Sciences at University of Manitoba (Winnipeg, Manitoba, Canada) and is co-editor of the *Journal of Paleolimnology.*

John P. Smol is a professor in the Biology Department at Queen's University (Kingston, Ontario, Canada), with a cross-appointment at the School of Environmental Studies. He co-directs the Paleoecological Environmental Assessment and Research Lab (PEARL). Professor Smol is co-editor of the *Journal of Paleolimnology* and holds the *Canada Research Chair in Environmental Change.*

AIMS AND SCOPE OF *DEVELOPMENTS IN PALEOENVIRONMENTAL RESEARCH* BOOK SERIES

Paleoenvironmental research continues to enjoy tremendous interest and progress in the scientific community. The overall aims and scope of the *Developments in Paleoenvironmental Research* book series are to capture this excitement and document these developments. Volumes related to any aspect of paleoenvironmental research, encompassing any time period, are within the scope of the series. For example, relevant topics include studies focused on terrestrial, peatland, lacustrine, riverine, estuarine, and marine systems, ice cores, cave deposits, palynology, isotopes, geochemistry, sedimentology, paleontology, etc. Methodological and taxonomic volumes relevant to paleoenvironmental research are also encouraged. The series will include edited volumes on a particular subject, geographic region, or time period, conference and workshop proceedings, as well as monographs. Prospective authors and/or editors should consult the series editors for more details. The series editors also welcome any comments or suggestions for future volumes.

EDITORS AND BOARD OF ADVISORS OF *DEVELOPMENTS IN PALEOENVIRONMENTAL RESEARCH* BOOK SERIES

Series Editors:

John P. Smol
Paleoecological Environmental Assessment and Research Lab (PEARL)
Department of Biology
Queen's University
Kingston, Ontario, K7L 3N6, Canada
e-mail: SmolJ@BIOLOGY.QueensU.Ca

William M. Last
Department of Geological Sciences
University of Manitoba
Winnipeg, Manitoba R3T 2N2, Canada
e-mail: WM_Last@UManitoba.ca

Advisory Board:

Professor Raymond S. Bradley
Department of Geosciences
University of Massachusetts
Amherst, MA 01003-5820 USA
e-mail: rbradley@climate1.geo.umass.edu

Professor H. John B. Birks
Botanical Institute
University of Bergen
Allégaten 41
N-5007 Bergen
Norway
e-mail: John.Birks@bot.uib.no

Dr. Keith Alverson
Science Officer
IGBP-PAGES International Project Office
Barenplatz 2
3011 Bern
Switzerland
e-mail: alverson@pages.unibe.ch

CONTENTS OF VOLUMES 1 TO 4 OF THE SERIES

Contents of Volume 1: ***Tracking Environmental Change Using Lake Sediments: Basin Analysis, Coring, and Chronological Techniques.***

An introduction to basin analysis, coring, and chronological techniques used in paleolimnology. *William M. Last & John P. Smol*

Applications of seismic sequence stratigraphy in lacustrine basins. *Christopher A. Scholz*

Ground penetrating radar applications in paleolimnology. *Brian J. Moorman*

Shoreline and basin configuration techniques in paleolimnology. *Dorothy Sack*

Sediment core collection and extrusion. *John R. Glew, John P. Smol & William M. Last*

Coring and drilling equipment and procedures for recovery of long lacustrine sequences. *Suzanne A. G. Leroy & Steve M. Colman*

Sediment logging techniques. *Bernd Zolitschka, Jens Mingram, Sjerry van der Gaast, J. H. Fred Jansen & Rudolf Naumann*

Logging of magnetic susceptibility. *Norbert R. Nowaczyk*

Chronostratigraphic techniques in recent sediments. *P. G. Appleby*

^{14}C chronostratigraphic techniques in paleolimnology. *Svante Björck & Barbara Wohlfarth*

Varve chronology techniques. *Scott Lamoureux*

Luminescence dating. *Olav B. Lian & D. J. Huntley*

Electron spin resonance (ESR) dating in lacustrine environments. *Bonnie A. B. Blackwell*

Use of paleomagnetism in studies of lake sediments. *John King & John Peck*

Amino acid racemization (AAR) dating and analysis in lacustrine environments. *Bonnie A. B. Blackwell*

Tephrochronology. *C. S. M. Turney & J. J. Lowe*

Glossary, Acronyms and Abbreviations

Subject Index

Contents of Volume 2: ***Tracking Environmental Change Using Lake Sediments: Physical and Geochemical Methods.***

An introduction to physical and geochemical methods used in paleolimnology. *William M. Last & John P. Smol*

Recognition and analysis of bedding and sediment fabric features. *Alan E. S. Kemp, Jean Dean, Richard B. Pearce & Jennifer Pike*

Image analysis techniques. *Timo Saarinen & Gunilla Petterson*

Textural analysis of lake sediments. *William M. Last*

Inorganic geochemical methods in paleolimnology. *J. F. Boyle*

Mineralogical analysis of lake sediments. *William M. Last*

Fluid inclusions in paleolimnological studies of chemical sediments. *Tim Lowenstein & Sean T. Brennan*

Application of mineral magnetic techniques to paleolimnology. *Per Sandgren & Ian Snowball*

Sediment organic matter. *Philip A. Meyers & Jane L. Teranes*

Paleolimnological methods and applications for persistent organic pollutants. *Jules M. Blais & Derek C. G. Muir*

Near-Infrared spectrometry (NIRS) in paleolimnology. *Tom Korsman, Eigil Dåbakk, Mats B. Nilsson & Ingemar Renberg*

Fly-ash particles. *Neil Rose*

Application of stable isotope techniques to inorganic and biogenic carbonates. *Emi Ito*

Carbon and oxygen isotope analysis of lake sediment cellulose: methods and applications. *Brent B. Wolfe, Thomas W. D. Edwards, Kristina R. M. Beuning & Richard J. Elgood*

Nitrogen isotopes in palaeolimnology. *Michael R. Talbot*

Glossary, Acronyms and Abbreviations

Subject Index

Contents of Volume 3: ***Tracking Environmental Change Using Lake Sediments: Terrestrial, Algal, and Siliceous Indicators.***

Using biology to study long-term environmental change. *John. P. Smol, H. John B. Birks & William M. Last*

Pollen. *K. D. Bennett & K. J. Willis*

Conifer stomata. *Glen M. MacDonald*

Plant macrofossils. *Hilary H. Birks*

Charcoal as a fire proxy. *Cathy Whitlock & Chris Larsen*

Non-pollen palynomorphs. *Bas van Geel*

Protozoa: testate amoebae. *Louis Beyens & Ralf Meisterfeld*

Diatoms. *Richard W. Battarbee, Laurence Carvalho, Vivienne J. Jones, Roger J. Flower, Nigel G. Cameron, Helen Bennion & Stephen Juggins*

Chrysophyte scales and cysts. *Barbara A. Zeeb & John P. Smol*

Ebridians. *Atte Korhola & John P. Smol*

Phytoliths. *Dolores R. Piperno*

Freshwater sponges. *Thomas M. Frost*

Siliceous protozoan plates and scales. *Marianne S. V. Douglas & John P. Smol*

Biogenic silica. *Daniel J. Conley & Claire L. Schelske*

Sedimentary pigments. *Peter R. Leavitt & Dominic A. Hodgson*

Glossary, Acronyms and Abbreviations

Subject Index

Contents of Volume 4: ***Tracking Environmental Change Using Lake Sediments: Zoological Indicators.***

Zoological indicators in lake sediments: an introduction. *John. P. Smol, H. John B. Birks & William M. Last*

Cladocera and other branchiopod crustaceans. *Atte Korhola & Milla Rautio*

Midges: Chironomidae and related Diptera. *Ian R. Walker*

Coleoptera and Trichoptera. *Scott A. Elias*

Oribatid mites. *Torstein Solhøy*

Bryozoan statoblasts. *Donna R. Francis*

Ostracoda. *Jonathan A. Holmes*

Freshwater molluscs. *Barry B. Miller & Michael J. S. Tevesz*

Fish. *W. P. Patterson & G. R. Smith*

Glossary, Acronyms and Abbreviations

Subject Index

SAFETY CONSIDERATIONS AND CAUTION

Paleolimnology has grown into a vast scientific pursuit with many branches and subdivisions. It should not be surprising, therefore, that the tools used by paleolimnologists are equally diverse. Virtually every one of the techniques described in this book requires some familiarity with standard laboratory or field safety procedures. In some of the chapters, the authors have made specific reference to appropriate safety precautions; others have not. The responsibility for safe and careful application of these methods is yours. Never underestimate the personal risk factor when undertaking either field or laboratory investigations. Researchers are strongly advised to obtain all safety information available for the techniques they will be using and to explicitly follow appropriate safety procedures. This is particularly important when using strong acids, alkalies, or oxidizing reagents in the laboratory or many of the analytical and sample collection/preparation instruments described in this volume. Most manufacturers of laboratory equipment and chemical supply companies provide this safety information, and many Internet and other library resources contain additional safety protocols. Researchers are also advised to discuss their procedures with colleagues who are familiar with these approaches, and so obtain further advice on safety and other considerations.

The editors and publisher do not necessarily endorse or recommend any specific product, procedure, or commercial service that may be cited in this publication.

LIST OF CONTRIBUTORS

Kristina R. M. Beuning
Department of Earth and Environmental Sciences
Wesleyan University
Middletown, CT, 06459, USA
e-mail: kbeuning@wesleyan.edu

Jules M. Blais
Program for Environmental and Chemical Toxicology
Department of Biology
University of Ottawa
30 Marie Curie St.
P.O. Box 450, Stn. A
Ottawa, Ontario, K1N 6N5, Canada
e-mail: jblais@science.uottawa.ca

J. F. Boyle
Department of Geography
University of Liverpool
PO Box 147
Liverpool L69 3BX, UK
e-mail: jfb@liverpool.ac.uk

Sean T. Brennan
Department of Geological Sciences & Environmental Studies
State University of New York at Binghamton
Binghamton, NY 13902, USA

Eigil Dåbakk
Department of Organic Chemistry
Umeå University
SE-901 87 Umeå, Sweden
e-mail: eigil.dabakk@chem.umu.se

Jean Dean
School of Ocean and Earth Sciences
University of Southampton
Southampton Oceanography Centre
European Way
Southampton, SO14 3ZH, UK

Thomas W. D. Edwards
Department of Earth Sciences
University of Waterloo
Waterloo ON, N2L 3G1, Canada
e-mail: tedwards@sciborg.uwaterloo.ca

Richard J. Elgood
Department of Earth Sciences
University of Waterloo
Waterloo, ON, N2L 3G1, Canada

Emi Ito
Department of Geology and Geophysics
and Limnological Research Center
University of Minnesota
310 Pillsbury Drive, SE
Minneapolis, MN 55455, USA
e-mail: eito@umn.edu

Alan E. S. Kemp
School of Ocean and Earth Sciences
University of Southampton
Southampton Oceanography Centre
European Way
Southampton, SO14 3ZH, UK
e-mail: aesk@soc.soton.ac.uk

Tom Korsman
Department for Ecology and Environmental Science
Umeå University
S-901 87 Umeå, Sweden
e-mail: tom.korsman@eg.umu.se

William M. Last
Department of Geological Sciences
University of Manitoba
Winnipeg, Manitoba, R3T 2N2, Canada
e-mail: WM_Last@UManitoba.ca

Tim K. Lowenstein
Department of Geological Sciences & Environmental Studies
State University of New York at Binghamton
Binghamton, NY 13902, USA
e-mail: lowenst@Binghamton.edu

Phillip A. Meyers
Department of Geological Sciences
The University of Michigan
Ann Arbor, MI 48109-1063 USA
e-mail: pameyers@umich.edu

Derek Muir
Environment Canada
Canada Centre for Inland Waters
867 Lakeshore Road
Burlington, Ontario, L7R 4A6 Canada
e-mail: derek.muir@cciw.ca

Mats B. Nilsson
Department of Forest Ecology
Swedish University of Agricultural Sciences
SE-901 83 Umeå, Sweden
e-mail: Mats.B.Nilsson@sek.slu.se

Richard B. Pearce
School of Ocean and Earth Sciences
University of Southampton
Southampton Oceanography Centre
European Way
Southampton, SO14 3ZH, UK

Gunilla Petterson
Department of Ecology and Environmental Science
Umeå University
S-901 87 Umeå, Sweden
e-mail: gunilla.petterson@eg.umu.se

Jennifer Pike
Department of Earth Sciences
Cardiff University
P.O. Box 914
Cardiff, CF1 3YE, UK

Ingemar Renberg
Department for Ecology and Environmental Science
Umeå University
S-901 87 Umeå, Sweden
e-mail: ingemar.renberg@eg.umu.se

Neil Rose
Environmental Change Research Centre
University College London
26 Bedford Way, London WC1H 0AP, U.K.
e-mail: nrose@geog.ucl.ac.uk

Timo Saarinen
Geological Survey of Finland
Betonimiehenkuja 4
FIN-02150 Espoo, Finland
e-mail: timo.saarinen@gsf.fi

Per Sandgren
Department of Quaternary Geology
Tornavägen 13
SE-223 63 Lund, Sweden
e-mail: Per.Sandgren@Geol.lu.se

John P. Smol
Paleoecological Environmental Assessment and Research Lab (PEARL)
Department of Biology
Queen's University
Kingston, Ontario, K7L 3N6, Canada
e-mail: SmolJ@BIOLOGY.QueensU.Ca

Ian Snowball
Department of Quaternary Geology
Tornavägen 13
SE-223 63 Lund, Sweden
e-mail: Ian.snowball@geol.lu.se

Michael R. Talbot
Geological Institute
University of Bergen
Allégaten 41
5007 Bergen, Norway
e-mail: michael.talbot@geol.uib.no

Jane L. Teranes
Geosciences Research Division
Scripps Institution of Oceanography
University of California San Diego
La Jolla, CA 92093-0244, USA
e-mail: jteranes@ucsd.edu

Brent B. Wolfe
Department of Earth Sciences
University of Waterloo
Waterloo ON, N2L 3G1, Canada
e-mail: bwolfe@sciborg.uwaterloo.ca

1. AN INTRODUCTION TO PHYSICAL AND GEOCHEMICAL METHODS USED IN PALEOLIMNOLOGY

WILLIAM M. LAST (WM_Last@UManitoba.ca)
Department of Geological Sciences
University of Manitoba
Winnipeg, Manitoba
R3T2N2, Canada

JOHN P. SMOL (SmolJ@Biology.QueensU.Ca)
Paleoecological Environmental Assessment and Research Lab (PEARL)
Department of Biology
Queen's University
Kingston, Ontario
K7L 3N6, Canada

Paleolimnology is the study of past conditions and processes in lake and river basins and the interpretation of the histories of these systems. It is a multidisciplinary science whose roots extend back nearly two centuries. As pointed out by Gierlowski-Kordesch & Kelts (1994), the scientific investigation of the history of lake basins was already an important theme in the early 1800's (e.g., Lyell, 1830; Agassiz, 1840), and played a significant role in the development of early thoughts about glaciation and eustasy. Modern paleolimnology is also a rapidly developing science that has seen tremendous progress over the past several decades. It is now clear that lacustrine sediments and sedimentary rocks represent one of the best archives for paleoenviromental information available within the entire realm of terrestrial settings. Not only does paleolimnology assume a pivotal role in paleoclimatic and global change investigations, but its importance and relevance are further enhanced by the fact that lake sediments are hosts to a wide variety of economically valuable resources. Moreover, recent lacustrine sediments provide an excellent means of monitoring and tracking environmental contaminants.

This explosion of interest in lake deposits and the associated dramatic increase in primary literature devoted to paleolimnology of all types has been accompanied by an equally rapid development and advance in the techniques and methods used in paleolimnological research. Today paleolimnologists use a large range of often sophisticated instruments and equipment in their studies, in addition to more traditional discipline-based field and laboratory techniques. There are few other fields of science in which such a vast array of interdisciplinary tools, methods, and techniques are involved. Paleolimnologists routinely use and must have working knowledge of methods and tools normally within the realms



W. M. Last & J. P. Smol (eds.), 2001. *Tracking Environmental Change Using Lake Sediments. Volume 2: Physical and Geochemical Methods.* Kluwer Academic Publishers, Dordrecht, The Netherlands

of agronomy and soil science, botany, chemistry and geochemistry, ecology, engineering, geography, geology, hydrology, physics and geophysics, and zoology to name a few. It is not surprising, therefore, that many of the advances in paleolimnological techniques have come about because of new developments in these allied fields. Previous methodology compilations and techniques monographs, such as Kummel & Raup (1965), Bouma (1969), Carver (1971), Berglund(1986), Gray (1988), Tucker (1988), Warner (1990), and Rutter& Catto (1995), were very important contributions to selected areas of paleolimnology. These (and many others) continue to serve as essential handbooks. However, the development of new and different methods for studying lake sediments, as well as advancements and modifications to old methods, have provided impetus for a new series of monographs for this rapidly expanding topic.

The objective of this volume is to provide a state-of-the-art summary of the major physical, mineralogical, and geochemical laboratory techniques used in the study of lacustrine deposits. Four additional books from this series deal with other components of paleolimnology. Volume 1 (Last & Smol, 2001) summarizes the critical techniques and methods used by paleolimnologists in field and sample/core collection, chronostratgraphy, and large-scale basin analysis. Volumes 3 and 4 (Smol et al., 2001a, b) focus on the vast range of biological techniques that can be applied to the interpretation of lake histories. Although chapters in each of these books discuss the quantitative aspects of lake sediment interpretations, a separate volume on statistical and data handling approaches in paleolimmnology is currently in preparation (Birks et al., in preparation). Our intent with this series of volumes is to provide sufficient methodological and technical detail to allow both practitioners and newcomers to the area of paleolimnology to use them as handbooks/laboratory manuals and as primary research texts.

Although we recognize that the study of pre-Quaternary lakes is a very rapidly growing component in the vast arena of paleolimnology, this volume and the other three in this series are directed primarily towards those involved in Quaternary lacustrine deposits and Quaternary environmental change. Nonetheless, many of the techniques and approaches are applicable to other time frames. Finally, we anticipate that many of the techniques discussed in these volumes apply equally well to marine, estuarine, and other depositional environments, although we have not specifically targeted non-lacustrine settings.

As illustrated in Figure 1, this volume addresses the techniques and methods used in the investigation of mainly physical and chemical paleolimnological pursuits. The 15 chapters are divided into three parts. Following this short introduction, Part I of this volume deals with physical lithostratigraphic techniques. Much valuable paleoenvironmental information can be deciphered from bedding characteristics of the sediment fill in a basin. Traditionally, sedimentologists have generally approached this topic from a qualitative and largely visual descriptive standpoint. However, the first two chapters in Part I highlight many of the new methods that can be applied in preparation and analysis of well-bedded lacustrine deposits (Kemp et al.) and in the techniques of obtaining quantitative information by computer-assisted digital image analysis (Saarinen & Petterson). Methods of quantitatively examining texture of the sediment, long considered one of the most fundamental descriptors of a deposit, are summarized by Last.

Part II discusses mineralogical and geochemical techniques. In the first chapter of this section, Boyle provides a comprehensive overview of the important topic of inorganic geochemical analyses of lake sediments. Although inorganic geochemistry has enjoyed a

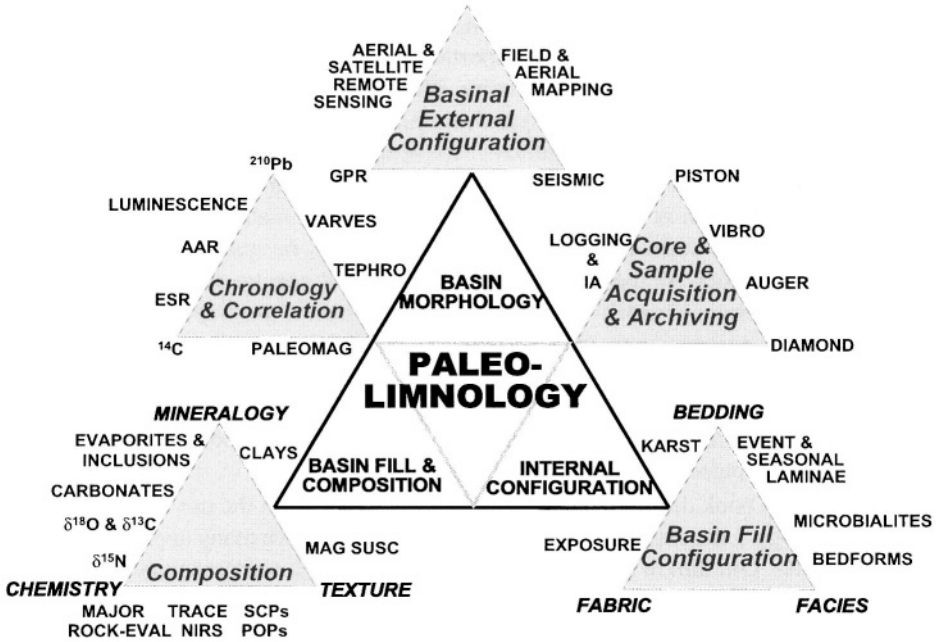


Figure 1. Schematic representation showing the spectrum of physical and chemical techniques and coring methods used in paleolimnology. This volume deals with the broad areas of basin fill and composition, and internal configuration, whereas Volume 1 (Last & Smol, 2001) covers the large-scale basin configuration, chronology and correlation, and core and sample acquisition

long and profitable history of use in paleolimnology, the rapid development of analytical instrumentation during the past few years has opened many new opportunities and avenues of investigation. In addition to variations in the elemental composition of lake sediments, changes in how these elements are chemically combined in a deposit are also important. The techniques for mineralogical assessment of lake deposits are summarized by Last. Crystals of minerals that originate by chemical precipitation within the water column or within the pore spaces of the sediment column can contain fluid-filled vacuoles, or fluid inclusions, which retain valuable information about past water compositions, temperatures and other environmental parameters. Lowenstein & Brennan discuss the methods of fluid inclusion research in paleolimnology and summarize the major advances that have taken place in this rapidly developing field. The magnetic characteristics of a deposit can be used to help establish a chronology and to assist in correlating the lacustrine sequence retrieved at one site to that of another, topics that are covered in Volume 1 of this series. In addition, the type, concentration and grain size of magnetic minerals found in lake sediments can be used to better understand the variety of processes operating in the lake and its catchment in response to changes in climate, human activity and limnology. Sandgren & Snowball summarize the various analytical components and techniques of environmental magnetism. Although organic matter comprises a relatively minor proportion of most lake deposits, this organic content provides a wealth of information from a variety of indicators that can be used to reconstruct paleoenvironments of lakes and their watersheds, and to infer histories of regional climate change as summarized by Meyers & Teranes. The use of lake sediments

to track contaminant loading of the environment through time and to help identify sources of chemical pollutants is an extremely important application of paleolimnology that will assume an even more critical role in the future. Blais & Muir review the analytical methods for persistent organic pollutants (POPs) and summarize the processes that govern the fate of these contaminants in the environment. Conventional chemical analyses of 'organic element' components, such as carbon, nitrogen and phosphorus, in a core can be slow and expensive. Korsman et al. discuss near-infrared spectrometry (NIRS), a method by which stratigraphic fluctuations in organic molecules can be quantified in a rapid and non-destructive manner. As the authors point out, the NIR spectra also have potential for reconstruction of water chemistries and other environmental parameters from sediment cores. Spheroidal carbonaceous particles (SCPs) and inorganic ash spheres (IASs), collectively termed fly-ash particles, are produced from industrial combustion of fossil fuels. Because they have no natural source, these particles make ideal stratigraphic markers. In the final chapter of Part II, Rose examines the concepts and methodology of the use of fly-ash particles in paleolimnological investigations.

Part III of this book discusses the techniques associated with the use of stable isotopes in paleolimnology. Like chronostratigraphy, stable isotopes have many applications in lake sediment studies. Our aim in this section was not to provide a comprehensive treatment of all possible isotopic applications in paleoenvironmental research, but rather to highlight a few of the most commonly used techniques that have been shown to yield useful paleoclimatologic and paleohydrologic information. The first two chapters of Part III both deal with carbon and oxygen isotope analyses. Ito provides a guide for the isotopic analysis of lacustrine carbonates and examines some of the potential technical and interpretive pitfalls. A complementary discussion of $\delta^{13}C$ and $\delta^{18}O$ of lake sediment cellulose is provided by Wolfe et al. Finally, in the last chapter of the section, Talbot discusses the methodology and application of nitrogen isotope geochemistry in paleolimnology.

Although we have assumed readers will have a basic knowledge of earth and environmental science jargon, we have included a comprehensive glossary and list of acronyms and abbreviations to assist with the large and perhaps unfamiliar vocabulary. This is followed by a subject index.

As in many other areas of environmental earth science, the continued development of our understanding of the histories of lake basins will depend on the interaction of specialists in a wide range of disciplines. The tools and investigative techniques these specialists bring to bear on the task of characterizing the sediments and fluids within these basins are continuing to advance at a rapid pace. The applications and research avenues fronting paleolimnology are immense, but so are the potential analytical and logistical problems. One of the greatest challenges facing the next generation of paleolimnologists is to maintain the integrated multidisciplinary approach to the study of lake sediments that has evolved over the past decade. We see no evidence that the accelerated rate of progress that this field has enjoyed will be slowing down in the near future. Many new approaches and applications are certainly soon to be discovered, and will hopefully be covered in subsequent volumes of this series.

References

Agassiz, L. J., 1840. Études sur les Glaciers. Neuchâtel, privately published, 346 pp.

Berglund, B. E. (ed.), 1986. Handbook of Holocene Palaeoecology and Palaeohydrology. John Wiley & Sons, New York, 869 pp.

Birks, H. J. B., S. Juggins, A. Lotter & J. P. Smol. Tracking Environmental Change Using Lake Sediments: Data Handling and Statistical Techniques. Kluwer Academic Publishers, Dordrecht, The Netherlands, in preparation.

Bouma, A. H., 1969. Methods for the Study of Sedimentary Structures. John Wiley & Sons, New York, 458 pp.

Carver, R. E. (ed.), 1971. Procedures in Sedimentary Petrology. Wiley Interscience, New York, 653 pp.

Gierlowski-Kordcsch, E. & K. Kelts (eds.), 1994. Introduction. In Gierlowski-Kordesch, E. & K. Kelts (eds.) Global Geological Record of Lake Basins. Volume 1. Cambridge University Press, Cambridge: xvii–xxxiii.

Gray, J. (ed.), 1988. Paleolimnology: Aspects of Freshwater Paleoecology and Biogeography. Elsevier, Amsterdam, 678 pp.

Kummel, B. & D. Raup (eds.), 1965. Handbook of Paleontological Techniques. W. H. Freeman and Company, San Francisco, 862 pp.

Last, W. M. & J. P. Smol (eds.), 2001. Tracking Environmental Change Using Lake Sediments. Volume I: Basin Analysis, Coring, and Chronological Techniques. Kluwer Academic Publishers, Dordrecht, The Netherlands, 548.

Lyell, C., 1830. Principles of Geology. Volume 1. J. Murray. London, 546 pp.

Rutter, N. W. & N. R. Catto (eds.), 1995. Dating Methods for Quaternary Deposits. GEOtext 2, Geological Association of Canada, St. John's, NF., 308 pp.

Smol, J. P., H. J. B. Birks & W. M. Last (eds.), 2001a. Tracking Environmental Change Using Lake Sediments. Volume 3: Terrestrial, Algal, and Siliceous Indicators. Kluwer Academic Publishers, Dordrecht, The Netherlands, 371 pp.

Smol, J. P., H. J. B. Birks & W. M. Last (eds.), 2001b. Tracking Environmental Change Using Lake Sediments. Volume 4: Zoological Indicators. Kluwer Academic Publishers, Dordrecht, The Netherlands.

Tucker, M. E. (ed.). 1988. Techniques in Sedimentology. Blackwell Scientific Publications Ltd., Osney Mead, Oxford, UK, 394 pp.

Warner, B. G. (ed.), 1990. Methods in Quaternary Ecology. Geoscicnce Canada Reprint Series 5, St. John's, NF., 170pp.

2. RECOGNITION AND ANALYSIS OF BEDDING AND SEDIMENT FABRIC FEATURES

ALAN E. S. KEMP (aesk@soc.soton.ac.uk)
JEAN DEAN AND RICHARD B. PEARCE
School of Ocean and Earth Science
University of Southampton
Southampton Oceanography Centre
European Way, Southampton SO14 3ZH
UK

JENNIFER PIKE
Department of Earth Sciences
Cardiff University
P.O. Box 914
Cardiff
CF10 3YE
UK

Keywords: laminated sediments, scanning electron microscopy, sediment fabric, resin embedding

Introduction

The first step in any investigation of a lacustrine paleo-archive is the detailed visual description of the core or outcrop section. This careful visual description accompanied by core photography will usually form the basis for further studies and, most importantly, for developing an analytical strategy for the investigation. In this chapter we give an account of the further methods available for extending the visual description of bedding features from the macroscopic to the microscopic. A number of case studies are included to illustrate the various scenarios possible and strategies for identifying the origins of fabric elements. The purpose of this chapter is to take the reader sequentially through the step by step core description methods normally employed in the study of lacustrine sediments. While many of the techniques and examples given have been employed on marine sediment cores and reflect the experience of the authors, the methods are equally applicable to lacustrine sediments. This compilation builds on previous work by the authors to which the reader is also referred including Pike & Kemp (1996) and Dean et al. (1999).



W. M. Last & J. P Smol (eds.), 2001. *Tracking Environmental Change Using Lake Sediments. Volume 2: Physical and Geochemical Methods.* Kluwer Academic Publishers, Dordrecht, The Netherlands.

Approach

The initial approach and sequence of techniques employed in core description commences with non-invasive photography and imaging and progresses through sequential sub-sampling (Fig. 1). The primary objective of these combined approaches is to provide information on the sequence and recurrence of depositional processes and events that have produced the sediment record. The guiding principal is to use whatever techniques are necessary to identify and interpret the bedding features within the core at whatever scale they occur. It is worth bearing in mind that even in sediments that may appear outwardly homogenous from visual examination, other techniques such as radiography may reveal fine structure. It should also be emphasized that for sediments with millimetre-scale features such as laminae, the production of thin sections is an essential prerequisite to further understanding. Examples of how the approaches outlined may be applied to bedding feature recognition are shown in Figure 2. Of course, our ideal scenario is to have a continuously laminated sediment record, but commonly laminae are interupted by intervals that may outwardly appear structureless or massive. A key step in interpretating such a record is to identify whether the lack of laminae is due simply to bioturbation, or whether some form of mass flow deposit is present. These two interpretations would form important but contrasting input to paleoenvironmental analysis. The incidence of bioturbation gives important information about the physical mixing of the lake and the history of eutrophication whereas the identification of mass flow deposits may inform about clastic sediment input to the lake or paleoseismicity (e.g., Blais-Stevens, et al., 1997).

Photography and imagery of the core surface

Following coring and core splitting detailed visual core description is generally accompanied by photography and also digital imagery. Careful preparation of the core surface is imperative and this is usually accomplished using the electro-osmotic knife (Chmelick, 1967; Schimmelmann et al., 1990) or by careful scraping with a sharp blade or microscope slide. In addition to conventional core photography (accomplished using a tripod-mounted camera in the field or on a photographic table under appropriate illumination in the laboratory) color reflectance and digital imaging techniques may be employed.

Color reflectance

Traditional descriptions of core color using Munsell charts are time consuming and of dubious value due to the variations in illumination and spectral response of the human eye. Quantification of sediment color has been increasingly used in the systematic down-core description of marine sediments (e.g., Nagao & Nakashima; 1992; Gersonde, et al., 1999). The most commonly available and widely used method adopts the Minolta spectrophotometer or chroma-meter which produces measurements in L* a* b* color space (Nagao & Nakashima, 1992). These instruments are deployed hand-held or on a rail-guide above the core. The minimum spot size (and therefore resolution) in commercially available instruments is 4 mm. Other instruments with similar resolution include the Oregon State

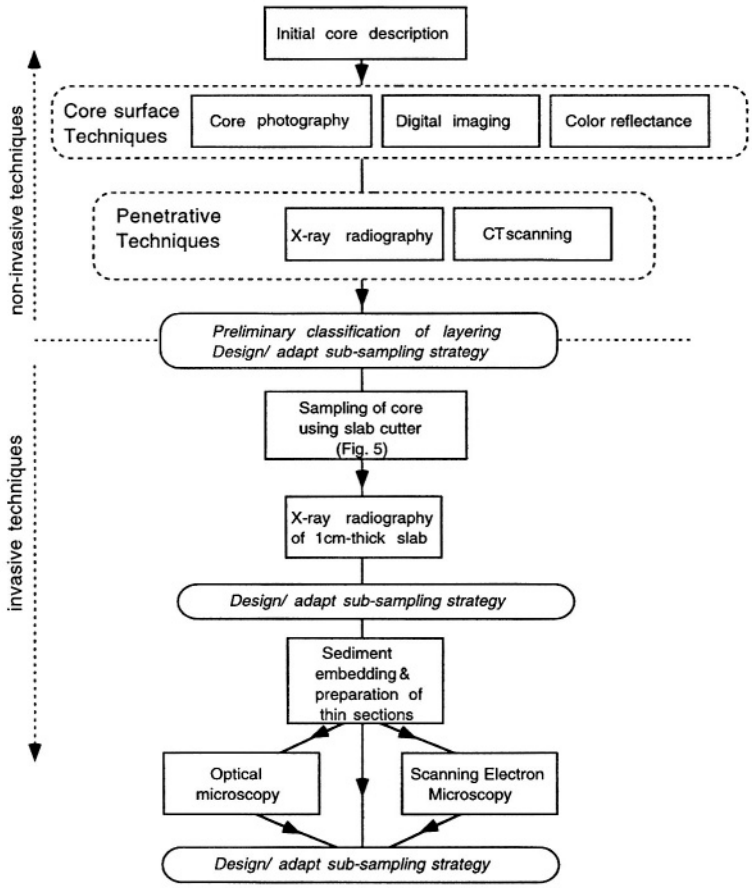


Figure 1. The initial approach to sediment core description and sub-sampling.

University spectral reflectometer (Mix et al., 1992). Color data can provide important information on compositional variation in the core including, for example, carbonate content, iron content, redox state.

Digital imaging

Digital imaging is a powerful and rapid technique for analysing high frequency down-core variations such as sedimentary laminae or varves. Digital scanners (e.g., Optotech) are used with commonly attainable resolutions of 0.1 mm (Schaaf & Thurow, 1994). A line scan of the gray values from such digital images may be used to generate time series from regular laminae or annual varves (e.g., Schaaf & Thurow, 1998). However, in data processing, care must be taken to subtract voids and cracks, to correct for non-uniform light distribution and to stack images into a continuous time series.

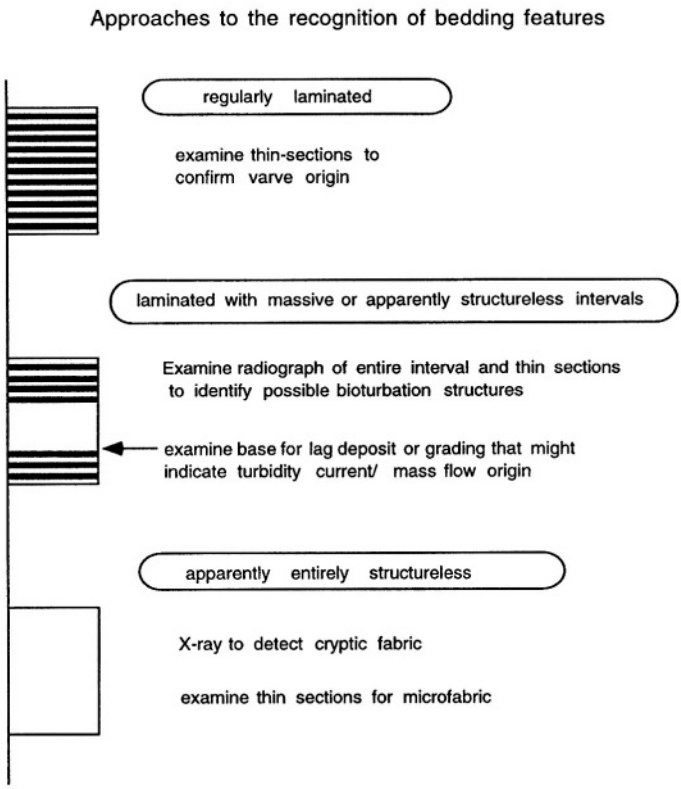


Figure 2. Approaches to the recognition of bedding features.

Penetrative imaging of the core

Radiography and X-ray imaging

Radiography has been used for some decades to provide insight into the layering and internal structures of sediments. The identification of bedding features, such as compositional layering as well as bioturbation fabrics, is often greatly enhanced. The resolution of the X-radiograph is generally limited by the thickness of the sediment sample and it is common practise to X-ray an approx. 1 cm-thick slab of sediment taken from the core with a slab cutter where resolution of 0.3 mm is attainable (Figs. 3, 4). A digital X-ray imaging system has recently been developed (Migeon et al., 1999) with 0.2mm resolution. This permits image enhancement techniques to be used which can vastly improve the differentiation and sensitivity of radiographic images. Digital gray scale images may be produced and processed in a similar method to core surface scans (above).

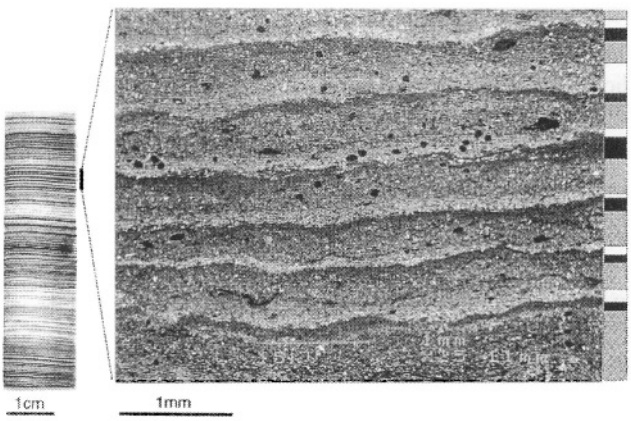


Figure 3. Laminated sediment from Lake Kassjön, Sweden: (a) X-radiograph; (b) BSEI photograph showing three-component varves. Key: (1) terrigenous, graded silts (white) deposited during snow melt in May; (2) organic/fine silt (gray) deposited during a period of biological production throughout June-September; and (3) clay/fine-grained organic material deposited when the lake is ice-covered, i.e. between November–April (black).

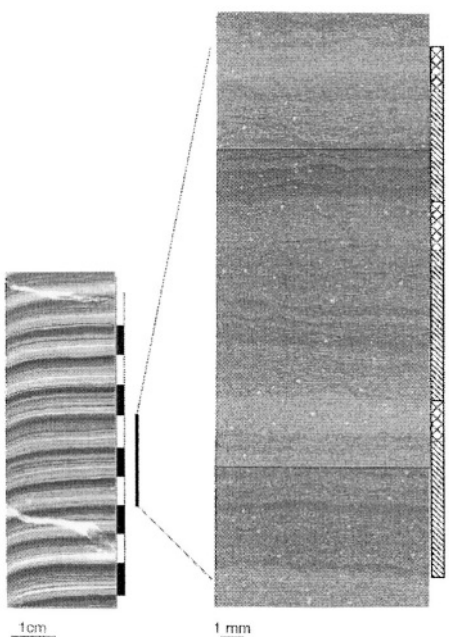


Figure 4. Laminated sediment from Saanich Inlet, British Columbia, Ocean Drilling Program drill Site 1093: (a) X-radiograph, individual varves are indicated by the black/white banding on the RH side of the image; (b) BSEI photograph showing two-component varves. Key: (1) diatom ooze/diatomaceous mud, these sediments are equivalent to spring-autumn deposition (diagonal shading); (2) silty-clay deposited during the winter months (cross-hatch shading).

CT-scanning

The use of medical body-scanners to image core material gives an important additional method of applying X-rays (Kenter, 1989). In this technique large samples may be scanned by a rotating X-ray beam to produce tomographic images of slices as thin as 2 mm. This has the considerable advantage that intact whole-round core samples may be scanned as well as split cores or slabs.

Sampling wet, unconsolidated or semi-consolidated sediment

Sub-sampling of wet sediment from cores is best accomplished with a sediment slab cutter (Schimmelmann et al., 1990) (Figs. 5, 6). The cutter, which uses the osmotic knife principle, provides undisturbed, 1 cm-thick sediment slabs which may then be X-radiographed for a permanent record of internal structure (Figs. 5, 6). Where strong sediment fabrics preclude the use of the slab cutter (e.g., by the presence of mesh-like diatom mats); slabs of sediment should be cut using either a large scalpel or 'autopsy' blade. Slabs may then be sub-divided for thin section preparation, micropalaeontological, geochemical and granulometric analyses. For thin section preparation, sediment blocks are initially cut from the slab using a scalpel.

Sediment drying and resin-embedding

For a range of analytical methods it is necessary first to dry out wet sediment. The technique that many researchers have found best-suited to this is fluid displacive embedding. A number of other methods are also employed.

Critical point drying

Above a critical point of temperature and pressure, the phase boundary between liquid and gas disappears (Bouma, 1969). The critical point of water is very high so pore-fluids are usually replaced by an alcohol (e.g., ethanol), followed by liquid CO_2. After the sample has been subjected to the appropriate temperature and pressure, gaseous CO_2 is removed and the dry sample is ready for resin-impregnation (Bennet et al., 1981; Reynolds & Gorsline 1992).

Freeze drying

Freeze drying is carried out using liquid nitrogen (Bouma, 1969). Samples must be in contact with the nitrogen at one face only so that it can move through the sediment block as a front. Quick freezing turns water into ice without ice-crystal growth. Frozen samples are placed into a freeze-drier immediately, and water is removed by sublimation (Crevello et al., 1981). A variant of this method is used in the process of resin-embedding of freeze cores (Lamoureux, 1994; 2001).

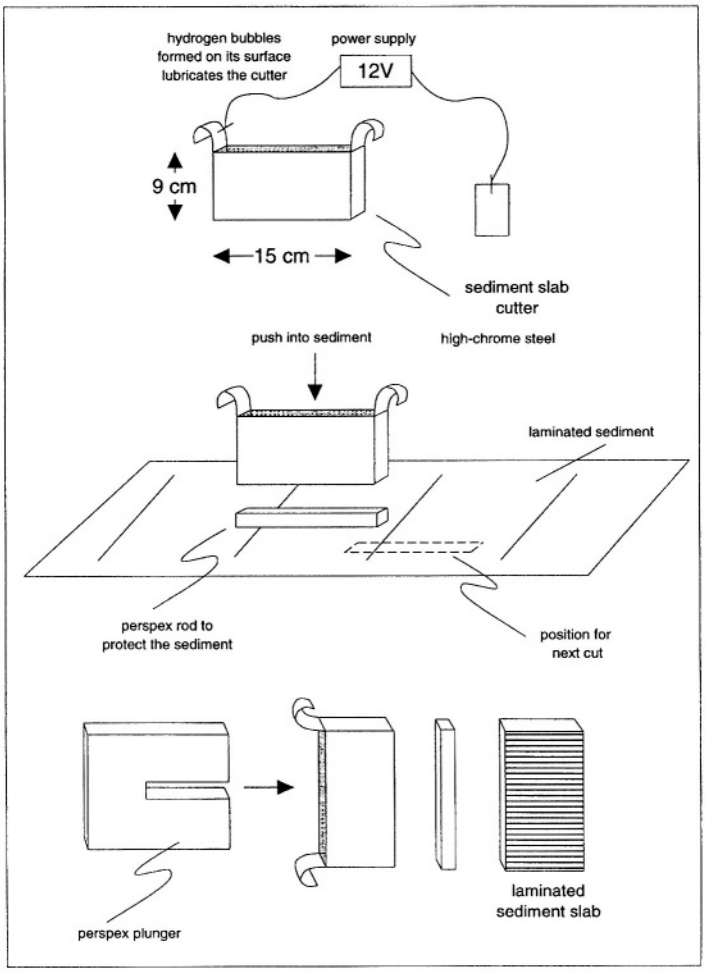


Figure 5. The Schimmelmann sediment slab cutter, described in Schimmelmann et al. (1990) (modified after Pike & Kemp, 1996).

Vacuum drying

During vacuum drying, the sample chamber is evacuated, removing any sediment pore-fluids. This is carried out using a vacuum impregnation unit (e.g., Bull & Kemp, 1995) such as that manufactured by Logitech. This unit introduces low-viscosity epoxy resin into the evacuated sample chamber aiding resin penetration. After releasing the vacuum, the resin-impregnated block is then cured in an oven. This is effective either for sediments which are already dry or for porous (e.g., diatom-rich) sediments, but is not effective for clay-rich sediment.

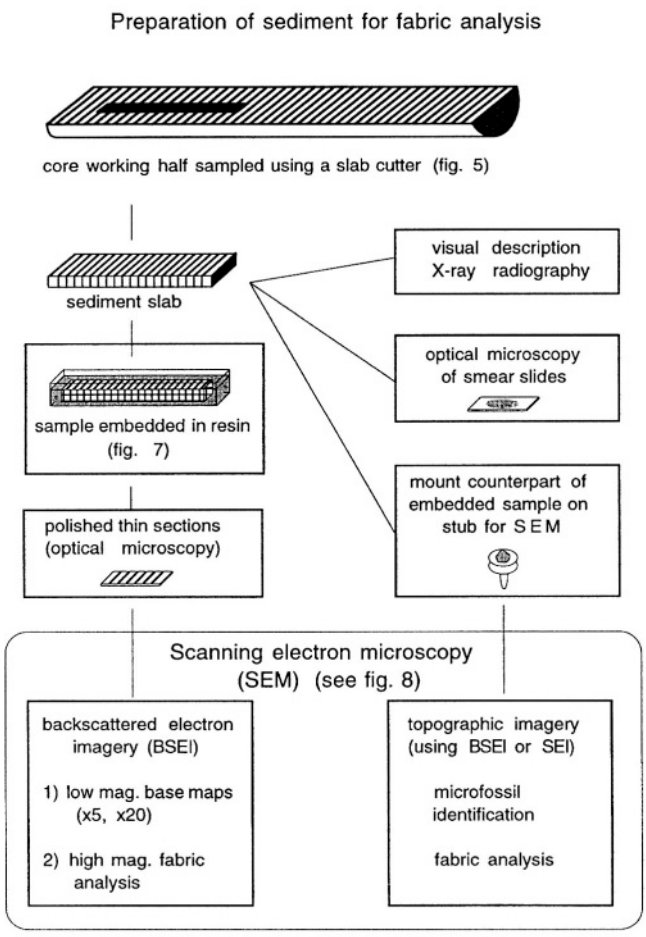


Figure 6. Preparation of wet sediment core for fabric analysis.

Fluid displacive drying and resin-embedding of wet sediments

This technique of drying and resin-embedding provides the best quality thin sections for microscopy. The method (described in Appendix I and illustrated in Figure 7) is adapted after Jim (1985), Polysciences Inc. (1986), Lamoureux (1994) and Pike & Kemp (1996) and uses low-viscosity Spurr epoxy resin (Spurr, 1969). Some of the component chemicals of this resin are toxic, and the operation requires a fume cupboard.

Fluid displacive resin-embedding of wet sediment is a passive procedure, samples are never physically dry and the fabric is supported by fluid throughout. Chemical dehydration prevents the cracking (common in vacuum dried sediment), and the technique requires no specialized drying, or resin-impregnating equipment. Water-saturated samples are more successfully embedded using fluid replacement than those which are partially dry.

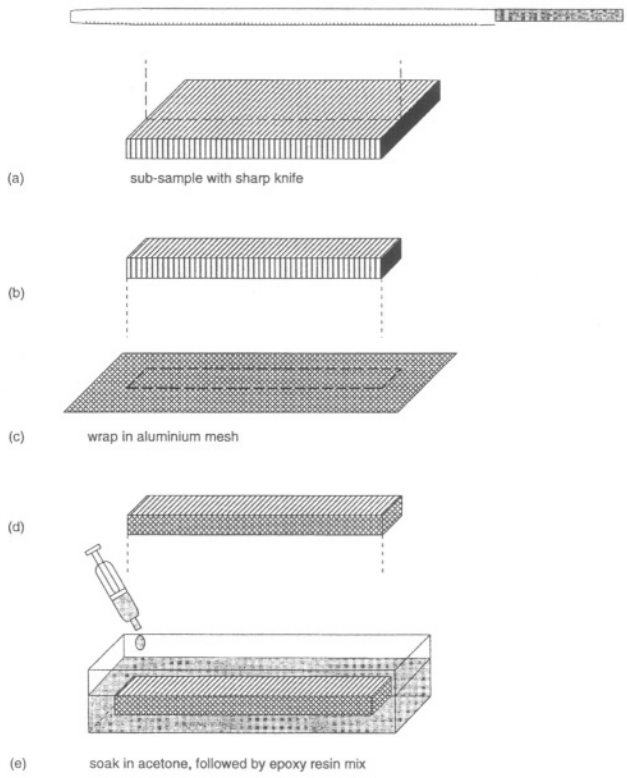


Figure 7. Preparation of wet, unconsolidated sediment samples for resin embedding.

Increasing the number of replacements of solvent and resin aids the embedding of less porous sediment. Thin sections produced by this technique show no sediment fabric disturbance and preserve the most detail for SEM-scale studies (Figs. 3, 4).

Thin section preparation

Very little preparation is required to produce thin sections from indurated rocks (Krinsley et al., 1983). Friable lithologies (e.g., diatomite), however, may require resin-impregnation to hold them together. Once this has been completed either impregnated blocks, or saw-cut samples of rock are glued to a glass microscope slide, the major portion of the block cut away, and the remaining sample ground and polished (avoiding the use of water-based lubricants which may cause swelling and rearrangement of the clay minerals and fabric disturbance).

Thin sections of resin-impregnated blocks are prepared in the same way as saw-cut rock samples. Oil-based rather than water-based lubricants should be used for cutting. For SEM analysis, thin sections should be highly polished, using a range of grits down to 1 μm,

particularly for BSEI (Krinsley et al., 1983). If thin sections are to be used for optical, as well as electron, microscopy they should be polished down to at least 35 μm. Thin sections are carbon-coated before being analysed in the SEM (Goldstein et al., 1992).

SEM analysis of laminated sediment

With digital imaging and X-radiography, variations in the thickness of the annual varve and the thickness of the light and dark components may be obtained. To proceed further into intra-annual resolution, scanning electron microscopy (SEM) must be adopted. The use of SEM methods can unlock a plethora of paleoenvironmental information such as interannual variability in the occurrence of individual microfossil species (e.g., Pike & Kemp, 1997). A comprehensive summary of the principles and practice of SEM, and types of analyses possible, is provided by Goldstein et al. (1992). The following is a description of BSEI, SEI and X-ray microanalysis applied to fine grained sediments and the approach is summarized in Figure 8.

Backscattered electron imagery (BSEI)

Analytical technique. Backscattered electrons are the result of elastic collisions between energetic beam electrons and atoms within the specimen (Goldstein et al., 1992). The number of backscattered electrons generated (backscatter coefficient, η) is primarily related to the average atomic number of the target (when using polished thin sections), and is recorded on a photograph as image brightness. Mineral grains such as pyrite, quartz and carbonate have relatively high average atomic numbers, and therefore have higher backscatter coefficients and produce brighter images than organic matter and carbon-based resin, which have low average atomic numbers, low backscatter coefficients, and produce dark images, i.e., black. BSEI photomosaics of laminated sediments provide compositional data, but may also be regarded as porosity maps which give sediment fabric information. Biogenic laminae comprising diatoms, for example, have high porosity and are recorded as dark layers on the photomosaic (carbon-based resin fills the frustules — Figs. 3, 4). Lithogenic laminae, comprising silt and clays, have low porosity and are characterised by bright layers. This contrast between components and resin, and the shallower sampling depth within the thin section, provides greatly improved resolution images over optical micrographs.

Sediment fabrics, such as bioturbation, may be investigated using BSEI photomosaics (e.g., Brodie & Kemp, 1995). Porosity contrasts highlight biogenic and lithogenic material redistributed by burrowing. BSEI can also be used for facies analysis of fine grained rocks (e.g., the Jurassic Kimmeridge Clay Formation (UK); Macquaker & Gawthorpe, 1993).

Secondary electron imagery (SEI)

Analytical technique. Secondary electrons are produced by inelastic collisions between high-energy beam electrons and atoms within the specimen (Goldstein et al., 1992). The number of secondary electrons emitted, and the resulting secondary electron coefficient, is

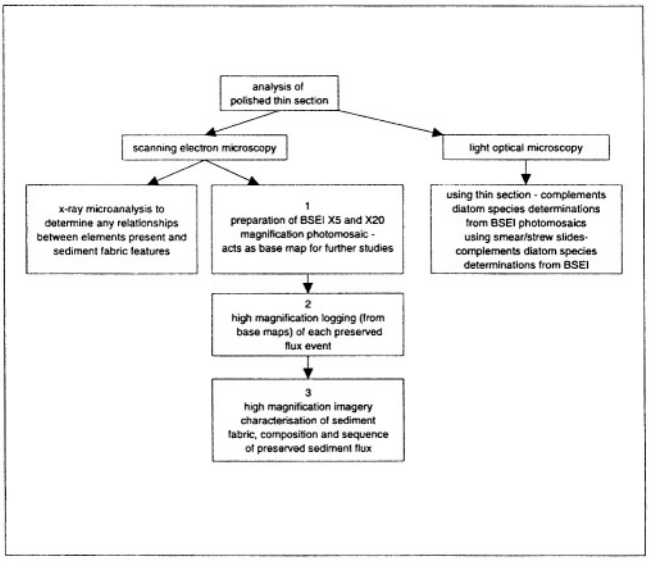


Figure 8. Summary of the analysis of polished thin sections using scanning electron microscopy and optical microscopy (after Pike & Kemp, 1996).

affected by the topography of the specimen, therefore the images produced are topographic and may be considered analogous to binocular optical microscopy images.

High-magnification SEI images of gold-coated, fractured sediment surfaces mounted on SEM stubs are used to aid characterization of laminations, e.g. component and microfossil taxa identification. If polished thin sections are thin enough, optical microscopy (utilising the depth of view within the section) can be used to reduce the amount of SEI imagery required.

Low vacuum scanning electron microscope (LVSEM)

Analytical technique. The LVSEM uses back-scatter electrons which are energetic enough to move through the low vacuum in the specimen chamber to the detector; these contrast with secondary electrons which have insufficient energy to pass through the low vacuum. Thus, either wet sediment blocks or strew mounts may be analysed directly and topographic images are produced without the need for carbon/gold coating. High magnification LVSEM images have the same uses as traditional SEI images.

Summary

The aim of this chapter has been to provide a comprehensive introduction to the various techniques involved in visualising bedding features at the appropriate scale required for their identification. Of course, this is just the first step along the road of analysis, quantifi-

cation and interpretation, but use of the optimal approaches can save time and aid in the development of cost-effective and efficient exploitation of paleo-archives.

Our main recommendation to anyone embarking on the analysis of lake sediments would be to adopt a systematic approach as outlined in Figure 1. Core material is generally hard to obtain and precious, so the correct sequencing of the different analytical methods is essential if the scientific outcome is to be maximized.

Acknowledgements

The approaches outlined were developed during research funded by the Natural Environment Research Council (UK) and the University of Southampton. We are most grateful to Bob Jones and John Ford for their help, advice and skill on all aspects of sediment embedding and thin section preparation.

Appendix 1

Fluid displacive low viscosity resin embedding technique

This technique is ideal for resin embedding of wet sediment samples for the purpose of fabric studies using the scanning electron microscope (SEM). By the nature of the method, the more water-saturated the samples, the better the results are as there will be a greater pathway for the acetone, and subsequently resin, to enter the sediment block. Accordingly sediment material should not be allowed to dry out, even slightly. The number of replacements needed, of both acetone and resin, will vary with the type of material. Coarser-grained, drier and/or thicker samples will require a greater number of replacements. It is advisable to vary the replacements of both acetone and resin, until a suitable combination is found. The succeeding method details 5 replacements only, and is suited to porous sediments such as diatom oozes; for less porous sediments, such as those with a significant clay fraction, more resin replacements (up to 12) are likely to be necessary.

Spurr Resin impregnation kits are available from Polysciences Ltd., Handelsstr. 3, Postfach 1130, D-6904 Eppelheim, Germany. These kits contain the chemicals and some of the equipment that is needed. However, the chemicals are supplied in significant mis-proportions for the resin standard mixture used, so it is more cost effective to purchase the individual chemicals.

Samples should be taken from the cores using a sediment slab cutter (Fig. 5) or rigid plastic u-channels, or a similar rigid, box-like container. Care is needed to ensure disturbance of the sediment is kept to a minimum. The sample and its container should be securely taped together and a number of samples may be wrapped together, with a piece of water-soaked oasis, and enclosed with cling film. This is to prevent the samples from drying out. The wrapped samples should then be refrigerated at 4–6 °C until such time as they are to be processed.

Method

Place the container (high density polyethylene — HDPE) to be used on a balance and tare. Fill with water to required depth (approx. 0.75–1.0 cm — enough to cover the sample when it is placed into the container). This is the mass of resin mixture needed for each replacement (round up to nearest gram), and the required mass of each reagent may be calculated using the standard below.

Standard:

Vinyl cyclohexene dioxide, VCD	10.0 g
diglycidol ether of polypropyleneglycol, DER	6.0 g
Nonenyl succinic anhydride, NSA	26.0 g
Dimethylaminoethanol,DMAE	0.2 g

Label containers by scratching the sample details and direction (way-up) arrow on the side. Any pen-drawn marks are likely to disappear in the acetone environment within the desiccator.

Samples should be as small as possible, i.e. less than 1 cm thick, 0.75 cm wide with length depending on the size of the containers. They should be prevented from drying out as much as possible (before addition of acetone) as wet samples are better suited to this technique. Place samples in either close-fitting foil, or fine wire mesh 'boats' so that samples may be moved without disturbing the sediment. After placing samples into wire mesh/foil containers, de-ionised water may be added using a syringe and replaced every couple of hours, this process can be repeated 2–3 times. If the samples have previously dried out, soaking them in water first is not advised, as some sediments are prone to expansion after the addition of water. During the soaking of samples, the sediments should be left in a sealed container to avoid desiccation.

Place the containers in a glass desiccator, over silica gel, and cover the samples with acetone by adding the acetone slowly from a small syringe so that it flows down the side of the container. Do not add to the tops of the samples. It is best to add small amounts of acetone gently, as a strong stream may disturb the samples, which can have a tendency to float, especially if broken or fragmented. A greater depth of acetone is required overnight as it is volatile, and the samples must not be allowed to dry out.

Change acetone 3 times a day (at least 3 hrs between each change) and complete 10–15 soakings, removing the "waste" acetone from the container using a syringe. The first 7 soakings are made using technical acetone and the final 8 using analytical acetone.

Prepare resin mixture immediately before adding to the containers. Contact of VCD and DMAE may cause an exothermic reaction so it is important to weigh out the reagents using separate syringes. Weigh the VCD, DER, NSA in separate tared containers (HDPE), add together and stir gently. Then add the DMAE and stir thoroughly.

The initial resin replacements are diluted with acetone to facilitate the embedding procedure. The resin content of each replacement is increased by stages in the following way: (1) the first addition of the acetone/resin mixture were in the proportion 50:50, (2) the second in the proportion 25:75, (3) the third in the proportion 10:90, and (4) the remaining two consisted of resin only. An example calculation is given at the end of the method.

Add the resin (or resin:acetone mixture) to the container, using a syringe, after the last quantity of acetone has been removed. Gently move the samples, lifting them slightly after each addition, to ensure fresh resin mixture reaches all around the sample. Keep the containers in the desiccator as moisture will make the resin go milky. This does not cause a major problem for backscatter electron imagery work because the resin will still appear black in the SEM. However, it is not a good idea to let it go to cloudy as it will hinder any comparisons between the slide and the remaining resin embedded block. Change the resin once a day to prevent difficulties arising from increases in the viscosity, and complete 5 soakings. After the final addition of resin, leave samples to soak for up to four weeks before curing. Ideally resin replacements should be made 24 hours apart, and for safety reasons resin replacements should be undertaken during normal working hours.

Samples are cured in stages, initially at a temperature of 30 °C for 72 hrs. Thereafter, samples are cured at 45 °C and 60 °C for 24 hours each. The resin should be left to cool after each heating stage, and it is important to allow the oven temperature to stabilize for a couple of hours before you put the samples in. It is important not to overheat the resin as it will bubble and destroy the fabric of the sediment. If the resin is slightly soft after the first stage of curing at 30 °C, this part of the process should be continued until the resin has hardened, and no longer deforms under moderately applied pressure.

After curing, the casting is relatively inert and should be very hard. This can be mounted, cut, ground and polished to give a polished thin section for optical microscopy or SEM work. This polished thin section should be carbon-coated before examination in the SEM using a back-scattered electron detector.

Example Calculation for a Container Requiring 12.5 g Resin

	Standard	Ratio
VCD	10.0 g	0.237
DER	6.0 g	0.142
NSA	26.0 g	0.616
DMAE	0.2 g	0.005

For 12.5 g resin:-

VCD: 0.237 × 12.5 = 2.96 g needed for 12.5 g of resin mixture. Apply same principle to other reagents.

Multiply this figure by the number of containers for the total amounts of the reagents needed for each resin replacement involving a 100% resin mixture.

To estimate the acetone and resin contents of the resin:acetone mixtures: (1) calculate the total mass, M of resin required for a 100% resin mixture (see above); (2) calculate 50%, 25%, and 10% of M to give mass of acetone required for each mixture; (3) calculate new figures for chemical components to make up a pure resin mixture for a mass of M/2, M/4, and M/10.

References

Bennett, R. H., W. R. Bryant & G. H. Keller, 1981. Clay fabric of selected submarine sediments: Fundamental properties and models. J. Sed. Petrol. 51: 217–232.

Blais-Stevens, A., J. J. Clague, P. T. Brobowsky & R. T. Patterson, 1997. Late Holocenc sedimentation in Saanich Inlet, British Columbia, and its paleoseismic implications. Can. J. Earth Sci. 34: 1345–1357.

Bouma, A. G., 1969. Methods for the Study of Sedimentary Structures. Wiley, N.Y., 458pp.

Brodie, I. & A. E. S. Kemp, 1985. Pelletal structures in Peruvian sediments upwelling sediments. J. Geol. Soc. Lond. 152: 141–150.

Bull, D. & A. E. S. Kemp, 1995. Composition and origins of laminae in late Quaternary and Holocene sediments from Santa Barbara Basin. In Kennett, J. P., J. G. Baldauf & M. Lyle (eds.) Proc. ODP, Sci. Results 146 (Pt 2): College Station TX (Ocean Drilling Program): 77–87.

Chmelick, F. B., 1967. Electro-osmotic core cutting. Mar. Geol. 5: 321–325.

Crevello, P. D., J. M. Rine & D. E. Lanesky, 1981. A method for impregnating unconsolidated cores and slabs of calcareous and terrigenous muds. J. Sed. Petrol. 51: 658–660.

Dean, J. M., A. E. S. Kemp, D. Bull, J. Pike, G. Petterson & B. Zolitschka, 1999. Taking varves to bits: Scanning electron microscopy in the study of laminated sediments and varves. J. Paleolim. 22: 121–136.

Gersonde, R., D. A. Hodell, P. Blum, et al., 1999. Proc. ODP, Init. Repts., 177 [CD-ROM]. Available from: Ocean Drilling Program, Texas A&M University, College Station, TX 77845-9547, USA.

Goldstein J. I., D. E. Newbury, P. Echlin, D. C. Joy, C. E. Romig Jr., C. Lyman, C. Fiori & E. Lifshin, 1992. Scanning Electron Microscopy and X-ray Microanalysis. 2nd ed. Plenum, New York, 820p.

Jim, C. Y., 1985. Impregnation of moist and dry unconsolidated clay samples using Spurr resin for microstructural studies. J. Sed. Petrol. 55: 597–599.

Kenter, J. A. M., 1989. Applications of computerized tomography in sedimentology. Mar. Geotechnol. 8: 201–211.

Krinsley, D. H., K. Pye & A. T. Kearsley, 1983. Application of backscattered electron microscopy in shale petrology. Geol. Mag. 120: 109–114.

Lamoureux, S. F., 1994. Embedding unfrozen lake sediments for thin section preparation. J. Paleolim. 10: 141–146.

Lamoureux, S., 2001. Varve chronology techniques. In Last, W. M. & J. P. Smol (eds.) Tracking Environmental Change Using Lake Sediments. Volume 1: Basin Analysis, Coring, and Chronological Techniques. Kluwer Academic Publishers, Dordrecht, The Netherlands: 247–260.

Macquaker, J. H. S. & R. L. Gawthorpe, 1993. Mudstone lithofacies in the Kimmeridge Clay Formation, Wessex Basin, southern England: implications for the origin and controls of the distribution of mudstones. J. Sed. Petrol. 63: 1129–1143.

Migeon, S. O. Weber, J.-C. Faugeres & J. Saint-Paul, 1999. SCOPIX: A new X-ray imaging system for core analysis. Geo-Marine Lett. 18: 251–255.

Mix, A. C., W. Rugh, N. G. Pisias, S. Viers, T. Hagelberg, S. Hovan, A. E. S. Kemp, M. Leinen, M. Levitan & C. Ravelo, 1992. Color reflectance spectroscopy: a tool for the rapid characterization of deep-sea sediments. Proc. ODP, Init. Repts, 138. College Station, TX. (Ocean Drilling Program): 67–77.

Nagao, S. & S. Nakashima, 1992. The factors controlling vertical colour variations of North Atlantic Madiera Abyssal Plain sediments. Mar. Geol. 109: 83–94.

Polysciences Inc., 1986. Spurr Low-viscosity Embedding Media. Polysciences data sheet 127.

Pike, J. & A. E. S. Kemp, 1996 Preparation and analysis techniques for studies of laminated sediments. In Kemp, A. E. S. (ed.) Palaeoceanography and Palaeoclimatology from Laminated Sediments. Geol. Soc. Spec. Publ. 116: 37–48.

Pike, J. & A. E. S. Kemp, 1997. Early Holocene decadal-scale ocean variability recorded in Gulf of California laminated sediments. Paleoceanog. 12: 227–238.

Reynolds, S. & D. S. Gorsline, 1992. Clay microfabric of deep-sea, detrital mud(stone)s, California continental borderland. J. Sed. Petrol. 62: 41–53.

Schaaf, M. & J. Thurow, 1994. A fast and easy method to derive highest-resolution time-series datasets from drillcores and rock samples. Sed. Geol. 94: 1–10.

Schaaf, M. & J. Thurow, 1998. Two 30,000 year, high resolution grey values time series from the Santa Barbara Basin and the Guaymas Basin. Geol. Soc. Spec. Publ. 131: 101–110.

Schimmelmann, A., C. B. Lange & W. H. Berger, 1990. Climatically controlled marker layers in Santa Barbara Basin sediments and fine-scale core-to-core correlation. Limnol. Oceanogr. 35: 165–173.

Spurr, A. R. 1969. A low-viscosity epoxy resin embedding medium for electron microscopy. J. Ultrastruct. Res. 26: 31–43.

3. IMAGE ANALYSIS TECHNIQUES

TIMO SAARINEN (timo.saarinen@gsf.fi)
Geological Survey of Finland
Betonimiehenkuja 4
FIN-02150 Espoo
Finland

GUNILLA PETTERSON
Department of Ecology
and Environmental Science
Umeå University
S-901 87 Umeå
Sweden

Keywords: digital image analysis, image processing, paleolimnology, lake sediments, varve counting, documentation, grey-scale, scanning

Introduction

In recent time, the interest in proxy archives with annual time-resolution has increased because of their potential as records for studying environmental change on a precise and high-resolution time-scale (e.g.,Gasse et al., 1997; Maslin & Berger, 1997; Alverson, 1999). The identification and analysis of rapid climatic changes is one example of a study, which requires not only a high-resolution archive but also a method suitable for such an investigation. Palaeolimnological studies are, however, often based on the visual inspection of microscope views, photos, or sediment core surfaces, and verbal descriptions of the character of the sediment, making it difficult to obtain precise and objective measurements. Image analysis is a powerful tool for quantitative analyses of sedimentary structures. The appearance of the sediment is digitized without disturbing the sediment sample, and with the obtained images it is possible to enhance or smooth desired structures with a number of applications (Cooper, 1997). Description of colour changes and varve structures, together with varve thickness measurements and grain size analyses, are examples of parameters that benefit from an objective and fast high-resolution technique such as image analysis.

Image analysis has been defined as the technique of obtaining quantitative information by measuring objects within an image (e.g., Mainwaring & Petruk, 1989; Russ, 1994; Fortey, 1995). The human brain is excellent at detecting and recognising patterns and spatial relationships, but very poor at estimating quantitative information from images (e.g., Russ, 1994; Krinsley et al., 1998). Image analysis has become very useful for industrial



W. M. Last & J. P. Smol (eds.), 2001. *Tracking Environmental Change Using Lake Sediments. Volume 2: Physical and Geochemical Methods.* Kluwer Academic Publishers, Dordrecht. The Netherlands.

purposes and in research because of its ability to process digital images and objectively, without disturbing the sample, analyse parameters such as size, distance, colour, number of particles, etc. (e.g., Rosenfeld & Kak, 1982; Pratt, 1991; Gonzales & Woods, 1992; Russ, 1994; Jähne, 1997).

The very rapid development of computers, hardware and image analysis programs during the last few years has opened up the opportunity of using image analysis as a standard method in palaeolimnolgy. Until the late 1990s, image analysis had seldom been used in palaeolimnology, although the technique had been successfully applied in related research areas such as tree-ring analysis, geology, petrology, marine sedimentology and soil morphology. Image analysis has three main advantages compared to conventional descriptive sedimentology. (i) The technique is objective, i.e., every colour shade is given a precise grey-scale or colour value compared to the subjective human description of a greyish sediment colour. (ii) Image analysis is a fast method, especially compared to the sub-sampling and subsequent analysis of biological parameters. (iii) Image analysis allows high-resolution analysis for example of seasonal layers in varved lake sediments. With the use of image analysis, either as a complement to other chemical, biological and physical parameters, or as a substitute for some of them, new and important information about past environmental changes can be gained.

An image can be obtained from different sources, but in a palaeolimnological context images are often acquired from fresh sediments or thin sections using different cameras and digitizing techniques. Working with image analysis involves three major steps: data acquisition, image processing and image analysis, i.e., the actual measurement of the object of interest (Fig. 1). In this chapter we will outline a basic approach for image analysis in palaeolimnology, describe some of the problems, give some examples of research results and discuss future prospects for the technique.

Image analysis in paleolimnology

The main application for image analysis in palaeolimnolgy has hitherto been varve counting and varve thickness measurements. Thetford et al. (1991) and Ripepe et al. (1991) showed how image analysis could be used to count and measure the thickness of tree-rings and varved oil shales, respectively. Since then, image analysis has also been applied to laminations and varves from lake sediments (Petterson et al., 1993; 1999; Dean et al., 1994; Zolitschka, 1996), postglacial clays (Anderson, 1996; Godsey et al., 1999; Lindeberg & Ringberg, 1999) and marine sediments (Schaaf & Thurow, 1994, 1997). The time-consuming work using manual equipment such as a tree-ring-measuring microscope can be replaced with image analysis. Varves or laminations are identified via alternating changes in colour or grey-scale depending on changes in density, grain-size or sediment composition. With methods developed for semi-automatic varve thickness measurements, artificial trends caused by heterogeneous illumination and noise from disturbances within the sediment can be handled (Ripepe et al., 1991; Bond et al., 1992; Schaaf & Thurow, 1994; 1997).

Image analysis can also be used to record changes in sediment composition. Relationships have been established between absolute grey-scale values or relative changes in grey-scale versus light-coloured sediment components such as mineral grains and calcium carbonate. Petterson et al. (1999) developed a model to infer the annual minerogenic matter accumulation rate by calibrating corrected grey-scale values (mean grey-scale per varve ×

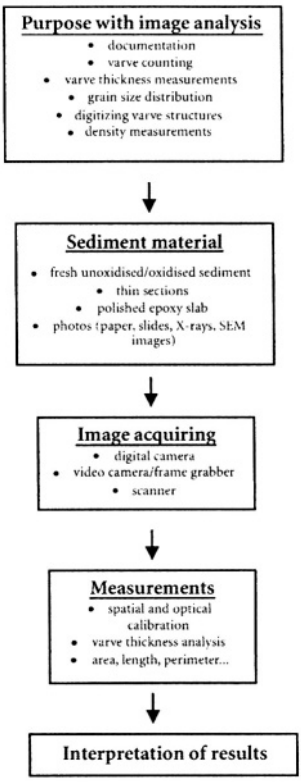


Figure 1. The flow chart illustrates the advantages and flexibility of image analysis. Image acquiring, processing and measurements can be applied according to the purpose of the study and the sediment material available.

varve thickness) against sediment component accumulation rates. Bond et al. (1992) used relative changes in grey-scale to study the concentration of calcium carbonate in marine sediments during different isotopic stages, and Anderson (1996) demonstrated a relationship between grey-scale density and percentage calcium carbonate in glacial laminations from Lake Estancia (New Mexico). Hughen et al. (1996) used grey-scale as a proxy for changes in biogenic productivity.

Data obtained by image analysis has often been used in climatic contexts such as the detection of cycles (Ripepe et al., 1991; Schaaf &Thurow, 1994, 1997) or identification of major climatic changes (Bond et al., 1992; Hughen et al., 1996).

Another application for image analysis is to count and analyse the shape and size of particles. This technique has successfully been applied in petrology (Petruk, 1989), structural geology (Bons & Jessell, 1996) and soil morphology (Tovey et al., 1992; Tovey & Hounslow, 1995). For palaeolimnological purposes, image analysis can be used to identify diatoms (Stoermer, 1996), and to count and characterise charcoal particles (Clark & Hussey, 1996; Goni, 1996; Earle et al., 1996) and mineral grains (Spooner, 1998; Bonardi & Tosi, 1995).

Image analysis has also been used to process back-scattered electron images to analyse the grain-size distribution of clastic minerals (Francus, 1998) and for sedimentological analyses (Krinsley et al., 1998). Finally, digital imaging is an excellent method for the documentation of sediment cores (e.g., Dartnell & Gardner, 1993). Cores are often sub-sampled and thus destroyed immediately after recovery, or left uncovered during, for example, varve counting which causes some drying and subsequent change of the appearance. Images of the cores can be preserved permanently and parameters analysed and reanalysed long after the cores have disappeared. Digital images do not loose their colour information during storage as conventional photographs do. The images are invaluable for core matching if new cores must be taken, which is not unusual in palaeolimnology.

Material and methods

It is important to remember that the final outcome of a study involving digital images depends on the quality of the sediment material used. It is easier and more reliable to generate quantitative information from high quality original images rather than strongly processed ones. Processing may modify image information, which can affect the grey-scale and particle characteristics, producing results not in accordance with the original sediment material.

Image acquisition and storing

A digital image is a two-dimensional array (x, y) of pixels where every pixel has a value related to the characteristics of the image, for example light reflection from a sediment sample (colour or grey-scale variation), density (x-ray radiography) or mean atomic number (back-scattered electron image). The resolution of the images varies with the equipment; if the sediment is digitized in a 8-bit grey-scale, each pixel represent a value ranging from 0 (black) to 255 (white). Digital images can be obtained from a number of macroscopic as well as microscopic sediment sources. Images can be acquired directly with a digital camera, which digitizes the sediment surface, or indirectly by a scanner, which digitizes a photograph of a sediment surface (Table I). The aim of the study and the sediment material determines the optimal technique to be used.

Digital cameras

Digital cameras produce high quality images from fresh sediment surfaces (Fig. 2a). Time is saved compared to the use of conventional photographs since the work with development and scanning can be omitted. It is, however, very important to prepare the sediment correctly in order to obtain images with a high quality. Video cameras with a frame grabber system have often been used to acquire digital images, but there is a trend towards replacing video cameras with multipurpose digital cameras.

Procedure for digitizing a fresh sediment surface with a digital camera

1. Prepare a flat core surface. For example, curved surfaces of cores sampled with a Livingstone or Russian corer must first be levelled off (Petterson et al., 1993, 1999).

Table 1. Examples from articles and the Geological Survey of Finland (GSF) on sediment sources and digitizing techniques.

Sediment source	Digitizing method
Fresh sediment surface	Digital camera
	Video camera
	Scanner
Frozen sediment surface	Digital camera
	Video camera
Photograph	Digital camera
	Table scanner
Slide	Slide scanner
X-ray film	Film scanner (dual bed scanner)
Polished epoxy slab	Scanner
	Microscope + digital camera
Thin section	Scanner
	Microscope + digital camera
SEM	Scanner
	Built-in digitizer

2. Proceed immediately with step 3, 4 and 5 if images of the fresh sediment surface are desired. In varved sediments, the colour of the fresh sediment is sometimes determined by iron species and the sediment must be oxidised for a couple of days before digitizing (Renberg, 1981a; Petterson et al., 1993, 1999).

3. Clean and moisten the sediment surface and cover it with stripes of transparent plastic film (Renberg, 1981b; Petterson et al., 1993, 1999). Water enhances the visibility of sediment structures and plastic film prevents drying and water reflections.

4. Day light lamps, flashes or fluorescent tubes can be used to illuminate the sediment. The lamps are placed on each side of the core, often with a direction of 45 ° towards the sediment surface. There are two problems with digitizing cores, uneven illumination and ageing of the lamps. If the room is dark apart from the sediment lighting, it is easier to control the light-conditions. Mathematical routines, e.g., polynomial regressions, can be used to correct for increasing grey-scale values towards the centre of the image (Bond et al, 1992;Schaaf & Thurow, 1994, 1997; Godsey et al., 1999). If a Kodak grey-scale is ditized as a standard in every image (Petterson et al., 1993, 1999) or regularly (Lindeberg & Ringberg, 1999), changes in light intensity due to ageing lamps can be compensated for.

5. Digitize, review the image and adjust the settings of the camera and the lighting. The work is facilitated if the quality of the images can be seen immediately, either by using a digital camera with a built-in LCD (liquid crystal display) screen or by adding

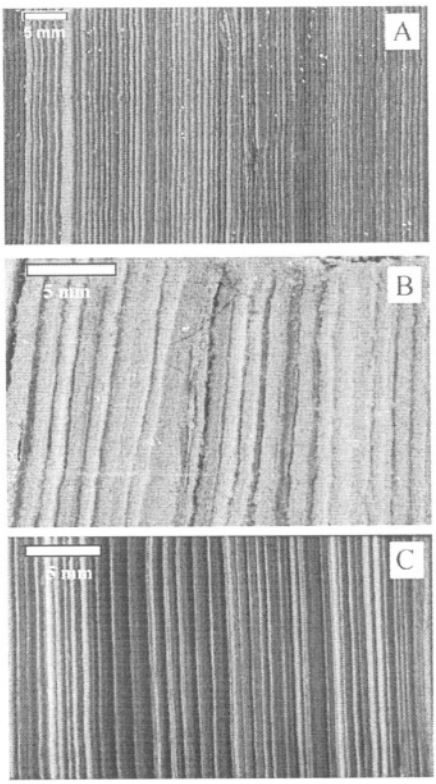


Figure 2. Digital images can be acquired from different sediment sources using a number of techniques. A. Fresh sediment surface digitized with a digital camera (Lake Jaatilanjärvi, Finland). B. Fresh sediment sample scanned directly using a table scanner with a resolution of 1000 dpi (Lake Lehmilampi, Finland). C. Scanned X-ray film from Lake Korttajärvi, Finland.

a video-screen to the camera. Random noise caused by the equipment can be eliminated if several identical images are acquired automatically and averaged into one image.

Scanners

With a scanner it is easy to obtain high-quality digital images from conventional photographs, thin-sections, X-ray films etc. (Table I). Film manufactures and developers may also produce high-resolution slides and photographs in digital form on request. Manufacturers of scanners sometimes advertise high-interpolated resolution, but this does not really improve the resolution of an image. A table scanner equipped with a transparent adapter or a special tray for transparent films can be used to scan large negatives and X-ray films. Slide scanners, which often have a higher resolution than table scanners, can be used for thin sections. Polarizing images can be acquired with a slide scanner if thin polarize sheets are added on both sides of the thin section during scanning (de Keyser, 1999). Zolitschka

(1996) discusses possibilities and problems with scanning of thin-sections of laminated sediments, e.g., uneven sample thickness.

Highly polished epoxy slabs and fresh sediment samples (Fig. 2b) can also be digitized with a scanner, but do not forget to add a plastic sheet on the glass plate before placing the sediment in the scanner. The advantage of scanning epoxy slabs compared to a digital camera equipped with a flash is that it is easier to control the lighting. However, fresh sediment samples and polished epoxy slabs are often very dark, and scanning fails because of the scanner's incapability to separate the darker tones. When dark originals are used, the result is sometimes improved if a 10- or 12-bit grey-scale is used during scanning. The brightness and contrast have to be adjusted before the image is transformed into a 8-bit grey-scale for further analysis. Reflections caused by imperfect polishing of epoxy slabs can be reduced by adding a thin film of water between the glass plate of the scanner and the epoxy slab.

With digital scanning it is possible to acquire high-resolution images from both thin sections and epoxy slabs, which bridges the gap between conventional photography and photomicroscopy, and opens up new possibilities in varve analysis. As an example of work completed at the Geological Survey of Finland in 1999, an AGFA Duoscan II was used to scan 12 cm long thin sections, polished epoxy slabs and 21 × 26 cm long X-ray films (Fig. 2c) using 1000-dpi resolution. The thin sections and X-rays were scanned using a transparent tray and the epoxy slabs were scanned directly on the glass plate (Tiljander et al.; unpublished). Several thin sections or epoxy slabs can be scanned simultaneously.

Procedure for digitizing a photograph with a scanner

1. Acquire a high quality photograph. Avoid dark photos, since the resolution of a scanner is often better for lighter tones than for darker tones.
2. Remove dust from the photograph and the glass plate of the scanner with an air duster.
3. Avoid fingerprints when placing the photograph on the glass plane.
4. Preview the image and adjust the contrast and brightness. By optimizing the image in this step, the need for additional touch-up and enhancement during image processing can be reduced or eliminated.
5. Perform the final scan. The resolution, grey-scale or colour-scale depends on the aim of the study and the properties of the hardware/software.

Storing of images

Digital images are often saved as disk files when working with computer-based image analysis systems. It is important to save both the original and processed images. There are several convenient media for storing of images, e.g., tape drivers, CD- or DVD-ROMs. Digital cameras, scanning programs and photo processing programs usually provides several image formats suitable for data storage. Avoid file formats that use compression, e.g., JPEG. During compression, pixels can be lost, which decreases the quality of the images. If the images are going to be moved between different computer platforms, it is advantageous

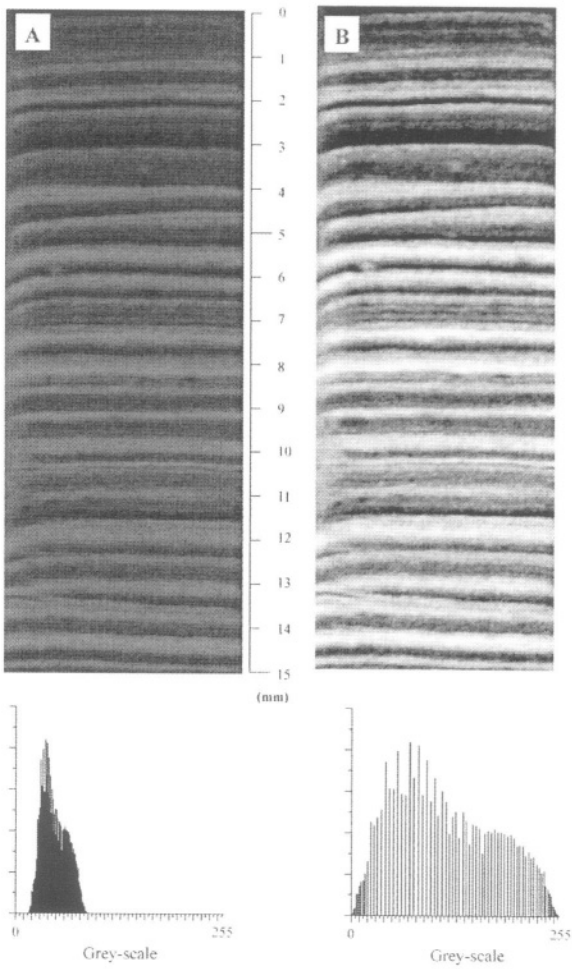


Figure 3. The contrast and brightness of an image; in this example an X-ray image, can be enhanced using the histogram operation equalize. Histograms of both images are shown below the X-ray images.

to use a common image formats like TIFF (tagged image file format). Certain formats may be unique to a particular type of computer.

Image processing

The main purpose of image processing is to enhance the quality of the images prior to further analysis. The graphical presentation of an image usually also benefits from enhancement (Fig. 3). The most common type of enhancement is to adjust the contrast and brightness of an image. A more thorough correction using filters is needed if erroneous pixels from reflections, dust particles or scratches on a photograph are present in the image.

Contrast and brightness

The contrast and brightness of an image can be modified using histogram operations such as equalize and stretch. Sometimes an image does not include the total grey-scale range and consequently results in low contrast. The visual impact of the image can be improved by expanding the grey-scale using histogram functions (Fig. 3). With equalize, the grey-level values within the image are redistributed in order to place an equal number of pixels at each grey-level (Marion, 1991; Cooper, 1997). If the histogram does not cover the entire spectrum, i.e., the image does not include the almost black and/or white values, the stretch operation adjusts the grey-scale range to cover the entire spectrum.

Filters

There are a number of filters available with which it is possible to, for example, reduce noise (e.g., median filter), enhance the contrast of edges (e.g., Laplacian filter), and outline or skeletonize objects within an image (e.g., Russ, 1994). During smoothing with a mean or median filter, a 'neighbouring operation' is performed, i.e., the new grey-scale value of an individual pixel depends on the values of the surrounding pixels. A mean filter calculates the mean value of a selected number of pixels and a median filter ranks a chosen number of pixels and calculates a median value. Medium filters are often better in reducing noise since mean filters smooth sharp lines and edges (Cooper, 1997). Modification of contrast or brightness are 'pixel operations', i.e., the new grey-scale value of a specific pixel is independent of the surrounding grey-scale values. If the *x*- and *y*-axis of an image consist of an equal number of pixels (e.g., 256 × 256 or 512 × 512 pixels), it is possible to enhance an image using Fourier transformation. Processing images in the frequency domain is useful for removing certain types of noise, enhance periodic structures, and measure images to determine periodicity or preferred orientation (Russ, 1994). When filters are used, care is needed to select the most suitable filter for each specific operation. In Figure 4, the effect of using median, outline and shadow filters on a BSE-image is demonstrated.

Segmentation

The purpose of segmentation and thresholding is to divide the image into regions that hopefully correspond to structural units in the sediment, and to distinguish objects of interest for further measurements (Russ, 1994). Density slicing can be used to highlight pixels within a chosen grey-scale range. This method is useful for selecting specified minerals within BSE-images and to identify, for example, dark-coloured winter layers in a varved sediment. Thresholding produces a binary image since pixels with a grey-scale value greater than the threshold turns black and those below the threshold turns white.

Binary images

In a binary image the background is white and the foreground or objects of interest is black (or vice versa). Binary images generally contain small artefacts. Rank filters (e.g., median filters) may be used to clean the image, but they also slightly modify the contour of the

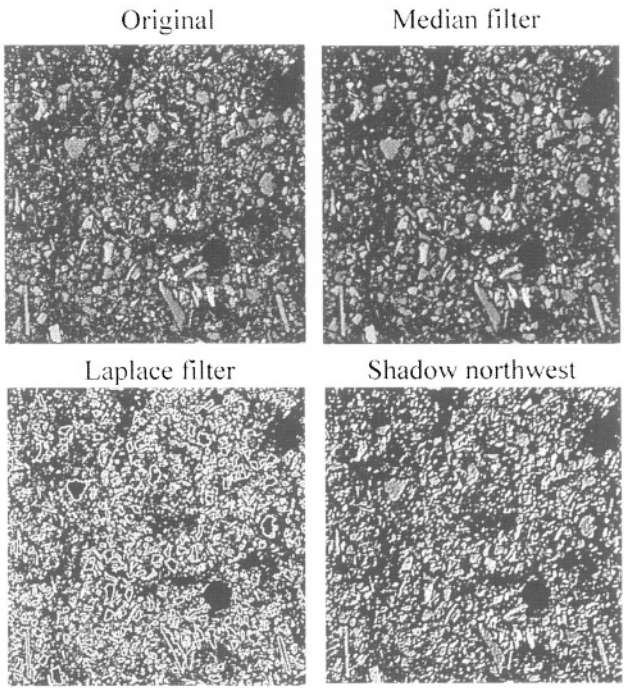


Figure 4. The effect of using median, outline and shadow filters on a BSE-image from Lake Korttajärvi, Finland.

objects. Erosion and dilation are morphological operations that correct specific erroneous pixels. Erosion removes pixels and dilation add pixels, either by filling small holes within the object or by adding a layer of pixels around the border of the object. Dilation slightly increases the size of the object. The two operations are often combined into an opening, where erosion is performed prior to dilation, or a closing where dilation precedes erosion. Dilation and erosion can also be used to separate adjoining objects. It is important that individual objects are clearly separated to avoid incorrect results when parameters such as area and perimeter are measured.

Image analysis

Once the images have been processed, several measurements can be performed. However, care must be taken not to perform measurements on highly processed images if the results are going to be related to, for example, the actual appearance of the sediment surface.

Calibration

The unit in image analysis is the pixel. The actual size of one pixel has to be calculated in order to transform the results into metric scale. Spatial calibration of images is included in

all image analysis software packages. If the scanning resolution is stored in the header of the image files, some programs automatically use this information. Within an image, the actual length of a distance or the actual size of an object can be used for calibration. Pixel size can also be calculated by placing a scale at the sediment surface prior to digitization or by measuring the size of the digitized sediment surface. Optical and X-ray densities can be calibrated by using a standard sample with known density. Bresson & Moran (1998) calibrated X-ray radiography images to obtain high-resolution bulk density data from impregnated soil slices.

Objects and grain-size

Binary images are commonly used for measurements of objects, although some analyses, such as spatial measurements (distance, length and angle) of particles, can be done from non-treated images. The most common operation is to count objects, but other measurements can be routinely made, such as: area, perimeter, roundness, elongation, centre point, and orientation and length of major and minor axes. All objects have to be separated from each other before they are counted, either by morphological operations or manually by drawing lines between them using the background colour. Results from measurements can be saved as computer files and imported to spreadsheet programs for further analyses.

The grain size distribution in a varved or laminated sediment sequence is often related to the inflow of clastic material to the lake. For example, during spring the high water discharges cause erosion in the catchment, which transports both more mineral matter and coarser grain sizes to the deep basin of the lake. BSE-images of polished thin sections (Fig. 5) can be used to determine grain-size variations (Francus, 1998). In varved sediments, BSE images can be used to study palaeodischarge conditions, which in a boreal environment presumably reflects winter/spring conditions in the lake catchement. During image processing, it is recommended to remove noise by excluding objects less than, for example, five pixels. The mineral content of varves can also be estimated from BSE-images by counting the number of black and white pixels along every line in the binary image (Fig. 6).

Grey-scale, varve thickness and varve counting

In varved or laminated sediments, it is common to define individual varves, measure varve thickness or analyse seasonal variability by using line plots, which is a useful tool in many image analysis programs. A line is drawn perpendicular to the varves or laminations and the grey-scale values are presented in a line plot (Fig. 7). Depending on the software, varves can be defined either by manual selection in the plot or by semi-automatic or automatic selection (Ripepe et al., 1991; Thetford et al., 1991; Schaaf & Thurow, 1997). The beginning of a varve is often defined as a turning point in the grey-scale record, which means that automatic selection seldom can solve problems with disturbances or define varves containing complicated structures, e.g., several alternating light and dark laminae. With the use of X-ray-images or strongly processed images, the contrast between different layers can be enhanced and the counting facilitated. Semi-automatic programs, e.g., programs developed for tree-ring analysis, produce reliable results since the automatic processing is followed by a manual final correction. If the varve boundaries are sharp, the

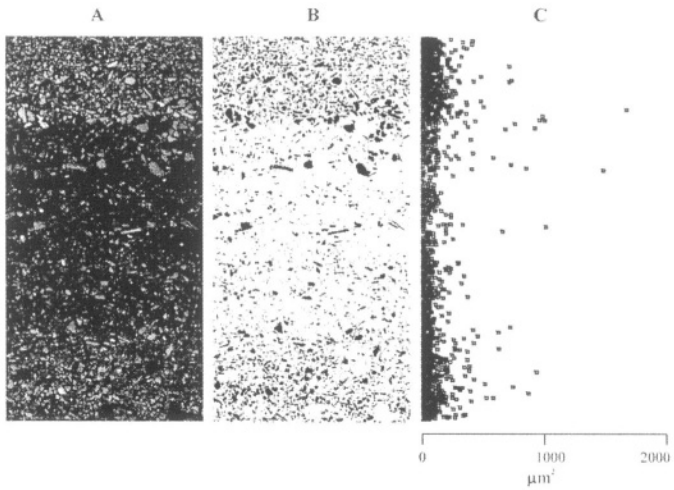


Figure 5. A BSE-image from the varved Lake Korttajärvi in Finland is processed with thresholding and open binary operation. The obtained binary image can be used to analyse the grain size variation (μm^2).

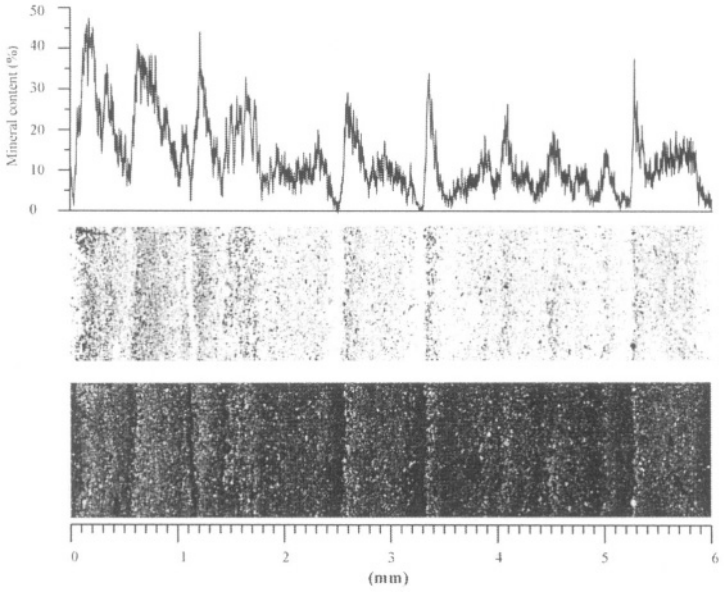


Figure 6. The mineral content in a polished thin section from Lake Korttajärvi obtained from a processed BSE-image.

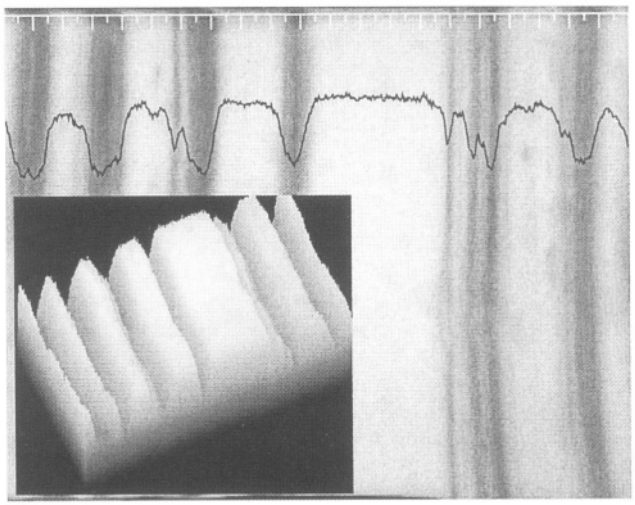


Figure 7. A line scan and surface plot from an X-ray image from Lake Korttajärvi. Units in mm.

program can count with an exactness of about 95% compared to the human eye. Figure 8 demonstrates automatic varve counting before and after correction by an operator. Image analysis can also be used to measure density changes in X-ray films, for example annual relative density, annual sum density (all pixel together), maximum and minimum densities. Figure 9 compares density data and varve thickness data obtained from an epoxy slab from the varved Lake Korttajärvi in Finland.

The methods for producing line plots differ from using a one pixel wide line perpendicular to the varves (Schaaf & Thurow, 1994, 1997) to averaging several lines (Ripepe et al., 1991; Dean et al., 1994; Petterson et al., 1993, 1999; Godsey et al., 1999). The quality of a grey-scale record is enhanced by (i) manually selecting the lines from which the record is obtained, i.e., local disturbances within the varves can be avoided, and (ii) using several lines and calculating a mean grey-scale record, which is more representative since a wider area of the sediment surface is used. The grey-scale variability within the whole image can be presented in a surface plot, where every grey-scale value is shown (Fig. 7). This presentation is useful to emphasis gradient changes and to visualise the structure of the image.

Future perspectives

Today, image analysis has made it possible to speed up time-consuming analyses and to perform manual work automatically, but the technique has also laid the base for expanding analyses to new parameters. By using a colour system instead of a black and white system, additional information about sediment composition and appearance can be gained, especially if the cores contain colour banding from bacteria or minerals. This chapter has only discussed digitizing during normal light-conditions, but with the use of other wave-lengths, new and exciting information about sediment composition might be obtained. One example

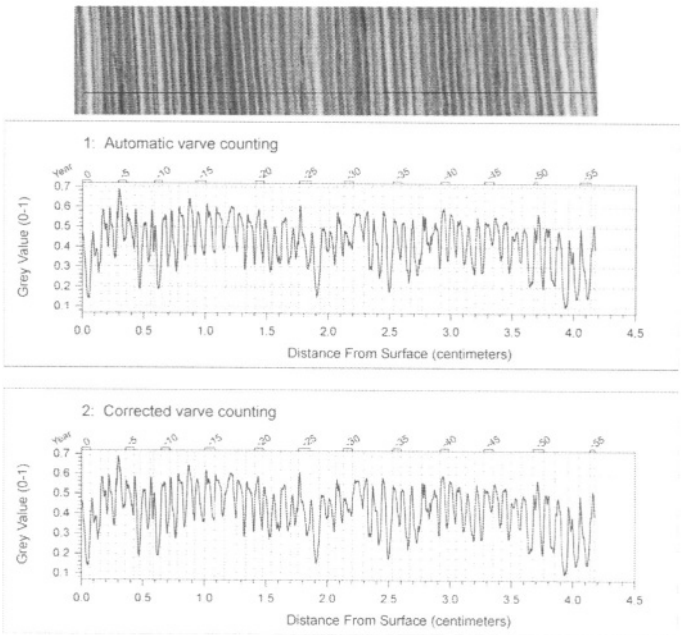


Figure 8. The result from an automatic varve counting using the DendroScan image analysis program slightly improves when an operator corrects the result.

is the near-infrared spectrum, which might give information about the organic content or characterise the organic matter present in a thin section or a fresh sediment sample. NIR has already been used in palaeolimnology but for other purposes (Korsman et al., this volume).

Provided that a statistical relationship between grey-scale and sediment composition can be established, image analysis can be used to infer fluxes of sediment components in records containing thousands of years. If a varved sediment is used, annual or perhaps even seasonal resolution can be obtained. Petterson et al. (unpublished) have inferred the annual accumulation rate of minerogenic matter for 6400 years in Kassjön (Sweden).

Because of the constant progress in the development of computers, hardware and software, image analyses is a rapidly developing technique where the only limit to future use in palaeolimnolgy is the researcher's imagination!

Conclusion

Image analysis is definitively a tool that will provide palaeolimnologists with new and exciting information about past environmental changes. The method is fast, objective and non-destructive, and performs high-resolution measurements on a regular basis. Image analysis is very suitable for documentation of cores, varve counting, varve thickness measurements, analyses of sediment composition, and studies of grain size variability and mineral content. On the Internet, there are several freeware image analysis program with versatile properties, which are quite easy to learn. Due to the rapid development of

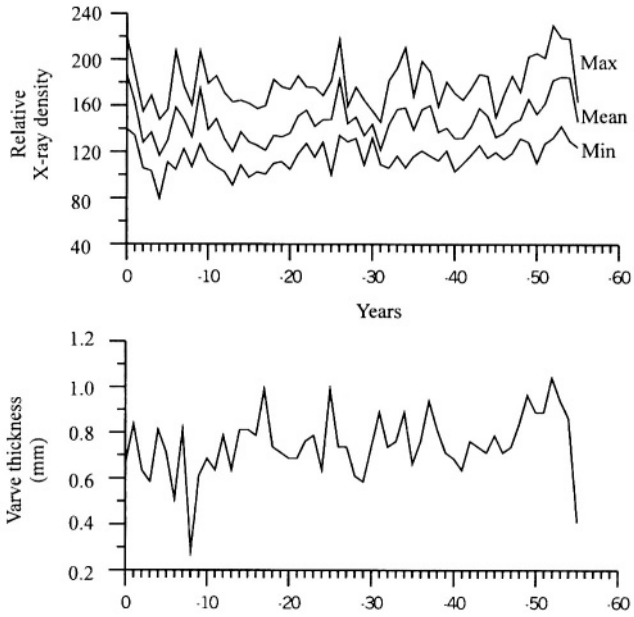


Figure 9 Annual relative X-ray density and annual minimum and maximun values and varve thickness obtained from Figure 8.

computers, images will continue to be shared via the Internet or FTP (file transfer protocol), and problems concerning interpretation of results will be more effectively discussed.

Summary

Image analysis is a high-resolution technique that provides new possibilities for the study of sedimentary structures. The often subjective visual study of for example sediment core surfaces can today be replaced by the objective analysis of digital images which is both fast and non-destructive. The images, acquired by a digital camera or a scanner, can be transformed by a number of applications to enhance or smooth desired structures. Image analysis has proved to be useful for the rapid documentation of cores, varve counting and varve thickness measurements together with quantitative and qualitative analyses of grain size and sediment composition. The applications of image analysis in palaeolimnology will continue to increase and develop in the future, especially due to the ongoing development of computers, hardware and software.

Acknowledgements

TS received financial support from EU (ENV4-CT97-0557). We are grateful to Kan Kinnunen and Ingemar Renberg for giving valuable comments on the manuscript and to Richard Bindler for correcting the English.

References

Alverson, K., 1999. The PAGES/CLIVAR Intersection: providing the paleoclimate perspective needed to understand climate variability. Global Change News 40: 11–14.

Anderson, R. Y, 1996. Seasonal sedimentation: a framework for reconstructing climate and environmental change. In Kemp, A. E. S. (ed.) Palaeoclimatology and Palaeooceanography from Laminated Sediments. Geological Society Special Publication, London 116: 1–15.

Bonardi, M. & L. Tosi, 1995. Image analysis: A tool for sedimentological investigations. European Microscopy and Analysis, May: 17–19.

Bond, G., W. Broecker, R. Lotti & J. McManus, 1992. Abrupt color changes in isotope stage 5 in North Atlantic deep sea cores: implications for rapid change of climate-driven events. In Kukla, G. J. & E. Went (eds.) Start of a Glacial. NATO ASI Series I 3. Springer-Verlag; Berlin Heidelberg: 185–205.

Bons, P. & M. W. Jessell, 1996. Image analysis of microstructures in natural and experimental samples. In De Paor, D. G. (ed.) Structural Geology and Personal Computers. Pergamon, Oxford: 135–166.

Bresson, L. M. & C. J. Moran, 1998. High-resolution bulk density images, using calibrated X-ray radiography of impregnated soil slices. Soil Sci. Soc. of Am. J. 62: 299–305.

Cooper, M. C., 1997. The use of digital image analysis in the study of laminated sediments. J. Paleolim. 19: 33–40.

Clark, J. S. & T. C. Hussey, 1996. Estimating the mass flux of charcoal particles from sedimentary records: effects of particle size, morphology and orientation. The Holocene 6: 129–144.

Dartnell, P. & J. V. Gardner, 1993. Digital imaging of sediment cores for archives and research. J. Sed. Petrol. 63: 750–751.

Dean, W. E., J. P. Bradbury, R. Y. Anderson, L. Ramirez Bader & K. Dieterich-Rurup, 1994. A high-resolution record of climatic change in Elk Lake, Minnesota for the last 1500 years. U.S. Geological Survey. Open-File Report: 94–578.

de Keyser, T. L., 1999. Digital scanning of thin sections and peels. J. Sed. Res. 69: 962–964.

Earle, C. J., L. B. Brubaker & P. M. Anderson, 1996. Charcoal in northcentral Alaskan lake sediments: relationships to fire and late-Quaternary vegetation history. Rev. Paleobot. Palyn. 92: 83–95.

Fortey, N. J. 1995. Image analysis in mineralogy and petrology. Mineralogical Magazine 59: 177–178.

Francus, P., 1998. An image-analysis technique to measure grain-size variation in thin sections of soft clastic sediments. Sed. Geol. 121: 289–298.

Gasse, F., F. Oldfield & S. Kroepelin (eds.), 1997. PEP III: The Pole-Equator-Pole Transect Through Europe and Africa. PAGES Report 97–5. PAGES International Project Office, Switzerland, 64 pp.

Godsey, H. S., T. C. Moore Jr., D. K. Rea & L. C. K. Shane, 1999. Post-younger Dryas seasonality in the North American midcontinent region as recorded in Lake Huron varved sediments. Can. J. Earth Sci. 36: 533–547.

Goni, M. F. S., 1996. Image analysis of charcoal particles: Application to environmental studies. European Microscopy and Analysis, July: 5–7.

Gonzalez, R. C. & R. E. Woods, 1992. Digital Image Processing. Addison-Wesley, Reading M.A., 716 pp.

Hughen, K. A., J. T. Overpeck, L. C. Peterson & S. Trumbore, 1996. Rapid climate changes in the tropical Atlantic region during the last deglaciation. Nature 380: 51–54.

Jähne, B., 1997. Practical Handbook on Image Processing for Scientific Applications. CRC Press, Boca Raton CA., 589 pp.

Krinsley, D. H., K. Pye, S. Boggs Jr. & N. K. Tovey, 1998. Back-scattered Scanning Electron Microscopy and Image Analysis of Sediments and Sedimentary Rocks. Cambridge University Press, New York, 193 pp.

Lindeberg, G. & B. Ringberg, 1999. Image analysis of rhythmites in proximal varves in Blekinge, southeast Sweden. GFF 121: 182–186.

Mainwaring, P. R. & W. Petruk, 1989. Introduction to image analysis in the Earth and mineral science. In Petruk, W. (ed.) Image Analysis in Earth Sciences. Mineralogical Association of Canada, Short Course Handbook 16: 1–5.

Marion, A., 1991. An Introduction to Image Processing. Chapman & Hall, London, U.K., 314 pp.

Maslin, M. A. & A. Berger, 1997. A European view of the future of palaeoclimate research. Quat. Sci. Rev. 16: 501–504.

Petruk, W. (ed.), 1989. Image analysis in the earth sciences: a short course held…Ottawa, Ontario, May 18–20, 1989. Short course handbook / Mineralogical Association of Canada: 16, 156 pp.

Petterson, G., I. Renberg, P. Geladi, A. Lindberg & F. Lindgren, 1993. Spatial uniformity of sediment accumulation in varved lake sediments in northern Sweden. J. Paleolim. 9: 195–208.

Petterson, G., B. V. Odgaard & I. Renberg, 1999. Image analysis as a method to quantify sediment components. J. Paleolim. 22: 443–455.

Pratt, W. 1991. Digital Image Processing. J. Wiley & Sons, N.Y., 720 pp.

Renberg, I., 1981a. Formation, structure and visual appearance of iron-rich, varved lake sediments. Verh. Int. Ver. Limnol. 21: 94–101.

Renberg, I., 1981b. Improved methods for sampling, photographing and varve-counting of varved lake sediments. Boreas 10: 255–258.

Ripepe, M., L. T. Roberts & A. G. Fischer, 1991. ENSO and sunspot cycles in varved Eocene oil shales from image analysis. J. Sed. Petrol. 61: 1155–1163.

Rosenfeld, A. & A. Kak, 1982. Digital Picture Processing, vol. 1, 2nd ed. Academic Press, N.Y., 349 pp.

Russ, J. C, 1994. The Image Processing Handbook. CRC Press, Boca Raton, 674 pp.

Schaaf, M. & J. Thurow, 1994. A fast and easy method to derive highest-resolution time-series datasets from drillcores and rock samples. Sed. Geol. 94: 1–10.

Schaaf, M. & J. Thurow, 1997. Tracing short cycles in long records: the study of inter-annual to inter-centennial climate change from long sediment records, examples from the Santa Barbara Basin. Journal of the Geological Society, London 154: 613–622.

Spooner, I. S., 1998. Changes in lake-sediment stratigraphy associated with late glacial climate change: examples from western Nov Scotia. Atlantic Geology 34: 229–240.

Stoermer, E. F., 1996. A simple, but useful, application of image analysis. J. Paleolim. 15: 111–113.

Thetford, R. D., R. D. D'Arrigo & G. C. Jacoby, 1991. An image-analysis system for determing densiometric and ring-width time-series. Can. J. For. Res. 21: 1544–1549.

Tovey, N. K., D. H. Krinsley, D. L. Dent & W. M. Corbett, 1992. Techniques to quantitatively study the microfabric of soils. Geoderma 53: 217–235.

Tovey, N. K. & M. W. Hounslow, 1995. Quantitative micro-porosity and orientation analysis in soils and sediments. J. Geol. Soc. 152: 119–129.

Zolitschka, B., 1996. Image analysis and microscopical investigation of annually laminated lake sediments from Fayetteville Green Lake (NY, USA), Lake C2 (NWT, Canada) and Holzmaar (Germany): a comparison. In Kemp, A. E. S. (ed.) Palaeoclimatology and Palaeoceanography from Laminated Sediments. Geological Society Special Publication No. 116: 49–55.

4. TEXTURAL ANALYSIS OF LAKE SEDIMENTS

WILLIAM M. LAST (WM_Last@UManitoba.ca)
Department of Geological Sciences
University of Manitoba
Winnipeg, Manitoba
R3T 2N2, Canada

Keywords: texture, particle size, shape, fabric, laser diffraction, X-ray attenuation, sedimentation, particle counter, grain size distribution

Introduction and importance of texture

Texture is the general physical appearance or character of a sediment or rock. It is used to describe the geometric aspects and mutual relationships among the component particles or crystals and, as emphasized by Lewis (1984), is one of the three basic descriptors of a sedimentary deposit, the others being structure and composition. Within the sedimentary realm of Earth science, the term "texture" usually includes the fundamental attributes of: (i) size, (ii) shape, and (iii) arrangement or fabric as listed in Table I. Pettijohn (1975) defines texture as essentially the microgeometry of sediment, a definition which emphasizes the characteristics of individual grains and grain-to-grain relations, versus larger scale features of the deposit, such as sedimentary structures, bedding character or stratigraphic sequence. It is also important to differentiate these primary textural attributes of sediment (e.g., size, shape, fabric) from derived properties. For example, porosity, permeability, bulk density, and color are all very important properties of sediments that are largely derived from, or strongly dependant on, the primary textural properties.

Much of the importance of texture, as with composition and structure, lies in its inherent role as a means of description and communication. Just as we might describe a lacustrine deposit as black, organic-rich sediment or finely laminated, siliciclastic-dominated sediment, we also routinely use the textural aspects of the material for classification and communication: fine sand, well-sorted silt, poorly-sorted mud, matrix-supported gravel all convey an explicit and quantitative meaning. Secondly, in addition to fundamental description, classification, and communication, careful study of the various textural parameters can lead to important clues about: (i) source (provenance), (ii) the mechanisms responsible for the transport of the material, (iii) past physical and chemical environmental and limnological conditions at the depositional site within the basin, and (iv) paleoclimatic and paleohydrological conditions within the surrounding watershed. Thirdly, knowledge of the texture of a lacustrine deposit is important because of its influence on other key properties of the sediment. For example, much engineering construction design is dependant upon



W. M. Last & J. P. Smol (eds.), 2001. *Tracking Environmental Change Using lake Sediments. Volume 2: Physical and Geochemical Methods.* Kluwer Academic Publishers, Dordrecht, The Netherlands

Table 1. Basic and derived attributes of sediments.

Selected Physical Characteristics and Properties	Internal	Texture	Size	Average Size Range of Sizes Sorting
			Shape	Roundness (angularity) Sphericity Surface texture
			Arrangement (fabric)	Packing Orientation
		Sedimentary Structures		Bedding Interbedding Directional Features Post-depositional features
	External	External Form/Geometry		Size (thickness, width, length) Configuration/Shape Nature of boundaries
		Relation to Basin Framework		Position in Stratigraphic Sequence or Cycle Overall vertical trend Overall lateral trend
Selected Compositional Properties and Characteristics		Mineralogy and Geochemistry		Detrital Components Endogenic Components Authigenic Components Major & Minor Element Trace Element & Contaminant Isotopic Organic
			Biological	
Selected Derived Mass Properties		Porosity	Pore Size	Permeability
		Hardness	Acoustic Velocity	Strength
		Density	Colour	Magnetic properties

textural data because factors such as slope stability, compaction, and strength are all, in part, a function of texture. Similarly, the mechanisms and rate of transfer of solutes between the pore waters, the sediment, and any overlying lake water are controlled by textural properties. Finally, from a practical perspective, the texture of a sedimentary deposit is an essential component in the analytical schemes of many other parameters of the sediment. For example, if we wanted to know about the clay *mineralogy* of a lake deposit, it is necessary to fractionate the sediment according to size and undertake mineralogical analyses of only the clay sized component. Similarly, many inorganic geochemical analytical techniques call for examination of only certain size fractions of the deposit.

As fundamental as these textural parameters are, unfortunately, we are faced with an often bewildering array of techniques and equipment used to evaluate aspects of texture, and an equally diverse and sometimes confusing system of nomenclatures. Although over twenty years have passed since Potter et al. (1980) contended that our understanding of *how* to measure and interpret texture lags far behind that of composition, it is still valid to say that sediment textural analysis, particularly of fine-grained material, is at the petrographic frontier of sedimentary studies.

The objectives of this chapter are to provide an overview of the basic concepts involved in texture, summarize the main techniques and methods of textural analysis, and demonstrate how an understanding of textural parameters can assist in paleoenvironmental research by briefly outlining a study from a lake in western Canada in which detailed particle size and shape data help decipher the recent history of the basin. Much of the emphasis of this chapter is on the textural component of size and specifically size characterization of relatively fine-grained sediment. This emphasis is for two reasons. First, most paleolimnological research (but certainly not all) is done on sedimentary sequences from the offshore areas of the lake basin. The materials comprising the lacustrine deposits in these offshore areas are usually fine particles. Second, although geoscientists have long recognized the paleoenvironmental importance of shape, particle surface morphology, and fabric, there have been surprisingly few efforts made to apply these non-size components of textural analysis to lake sediments.

Size

The concept of size

Intuitively, size should be an easy concept to understand. If we were given a beaker full of spherical glass beads, we would likely have no problem determining the size of the beads: we would simply evaluate the size of each bead by measuring the distance from one side of the bead to its opposite side (i.e., the diameter). For a spherical particle, the size is uniquely defined by its diameter. Alternatively, if our container held small cubes, we could, likewise, easily measure the length of one side of each cube and thereby describe the size characteristics of the material. It would take little effort to apply this simple concept of size to other regularly shaped particles, such as a container full of cones or cylinders. We would quickly realize, however, in most cases it is necessary to measure more than one dimension in order to evaluate the size (e.g., both diameter and height for the cones). To illustrate this point, attempt to assign a size to each of the following items: a golf ball, a needle, and a 35mm film cartridge. Each has at least one linear measurement approximately equal: the golf ball is ~40mm in diameter; both the needle and the film cartridge have a long dimension of ~40 mm. However, few would argue that these three simple, regularly shaped items are all the same size.

To further complicate size measurement, most naturally occurring particles are irregular in shape and many are non-equant. Hence, the problem with conceptualizing the size of particles comprising a sediment is threefold: (i) because the particles are irregularly shaped, it becomes difficult to assign one or even a few simple measurements as *the* 'size' parameter; (ii) the farther the particle is from an equant shape (i.e., sphere or cube), the greater the discrepancy between the various measures of size; and (iii) particles having the same "size" can have vastly different shapes.

This dilemma of attempting to evaluate the size of irregularly shaped solids has attracted the interest of geoscientists for many years. Krumbein & Pettijohn (1938) provide an eloquent and detailed summary of the various measures of size and the properties of sediments that can be used to evaluate size. More recently, excellent overviews appear in many of the papers in Knapp et al. (1996) and Syvitski (1991). In fact, for naturally-occurring material we have the rather unusual situation that the size parameter of texture is determined entirely by the method, technique, or equipment used to do the measuring. For example, it is common practice to evaluate the size characteristics of a sandy sediment by passing the sand through a series of nested sieves. The 'sieve diameter', then, is defined as the length of the side of the minimum square aperture through which the particle will pass. In our example above with a golf ball, needle, and film cartridge, a sieve with aperture size of 38 mm will not allow the golf ball to pass through but, with enough bouncing, both the film cartridge and the needle will eventually pass through.

Table II summarizes some of the many definitions of size. Although by no means consistent, many of these attempts to identify and quantify the parameter of size do so by trying to relate the irregularly shaped particle to the diameter of a sphere that is in some way equivalent to the particle being measured. This diameter is referred to as the equivalent diameter. For example, for a large particle we could conceivably measure its weight and density and thereby find the particle's volume. The volume diameter, then, would be the diameter of a sphere having the same volume as the irregularly shaped particle. Similarly, we could evaluate the surface area of the irregular grain and characterize the size of this particle by relating it to the diameter of a sphere having the same surface area (i.e., the surface diameter in Table II).

Terminology

Sediment grade scale

Lacustrine sediments can contain a wide range of particle sizes, with diameters spanning as much as seven orders of magnitude. This large range in sizes, from material measured in terms of tens of centimeters to submicron particles, necessitates the use of a logarithmic scale in describing and classifying the deposit. Udden (1898, 1914) first recognized this over a century ago and devised a grade scale consisting of a series of size classes that had a constant geometric relationship to one another based on the factor of 2 (or 0.5). The original terminology suggested by Udden was modified by Wentworth (1922) to create the now commonly-used Udden-Wentworth size classification shown in Table III.

Phi scale

In order to circumvent the problem of unwieldy numerical fractions having several digits (e.g., the clay-silt boundary at 0.001953mm) and to simplify (at that time) the laborious hand calculations of various statistical parameters for the particle size distributions, Krumbein (1934) subsequently proposed that the size of particles should be measured in dimensionless units of ϕ (phi). Phi is defined as:

$$\phi = -\log_2 d_{mm}, \tag{1}$$

where d_{mm} is the diameter measured in millimeters. Note that this logarithmic scale is based on 2 (rather than the more conventional 10 or *e)* and that coarser sediments are more

Table II. Definitions of particle size (modified from Allen, 1981, and Müller, 1967).

Size Name	Definition
Volume Diameter	Diameter of a sphere having the same volume as the particle
Surface Diameter	Diameter of a sphere having the same surface area as the particle
Surface Volume Diameter	Diameter of a sphere having the same external surface area to volume ratio as the particle
Drag Diameter	Diameter of a sphere having the same resistance to motion as the particle in a fluid of the same viscosity and at the same velocity
Free-falling Diameter	Diameter of a sphere having the same density and the same free-falling speed as the particle in a fluid of the same density and viscosity
Stokes' Diameter	The free-falling diameter of a particle in a fluid with laminar flow
Projected Area Diameter	Diameter of a circle having the same area as the projected areas of the particle resting in a stable position OR in a random position
Perimeter Diameter	Diameter of a circle having the same perimeter as the projected outline of the particle
Sieve Diameter	The width of the minimum square aperture through which the particle will pass
Feret's Diameter	The distance between a pair of parallel lines which are oriented in a given direction (normally parallel to the vertical cross-hair in a microscope field of view) and which touch the extreme points on the perimeter of the projected outline of the particle
Martin's Diameter	The length of a line which divides the projected outline of the particle into two equal areas and is parallel to a given direction (normally the horizontal cross-hair in a microscope field of view)
Krumbein's Diameter	The length of the longest line in a given direction (normally parallel to the horizontal cross-hair in a microscope field of view) that is bounded by the projected outline of the particle
Long Diameter	The distance between the two most distant points on the particle
Middle Diameter	The smallest possible distance between two points on the particle, between which the projection of the particle can pass
Unrolled Diameter	The mean chord length through the center of gravity of the particle

negative and finer sediments are more positive (see Table III). Although equation (1) is the usual statement of the phi-mm relationship, as pointed out by numerous authors (e.g., Håkanson & Jansson, 1983; Leeder, 1982), to be dimensionless, the correct equation is:

$$\phi = -\log_2 (d_{mm}/d_{1mm}), \tag{2}$$

where d_{1mm} is the grain diameter of 1 mm. Conversion between ϕ and metric units can be done graphically (Fig. 1) or by equations (1), (2) or (3):

$$\phi = -(\log_{10} d_{mm}/\log_{10} 2). \tag{3}$$

Clearly, with today's widespread use of electronic hand calculators and computers, the advantage gained in ease of calculation using the phi-based numbers is largely negated.

Table III. Udden-Wentworth grain size scale (modified from Friedman & Sanders, 1992).The limiting particle diameter numeric values are the boundaries corresponding to the adjacent descriptive terms. For example, the boundary between Very Large and Large Boulder is at 2048 mm diameter.

Limiting Particle Diameter (ϕ units)	(mm)		Descriptive Terms			
−11	2048		Very Large	Boulder		Gravel
−10	1024		Large			
−9	512		Medium			
−8	256		Small			
−7	128		Large	Cobble		
−6	64		Small			
−5	32		Very Coarse	Pebble		
−5	16		Coarse			
−3	8		Medium			
−2	4		Fine			
−1	2		Very Fine			
0	1		Very Coarse	Sand		
	mm	μm				
+1	0.5	500	Coarse			
+2	0.25	250	Medium			
+3	0.125	125	Fine			
+4	0.0625	62.5	Very Fine			
+5	0.03125	31.25	Very Coarse	Silt	Coarse	Mud
+6	0.01563	15.63	Coarse		Medium	
+7	0.00781	7.81	Medium		Fine	
+8	0.00391	3.91	Fine		Very Fine	
+9	0.00195	1.95	Very Fine	Clay	Clay	

However, despite this and the observation that phi notation is essentially meaningless to other groups of scientists (Lindholm, 1987; Pierce & Graus, 1981), it still remains deeply infused in sedimentological and geolimnological literature. Virtually all current university-level sedimentology and stratigraphy textbooks describe and use phi notation. Over 60% of the papers using or discussing particle size published in the past decade (1990–1999) in *Journal of Sedimentary Research, Sedimentology, Sedimentary Geology,* and *Journal of Paleolimnology* cite phi units.

Although the boundaries of the various size classes are generally well agreed upon (see, for example, Table 3-3 in Blatt et al., 1980, or Fig. 16 in Müller, 1967), for researchers dealing with relatively fine sediments, unfortunately the very important division between silt and clay still remains ambiguous. Despite a call for standardization of this boundary at 9 ϕ ($\sim$2 μm; Friedman et al., 1992; McCave & Syvitski, 1991; Jackson, 1985; Friedman & Johnson, 1982;Tanner, 1969), in most sedimentological literature the use of 8ϕ

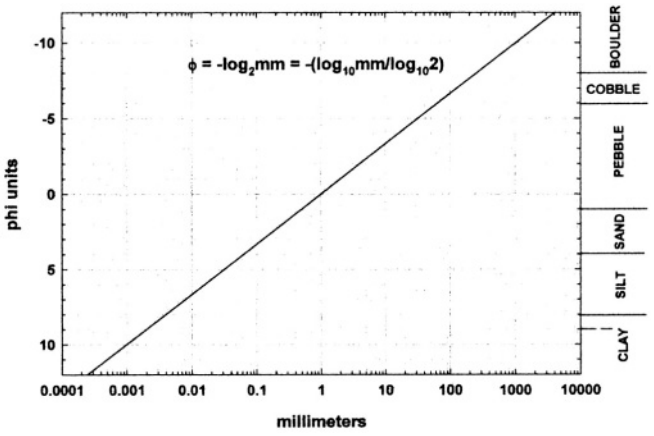


Figure 1. Graphical conversion between phi (ϕ) scale and metric measures of diameter.

(3.9 μm) is more common (e.g., Boggs, 1995; Blatt, 1992; McManus, 1988; Leeder, 1982; Brownell, 1978).

Naming the sediment

In addition to the specific textural class of individual particles, the range of particle sizes common in naturally-occurring lake sediments necessitates use of an additional sediment mixture classification system to actually name the material. Several such systems are in common use (Fig. 2), and, as with sediment compositional classification systems, there is little uniformity of practice or nomenclature.

Techniques and instruments

Because there are many ways to define particle size, it follows that there are many different methods for analysis of size involving an equally diverse array of instruments and techniques. Up-to-date summaries of these methods and instruments, and the theory behind the size determination, can be found in Knapp et al. (1996), Washington (1992), Syvitski (1991) and McManus (1988). The more traditional techniques (i.e., non-automated and generally non-electronic) have been discussed in Krumbein & Pettijohn (1938), A.S.T.M. (1959), Irani & Callis (1963), Müller (1967) and Jelínek (1971), and are also summarized in most standard sedimentological textbooks and laboratory manuals (e.g., Lewis & McConchie, 1994a, b; Boggs, 1995; Lewis, 1984; Friedman & Johnson, 1982; Blatt et al., 1980).

In any discussion of particle size analysis techniques, it is important to re-emphasize several points made by McCave & Syvitski (1991). During the past several decades, advances in particle size instrumentation have been so rapid that most electronic instruments are outdated by the time they are purchased. Similarly, it must be realized that most of the sizing instrumentation used by Earth scientists today was designed for different purposes and different areas of investigation (e.g., pharmaceutical sciences, medical research, paint

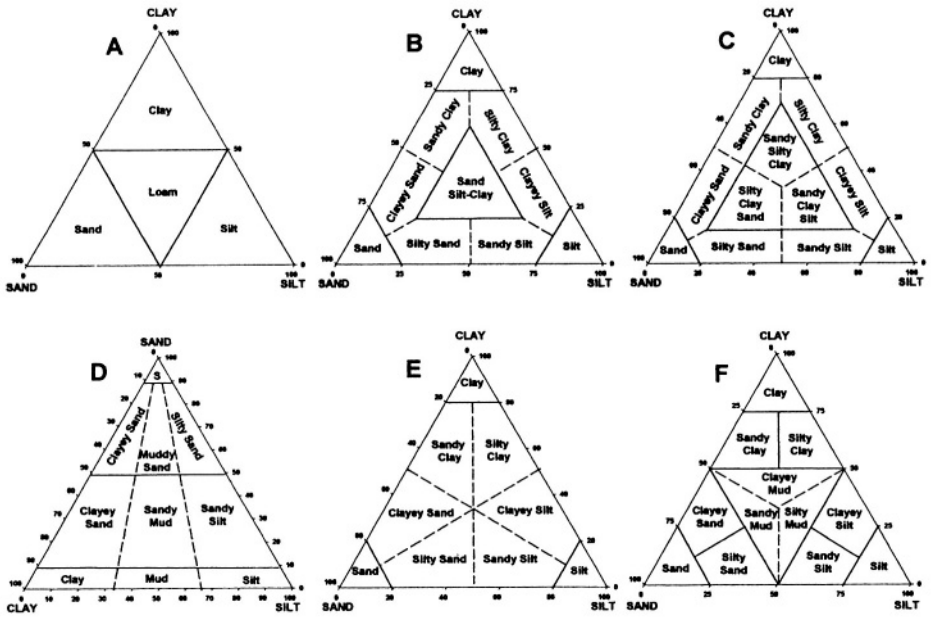


Figure 2. Examples of textural classifications of sediments. A: Robinson (1949); B: Shepard (1954); C: Trefethen (1950); D: Folk (1980); E: Krumbein & Sloss (1963); F: Picard (1971). See also summaries and classification systems in Pettijohn (1974), Stevens (1984), Lewis & McConchie (1994b) and Nichols (1999).

and pigment industries, food and beverage monitoring, etc.). Thus, there may be inherent design factors and other constraints that can significantly limit the widespread application of the particular technique or equipment in paleolimnological research. It is imperative the researcher knows what is being measured (i.e., specifically what component of size is being evaluated) and understands the limitations and constraints of the technique and equipment. Particularly within the realm of automated and electronic sizing equipment, Washington's (1992) contention that the less we understand about the technique the more likely we are to blindly accept the data is not far from the truth.

Finally, the researcher contemplating acquisition of size data or use of particle size information in any paleolimnological effort must be cognizant of data quality. Many criteria must be considered when examining scientific data quality, including technician and operator factors, sample character, equipment conditions, detection level, etc. Most (if not all) modern particle size equipment is probably best characterized as precisely inaccurate. However, given the many definitions of size and the wide variety of parameters that are evaluated as size, the concept of accuracy (i.e., how close our measured value is to the true value) with respect to size analysis of natural materials is meaningless. Although a variety of synthetic reference materials exist (e.g., glass beads, polymer latex spheres; see Xu, 1996) from which standard mixtures of given particle sizes can be prepared, in a comparison study of seven automated electronic size analyzers, Syvitski et al. (1991a) found that none of the instruments tested provided truly accurate results (Fig. 3). This same study found

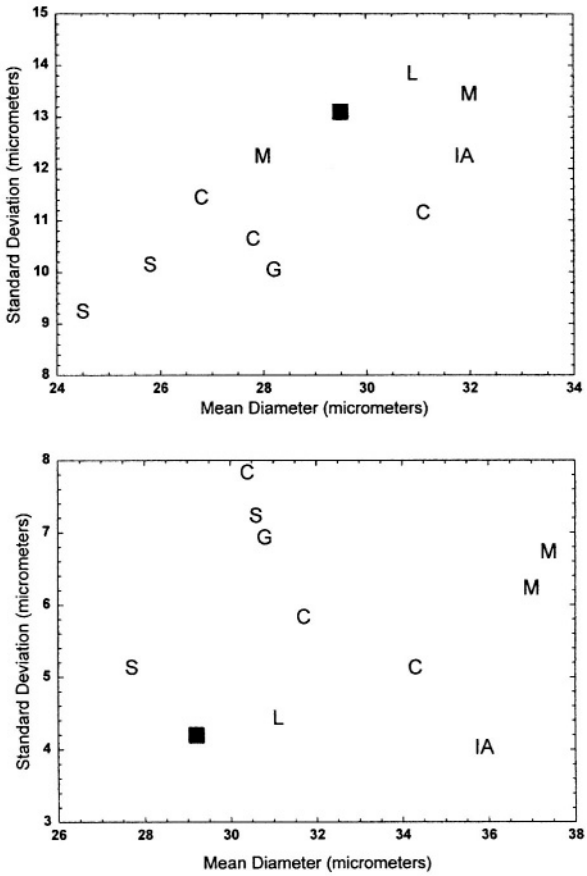


Figure 3. Plots of mean particle size versus standard deviation of two prepared mixtures of standards analyzed by selected automated electronic particle size analysers (from Syvitski et al., 1991a). The expected value is shown with a black box. S: SediGraph; C. Coulter Counter; M: Malvern laser particle sizer; G: Galai CIS-1, L: Lumosed photosedimentometer; IA: Image analysis (Syvitski et al., 1991a).

that nearly all commercial size analytical devices were very precise (i.e., the instrument provided consistent results).

Because of the great diversity of size analysis equipment that is available to paleolimnologists and the often significantly different sample preparation techniques that are required for the various techniques discussed below, it is not practical to recommend any specific analytical sequence. Clearly, the sample handling and preparation flow chart used in a laboratory in which particle size analysis is done by equipment such as Galai CIS would not be applicable to a researcher interested in acquiring size data by SediGraph, laser diffraction or Coulter Counter. General-purpose analytical sequence guidelines that can be modified to the individual researcher's situation and equipment have been prepared by numerous authors. Probably the best of these appear in Lewis & McConchie (1994a).

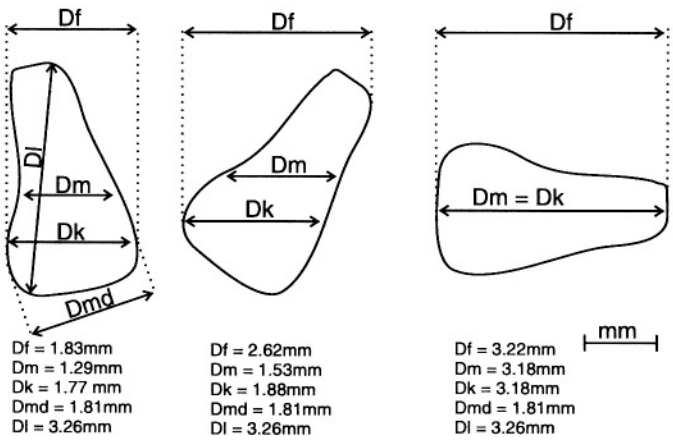


Figure 4. Selected measures of size on a single particle (modified from Müller, 1967). See Table II for definitions. *Df*: Feret's diameter; *Dm*: Martin's diameter; *Dk*: Krumbein's diameter; *Dmd*: Middle diameter; *Dl*: Long diameter.

It must be emphasized, however, that many of today's automated electronic size analysis instruments require very small quantities of sample for optimum performance. This places considerable importance on the pretreatment, sample splitting, and preparation techniques (see also discussions in Matthews, 199la; McManus, 1988).

Direct measurement of particle size

Measurement of particle size directly by visual observation is one of the oldest and most straightforward techniques available. Today, with widespread use of desktop image analysis equipment and other computer-assisted techniques, direct estimation of size still holds considerable promise as a routine paleolimnological tool.

Direct visual estimation of size is routinely done in the field with relatively coarse sediments (coarser than silt) using calipers for the gravels or a particle size comparator (with the assistance of a hand lens or low power binocular microscope) for sands (see, for example, sheets 16-1 and 16-2 in Dietrich et al., 1982, Fig. 4-1 in Blatt,1982, or Fig. 7 in Müller,1967).

In the laboratory, unconsolidated grains can be mounted in epoxy using a simple hydraulic press, or thin sections of either unconsolidated or consolidated sediments can be prepared (e.g., Kemp et al., this volume; Pike & Kemp, 1991; Murphy, 1986), and examined using higher-power transmitted or reflected light microscopy in conjunction with standard petrographic analysis (Nesse, 1991; Fleischer et al., 1984; McCrone et al, 1978). It is beyond the scope of this chapter to discuss the details of this petrographic analysis, but the topic is well covered in most introductory petrology textbooks (e.g., Boggs, 1992; Blatt, 1992; Williams et al., 1982; Müller, 1967). Delly (1996) provides an up-to-date summary of the recommended equipment and procedures for size analysis in the microscope lab.

Because of the array of possible diameters that can be evaluated (Fig. 4), traditional textural analysis by this type of direct measurement can be labor intensive. In addition, the number of particles that must be counted in order to provide a statistically significant

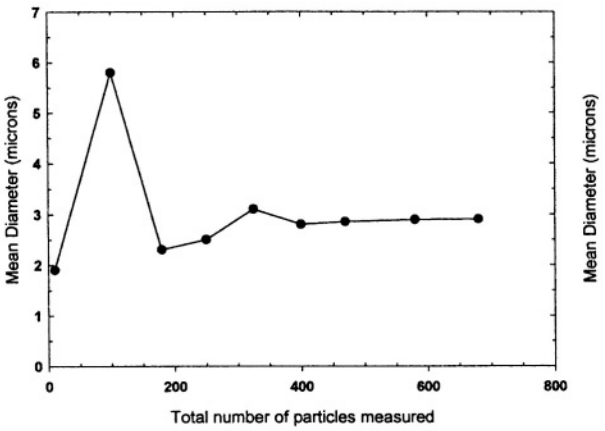


Figure 5. Average diameter per total number of particles counted in a thin section or grain mount (modified from Irani & Callis, 1963).

evaluation can significantly increase data collection time: As shown in Figure 5, a 95% confidence level is achieved only after measuring approximately 400 grains in a well sorted sample on a standard petrographic slide (see also Solomon, 1963; Solomon & Green, 1963: Friedman, 1958; Chayes, 1956). Kennedy & Mazzullo (1991) indicate that samples with more complex size distributions may require on the order of 1000 grains. However, microscopic image analysis systems, such as those described by Barber (1996), Kennedy & Mazzullo (1991), and Tianrui (1991) are now in fairly widespread use in most sedimentological laboratories. These computer assisted image analysis (IA) techniques have the capability of extending direct measurement of particle size down to the micrometer level. Russ (1991) summarizes this IA sizing and associated statistical techniques using mainly non-geological examples. These techniques have already been used successfully to characterize components of texture of *selected* particles (e.g., the size of charcoal, quartz, salt minerals, porosity, etc.; Clark & Hussey, 1996; Stirling, 1989; Smith, 1989; Ehrlich et al., 1980; Murphy et al., 1977). However, the inability to readily distinguish boundaries between adjacent particles and poor resolution of the fine components in low magnification images are problems that have constrained the widespread application of these IAS sizing techniques in lake sediment research. Nonetheless, perhaps the success demonstrated by Francus (1998) in his study of grain size variation of clay-silt laminae from Lake Baikal will provide the impetus needed for continued refinement of 'whole sediment' particle size by image analysis techniques.

Single particle counters

One of the earliest electronic particle sizing devices available was developed in the late-1940's and was originally designed to count blood cells (Coulter, 1956). The Coulter Counter rapidly gained immense popularity in many industry and research applications, including the Earth sciences, and is still a very commonly used instrument in sedimentological laboratories. The "Coulter Principle" is sufficiently well established to be included in many A.S.T.M. (American Society for Testing Materials) reference method standards.

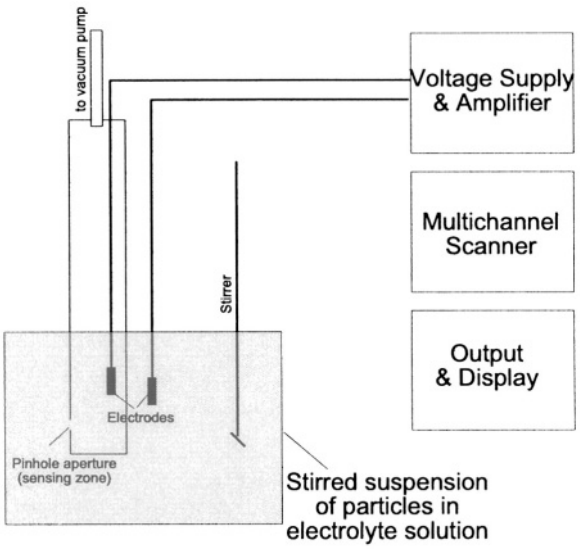


Figure 6. Basic electrical resistance particle counter (modified from Lieberman, 1996).

The basic principle of size measurement employed by the Coulter Counter and similar sizing equipment (e.g., Elzone) is remarkably simple: A tube containing a small pinhole opening (aperture) between electrodes is immersed in a suspension of particles (Fig. 6). The application of a negative pressure inside the tube will cause the suspended particles to be sucked into the tube through the pinhole. As a single particle passes through the opening, it partially closes the orifice which, in turn, reduces the amount of electrical current passing between the electrodes (i.e., increases the electrical resistance). A small diameter particle causes only a small change in resistance; a larger particle generates a proportionally larger resistance fluctuation. Thus, the amplitude of the voltage pulse produced by the particle is proportional to the size (i.e., projected area diameter) of the particle. The equipment then simply counts and classifies the pulses according to size. Counting rates are about 2000–5000 particles per second, with a total of 100,000 to 250,000 counts being typical per sample. The equipment reports equivalent spherical diameter. Current top-line models of Coulter equipment (e.g., Multisizer 3) are autocalibrated (earlier models had to be calibrated by running a latex sphere standard) and can subdivide the acquired size data into 256 classes (channels) over the spectrum of sizes being evaluated. Because size sensing is, in part, a function of the aperture size, multiple tubes with different aperture sizes can evaluate a wide range of sizes from 0.4 μm–1200 μm.

The advantages of electrical resistance pulse measurement sizing equipment like the Coulter Counter and Elzone Analyzer are their speed of analyses (typically 10 to 100 seconds per sample), the absence of problems associated with varying indices of refraction caused by variable mineralogy, and the ability to analyze small quantities of sample (see also discussions in Lines, 1996; Milligan & Krank, 1991; McCave & Jarvis, 1973). However, the small sample size (typically milligrams of sample) also presents splitting problems and

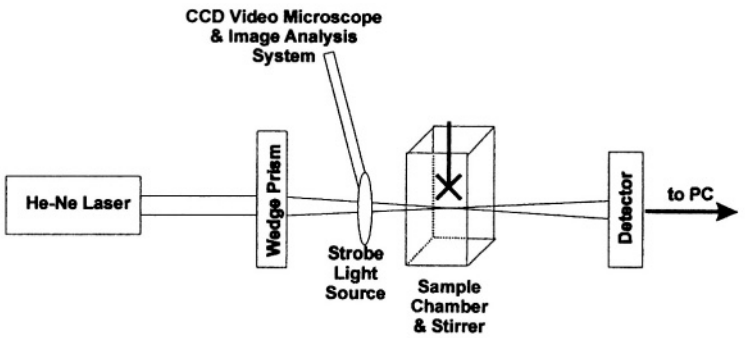


Figure 7. Basics of the Galai CIS particle size-shape equipment (modified from Galai Ltd., 1989).

raises concerns about whether the sample being analyzed is actually representative of the whole population. This aspect of subsample "representativeness" is a problem common to most of the modern electronic size equipment. For the Coulter Counter, the amount of dilution required by the equipment in order to avoid the phenomenon of "coincidence" (i.e., more than one particle passing through the sensing zone at once) is significant; particle concentrations of less than 1000 ppm are recommended. Other disadvantages noted by researchers are frequent clogging of the orifice, the necessity of having to use an aqueous electrolytic solution (typically about 1% salinity), and particle breakage associated with the high shears experienced as the particle passes through the aperture (Lieberman, 1996; Washington, 1992; McCave & Syvitski, 1991). Because of their popularity for many decades, the published literature on these electroresistance analyzes is large; guidelines for optimum laboratory procedures can be found in Lines (1996), Milligan & Kranck (1991), Shideler (1976), and McCave & Jarvis (1973).

Another newer-generation type of particle counting device, the Galai CIS particle size analyzer, uses a "time-of-transition" phenomenon to directly measure particle size. A finely focused He-Ne laser beam ($\sim$1 μm) is rotated through a solution containing the particles (Fig. 7). As the particles within the solution intersect the beam, the light is blocked from the detector. This creates an electrical pulse. The size of each individual particle is calculated by the duration (i.e., time-of-transition) of the pulse. The form of the detector signal is used to reject out-of-focus or off-center interactions. Signals are collected and reported in 300 size intervals per measurement spectrum. The size of the focused beam controls the size resolution and the range of sizes evaluated. By changing the focusing lenses, it is possible to examine ranges from 0.5 μm to 150 μm, 2 μm to 300 μm and 5 μm to 1200 μm, although the top-of-line model (CIS-100) provides a range from 0.5 μm to 3600 μm.

The advantages of the Galai equipment are similar to those described above for the electroresistance analyzers (e.g., small sample size, rapid analysis) plus the problems associated with coincidence and orifice clogging are also avoided. Analyses can be run until either a specified number of particles are counted (generally >200,000) or until a desired level of confidence in the distribution is reached (95%, 98% or 99%). Because the solution in which the particles are suspended does not have to be either aqueous nor

electrolytic, the system offers a distinct advantage over Coulter-type of counters for the study of highly soluble materials or freshwater sediments that may undergo flocculation upon introduction to a saline solution. The Galai size analyzer is also integrated with a powerful image viewing, acquisition, and analysis system which, together with the sizer, provides an impressively comprehensive approach to textural analysis. The major disadvantage is, like that of the electroresistance equipment, sample "representativeness". Also, the laser equipment is particularly susceptible to alignment problems and laboratory bench (and building) vibrations, and requires moderate to high level of technician skill and training. The Galai unit in the author's laboratory uses a magnetic stirrer to keep the particles suspended during analyses; this undoubtedly biases the data when samples containing abundant magnetic grains are examined.

Sieving

After direct visual estimation, sieving is probably the earliest particle sizing technique known. According to Agricola (1556), it was in common use during the 16th century, although high precision sieves were not available until the mid-19th century. Today, woven metal wire sieves of standard 200 mm diameter are available from 20 μm (coarse silt) up to 125 mm (cobble) (Table IV). Finer sieves, down to 5 μm openings, can be made by metal foil etching technology, although these are generally too delicate for most sedimentological work. Most sedimentology laboratories are equipped with sieves spanning the range of particle size from sand/silt (62 μm) through pebble (32 mm), and sieving still remains the most commonly used method of size analysis of unconsolidated materials coarser than silt.

In standard sieve analysis, a weighed[1] subsample of dry sediment is put into the top of a series of vertically stacked sieves. This column of nested sieves is then placed in a mechanical or sonic shaker/vibrator device (e.g., Ro-Tap, Allen-Bradley, Haver-Tyler, and Gilsonic are the most commonly used in North America) and after a suitable period of shaking (generally 15–20 minutes; Fig. 8), the contents of each sieve are weighed. As mentioned above, the sieve diameter is defined as the size of a sphere which passes through the mesh of a particular sieve but not through the underlying sieve, and as we saw in our example with sizing the golf ball, needle, and film cartridge, sieving generally measures the *minimum* cross-sectional dimension. Numerous texts and laboratory manuals provide details on the sieving procedure and templates for data collection and manipulation (e.g., Lewis & McConchie, 1994a; Lindholm, 1987; Lewis, 1984; Friedman & Johnson, 1982; Müller, 1967). The classic manual on sieve (and pipette) size analysis, *Petrology of Sedimentary Rocks,* by R. L. Folk (1980), is now available at no cost on the internet at: http://www.lib.utexas.edu/Libs/GEO/FolkReady/folkprefRev.html.

Sedimentation/settling rate

It is axiomatic that a large particle settles through a water column faster than a small particle. Following elucidation of the basic parameters and force relationships that govern the velocity of an object falling through a liquid by Stokes in the mid- 1800's (Stokes, 1851),

[1] A large amount of sample may result in clogging of the screens, mass-trapping effects, or even screen distortion and damage, whereas a small amount of sample may result in lowered statistical significance. Lewis & McConchie (1994a) recommend "the greatest load on a sieve should not exceed 5 grain diameter thickness". Folk (1980) recommends 30–70 g; if there are many screens, a larger amount should be used; if there are only 4–6 screens in the stack, a smaller amount should be used.

Table IV. Dimensions of A.S.T.M. (American Society for Testing Materials) standard wire cloth sieves.

Sieve Designation		Permissible Variation	Wire Diameter
Standard	Alternative		(mm)
125 mm	5 inch	±3.70 mm	8
106 mm	4.24 inch	±3.20 mm	6.3
100 mm	4 inch	±3.00 mm	6.3
90 mm	3.5 inch	±2.70 mm	6.3
75 mm	3 inch	±2.20 mm	6.3
63 mm	2.5 inch	±1.90 mm	5.6
53 mm	2.5 inch	±1.60 mm	5
50 mm	2 inch	±1.50 mm	5
45 mm	1.75 inch	±1.40 mm	4.5
37.5 mm	1.5 inch	±1.10 mm	4.5
31.5 mm	1.25 inch	±1.00 mm	4
26.5 mm	1.06 inch	±0.800 mm	3.55
25.0 mm	1.00 inch	±0.800 mm	3.55
22.4 mm	0.875 inch	±0.700 mm	3.55
19.0 mm	0.75 inch	±0.600 mm	3.15
16.0 mm	0.625 inch	±0.500 mm	3.15
13.2 mm	0.530 inch	±0.410 mm	2.8
12.5 mm	0.5 inch	±0.390 mm	2.5
11.2 mm	7.0625 inch	±0.350 mm	2.5
9.5 mm	0.375 inch	±0.300 mm	2.24
8.0 mm	0.3125 inch	±0.250 mm	2
6.7 mm	0.265 inch	±0.210 mm	1.8
6.3 mm	0.25 inch	±0.200 mm	1.8
5.6 mm	No. 3.5	±0.180 mm	1.6
4.75 mm	No. 4	±0.150 mm	1.6
4.0 mm	No. 5	±0.130 mm	1.4
3.35 mm	No. 6	±0.110 mm	1.25
2.8 mm	No. 7	±0.095 mm	1.12
2.36 mm	No. 8	±0.080 mm	1
2.0 mm	No. 10	±0.070 mm	0.9
1.7 mm	No. 12	±0.060 mm	0.8
1.4 mm	No. 14	±0.050 mm	0.71
1.18 mm	No. 16	±0.045 mm	0.63
1.0 mm	No. 18	±0040 mm	0.56
850 μm	No. 20	±35 μm	0.5
710 μm	No. 25	±30 μm	0.45
600 μm	No. 30	±25 μm	0.4
500 μm	No. 35	±20 μm	0.315
425 μm	No. 40	±19 μm	0.28
355 μm	No. 45	±16 μm	0.224

Table IV. Dimensions of A.S.T.M. (American Society for Testing Materials) standard wire cloth sieves (continued).

Sieve Designation		Permissible Variation	Wire Diameter
Standard	Alternative		(mm)
300 μm	No. 50	±14 μm	0.2
250 μm	No. 60	±12 μm	0.16
212 μm	No. 70	±10 μm	0.14
180 μm	No. 80	±9 μm	0.125
150 μm	No. 100	±8 μm	0.1
125 μm	No. 120	±7 μm	0.09
106 μm	No. 140	±6 μm	0 .071
90 μm	No. 170	±5 μm	0.063
75 μm	No. 200	±5 μm	0.05
63 μm	No. 230	±4 μm	0.045
53 μm	No. 270	±4 μm	0.036
45 μm	No. 325	±3 μm	0.032
38 μm	No. 400	±3 μm	0.030
32 μm	No. 450	±3 μm	0.028
25 μm	No. 500	±3 μm	0.025
20 μm	No. 635	±3 μm	0.02

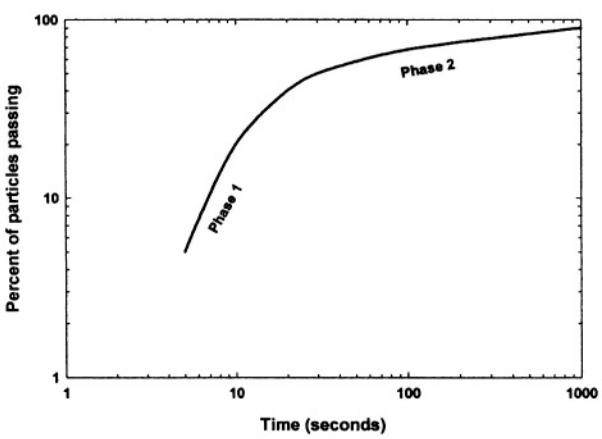


Figure 8. Plot of the proportion of particles finer than the sieve mesh that have passed through the sieve per time (modified from Irani & Callis, 1963). Phase 1 is due to the passage of particles which are smaller than the sieve mesh in all dimensions; Phase 2 is due to the more gradual passage of particles which at least one dimension larger than the sieve mesh.

fine particle size analysis during much of the past century was dominated by the technique of sedimentation.

A great range of instruments have been produced to evaluate size of particles controlled by this differential settling rate, but they all exploit the basic concept of Stokes' Law, namely that the settling velocity of fine-grained material varies according to the square root of the diameter of the grain. When a particle is put into a liquid, it will be exposed to the force of gravity (F_g) pulling it downward and to the viscous drag force (F_v) in the opposite direction. These are related according to:

$$F_v = 3\pi\eta d v, \tag{4}$$

and

$$F_g = \pi d^3 g(\rho_s - \rho_l)/6, \tag{5}$$

where d is the particle diameter, v is the dynamic velocity, g is the acceleration due to gravity, η is the viscosity of the fluid, ρ_s is the particle density, and ρ_l is the liquid density. Since the gravitational force is fixed and constant and F_v is initially zero, the particle begins to accelerate downward, thereby resulting in increased drag from the fluid. Soon the net forces control the movement and the particle will fall with a constant velocity (i.e., terminal velocity), represented by:

$$3\pi\eta d v = \pi d^3 g(\rho_s - \rho_l)/6 \tag{6}$$

or

$$v = d^2 g(\rho_s - \rho_l)/18\eta. \tag{7}$$

Thus, the particles can be characterized according to diameter,

$$d = \left[18\eta v / g(\rho_s - \rho_l)\right]^{0.5} \tag{8}$$

by placing them into the top of a particle-free column of liquid and measuring the quantity of particles which have settled to a particular level in the column as a function of time.

There are a number of important limitations to the practical application of Stokes' Law. First, it applies only to spherical particles. Anything not spherical will be described in terms of Stokes' equivalent diameter (Table II), which can be significantly different than the equivalent diameters evaluated by electroresistance analyzers for example. Second, the application of Stokes' Law assumes dilute suspensions. If the particle concentration is not low (as is frequently the case), the falling particles interact with one another and the settling velocity is lower than it should be. Similarly, Stokes' Law assumes the particles are settling under laminar flow conditions. Unfortunately, relatively large particles settle with such velocity as to set up turbulence within the water column, again adversely affecting the settling rate of the small particles. Finally, and most important from the perspective of analyzing naturally occurring materials, Stokes' Law assumes constant densities (or a constant difference in densities between the liquid and the solid). Clearly, this is not the case in a multimineralic sample consisting of, for example, feldspars ($\rho = 2.5\,\mathrm{kg\,m^{-3}}$), quartz ($2.65\,\mathrm{kg\,m^{-3}}$), calcite ($2.7\,\mathrm{kg\,m^{-3}}$), dolomite ($2.9\,\mathrm{kg\,m^{-3}}$) and micas ($3.0\,\mathrm{kg\,m^{-3}}$). Furthermore, minor temperature changes within the liquid during the course of the settling experiment change the viscosity of the liquid.

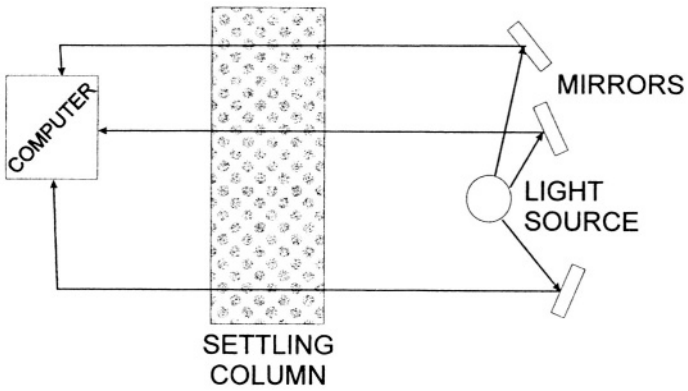


Figure 9. Schematic of a gravity sedimentometer.

It is beyond the scope of this chapter to summarize all of the many types of equipment that evaluate size by the sedimentation technique. Some, such as settling tubes, are one-of-a-kind type of instruments. Settling tube design is summarized by Syvitski et al. (1991b). Most of the classical approaches are reviewed and described in Müller (1967), Irani & Callis (1963), Milner (1962), and Krumbein & Pettijohn (1938). Few of these techniques are in common use today. Folk (1980), as well as many other sedimentology textbooks (e.g., Lewis & McConchie, 1994a; Lindholm, 1987; Lewis, 1984; Friedman & Johnson, 1982) describe the step-by-step procedure for the classical pipette method, which, for many years was the mainstay for size analysis of sediment finer than 62 μm. In essence, the technique involves taking multiple samples over time of a solution through which particles are settling. By knowing the depth at which the sample was taken (i.e., the distance the particles have settled) and the length of time the particles have been settling, it is possible to calculate the diameter of the grains that have settled past the sampling point.

Other than the amount of laboratory space and technician time required for classical pipette analysis, the major practical problem with the pipette method is that withdrawal of multiple samples, even if done carefully, disturbs the sedimentation column. So a variety of other techniques were designed to 'remotely' estimate the amount of material in suspension at a given point. Intuitively, it would appear the most straight-forward technique, instead of actually removing samples, is rather simply shine a light through the settling column and evaluate the amount of light attenuation at a given point with time. The photosedimentometer (e.g., Lumosed) uses multiple light beams at different levels within the column to evaluate changes in the concentration of solid material (Fig. 9). A uniform suspension of particles is placed in a settling column and, as the particles move to the bottom of the column, their decreasing concentration is recorded at the different levels by the increasing light transmission through the column.

However, gravitational settling of fine material is slow (a 1 μm particle requires nearly 15 hours to settle 5cm in a water column). Thus, to further decrease the time required to measure slowly settling particles, some instruments (e.g., Fritsch Scanning Photosedi-

mentograph) use a gradually moving light and detector system so that the smaller particles towards the top of the sedimentation column are measured after having settled through much shorter distances. The moving photometer records optical density as it travels upwards along a sedimentation column and the equipment uses the change in the concentration of settling particles as a function the height to calculate particle diameter.

Alternatively, other devices (e.g., Brookhaven Bl-DCP Disk Centrifuge; Chemical Process Specialists Disc Centrifuge) have been manufactured that use a similar detection scheme but increase the rate of sedimentation by applying a centrifugal force. The time for a particle to travel from the initial point at the surface or edge of the rotating disk to the detector can be calculated according to:

$$t = \left[18\eta \ln\left(R_d/R_i\right)\right]/\left[\omega^2 d^2\left(\rho_s - \rho_l\right)\right], \tag{9}$$

where t is the time, η is the fluid viscosity, R_d and R_i are the final and initial radii, respectively, ω is the centrifuge angular velocity, and ρ_s and ρ_l are the densities of the solid and liquid, respectively. By varying rotational speed and fluid viscosities, analyses down to 0.01 μm are claimed.

Photosedimentometers, whether gravitational or centrifugal, all have one distinct theoretical disadvantage: they are based on the assumption that the light cut off by a particle is equal to its projected area. Unfortunately, the particles not only directly block the light by simple absorption, but they also scatter the light by refraction. This ability to scatter the light varies according to size and composition of the material. Thus, a detailed knowledge of the mineralogy, or at least the index of refraction, of the solid material is essential so that appropriate corrections can be made. This significantly limits the use of photosedimentometers in analyzing the size of material a naturally occurring sample with variable (and probably unknown) mineralogy. Other problems are that it is assumed the particles are opaque (probably not the case for many fine-grained solids) and that the concentration of the particles in suspension is low enough that no two particles fall on the same line parallel to the light beam.

To circumvent the problems of using light, remarkable success has been achieved by using X-rays (Hendrix & Orr, 1972). The extremely short wavelength of X-rays prevents the waves from being diffracted by the particles. Thus, the attenuation of the beam is due entirely to absorbance and is proportional to the amount of material in the beam such that the relative transmittance of the X-rays (T) is:

$$T = e^{-C(\mu p - \mu l)L}, \tag{10}$$

where μ_p and μ_l are the X-ray absorption coefficients of the particles and liquid, respectively, C is the particle mass concentration, and L is the length of the path. The most widely known of these X-ray attenuation devices, the SediGraph manufactured by Micromeritics, is the equipment most commonly used to analyze fine-grained sediment over the past decade and is the preferred method for finer-than-sand analyses in many major sedimentological laboratories (see summary provided by Micromeritics at their internet web site: http://www.micromeritics.com/ps_sedigraph.html).

The principle of operation of this equipment has been described in many other places (e.g., Washington, 1992; Coakley & Syvitski, 1991; Singer et al., 1988; Jones et al., 1988;

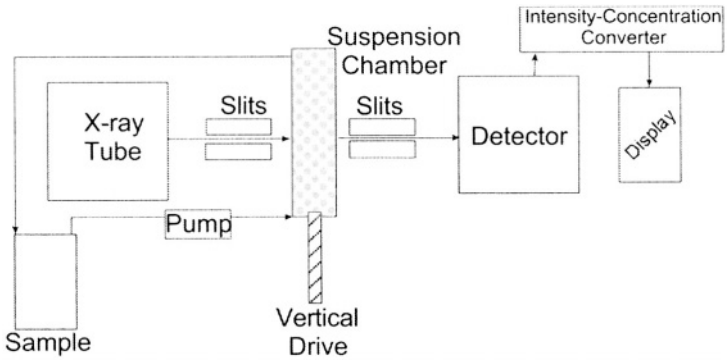


Figure 10. Schematic of an X-ray attenuation size analyzer such as the SediGraph.

Stein, 1985). The dispersed sample is placed in a chamber through which a narrow beam of X-ray radiation is passed (Fig. 10). As with the photosedimentometers described above, as the particles settle through the chamber, the density of material in the beam falls and the X-ray intensity at the detector increases. Initially the X-ray beam is passed through the solution near the base of the chamber, but as the analysis continues the chamber moved downward so that the very slowly settling fine-grained material near the top of the chamber can be evaluated.

The popularity of X-ray attenuation equipment for routine size analysis of relatively fine material lies in the combination of moderately rapid speed of analysis (~40 minutes for an analysis of a sample from fine sand to clay), moderate sample size requirements (1–5 g sample), and the lack of interference from variable indices of refraction. However, several disadvantages are evident. First, the size of the sample (and the density of particles in the sample chamber) required to obtain optimum results limits the analysis of individual laminae or small subsamples such as might be obtained from sediment traps. Second, the absorption of X-rays varies considerably depending on the elemental composition of the material. Light elements (e.g., carbon, oxygen) absorb X-rays only weakly, whereas relatively heavy elements (e.g., iron, titanium, magnesium) absorb much more strongly. Thus, in a multimineralogic sample, it is possible particles such as illmenite, hornblende, or chlorite could 'blind' the equipment from detecting particles composed of elements less effective at blocking the X-rays, as shown by Coakley & Syvitski (1991) and Jones et al. (1988) and, conversely, ignore particles such as charcoal and other organic materials. The use of a magnetic stirrer presents the same problem as that described above for the Galai device. Finally, the SediGraph equipment in the author's laboratory has experienced an unusually high frequency of pump failures. These mechanical problems have also been noted by others (e.g., Coakley & Syvitski, 1991).

Laser diffraction

It was mentioned above that a significant problem with size analysis using the attenuation of a light beam passing through a settling tube is that the small particles scattered the light rather than blocked it. However, with the advent of laser technology coupled with high

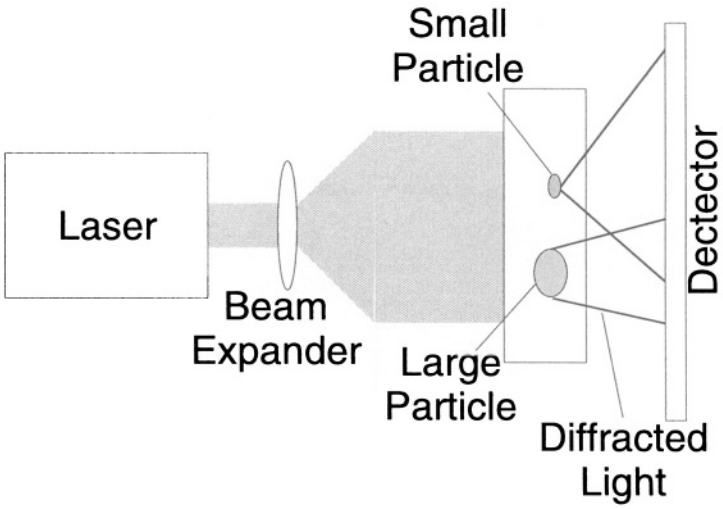


Figure 11. Schematic of a laser diffraction size analyszer.

speed computer manipulation of data, in the past several decades is has become possible to use the physics of this light scattering to actually deduce the size of the particles responsible for the scattering.

As light impinges on a particle, a combination of absorption and refraction takes place. The net result, the relative refractive index, is controlled by the composition of the material and the medium. In addition, the size of the particle (relative to the wavelength of the light) also affects its light scattering ability. If the particle is large, scattering occurs in all directions; as the particle becomes progressively smaller, scattering becomes more and more in the forward direction. A detailed quantification of these principles (i.e., Mie theory) is covered in Bohren & Huffman (1983). Essentially, if a column of liquid containing particles is illuminated by a laser beam, particles in the size range of about 0.7 to 700 μm scatter light in the forward direction at angles inversely proportional to their size but at intensities directly proportional to size (Fig. 11). The resulting patterns can be resolved mathematically using a series of data fitting processes as summarized by Agrawal et al. (1991).

Despite the ease of operation of most of the laser diffraction sizing equipment and the manufacturers' claims about analytical size range (e.g., 0.02 μm to 2000 μm for the Malvern's Mastersizer 2000; 2 nanometers to 3 μm for Brookhaven's 90Plus Dynamic Light Scattering Analyzer), diffraction equipment has not been used extensively in sedimentological laboratories. Although this is one of the newest techniques in the particle size field and the equipment is undoubtedly rapidly evolving, many authors within the past decade have reported less than desirable resolutions at the fine end of the spectrum, inappropriate data fitting algorithms for polymodal distributions, and systematic errors inherent in the analysis of non-equant particles (e.g., Washington, 1992; McCave&Syvitski, 1991; Singer et al., 1988; and McCave, 1986).

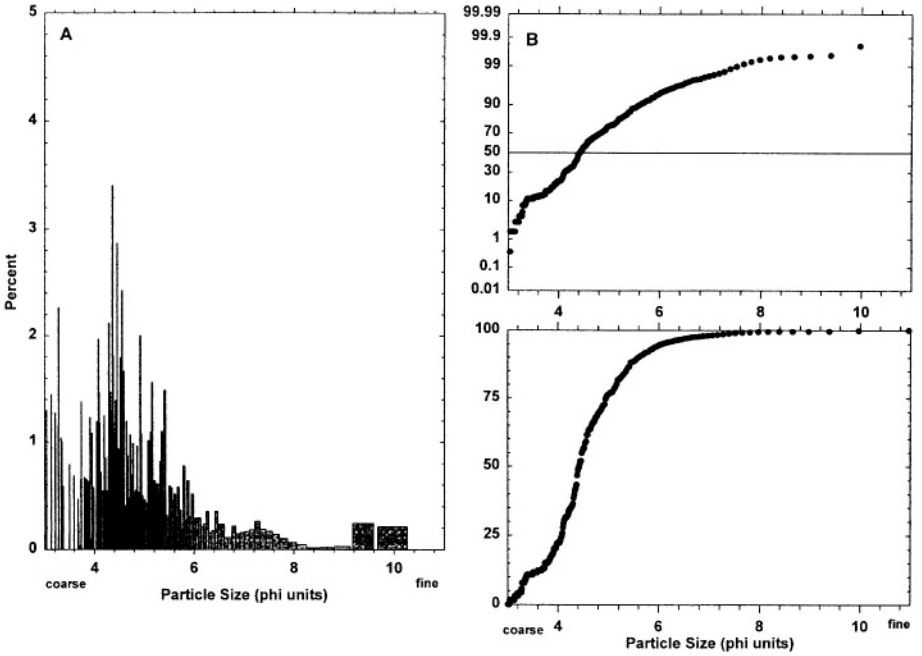


Figure 12. Results of particle size analysis of a sample from West Basin Lake, Australia. A: Histogram; B: Cumulative frequence curve plotted using arithmetic-ϕ scales; C: Cumulative frequency curve plotted using probability-ϕ scales.

Particle size distributions

Many of the automated electronic size analyzers summarized above also provide an impressive array of graphing and statistical manipulation capabilities. Data presentation and treatment of the size data from a statistical perspective are clearly very important parts of textural analysis and the literature in this area is immense (see, for example, references listed in Lewis, 1984). Traditionally, sedimentologists have used mainly graphical means of describing and analyzing the particle size data. Simple histograms, size frequency curves, and cumulative frequency curves are all straight-forward graphical displays of the collected size data (Fig. 12). Histograms are usually plotted with arithmetic-log or arithmetic-ϕ scales, with each bar coinciding with a single size class. The traditional use of % (increasing upward on the vertical axis) versus ϕ size (ϕ numbers increasing to the right on the horizontal axis), following Krumbein & Pettijohn's (1938) recommendation, is still in common use, although there is now a tendency to plot the size data in reverse (i.e., the absolute size of the particle class increasing to the right). A frequency curve can be drawn by joining the midpoints of each size bar. The cumulative frequency curve, particularly when drawn using log-ϕ scales, is useful for quickly assessing the distribution's characteristics. Much early work with mainly sandy sediments assumed normal (Gaussian) distributions. In a normal distribution, the central part of the population contains the bulk of the particle

Table V. Descriptive statistical measures of particle size (from Folk, 1980; Griffiths, 1967).

Measures of Central Tendency	
Folk's Graphic Mean	$M_z = (\phi_{16} + \phi_{50} + \phi_{84})/3$
Inman Mean	$M = (\phi_{16} + \phi_{84})/2$
Median	$M_d = \phi_{50}$
Mode	M_0 = Most frequently occurring particle size. On a histogram it is the midpoint of the most abundant class interval; on a cumulative frequency curve it is the size corresponding to the steepest part of the curve.
Measures of Uniformity	
Trask's Sorting Coefficient	$S_0 = (\mathrm{mm}_{25}/\mathrm{mm}_{75})^{0.5}$
Phi Quartile Deviation	$QD_\phi = (\phi_{75} - \phi_{25})/2$
Graphic Standard Deviation	$\sigma_g = (\phi_{84} - \phi_{16})/2$
Inclusive Graphic Standard Deviation	$\sigma_i = [(\phi_{84} - \phi_{16})/4] + [(\phi_{95} - \phi_{50})/6.6]$
Measures of Symmetry	
Phi Quartile Skewness	$S_{kq\phi} = (\phi_{25} + \phi_{75} - 2M_d)/2$
Graphic Skewness	$S_{kg} = (\phi_{16} + \phi_{84} + 2\phi_{50})/(\phi_{84} - \phi_{16})$
Inclusive Graphic Skewness	$S_{ki} = [(\phi_{16} + \phi_{84} + 2\phi_{50})/2(\phi_{84} - \phi_{16})] + [(\phi_5 + \phi_{95} + 2\phi_{50})/2(\phi_{95} - \phi_5)]$
Measures of Frequency Curve Peakedness	
Kurtosis	$K_g = (\phi_{95} - \phi_5)/2.44(\phi_{75} - \phi_{25})$

sizes and the coarser and finer parts are equally distributed on each side of this central part. When plotted as a frequency curve, the classic bell-shaped curve results; when plotted as a cumulative curve using log-ϕ scales, the data approximate a straight line (i.e., the distribution is referred to as lognormal).

From this basic assumption of lognormalcy, a large number of descriptive statistics have been defined and are regularly used. Table V lists the formulae used to calculate these descriptive statistics from the cumulative frequency curve. Mean (average) and median (size at the middle of the population) are the most frequently used descriptors. Sorting, which refers to uniformity of the size distribution, is usually expressed as the inclusive graphical standard deviation. Material that is well sorted (i.e., contains only a small range of particle sizes) has a low standard deviation, whereas high standard deviations indicate the sediment has a wide range of sizes and is poorly sorted. Table VI lists the numerical subdivisions of sorting. In a normal bell-shaped distribution (i.e., the mean is equal to the median), the two halves of the distribution are mirror images. However, if the distribution is asymmetrical, or skewed, the mean does not equal the median. If the deposit has excess fine particles, it is referred to as positively skewed; negatively skewed deposits have an excess of coarse material. The inclusive graphic skewness parameter is used to quantify this asymmetry. Finally, the peakedness of the frequency curve can be evaluated by calculating the graphic kurtosis. Kurtosis measures the ratio between the sorting in the tails of the distribution and the sorting in the central portion of the distribution. If the central portion is better sorted

Table VI. Sorting, skewness, and kurtosis classes (after Folk, 1980).

Sorting (σ_1)	
$<0.35\phi$	Very well sorted
0.35ϕ–0.50ϕ	Well sorted
0.50ϕ–0.71ϕ	Moderately well sorted
0.71ϕ–1.00ϕ	Moderately sorted
1.00ϕ–2.00ϕ	Poorly sorted
$>2.00\phi$	Very poorly sorted
Skewness (S_{ki})	
>0.30	Strongly fine-skewed
0.30–0.10	Fine-skewed
0.10–−0.10	Near-symmetrical (unskewed)
−0.10–−0.30	Coarse-skewed
<−0.30	Strongly coarse-skewed
Kurtosis (K_g)	
>3.0	Extremely leptokurtic
1.5–3.0	Very leptokurtic
1.11–1.50	Leptokurtic
0.90–1.11	Mesokurtic
0.67–0.90	Platykurtic
<0.67	Very platykurtic

than the tails, the distribution is excessively peaked or leptokurtic. Conversely, if the tails are better sorted than the central portion, the distribution is 'flat peaked' (deficiently peaked) or platykurtic.

With automated size analyzers and ready computer access, various analogous descriptive parameters can be much more easily and accurately calculated by moment statistics. Most sedimentology texts provide introductions to moment measures, but see the discussions in Friedman et al. (1992) and Friedman & Johnson (1982) for particularly lucid descriptions of the computation technique. Lindholm (1987), Lewis (1984), and Griffiths (1967) provide several worked examples using sieve-derived size data. Swan et al. (1979) report the results of an interesting comparison study of moment and graphic statistics.

In the method of moments, the measure of central tendency is the first moment (arithmetic mean):

$$m_1 = \Sigma(DW)/\Sigma W, \tag{11}$$

where D is the midpoint of each size group and W is the weight of each size group. Alternatively, if frequency data are being used (see also Lindholm, 1987, Blatt et al, 1980, and Swan et al., 1978, for discussion of the inherent limitations of using frequency versus weight data), equation (11) becomes:

$$m_1 = \Sigma(DF)/\Sigma 100, \tag{12}$$

where F is the frequency in weight percent. Once the first moment (average) is established, higher order moments are usually calculated about this value according to:

$$\text{second moment or variance} = m_2 = \sigma^2 = \Sigma W(D - m_1)^2 / \Sigma W, \quad (13)$$

$$\text{third moment} = m_3 = \Sigma W(D - m_1)^3 / \Sigma W, \quad (14)$$

$$\text{fourth moment} = m_4 = \Sigma W(D - m_1)^4 / \Sigma W. \quad (15)$$

The values analogous to the graphic statistics are:

$$\text{standard deviation} = \sigma = m_2{}^{0.5}, \quad (16)$$

$$\text{skewness} = m_3 / (m_2{}^{1.5}), \quad (17)$$

$$\text{kurtosis} = m_4 / (m_2{}^2). \quad (18)$$

Although these moment statistics are, today, very easily acquired, it must be emphasized that their use implies a knowledge of the *complete* size distribution. For example, in sieving, the grain size distribution is often open-ended (i.e., undifferentiated fines that have passed through the finest sieve in the stack). Alternatively, in the analysis of many relatively fine-grained sediments by any of the electronic size analyzers discussed above, there is an upper limit above which the equipment cannot evaluate. In these situations, the moment statistics can provide misleading, if not meaningless, results (McManus, 1988; Lewis, 1984). Finally, both sets of descriptive statistics (i.e., graphical and method of moments) assume the particle size distribution is normal or lognormal. In fact, it has been repeatedly shown that this assumption is generally false. This has lead to the view that use of the more sophisticated moment measures or other complex statistical handling of the data (e.g., factor analysis; see papers in Syvitski, 1991) may be unwarranted (Lindholm, 1987; Krumbein, 1975).

What does it all mean?

The interpretive use (versus descriptive use) of particle size data is one of the more controversial areas in the entire realm of sedimentology. Despite many decades of effort, there has been little agreement about the application of size data in the area of paleoenvironmental research (e.g., see discussions in Pettijohn, 1975; Ehrlich, 1983; Lindholm, 1987; McManus, 1988). For fine-grained sediments, for example, although precise data can be collected from a stratigraphic sequence and statistically significant summary parameters can be calculated, these numbers may be meaningless in terms of paleohydrological interpretations. This is because most fine particles are deposited as fragile but often larger aggregates (e.g., inorganic floccules, organic fecal pellets) which respond differently to hydrological conditions than if they were individual particles. Even with coarser sediments, the simple intuitive relationship between particle size, energy level, and water depth can be ambiguous as reviewed by Teller & Last (1990). Krumbein (1975) concludes that it is still questionable whether the grain size distribution is indicative of any particular erosion/transport agent and/or specific environmental setting. Nonetheless, particle size still remains one of the primary indicators of energy level in lacustrine sequences (e.g., Sly, 1978, 1977).

Form and fabric

Most naturally occurring particles are of irregular shape. This presents considerable problem not only in simply defining what we mean by size as discussed above, but also, from a more practical standpoint, in deciphering effect that irregular grain shape has on size measurement. The difficulties of quantitatively assessing particle shape are not trivial (e.g., Matthews, 1991b; Orford & Whalley, 1991; Allen, 1981; Barrett, 1980) and a considerable amount of geoscientific literature has accumulated dealing with this. As with many other aspects of textural analysis, future advances in the area of particle shape and fabric will be largely tied to developments in automated image analysis systems (e.g., Persson, 1998) combined with advanced statistical approaches (e.g., Nelson & Full, 1998; Thomas et al., 1995; Lilje, 1991). Boggs (1992) provides a very readable summary of the most promising of these tools, Fourier analysis. Orford & Whalley (1991,1987, 1983) summarize the application of fractals and harmonics (together with Fourier analysis).

Sphericity and its measurement

The classification of particle shapes by symmetry, a system used by crystallographers, or by pure geometrical standards (cubes, cylinders, spheres, cones, etc.), is neither convenient nor applicable in most cases. The simplest concept of shape that can be applied to most common non-clay mineral particles is sphericity (i.e., the degree to which the shape of the particle approaches that of a sphere). The sphere is a convenient shape for reference because it has certain unique properties. Of all possible shapes for a given volume, the sphere has the least surface area, the greatest settling velocity, and the greatest tendency to roll. Ideally, the sphericity of a particle is the ratio of the surface area of a sphere of the same volume to the surface area of the particle. However, because of measurement difficulties, sphericity is generally calculated as the ratio of the diameter of a sphere of the same volume as the particle to the diameter of a circumscribing sphere (Fig. 13). Even this presents some measurement difficulties unless the researcher is working with gravels or is undertaking image analysis. The most practical method for estimating sphericity involves simple visual comparison of the projected two-dimensional image of the particles to images of calculated sphericity. Numerous charts have been prepared for this purpose (e.g., Zingg, 1935; Rittenhouse, 1943; Blatt et al., 1980), and, for gravels, a variety of quantitative methods of classifying the shapes (Fig. 14; Sneed&Folk, 1958; Krumbein, 1941).

Roundness and its measurement

Roundness or angularity has to do with the sharpness of the edges or corners of a particle. It is independent of shape. Roundness has been expressed as the ratio of the average radius of curvature of the corners to the radius of the maximum inscribed sphere (Fig. 13). For practical purposes this definition is normally applied to the two-dimensional case, commonly a section or projection of the particle. Without IAS, calculation of roundness is tedious, and the most common method of measurement is by visual comparison of grains or grain images with standards of calculated degrees of roundness as furnished by Powers (1953) or Krumbein (1941) and reproduced in most modern sedimentology textbooks.

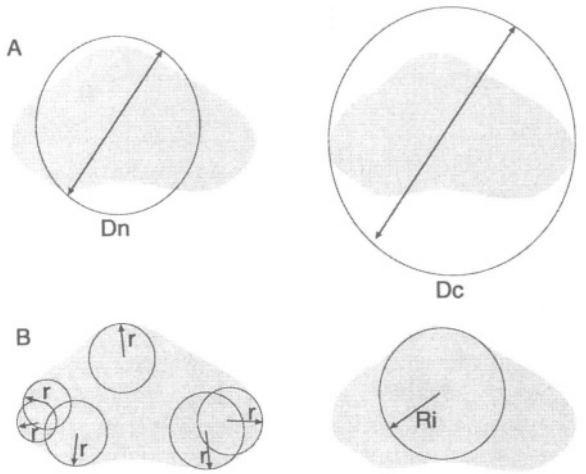


Figure 13. A. General method for determining particle sphericity from a two dimensional image (e.g., thin section photomicrograph). A sphericity value, S_p, is defined as the ratio of the diameter of a circle of the same area as the projected image of the particle (Dn) to the diameter of a circumscribing circle (Dc). Perfect sphericity has a value of 1. B. General method for determining particle roundness from a two dimensional image (e.g., thin section photomicrograph). A roundness value, Rd, is defined as the ratio of the average radii of curvatures of the corners to the radius of the maximum inscribed circle (Ri). A perfectly round particle has a value of 1 (after Wadell, 1932)

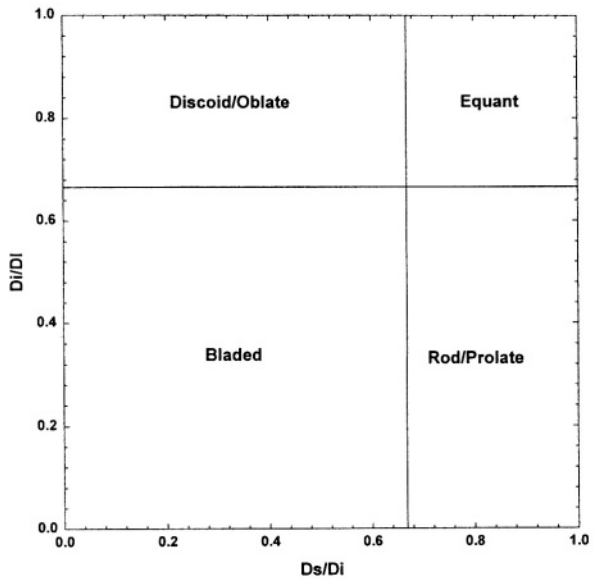


Figure 14. Classification of particle shapes according to Zingg (1935). Ds, Di, and Dl refer to the lengths of the short, intermediate and long axes, respectively.

Surface texture

Another attribute of particles is their surface texture. Surface textures are exceedingly diverse but Pettijohn (1975) has grouped them into two categories. One class is concerned with dullness or polish of the surface; the other has to do with surface markings, such as striations, percussion scars, etc. The widespread use of the scanning electron microscope by sedimentologists beginning in the 1970s provided the impetus for considerably more detail and improved methodology for studying particle surface texture. For example, Bull (1986) distinguished some 60 different types of surface features on quartz grains, many of which hold potential for paleoenvironmental interpretation. Krinsley & Trusty (1986) summarize the major applications of quartz surface texture analysis.

The application of particle form in geolimnological studies has, to date, lagged behind that of other environments. Although this avenue of research has not been extensively applied by paleolimnologists, the area hold considerable promise as a means of better understanding climatic and hydrological conditions within a lake's watershed, and the chemical and diagenetic conditions at the depositional site. Studies of particle form will also give paleolimnologists the ability to make better interpretations about the provenance (source areas) of the materials in the lake and inferences of transport distances and genesis.

Fabric

The concept of fabric in sediments refers to the arrangement of particles in terms of their (i) sorting (discussed above), (ii) packing, and (iii) spatial relationship (orientation) of individual non-equant grains. The literature on this topic is at least as voluminous as that on size because of the obvious importance of fabric to derived properties like porosity, permeability, and strength. An understanding of sedimentary fabric is also essential in deciphering flux and in modeling diagenetic and transport processes within sediments as discussed by Boudreau (1997), Berner (1980) and Lerman (1979). Despite this wealth of literature, few would argue with Pettijohn's (1975) assessment that the results of particle fabric investigation have not been commensurate with the efforts made.

The spatial density of particles, or packing, is easily understood if we imagine that the particles in our sediment are all uniform, perfectly sorted spheres. These spheres can be arranged in a container in a loose (open) packing pattern or in a tight (close) pattern. A cubic arrangement of the particles is the most open, whereas a rhombohedral pattern produces the tightest packing. Unfortunately, naturally occurring sediments are not spherical, nor are the deposits perfectly sorted, so simple descriptions and classifications based on these assumptions have little relevance. Sedimentary particle packing is a complex phenomenon controlled by the interplay of many factors including: (i) the shapes and sorting of the particles, (ii) the depositional processes, and (iii) postdepositional modification by compaction, organism activity, authigenic mineral formation, etc. Packing of sedimentary deposits plays a significant role in how the material behaves from an engineering perspective. Some clay-rich lacustrine (and marine) sediments can be troublesome for foundations because the deposits can undergo a rapid change in packing, resulting in spontaneous liquefaction (Graham & Shields, 1985; Rahn, 1996). Liquefaction, or the loss of shear strength, affects the sediment's ability to support the load of a structure or the stability on a slope. Several attempts have been made to quantify the aspect of packing (see overviews in Boggs, 1992;

Pettijohn et al., 1987; Pandalai & Basumallick, 1984; Griffiths, 1967), but these have not yet been applied to lacustrine sequences or paleolimnological efforts.

Studies of the orientation of non-equant particles within a sediment have been directed primarily toward the coarse fraction of the deposit with particular emphasis placed on the usefulness of a preferred orientation (versus an isotropic or random orientation) in paleocurrent analysis (Martini, 1978; Potter & Pettijohn, 1977; Bonham & Spotts, 1971; Griffiths, 1967). In finer grained sediments, use of scanning electron microscopy and xradiography techniques in conjunction with petrographic studies are essential (e.g., Potter et al., 1980; Keller, 1976; 1970; O'Brien, 1970; Heling, 1970; Gilliot, 1969) and hold consider promise in helping to identify exposure horizons and flocculation changes (i.e., water chemistry fluctuations) in lacustrine sequences.

Example of application of textural studies

As pointed out in the introductory comments, the textural investigation of lake sediments is very common and is undertaken for a great many purposes. There is a wealth of published work using sediment texture to describe lacustrine deposits, understand the mechanisms of modern and past depositional and diagenetic processes, assess the environmental and contaminant chemical dynamics of the lake, and decipher past changes in hydrology, climate, source areas, and limnology of lacustrine basins and their watersheds. Much of this vast literature is reviewed in a number of excellent synthesis papers and monographs including Talbot & Allen (1996), Gierlowski-Kordesch & Kelts (1994), Anadón et al. (1991), Håkanson & Jansson (1983), Sly (1978), Matter & Tucker (1978), Jopling (1975), Picard & High (1972), and Reeves (1968). Among the many examples that can be cited, the classic work on the Great Lakes of North America (e.g., Cahill, 1981; Sly, 1977; Thomas et al.,1976, 1972) and the efforts of Håkanson (e.g., 1982, 1981,1977, 1974) and his associates on the sedimentary regime of Swedish lakes deserve special mention.

An example from western Canada

The following is a somewhat unusual example of textural analysis of lake sediments using the size and shape of endogenic rather than detrital components in the stratigraphic record. The northern Great Plains of western Canada form a unique setting for literally millions of saline and hypersaline, closed basin lakes. The lakes are generally small and shallow; many exhibit playa characteristics. However, the region also contains several of North America's largest and deepest salt lakes. The subject of over thirty papers, technical reports and theses, Waldsea Lake(52°10'N; 105° 10'W), located in south-central Saskatchewan, has received considerable attention from the scientific community over the past three decades, and is one of Canada's best-studied perennial saline lakes. Much of the scientific interest in Waldsea Lake stems from the fact that it is one of only four meromictic lakes in the entire Plains region of Canada. Absence of both bioturbation and reworking of the sediments by waves permits excellent preservation of sedimentary structures in the offshore areas of the lake. Summaries of the geolimnology, hydrology, and neolimnology of the lake can be found in Hammer (1978, 1986), Hammer et al. (1978), Lawrence et al. (1978), Parker et al. (1983),

Schweyen & Last (1983), Schweyen (1984), Last & Schweyen (1985), and Last & Slezak (1986, 1988).

The water in Waldsea Lake is saline to hypersaline, with an average salinity of the mixolimnion of 25ppt TDS and 70ppt TDS for the monimolimnion. Both water masses are alkaline, strongly dominated by Na^+, Mg^{2+} and SO_4^{2-}, and saturated or supersaturated with respect to various carbonate minerals at all times of the year. Because of the high Mg/Ca ratio of the brines, aragonite is the stable $CaCO_3$ phase being precipitated in the lake today. The monimolimnion is also perennially saturated with respect to gypsum, as is the upper meter of the mixolimnion during winter. During winter, the surface water can also approach saturation with respect to various hydrated sodium and magnesium sulfates. The offshore stratigraphic record of the past 6000 years consists of laminated to massive, chemically-precipitated sediments (mainly aragonite with some gypsum, mirabilite, magnesite, hydromagnesite, and protodolomite) mixed with relatively fine-grained siliciclastics.

Aragonite laminae petrography

The particle size and shape characteristics of the aragonite in the deep-water laminated sequence of the lake offer considerable insight into the paleolimnology of the basin.

The aragonite laminae, which range in thickness from ~0.2 mm to 2 mm, are irregularly spaced from 2–3 laminae per centimeter to much closer spacing. Individual laminae are composed entirely of extremely well-sorted, euhedral, micrometre-sized $CaCO_3$ crystals. There is an almost complete absence of biological and other non-carbonate grains, suggesting that the layers represent rapid inorganic precipitation and accumulation without dilution by non-carbonate endogenic minerals, siliciclastics, or organic debris.

These aragonite crystals show considerable variation in both size and morphology. Individual $CaCO_3$ crystals range from acicular to ellipsoidal, but are usually uniform in any single layer (Fig. 15). Many of the laminae have fine, needle-like crystals that are typical of the aragonite formed in many other perennial saline lakes in the northern Great Plains region. The aragonite in other laminae, however, have a distinctive wheat grain or rice grain morphology. This ellipsoidal aragonite has been noted in other deep water saline lakes in Canada and Australia , as well as from the Black Sea, and is indicative of newly-formed $CaCO_3$ crystals settling through a relatively deep, stagnant, somewhat undersaturated water column (Sack & Last, 1994; Last & De Deckker, 1990; Hsü, 1978).

Conditions in Waldsea Lake today are such that ellipsoidal aragonite does not form and the modern bottom sediments contain only acicular $CaCO_3$. However, geochemical modeling (Schweyen, 1984) indicates that shallowing of the chemocline by about 4 m would produce undersaturated conditions in the lower water mass and, in turn, create conditions favorable for the generation of rice-grain aragonite crystals. Thus, laminae with ellipsoidal aragonite crystals indicate the presence of a stratified water column in which the chemocline was considerably shallower than that of the modern lake, or, alternatively, the monimolimnion was less saturated (more undersaturated) with respect to $CaCO_3$.

As shown in Figure 16, the proportion of euhedral acicular aragonite crystals relative to other shapes in laminae from one of the cores near the basin center increased dramatically at about 500 years B.P. This suggests that the depth to the chemocline increased significantly in the lake about that time possibly due to the influx of more freshwater via precipitation

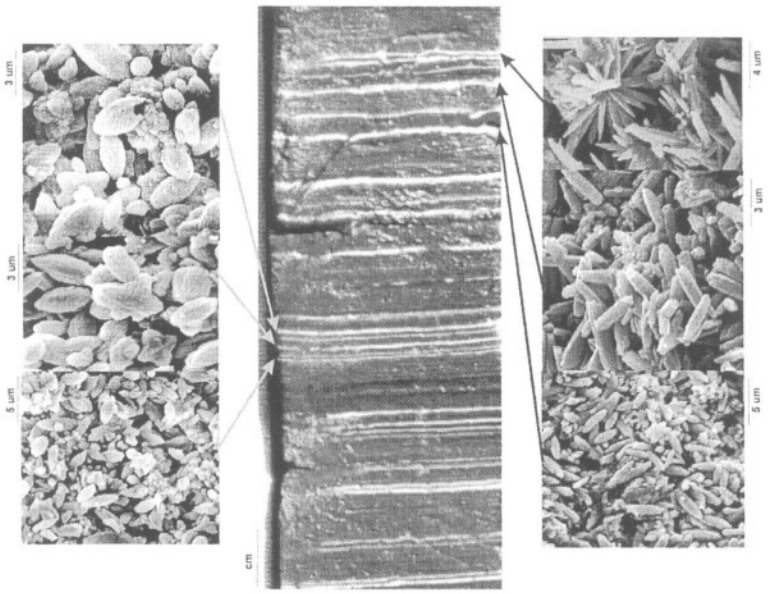


Figure 15. Variations in aragonite crystal shapes in selected laminae from an offshore core in Waldsea Lake, Saskatchewan. Examples shown on the left illustrate laminae composed mainly of ellipsoidal (rice-grained) crystals; examples on the right show laminae in which the aragonite is mainly of acicular morphology (modified from Greengrass et al., 1999; Deliqiat et al., 1999).

and steam runoff, increased wind mixing of the mixolimnion, or an increase in the degree of saturation with respect to $CaCO_3$ of the monimolimnion.

The crystals in individual laminae are extremely well sorted (average $\sigma < 1.0\,\mu m$) and have a mean size ranging from less than $2\,\mu m$ to more than $20\,\mu m$ (Fig. 17). There is a general trend toward increasing crystal size upward in the cores. Although many geochemical and environmental factors combine to determine the size of precipitated inorganic crystals, one of the most important is the length of time the crystal resides in the supersaturated solution. Thus, the stratigraphic variation in aragonite crystal size in the laminae is a reflection of the depth of the supersaturated water column. In the modern lake, this is essentially the depth of the mixolimnion (or the depth to the chemocline). Using aragonite crystals collected in sediment traps from modern Waldsea Lake and other aragonite-precipitating basins, it is possible to calibrate the stratigraphic variation in crystal size in terms of approximate depth to the paleochemocline (or, more correctly, the vertical extent of the supersaturated water column; Greengrass et al., 1999; Deleqiat et al., 1999). Other factors, such as the degree of supersaturation and the amount of crystal size modification that may take place during settling through an undersaturated monimolimnion, may affect these estimates, but this crystal size parameter should offer a reliable means of estimating past chemocline depths.

Figure 18 shows the fluctuation in interpreted chemocline depth of Waldsea Lake over the past 2000 years based on the mean crystal size of aragonite crystals in two cores in the basin. The Core A, the same core on which the detailed aragonite shape analysis was done, is located near the deepest (14 m) part of the basin. Core B is located about a kilometer

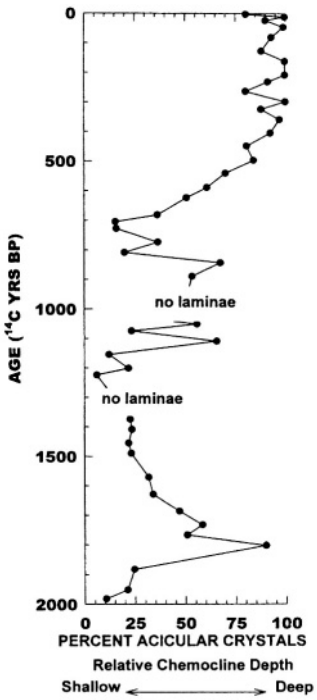


Figure 16. Stratigraphic variation in the percent of acicular crystals in individual aragonite laminae from an offshore core in Waldsea Lake, Saskatchewan. Laminae with relatively low proportions of acicular crystals indicate relatively shallow chemocline depths and slightly undersaturated monimolimnion conditions, whereas laminae with high proportions of acicular crystals suggest relatively greater chemocline depths and near-saturated conditions in the bottom water. Shape data were collected using a Galai CIS-1 Shape Analyzer. (modified from Greengrass et al., 1999; Deleqiat et al., 1999).

north in ~ 10 m water depth. Although the fluctuations do not match precisely, there is good general correspondence between the two cores. Both cores show a significant increase in interpreted chemocline depth during the most recent ~500 year period and generally shallower chemocline depths between about 500 and 1700 years B.P. This corresponds well with the changes in water column conditions interpreted from the aragonite crystal shape analyses.

Summary

Texture is the size, shape and arrangement of component particles in a sedimentary deposit. Texture has to do with the geometric characteristics of individual particles and the grain-to-grain relationships, whereas structure refers to larger features of the deposit and describes such characteristics as bedding features and stratigraphic sequence. Size, although an intuitively easy concept to understand, presents considerable practical problems in terms of measurement because most naturally occurring particles are irregular and non-equant.

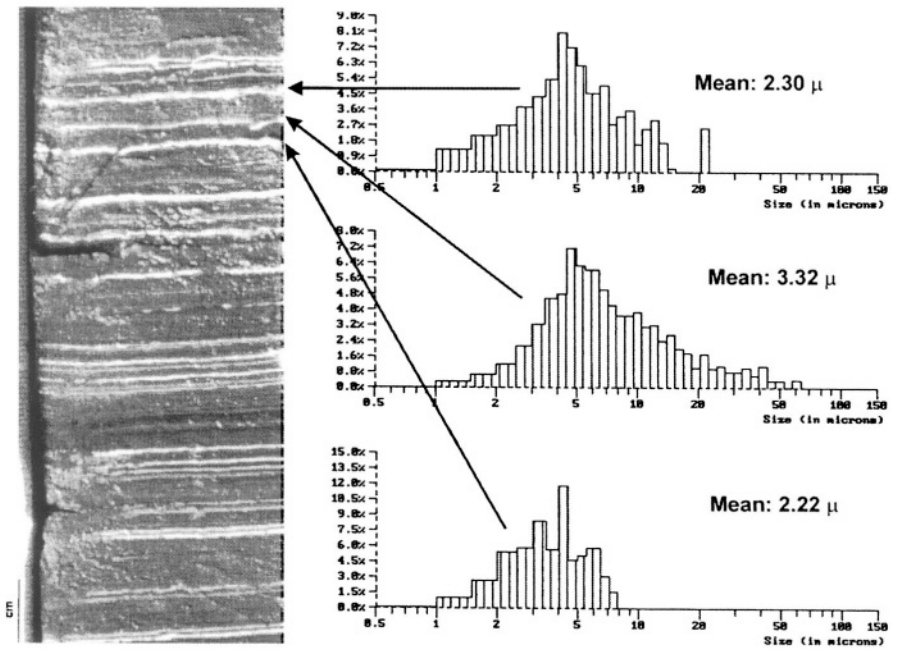


Figure 17. Examples of variations in mean aragonite crystal size in laminae from a Waldsea Lake core. Size spectra are shown as histograms of the relative abundance of the crystals in each size category. Note the logarithmic scale of the size axes (modified from Greengrass et al., 1999; Deleqiat et al., 1999).

A wide range of definitions of size have been proposed and the equipment designed to measure size records a similarly great diversity of size-related components. Traditional methods of particle size analysis, which tended to be time consuming, have been, over the past several decades, largely replaced by automated and electronic methods. Probably the most successful of these are the single particle counters, several of which also offer particle shape analysis systems. There has been a long history of debate and discussion about the interpretive use particle size distributions. Traditional graphic-based summary descriptive statistics have given way to more sophisticated methods but some contend that the errors inherent in the data collection do not warrant the higher level of refinement.

Acknowledgments

I gratefully acknowledge the financial support provided by the Natural Sciences and Engineering Research Council of Canada which allowed me to equip the Lake Sedimentology Laboratory at University of Manitoba. Enormous thanks go to Jenny Deliqiat, Pierre Francus, Bob Gilbert, Scott Lamoureux, John Smol, and Anke Tugulea for the many helpful and thoughtful comments and suggestions made on an earlier version of this chapter. Finally, special thanks to Professor Jim Teller, who introduced me to the importance of lake sediment textural analyses many years ago.

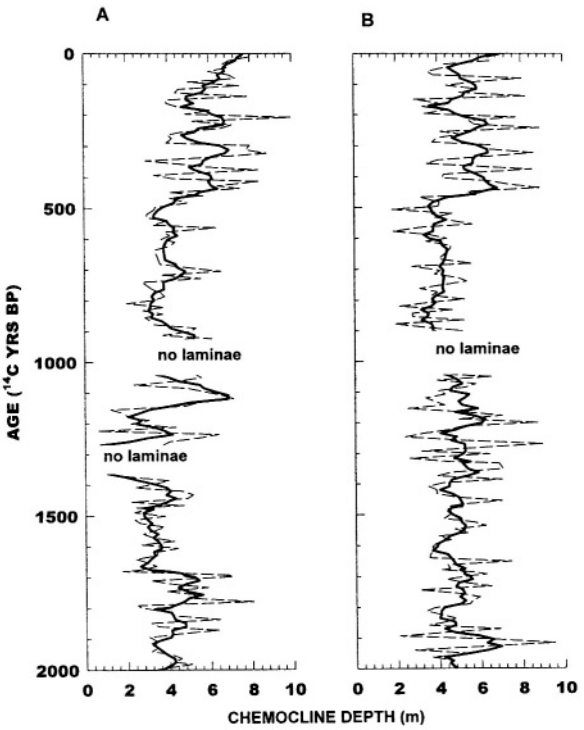


Figure 18. Stratigraphy variation in interpreted chemocline depth based on detailed aragonite crystal size spectra collected from laminae of two offshore cores from Waldsea Lake. The dark continuous line is a 3 sample running average (modified from Greengrass et al., 1999; Deleqiat et al., 1999).

References

Agricola, G., 1556. De re Metallica. Translated from the first Latin edition of 1556 by H. C. Hoover & L. H. Hoover in 1950. Dover Press, New York, 639 pp.

Agrawal,Y. C., I. N. McCave & J. B. Riley, 1991. Laser diffraction size analysis. In Syvitski, J. P. M. (ed.) Principles, Methods, and Application of Particle Size Analysis. Cambridge University Press, New York: 119–128.

Allen, T., 1981. Particle Size Measurement (3rd edition). Chapman and Hall, London, 678 pp.

Anadon, P., Ll. Cabrera & K. Kelts (eds.), 1991. Lacustrine Facies Analysis. International Association of Sedimentologists Special Publication No. 13, Blackwell Scientific Publications, Oxford, 318pp.

A.S.T.M. (American Society for Testing Materials), 1959. Symposium on Particle Size Measurement. Special Technical Publication 234, 303 pp.

Barber, T. A., 1996. Image analysis (automated microscopy) for particle size. In Knapp, J. Z., T. A. Barber & A. Lieberman (eds.) Liquid- and Surface-borne Particle Measurement Handbook. Marcel Dekker, Inc., New York: 61–112.

Barrett, P. J., 1980. The shape of rock particles, a critical review. Sedimentology 27: 291–303.

Berner, R. A., 1980. Early Diagenesis: A Theoretical Approach. Princeton University Press, Princeton, New Jersey, 241 pp.

Boggs, S., 1995. Principles of Sedimentology and Stratigraphy. Merrill Publishing Company, Toronto, 784 pp.

Boggs, S. 1992. Petrology of Sedimentary Rocks. Macmillan Publishing Company, New York, 707 pp.

Bohren, C. F. & D. R. Huffman, 1983. Absorption and Scattering of Light by Small Particles. Wiley Interscience, New York, 530 pp.

Bonham, L. C. & J. H. Spotts, 1971. Measurements of grain orientation. In Carver, R. E. (ed.) Procedures in Sedimentary Petrology. Wiley Interscience, New York: 285–312.

Boudreau, B. P., 1997. Diagenetic Models and Their Implementation. Springer, New York, 414 pp.

Blatt, H., 1992. Sedimentary Petrology (2nd edition). W. H. Freeman and Company, New York, 514 pp.

Blatt, H. 1982. Sedimentary Petrology. W. H. Freeman and Company, New York, 564 pp.

Blatt, H., G. Middleton & R. Murray, 1980. Origin of Sedimentary Rocks. Prentice-Hall, Inc., Englewood Cliffs, New Jersey, 781 pp.

Brownell, W. E., 1978. Clay. In Fairbridge, R. W. & J. Bourgeois (eds.) The Encyclopedia of Sedimentology. Dowden, Hutchinson & Ross, Inc., Stroudsburg, Penn.: 136–138.

Bull, P. A., 1986. Procedures in environmental reconstruction by SEM analysis. In Sieveking, G. de G. & M. B. Hart (eds.)The Scientific Study of Flint and Chert. Fourth International Flint Symposium, Brighton, UK. p. 221–226.

Cahill. R. A., 1981. Geochemistry of Recent Lake Michigan Sediments. Illinois State Geological Survey Circular 517, 94 pp.

Chayes, F., 1956. Petrographical Modal Analysis — an Elementary Statistical Approach. John Wiley and Sons, Inc., New York, 113 pp.

Clark. J. S. & T. C. Hussey, 1996. Estimating the mass flux of charcoal from sedimentary records: effects of particle size, morphology, and orientation. The Holocene 6: 129–144.

Coulter, W. H., 1956. High speed automatic blood cell counter and cell size analyser Proceeding. National Electronics Conference 12: 1034–1040.

Delly, J. G., 1996. Microscopy: the setup and operation of the polarized-light microscopy lab for particle identification. In Knapp, J. Z., T. A. Barber & A. Lieberman (eds.) Liquid- and Surface-Borne Particle Measurement Handbook. Marcel Dekker, Inc., New York: 29–59.

Deleqiat, J., W. M. Last, K. Greengrass & S. Sukhan, 1999. Waldsea Lake, Saskatchewan: the recent history of one of western Canada's best studied mermomictic lakes. Abstracts Volume, 2nd International Congress of Limnogeology. Brest, France: 14.

Dietrich, R. V., J. T. Dutro & R. M. Foose, 1982. AGI Data Sheets for Geology in the Field, Laboratory, and Office. American Geological Institute, Falls Church, Virginia.

Ehrlich, R., 1983. Editorial — Size analysis wears no clothes, or have moments come and gone? J. Sed. Petrol. 53: 1.

Fleischer, M., R. E. Wilcox & J. J. Matzko, 1984. Microscopic Determination of the Nonopaque Minerals. United States Geological Survey Bulletin 1627, Washington, 453 pp.

Folk, R. L., 1980. Petrology of Sedimentary Rocks. Hemphill Publishing Company, Austin, 182 pp.

Francus, P., 1998. An image-analysis technique to measure grain-size variation in thin section of soft clastic sediments. Sed. Geol. 121: 289–298.

Friedman, G. M., 1958. Determination of sieve-size distribution from thin-section data for sedimentary petrological studies. J. Geol. 66: 394–416.

Friedman, G. M. & K. G. Johnson, 1982. Exercises in Sedimentology. John Wiley & Sons, New York, 205 pp.

Friedman, G. M., J. E. Sanders & D. C. Kopaska-Merkel, 1992. Principles of Sedimentary Deposits. Macmillan Publishing Company, New York, 717 pp.

Galai Ltd., 1989. The PSA Operation Manual, 189 pp.

Gierlowski-Kordesch.E, & K. Kelts (eds.), 1994. Global Geological Record of Lake Basins Volume I. Cambridge University Press, Cambridge, UK, 427 pp.

Gilliot, J. E., 1969. Study of the fabric of fine-grained sediments with the scanning electron microscope. J. Sed. Petrol. 39: 90–105.

Gilliot, J. E., 1970. Fabric of Leda Clay investigated by optical, electron-optical and X-ray diffraction methods. Engin. Geol. 4: 133–153.

Gipson, M., 1965. Application of the electron microscope to the study of particle orientation and fissility in shale. J. Sed. Petrol. 35: 408–14.

Graham, J. & D. H. Shields, 1985. Influence of geology and geological processes on the geotechnical properties of a plastic clay. Engin. Geol. 22: 109–126.

Greengrass, K., W. M. Last, J. Deleqiat & S. Sukhan, 1999. Waldsea Lake revisited: another look at the recent history of one of Western Canada's best-studied meromictic lakes. In Koster, R. (ed.) Prairie Perspectives: Geographical Essays, Volume 2: 89–115.

Griffiths, J. C., 1967. Scientific Methods in Analysis of Sediments. McGraw-Hill, New York, 508 pp.

Håkanson, L., 1982. Bottom dynamics in lakes. In Sly. P. G. (ed.) Sediment/Freshwater Interaction, Junk. The Hague: 1–22.

Håkanson, L., 1981. Determination of characteristic values for physical and chemical lake sediment parameters. Water Resources Res. 17: 1625–1640.

Håkanson, L., 1977. The influence of wind, fetch and water depth on the distribution of sediments in Lake Vanern, Sweden. Can. J. Earth Sci. 14: 397-412.

Håkanson, L., 1974. A mathematical model for establishing numerical values of topographical roughness for lake bottoms. Geogr. Annaler 56A: 183–200.

Håkanson, L. & M. Jansson, 1983. Principles of Lake Sedimentology. Springer-Verlag, New York, 316 pp.

Hammer, U. T., 1986. Saline Lake Ecosystems of the World. Dr W. Junk Publishers, Dordrecht, 616 pp.

Hammer, U. T., 1978. The saline lakes of Saskatchewan, III. Chemical characterization. Intern. Rev. ges. Hydrobiol. 63: 311–335.

Hammer, U. T., R. C. Haynes, J. R. Lawrence & M. C. Swift, 1978. Meromixis in Waldsea Lake, Saskatchewan. Verh. Intern. Verein. Limnol. 20: 192–200.

Heling, D., 1970. Micro-fabrics of shales and their rearrangement by compaction. Sedimentology 15: 247–260.

Hendrix, W. P. & C. Orr, 1972. Automatic sedimentation size analysis instrument. In Groves, M. J. & J. L. Wyatt-Sargent (eds.) Particle Size Analysis 1970. Society for Analytical Chemistry, London: 133–146.

Hsü, K. J., 1978. Stratigraphy of the lacustrine sedimentation in the Black Sea. In Usher, J. L. & P. Supko (ed.) Initial Reports of the Deep Sea Drilling Project, XLII: 509–524.

Irani, R. R. & C. F. Callis, 1963. Particle Size: Measurement, Interpretation, and Application. John Wiley & Sons, New York, 163 pp.

Jelínek, Z. K., 1971. Particle Size Analysis. John Wiley & Sons, New York, 178 pp.

Jopling, A. V. & B. C. McDonald (eds.), 1975. Glaciofluvial and Glaciolacustrine Sedimentation. SEPM Special Publication No. 23, Tulsa, 320 pp.

Jones, K. P. N., I. N. McCave & P. D. Patel, 1988. A computer-interfaced SediGraph for model analysis of fine-grained sediment. Sedimentology 35: 163–172.

Keller, W. D., 1976. Scanning electron micrographs of kaolins collected from diverse environments of origin - I. Clays and Clay Minerals 24: 107–113.

Kennedy, S. K. & J. Mazzullo, 1991. Image analysis method of grain size measurement. In Syvitski, J. P. M. (ed.) Principles, Methods, and Application of Particle Size Analysis. Cambridge University Press, New York: 76–87.

Knapp, J. Z., T. A. Barber & A. Lieberman (eds.), 1996. Liquid- and Surface-borne Particle Measurement Handbook. Marcel Dekker. Inc., New York. 915 pp.

Krinsley, D. H. & P. Trusty, 1986. Sand grain surface textures. In Sieveking, G. de G. & M. B. Hart (eds.) The Scientific Study of Flint and Chert. Fourth International Flint Symposium, Brighton, UK. p. 201–207.

Krumbein, W. C., 1934. Size frequency distribution of sediments. J. Sed. Petrol. 4: 65–77.

Krumbein, W. C., 1941. Measurement and geological significance of shape and roundness of sedimentary particles. J. Sed. Petrol. 11: 64–72.

Krumbein, W. C. & F. J. Pettijohn, 1938. Manual of Sedimentary Petrography. Appleton- Century Company, Inc., Reprinted by Society of Economic Paleontologists and Mineralogists, Tulsa, 549 pp.

Krumbein, W. C. & L. L. Sloss, 1963. Stratigraphy and Sedimentation (2nd edition). W. H. Freeman and Company, San Francisco, 660 pp.

Last, W. M. & P. De Deckker, 1990. Modern and Holocene carbonate sedimentology of two saline volcanic maar lakes, southern Australia. Sedimentology 37: 967–981.

Last, W. M. & T. H. Schweyen, 1985. Late Holocene history of Waldsea Lake, Saskatchewan, Canada. Quat. Res. 24: 219–234.

Last, W. M. & L. A. Slezak, 1988. The salt lakes of western Canada: a paleolimnological overview. Hydrobiologial 58: 301–316.

Last, W. M. & L. A. Slezak, 1986. Paleohydrology, sedimentology, and geochemistry of two meromictic saline lakes in southern Saskatchewan. Geog. phys. Quat. XL: 5–15.

Lawrence, J. R., R. C. Haynes & U. T. Hammer, 1978. Contribution of photosynthetic bacteria to total primary production in a meromictic saline lake. Verh. Intern. Verein. Limnol. 20: 201–207.

Leeder, M. R., 1982. Sedimentology Process and Product. Allen & Unwin, London, 344 pp.

Lerman, A. 1979. Geochemical Processes: Water and Sediment Environments. Wiley Interscience, New York, 481 pp.

Lewis. D. W., 1984. Practical Sedimentology. Hutchinson Ross Publishing Company. New York, 227 pp.

Lewis, D. W. & D. M. McConchie, 1994a. Analytical Sedimentology. Chapman & Hall, New York, 197 pp.

Lewis, D. W. & D. M. McConchie, 1994b. Practical Sedimentology. Chapman & Hall, New York, 213 pp.

Lieberman, A., 1996. Particle characterization in liquids: background information. In Knapp, J. Z., T. A. Barber & A. Lieberman (eds.) Liquid- and Surface-Borne Particle Measurement Handbook. Marcel Dekker, Inc., New York: 1–28.

Lilje, A., 1991. The fractal A/P method; a new robust fractal method for characterizing grain shape with applications to clastic sediments of the San Jacinto Valley, California. Geol. Soc. Amer., Abstracts with Programs 23: 289,

Lindholm, R., 1987. A Practical Approach to Sedimentology. Allan and Unwin, Inc., Winchester, Mass., 276 pp.

Lines, R. W., 1996. The electrical sensing zone method (The Coulter Principle). In Knapp, J. Z., T. A. Barber & A. Lieberman (eds.) Liquid- and Surface-Borne Particle Measurement Handbook. Marcel Dekker, Inc., New York: 113–154.

Martini, I. P., 1978. Sedimentary fabric. In Fairbridge, R. W. & J. Bourgeois (eds.) The Encyclopedia of Sedimentology. Dowden, Hutchinson & Ross. Inc., Stroudsburg, Penn.: 320–322.

Matter, A. & M. E. Tucker (eds.), 1978. Modern and Ancient Lake Sediments. International Association of Sedimentologists Special Publication No. 2, Blackwell Scientific Publications, Oxford, 290 pp.

Matthews, M. D., 1991a. The effect of pretreatment on size analysis. In Syvitski, J. P. M. (ed.) Principles, Methods, and Application of Particle Size Analysis. Cambridge University Press, New York: 34–42.

Matthews, M. D., 1991b. The effect of grain shape and density on size measurement. In Syvitski, J. P. M. (ed.) Principles, Methods, and Application of Particle Size Analysis. Cambridge University Press, New York: 22–33.

McCave, I. N. & J. Jarvis, 1973. Use of the model T Coulter Counter in size analysis of fine to coarse sand. Sedimentology 20: 305–315.

McCave, I. N. & J.P. M. Syvitski, 1991. Principles and methods of geological particle size analysis. In Syvitski, J. P. M. (ed.) Principles, Methods, and Application of Particle Size Analysis. Cambridge University Press, New York: 3–21.

McCrone, W. C., L. B. McCrone & J. G. Delly, 1978. Polarized Light Microscopy. Ann Arbor Science, Ann Arbor, Michigan, 251 pp.

McManus, J. M., 1988. Grain size determination and interpretation. In Tucker, M. (ed.) Techniques in Sedimentology. Blackwell Scientific Publications, London: 63–85.

Milligan,T. G. & K. Kranck, 1991. Electroresistance particle size analysers. In Syvitski, J. P. M. (ed.) Principles, Methods, and Application of Particle Size Analysis. Cambridge University Press, New York: 109–118.

Milner, H. B., 1962. Sedimentary Petrography, Volume 1. MacMillan Company, New York, 643 pp.

Müller, G., 1967. Methods in Sedimentary Petrography. Hafner Publishing Company, New York, 281 pp.

Murphy, C. P., 1986. Thin Section Preparation of Soils and Sediment. AB Academic Press, Berkhamstead, U.K., 149 pp.

Murphy, C. P., P. Bullock & R. H. Turner, 1977. The measurement and characterisation of voids in soil thin sections by image analysis, I. Principles and techniques. J. Soil Science 28: 498–508.

Nelson, D. D. & W. E. Full, 1998. An improved program for the calculation of high-resolution Fourier coefficients used for shape analysis. Comp. & Geosci. 24: 237–242.

Nesse, W. D., 1991. Introduction to Optical Mineralogy (2nd edition), Oxford University Press, New York, 335 pp.

Nichols, G., 1999. Sedimentology and Stratigraphy. Blackwell Science, London, 355 pp.

O'Brien, N. R., 1970. The fabric of shale — an electron-microscope study. Sedimentology 15: 229–246.

Orford, J. D. & W. B. Whalley, 1991. Quantitative grain form analysis. In Syvitski, J. P. M. (ed.) Principles, Methods, and Application of Particle Size Analysis. Cambridge University Press, New York: 88–108.

Orford, J. D. & W. B. Whalley, 1987. The quantitative description of highly irregular sedimentary particles: the use of the fractal dimension. In Mashall, J. R. (ed.) Clastic Particles. Van Nostrand Reinhold, New York: 267–280.

Orford, J. D. & W. B. Whalley, 1983. The use of thefractal dimension to quantify the morphology of irregular-shaped particles. Sedimentology 30: 655–668.

Pandalai, H. S. & S. Basumallick, 1984. Packing in a clastic sediment: concepts and measurements. Sed. Geol. 39: 87-93.

Parker, R. D., J. R. Lawrence & U. T. Hammer, 1983. A comparison of phototropic bacteria in two adjacent saline meromictic lakes. Hydrobiologia 105: 53–62.

Persson, A.-L., 1998. Image analysis of shape and size of fine aggregates. Eng. Geol. 50: 177–186.

Pettijohn, F. J., 1975. Sedimentary Rocks (3rd edition). Harper & Row, New York, 628 pp.

Pettijohn, F. J., P. E. Potter & R. Siever, 1987. Sand and Sandstone (2nd edition). Springer-Verlag, New York, 553 pp.

Picard, M. D., 1971. Classification of fine-grained sedimentary rocks. J. Sed. Petrol. 41: 179-195.

Picard, M. D. & L. R. High, 1972. Criteria for recognizing lacustrine rocks. In Rigby, J. K. & W. K. Hamblin (eds.) Recognition of Ancient Sedimentary Environments. SEPM Special Publication No. 16, Tulsa: 108–145.

Pierce, J. W. & R. R. Graus, 1981. Use and misuses of the ϕ-scale: Discussion. J. Sed. Petrol. 51: 1348–1350.

Pike, J. & A. E. S. Kemp, 1996. Preparation and analysis techniques for studies of laminated sediments. In Kemp, A. E. S. (ed.) Palaeoclimatology and Palaeoceanography from Laminated Sediments. Geol. Soc. Spec. Paper No. 116: 37–8.

Potter, P. E., J. B. Maynard & W. A. Pryor, 1980. Sedimentology of Shale. Springer-Verlag, New York, 306 pp.

Potter, P. E. & F. J. Pettijohn, 1977. Paleocurrents and Basin Analysis (2nd edition). Springer-Verlag, New York. 425 pp.

Rahn, P. H., 1996. Engineering Geology: An Environmental Approach (2nd edition). Prentice Hall, New Jersey, 657 pp.

Reeves, C. C., 1968. Introduction to Paleolimnology. Elsevier Publishing Company, New York, 268 pp.

Rittenhouse, G., 1943. A visual method of estimating two-dimensional sphericity. J. Sed. Petrol. 13: 79–81.

Robinson, G. W., 1949. Soils, Their Origin, Constitution and Classification (3rd edition). Murby, London, 573 pp.

Russ, J. C., 1991. Computer-assisted Microscopy: The Measurement and Analysis of Images. Plenum Press, New York, 453 pp.

Sack, L. A. & W. M. Last, 1994. Lithostratigraphy and recent sedimentation history of Little Manitou Lake, Saskatchewan, Canada. J. Paleolim.10: 199–212.

Shepard, F. P., 1954. Nomenclature based on sand-silt-clay ratios. J. Sed. Petrol. 24: 151–158.

Schweyen, T. H., 1984. The Sedimentology and Paleohydrology of Waldsea Lake, Saskatchewan, an Ectogenic Meromictic Saline Lake. M.Sc. Thesis, Geological Sciences Department, Univ. Manitoba, Winnipeg, 192 pp.

Schweyen, T H. & W. M. Last, 1983. Sedimentology and Paleohydrology of Waldsea Lake, Saskatchewan. In Scott, M. D. (ed.) Third Biennial Plains Aquatic Research Conference Proceedings. Canadian Plains Research Center, Regina: 96–113.

Shideler, G. L., 1976. A comparison of electronic particle counting and pipette techniques in routine mud analysis. J. Sed. Petrol. 46: 1017–1025.

Singer, J. K., J. P. Anderson, M. T. Ledbetter, I. N. McCave, K. P. N. Jones & R. Wright, 1988. An assessment of analytical techniques for the analysis of fine-grained sediments. J. Sed. Petrol. 58: 534–543.

Sly, P. G., 1978. Sedimentary processes in lakes. In Lerman, A. (ed.) Lakes Chemistry Geology Physics, Springer-Verlag, New York: 65–89.

Sly, P. G., 1977. Sedimentary environments in the Great Lakes. In Golterman, H. L. (ed.) Interactions Between Sediments and Freshwater. Junk, The Hague: 76–82.

Smith, M. M., 1989. Shape of analysis of loose particles: from shape factor to fractals to fourier. In Petruk, W. (ed.) Mineralogical Association of Canada Short Course on Image Analysis Applied to Mineral and Earth Sciences 16: 106–118.

Sneed, E. D. & R. L. Folk, 1958. Pebbles in the lower Colorado River, Texas, a study in particle morphogenesis. J. Geol. 66: 114–150.

Solomon, M., 1963. Counting and sampling errors in modal analysis by point counting. J. Petrology 4: 367–382.

Solomon, M. & R. Green, 1963. A chart for designing model analysis by point counting. Geologische Rundschau 55: 844–848.

Stein, R., 1985. Rapid grain-size analyses of clay and silt fractions by Sedi-Graph 5000D: comparison with Coulter Counter and Atterberg methods. J. Sed. Petrol. 55: 590–593.

Stevens, R., 1983. A new sand-silt-clay triangle for textural nomenclature. Geologiska Foereningen i Stockholm Foerhandlingar 105: 245–250.

Stirling, J. A. R., 1989. Image analysis techniques applied to potash ores. In Petruk, W. (ed.) Mineralogical Association of Canada Short Course on Image Analysis Applied to Mineral and Earth Sciences 16: 141–150.

Stokes, G. G., 1851. On the effect of the internal friction of fluids on the motion of pendulums. Trans. Cambridge Phil. Soc. 9: 8–106.

Swan, D., J. J. Clague & J. L. Luternauer, 1978. Grain-size statistics I: evaluation of the Fold and Ward graphic measures. J. Sed. Petrol. 48: 863–878.

Swan, D., J. J. Clague & J. L. Luternauer, 1979. Grain-size statistics II: evaluation of grouped moment measures. J. Sed. Petrol. 49: 487–500.

Syvitski, J. P. M. (ed.), 1991. Principles, Methods, and Application of Particle Size Analysis. Cambridge University Press, New York, 367 pp.

Syvitski, J. P. M., K. W. G. LeBlanc & K. W. Asprey, 1991a. Interlaboratory, interinstrument calibration experiment. In Syvitski, J. P. M. (ed.) Principles, Methods, and Application of Particle Size Analysis. Cambridge University Press, New York: 174–193.

Syvitski, J. P. M., K. W. Asprey & D. A. Clattenburg, 1991b. Principles, design, and calibration of settling tubes. In Syvitski, J. P. M. (ed.) Principles, Methods, and Application of Particle Size Analysis. Cambridge University Press, New York: 45–63.

Talbot, M. R. & P. A. Allen, 1996. Lakes. In Reading, H. G. (ed.) Sedimentary Environments: Processes, Facies and Stratigraphy (3rd edition). Blackwell Science, London: 83–124.

Tanner, W. F., 1969. The particle size scale. J. Sed. Petrol. 39: 809–812.

Teller, J. T. & W. M. Last, 1990. Paleohydrological indicators in playas and salt lakes, with examples from Canada, Australia, and Africa. Palaeog. Palaeoclim. Palaeoecol. 76: 215–240.

Tianrui, S., 1991. Textural maturity of arenaceous rocks derived by microscopic grain size analysis in thin section. In Syvitski, J. P. M. (ed.) Principles, Methods, and Application of Particle Size Analysis. Cambridge University Press, New York: 163–173.

Thomas, M. C., R. J. Wiltshire & A. T. Williams, 1995. The use of Fourier descriptors in the classification of particle shape. Sedimentology 42: 635–645.

Thomas, R. L., A. L. W. Kemp & C. F. M. Lewis, 1972. Distribution, composition and characteristics of the surficial sediments of Lake Ontario. J. Sed. Petrol. 42: 66–84.

Thomas, R. L., J.-M. Jaquet, A. L. W. Kemp & C. F. M. Lewis, 1976. Surficial sediments in Lake Erie. J. Fish. Res. Bd. Can. 33: 385–403.

Trefethen, J. M., 1950. Classification of sediments. Amer. J. Sci. 248: 55–62.

Tucker, M. E., 1991. Sedimentary Petrology (2nd edition). Blackwell Scientific Publications, Oxford, 260 pp.

Udden, J. A., 1898. Mechanical Composition of Wind Deposits. Augustana Library Publication 1, 69 pp.

Udden, J. A., 1914. Mechanical composition of clastic sediments. Geol. Soc. Amer. Bull. 25: 655–744.

Wadell, H., 1932. Volume, shape and roundness of rock particles. J. Geol. 40: 443–51.

Washington, C., 1992. Particle Size Analysis in Pharmaceutics and Other Industries, Theory and Practice. Ellis Horwood, New York, 243 pp.

Wentworth, C. K., 1922. A scale of grade and class terms for clastic sediments. J. Geol. 30: 377–392.

Williams, H., F. J. Turner & G. M. Gilbert, 1982. Petrography: an Introduction to the Study of Rocks in Thin Sections (2nd edition). W. H Freeman and Company, New York, 626 pp.

Xu, R., 1996. Reference materials in particle measurements. In Knapp, J. Z., T. A. Barber & A. Lieberman (eds.) Liquid- and Surface-Borne Particle Measurement Handbook. Marcel Dekker, Inc., New York: 709–720.

Zingg, Th., 1935. Beiträge zur Schotteranalyse. Schweiz. Mineralog. Petrog. Mitt. 15: 39–140.

5. INORGANIC GEOCHEMICAL METHODS IN PALAEOLIMNOLOGY

J. F. BOYLE (Jfb@liv.ac.uk)
Department of Geography
University of Liverpool
PO Box 147
Liverpool L69 3BX
UK

Keywords: Lake, sediment, geochemistry, palaeolimnology. trace elements, environmental change, human impact

History & scope

Introduction

Inorganic geochemical analysis of sediment has played a central role in palaeolimnology since its establishment as a research field. This chapter outlines methods that can be applied, explores the issues affecting reliability of interpretations, and refers readers to the appropriate literature.

A distinction is made between inorganic geochemical palaeolimnology and inorganic geochemistry in general. While sharing many techniques and information sources, the two subjects differ fundamentally in purpose. Inorganic geochemistry aims to understand the chemical properties of the natural world, and the behaviour of chemical substances within it. Geochemical palaeolimnology uses such information to describe and quantify the environment. Furthermore, whereas palaeolimnological analysis is about lake, catchment or even landscape scale processes, geochemistry often considers minute scales. This contrast in scale has lead to conflicting interpretations. Geochemists working with laboratory experiments, and studying speciation and small-scale mobility, emphasize complexity. Palaeolimnologists, on the other hand, tend to look at large scale phenomena, and often find consistent patterns, even where a full geochemical understanding is lacking.

The two disciplines should not be seen as separate. Inorganic geochemistry feeds into geochemical palaeolimnology because it is important to have a good understanding of the behaviour of the elements being measured. Conversely, palaeolimnological data can help to constrain geochemical models. Nevertheless, the contrasts in purpose and scale must be kept firmly in mind.

A further distinction is made between organic and inorganic methods. For many inorganic elements, behaviour is highly dependent upon organic substances, and the two topics cannot be treated in isolation. Rather, inorganic methods must include a basic evaluation of organic components.



W. M. Last & J. P. Smol (eds.), 2001. *Tracking Environmental Change Using Lake Sediments. Volume 2: Physical and Geochemical Methods.* Kluwer Academic Publishers, Dordrecht, The Netherlands.

Scope of inorganic geochemical palaeolimnology

Inorganic geochemical palaeolimnology is constrained by the available analytical tools. Geochemists have sought to describe the elemental compositions of soils and sediment, and to understand the interactions between different parts of the environment. They have also sought to understand the transport mechanisms of elements through the atmosphere, living organisms, surface waters, soils, and sediment. In doing this they have devised analytical procedures to quantify elemental compositions, and have developed models to explain variation in the environment. Palaeolimnologists have used these methods, and the knowledge thus gained about environment-composition links, to infer environmental change from lake sediment chemical stratigraphy. However, many substances examined by geochemists leave no record in sediments. Furthermore, there is a difference in how the geochemical tools are applied. In palaeolimnological geochemistry, there is less emphasis on the molecular scale, and much more emphasis on macroscale patterns. While the inorganic geochemist isolates components in lake sediments, with the hope of constructing rigorous chemical models, the palaeolimnologist works at a larger scale, perhaps applying the geochemist's models, but basically using an inductive/deductive empirical methodology to link macroscale features of the sediment with gross environmental factors.

This empirical emphasis in palaeolimnology is unfortunate, but at present necessary. Natural materials, such as lake water and sediment, are chemically highly complex heterogeneous materials, in which most separate components are poorly characterized. Geochemists are making progress in studying the different components present, but we are a very long way from having comprehensive chemical models. In the mean time, the empirical approach can still be usefully applied to constraining present or past lake environments.

Some aspects of organic chemistry fall within the scope of inorganic geochemical palaeolimnology. A central aim of the discipline is characterization of particle types within the sediment. Many of these particles are partially or wholly organic in origin. A minimum quantitative description of these components is thus essential to inorganic analysis of sediments. Basic characterization of the organic matter, at least determination of total C, but preferably N and H as well, is a minimum requirement.

In summary, inorganic geochemical palaeolimnology can be defined as the application of mainly inorganic geochemical techniques (chiefly elemental determinations and models) to sediment core samples with a view to shedding light on past environments.

Historical development

Geochemical analysis in palaeolimnology can be traced back to Mackereth (1966) who attempted to construct an interpretational framework from observations on Holocene sediments in the English Lake District. Three particularly influential palaeolimnological principles (for freshwater, clastic-dominated lake systems) were established. First, stratigraphic changes in lake sediment composition could be most easily explained if they were viewed as a sequence of soils derived from the catchment. Second, sediment composition is largely governed by the catchment. Third, peaks in the mineral matter concentration in lake sediment correspond with erosion events. In addition, he showed how both the catchment and lake conditions influence the concentrations of Fe and Mn, and he established proto-

cols for distinguishing catchment effects from within-lake redox effects using Fe and Mn concentrations and ratios.

The work of Mackereth (1966) was based largely on total element concentrations, and was undertaken at a time when relatively little was known about the geochemistry of lake sediments. This situation changed in the two decades that followed, as more sophisticated methods were developed for extracting and analyzing elements in soils and sediments. At the same time, dating tools for recent sediments, based on radioisotope concentrations (particularly ^{137}Cs and ^{210}Pb) and exotic pollen from introduced weeds in North America, allowed sediment cores to be used in the study of recent human impact. During the 1970s, human impact histories were published from both Europe and North America (e.g., Shapiro et al., 1971; Digerfeldt, 1972, 1975; Likens & Davis, 1975; Renberg, 1976; Huttunen & Tolonen, 1977; Davis & Norton, 1978; Huttunen et al., 1978).

The work up to the 1980s is reviewed by Engstrom & Wright (1984) in what is probably the most influential text on chemical palaeolimnology. A number of the general principles laid down by Mackereth (1966) were supported, but others were rejected or modified. They concluded that:

- Mackereth's evidence for chemical weathering of soils was flawed.
- In oligotrophic systems the sediment reflects catchment as suggested by Mackereth; but in richer systems, sediments are strongly modified by the lake. Lake and catchment effects are superimposed in such lakes.
- Chemical stratigraphy is best interpreted alongside biological methods.

By the 1980s, much more was known about the many mineral and biological particles which make up lake sediments. Studies in the oceans had lead to greater appreciation of the role of early diagenesis in altering sediment composition. Yet, in spite of these advances, Engstrom & Wright (1984) argued that ignorance both about the nature of the particles and about their sources, prevented optimal interpretation of lake chemical stratigraphies. As a step towards solving these problems they championed chemical fractionation of sediments, separating a residual fraction from a more available element pool. They argued strongly that the use of total element concentrations had obscured interpretation of lake sediments.

The refinement of geochemical palaeolimnological methods described by Engstrom & Wright (1984) coincided with a growing awareness of anthropogenic trace element contamination in lake sediment (e.g., Thomas, 1972; Crecelius & Piper, 1973; Kemp & Thomas, 1976; Förstner, 1976; Bertine & Mendeck, 1978; Hamilton-Taylor, 1979; Rippey et al., 1982; Norton, 1986). The role of atmospheric pollution was recognized, and procedures were developed for distinguishing natural from anthropogenic sources of the elements (Hilton et al., 1985; Renberg, 1986; Norton & Kahl, 1987).

During the 1980s and 1990s this work continued, benefiting from a number of advances in geochemical understanding of lakes and catchments. Some particularly important topics include:

- Fe and Mn cycling in lakes (e.g., Davison, 1993; Nürnberg & Dillon, 1993; Bryant et al., 1997).

- Trace elements in sediments (e.g., Norton et al., 1992) and lake systems (e.g., Schindler, 1975; Imboden et al., 1980; Santschi, 1984; Diamond et al., 1990).

- Particles, surfaces, and trace elements (e.g., Tessier et al., 1996; Benoit & Rozan, 1999).

- The role of diffusion in transferring elements from lake to sediment (e.g., Carignan & Tessier, 1985; Diamond et al., 1990).

In addition, there is a better understanding of chemical fractionation methods (e.g., Mester et al., 1998; Sahuquillo et al., 1999).

At present, inorganic geochemical methods are best used as a supporting tool in general palaeolimnology, as was suggested by Engstrom & Wright (1984). However, there is no doubting the magnitude of the contribution of sediment geochemistry to multidisciplinary studies of lake history (e.g., Digerfeldt, 1975; Mathewes & D'Auria, 1982; Gaillard et al., 1991; Punning et al., 1997; Valero-Garcés et al., 1997). Together with diatom and pollen data, sediment chemical data provide a comprehensive picture of long-term environmental change, or of recent human impact. In the absence of biological methods, geochemical palaeolimnology is more speculative. However, it remains valuable because of its relatively low cost (e.g., Boyle, 2000). For preliminary data analysis, and for extrapolation from more comprehensively studied sites, it has a great deal to offer as an independent method.

Objectives of inorganic geochemical research

The principal objective of this branch of inorganic geochemistry is palaeoenvironmental reconstruction. To achieve this it is necessary to characterize both contemporary and past sediments, and to establish the link between sediment composition and environment. At the heart of this are characterization, classification and measurement of sediment chemical components.

Classification of sediment components

Sediments are mixtures; analysis of their component parts is essential to their geochemical interpretation. For example, the palaeolimnological significance Si depends upon whether it is in diatoms or clay minerals. Before such sediment components can be identified or measured, they must be classified.

The palaeolimnological research community has long used the terms 'authigenic' and 'allogenic' at the heart of sediment component classification. While this remains appropriate, there is a need for clarity in the way these terms are used. At present, the term 'authigenic' is used in three different ways. First, in the geological literature it is used of minerals formed within the sediment after burial (e.g., Jones & Bowser, 1978). Second, in most palaeolimnological literature it refers to a sediment component formed within the lake water or at the surface of the sediment (e.g., Engstrom & Wright, 1984), and is essentially synonymous with the term 'endogenic' (see Jones & Bowser, 1978). Under this definition, components formed within the sediment are termed 'diagenetic'. Third, some operational

classification schemes use 'authigenic' to refer to the readily extractable element fraction, thereby including any extractable allogenic contribution (see Engstrom & Wright, 1984).

Before considering which of these definitions is most appropriate, there are a number of more general problems with defining sediment compositional components which must be considered. At the heart of this is interference between three contrasting approaches to classification:

- Classification based on particle origin (genetic classification): *authigenic* (= endogenic, particles formed within the lake of inorganic and/or biological origin), *hydrogenic* (particles formed within the lake of inorganic origin), *biogenic* (= biophile, derived from biological sources), *allogenic* (particles derived outside the lake), *anthropogenic* (= technogenic, materials derived from human sources); *cosmogenic* (from space); *aeolian* (windblown allogenic particles), *minerogenic* (= lithogenic, terrigenous, derived from catchment mineral sources), *diagenetic* (supplied through post-burial modification of the sediment).

- Classification based on idealized compositional components in the sediment: *organic* (elements bound to organic matter); *sorbed* (elements sorbed to particle surfaces); Fe-Mn oxide (elements bound to or within oxides), *lattice* (= mineral-bound, elements contained within the structure of allogenic rock-forming mineral).

- Classification based on measurable fractions (operational classification). There are numerous schemes. A typical example might include: *acid extractable* (dilute acid reagent); *reducible* (reducing agent); *oxidizable* (oxidizing agent); *residual* (total digestion).

Each of these schemes has both merits and limitations. Problems arise where different schemes use similar or identical labels. As mentioned above, the label 'authigenic' is sometimes used for the acid-extractable fraction. The danger is that this brings with it concepts associated with its definition under the genetic classification scheme.

Genetic classification of some kind is essential; palaeolimnological interpretation depends upon subdivision of components by origin. However, such a scheme must be treated as strictly hypothetical for a number of reasons. First, even authigenic materials are of external origin; only the particle formation is authigenic (Engstrom & Wright, 1984). Second, many components will be from mixed sources; allogenic particles that capture metals from the water column are both allogenic and authigenic in origin (Engstrom & Wright, 1984).

Compositional classification avoids the difficulty of linking components to sources. As a compositional component, the Fe-Mn oxyhydroxide fraction is unambiguous even if its origin is uncertain (mixed allogenic, authigenic, and diagenetic), and we cannot, in practice, measure it with certainty. Nevertheless, this classification scheme is the one to keep most clearly in mind, as it can be used to infer origin, and can be deduced from data analysis and/or sequential extraction.

Operational classification (by extraction agent, or procedure) has the advantage of being unambiguous (though not necessarily repeatable unless very strict conditions are adhered to). However, numerous schemes exist leading to problems with comparability. There is also the problem of what to call the fractions, and how the fraction labels link with the genetic and composition classifications. The fractions are operationally defined and should

be named accordingly. Engstrom & Wright (1984) introduced an 'operational' definition of 'allogenic' (i.e., it 'consists entirely of mineral particles resulting from erosion of the catchment soils') allowing the term to be used for the residual fraction. Conflict between this definition and their more general definition of 'authigenic' (Engstrom & Wright, 1984) has led to considerable confusion in subsequent literature.

A number of genetic terms are widely used in the recent literature. These are generally well defined, and are useful where clearly distinguished from any operational definitions. Included are: *authigenic, diagenetic, allogenic, anthropogenic* and *minerogenic.* Some compositional terms are also widely used: *organic, aluminosilicate, oxide,* etc. Again, these are useful where distinguished from operational definitions. The real problem is what terms to use for the sequentially extracted fractions. The original labels of Tessier et al. (1979) are cumbersome (C1 to C5), which has encouraged substitution by genetic or composition labels.

Some conclusions can be drawn from this.

- The term 'authigenic' should be used as discussed by Engstrom & Wright (1984), having the same meaning as 'endogenic' (see Jones & Bowser, 1978).
- When using multifraction schemes, e.g., that of Tessier et al. (1979), the labels should refer to the extraction methods (e.g., mildly reducible).
- In simpler two stage schemes, such as that of Engstrom & Wright (1984), the terms 'extractable' or 'labile', and 'residual' are appropriate, and the terms 'authigenic' and 'allogenic' should not be used.

Measurement of components

Once a system for classifying sediment components has been devised, there remains the problem of identifying and quantifying these in the sediment. There are two approaches to this problem. First, selective chemical extractions can be used to measure the components directly (described above). This has the advantage of being direct, but there are problems with specificity of the extractions. Second, inter-element correlations can be used to 'unmix' the whole-sample compositions. This has the advantage of not altering the sample, but has the problem that correlated component cannot be unambiguously separated. Fortunately, there is little overlap between the various advantages and disadvantages of these two approaches, and they may therefore be used effectively in tandem. Current methods for both techniques are discussed below.

Component-environment links

Where did the sediment component come from? What mechanism transported the component? These are key questions in palaeolimnology. Passive tracing methods are widely used to provide answers. To achieve this the components must be quantitatively characterized in the sediment, and the composition of potential source materials must be known. For example, Punning et al. (1997) showed that a new minerogenic component had appeared in

the sediment, and that its composition resembled mining waste but not the other potential sources. Multivariate analysis of elemental variations makes identification of end-member compositions relatively simple. However, much more work needs to be done on characterization of potential source materials, and allowing for the effect of particle size fractionation in the catchment/lake system on changes in elemental concentrations (e.g., Moalla, 1997). Techniques in this area need development.

In addition to component identification, we need to know how lake and catchment environments influence the component concentrations. Many observations have been made over the last c. 40 years, and there is a steadily growing number of case studies which examine stratigraphic changes, and which attempt to explain these in terms of environmental change. These topics are described in detail in the section *Inorganic geochemical data in palaeolimnology*, including the impacts of acidification, eutrophication, water balance and human physical disturbance, etc. on lake sediments.

Elemental analysis

Most chemical analytical procedures applied in palaeolimnological inorganic geochemistry involve determining the total concentration of chemical elements. Even where speciation is involved, this does not usually conform to definite chemical species, and in essence involves determination of the concentration of chemical elements in a specified chemical extract. Basic approaches to elemental analysis are outlined in Figure 1. Procedures fall into two main categories. First, total elemental concentrations can be determined in the original solid material. Second, total elemental concentrations can be determined in extracted solutions. The relative merits of these depend both on the technique and the objectives. Directly analyzing the solid material means that total elemental concentrations are measured. This is not suitable if any kind of analytical partitioning is required. However, some methods for the analysis of solids are non-destructive, which may be an advantage where little sediment is available. It also minimizes sample handling, reducing the risk of contamination or handling error.

Analysis of derived solutions is more versatile, as total or partial determinations are both possible (Fig. 1). It is always destructive, but sample size is usually small so this need not be a problem. Generally, there is greater handling of the samples, which increases the risk of contamination or handling errors.

Many chemical extraction methods involve the use of reagents that are highly hazardous; particularly hydrofluoric and perchloric acids; great care must be taken in using them. Authoritative advice (conforming with national legislation) must be sought on risk assessment, appropriate fume cupboards, protective clothing, safe working practices, and emergency procedures.

Analysis of solid material

Methods for analysis of the solid material can be classified in a number of ways, depending upon the physical basis and sample size. One class of techniques is based on nuclear processes, stimulated by neutron irradiation. However, most techniques are based on inner electron shell atomic properties, centred on x-ray fluorescence stimulated by irradiation

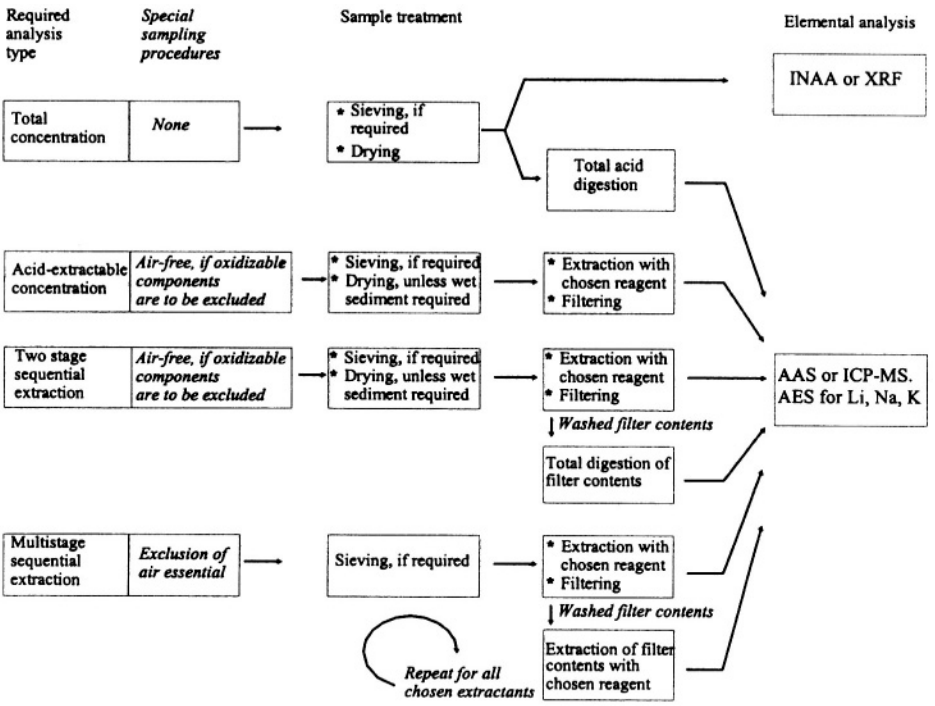


Figure 1. Comparison of procedures for the elemental analysis of sediment. See text for discussion.

of the sample by primary x-rays or electrons. X-ray methods are further subdivided by detector type, e.g., wavelength dispersive or energy dispersive, and sample size e.g., x-ray fluorescence spectrometry (XRF) on powder, and microprobe or EDS (electron microscopy with energy dispersive analysis capability) on individual crystals or particles.

Instrumental neutron activation analysis (INAA)

The are a number of different procedures, the most popular of which is termed the K_0 method (e.g., Negi et al. 1997). Small samples of sediment (c. 0.15 g) are irradiated by neutrons from a nuclear reactor for a few tens of hours. This activates the nuclei of atoms in the sample, leading to gamma emission which can be measured using a Ge detector. The method can measure a wide range of elements simultaneously, with excellent sensitivity and detection limits for some elements (e.g., Smodiš et al., 1993; Negi et al., 1997).

X-ray fluorescence spectrometry (XRF)

The basis of any XRF technique is the photoelectric fluorescence of characteristic secondary x-rays from a sample. These are stimulated by irradiation with suitable primary photons. In isotope source systems, primary photons are provided by radioisotopes that emit photons in the x-ray energy band. In tube source instruments, x-rays are generated by accelerating electrons onto a suitable target in the tube. In both cases, energies of the secondary x-rays

generated within the sample are characteristic tor the elements present, and the rate of emission is largely a function of the concentration of the element and absorption of the outgoing x-rays by the sample. Instruments are calibrated using known reference materials (e.g., Boyle, 2000).

A further distinction in XRF instruments is the method of x-ray detection. Wavelength dispersive instruments (XRF-WD) are more precise, but more time consuming. Energy-dispersive instruments (XRF-ED) are more rapid, but less precise and with poorer detection limits. An isotope-source energy-dispersive system can process 70 samples per day for 14 elements (Boyle, 2000).

For most elements, XRF has far poorer detection limits than the solution techniques described below. However, for many elements of interest this is not important, as observed concentrations are far above the detection limit. In such cases the minimal handling, and excellent precision of XRF make it highly suitable for the analysis of sediments.

Energy dispersive x-ray spectroscopy (EDS) and Microprobe

Both of these methods share similarities with XRF in that they stimulate and measure x-rays. They can be energy-dispersive or wave-length dispersive (microprobe only). They differ from XRF in two main respects. First, they stimulate x-rays using an electron beam. Second, the beam is narrow, so individual minerals can be determined. Application in palaeolimnology is relatively restricted. EDS has been used for automatic characterization of spheroidal carbonaceous particles (Watt, 1998), which could equally well be applied to minerals in sediments. Microprobe can also be used to characterize fine-grained sediments by measuring localized whole-sample composition (by defocusing the electron beam) at random locations. The observed variation in element concentrations can be unmixed using numerical methods (Boyle, 1984). A microprobe can also be used to measure total element concentrations in small samples by preparation of small beads by fusion (comparable to the laser ICP-MS technique of Fedorowich et al., 1993).

Carbon

In palaeolimnological studies carbon has been divided into two fractions: organic carbon, which is the residual remains of plant and animal tissues; and inorganic carbon, mainly calcium carbonate (e.g., Dean, 1981). Both these fractions can be measured accurately, under favourable circumstances, by determining the weight loss on heating (Dean, 1974).

Dry samples thoroughly at 105 °C, cool and weigh (W_{105}). Heat for 4 hours at 550 °C, cool and reweigh (W_{550}). Heat again for 2 hours at 1000 °C, cool and reweigh (W_{1000}).

Weight percent organic matter = $100\ (W_{105} - W_{550})/W_{105}$

Weight percent carbonate = $100\ (W_{550} - W_{1000})/W_{105}$

The accuracy of the loss-on-ignition (LOI) method depends on both the organic matter concentration and the nature of the sediment. The main problem is that most minerals contain structurally bound water that is released progressively on heating. Some clay minerals contain ten weight percent structural water; thus an LOI of 10% need not indicate that organic matter is present. Mackereth (1966) discusses this problem, and shows that there is significant discrepancy between measured carbon and LOI if the LOI is less than c. 10% (Fig. 2). The problem can be minimized by not igniting above 375 °C for organic matter (Ball, 1964). However, not all organic carbon will be ignited at this temperature, and a compromise must be identified, based on the abundance of organic matter and the

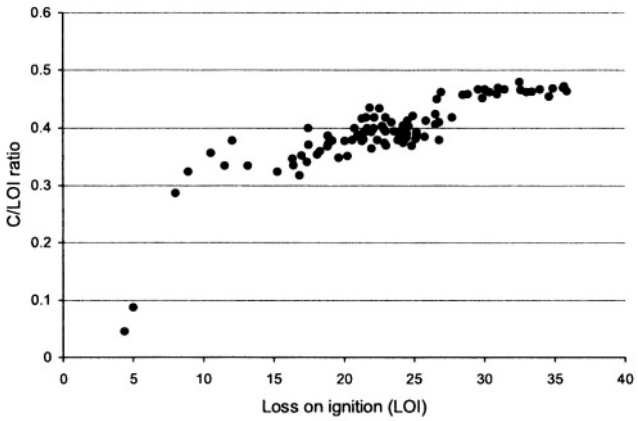


Figure 2. At values below 10%, LOI can seriously underestimate organic carbon. Graph re-drawn from Mackereth (1966).

questions being addressed. Generally, where LOI is low, the relationship of LOI to C should be evaluated by direct C determination, and a correction applied if necessary.

There are two classes of method for C determination. If only occasional measurements are required, then wet oxidation and titration are suitable (e.g., Tinsley, 1950). If large numbers of samples are to be determined, an instrumental carbon analyzer is preferred. This has the added advantage that with many instruments S, N and H can be analyzed at the same time. However, the technique has high consumable costs and is not likely to replace LOI as a routine method for organic matter determination in palaeolimnology.

Analysis of solutions

Atomic emission spectrometry (AES)

Thermal excitation of atoms results in emission of narrow radiation lines of characteristic wavelength within the visible spectrum. With an appropriate experimental setup, line intensity is proportional to element concentration, an effect that has been employed by chemical analysts since the middle of the 19th century. The analytical value of the technique is severely limited due to the large number of lines emitted by each element, and the consequent spectral interferences. This is not a problem for the alkalis, and AES, usually by propane flame photometers, is better than AAS for the measurement Na, K and Li.

A more recent addition to the AES family uses high temperature plasma to promote emission. Inductively coupled plasma atomic absorption spectrometry (ICP-AES) has the advantage that a wide range of elements may be measured simultaneously. However, great problems with spectral interferences restrict the value of this technique for complex mixture such as sediments.

Atomic absorption spectrometry (AAS)

Atomic absorption analysis is based on the absorption by free atoms of light at a specific wavelength. Near-monochromatic light of the appropriate wavelength is usually provided by a hollow cathode lamp. Absorption is generally free from spectral interferences, and is linearly related to concentrations over a wide concentration range. There are non-specific background effects varying with the matrix, so background correction is essential in trace element analysis, particularly for electrothermal methods. This is simply achieved using a deuterium lamp.

AAS is split into two types according to the method by which the sample is atomized. In flame atomic absorption spectrometry (FAAS) the sample is aspirated into a flame which is placed in the path of the light. In electrothermal atomic absorption (EAAS) the sample is placed in a graphite tube and heated in a brief pulse by passing an electric current through the tube. Generally, EAAS is more sensitive, giving better detection limits, but suffers from more matrix interference effects than FAAS.

Recent improvements in FAAS include the addition of a flow injection sample delivery system. This allows for automatic dilution and reagent addition, and also provides for automated cold vapour or hydride generation needed for As, Se and Hg (e.g., Saraswati et al., 1995). Other new techniques are improving the sensitivity of FAAS. A slotted silica tube placed in the flame improves the sensitivity 8 fold for Cd and c. 3 fold for Cu, Pb, and Zn. Experimental application of graphite tubes in the flame can improve Pb sensitivity 50 fold (Alvarado & Jaffé, 1998).

Cost, simplicity, and sensitivity make FAAS an ideal instrument for measuring a wide range of elements appropriate to palaeolimnological inorganic geochemistry.

Inductively coupled plasma mass spectrometry (ICP-MS)

ICP-MS uses a high-temperature plasma to atomize samples for mass spectrometric analysis. In contrast with ICP-AES, the method is highly selective and has excellent detection limits (e.g., Catterick et al., 1995). For most elements, ICP-MS is the method giving best accuracy and detection limits. The disadvantages are its high cost compared with FAAS, and greater sample handling when compared with XRF.

Colorimetric methods

Colorimetric methods, whereby chemical species are determined by their ability to alter the colour intensity of a dye, have limited application in palaeolimnology, because there are more suitable alternative methods for most elements. However, colorimetry remains the method of choice for P (e.g., APHA, 1980). A flow injection method can be used to automate the analysis (e.g., Mas et al., 1990). If the total P concentration of a sample is required, wavelength dispersive XRF is a good alternative.

Summary of methods: comparison of detection limits

The figures in Table I are based on the assumption of good practice with respect to clean water, glassware and laboratory working practices. The detection limits in solid material for the solution techniques are based on 0.5 g samples diluted to 25 ml. For the last three columns, the data are two standard deviations for fitted values through reference materials. They are essentially measures of precision.

Table I. Guide to approximate detection limits. Blank cell: absence of data. A dash indicates that the method is poor for typical concentrations. All concentrations are in μg/g. For solution methods, the detection limit in solid form is based on 0.5 g solid in 25 ml solution

Element	FAAS[1]	EAAS[1]	ICP-AES[1]	ICP-MS[1]	XRF ED[2]	XRF WD[3]	INAA[4]
Al	1.5	0.002	0.2	0.005	-	500	
Sb	1.5 (0.005)	0.01	3	0.001	-		0.1
As	5 (0.001)	0.01	1	0.0025	-		2.2
Ba	0.4	0.005	0.005	0.001	-	11	32
B	35	1	0.1	0.005	-		
Cd	0.025	0.00015	0.05	0.001	-		40
Ca	0.05	0.0025	0.004	0.25	1200	300	
Cl				0.5	1300		
Cr	0.1	0.0005	0.1	0.001		6	8
Co	0.3	0.0005	0.1	0.001	-		2
Cu	0.05	0.001	0.045	0.0015	-	1	2000
Eu	1			0.001	-		0.2
Ga	2.5	0.005	0.5	0.004	-		12
Fe	0.15	0.001	0.05	0.05	600	300	2400
La	100		0.05	0.005	-	2	4
Pb	0.5	0.0025	1	0.001	27	3	
Li	0.025	0.0025	0.045	0.005	-		
Mg	0.005	0.0002	0.004	0.005	-	300	
Mn	0.05	0.0005	0.02	0.002	700	70	
Hg	10(0.0004)	0.05	1	0.0015	-		0.2
Mo	1.5	0.002	0.25	0.004	-		6
Nd	50			0.001	-	1	6
Ni	0.2	0.005	0.2	0.0015	25	1	
Nb	50		0.15	0.001	4	1	
P	2500	1.5	1.5	1	-	30	
K	0.1	0.001	2.5	0.5	1700	50	3000
Rb	0.1	0.0025		0.001	9	1	7
Sc	1		0.01	0.004	-	1	0.6
Se	3.5 (0.001)	0.01	3	0.025	-		
Si	3	0.02	0.15	0.5	6000	900	
Ag	0.045	0.00025	0.05	0.002	-		0.5
Na	0.01	0.0025	0.2	0.003	-	400	
Sr	0.1	0.001	0.0025	0.001	24	8	60
S			2.5	25	1200		
Sn	5	0.01	2	0.0015	-		30
Ti	2.5	0.05	0.025	0.003	220	60	
V	2	0.01	0.1	0.0015	-	7	
Y	2.5		0.01	0.001	-	1	
Zn	0.04	0.0005	0.05	0.004	30	2	2
Zr	15		0.04	0.0015	28	2	60

[1] Data from Perkin Elmer, Guide to Techniques and applications of atomic spectroscopy, (1988)
[2] Boyle (2000)
[3] Fitton et al. (1984)
[4] Smodiš et al. (1993).

Note that Cr is particularly problematic with AAS and ICP-AES methods due to matrix enhancement effects (Liu et al., 1996).

Extraction methods

Total digestion

Total digestion of mineral-bearing material can be achieved by fusion or acid attack using hydrofluoric acid (HF). Fusion methods are rarely used today. A recent review by Kowalewska et al. (1998) found no advantage of fusion over acid digestion. The preferred method is total digestion by a mixture of hydrofluoric and perchloric acids. There are two main approaches. Allen et al. (1974) uses perchloric acid in open vessels to fume off the hydrofluoric acid and silica. This has the advantage of improving analytical accuracy by eliminating Si interferences. It has the disadvantage of preventing Si determination. The alternative method (e.g., Buckley & Cranston, 1971; Kowalewska et al. 1998) is to use a sealed PTFE (polytetrafluoroethylene) bomb, which retains the silica. The free hydrofluoric acid is made safe by adding boric acid.

Partial and sequential extraction

Sediment can be separated simply into two fractions (easily extractable and the rest), or in a more complex way where progressively more aggressive chemical attacks are applied in succession. Issues relating to this are discussed at length below.

Partial extraction techniques aim to bring 'readily available' ions into solution, while leaving behind those that are inert with respect to the lake system (i.e., lattice bound elements). The problem is to find a reagent which will efficiently extract the available ions, while not significantly attacking the aluminosilicate minerals. A good review is offered by Malo (1977), who recommended using 0.3 M HCl. Engstrom & Wright (1984) basically support this, but add an oxidizing step (using H_2O_2). This is then not very different from other oxidizing acid attacks, such as aqua regia (e.g., Hornburg & Luer, 1999) or nitric acid.

Sequential analysis aims to distinguish a greater number of fractions. The validity of this approach is discussed below. The most widely used method for lake sediment is that of Tessier et al. (1979). This defines five classes of element associations, but can only be applied if suitable precautions are taken with the samples, such as sampling and storing under nitrogen. An alternative approach is that of the European Community Bureau of Reference (BCR). This has the advantage that it has been critically tested against a standard reference material (Quevauviller et al., 1997; Mester et al., 1998).

Some elements may require special extraction procedures, e.g., **Phosphorus** (Pardo et al., 1999); **Sulphur** (Fiedler et al., 1999); **Arsenic** (Yehl & Tyson, 1997); **Silica** (Ragueneau & Treguer, 1994); **Mercury** (Quevauviller et al., 1996).

Sampling

Lake sediments are commonly highly heterogeneous, showing strong lateral and stratigraphic variation. These variations are typically far greater than analytical uncertainty, and lateral variation may be as great as stratigraphic variations. If it is intended that surface sample concentrations should represent averages for the lake, or that cores should

represent the average profile, then great care must be taken in sampling. The problem of sampling surface sediments, and a protocol for determining average values, is discussed by Baudo (1989) for Lake Orta in Italy. The number of cores and choice of sites required for determining an average profile is discussed by Rowan et al. (1995a; 1995b). They suggest that 5–10 cores are needed to give a good indication of the mean profile. Engstrom & Swain (1986) clearly illustrate the value of multiple core studies within a single basin, as this allows far better discrimination between the possible causal factors.

An additional, and frequently disregarded, problem is the role of particle size. Stratigraphic variation in sediment particle size will cause corresponding variations in elemental concentrations. It may be desirable to size fractionate sediment samples by sieving or settling prior to elemental analysis.

Quality control and reference materials

Accurate and precise elemental determinations are essential and relatively easily achieved. A number of steps can be taken to avoid problems, detect contamination and verify accuracy.

Reagents, laboratory, and equipment

Issues of cleanliness in the laboratory are discussed by APHA (1980). The essentials are: **Water**: double distilled, deionized water, with regular quality control. All reagents should be prepared using this water. **Laboratory**: for major elements a regularly cleaned laboratory is sufficient. For most trace elements it is essential that the laboratory is dust-free. **Equipment**: the most important factor is proper cleaning of all items which come in contact with extractant solutions. All beakers, in addition to standard cleaning, should be acid-washed in concentrated HCl, and rinsed thoroughly in double distilled water.

Blanks and quality control samples

The use of reagent blanks, prepared at the same time as the samples using identical procedures and the same quantity of reagents, is an essential step in evaluating contamination (APHA, 1980). At least 5% of the sample number, or a minimum of six blanks, should be prepared. High, but constant, blank values point to contaminated reagents. Subtraction of the mean blank value from the solution concentrations for the samples is the remedy if the contamination is minor. If blanks are high with respect to the measured values, ways to reduce the blank values must be found. Erratic high blanks point to contamination either by dust or dirty glassware. This can be serious if it is significant. Running a number of suitable blanks allows such effects to be identified. Analysis of 5% or more of the samples as duplicates serves to evaluate overall precision.

Reference materials

With the relative analysis techniques described above, accuracy is best evaluated by reference to external standards. Inter-laboratory comparisons have a role to play in multi-laboratory projects, but the basic tool is the certified reference material. These are natural materials which have been homogenized and analyzed by a range of laboratories, and have agreed, or 'certified', concentrations for some of the elements they contain.

Most reference materials have been certified for total concentrations only. They can, however, still be used for partial extractions, as they provide constraints on concentrations,

Table II. Some standard reference materials appropriate for lake sediment studies.

Name	Source	Type
CRM277	BCR	Estuarine sediment
CRM280	BCR	Lake sediment
CRM320	BCR	River sediment
CRM601	BCR	Lake sediment
CRM 2	NIES	Pond sediment
GBW7309	MC	Stream sediment
GBW7602	MC	Bush branch & leaves
GBW7603	MC	Bush branch & leaves
GBW7604	MC	Poplar leaves
GBW7605	MC	Tea
NBS-1B	NBS	Argillaceous limestone
NBS-88a	NBS	Magnesian limestone
SRM1632b	NIST	Trace elements in coal
SRM1646a	NIST	Estuarine sediment
SRM2704	NIST	Buffalo River Sediment
SRM2709	NIST	San Joaquin Soil
SRM2710	NIST	Silver Bow Creek Soil

BCR Community Bureau of Reference, Commission of the European Communities.
MC National Research Centre for Certified Reference Materials, China.
NBS National Bureau of Standards
NIES National Institute for Environmental Studies, Environment Agency of Japan.
NIST National Institute of Standards and Technology, United States Department of Commerce

and some published data exist, providing a guide to expected results (e.g., Hall et al. 1996). Furthermore, a laboratory can ensure internal consistency by monitoring results through time. More recently, there has been an attempt to develop reference materials with certified values for extractable ions. The best studied of these at present is a lake sediment from Italy, CRM601 (From Lake Flumendosa, Quevauviller et al. 1997; López-Sánchez et al., 1998).

In every batch of determinations, a range of appropriate reference materials should be included. There are a number of considerations affecting the choice of reference materials.

- Ideally, the range of concentrations should bracket those of the study. It is as important to have low concentration materials as to have high concentration materials.
- Ideally, the matrices should be similar.

In studies where successive batches are analyzed, it is particularly important that a suitable set of reference materials is analyzed in each batch. An internal reference material (or set of materials) can be useful; these can be ideally matched for concentration range and matrix. Issues relating to the preparation and validation of reference materials are discussed by Quevauviller (1998). Table II shows a range of suitable international reference materials. Note that there are no standard reference materials for peat. For highly organic sediments or peats, plant tissue materials are a reasonable alternative.

Identifying, characterizing, and quantifying sediment components

Characterization of sediment components can be achieved directly using sequential chemical extractions. The advantages and limitations of this approach are discussed in the section, *Partial chemical extractions and sediment sourcing.* In this section, numerical approaches to determining the sediment components are addressed.

Graphing, correlation, and regression

Graphical representation of inter-element relationships is the most basic method in the discipline, and is valuable even where more sophisticated numerical methods are employed. There are numerous examples in the literature, from the earliest studies (Mackereth, 1966) through to the present (e.g., Boyle & Birks, 1999). Graphical methods serve to evaluate the strength of a relationship robustly regardless of distribution and linearity, in a way that no numerical method can. Indeed, while correlation coefficients are valuable, they should not be used without supporting graphical analysis. This is not to underestimate the usefulness of the R value. Where graphical analysis shows that linear regression is a reasonable model, R^2 values are a very useful way of quantifying inter-element associations (e.g., Boyle et al., 1998). Where R^2 values are very high, regression is a useful tool for determining element ratios in components of the sediment. This is particularly effective where elements are distributed between only a few sediment components. For example, Hilton et al. (1985) use regression analysis to apportion the trace elements to a constant background parameter and to the mineral fraction, and Ochsenbein et al. (1983) use regression analysis to determine the association of Mg with chlorite in Blelham Tarn. Figure 3 illustrates the use of regression to find the relationship between Zn and residual Fe, a tracer for natural supply, in Antonelli Pond, California.

Simple bivariate scatter plots have the disadvantage that dilution distorts the relationship. Triangular diagrams have the advantage of eliminating dilution effects, and of increasing the number of elements represented. This approach is particularly useful for highlighting compositional differences (e.g., Englund & Jørgensen, 1973).

Matrix methods and unmixing

The process of determining the end-members that make up a mixture can be referred to as unmixing. Simple approaches to unmixing often use ratios to an index element. For example, Norton & Kahl (1987) use element: Ti ratios to quantifying trace element baselines, and ten Hulscher et al. (1992) use Sc as a sediment source tracer. However, if there is prior knowledge of end-member compositions, then their contributions to the mixture can be found by least-squares approximation (e.g., Bryan et al., 1969). Such end-members can be selected in many ways. The method of Miesch (1981), discussed below (*Positive subspace and unmixing*), offers a method based on observed data structure. Alternatively, extreme compositions may be used, or expected end-members such as mineral compositions (A good basic source reference for mineral chemical compositions is Deer et al. 1966). The method is easily coded on a computer; code and discussion are offered by Davis (1986).

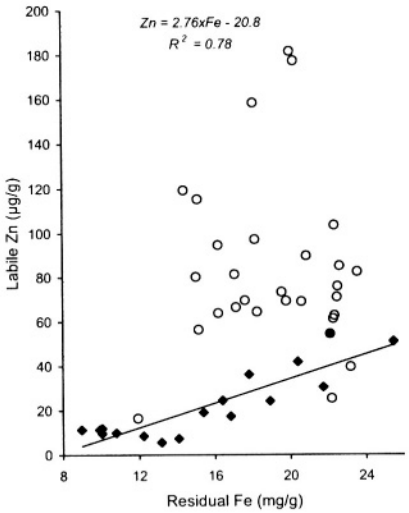


Figure 3. Regression is used to quantify the relationship between acid-extractable Zn and residual Fe in Antonelli Pond, California, using the method of Hilton et al. (1985). Unpublished data.

A different approach to unmixing involves the use of multivariate discriminant functions. Collins et al. (1996, 1997) successfully apply this technique to sediment source discrimination in suspended river particulates and river over-bank deposits.

PCA and related methods

Description and pitfalls

Principal components analysis (PCA), and other techniques based on eigen analysis (factor analysis), have been widely applied to geological data since the 1970s. An excellent general introduction and FORTRAN computer code are given by Davis (1986). The methods can also be performed using many modern data analysis software packages. The following brief description of eigen analysis introduces aspects relevant to unmixing of multivariate data sets.

For any data set comprising objects (e.g., sediment samples) on which a number of variables have been measured (e.g., element concentrations), an abstract composition space can be defined in which the variables are the dimensions. Within this space, the position of a sediment sample is determined by its elemental concentrations. Dissimilarity between sediment samples is measured by the Euclidean distances between them in the composition space. If all of the elements varied in concentration independently (i.e., they were uncorrelated), then the concentrations of all elements would be needed to describe the positions and inter-relationships of the samples. However, in all real sediment data sets, the element concentrations are partially interrelated; sediment samples can be seen as mixtures of a small number of independent multi-element sediment components. In such a case, the composition space can be accurately represented by fewer axes (dimensions). The

number of axes is equal to one less than the number of independent sediment components. Thus, if the mixture contained only two minerals, then variation across the samples can be represented by only one axis, the opposite ends of which represent the two minerals. More commonly there 3–4 significant axes, but that is a lot better than the sometimes tens of original variables. Eigen analysis is simply a mathematical procedure for identifying these combination axes.

There are several key issues in the application of these techniques.

- Euclidean distance is not the only possible measure of dissimilarity. It is, however, ideal for dealing with mixtures.

- Data transformation and re-scaling may be appropriate. As with all methods based on Euclidean distances, outlying objects have a disproportionately great influence on the outcome. Data cleaning or transformation is necessary to deal with this. Furthermore, in the most basic form of PCA (in which a simple cross product matrix is used), high magnitude variables have more influence than low. This can be overcome by scaling. The most common practice is to standardize the variables.

- Should factors be defined? In its most basic form, PCA provides a relatively objective assessment of the relationships between both the samples and variables (it is not, however, without subjectivity, as decisions have to be made about inclusion of variables, and about transformation and scaling). In factor analysis, there is further erosion of the objectivity. Instead of simply displaying the patterns, factor analysis attempts to determine the number of independent components (or factors) which underlie the data set, and to find their composition. While there are procedures to help choose the appropriate number (e.g., Hsu et al., 1986), in practice the approach tends to be rather arbitrary (see Dean et al., 1988; 1993). Nevertheless, in its Q-mode form, factor analysis has been widely applied to unmixing problems.

- Correlated components. The method can only work perfectly if all of the contributing sediment sources are uncorrelated. If they are correlated, then even if they are functionally independent, no amount of rigid rotation of the axes can fully separate them.

Q-mode factor analysis

The various factor analysis methods which became widely available during the 1970s are ideally suited to the examination of conservative mixing (Klovan & Imbrie, 1971). They can be used to simultaneously classify sites and identify independently varying compositional components. Dean et al. (1988; 1993) apply Q-mode factor analysis to total elemental analyses of lake surface sediments, with a view to regional classification and sediment source characterization. The approach uses a varimax rotation. This is a numerical procedure that rigidly rotates the selected axes to maximize or minimize the variable scores on each axis. This helps in the interpretation of the factors as real end-members.

Such techniques have the distinct advantage that once the elements are selected, the method is not subject to user-bias, beyond the choice of the number of factors to be included in the varimax rotation. The resulting factors are truly independent of each other, and faithfully reflect the composition of the original data set, within certain transparent

limits. However, there are problems. Once the analysis is complete, the normal practice is to interpret the factors by identifying them with known actual processes or sediment components on the basis of the element loadings. This process is subjective, reducing any advantage of factor analysis over more basic PCA methods.

In conclusion, the appeal of 'objective' factors is great. However, except in simple cases, there is little advantage in this approach compared with using PCA biplots to examine multivariate relations and possible end-members (see Birks, 1987).

Positive subspace and unmixing

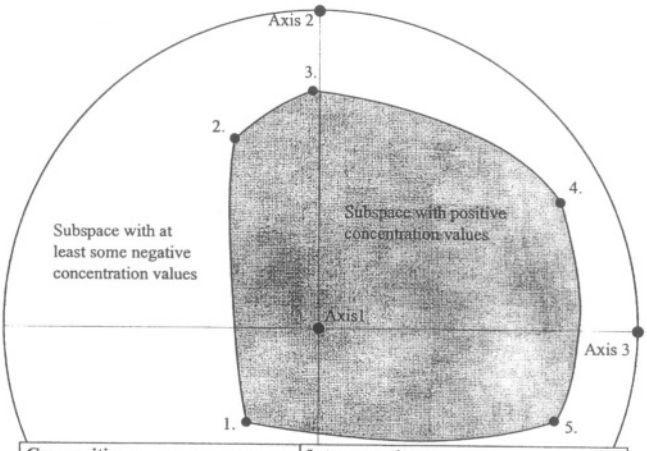
The factor analysis methods described above can be used to explore mixing, and to identify components. However, they do not yield estimates of the end-member compositions. Miesch (1981) proposed an alternative method, starting with Q-mode factor analysis, which aims to identify and quantify sensible end-member compositions based on the structure of the data. The concept is developed as follows;

- No components of a real mixture have any elements with negative concentrations.
- In a Q-mode factor analysis of data that have not been standardized, the first axis will have positive values for all elements, but the remaining axes will contain some negative elements.
- The second and further axes cannot represent real end-members, because of the negative values they contain. However, there is a region of composition space close to the first axis where all compositions are positive. This contains all the realistic end-member vectors.
- For a simple mixture, the boundary of this positive composition space describes a shape with straight sides and intervening apices. The number of apices equals the number of axes, or end-members if fewer. Thus, if three end-members are found, the shape bounding the positive solutions is triangular. The apices of the shape give the best possible estimates of the end-member compositions.

In the ideal case, where one element at least of each actual end-member is zero, then this method perfectly identifies the end-members in artificial data sets (Miesch, 1981). Furthermore, in such a case the end-member vectors are orthogonal and the data set is perfectly accounted for. If, however, no elements are zero in the true end-members, then perfect unmixing is not achieved, and the axes are not orthogonal. The end-members found this way only imperfectly account for the original data.

The method is easy to apply to three axes, yielding a maximum of three end-members. Because real data sets are complex, a perfectly triangular positive subspace is rarely observed. However, by considering the changing compositions around the perimeter of the subspace, realistic estimates of the end-members can be identified. For example, the sediment in Pinto Lake, California (Fig. 4) has a broadly triangular subspace, with five apices. By comparing the compositions represented by these apices, it is possible to constrain the end-member compositions.

In spite of the obvious merits of this approach to dealing with conservative mixing in soils and sediments, it has been little applied.



Compositions.

	#1.	#2.	#3.	#4.	#5.
SiO_2	66.7	88.3	89.0	34.1	22.6
TiO_2	1.2	1.5	1.4	0.0	0.2
CaO	0	4.0	5.9	8.3	0.0
K_2O	1.7	2.4	2.5	0.4	0.0
Fe_2O_3	13.4	3.8	0.0	0.3	17.1
S	0.0	0.0	1.1	8.5	4.9
LOI	17.0	0.0	0.0	48.0	55.1

Interpretation

- End-member 1. As #1: A terrigenous component rich in clays and detrital Fe.
- End-member 2. As #2 & #3. A terrigenous component rich in Si (quartz?) and Ca + K (feldspar?).
- End-member 3. As #4 & #5. An authigenic component rich in S and LOI (organic matter). May have two sub-members; 1) Fe-rich, 2) Ca-rich.

Figure 4. The Miesch (1981) procedure for identifying compositional end-members. A subset of composition vectors surrounding Axis 1 yield compositions with positive values for all elements. Outside this area, some of the elements have negative concentration values. Compositions corresponding to the numbered points are given in the inset table. Data from Pinto Lake, Santa Cruz, California (Unpublished data).

Normative calculations

Calculation of normative mineral concentrations is common practice in igneous petrology. This is a standardized scheme for deducing the concentration of idealized, or 'normative', minerals from whole-sample elemental concentrations. Garrels & MacKenzie (1971) propose a normative method for sedimentary rocks. As they state, it is not intended that the 'norms' so calculated should portray the actual minerals present, rather that a feel for the mineralogy is given. The method below is slightly modified to allow for the different mineral assemblages found in lake sediments; illite, organic matter, and Mn have been added, and a mixed Fe and Mg chlorite is used in place of the original Fe-free chlorite. The method is appropriate only for fine-grained sediments, and is likely to work best on clastic dominated systems.

To apply the method, all the major elements must be known. Then a series of steps must be taken:

1. Recalculate the elements as wt. % oxides (SiO_2 = Si × 2.14; Al_2O_3 = Al × 1.89; total FeOOH = Fe × 1.43; MgO = Mg × 1.66; CaO = Ca × 1.40; Na_2O = Na × 1.35; K_2O = K × 1.21; MnO_2 = Mn × 1.58; TiO_2 = Ti × 1.67).

   Organic matter = wt. % LOI.

2. Sum the oxides, LOI, and CO_2 (if significant) for each sample, and make sum equal to 100 (i.e. multiply each value by 100/sum).

3. Divide each oxide by its molecular weight; the components will then be in moles/100g of sediment.

Idealized minerals assumed to be present; calcite ($CaCO_3$); Ca-feldspar ($CaAl_2Si_2O_8$); magnesite ($MgCO_3$); chlorite ($Mg_{3.5}Fe_{1.5}Al_2Si_3O_{14}$); Na-feldspar ($NaAlSi_3O_8$); illite ($K_1Ti_{0.1}Al_3Si_7O_{24}$); kaolinite ($Al_2Si_2O_7$); K-feldspar ($KAlSi_3O_8$); silica ($SiO_2$); Fe oxy-hydroxide (FeOOH); Mn oxide (MnO_2).

Progressively apportion the elements (as oxides) to the minerals using the following sequence. After each step subtract from the element totals *all* of the elements contained within the mineral of that step.

1. If $CO_2 < CaO$ **calcite** = CO_2, and Ca -**feldspar** = remaining CaO

   If $CO_2 > CaO$ then **calcite = CaO, and magnesite** = remaining CO_2

2. **Chlorite** = remaining MgO/3.5

3. Na-**feldspar** = $2 \times Na_2O$

4. **Illite** = $10 \times TiO_2$

5. K-**feldspar** = remaining $2 \times K_2O$

6. **Kaolinite** = remaining Al_2O_3

7. **Silica** = remaining SiO_2

8. Fe **oxyhydroxide** = remaining FeOOH

9. Mn **oxide** = MnO_2

Finally multiply the sum for each mineral by its molecular weight to get its weight percent concentration (calcite; 100.09; Ca-feldspar, 278.2; magnesite 84.3; chlorite, 531.0; Na-feldspar, 262.2; illite, 705.4; kaolinite; 222.1; K-feldspar, 278.3; silica 60.1; Fe oxyhydroxide, 88.8; Mn oxide 86.9).

This system can be applied very easily using a spreadsheet. It must be remembered that the minerals identified are hypothetical. At any one site the method can be improved by refining the mineral compositions on the basis of local knowledge. For example, in a site with low chemical weathering, mica (muscovite, $K_2Ti_{0.1}Al_{5.4}Si_{6.5}O_{20}$) might be more appropriate than illite. Alternatively, if significant Ti is present in minerals other than micas or illite, this will need to be allowed for.

Calculating trace element baselines in pollution studies

As Norton & Kahl (1987) state, identification of the natural trace element contribution is essential if lake sediments are to be used as recorders of pollution. Early studies simply

used ratios to Al to allow for variations in the natural supply (e.g., Kemp & Thomas, 1976; Bertine & Mendeck, 1978). Norton & Kahl (1987) instead apply a correction using element: TiO_2 ratios. The principle is that the natural trace element supply can be divided into two fractions; soil minerals with associated trace elements, and the rest of the sediment lacking trace elements. Thus, unpolluted sediments will have trace element concentrations that vary with a soil mineral tracer, for example TiO_2. The anthropogenic fraction can be found by subtracting the background fraction from the total concentration. i.e.,

$$Pb_{a(x)} = Pb_{\text{total},(x)} - \left[\frac{TiO_{2(x)}}{TiO_{2(b)}}\right][Pb_b], \quad (1)$$

where: suffix a = anthropogenic, (x) is any depth, and b = background.

This approach is particularly appropriate where total element concentrations are used, because a high fraction of elements such as Zn, Cu, Ni, Co and V are firmly bound in mineral lattices. For elements such as Hg, Cd and Pb, the labile fraction is generally greater. When acid extractable concentrations are measured, the strength of the correlation between trace elements and TiO_2 weakens, reducing the value of the method. Further, given the key role of organic matter in binding elements such as Hg, Cd, Cu and Pb, it may actually introduce errors. Renberg (1986), for example, working with extractable trace element concentrations, concluded that normalization to organic matter can be appropriate, in complete contrast to Norton & Kahl (1987). A further potential problem in highly organic sediments is that acid-extractable TiO_2 can be significant (Engstrom & Wright, 1984).

An alternative model was suggested by Hilton et al. (1985). Rather than assume a fixed ratio of trace elements (total concentrations) to the catchment source tracer, they use regression to determine a model. The method is compared with that of Norton & Kahl (1987), using data for Zn from Antonelli Pond, California. Residual Fe is used here as a natural source tracer (Fig. 5). The method is not without problems. Hilton et al. (1985) argued that, in addition to the soil particulate component, some of the trace element would be supplied in solution leading to a positive value for the regression intercept. However, in practice, they found negative intercepts for all trace elements for which a significant regression model was found, suggesting that the theoretical basis is incorrect. A plausible explanation for the discrepancy may be vertical differentiation of the source soils. The ratio of natural trace elements to TiO_2 (or any other passive tracer such as Mg or residual Fe is unlikely to be constant throughout the soil profile. Alternatively, if TiO_2 and trace elements are associated with different particle sizes, mechanical sorting in the lake system may cause separation (e.g., Norton et al., 1992). This problem does not mean that the method of Hilton et al. (1985) should not be used; it remains the best available method. It may well be better, however, to look for tracers which discriminate between parts of the soil profile, or which correlate better with trace elements in soils.

Two possible alternative soil tracers are organic matter and acid-extractable Al. Organic matter has a well-known association with trace elements in sediment cores (Renberg, 1986). Boyle et al. (1998) also observed this effect in Lake Baikal, as do Boyle et al. (in prep) in Spitzbergen. However, variable amounts of authigenic organic matter prevent the use of total organic matter as a normalizing index. On the other hand, a measure of soil organic matter, based on N : P : C ratios, might be a suitable tracer to soil trace elements in many lakes. An alternative is acid-extractable Al, which, like trace elements, is strongly associated with the soil organic fraction. In a system where physical transport of soil particles to the

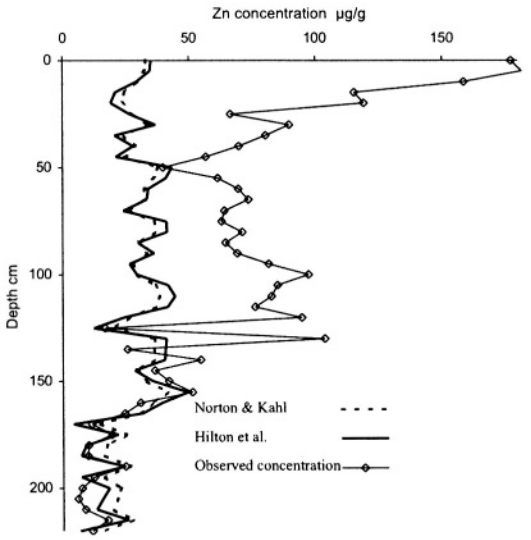


Figure 5. Estimation of baseline concentration for Pb using the methods of Hilton et al (1985) and Norton & Kahl (1986). Data from Antonelli Pond, Santa Cruz, California (Unpublished data).

lake dominates the supply of trace elements (i.e., not acidic), acid-extractable Al may be a suitable tracer. The chosen tracer can then be applied using the procedure of Hilton et al. (1985). As an example, consider concentration profiles from Nunatak Lake, Greenland (Fig. 6). A striking similarity is seen between the Pb and the acid-extractable Al and Mn profiles.

Areas of contention

Partial chemical extractions and sediment sourcing

Chemical fractionation by sequential extraction has been developed as a tool in environmental geochemistry for two main reasons. First, to understand the behaviour and fate of elements. Second, to predict aqueous speciation, mainly for toxicological reasons. The various techniques employed have greatly advanced our understanding in environmental geochemistry, though they are not without their problems. Palaeolimnologists would like access to such methods and information, but are faced with additional problems; has the speciation changed since accumulation?

There are two main issues. First, are the extracted chemical fractions specific and free from redistribution? Second, can the methods be applied to buried sediment. The second question involves three different points. Does speciation change on sampling? Does it change during diagenesis? Most importantly, is any useful palaeolimnological information recorded in the extracted fractions?

There are a number of studies which have looked at speciation in aqueous particulates. The method of Tessier et al. (1979) is a good example. These methods have been

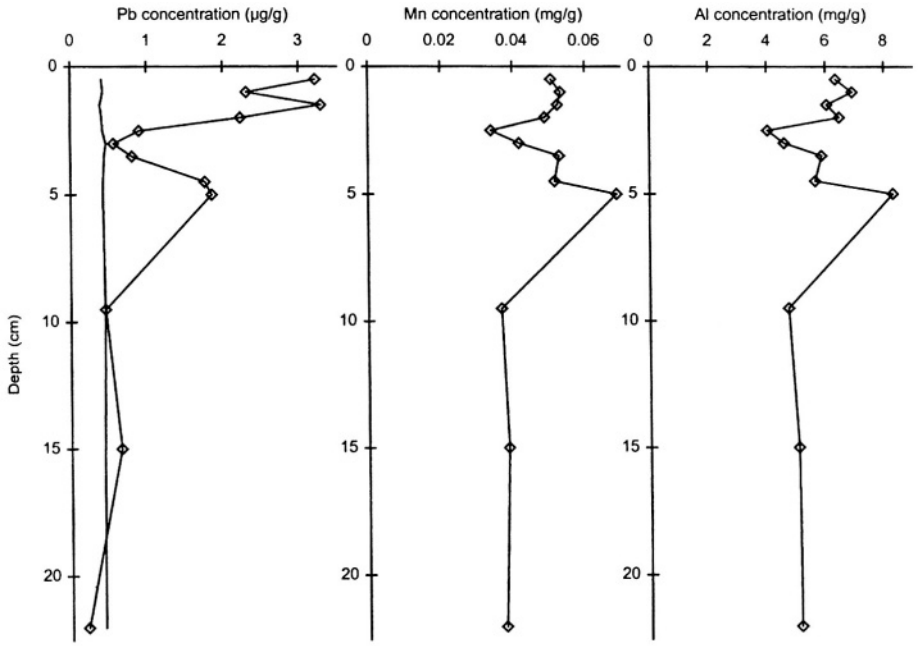


Figure 6. At Nunatak lake, Greenland, the sediment Pb concentration profile shows a slight surface enrichment. The baseline Pb concentration (line with no symbols), estimated using the method of Norton & Kahl (1987), does not account for this surface enrichment, which might be taken as evidence for an atmospheric pollution signal. However, the acid-extractable Mn and Al profiles resemble that of Pb. The similarity of the profiles for elements with such differing mobility can only be explained by a physical transport/sorting mechanism. A plausible explanation is that all three elements are associated with fine particles formed in catchment inceptisols. A small excess of Pb above both Mn and Al in the top c. 2 cm *may* indicate an atmospheric pollution component.

used to explore geochemical processes relating to contemporary sediments (Tessier et al., 1989). The European Community Bureau of Reference (BCR) has also developed a method (e.g., Sahuquillo et al., 1999). The reproducibility of such techniques has been recently improved by the development of appropriate reference materials (Sahuquillo et al., 1999; Lopez-Sánchez, 1998: Quevauviller et al., 1997). However, there remain concerns about the interpretation of these extractions. Raksasataya et al. (1996), comparing the Tessier et al. (1979) and BCR methods, found that on synthetic soils and spiked natural soils, both methods failed to correctly characterize Pb. Both methods removed Pb in early stages in spite of the fact that most was actually associated with humic substances. Nevertheless, sequential extraction methods are well established as a technique for examining contemporary sediments.

The same techniques have been applied to sediment cores (e.g., Reuter et al., 1981;Tsai et al., 1998), but it is not possible to verify that the data can be interpreted in the same way as for surface sediments. White & Gubala (1990) found that speciation changes rapidly on exposure to the air, requiring very careful handling of the sediment material, and argue that the initial particulate speciation is unlikely to be preserved. They conclude, as did Engstrom

& Wright (1984), that only the residual, aluminosilicate fraction, is resistant to alteration. This suggests that only two fractions can realistically be measured; the residual fraction, and the rest.

If a two-part division is made of the sediment, it is important to be very clear about the environmental significance of the fractions. The residual, or lattice-bound, fraction is largely bound up in insoluble silicate minerals, and thus is completely inert with respect to the lake system. The only information derived by measuring this fraction is about the character of the drift and bedrock of the catchment, and any aeolian mineral influx. The non-residual fraction is more complex. From the lake water, it can derive pore-water ions, sorbed ions, organic residue from partially decomposed organisms, biogenic silica, biogenic carbonate, sulphides, precipitated humic substance and oxyhydroxides of Mn and Fe, with associated organic matter and trace elements. From the catchment, it receives residues from decomposed plant tissues, soil oxyhydroxides of Fe and Mn with associated organic matter and trace elements. In other words, whereas the residual fraction is entirely allogenic in origin, the non-residual fraction is a complex mixture of allogenic and authigenic components. Clearly, it is very important to be cautious about interpreting the origin of lake sediment materials on the basis of partial extractions.

Finally, it is important that the objectives of the sequential extraction are kept in mind. If speciation is being studied, then sequential extraction must be used, and interpreted with due caution. If a palaeolimnological analysis is the objective, then it is necessary to consider the reliability of the speciation in the context of the questions being addressed.

Concentrations versus accumulation rates; issues, problems and models

Issues

Chemical elements in lake sediments are measured as concentrations. Yet, for a number of reasons, it is often desirable to convert the concentrations to accumulation rates. This issue is reviewed at length by Engstrom & Wright (1984). Concentrations are measured relative to the sample mass, and are therefore not independent from each other. If the rate of supply of one component increases relative to the others, then its concentration increases, while the others decrease. Thus, an up-core increase in the concentration of any particular element might be explained either by an increase in its supply rate, or by a decrease in the supply rate of one or more of the other components. Only accumulation rate data can unambiguously distinguish these cases. The obvious solution is to express the elements as fluxes. However, this is not straightforward for a number of reasons. First, even where ^{210}Pb data are available, sediment accumulation rate data are considerably less precise than the concentration data. Therefore, presenting results as accumulation rates reduces precision. Second, ^{210}Pb accumulation rate values are not usually measured for every sampling interval. Interpolation is required, adding unknown biases to the data. Third, accumulation rate data from any one core may differ greatly from the accumulation rate history of the lake as a whole. A variety of redistribution processes ensure that local effects dominate the accumulation rate history at any one location within a lake. In consequence, the measured accumulation rate history will be noisier than that of the whole lake. Any observed accumulation rate events (maxima, minima, steps, etc.) might be either redistribution events or supply rate change events, having very different significance for the element supply

fluxes. To eliminate these effects it is necessary to study many cores; Rowan et al. (1995a) argue that 5–10 cores are needed to obtain reasonably precise estimates of whole-lake sedimentation rates. A procedure for determining an optimal number of sediment cores has been proposed (Rowan et al., 1995b).

Concentration data are precise by comparison, recording subtle changes in the supplied sediment. If the relative importance of any component changes, then this is faithfully recorded in the sediment record. To determine which of the components has changed, two approaches are possible. First, accumulation rate data, if they exist, can be used to show which components show greatest flux changes. Second, a logical analysis of variation in the components may indicate which is most likely to have changed. For example, if one component goes down, while the three other independent components go up, then it is most *likely* that the flux of the single component has changed.

These arguments lead to the conclusion that concentrations are the primary data type; by comparison with accumulation rates, they are more precise, less open to interference, and often easier to interpret. Nevertheless, accumulation rate data are often necessary to interpret concentration changes, and a case can be made for displaying graphs of both concentration and accumulation rates (Engstrom & Wright, 1984; Renberg, 1986).

There is, however, an additional dimension to the problem of accumulation rates. The interpretation of two specific types of component is very sensitive to mass accumulation rate. First, elements that are transported to the lake in a soluble form, and only partially captured by the lake, have concentrations which can be highly sensitive to the sediment accumulation rate. Second, any component for which the supply rate is completely independent of catchment particle supply rates, is sensitive to variable dilution. For many atmospherically supplied trace elements both of these situations apply. The model described below can be used to evaluate these effects.

Models linking flux and concentration

The role of water column particles in capturing dissolved trace elements has been known for a long time (e.g., Schindler, 1975). The practical significance of this was demonstrated by Santschi (1984), who showed how the water column residence times of trace elements could be predicted from the particle flux. The simplest model which links fluxes of particles, supply of trace elements, and capture by sediments, is that of Schindler (1975). At the heart of the model is the distribution coefficient, K_d (sometimes referred to as the partition coefficient), which quantifies the relationship between the dissolved and particulate concentrations. Most subsequent formulations of the model are built around this concept (e.g., Imboden et al., 1980; Diamond et al., 1990; Hilton et al. 1995;Appleby, 1997). These models all assume reversible sorption of dissolved elements to particle surfaces. This simplistic view is broadly supported by recent studies of suspended particles in rivers (Findlay et al., 1996; Ferriera et al., 1997) and more rigorous chemical models of binding (e.g., Lofts & Tipping, 1998).

The model of Schindler (1975) can be expressed in terms of sediment concentration, which is convenient for palaeolimnological studies. The model derivation is outlined in Figure 7. A simpler steady state version of this, which is suitable for most purposes, is discussed at length by Boyle & Birks (1999). Both forms of the model exclude diffusion of dissolved elements into the sediment from the water column. This issue is discussed by

Basic sediment model

The metal mass balance for unit area of lake bed depends on the competing input and output fluxes. The input flux, J, is balanced by burial, outflow in dissolved form, and outflow as suspended solids. Each of these outputs can be expressed in terms of the metal concentration on particles, C. The mass balance can thus be expressed:

$$D\frac{d\bar{c}}{dt} = J - C\left\{P + \frac{1000Q}{K_d} + \frac{QP}{v}\right\} \qquad 1.$$

where D = depth (m)
$\bar{c}$ = total water held metal, dissolved and particulate (mg m^{-3})
J = areal metal input (mg m^{-2} yr^{-1})
C = metal bound to particles (mg kg^{-1})
P = areal particle flux (kg m^{-2} yr^{-1})
Q = areal water flux (m^3 m^{-2} yr^{-1})
K_d = distribution coefficient (m^3 $tonne^{-1}$)
v = particle mean settling velocity (m yr^{-1})

To solve this expression, the fluxes in the lake must be expressed in terms of the mean water held metal, $\bar{c}$, rather than concentration on particles. $\bar{c}$ is given by:

$$\bar{c} = C\frac{PK_d + 1000v}{vK_d} \qquad 2.$$

In terms of $\bar{c}$, the bass balance is:

$$D\frac{d\bar{c}}{dt} = J - \bar{c}\left\{\frac{vK_dP}{PK_d + 1000v} + Q\right\} \qquad 3.$$

Let
$$k = \frac{1}{D}\left\{\frac{vK_dP}{PK_d + 1000v}\right\} \qquad 4.$$

then,

$$\bar{c}_t = \bar{c}_0 \exp(-kt) + \bar{c}_e\left[1 - \exp(-kt)\right] \qquad 5.$$

Where $\bar{c}_0$ is the previous condition of the lake, and

$$\bar{c}_e = \frac{J}{Dk + Q} \qquad 6.$$

C, the concentration in sediment, can be found from $\bar{c}_t$ using expression 2.

Figure 7. Whole-lake trace element model.

Diamond et al. (1990), and suggests that omission of diffusion is a problem for highly soluble elements such as As, Cs and Ni, or acid sensitive elements (Cd, Co, Zn) in acidic lakes.

Variable dilution

If an element that is independent of the dominant panicle supply (i.e., in solution from catchment, or from the atmosphere) is captured efficiently by the lake system, then variation in the particle mass accumulation rate will cause an inverse variation in its sediment

concentration. This is due to variable dilution. As stated above, it is not sufficient to measure the accumulation rate of the specific core to correct this. The particle accumulation rate of the core will vary with redistribution, while the dilution will be controlled by particle supply to the whole lake. In principle, a sufficient number of cores from a lake can solve this problem.

If a significant proportion of the element remains dissolved in the water column, then the situation is more complicated. The proportion of the element retained by the lake sediment will then vary with the sediment supply rate. For example, for an atmospherically supplied trace element which is entirely sorbed to particles, doubling the particle accumulation rate will halve the sediment concentration. However, if only 10% of the element is bound to particles, then the sediment concentration is very nearly independent of the particle accumulation rate. Furthermore, the concentration will vary with the water flux. These effects can be evaluated using the simple partition model presented in Figure 7 and discussed by Boyle & Birks (1999). The model can be used to correct for the effect of changing particle accumulation rate. However, as discussed in the previous section, good accumulation rate data are rarely available. Instead, corrections for the effect of flux using local accumulation rate data can be used to constrain interpretation of changes, and to estimate average trace element supply rates. However, just as with the discussion about accumulation rate approaches above, the most reliable, and therefore primary, data type is concentration.

Deep lakes

The relationships between particle flux, trace element flux and trace element concentration in sediment are more complicated in deep lakes. In a deep lake, there may be a significant proportion of dissolved element held in the water column. If the water column dissolved element inventory approaches the magnitude of the annual flux for that element, then a steady state model is invalid. Instead, the dynamic model outlined in Figure 7 must be used to allow for the time delay in the response of the sediment to changes in trace element supply rate. The disadvantage of this, compared with the steady state situation, is that an observed trace element concentration profile does not lead back to a unique trace element supply history. However, a trace element supply history does lead to a definite trace element concentration profile, so it is possible to see if any particular supply history is compatible with the observed concentration data. A practical example of this from Lake Baikal is shown in Boyle et al. (1998), where the exceptional water depth makes this effect particularly strong.

The dynamic model of Figure 7 can be used to illustrate the impact of water depth on the response of the sediment to changes in trace element supply. The effects on the sediment composition are illustrated of five year episodes of doubled trace element supply rate (Fig. 8a), doubled particle deposition rate (Fig. 8b) and doubled K_d (Fig. 8c), for different combinations of water depth and initial K_d.

For a trace element with $K_d = 10^5$, doubling the trace element supply rate produces a smoothed sediment concentration record in even a 10 m deep lake. In 500 m, five years is not enough time for a well developed peak to form (Fig. 8a). Such a lake will be insensitive to short term changes in trace element supply. Clearly, in very deep lakes smoothing can seriously reduce the value of the sediment record.

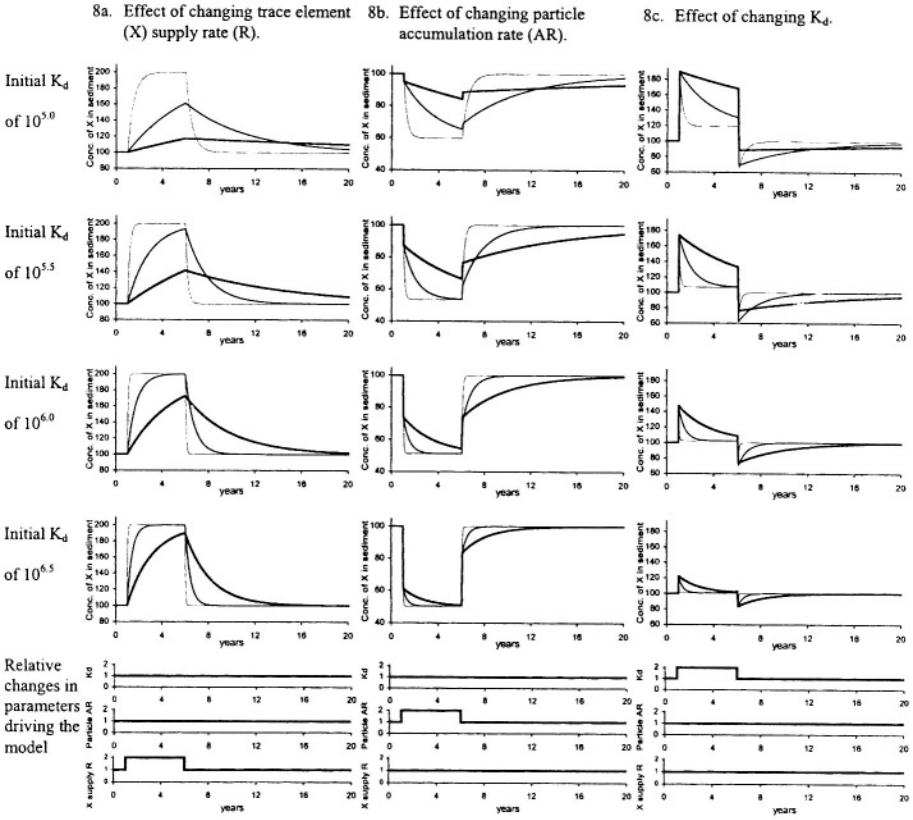


Figure 8. Modelled impact of changes in the lake system on the sediment concentration of a trace element (X). Thick line = 500 m water depth, medium line = 100 m water depth, thin line = 10 m water depth.

The insensitivity of the sediment record of deep lakes to changes in trace element supply, does not mean that the trace element concentration profile in the sediment cannot show sharp changes. A change in the particle deposition rate will cause an instantaneous change in sediment composition through dilution. However, for deep lakes, particularly for low K_d values, this dilution effect is reduced by the high water column trace element inventory (Fig. 8b). This means that in deep lakes it is important not to infer external trace element supply simply using sediment trace element accumulation rates.

Rapid changes in sediment composition can also be caused by changes in K_d. An increase in K_d can result from an increased proportion of algal matter, while a decrease in K_d can be caused by increasing calcium carbonate (Sigg et al., 1987) and biogenic silica (Boyle & Birks, 1999). Increasing the K_d causes an instantaneous increase in trace element concentration because the particles can take elements from the water column reservoir (Fig. 8c). Of course, this reservoir is not inexhaustible, and eventually a new steady state will be reached in which the concentrations return approximately to their pre-change values (not quite the same, as the change in K_d will have altered the outflow losses). This effect

increases with the solubility of the trace element, and the depth of the lake. In the 10 m deep lake (Fig. 8c), for the K_d values typical for Pb (c. $10^{6.4}$), we see that the increase in concentration is very short lived; the panicles take more Pb, but rapidly deplete the reservoir and establish a new equilibrium. When the K_d returns to normal the reverse happens. In a shallow lake, and with typical sedimentation rates, sediment mixing, and sampling intervals, such an event is probably undetectable for Pb. However, for the more soluble Zn ($K_d < 10^{5.8}$) there is a chance of seeing an effect in even a shallow lake, while at 500 m water depth (Fig. 8c) even Pb shows distinct peaks associated with changes in K_d.

The various effects of deep water, illustrated in Figure 8, mean that a trace element concentration peak in the sediment of a deep lake need not imply a supply event. While the model makes this clear, as discussed above, unique deconvolution of the smoothed and distorted sediment record is not possible. However, the model does allow constraints to be placed on possible interpretations of the record. For example, in Lake Baikal the model served to demonstrate that the sediment Pb record is compatible with the expected Pb supply history (Boyle et al., 1998). It also showed that observed stratigraphic changes in the sediment trace element concentration were too sharp to be explained by supply effects, and that changes in K_d needed to be considered.

Diagenesis, diffusion and signal preservation

If palaeolimnological methods are to be reliably applied to element concentration profiles, then two, often unstated, assumptions must hold true.

- At any one time the sediment concentration must be proportional to the external element loading.
- The sediment concentrations must not change after burial.

The former seems generally true, within the constraints of water depth (see section above) and sediment mixing (this important topic, relevant to all branches of palaeolimnology, is not addressed here. See Boudreau, 1999). However, the latter has long been known not to be true for some metals (Fe and Mn), and there has been much conflicting evidence and conjecture about other elements. This topic has been thoroughly reviewed by Hamilton-Taylor & Davison (1995) and Boudreau (1999), and it is concluded that remobilization of trace elements in sediment is not an overriding factor in most situations. The topic is, however, of such significance to inorganic geochemical palaeolimnology, that it is worth looking in detail at the evidence.

This section will consider three specific issues of relevance to palaeolimnology: surface sediment trace element enrichment; diffusion of elements within the sediment; and the role of Fe and Mn reduction in the potential remobilization of trace elements.

Surface sediment trace element enrichment

Enrichment of the sediment surface in trace elements, such as Cd, Cu, Zn and Ra, is not uncommon (e.g., Boyle et al., 1998). What do such enrichments mean? How can the sediment preserve an element supply record, when there is a mechanism generating surface enrichments?

The enrichments are usually reported only on the surface of the sediment. Three situations could explain this.

- Coincidence of trace element supply increase with the present; implausible as these have been observed for years without sign of burial.
- Constant surface enrichment due to continuous upward migration, and dissolution upon burial.
- Ephemeral surface enrichment due to cycling in processes in the water column.

At present, evidence points to the third alternative. Morfett et al. (1988) made repeat observations of lake sediment composition profiles, which showed that the surface enrichment was indeed temporary, and was coupled with trace element cycling in the water column. While few detailed studies of this kind exist, the generality of the phenomenon is attested to by studies of element cycling in lakes. Hamilton-Taylor et al. (1984) showed that C, Cu and Mn in particular were being recycled in the lower part of Windermere, Britain. Cu was released by rapid microbial decomposition of diatoms in the surface sediment, while Mn release was linked to redox cycling in the sediment. Some evidence for cycling of Pb and Zn was also found, but no clear cause could be demonstrated. A similar result was found in Greifensee, Switzerland, by Xue et al. (1997). Other studies have emphasized the instability of the fresh surface sediments and the rapid mineralization of the organic matter (McKee et al., 1989; Jonsson & Jansson, 1997). The significance of this mineralization for trace element release from river sediments has also been demonstrated (Song & Müller, 1995; Petersen et al., 1995). The trace elements released by the mineralization move dominantly upward into the water column because of the far greater upward diffusivity. Hamilton-Taylor et al. (1996) found that the downward diffusive flux for Cu and Zn was only about 1% of the total trace element sedimentation rate.

The escape of the trace elements back to the water column could be prevented by burial, thereby preserving a sediment record. However, such fossilized enrichments might be difficult to detect; the surface sediments commonly have extremely low densities, and thus comprise very little material. On burial, we can expect that any enrichment will be strongly diluted by the 'normal' underlying and overlying sediment. There are, however, some potential examples in the sediment of Lake Baikal (Boyle et al., 1998), where frequent small turbidity flows provide an ideal mechanism for burying the surface enrichments.

In conclusion, surface trace element enrichments are most likely to be linked to trace element cycling in lakes. This need not, however, have much impact on the longer term sediment record. The trace elements scavenged and re-released by the organic sediment are returned to the water column, mostly to be recaptured by falling particles at a later date. Simply, there are two scales of trace element cycling; one fast and temporary; the other slow and long-lived. The former appears to have little impact on the latter.

Diffusion of trace elements

There are problems for palaeolimnological interpretation of element concentration profiles if: diffusion from the water column to the sediment is greater than sedimentation; and if elements migrate within the sediment after burial. Diffusion between the water column and the sediment is potentially a huge problem. Diffusive loss or gain to the upper surface of the sediment would matter little, as the effect would be similar to sedimentation. If,

however, diffusive exchange occurs between the water column and deeper layers, then severe limitations could be placed on the temporal resolution of the record.

The first firm evidence for diffusive transport from water to sediment came from Carignan & Tessier (1985). In two lakes in Ontario (Clearwater and Tantaré Lakes), they showed that the diffusive flux of Zn exceeded the sedimentation flux. These results were supported by Tessier et al. (1989), who showed how widespread the effect was. Other studies showed significant, though lower, diffusion of Cu (Carignan & Nriagu, 1985). At both sites, they found highly significant diffusion of Ni, which at least equaled the sediment settling component. For both Ni and Cu, subsurface peaks were attributed to this effect. For all three metals these sites are rather unusual. The sediment concentrations are high through proximity to the Sudbury smelter, and the dissolved concentrations are high because of acidification, leading to high diffusive fluxes. In the long run, metal mobility at these sites is thought to be very low because of sulphide available in the sediment (Huerta-Diaz et al., 1998). An important question is whether significant diffusion of these or other trace elements is occurring at other less acidic and less polluted sites, and in sites where sediments are sulphide-free. Direct evidence from sediment studies is scarce. However, Diamond et al. (1990) present a simple model of diffusion of trace elements from the water column to the sediment. This is useful in that it predicts the relative importance of diffusion as a transport mechanism based on the K_d value (Fig. 9). However, this model is designed to study water quality, and does not deal specifically with where the trace element goes. The model gave a best fit if the depth of sediment involved in diffusion is 1 cm, which is similar to the depth for diffusive accumulation of Zn observed by Carignan & Tessier (1985). Using the model of Diamond et al. (1990), knowing the sediment accumulation rate, and assuming a 1 cm diffusive penetration, it is possible to place crude constraints on the impact of diffusion on a sediment trace element profile. It must be stressed, however, how crude this is. It would not be difficult to construct a more sophisticated model, using, for example, approaches suggested by Golterman (1995), but it is difficult to collect the kind of data needed to parameterize the model.

Evidence for diffusive redistribution of elements within the sediment must also be considered. Redox impacts are considered in the next section. However, diffusion in sediments need not be related to redox effects. There is no doubt that ^{137}Cs can migrate in sediments (e.g., Davis et al., 1984). However, this is complex matter, and profiles examined by Crusius & Anderson (1995) could not be interpreted with a single K_d value. A fraction of more mobile Cs had to be present with a K_d of about 5000.

Pore water data have been presented by Benoit & Hemond (1991) to support redistribution of ^{210}Pb. Such a finding has not been reported by other researchers. Indeed, studies of ^{210}Pb in varved sediments have failed to detect migration (e.g., Appleby et al., 1979; Crusius & Anderson, 1995). While not being able to explain this discrepancy, Hamilton-Taylor & Davison (1995) conclude that an overwhelming body of evidence supports the view that Pb is only minimally mobile in lake sediments.

From these examples, it is clear that diffusion can be a problem under some circumstances. From the palaeolimnologist's perspective, it is important to be able to predict where such problems will occur, and what their potential significance is. A promising approach to this is via modeling. Some hope is also offered by the diffusive gradients in thin-films (DGT) technique (e.g., Harper et al., 1998), because it may then be possible to estimate at each site the relative mobility of the elements under study.

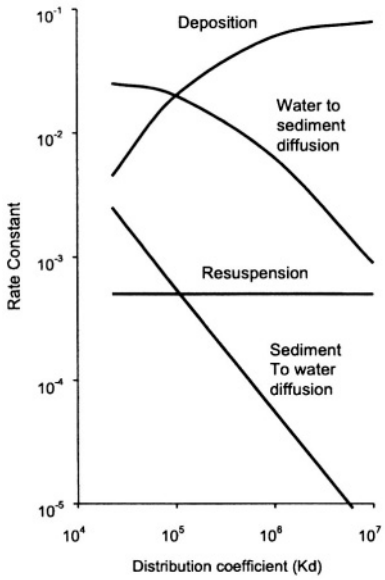


Figure 9. Influence of distribution coefficient on the contributions of diffusive and advective fluxes to the total sediment flux of an element as predicted by the model of Diamond et al. (1990) for a lake enclosure.

Redox effects and trace elements

The affinity of trace elements for Fe and Mn oxides has been known for a long time. It has also long been known that redox cycling of Fe and Mn takes place in lake sediments (e.g., Mackereth, 1966). What is less certain is whether redox remobilization of Fe and Mn oxides causes remobilization of trace elements (e.g., Förstner & Wittmann, 1979).

Correlation of trace elements with Fe-Mn oxide concentrations within sediment profiles has been attributed to remobilization. This is particularly the case for surface sediment enrichments (e.g., Cornwell, 1986; Williams, 1992), but also for subsurface sediments (e.g., Boyle et al., 1998). In all of these cases, redox remobilization is plausible, but not demonstrated as there are a number of alternative possible explanations. Many sediment cores have elevated Fe and Mn in their surface sediment due to redox recycling. Many sediment cores likewise have elevated trace elements due to the cycling within the water column. If sampling intervals are coarse with respect to these effects, then a good correlation between Fe-Mn oxides and trace elements is inevitable for many cores (e.g., Cornwell, 1986, for Cu, Pb and Zn). Looking in detail at six fine-resolution Lake Baikal cores, Boyle et al. (1998) show that apart from the surface samples, which are typically elevated in both Fe-Mn oxides and trace elements, there is either no correlation or a negative correlation between Fe-Mn oxides and trace elements. This suggests that far from capturing trace elements, the diagenetic Fe-Mn oxides simply dilute them. This is not the case for all trace elements; Flower et al. (1995) found that Co correlated with Mn in a sediment core from Lake Baikal, supporting mobilization of Co on reduction.

The evidence presented above does not discount redox remobilization, but does serve to show that patterns in sediment composition are not likely to prove anything. To demonstrate redox remobilization it is necessary to find evidence for change. The most direct approach

is to look for gradients in pore water concentrations. Both Co (Wang et al., 1986; Williams, 1992; Petersen et al., 1995; Achterberg et al., 1997) and Cr (Petersen et al., 1995) remobilization have been demonstrated in freshwater sediments. Arsenic is also shows strong pore water gradients. Cornett et al. (1992) studied the As polluted Moira Lake (Ontario) and found that the diffusive flux of As was greater than the current external loading. K_d declined sharply with depth, as the sediment becomes more reducing. In Loch Lomond, Scotland, a strong sub-surface sediment enrichment in As is observed, driven by pore-water fluxes towards an oxidation front just below the sediment surface (Farmer & Lovell, 1986; Farmer, 1994).

As, Co and Cr can become remobilized because they have multiple oxidation states in sediments. A crucial question is whether trace elements that do not change oxidation state are remobilized in response to redox changes in Fe and Mn. The pore water data of Williams (1992) offers some evidence for movement of Cu and Zn, though the patterns are complex. Klinkhammer (1980) and Klinkhammer et al. (1982) show that Cu and Ni diffuse upward in anoxic marine sediments in the equatorial Pacific; but the higher accumulation rates observed in lake sediments make any comparison problematic. Shaw et al., (1990) also find migration of transition elements, but in faster accumulating marine sediments. They find a striking similarity between the Mn and Co pore water profiles. They conclude that there is significant decoupling between transport and burial processes. The strength of this finding depends upon the assumption that water centrifuged from sediment is a good proxy for pore water.

Thus, pore water studies provide evidence that some trace elements (As, Co, Cr) become more soluble on redox dissolution of Mn-Fe oxides in marine and sediments. However, these studies have failed to detect a parallel release of trace elements (other than Co) with Fe and Mn during redox events (Sakata, 1985; Morfett et al., 1988; Achterberg et al., 1997). It appears that in spite of the loss of labile organic matter and oxides of Fe and Mn, the trace elements remain relatively immobile. In oceanic or estuarine sediments it has been proposed that sulphides have a role to play in fixing the trace elements under reducing conditions. This has also been demonstrated in sulphate-rich freshwater systems (Huerta-Diaz et al., 1998). However, Cu and Pb, at least, clearly remain firmly attached to freshwater sediment even in the absence of measurable sulphides, and where Mn and Fe are being actively released via reduction (Sakata, 1985).

One question to consider is why the trace elements are not released. If a key binding site for trace elements is brought into solution (Mn-Fe-oxides), how is it that the trace elements are not also dissolved? The logical argument that trace elements should go into solution when their binding surfaces are disrupted appears to be based on too simplistic a model. Substantial loss of Fe and Mn are experienced on reduction, yet this does not necessarily mean total loss of oxide binding sites. In fact, reduction of oxides is rarely complete even where conditions are sufficiently reducing that sulphides are present (Davison, 1994). Thus, reduction need not eliminate oxides, while at the same time offering fixation by sulphide.

Furthermore, it may be that the significance of Fe and Mn oxides for binding trace elements in freshwaters has been overestimated. There is good evidence that in freshwater systems humic substances are as important. Indeed, Tipping (1980) showed that in the presence of dissolved humic substances Fe oxyhydroxides became coated and behaved as humic substances. Further studies have emphasized this effect, stressing its importance in acidic systems (Tessier et al. 1996). Given the effectiveness of humic substances in binding

trace elements (e.g., Tipping & Hurley, 1992; Tipping, 1994; Lofts & Tipping, 1998), and their tendency to coat oxide particles present in freshwater systems (Findlay et al., 1996), it need not be concluded that removing the Fe must have a dramatic effect on total binding.

Finally, diffusive fluxes are driven by solution gradients. Fe and Mn diffuse out of sediments on reduction because they become 2–3 orders of magnitude more soluble. For trace elements such as Cu, Pb and Zn, any increase in solubility due to loss of binding sites is very small by comparison. Therefore, relative diffusive losses are expected to be far lower.

In conclusion, it is not possible to prove or disprove the existence of redox remobilization of the common pollutant trace elements (Cd, Cu, Hg, Pb and Zn). However, evidence at present suggest that any effect is usually too small to be detected against the larger advective fluxes (Hamilton-Taylor & Davison, 1995).

Uses of inorganic geochemical data in palaeolimnology

Inorganic geochemical data have been used in palaeolimnological studies for a long time, and a number of key environment-composition associations have been studied. There is a danger that such methods get used blindly, without adequate consideration of alternative interpretations. In particular, there has been a tendency to disregard particle size effects when interpreting variation in elemental composition (See Moalla, 1997, for an example of how great such effects can be). Most of this section is devoted not to specific elements, but to environmental factors and the effect they have on the inorganic chemistry of lake sediments. Table III provides information about some elements that have been used in palaeolimnological studies, listing their properties and providing some references to the literature.

Changes in the lake environment

Trophic status

At an early stage in palaeolimnological method development, it was argued that autochthonous organic matter was so susceptible to oxidation, that it contributed little to the sediment carbon record (Mackereth, 1966). While other studies have concluded that within-lake sources can be important in some cases, most studies have supported Mackereth's conclusion (e.g., Engstrom & Wright, 1984; Rowan et al., 1992). Dean & Gorham (1998), on the other hand, argue that in all but the most oligotrophic systems, organic matter is mostly autochthonous. This uncertainty, and the susceptibility of organic carbon to mineralization (e.g., Dean, 1981), severely limits its use as an indicator of lake productivity.

Phosphorus, on the other hand, has long been used to reconstruct lake productivity. The early work is reviewed in detail by Engstrom & Wright (1984). Under favourable conditions, sedimentary P is a useful productivity indicator. The problem is that it is hard to be certain about when the conditions are not favourable. For these reasons, and because diatom transfer functions have proved so reliable (Hall & Smol, 1999), this technique is less used than it might be.

Engstrom & Wright (1984) noted that some fractionation of the sediment P is desirable because there is a detrital component. Since then, many studies have applied a number of

Table III. Chemical properties and source references for some elements. The references are reviews where these exist, and recent case studies if not.

Name		log K_d	log K_d pH 4.8	Conc. in average shale. µg/g[5]	Goldschmidt classification[4]	References
Aluminium	Al			92 000	lithophile	Ochsenbein et al. 83; Engstrom & Wright 84; Boyle 94.
Arsenic	As	5.2[2]		10	chalcophile	Cornett et al. 92; Farmer 94.
Barium	Ba			600	lithophile	Cornwell 86; Stone et al. 97.
Boron	B			100	lithophile	Mackereth 66; Goodarzi & Swain 94.
Bromine	Br			5		Mun & Bazilevich 62; Mackereth 66; Farmer 94.
Cadmium	Cd	6.3[1]		0.3	chalcophile	Evans et al. 83.
Calcium	Ca			25 000	lithophile	Engstrom & Wright 84; Kelts & Hsü 78.
Carbon	C			1 000		Engstrom & Wright 84; Rowan et al. 92; Dean 99.
Chlorine	Cl			170		Lerman & Weiler 70.
Chromium	Cr			100	lithophile	Achterberg et al. 97; Schaller et al. 97.
Cobalt	Co	7.1[2], 6.3[3]	3.3[3]	20	siderophile	Achterberg et al. 97; Williams 92.
Copper	Cu	5.4[1]		50	chalcophile	Norton et al. 92; Hamilton-Taylor et al. 96.
Iron	Fe	6.0[3]	4.3[3]	47 000	siderophile	Engstrom & Wright 84; Davison 93; Nürnberg & Dillon 93
Lead	Pb	6.4[1]		20	chalcophile	Norton et al. 92.
Magnesium	Mg			14 000	lithophile	Ochsenbein et al. 83; Engstrom & Wright 84.
Manganese	Mn	5.2[3]	3.8[3]	850	lithophile	Engstrom & Wright 84; Davison 93; Bryant et al. 97.
Mercury	Hg	5.6[2], 5.5[3]	5.5[3]	0.3	chalcophile	Engstrom et al. 94; Fitzgerald et al. 98.
Molybdenum	Mo			2	chalcophile	Schaller et al. 97.
Nickel	Ni			80	siderophile	Cornett et al. 89; Achterberg et al. 98.
Phosphorus	P			750	siderophile	Engstrom & Wright 84; Brezonik & Engstrom 98.
Potassium	K			25 000	lithophile	Ochsenbein et al. 83; Engstrom & Wright 84.
Rubidium	Rb			140	lithophile	Gelinas et al. 2000.
Scandium	Sc			15	lithophile	ten Hulscher et al. 92.
Selenium	Se	5.0[3]	4.0[3]	0.6	chalcophile	Peters et al. 99.
Silicon	Si			238 000	lithophile	Coleman et al. 95; Verschuren et al. 98.
Silver	Ag	5.8[1], 5.3[3]	5.3[3]	0.1	chalcophile	Horowitz et al. 95.
Sodium	Na			9 000	lithophile	Engstrom & Wright 84.
Strontium	Sr			400	lithophile	Engstrom & Nelson, 91; Xia et al. 97; Stone et al. 97.
Sulphur	S			2 500	chalcophile	Baker et al. 92; Evans et al. 97.
Tin	Sn	6.5[2], 6.2[3]	6.0[3]	6	siderophile	Gelinas et al. 2000.
Titanium	Ti			4 500	lithophile	Norton et al. 92.
Vanadium	V			130	lithophile	Norton et al. 92; Schaller et al. 97.
Zinc	Zn	5.8[1], 5.0[2]	3.8[3]	90	chalcophile	Hamilton-Taylor et al. 96; Carignan & Tessier 85.
Zirconium	Zr			180	lithophile	Stone et al. 97; Wolfe & Hartling 97.

Sources:

[1] Benoit & Rozan (1999), filter method, at 1 mg/l particle concentration.

[2] Diamond et al. (1990), filter method, at ca. 1 mg/l particle concentration.

[3] Santschi et al. (1984), filter method.

[4] Krauskopf (1982): elements preferentially occur

earth's iron core (siderophile), sulphide ores (chalcophile), silicate minerals (lithophile) or the atmosphere (atmophile).

different sequential extraction procedures. Most of these determine *non-apatite inorganic phosphorus* (NAI-P), *apatite phosphorus* (AP) and *organic phosphorus* (OP), but a number of finer distinctions are also made. The method of Williams et al. (1976) is the most widely used, but there are both alternative procedures (e.g., Oluyedin et al., 1991), and objections to steps in the Williams method (e.g., Golterman et al. 1998). There are currently attempts to develop standard reference materials for a modified Williams method (Pardo et al., 1999).

Both the OP and NAI-P fractions are potentially related to lake productivity. However, a series of factors affect the retention of P by lake sediments (Engstrom & Wright, 1984).

- In lakes rich in authigenic Fe, stratigraphic variations in P correlate with stratigraphic variations in extractable Fe.
- In lakes poorer in authigenic Fe, P does not correlate with extractable Fe.
- Hypolimnetic anoxia causes loss of sediment P. Thus, in cases of excessive productivity leading to hypolimnetic anoxia, sediment P can be anticorrelated with water column P. Bacterial processes are thought to cause the release of the P (Davison, 1993; de Montigny & Prairie, 1993).
- Reductive remobilization of P can lead to a stationary surface maximum which could be falsely interpreted as indicating recent eutrophication (Farmer, 1994).

In addition to these problems, Belzile et al. (1996) show that lateral fluxes of P in a eutrophic lake can make up a significant part of the local load, and can exceed vertical diagenetic remobilization. On the other hand, Dillon & Evans (1993) observed good agreement between mass balance data and sediment core evidence for P loadings to lakes in Ontario. They suggest that sediment cores make a good alternative to the logistically more difficult mass balance studies, provided that several cores are used. So, if a lake has not become severely anoxic, and if sediment mass accumulation rates are high enough to minimize diagenetic effects, and the P signals being looked for are not subtle, then P reconstruction can be achieved (Engstrom & Wright, 1984). For some successful case studies see Shapiro et al. (1971), Williams et al. (1976), Farmer (1994), Heathwaite (1994) and Brezonik & Engstrom (1998).

Another approach to quantifying lake productivity is to measure biogenic silica (e.g., Mortlock & Froelich, 1989). This, again, is reviewed by Engstrom & Wright (1984). The principle is that the extractable silica will measure biogenic silica, chiefly diatoms, and will thus be a measure of biological productivity. Engstrom & Wright (1984) explore the weaknesses in this argument, which may be summarized as follows.

- NaOH (or other reagents) attacks readily soluble clays in addition to biogenic silica. Conversely, not all of the biogenic silica is dissolved. Thus, extractable Si may be a poor measure of biogenic silica.
- Biogenic silica is subject to variable and rather unpredictable dissolution on burial in sediment, which interferes with the method. There are ways to estimate the amount of dissolution using electron microscopic methods (Battarbee, 1980).

- Diatoms make up only a portion of the total phytoplankton population; variations in diatoms need not reflect general productivity.

This much said, there are examples of lake sediment studies where estimates of biogenic silica, or diatom counts, have contributed to the overall picture emerging from holistic palaeoecological analysis (e.g., Coleman et al., 1995; Flower et al., 1995; Verschuren et al., 1998).

Lake trophic status can also affect calcium carbonate. Increased productivity in lakes can lead to biological CO_2 consumption, consequent increased pH, and precipitation of calcium carbonate. Under the right circumstances this can be preserved in the sediment (Kelts & Hsü, 1978; Dean, 1981; 1999).

Lake redox

Mackereth (1966) studied the link between lake redox conditions and the capture of Fe and Mn by lake sediments. In reducing conditions both Fe and Mn can become soluble, but Mn more readily. Mackereth interpreted the redox history of lakes in the English Lake District using this principle. He also recognized that it was difficult to separate source changes from lake redox effects. He proposed, however, that this could be done by comparing the Fe profiles with the Fe : Mn ratio profiles. If peaks in Fe concentration coincided with peaks in the Fe : Mn ratio, then he argued that this was most simply explained by changes in supply from the catchment. However, if peaks in Fe coincided with minima in the Fe : Mn ratio, then it was best explained by reducing conditions in the lake. These arguments, and related evidence based on Fe and Mn enrichment with respect to lithospheric concentrations, are illustrated in Figure 10. This is one of the most widely applied tools in chemical palaeolimnology. Many studies of lake history have invoked related arguments (see Engstrom & Wright, 1984).

Engstrom & Wright (1984) point out a number of problems with this simple view.

- Remobilization of reduced Fe and Mn within the sediment causes changes in the Fe : Mn ratios. This means that small scale changes in the ratio need have nothing to do with either supply or capture (e.g., Bryant et al., 1997).

- In some systems, chemical reduction of the sediment leads to sulphide production, and capture of Fe with loss of Mn. However, in sulphate depleted systems, there is insufficient sulphide, and Fe is also lost.

- Acidification can cause reduced Mn in sediments (e.g., Renberg, 1985).

- There is poor agreement on redox conditions between chironimid data and that of Mackereth.

These concerns are reinforced by Davison's (1993) review of the aqueous chemistry of Fe and Mn in lakes, emphasizing their complex behaviour. While the key role of redox in governing concentrations is reinforced, many exceptions are identified. It is stressed that both Fe and Mn have substantial colloidal fractions, which allows aqueous transport of both in oxidizing conditions. In addition, photoreduction of Fe and Mn is active, particularly in the presence of organic substances, and leads to measurable amounts of reduced Mn and Fe

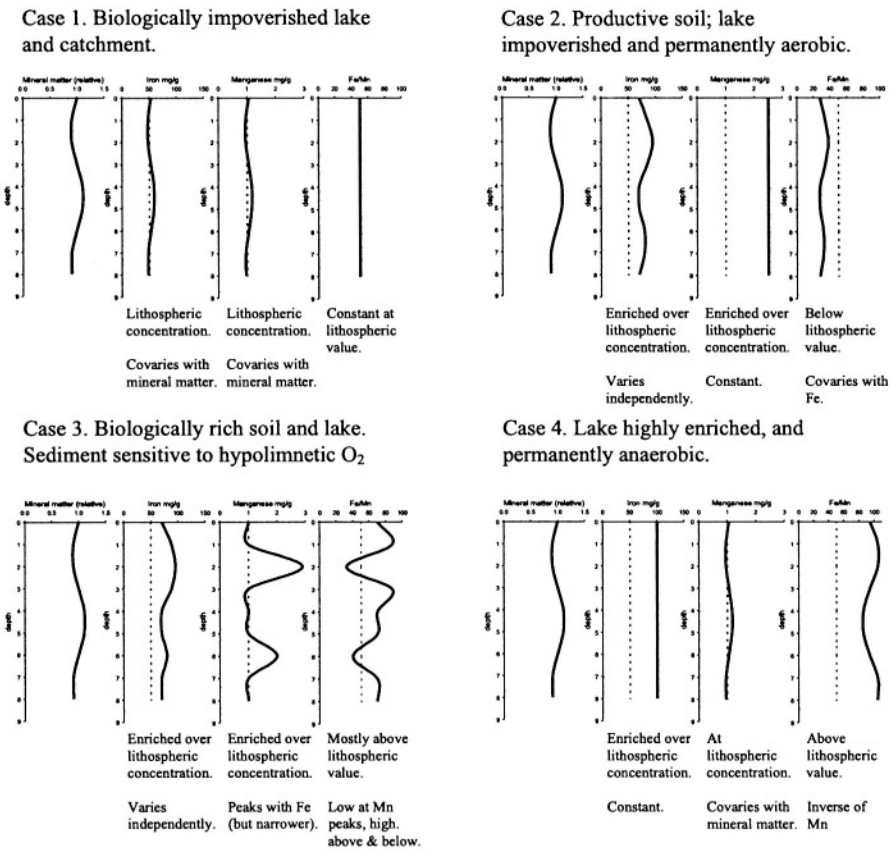


Figure 10. Mackereth's (1966) hypothesis for the palaeolimnological interpretation of Fe and Mn. Dashed line = Mackereth's lithospheric concentration value.

even in oxygenated water. It is also noted that geochemical models that predict the survival of oxyhydroxide under reducing conditions are inadequate; Fe oxyhydroxides are capable of coexisting with sulphide.

There are some additional considerations. The Fe and Mn fluxes to a lake can be altered by acidification (Davis et al., 1983; Dillon et al., 1988). Further, if major changes in the acid-soluble allogenic sediment fraction occur, the Fe : Mn ratio can alter substantially without this meaning anything about the lake conditions.

A number of additional chemical species can be used to validate an interpretation based on Fe and Mn. A promising approach is proposed by Schaller et al. (1997), who include additional information from the distribution of Cr, Mo, V and As to better constrain possible interpretations. Alternatively, the presence of sulphide in the lake sediment can be used (detected by correlated stratigraphic increases in Fe and S, Engstrom & Wright, 1984; Carignan & Tessier, 1988), though interpretation is not simple. An increase in the concentration of sulphides in the sediment can indicate a reduction in hypolimnetic oxygen, but might instead be due to an increase in reducing capacity of the sediments. Both are

likely to accompany increased lake productivity, but may also indicate reduced mixing, as might accompany isolation of a lake basin or onset of meromixis. All three of these have been invoked to explain the presence of sulphides (Engstrom & Wright, 1984). However, there are more problems. At low concentrations, sulphide in sediment is usually determined from total sulphur. This, however, can be enriched through diagenesis of sulphur-rich humic substances (Ferdelman et al., 1991), and can be affected by atmospheric loading (Baker et al., 1992). Clearly, it is necessary to fully understand the S budget before interpreting sulphur variations in the sediment (e.g., Evans et al., 1997).

Human impact

Acidification

A number of significant impacts of acidification on lake sediment chemical composition have been documented. Enhanced supply of trace metals leached from the catchment can compete with reduced capture of trace metals by lake sediments, leading to a complex response.

Catchment acidification has been invoked to explain increases in the catchment contribution of Mn in Sweden (Renberg, 1985) and Fe in Norway (Davis et al., 1983). Enhanced supply of Al due to catchment acidification is also reported (White & Gubala, 1990). The export of trace metals is demonstrated in acidified parts of Sweden, where stream water concentrations of Cd and Zn are enhanced in acidified areas (Johansson et al., 1995). In a study of catchment and lake budgets in the highly acidified area around Sudbury, Ontario, Dillon et al. (1988) found that the acidified catchments were sources for Al, Mn and Ni, but sinks for Cu and Zn. An enhanced supply from the catchment is supported by lake sediment studies for Al and Zn, but not for Pb.

Reduced capture of trace metals in lakes or enhanced leaching must also be considered. In laboratory experiments, great effects on sediment leaching have been observed (e.g., Matschullat & Wyrobek, 1993). Field observations suggest that the effects are more muted. Borg et al. (1989), working on forest lakes in southern Sweden (Holmeshultasjön, Fiolen, St. Skärshultasjön, Klintsjön and Gyslättsjön), found little correlation of trace metals with pH between lakes, but did find that for Zn, Cd and Mn there was reduced capture by sediments in the acidified lakes. In contrast, pH had little effect on Fe, Al, Cu and Pb, which were still dominantly captured by the sediment. Whole lake acidification at Little Rock Lake (Wisconsin) found significant increases in dissolved concentrations for Al, Mn and Fe (Mach & Brezonik, 1989), but not of Cd, Cu, Pb and Zn for pH values of 5.1 Their limnocorral experiments suggest that dissolved concentrations of Cd and Zn would increase at pH values at 4.6. Sprenger & McIntosh (1989) found elevated dissolved concentrations of Cd, Al, Zn and Pb in acid lakes, attributing it to reduced affinity for particles. Experimental work using isotope tracers also shows a strong effect on Co (Santschi et al., 1984). All this information from lake water is difficult to interpret because trace metal pollution and acid pollution are correlated in both space and time. Studies of sorption by particles in lakes, thereby avoiding pollution effects, suggest that pH has no impact on Pb over observed ranges, but could affect Cu and Zn (Hamilton-Taylor et al. 1997).

Palaeolimnological studies support reduced sediment capture of some elements in acidified lakes. Lake acidification has been invoked to explain near surface decreases in the

sediment concentration of Mn and Ca (Renberg, 1985; Norton & Kahl, 1991; Norton et al., 1992), and Zn (Norton et al., 1992). In a study of labile sediment Al, Boyle (1994) found both enhanced and diminished accumulation of Al depending on lake water pH, suggesting that labile Al is a useful palaeolimnological indicator of acidification thresholds.

Subsurface peaks in Zn have also been explained by diffusion to sulphide-enriched layers in acidified lakes (Carignan & Tessier, 1985; Tessier et al., 1989). However, reduced capture of Zn by most acid lakes suggests that diffusive fluxes are less important than advective fluxes overall.

A debate has taken place about whether it is remobilization or reduced capture that has led to elevated dissolved trace metal concentrations in lakes (e.g., Norton & Hess, 1980). Some experimental work suggests leaching from lake sediments (e.g., Matschullat & Wyrobek, 1993). Others have argued that the sharp increase in water pH at the water-sediment interface would prevent remobilization (Renberg, 1985), and that binding of the metals to relatively stable sediment chemical fractions was too strong (e.g., Reuter et al., 1981). Experimental work using tracers tends to support decreased capture as the dominant effect (Santschi et al., 1984).

Atmospheric pollution

Thomas (1972) reported a sediment record of recent mercury contamination in Lake Ontario. The following year a similar result was reported from the more rural Lake Windermere (Aston et al., 1973), and a sedimentary record of Pb contamination was reported from Lake Washington (Crecelius & Piper, 1973). In the years that followed, similar results were found elsewhere, and for many trace elements in addition to Hg and Pb (Kemp & Thomas, 1976; Bertine & Mendeck, 1978; Norton & Hess, 1980; Rippey et al., 1982; Davis et al., 1983; Ochsenbein et al., 1983; Norton 1986; Verta et al., 1989; Norton et al., 1992; Engstrom et al., 1994). These studies have consistently shown enhanced accumulation of Cd, Cu, Pb, Zn and Hg. Generally, increases in Ni, Co and V have not been found, except where there are major local sources (e.g., Cornett et al., 1989).

The role of long-transported atmospheric pollution as a key factor in regional enrichment of surface sediments in Pb, Hg, Cd and Zn has been confirmed (Rognerud & Fjeld, 1993; Boyle & Birks, 1999; Fitzgerald et al., 1998). However, specific local sources have also been identified. For example, the Sudbury (Ontario) smelter caused widespread As, Cu, Ni and Zn contamination. In Scotland former mining activities have caused more localized pollution by Cd, Pb and Zn (Farmer, 1994). Simola & Lodenius (1982) found elevated Hg in core-tops in Finland, but attributed this to peatland drainage rather than atmospheric pollution. Other studies have focused on urban pollution, comparing urban with rural reservoirs (Foster et al., 1991). Such systems are highly complex, and require good knowledge of the hydrological systems involved.

There are a number of problems with interpreting atmospheric pollution from sediment records. First, there may be indirect effects due to acidification. Zn in particular must be treated with great caution, as there is often inconsistency between concentration profiles from the same lake (White & Driscoll, 1987; White & Gubala, 1990). Second, there may be diffusion within the sediment, particularly for As (Farmer & Lovell, 1986; Cornett et al., 1992). The potential impact of diffusion is greater at low sedimentation rates, and is worse for elements which are mobile under reducing conditions. As, Co, Fe and Mn all migrate readily in sediments under the appropriate redox conditions (see section *Diagenesis,*

diffusion, signal preservation). Third, there are temporary surface enrichment effects for many metals (see same section), which must not interpreted as changes in external loading. This problem is also greater where sediment accumulation rates are low. Fourth, there is always a natural catchment contribution to the element profiles. This is normally least important for Cd, Hg and Pb, but always needs to be addressed. This problem is worsened by high sediment accumulation rates. Fifth, there is evidence for direct diffusion of metals to lake sediments (e.g., Zn, Carignan & Tessier, 1985), which potentially weakens the integrity of the temporal record (See section *Diagenesis, diffusion, and signal preservation*). This effect is worsened by low sediment accumulation rates. Consideration of these points reveals that sedimentation rate is a crucial parameter. Low rates improve sensitivity, but worsen smoothing due to mixing and diffusion. The ideal sediment accumulation rate depends upon the objectives of the study.

While early studies of atmospheric contamination of lake sediment were undertaken close to long-established industrialized regions, much recent work has been directed at the newly industrialized countries, and also to areas remote from industry. It can be much harder to detect contamination in such areas. The low sedimentation rates generally found in upland Europe and North America, meant that small additions of trace elements significantly altered total budgets and, therefore, concentrations in the sediment. In the large lowland lakes in central China, even though current trace element pollution is comparable to that in Europe, the high sediment accumulation rates partially mask any atmospheric contamination (Boyle et al., 1999). In such environments it is necessary to pay very careful attention to estimation of the natural concentrations (e.g., Norton's TiO_2 normalization, Norton & Kahl, 1987). This is still more important in areas where atmospheric contamination is very minor. For example, in Lake Baikal, even though the sediment accumulation rate is low, the trace element supply rate is very low. Only Pb shows unambiguous evidence of atmospheric contamination, rising from a baseline of 10.9 ppm to a maximum of 14.8 ppm on average (Boyle et al., 1998). In such systems, natural variations in trace element concentration are greater than the anthropogenic forcing, and very great care must be taken in establishing the natural baseline. At such sites, it is necessary to be far more critical of the data, and to take full account of any natural processes which might lead to surface enrichments. If natural surface enrichments are present, it is then necessary to compare dated cores between sites to distinguish regional from local patterns. In any one core a slight up-core concentration increase could be interpreted in several ways. If, however, many cores are considered together it may be possible to arrive at firm conclusions about atmospheric contamination (e.g., Fitzgerald et al., 1998, review of global Hg contamination).

A further uncertainty is the transfer of atmospherically deposited pollutants from catchments to lakes. A number of studies have shown the dominance of direct atmospheric supply of metals to the lake for Pb (Dillon & Evans, 1982) and Cd and Zn (Evans et al., 1983), suggesting that the pollutants are being retained efficiently by the catchments. In a detailed multicore study of 11 lakes in Quebec and Ontario, Blais & Kalff (1993) conclude that Zn and Pb are retained entirely, but that Cu, Ni and Cr are being transferred to the lake from the catchment. Other studies suggests that the failure of catchment Pb to appear in the lakes may be due to disequilibrium (Miller & Friedland, 1994). This conclusion is shared by some theoretical studies (Tipping, 1996; Wang & Benoit, 1997). There is clearly need for work here.

Element concentration data are ideal as qualitative evidence for atmospheric contamination. However, it is desirable that lake sediment records can give quantitative estimates of loadings over time. Mackereth (1966) recognized that trace elements were supplied in labile form to the lake, and therefore their concentration in the sediment reflected capture efficiency as much as supply. Hamilton-Taylor (1979) echoed this concern, suggesting that in Windermere the metal concentrations: a) might be controlled by diatom flux and b) might be low due to outflow loss. The model outlined in the section *Models linking flux and concentration* can be used to estimate atmospheric fluxes from sediment concentration data (also, see Boyle & Birks, 1999).

Erosion

One of Mackereth's key conclusions, and one that has been highly influential, is the argument that high concentrations of minerogenic elements correspond with high erosion rates. He recognized that the same sediment signal could be explained by a reduced supply of organic matter, but argued that the former was more likely. He concluded that subsoil, richer in these elements, was preferentially supplied during catchment instability and erosion, diluting material from the more organic topsoil. Engstrom & Wright (1984) reviewed subsequent research on this topic, revealing that most studies supported Mackereth. Numerous studies have used the principles described above to infer periods of catchment stability and instability (e.g., Brubaker & Anderson, 1993). A major impact of recent human activity has usually been demonstrated (e.g., Foster & Lees, 1999). Thus, if due consideration is given to tests for the alternative, the link between mineral enrichment and erosion remains one of the most fundamental of geochemical environmental indicators.

Exotic sediment

Catchment disturbance can lead to a change in the source of clastic sediments. Source changes can be detected using variation in elemental composition (e.g., Stone et al., 1997). Such changes can be minor, such as the impact of enhanced soil erosion (e.g., Norton & Hess, 1980; Mathewes & D'Aura, 1982). Alternatively, source changes may be more radical, leading to a fundamental change in composition at the disturbance depth. For example, Punning et al. (1997) find a very great change in the composition of sediment in an Estonian lake following diversion of mine drainage water.

Characterization of the sediment composition is hindered by dilution effects. PCA biplots or simple triangular diagrams avoid this. In Figure 11, a PCA biplot clearly discriminates between different lake sediments from the Jianghan Plain (Boyle et al., 1999).

Long term catchment evolution

Catchment weathering

Mackereth argued that Na, K and Mg were preferentially supplied from the catchment by erosion, leading to enrichment of the sediment in those elements. However, he also showed that the ash-normalized concentrations increased in the minerogenic layers, which he interpreted as evidence of reduced leaching during high erosion periods. He argued that during periods of high erosion rate, deep less-weathered subsoils were supplied to the lake,

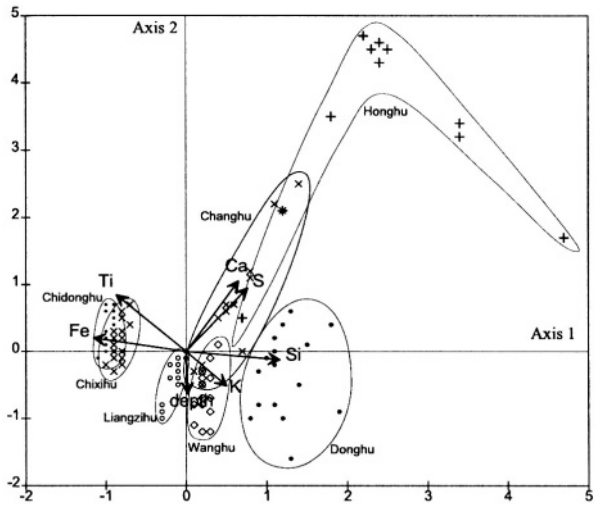


Figure 11. A principal components analysis (PCA) biplot can be used for comparing sediment compositions from different sites. A range of sediment compositions is seen for lakes from the Jianghan Plain, Central China (Figure from Boyle et al. 1999).

evidencing reduced leaching. During periods of greater catchment stability, there would be relatively more leaching, destruction of alkali bearing minerals, and thus formation of sediment relatively depleted in Na, K and Mg. This argument has been convincingly criticized by Engstrom & Wright (1984) who show that the ashed weight is a poor measure of catchment derived mineral matter, as it includes both authigenic Fe and biogenic silica. For their study lakes in Labrador, they found no increase in mineral-normalized Na, K and Mg in the mineral rich layers. However, they argue that progressive weathering of minerals in soils could reasonably appear in some long sediment records, and that their Labrador sites may simply have been too insensitive to show changes in recent weathering. Indeed, at Elk Lake, Minnesota, Dean (1997) found that the Na/Al ratio was high during the drier mid-Holocene period, and attributed this to reduced leaching of Na. This position is supported by Englund & Jørgensen (1973) who show that source area weathering is the principal factor governing between-site compositional variation in fine-grained sedimentary rocks.

Interpretation of variation in element ratios in terms of leaching must be undertaken cautiously. Such variation implies a marked alteration in sediment mineral assemblage. For example, a significant increase in clay formation would lead to reduced Na, K and Mg/mineral matter ratios. However, stratigraphic variation in mineralogy can also be caused by mechanical particle size sorting, or source heterogeneity. Changes in the proportion of top soil, degree of sediment focusing, or source of clastic material (such as an increase in sodic feldspar due enhanced aeolian influx), could all reasonably explain mineralogical change. A physical rather than chemical explanation is strongly supported by Ochsenbein et al. (1983) who show that Mg correlates with the mineral chlorite in Blelham Tarn. That an element as soluble as Mg should be bound firmly to a mineral component led them to

conclude that leaching was not a key factor. The importance of physical factors in governing element ratios is supported, for trace elements, by Moalla (1997).

Soil redox

As discussed in the section *Lake Redox,* Mackereth (1966) suggested that changes in the Fe and Mn concentrations can be used to infer changes in the redox status of the catchment soil. In essence, Mackereth argued that there were three states. First, oxidizing soil, in which neither Mn nor Fe were mobile. Second, partially reducing soil, in which Mn was mobile but Fe not. Third, reducing soil, in which both Fe and Mn were mobile. He suggested a protocol, summarized in Figure 10, for distinguishing these effects from within-lake impacts on Fe and Mn. The degree to which the effects can really be distinguished is addressed above (Section, *Lake redox*).

The assumption that soil redox governs the supply of Fe and Mn to the lake is criticized by Engstrom & Wright (1984). They argue instead that the flux of water-carried Fe and Mn is controlled dominantly by dissolved humic substances. In their Labrador study they note a striking agreement between vegetation change over time and the concentrations of Fe and Mn. Development of coniferous forest correlated with the build up of Fe and Mn, which was attributed to the association of coniferous forest with acid humic substances in soil. They report similar results from other studies, though they argue that the link remains speculative.

A more complex picture than that envisaged by Mackereth (1966) is also supported by Davison (1993), suggesting that caution must exercised when interpreting sediment Fe : Mn ratios in terms of catchment processes.

Natural environment and environmental change

Climate change

Climate change can affect many aspects of a lake system, and a number of these have been used to develop palaeolimnological proxies. Valero-Garcés et al. (1997) used the Sr and Mg contents of authigenic carbonate in a sediment core from Moon Lake, N. Dakota, along with other indicators, to reconstruct changes in effective moisture over the Holocene. Engstrom & Nelson (1991) and Xia et al. (1997) show that the Sr/Ca ratio in ostracod calcite increases with the Mg content, which is a function of the hydrological balance.

Long-term climate trends have been shown to correlate with variations in sediment biogenic silica in Lake Baikal (e.g., Coleman et al., 1995), while climatic change has been inferred from variations in aeolian supply of mineral matter to lakes in the USA (Dean, 1997).

Terrigenous source

Variation in the concentration of the minerogenic elements provides a sensitive method for discriminating between sediment sources. For example, using a PCA biplot based on five elements, Boyle et al. (1999) were able to demonstrate that each of seven lakes in the Jianghan Plain, China, had different sediment compositions (Fig. 11). This permitted rejection of a hypothesis that there was a single source of terrigenous sediment.

Palaeosalinity

Pore-water, or extractable, concentrations of Na and Cl cannot be used to reconstruct past salinity, because diffusion rates are too rapid (Lerman & Weiler, 1970). Likewise, pore-water studies of K, Mg and Ca have shown that a combination of diffusion and mineral reactions controls the present dissolved concentrations, thus eliminating any record of the initial values (Sasseville & Norton, 1975; Sasseville et al., 1975).

Slightly more promising results have been found for Br. Like the other halogens it is enriched in seawater, but unlike Cl it does become fixed to solid particles, particularly to organic matter. Mackereth (1966) observed between-lake agreement in Holocene scale total halogen (mostly Cl and Br) profiles in the English Lake District and concluded that this measured oceanicity. At Loch Lomond, Farmer (1994) attributes a Br enriched sediment horizon to a past marine incursion, supporting a link with seawater. Problems with interpreting Br come from its tendency to bind to organic matter. Thus, in lake sediment its distribution may be more a function of organic matter loading than Br loading (Mun & Bazilevich, 1962; Lange, 1970). Further, organic matter in soils also concentrates Br. Peats commonly contain 50–150 ppm Br. Thus, in upland temperate zones, a Br profile may be more an indicator of peat erosion than oceanicity. An additional problem is the possibility of Br loss from the sediment after burial, which has been demonstrated in marine sediments (Price et al., 1970).

Mackereth (1966) also proposed that B could be an indicator of oceanicity; it, too, is primarily derived from seawater. Good agreement between the B and total halogen concentration profiles led him to conclude that they were both likely to be indicators of oceanicity. However, he noted that progressive soil impoverishment could also explain the profiles. Alternatively, the successful application of B to assessing palaeosalinity in coals (e.g., Goodarzi & Swaine, 1994) suggests that it could be useful in highly organic sediments.

Future developments

Inorganic geochemistry will continue to play a central role in palaeolimnology. No techniques will replace chemical characterization of mineral matter as a basic indicator of catchment sources. As in the past, procedures will evolve, and interpretation will improve with the growing numbers of studies. With current interest in the environmental fate of pollutant trace elements in catchments, there has never been greater potential for chemical palaeolimnology to make a major contribution.

Sixteen years after the review by Engstrom & Wright (1984), problems still remain with chemical characterization of sediment components. However, the development of new reference materials promises better standardization of analytical procedures, and brings nearer the goal of more generalized interpretations.

Models for contaminant cycling in lake systems continue to improve. However, there are a number of limitations which need to be addressed. First, most models treat the lake as a single unchanging box. More realistic dynamic lake models, such as for Mn in Lake Greifen (Johnson et al., 1991) and for Hg (Diamond, 1999), need to be applied to palaeolimnological problems. Second, most current models are based on simple dissolved species. This is because the models are designed for toxicological studies (e.g., Tessier et al., 1993; Anderson & Håkanson, 1992). From a palaeolimnological point of view, precise

speciation is less important than distinguishing between trace element carried by water (dissolved, colloidal and particulate) and that captured by sediment. This is why the K_d definition of Boyle & Birks (1999) and Benoit (1995), though less chemically rigorous than that of Tessier et al. (1989), is more appropriate for palaeolimnological studies. However, if progress is to be made, the models need to be put on a sounder footing. Progress is being made with more realistic characterization of aqueous particulates, e.g., humic substances (Tipping & Hurley, 1992; Tipping, 1994), riverine particulates (Ferriera et al., 1997) and natural authigenic Fe and Mn minerals (Fortin et al., 1993; Tessier et al., 1996). Progress is also being made in the simplified functional classification of colloids in freshwaters (Buffle & Leppard 1995a,b; Buffle et al., 1998; Ledin et al., 1995; Pizarro et al., 1995), and models to predict colloid stability and floc formation are being developed (e.g., Droppo et al., 1997). Limnological models will remain crude until this vital section, linking mobility, toxicity and macro-particles, is better understood.

It is not enough, however, to know what happens in the lake. There are now numerous studies showing the importance of considering catchment sources and temporary sediment stores, and also showing that such stores can be evaluated via the study of over-bank deposits (Collins et al., 1997). Some studies have explored lake/catchment links (e.g., Hamilton-Taylor & Willis, 1990 and Cuthbert & Kalff, 1993), but there has been a tendency for geochemical palaeolimnologists to treat lakes independently of their catchments, or at most to simplify the role of the catchment. Studies of natural fallout isotope distributions may provide the key to improved models (He & Walling, 1996; He et al. 1996; Håkanson et al., 1986). Integration of lake, river and hillslope models also offers the chance to get the most out of lake sediment records. For example, a challenge to palaeolimnology is to work with the problem of evaluating the new generation of contaminant fate/flux models (e.g., Tipping, 1996; Wang & Benoit, 1997).

Finally, diffusion and mechanisms of element mobility need to be further addressed. There are good models for well-characterized dissolved components (e.g., Golterman, 1995), but trace elements remain a problem. It may be that the new DGT method (Harper et al., 1998) will offer a chance for direct evaluation of mobility at each site, and will help lead to a better general understanding.

Summary

Objectives and scope

- Inorganic geochemical palaeolimnology can be defined as the application of mainly inorganic geochemical techniques (chiefly elemental determinations and models) to sediment core samples with a view to shedding light on past environments.

- At present, inorganic geochemical methods are best used as a supporting tool in general palaeolimnology. For preliminary data analysis, and for extrapolation from more comprehensively studied sites, it has a great deal to offer as an independent method.

- The principal objective of this branch of inorganic geochemistry is palaeoenvironmental reconstruction. To achieve this it is necessary to characterize both contemporary

and past sediments, and to establish the link between sediment composition and environment. At the heart of this are characterization, classification and measurement of sediment chemical components.

Elemental analysis, sediment components, and extraction procedures

- Accurate and precise elemental determinations are essential and relatively easily achieved, with appropriate use of analytical blanks and standard reference materials.
- Element concentration is the primary data type; by comparison with accumulation rate, it is more precise, less open to interference, and often easier to interpret.
- Only the residual (aluminosilicate) fraction of the sediment is resistant to alteration. This suggests that at present only two sediment composition fractions can realistically be measured; the 'residual' fraction, and the rest ('extractable' or 'labile' fraction).
- The term 'authigenic' should be used as discussed by Engstrom & Wright (1984), having the same meaning as 'endogenic' (see Jones & Bowser, 1978). It should not be used in place of 'extractable' or 'labile'.

Palaeolimnological methods

- A wide range of useful palaeolimnological methods have been developed. Details are outlined in the sections above.
- There is a danger that palaeolimnological methods get used blindly, without adequate consideration of alternative interpretations. In particular, there has been a tendency to disregard particle size effects when interpreting variation in elemental composition
- Much more work needs to be done on characterization of potential source materials, and allowing for the effect of particle size fractionation in the catchment/lake system on changes in elemental concentrations.
- The procedure outlined by Hilton et al. (1985) remains the best available method for estimating trace element baselines. However, more work is needed to evaluate tracers which discriminate between different parts of the soil profile, or which correlate better with trace elements in soils.
- The relationships between particle flux, trace element flux and trace element concentration in sediment are complicated in deep lakes. The various effects of deep water mean that a trace element concentration peak in the sediment of a deep lake need not imply a supply event.
- It is not possible to prove or disprove the existence of redox remobilization of the common pollutant trace elements (Cd, Cu, Hg, Pb and Zn). However, remobilization of trace elements in sediment is unlikely to be an overriding factor in most situations.

Acknowledgements

Many people have influenced my view of geochemistry over the years. My thanks go to Peter Appleby, John Birks, Jorunn Larson, Helge Leivestad, Brian Price, Alastair Roberston and Tom Smayda. Thanks to Gareth Williams for the chemical data for Antonelli Pond, Santa Cruz, California, and to John Anderson for the chemical data from Nunatak Lake, Greenland.

References

Achterberg, E. P., C. M. G. van den Berg, M. Boussemart & W. Davison, 1997. Speciation and cycling of trace metals in Esthwaite Water: a productive English lake with seasonal deep-water anoxia. Geoch. Cosmoch. Acta 61: 5233–5253.

Allen, S. E., H. M. Grimshaw, J. A. Parkinson & C. Quarmby, 1974. Chemical Analysis of Ecological Materials. Blackwell Scientific, Oxford, 565 pp.

Alvarado, J. & R. Jaffé, 1998. Tube in flame atomisation: a way of enhancing detection limits in flame atomic absorption spectrometry. J. Analytical Atomic Spectrom. 13: 37–40.

Anderson, T. & L. Håkanson, 1992. Mercury content in lake sediments and suspended matter — temporal variation and relation to water chemistry. Hydrobiologia 235/236: 685–696.

American Public Health Association (APHA), American Water Works Association and Water Pollution Control Federation, 1980. Standard Methods for the Examination of Water and Wastewater. 15th Edition, 415 pp.

Appleby, P. G., 1997. Sediment records of fallout radionuclides and their application to studies of sediment-water interactions. Wat. Air Soil Pollut. 99: 573–586.

Appleby, P. G., F. Oldfield, R. Thompson & P. Huttunen, 1979. ^{210}Pb dating of annually laminated lake sediments from Finland. Nature 280: 53–54.

Aston, S. R., D. Bruty, R. Chester & R. C. Padgham, 1973. Mercury in lake sediments: a possible indicator of technological growth. Nature 241: 450–451.

Baker, L. A., D. R. Engstrom & P. L. Brezonik, 1992. Recent sulfur enrichment in the sediments of Little Rock Lake, Wisconsin. Limnol. Oceanogr. 37: 689–702.

Ball, D. F., 1964. Loss-on-ignition as an estimate of organic matter and organic carbon in non-calcareous soils. J. Soil. Sci. 15: 84–92.

Battarbee, R. W., 1980. Diatoms in lake sediments. In Berglund, B. E. (ed.) Palaeohydrological Changes in the Temperate Zone in the Last 15,000 years, Subproject B. Lake and Mire Environments, IGCP Project 158. University of Lund, Department of Quaternary Geology.

Baudo, R., 1989. Uncertainty in description of sediment chemical composition. Hydrobiologia 176/177: 441–448.

Belzile, N., J. Pizzaro, M. Filella & J. Buffle, 1996. Sediment diffusive fluxes of Fe, Mn and P in a eutrophic lake: contributions from lateral vs bottom sediments. Aquat. Sci. 58: 327–354.

Benoit, G. & H. F. Hemond, 1991. Evidence for diffusive redistribution of ^{210}Pb in lake sediments. Geoch. Cosmoch. Acta 55: 1963–1975.

Benoit, G., 1995. Evidence of the particle concentration effect for lead and other metals in fresh waters based on ultraclean techniques. Geoch. Cosmoch. Acta 59: 2677–2687.

Benoit, G. & T. F. Rozan, 1999. The influence of size distribution on the particle concentration effect and trace metal partitioning in rivers. Geoch. Cosmoch. Acta 63: 113–127.

Bertine, K. K. & M. F. Mendeck, 1978. Industrialization of New Haven, Conn., as recorded in reservoir sediments. Envir. Sci. Technol. 12: 201–207.

Birks, H. J. B., 1987. Multivariate analysis in geology and geochemistry: an introduction. Chemometric and Intelligent Laboratory Systems 2: 15–28.

Blais, J. M. & J. Kalff, 1993. Atmospheric loading of Zn, Cu, Ni, Cr and Pb to lake sediments: the role of catchment, lake morphometry, and physico-chemical properties of the elements. Biogeochem. 23: 1–22.

Borg, H., P. Andersson & K. Johansson, 1989. Influence of acidification of metal fluxes in Swedish forest lakes. Sci. Total Envir. 87/88: 241–253.

Boudreau, B. P., 1999. Metals and models: diagenetic modelling in freshwater lacustrine sediments. J. Paleolim. 22: 227–251.

Boyle, J. F., 1984. The Origin and Geochemistry of the Metalliferous Sediments of the Troodos Massif, Cyprus. Ph.D. Thesis. University of Edinburgh, 200 pp.

Boyle, J. F., 1994. Acidification and sediment aluminium: palaeolimnological interpretation. J. Paleolim. 12: 181–187.

Boyle, J. F., 2000. Rapid elemental analysis of sediment samples by isotope source XRF. J. Paleolim. 23: 213–221.

Boyle, J. F. & H. J. B. Birks, 1999. Predicting heavy metal concentrations in the surface sediments of Norwegian headwater lakes from atmospheric deposition: an application of a simple sediment-water partitioning model. Wat. Air Soil Pollut. 114: 27–51.

Boyle, J. F., A. W. Mackay, N. L. Rose, R. J. Flower & P. G. Appleby, 1998. Sediment heavy metal record in Lake Baikal: natural and anthropogenic sources. J. Paleolim. 20: 135–150.

Boyle, J. F., N. L. Rose, H. Bennion, H. Yang & P. G. Appleby, 1999. Environmental impact in the Jianghan Plain: evidence from lake sediments. Wat. Air Soil Pollut. 112: 21–40.

Brezonik, P. L. & D. R. Engstrom, 1998. Modern and historic accumulation rates of phosphorus in Lake Okeechobee, Florida. J. Paleolim. 20: 31–46.

Brubaker, H. U. & P. M. Anderson, 1993. A 12000 year record of vegetation change and soil development from Wien Lake, central Alaska. Can. J. Botany 71: 1133–1142.

Bryan, W. B., L. W. Finger & F. Chayes, 1969. Estimating proportions in petrographic mixing equations by least-squares approximation. Science 163: 926–927.

Bryant, C. L., J. G. Farmer, A. B. MacKenzie, A. E. Bailey-Watts & A. Kirika, 1997. Manganese behaviour in the sediments of diverse Scottish freshwater lochs. Limnol. Oceanogr. 42: 918–929.

Buckley, D. E. & R. E. Cranston, 1971. Atomic absorption analysis of 18 elements from a single decomposition of aluminosilicate. Chem. Geol. 7: 273–284.

Buffle, J. & G. G. Leppard, 1995a. Characterization of aquatic colloids and macromolecules. 1. Structure and behaviour of colloidal material. Envir. Sci. Technol. 29: 2169–2175.

Buffle, J. & G. G. Leppard, 1995b. Characterization of aquatic colloids and macromolecules. 2. Key role of physical structures on analytical results. Envir. Sci. Technol. 29: 2175–2184.

Buffle, J., K. J. Wilkinson, S. Stoll, M. Filella & J. W. Zhang, 1998. A generalized description of aquatic colloidal interactions: the three-colloidal component approach. Envir. Sci. Technol. 32: 2887–2899.

Carignan, R. & J. O. Nriagu, 1985. Trace metal deposition and mobility in the sediments of two lakes near Sudbury, Ontario. Geoch. Cosmoch. Acta 49: 1753–1764.

Carignan, R. & A. Tessier, 1985. Zinc deposition in acid lakes: the role of diffusion. Science 228: 1524–1526.

Carignan, R. & A. Tessier, 1988. The co-diagenesis of sulfur and iron in acid lake sediments of southwestern Québec. Geoch. Cosmoch. Acta 52: 1179–1188.

Catterick, T., H. Handley & S. Merson, 1995. Analytical Accuracy in ICP-MS Using Isotope Dilution and its Application to Reference Materials. Atomic Spectroscopy 16: 229–234.

Collins, A. L., D. E. Walling & G. J. L. Leeks, 1996. Composite fingerprinting of the spatial source of fluvial suspended sediment: a case study of the Exe and Severn River basins, UK. In: Proceedings CNRS Conference on floods, slopes and river beds, Paris, 1995. Environment 2: 41–54.

Collins, A. L., D. E. Walling & G. J. L. Leeks, 1997. Use of the geochemical record preserved in floodplain deposits to reconstruct recent changes in river basin sediment sources. Geomorphology 19: 151–167.

Coleman, S. M., J. A. Peck, E. B. Karabanov, S. J. Carter, J. P. Bradbury, J. W. King & D. F. Williams, 1995. Continental climate response to orbital forcing from biogenic silica records. Nature 378: 769–771.

Cornett, R. J., L. Chant & R. D. Evans, 1989. Nickel diagenesis and partitioning in lake sediments. Sci. Total. Envir. 87/88: 157–170.

Cornett, R. J., L. Chant & B. Risto, 1992. Arsenic transport between water and sediments. Hydrobiologia 235/236: 533–544.

Cornwell, J. C., 1986. Diagenetic trace-metal profiles in Arctic lake sediments. Envir. Sci. Technol. 20: 299–303.

Crecelius, E. A. & D. Z. Piper, 1973. Particulate lead contamination recorded in sedimentary cores from Lake Washington, Seattle. Envir. Sci. Technol. 7: 1053–1055.

Crusius, J. & R. F. Anderson, 1995. Evaluating the mobility of ^{137}Cs, $^{239+240}Pu$ and ^{210}Pb from their distributions in laminated lake sediments. J. Paleolim. 13: 119–141.

Cuthbert, I. D. & J. Kalff, 1993. Empirical models for estimating the concentrations and exports of metals in rural rivers and streams. Wat. Air Soil Pollut. 71: 205–230.

Davis, J. C., 1986. Statistics and Data Analysis in Geology. Wiley, New York, 2nd Ed, 646 pp.

Davis, R. B., C. T. Hess, S. A. Norton, D. W. Hanson, K. D. Hoagland & D. S. Anderson, 1984. ^{137}Cs and ^{210}Pb dating of sediments from soft-water lakes in New England (USA) and Scandinavia, a failure of ^{137}Cs dating. Chem. Geol. 44: 151–185.

Davis, R. B. & S. A. Norton, 1978. Paleolimnologic studies of human impact on lakes in the United States, with emphasis on recent research in New England. Pol. Arch. Hydrobiol. 25: 99–115.

Davis, R. B., S. A. Norton, C. T. Hess & D. F. Brakke, 1983. Paleolimnological reconstruction of the effects of atmospheric deposition of acids and heavy metals on the chemistry and biology of lakes in New England and Norway. Hydrobiologia 103: 113–123.

Davison, W., 1993. Iron and manganese in lakes. Earth Sci. Rev. 34: 119–163.

Dean, W. E., 1974. Determination of carbonate and organic matter in calcareous sediments and sedimentary rocks by loss on ignition: comparison with other methods. J. Sediment. Petrol. 44: 242–248.

Dean, W. E., 1981. Carbonate minerals and organic matter in sediments of modern north temperate hard-water lakes. Soc. Econ. Paleont. Mineral. Special Publication 31: 213–231.

Dean, W. E., 1997. Rates, timing, and cyclicity of Holocene eolian activity in north-central United States: evidence from varved lake sediments. Geology 25: 331–334.

Dean, W. E., 1999. The carbon cycle and biogeochemical dynamics in lake sediments. J. Paleolim. 21: 375–393.

Dean, W. E. & E. Gorham, 1998. Magnitude and significance of carbon burial in lakes, reservoirs and peatlands. Geology 26: 535–538.

Dean, W. E., E. Gorham & D. J. Swaine, 1988. Geochemistry of surface sediments in the English Lake District. In Round, F. E. (ed.) Algae and the Aquatic Environment: Bristol, England. Biopress Ltd.: 244–271.

Dean, W. E., E. Gorham & D. J. Swaine, 1993. Geochemistry of surface sediments of Minnesota lakes. Geol. Soc. Am. Spec. Paper 276: 115–133.

Deer, W. A., R. A. Howie & J. Zussman, 1966. An Introduction to the Rock-Forming Minerals. Longman, Harlow, 528 pp.

Diamond, M. L., 1999. Development of a fugacity/aquivalence model of mercury dynamics in lakes. Wat. Air Soil Pollut. 111: 337–357.

Diamond, M. L., D. Mackay, R. J. Cornett & L. A. Chant, 1990. A model of the exchange of inorganic chemicals between water and sediments. Envir. Sci. Technol. 24: 713–722.

Digerfeldt, G., 1972. The post-glacial development of Lake Trummen. Folia limnol. Scand. 16: 1–104.
Digerfeldt, G., 1975. The post-glacial development of Ranviken Bay in Lake Immeln. III. Palaeolimnology. Geol. För. Stockh. Förh. 97: 13–28.
Dillon, P. J. & R. D. Evans, 1982. Whole-lake lead burdens in sediments of lakes in southern Ontario, Canada. Hydrobiologia 91: 121–130.
Dillon, P. J. & H. E. Evans, 1993. A comparison of phosphorus retention in lakes determined from mass balance and sediment core calculations. Wat. Res. 27: 659–668.
Dillon, P. J., H. E. Evans & P. J. Scholer, 1988. The effect of acidification on metal budgets of lakes and catchments. Biogeochem. 5: 201–220.
Droppo, I. G., G. G. Leppard, D. T. Flannigan & S. N. Liss, 1997. The freshwater floc: a functional relationship of water and organic and inorganic floc constituents affecting suspended sediment properties. Wat. Air Soil Pollut. 99: 43–53.
Englund, J.-O. & P. Jørgensen, 1973. A chemical classification system for argillaceous sediments and factors affecting their composition. Geologiska Föreningen i Stockholm Förhandlingar 95: 87–97.
Engstrom, D. R. & S. R. Nelson, 1991. Paleolsalinity from trace metals in fossil ostracods compared with observational records at Devils Lake, North Dakota, USA. Palaeogeogr. Palaeoclim. Palaeoecol. 83: 295–312.
Engstrom D. R. & E. B. Swain, 1986. The chemistry of lake sediments in time and space. Hydrobiologia 143: 37–44.
Engstrom, D. R. & H. E. Wright Jr., 1984. Chemical stratigraphy of lake sediments as a record of environmental change. In Haworth, E. Y. & J. W. G. Lund (eds.) Lake Sediments and Environmental History. Leicester University Press, Leicester: 11–68.
Engstrom, D. R., E. B. Swain, T. A. Henning, M. E. Brigham & P. L. Brezonik, 1994. Atmospheric mercury deposition to lakes and watersheds — a quantitative reconstruction from multiple sediment cores. Advances in Chemistry Series 237: 33–66.
Evans, H. E., P. J. Dillon & L. A. Molot, 1997. The use of mass balance investigations in the study of the biogeochemical cycle of sulfur. Hydrological Processes 11: 765–782.
Evans, H. E., P. J. Smith & P. J. Dillon, 1983. Anthropogenic zinc and cadmium burdens in sediments of selected southern Ontario lakes. Can J. Fish. Aquat. Sci. 40: 570–579.
Farmer, J. G., 1994. Environmental change and the chemical record in Loch Lomond sediments. Hydrobiologia 290: 39–49.
Farmer, J. G. & M. A. Lovell, 1986. Natural enrichment of arsenic in Loch Lomond sediments. Geoch. Cosmoch. Acta 50: 2059–2067.
Fedorowich, J. S., J. P. Richards, J. C. Jain, R. Kerrich & J. Fan, 1993. A rapid method for REE and trace-element analysis using laser sampling ICP on direct fusion whole-rock glasses. Chem. Geol. 106: 229–249.
Ferdelman, T. G., T. M. Church & G. W. Luther, 1991. Sulfur enrichment of humic substances in a Delaware salt marsh sediment core. Geoch. Cosmoch. Acta 55: 979–988.
Ferriera, J. R., A. J. Lawlor, J. M. Bates, K. J. Clarke & E. Tipping, 1997. Chemistry of riverine and estuarine suspended particles from the Ouse-Trent system, UK. Colloids and Surfaces A: Physicochemical and Engineering Aspects 120: 183–198.
Fiedler, H. D., R. Rubio, G. Rauret & I. Casals, 1999. Acid volatile sulfide determination in sediment using elemental analyzer with thermal conductivity detector. Talanta 48: 403–407.
Findlay, A. D., D. W. Thompson & E. Tipping, 1996. Electrokinetic properties of oxide particles in natural waters. Colloids and Surfaces A: Physicochemical and Engineering Aspects 111: 203–212.
Fitton, J. G., D. E. James & M. F. Thirwall, 1984. A User's Guide to the X-Ray Fluorescence Analysis of Rock Samples. Internal report, Grant Institute of Geology, Edinburgh University.
Fitzgerald, W. F., D. R. Engstrom, R. P. Mason & E. A. Nater, 1998. The case for atmospheric mercury contamination in remote areas. Envir. Sci. Technol. 32: 1–7.

Flower, R. J., A. W. Mackay, N. L. Rose, J. F. Boyle, J. A. Dearing, P. G. Appleby, A. E. Kuzmina & L. Z. Granina, 1995. Sedimentary records of recent environmental change in Lake Baikal, Siberia. The Holocene 5: 323–327.

Fortin, D., G. G. Leppard & A. Tessier, 1993. Characteristics of lacustrine diagenetic iron oxyhydroxides. Geoch. Cosmoch. Acta 57: 4391–4404.

Förstner, U., 1976. Lake sediments as indicators of heavy metal pollution. Naturwissenschaften 63: 465–470.

Förstner, U. & G. T. Wittmann, 1979. Metal Pollution in the Aquatic Environment. Springer, New York, 486 pp.

Foster, I. D. L. & J. A. Lees, 1999. Changes in the physical and geochemical properties of suspended sediment delivered to the headwaters of LOIS river basins over the last 100 yrs: a preliminary analysis of lake and reservoir bottom sediments. Hydrological Processes 11: 1067–1086.

Foster, I. D. L., S. M. Charlesworth & D. H. Keen, 1991. A comparative study of heavy metals and pollution in four reservoirs in the English Midlands. Hydrobiologia 214: 155–162.

Gaillard, M.-J., J. A. Dearing, F. El-Daoushy, M. Enell & H. Håkansson, 1991. A multidisciplinary study of the lake Bjäresjösjön (S. Sweden): land-use history, soil erosion, lake trophy and lake-level fluctuations during the last 3000 years. Hydrobiologia 214: 107–114.

Garrels, R. M. & F. T. MacKenzie, 1971. Evolution of Sedimentary Rocks. Norton & Company, New York, 397 pp.

Gelinas, Y., M. Lucotte & J. P. Schmidt, 2000. History of the atmospheric deposition of major and trace elements in the industrialized St. Lawrence Valley, Quebec, Canada. Atmos. Envir. 34: 1797–1810.

Golterman, H. L., 1995. Remarks on numerical and analytical methods to calculate diffusion in water/sediment systems. Hydrobiologia 315: 69–88.

Golterman, H., J. Paing, L. Serrano & E. Gomez, 1998. Presence of and phosphate release from polyphosphates and phytate phosphate in lake sediments. Hydrobiologia 364: 99–104.

Goodarzi, F. & D. J. Swaine, 1994. The influence of geological factors on the concentration of boron in Australian and Canadian coals. Chem. Geol. 118: 301–318.

Håkanson, L., J. E. Brittain, L. Monte, R. Heling, U. Bergström & V. Suolanen, 1996. Modelling of radiocesium in lakes — the VAMP model. J. Envir. Radioactivity 33: 255–398.

Hall, G. E. M., G. Gauthier, J.-C. Pelchat, P. Pelchat & J. E. Vaive, 1996. Application of a sequential extraction scheme to ten geological certified reference materials for the determination of 20 elements. J. Analyt. Atom. Spectr. 11: 787–796.

Hall, R. I. & J. P. Smol, 1999. Diatoms as indicators of lake eutrophication. In Stoermer, E. F. & J. P. Smol (eds.) The Diatoms: Applications for the Environmental and Earth Sciences. Cambridge University Press, Cambridge: 128–168.

Hamilton-Taylor, J., 1979. Enrichments of zinc, lead, and copper in recent sediments of Windermere, England. Env. Sci. Technol. 13: 693–698.

Hamilton-Taylor, J. & W. Davison, 1995. Redox-driven cycling of trace elements in lakes. In Lerman, A., D. Imboden & J. Gat (eds.) Physics and Chemistry of Lakes. Springer-Verlag, Berlin, 334 pp.

Hamilton-Taylor, J., W. Davison & K. Morfett, 1996. The biogeochemical cycling of Zn, Cu, Fe, Mn, and dissolved organic C in a seasonally anoxic lake. Limnol. Oceanogr. 41: 408–418.

Hamilton-Taylor, J., L. Guisti, W. Davison, W. Tych & C. N. Hewitt, 1997. Sorption of trace metals (Cu, Pb, Zn) by suspended lake particles in artificial (0.005 M $NaNO_3$) and natural (Esthwaite Water) freshwaters. Colloids and Surfaces A; Physicochemical and Engineering Aspects 120: 205–219.

Hamilton-Taylor, J., & M. Willis, 1990. A quantitative assessment of the sources and general dynamics of trace metals in a soft-water lake. Limnol. Oceanogr. 35: 840–851.

Hamilton-Taylor, J., M. Willis & C. S. Reynolds, 1984. Depositional fluxes of metals and phytoplankton in Windermere as measured by sediment traps. Limnol. Oceanogr. 29: 695–710.

Harper, M. P., W. Davison, H. Zhang & W. Tych, 1998. Kinetics of metal exchange between solids and solutions in sediments and soils interpreted from DGT measured fluxes. Geoch. Cosmoch. Acta 62: 2757–2770.

He, Q. & D. E. Walling, 1996. Use of fallout Pb-210 measurements to investigate longer-term rates and patterns of overbank sediment deposition on the floodplains of lowland rivers. Earth Surf. Process. Landforms 21: 141–154.

He, Q., D. E. Walling & P. N. Owens, 1996. Interpreting the ^{137}Cs profiles observed in several small lakes and reservoirs in Southern England. Chem. Geol. 129: 115–131.

Heathwaite, A. L., 1994. Chemical fractionation of lake sediments to determine the effects of land-use change on nutrient loading. J. Hydrol. 159: 395–421.

Hilton, J., W. Davison & U. Ochsenbein, 1985. A mathematical model for analysis of sediment core data: implications for enrichment factor calculations and trace-metal transport mechanisms. Chem. Geol. 48: 281–291.

Hilton, J., E. Rigg, W. Davison, J. Hamilton-Taylor, M. Kelly & F. R. Livens, 1995. Modeling and interpreting element ratios in water and sediments: a sensitivity analysis of post-Chernobyl Ru : Cs ratios. Limnol. Oceanogr. 40: 1302–1309.

Hornburg, V. & B. Luer, 1999. Vergleich zwischen total-und königswasserextrahierbaren elementgehalten in natürlichen böden und sedimenten. J. Plant Nutrition Soil Sci. 162: 131–137.

Horowitz, A. J., K. A. Elrick, J. A. Robbins & R. B. Cook, 1995. The effects of mining and related activities on the sediment trace-element geochemistry of Lake Coeur D'Alene, Idaho, USA. 2: Subsurface sediments. Hydrological Processes 9: 35–54.

Hsu, Y.-S., J. J. Walker & D. E. Ogren, 1986. A stepwise method for determining the number of component distributions in a mixture. Math. Geol. 18: 153–160.

Huerta-Diaz, M. A., A. Tessier & R. Carignan, 1998. Geochemistry of trace metals associated with reduced sulfur in freshwater sediments. Applied Geochem. 13: 213–233.

ten Hulscher, Th. E. M., G. A. J. Mol & F. Lüers, 1992. Release of metals from polluted sediments in a shallow lake: quantifying resuspension. Hydrobiologia 235/236: 97–105.

Huttunen, P. & K. Tolonen, 1977. Human influence on the history of lake Lovojärvi, S. Finland, Suom. Mus. 1975: 68–105.

Huttunen, P., J. Meriläinen & K. Tolonen, 1978. The history of a small dystrophied forest lake, southern Finland. Pol. Arch. Hydrobiol. 25: 189–202.

Imboden, D. M., J. Tchopp & W. Stumm, 1980. Die Rekonstruktion früherer Stofffracten in einem See mittels Sedimentuntersuchungen. Schweiz. Z. Hydrol. 42: 1–14.

Johnson, C. A., M. Ulrich, L. Sigg, D. M. Imboden, 1991. A mathematical model of the manganese cycle in a seasonally anoxic lake. Limnol. Oceanogr. 36: 1415–1426.

Johansson, K., E. Bringmark, L. Lindevall & A. Wilander, 1995. Effects of acidification on the concentrations of heavy metals in running waters in Sweden. Wat. Air Soil Pollut. 85: 779–784.

Jones, B. F. & C. J. Bowser, 1978. The mineralogy and related chemistry of lake sediments. In Lerman, A. (ed.) Lakes — Chemistry, Geology, Physics. Springer, New York, 363 pp.

Jonsson, A. & M. Jansson, 1997. Sedimentation and mineralisation of organic carbon, nitrogen and phosphorus in a large humic lake northern Sweden. Arch. Hydrobiol. 141: 45–65.

Kelts K. & K. J. Hsü, 1978. Freshwater carbonate sedimentation. In Lerman, A. (ed.) Lakes — Chemistry, Geology, Physics. Springer, New York, 363 pp.

Kemp, A. L. W. & R. L. Thomas, 1976. Impact of man's activities on the chemical composition of the sediments of Lakes Ontario, Erie and Huron. Wat. Air Soil Pollut. 5: 469–490.

Klinkhammer, G., 1980. Early diagenesis in sediments from the eastern equatorial Pacific, II. Pore water metal results, Earth Planet Sci. Lett. 49: 81–101.

Klinkhammer, G., D. T. Heggie & D. W. Graham, 1982. Metal diagenesis in oxic marine sediments. Earth Planet Sci. Lett. 61: 211–219.

Klovan, J. E. & J. Imbrie, 1971. An algorithm and FORTRAN-IV program for large-scale factor

analysis and calculation of factor scores. J. Math. Geol. 3: 61–77.
Kowalewska, Z., E. Bulska & A. Hulanicki, 1998. The effect of sample preparation on metal determination in soil by FAAS. Fresnius. J. Analyt. Chem. 362: 125–129.
Krauskopf, K. B., 1982. Introduction to Geochemistry. 2nd edition, McGraw-Hill, Singapore. 617 pp.
Lange, J., 1970. Gcochemische Unteruchungen an Sedimenten des Persischen Golfes. Contr. Min. Petr. 28: 288–305.
Ledin, A., S. Karlsson, A. Düker & B. Allard, 1995. Characterisation of the submicrometer phase in surface waters — a review. Analyst 120: 603–608.
Lerman, A & R. R. Weiler, 1970. Diffusion and accumulation of chloride and sodium in Lake Ontario sediment. Earth Planet. Sci. Lett. 10: 150–156.
Likens, G. E. & M. B. Davis, 1975. Post-glacial history of Mirror Lake and its watershed in New Hampshire, USA: an initial report. Verh. int. Ver. Limnol. 19: 982–993.
Liu, J., R. E. Sturgeon, V. J. Boyko & S. N. Willie, 1996. Determination of chromium in marine sediment reference material BCSS-1. Fresnius J. Analyt. Chem. 356: 416–419.
Lofts, S. & E. Tipping, 1998. An assemblage model for cation binding by natural particulate matter. Geoch. Cosmoch. Acta 62: 2609–2625.
López-Sánchez, J. F., A. Sahuquillo, H. D. Fiedler, R. Rubio, G. Rauret, H. Muntau & P. Quevauviller, 1998. CRM 601, a stable material for its extractable content of heavy metals. Analyst 123: 1675–1677.
Mach, C. E. & P. L. Brezonik, 1989. Trace metal research at Little Rock Lake, Wisconsin: background data, enclosure experiments, and the first three years of acidification. Sci. Total Envir. 87/88: 269–285.
Mackereth, F. J. H., 1966. Some chemical observations on post-glacial lake sediments. Phil. Trans. R. Soc. Lond. B250: 165–213.
Malo, B. A., 1977. Partial extractions of metals from aquatic sediments. Envir. Sci. Technol. 11: 277–282.
Mas, F., J. M. Estella & V. Cerda, 1990. Determination of phosphate in water by flow injection analysis. Wat. Air Soil Pollut. 52: 359–368.
Mathewes, R. W. & J. M. D'Auria, 1982. Historic changes in an urban watershed determined by pollen and geochemical analyses of lake sediment. Can J. Earth Sci. 19: 2114–2125.
Matschullat, J. & M. Wyrobek, 1993. Controlled experimental acidification of lake sediments and resulting trace metal behaviour. Wat. Air Soil Pollut. 69: 393–403.
McKee, J. D., T P. Wilson, D. T. Long & R. M. Owen, 1989. Pore-water profiles and early diagenesis of Mn, Cu and Pb in sediments from large lakes. J. Great Lakes Res. 15: 68–83.
Mester, Z., C. Cresmisini, E. Ghiara & R. Morabito, 1998. Comparison of two sequential extraction procedures for metal fractionation in sediment samples. Analyt. Chim. Acta 359: 133–142.
Miesch, A. T., 1981. Computer methods for geochemical and petrologic mixing problems. In Merriam, D. F. (ed.) Computer Applications in the Earth Sciences: an Update on the 70s. Plenum Press, New York and London: 243–265.
Miller, E. K. & A. J. Friedland, 1994. Lead migration in forest soils: response to changing atmospheric inputs. Envir. Sci. Technol. 28: 662–669.
Moalla, S. M. N., 1997. Physical fractionation of trace and rare earth elements in the sediments of Lake Nasser. Talanta 45: 213–221.
de Montigny, C. & Y. T. Prairie, 1993. The relative importance of biological and chemical processes in the release of phosphorus from a highly organic sediment. Hydrobiologia 253: 141–150.
Morfett, K., W. Davison & J. Hamilton-Taylor, 1988. Trace metal dynamics in a seasonally anoxic lake. Envir. Geol. Wat. Sci. 11: 107–114.
Mortlock, R. A. & P. N. Froelich, 1989. A simple method for the rapid determination of biogenic opal in pelagic marine sediments. Deep-Sea Res. 30: 1415–1426.

Mun, A. I. & Z. A. Bazilevich, 1962. Distribution of bromine in lacustrine bottom muds. Geochemistry 2: 199–205.

Negi, B. S., V. Meenakshy & T. M. Krishnamoorthy, 1997. K_0 method of quantification in neutron activation analysis as applied to environmental samples. Envir. Monit. Assess. 47: 303–313.

Norton, S. A., 1986. A review of the chemical record in lake sediment of energy related air pollution and its effects on lakes. Wat. Air Soil Pollut. 30: 331–345.

Norton, S. A. & C. T. Hess, 1980. Atmospheric deposition in Norway during the last 300 years as recorded in SNSF lake sediments. I. Sediment dating and chemical stratigraphy. Proc. Int. Conf. Ecol. Impact Acid Precip. Norway 1980, SNSF Project.

Norton, S. A. & J. S. Kahl, 1987. A comparison of lake sediments and ombrotrophic peat deposits as long term monitors of atmospheric pollution. New Approaches to Monitoring Aquatic Ecosystems, ASTM STP 940, T. P. Boyle, American Society for Testing and Materials, Philadelphia, 40–57.

Norton, S. A. & J. S. Kahl, 1991. Progress in understanding the chemical stratigraphy of metals in lake sediments in relation to acidic deposition. Hydrobiologia 214: 77–84.

Norton, S. A., R. W. Bienert, M. W. Binford & J. S. Kahl, 1992. Stratigraphy of total metals in PIRLA sediment cores. J. Paleolim. 7: 191–214.

Nürnberg, G. K. & P. J. Dillon, 1993. Iron budgets in temperate lakes. Can. J. Fish. Aquat. Sci. 50: 1728–1737.

Ochsenbein, U., W. Davison, J. Hilton & E. Y. Haworth, 1983. The geochemical record of major cations and trace metals in a productive lake — analysis of thinly sliced sediment samples characterised by diatom stratigraphy. Arch. Hydrobiol. 98: 463–488.

Oluyedun, O. A., S. O. Ajayi & G. W. van Loon, 1991. Methods for fractionation of organic phosphorus in sediments. Sci. Total Envir. 106: 243–252.

Pardo, P., J. F. López-Sánchez, G. Rauret, V. Ruban, H. Muntau & P. Quevauviller, 1999. Study of the stability of extractable phosphate content in a candidate reference material using a modified Williams extraction procedure. Analyst 124: 407–41.

Peters, G. M., W. A. Maher, D. Jolley, B. I. Carroll, V. G. Gomez, A. V. Jenkinson & G. D. McOrist, 1999. Selenium contamination, resdistribution and remobilization in sediments of Lake Macquarie, NSW. Organic Geochem. 30: 1287–1300.

Petersen, W., K. Wallmann, P. Li, F. Schroeder & H.-D. Knauth, 1995. Exchange of trace metals at the sediment-water interface during early diagenesis processes. Mar. Freshwater Res. 46: 19–26.

Pizzaro, J., N. Belzile, M. Filella, G. G. Leppard, J. C. Negre, D. Perret & J. Buffle, 1995. Coagulation/sedimentation of submicron iron particles in a eutrophic lake. Water Res. 29: 617–632.

Price, N. B., S. E. Calvert & P. G. W. Jones, 1970. The distribution of iodine and bromine in the sediments of the southwestern Barents Sea. J. Mar. Res. 28: 22–35.

Punning, J.-M., J. F. Boyle, T. Alliksaar, R. Tann & M. Varvas, 1997. Human impact on the history of Lake Nômmejärv, NE Estonia: a geochemical and palaeobotanical study. The Holocene 7: 91–99.

Quevauviller, P., 1998. Operationally defined extraction procedures for soil and sediment analysis. Trends in Analytical Chem. 17: 632–643.

Quevauviller, P., G. U. Fortunati, M. Filippelli, F. Baldi, M. Bianchi & H. Muntau, 1996. Interlaboratory study to improve the quality control of methylmercury determination in sediment. Applied Organometallic Chem. 10: 537–544.

Quevauviller, P., G. Rauret, J.-F. López-Sánchez, R. Rubio, A. Ure & H. Muntau, 1997. Certification of trace metal extractable contents in a sediment reference material (CRM 601) following a three-step sequential extraction procedure. Sci. Total Envir. 205: 223–234.

Ragueneau, O. & P. Treguer, 1994. Determination of biogenic silica in coastal waters — applicability and limits of the alkaline digestion method. Mar. Chem. 45: 43–51.

Raksasataya, M., A. G. Langdon & N. D. Kim, 1996. Assessment of the extent of lead redistribution during sequential extraction by two different methods. Analyt. Chim. Acta 332: 1–14.

Renberg, I., 1976. Paleolimnological investigations in Lake Prästsjön. Early Norrland 9: 113–159.

Renberg, I., 1985. Influence of acidification on the sediment chemistry of Lake Gårdsjön, SW Sweden. Ecol. Bull. 37: 246–250.

Renberg, I., 1986. Concentration and annual accumulation values of heavy metals in lake sediments: their significance in studies of the history of heavy metal pollution. Hydrobiologia 143: 379–385.

Reuter, R., R. F. Wright & U. Förstner, 1981. Distribution and chemical form of heavy metals in sediment cores from two Norwegian lakes affected by acid precipitation. In Heavy Metals in the Environment, CEP Consultants, Edinburgh: 318–321.

Rippey, B., R. J. Murphy & S. W. Kyle, 1982. Anthropogenically derived changes in the sedimentary flux of Mg, Cr, Ni, Cu, Zn, Hg, Pb, and P in Lough Neagh, Northern Ireland. Envir. Sci. Technol. 16: 23–30.

Rognerud, S. & E. Fjeld, 1993. Regional survey of heavy metals in lake sediments in Norway. Ambio 22: 206–212.

Rowan, D. J., R. J. Cornett, K. King & B. Risto, 1995a. Sediment focusing and ^{210}Pb dating: a new approach. J. Paleolim. 13: 107–118.

Rowan, D. J., J. Kalff & J. B. Rasmussen, 1992. Profundal sediment organic content and physical character do not reflect lake trophic status, but rather reflect inorganic sedimentation and exposure. Can. J. Fish. Aquat. Sci. 49: 1431–1438.

Rowan, D. J., J. B. Rasmussen & J. Kalff, 1995b. Optimal allocation of sampling effort in lake sediment studies. Can. J. Fish. Aquat. Sci. 52: 2146–2158.

Sahuquillo, A., J. F. López-Sánchez, R. Rubio, G. Rauret, R. P. Thomas, C. M. Davidson & A. M. Ure, 1999. Use of a certified reference material for extractable trace metals to assess sources of uncertainty in the BCR three-stage sequential extraction procedure. Analyt. Chim. Acta 382: 317–327.

Sakata, M., 1985. Diagenetic remobilisation of manganese, iron, copper and lead in anoxic sediment of a freshwater pond. Wat. Res. 19: 1033–1038.

Santschi, P. H., 1984. Particle flux and trace metal residence time in natural waters. Limnol. Oceanogr. 29: 1100–1108.

Santschi, P., U. P. Nyffeler, R. F. Anderson, S. L. Schiff, P. O'Hara & R. H. Hesslein, 1984. Response of radioactive trace metals to acid-base titrations in controlled experimental ecosystems: evaluation of transport parameters for application to whole lake radiotracer experiments. Can. J. Fish. Aquat. Sci. 43: 60–77.

Saraswati, R., T. W. Vetter & R. L. Watters, 1995. Determination of arsenic, selenium and mercury in an estuarine sediment standard reference material using flow injection and atomic absorption spectrometry. Mikrochimica Acta 118: 163–175.

Sasseville, D. R. & S. A. Norton, 1975. Present and historic geochemical relationships in four Maine lakes. Limnol. Oceanogr. 20: 699–714.

Sasseville, D. R., S. A. Norton & R. B. Davis, 1975. Comparative interstitial water and sediment chemistry in oligotrophic and mesotrophic lakes, Maine, USA Verh. int. Ver. Limnol. 19: 367–371.

Schaller, T., H. C. Moor & B. Wehrli, 1997. Sedimentary profiles of Fe, Mn, V, Cr, As and Mo as indicators of benthic redox conditions in Baldeggersee. Aquatic Sciences 59: 345–361.

Schindler, P. W., 1975. The regulation of trace metal concentrations in natural water systems: a chemical approach. In: Proc. First Speciality Symp. Atmospheric Contribution to the Chemistry of Lake Water. Internat. Assoc. Great Lakes Res., 28 October 1975.

Shapiro, J., W. T. Edmondson & D. E. Allison, 1971. Changes in the chemical composition of sediments of Lake Washington 1958–1971. Limnol. Oceanogr. 16: 437–452.

Shaw, T. J., J. M. Gieskes & R. A. Jahnke, 1990. Early diagenesis in differing environments: the response of transition metals in pore water. Geoch. Cosmoch. Acta 54: 1233–1246.

Sigg, L., M. Sturn & D. Kistler, 1987. Vertical transport of heavy metals by settling particles in Lake Zurich. Limnol. Oceanogr. 32: 112–130.

Simola, H. & M. Lodenius, 1982. Recent increase in mercury sedimentation in a forest lake attributable to peatland drainage. Bull. Envir. Contam. Toxicol. 29: 298–305.

Smodiš, B., R. Jaćimović, G. Medin & S. Jovanić, 1993. Instrumental neutron activation analysis of sediment reference materials using the k_0-standardization method. J. Radioanalytical Nuclear Chem. 169: 177–185.

Song Y. & G. Müller, 1995. Biogeochemical cycling of nutrients and trace metals in anoxic freshwater sediments of the Neckar River, Germany. Mar. Freshwater Res. 46: 237–243.

Sprenger, M. & A. McIntosh, 1989. Relationship between concentrations of aluminum, cadmium, lead, and zinc in water, sediments and aquatic macrophytes. Arch. Envir. Contam. Toxicol. 18: 225–231.

Stone, P., P. M. Green & T. M. Williams, 1997. Relationship of source and drainage geochemistry in the British paratectonic Caledonides — an exploratory regional assessment. Trans. Inst. Mining Metall. B- Applied Earth Science 106: B79–B84.

Tessier, A., P. G. C. Campbell & M. Bisson, 1979. Sequential extraction procedure for the speciation of particulate trace metals. Analyt. Chem. 51: 844–851.

Tessier, A., R. Carignan, B. Dubreuil & F. Rapin, 1989. Partitioning of zinc between the water column and the oxic sediments in lakes. Geoch. Cosmoch. Acta 53: 1511–1522.

Tessier, A., Y. Couillard, P. G. C. Campbell & J. C. Auclair, 1993. Modeling Cd partitioning in oxic lake sediments and Cd concentrations in the freshwater bivalve *Anodonta grandis*. Limnol. Oceanogr. 38: 1–17.

Tessier, A., D. Fortin, N. Belzile, R. R. DeVitre & G. G. Leppard, 1996. Metal sorption to diagenetic iron and manganese oxyhydroxides and associated organic matter: narrowing the gap between field and laboratory measurements. Geoch. Cosmoch. Acta 60: 387–404.

Thomas, R. L., 1972. The distribution of mercury in the sediments of Lake Ontario. Can. J. Earth Sci. 9: 636–651.

Tinsley, J., 1950. The determination of organic carbon in soils by dichromate mixtures. Trans. 4th Int. Congr. Soil Sci. 1: 161–164.

Tipping, E., 1980. The adsorption of aquatic humic substances by iron oxides. Geoch. Cosmoch. Acta 45: 191–199.

Tipping, E., 1994. WHAM a chemical equilibrium model and computer code for waters, sediments, and soils incorporating a discrete site/electrostatic model of ion binding by humic substances. Computers & Geosciences 20: 973–1023.

Tipping, E., 1996. CHUM: a hydrochemical model for upland catchments. J. Hydrol. 174: 305–330.

Tipping, E. & M. A. Hurley, 1992. A unifying model of cation binding by humic substances. Geoch. Cosmoch. Acta 56: 3627–3641.

Tsai, L. J., K. C. Yu, J. S. Chang & S. T. Ho, 1998. Fractionation of heavy metals in sediment cores from the Ell-Ren River, Taiwan. Wat. Sci. Tech. 37: 217–224.

Valero-Garcés, B. L., K. R. Laird, S. C. Fritz, K. Kelts, E. Ito & E. C. Grimm, 1997. Holocene climate in the Northern Great Plains inferred from sediment stratigraphy, stable isotopes, carbonate geochemistry, diatoms, and pollen at Moon Lake, North Dakota. Quat. Res. 48: 359–369.

Verschuren, D., D. N. Edgington, H. J. Kling & T. C. Johnson, 1998. Silica depletion in Lake Victoria: sedimentary signals at offshore stations. J. Great Lakes Res. 24: 118–130.

Verta, M., K. Tolonen & H. Simola, 1989. History of heavy-metal pollution in Finland as recorded by lake sediments. Sci. Total Envir. 87–88: 1–18.

Wang, E. X. & G. Benoit, 1997. Fate and transport of contaminant lead in spodsols: a simple box model analysis. Wat. Air Soil Pollut. 95: 381–397.

Wang, Z. J., H. El Ghobary, F. Giovanoli & P.-Y. Favarger, 1986. Interpretation of metal profiles in a sediment core from Lake Geneva: metal mobility or pollution. Schweiz. Z. Hydrol. 48: 1–17.

Watt, J., 1998. Automated characterisation of individual carbonaceous fly-ash particles by computer controlled scanning electron microscopy: analytical methods and critical review of alternative methods. Wat. Air Soil Pollut. 105: 309–327.

White, J. R. & C. T. Driscoll, 1987. Zn cycling in an acidic Adirondack lake. Envir. Sci.Technol. 21: 211–216.

White, J. R. & C. P. Gubala, 1990. Sequentially extracted metals in Adirondack lake sediment cores. J. Paleolim. 3: 243–252.

Williams, T. M., 1992. Diagenetic metal profiles in recent sediments of a Scottish freshwater loch. Envir. Geol. Wat. Sci. 20: 117–123.

Williams, J. D. H., J. M. Jaquet & R. L.Thomas, 1976. Forms of phosphorus in the surficial sediments of Lake Erie. J. Fish. Res. Bd. Can. 33: 413–429.

Wolfe, A. P. & J. W. Hartling, 1997. Early Holocene trace metal enrichment in organic lake sediments, Baffin Island, Arctic Canada. Arctic and Alpine Res. 29: 24–31.

Xia, J., D. R. Engstrom & E. Ito, 1997. Geochemistry of ostracod calcite: part 2. The effects of water chemistry and seasonal temperature variation on *Candona rawsoni.* Geoch. Cosmoch. Acta 61: 383–391.

Xue, H. B., R. Gächter & L. Sigg, 1997. Comparison of Cu and Zn cycling in eutrophic lakes with oxic and anoxic hypolimnion. Aquat. Sci. 59: 176–189.

Yehl, P. M. & J. F. Tyson, 1997. Towards speciation of arsenic in a standard reference river sediment by high performance ion chromatography coupled with plasma-source mass spectrometry. Analyt. Communications 34: 49–51.

6. MINERALOGICAL ANALYSIS OF LAKE SEDIMENTS

WILLIAM M. LAST (WM_Last@UManitoba.ca)
Department of Geological Sciences
University of Manitoba
Winnipeg, Manitoba
R3T 2N2, Canada

Keywords: X-ray diffraction, optical microscopy, mineralogy, lake sediment, methods

Introduction and importance of mineralogy

The sedimentary records of many lakes are dominated by inorganic material. At some point, most paleolimnologists need to characterize or at least have a knowledge of the mineral composition of the deposit on which they are working. Minerals are fundamental components of sediments: Like texture and sedimentary structures, an understanding of the mineralogical composition of a sediment is essential in order to properly describe and discuss the material (Lewis, 1984). The field of sedimentary petrography, which is the description and systematic classification of sediments and sedimentary rocks, is based largely on mineralogy (Milner, 1978). Knowledge of the minerals comprising the deposits in a lake basin is also integral in understanding the genesis of the sediments, deciphering the transport mechanisms, and inferring past limnologic, hydrologic and climatic conditions.

From a genetic perspective, three distinct types of minerals exist in most lacustrine deposits (see also discussions in Boyle, this volume, and Engstrom & Wright, 1984). Minerals that are brought into the lake via surface streams, shoreline erosion, sheet flood, mass movement, and aeolian activity are referred to as allogenic or detrital material. Endogenic minerals are those inorganic components that originate within the water column of the lake, either by inorganic or biologically-induced chemical precipitation. Finally, authigenic material is derived by the diagenetic alteration of sediment that is already deposited (secondary minerals) or by chemical reactions within the pore water system of the deposit (primary or secondary minerals).

A tremendous range of paleoenvironmental information can be gained from an assessment of each of these three basic mineral components of lake sediments. Much of this vast literature has been summarized and reviewed in Talbot & Allen (1996), Smoot & Lowenstein (1991), Rodríguez-Clemente & Tardy (1987), Håkanson & Jansson (1983), Dean & Fouch (1983), Eugster & Kelts (1983), Watson (1983a, b), Dean (1981), Eugster & Hardie (1978), Kelts & Hsü (1978), Jones & Bowser (1978), Hardie et al. (1978) and Reeves (1968). Detrital minerals reflect the interaction of several factors: (i) tectonic



W. M. Last & J. P. Smol (eds.), 2001. *Tracking Environmental Change Using Lake Sediments. Volume 2: Physical and Geochemical Methods.* Kluwer Academic Publishers, Dordrecht, The Netherlands.

framework of the basin, (ii) place of origin (provenance) of the sediments, (iii) nature and intensity of weathering processes within the watershed, and (iv) transportation processes responsible for the delivery of the sediment to the lake. Thus, the allogenic component can often be used to quantitatively deduce past changes in drainage basin size and morphology (e.g., Henderson & Last, 1998; Olsen, 1990; Teller & Last, 1981a, b; Teller, 1976) and fluctuations in the climatic regime of the watershed (e.g., Schütt, 1998a, b; Menking, 1997; Dean, 1997, 1993; Webster & Jones, 1994; Last & Sauchyn,1993; Parry & Reeves, 1968).

The endogenic minerals usually provide the most straightforward and explicit paleoenvironmental interpretive potential because these components give a snapshot of the chemical and limnological conditions at the time of the minerals' formation. Carbonate minerals are among the most common endogenic constituents in many lakes (Dean & Fouch, 1983). Numerous studies, both on modern and ancient lacustrine deposits, have documented the applications of endogenic calcite, Mg-calcite, aragonite, dolomite, and magnesite in paleolimnology (e.g., Haskell et al., 1996; Valero-Garcés & Kelts, 1995; Dean & Megard, 1993; Coshell et al., 1988; Talbot & Kelts, 1986; von der Borsch & Lock, 1979; Müller et al., 1972). It has now become routine to use the stratigraphic variation of these endogenic carbonate species to deduce past Mg/Ca ionic ratios and salinities of the lake water (e.g., Campbell et al., 2000; Last & Vance, 2001; Last & De Deckker, 1992, 1990; Müller & Wagner, 1978; Last & Schweyen, 1985). These carbonate mineral data can be particularly useful when interpreted in conjunction with stable isotopic analyses of either the inorganic carbonates or biological components (e.g., Dean & Schwalb, 2000; Valero-Garcés et al., 1997; Gell et al., 1994; Last et al., 1994; Van Stempvoort et al., 1993; Rosen et al., 1988; Abell & McClory, 1986).

In lacustrine systems that have more complex endogenic mineral assemblages, as is the case for most brackish, saline, and hypersaline lakes, composition of the endogenic inorganic fraction is a foremost paleoenvironmental parameter because of the often limited application of some biological proxy indicators (Evans, 1993; Hammer, 1986). In these higher salinity settings, the mineralogy of the precipitated material is the single most direct and unambiguous indicator of past chemical composition of the lake water available to paleolimnologists. These endogenic minerals are generally thermodynamically and kinetically responsive to even relatively minor changes in water composition (Braitsch, 1971; Sonnenfeld & Perthuisot, 1989; Sonnenfeld, 1984). Explicit chemical paleo-reconstructions are now possible for lake waters once the detailed endogenic equilibrium mineral assemblage is known (e.g., Pienitz et al., 2000; Shang & Last, 1999; Wasson et al., 1984; Smith et al., 1979). Thus, the endogenic mineral fraction contains a precise and accurate record of salinity, water chemistry, and other limnological parameters that are useful in reconstructing lake-level changes, and climatic and hydrologic fluctuations.

Because authigenic minerals can result from essentially penecontemporaneous processes or can originate long after the sediment has been deposited, their paleolimnological interpretation is somewhat more intricate and can be ambiguous without detailed chronological support. Although more complex, the authigenic fraction of lake sediments can, nonetheless, provide important clues about the past environmental conditions in the basin (e.g., Lowenstein & Brennan, this volume; Salvany & Orti, 1994; Ordonez & Garcia del

Cura, 1994; Spencer & Lowenstein, 1990; Jones, 1986; Renaut et al., 1986; Smith & Friedman, 1986; Ziqiang & Zhiqiang, 1985).

Characterization of the mineral components in a lake sediment may involve only a small number of relatively simple analyses, such as one might undertake in a marl deposit, or it may require more complex and multi-component analyses, such as is required for most evaporite mineral and clay mineral assessments. Similarly, mineralogical examinations can be made of the entire inorganic assemblage of a lake deposit (i.e., bulk mineralogy) or of specific groups of minerals (e.g., carbonate minerals or layer silicate minerals), or of specific size fractions of the sediment (e.g., clay-sized or sand-sized fractions). In each instance, the sample preparation procedures, analytical methodologies, and quantification techniques can be considerably different. It is beyond the scope of this chapter to summarize all of the many techniques used in sedimentary petrography and mineralogy. Numerous excellent university-level textbooks and laboratory manuals already provide many of these essential details (e.g., Lewis & McConchie, 1994; Carozzi, 1993; Blatt, 1992; Boggs, 1992; Tucker, 1991, 1988; Barker & Kopp, 1991; Tucker & Wright, 1990; Ehlers, 1987; Phillips & Griffen, 1981; Folk, 1980; Greensmith, 1979; Allman & Lawrence, 1972; Carver, 1971; Müller, 1967). The intent of this chapter is to summarize two of the most commonly used analytical methods applicable to lake sediment studies: X-ray diffractometry and optical mineralogy. Emphasis will be placed on the investigation of unconsolidated sediments and, because the vast majority of paleolimnologists deal with offshore stratigraphic sequences, most of the overview will be directed toward examination of fine-grained sediments.

Mineralogy versus geochemistry

The inorganic composition of a lacustrine deposit may be expressed in terms of either chemistry or mineralogy. Techniques and applications of inorganic geochemistry in paleolimnology are summarized elsewhere in this volume (Boyle, this volume). As discussed by Boyle (this volume) and others (e.g., Bengtsson & Enell, 1986; Engstrom & Wright, 1984; Mackereth, 1966), a chemostratigraphic approach offers many attractive interpretive possibilities, particularly for investigation of erosion histories, tracking pollution and contaminant elements, and in eutrophication and nutrient studies. However, interpreting bulk elemental data can be exceedingly difficult without having a sound knowledge of the mineralogical assemblage present in the sediment. Indeed, as pointed out by others (e.g., Prothero & Schwab, 1996; Potter et al., 1980) describing a sediment using bulk chemistry can be misleading. Similar chemistries can imply identical sediment types and similar limnological histories when, in fact, important differences may exist. Jones & Bowser (1978) maintain that the treatment of lacustrine sediment as a chemically homogeneous phase significantly limits the interpretive potential of the analytical data. The importance of collecting mineralogical data (in addition to or, in some cases, instead of element geochemistry) in order to quantitatively reconstruct the history of a lake cannot be overemphasized. For example, knowing that a sediment sample contains quartz, plagioclase, hexahydrite, and halite provides essential genetic and paleolimnological interpretive detail unavailable through a chemical analysis identifying the analytical proportions of Si, Na, Ca, Mg,

Al, S, and Cl. Similarly, bulk elemental analyses cannot readily distinguish among oxidation states (e.g., Fe^{2+} and Fe^{3+}; Mn^{2+}, Mn^{3+} and Mn^{4+}) nor among polymorphs (i.e, minerals, such as calcite, aragonite, monohydrocalcite, vaterite, that have different structures and genetic relationships within a lacustrine system but share the same elemental stoichiometry).

Minerals in lake sediments

One of the most important and comprehensive summaries of the mineralogy of lake sediments is that of Jones & Bowser (1978). Although this overview concentrates mainly on the deposits of freshwater lakes, nonetheless, it provides all the essential background information and fundamental concepts necessary for neophytes as well as seasoned veteran paleolimnologists. Smoot & Lowenstein (1991), Warren (1989), Sonnenfeld & Perthuisot (1989), Sonnenfeld (1984), and Reeves (1968) offer complementary overviews of minerals in saline and hypersaline lacustrine deposits.

A mineral is a naturally occurring crystalline substance composed of an inorganic element or compound. Organic compounds also are often crystalline, but they are not considered minerals. In crystals, the atoms are arranged in a regular, orderly, three-dimensional pattern or structure, whereas amorphous material has no such internal arrangement. However, there is no sharp boundary between crystalline and amorphous materials. Some 'amorphous' substances, such as opal ($SiO_2 \cdot nH_2O$), are often comprised of submicron aggregates or spheres that form a more or less ordered internal structure, and are more properly referred to as mineraloids. Other noncrystalline inorganic compounds, such as the commonly occurring clay 'mineral' allophane ($Al_2O_3 \cdot 2SiO_2 \cdot nH_2O$), appear to be transitional between amorphous and crystalline, and are referred to as paracrystalline.

Assessing the mineral composition of a lacustrine deposit can be an immense undertaking, directly comparable to a researcher striving to identify and quantify all of the biological components within a sample. The diversity of minerals in lacustrine sediments (Table I) is characteristically much greater than that of marine or other continental (e.g., fluvial, aeolian) deposits because of the wide range of water compositions in lakes and the significant influence of local watershed geology and soil composition. In addition, because lake sediments can be a mixture of minerals formed elsewhere (allogenic), minerals precipitated from the water column (endogenic), and minerals formed by the alteration of previously deposited material or precipitated from pore fluids (authigenic), the assemblage is not necessarily in thermodynamic equilibrium. This is in striking contrast to igneous and metamorphic petrogenesis studies in which equilibrium is achieved at the time of formation and the resulting mineral assemblages are relatively simple. This nonequilibrium condition also curtails the use of simple normative calculation techniques for deciphering the mineral assemblage from an elemental geochemistry assessment (cf. Boyle, this volume; Rollinson, 1993; Garrels & MacKenzie, 1971).

A synopsis of methods

The study of minerals in a naturally occurring sediment sample can be, to a new investigator, an exceedingly complex, time-consuming, and labor-intensive task, often incorporating

Table I. Minerals in Quaternary lacustrine sediments.

Mineral Name	Composition	Occurrence[1]
	Carbonate Minerals	
Aragonite	$CaCO_3$	D, E, A
Artinite	$Mg_2CO_3(OH)_2 \cdot 3H_2O$	E, A
Ankerite	$Ca(Fe, Mg)(CO_3)_2$	E, A
Benstonite	$Ca_7Ba_6(CO_3)_{13}$	A
Burbankite	$Na_2(Ca, Sr, Ba, Ce)_4(CO_3)_5$	A
Calcite	$CaCO_3$	D, E, A
Dawsonite	$NaAl(CO_3)(OH)_2$	A
Dolomite	$CaMg(CO_3)_2$	D
Eitelite	$Na_2Mg(CO_3)_2$	A
Gaylussite	$Na_2Ca(CO_3)_2 \cdot 5H_2O$	E, A
Hydromagnesite	$Mg_5(CO_3)_4(OH)_2 \cdot 4H_2O$	E, A
Huntite	$CaMg_3(CO_3)_4$	E, A
Kutnohorite	$Ca(Mn, Mg)(CO_3)_2$	E, A
Magnesite	$MgCO_3$	E, A
Magnesian Calcite	$(Mg_xCa_{1-x})CO_3$	E
Monohydrocalcite	$CaCO_3 \cdot H_2O$	E
Minrecordite	$CaZn(CO_3)_2$	E, A
Nahcolite	$NaHCO_3$	E, A
Natron	$Na_2CO_3 \cdot 10H_2O$	E, A
Nesquehonite	$Mg(HCO_3)(CO_3)_4$	E, A
Pirssonite	$Na_2Ca(CO_3)_2 \cdot 2H_2O$	A
Protodolomite	$(Mg_xCa_{1-x})(CO_3)_2$	E, A
Rhodochrosite	$MnCO_3$	A
Scarbroite	$Al_2(CO_3)_3 \cdot 13Al(OH)_3$	A
Shortite	$Na_2Ca_2(CO_3)_3$	A
Siderite	$FeCO_3$	E, A
Strontianite	$SrCO_3$	E, A
Thermonatrite	$Na_2CO_3 \cdot H_2O$	E, A
Trona	$NaHCO_3 \cdot Na_2CO_3 \cdot 2H_2O$	E, A
Vaterite	$CaCO_3$	E, A
Witherite	$BaCO_3$	A
Zemkorite	$Na_2Ca(CO_3)_2$	E, A
	Phosphate Minerals	
Anapaite	$Ca_3Fe(PO_4)_3 \cdot 4H_2O$	A
Apatite	$Ca_2(PO_4)_3(OH, F)$	D, A
Brushite	$CaHPO_4 \cdot 2H_2O$	E
Fluorapatite	$Ca_{10}(PO_4)_6F_2$	A
Lipscombite	$Fe_3(PO_4)_2(OH)_2$	A
Ludlamite	$(Fe, Mn, Mg)_3(PO_4)_2 \cdot 3H_2O$	A
Lüneburgite	$Mg_3(PO_4)_2B_2O_3 \cdot 8H_2O$	E, A
Newberyite	$MgHPO_4$	E, A
Phosphoferrite	$(Mn, Fe)_3(PO_4)_2 \cdot 3H_2O$	A
Rockbridgeite	$(Fe, Mn)Fe_4(PO_4)_3(OH)_5$	E, A
Strengite	$FePO_4 \cdot 2H_2O$	E, A

Table I. Minerals in Quaternary lacustrine sediments (continued).

Mineral Name	Composition	Occurrence[1]
	Phosphate Minerals (continued)	
Struvite	$MgNH_4PO_4 \cdot 6H_2O$	E, A
Vivianite	$Fe_3(PO_4)_2 \cdot 8H_2O$	A
	Sulfate Minerals	
Alunite	$KAl_3(OH)_6(SO_4)_2$	E
Anhydrite	$CaSO_4$	D, E, A
Aphthitalite	$K_3Na(SO_4)_2$	A
Arcanite	$(K, NH_4)_2SO_4$	A
Barite	$BaSO_4$	E, A
Bassanite	$2CaSO_4 \cdot H_2O$	A
Bloedite	$Na_2Mg(SO_4)_2 \cdot 4H_2O$	E, A
Celestite	$SrSO_4$	A
Coquimbite	$Fe(SO_4)_3 \cdot 9H_2O$	E, A
Despujolsite	$Ca_3Mn(SO_4)_2(OH) \cdot 3(H_2O)$	E, A
Epsomite	$MgSO_4 \cdot 7H_2O$	E
Eugsterite	$Na_2Ca(SO_4)_3 \cdot 2H_2O$	E, A
Glauberite	$Na_2Ca(SO_4)_2$	E, A
Görgeyite	$K_2Ca_5(SO_4)_6 \cdot H_2O$	E, A
Gypsum	$CaSO_4 \cdot 2H_2O$	D, E, A
Hexahydrite	$MgSO_4 \cdot 4H_2O$	E, A
Hydroglauberite	$Na_{10}Ca_3(SO_4)_8 \cdot 6H_2O$	A
Jokokuite	$MnSO_4 \cdot 5H_2O$	E, A
Jarosite	$KFe_3(SO_4)_2(OH)_6$	A
Kalistronitite	$K_2Sr(SO_4)_2$	A
Kieserite	$MgSO_4 \cdot H_2O$	A
Krausite	$Fe_2(SO_4)_3 \cdot 2H_2O$	A
Langbeinite	$2MgSO_4 \cdot K_2SO_4$	A
Lecontite	$NaKNH_4SO_4 \cdot 2H_2O$	E, A
Leightonite	$K_2Ca_2Cu(SO_4)_4 \cdot 2H_2O$	A
Leonhardtite	$MgSO_4 \cdot 4H_2O$	E, A
Leonite	$MgK_2(SO_4)_2 \cdot 4H_2O$	E, A
Loeweite	$Na_{12}Mg_7(SO_4)_{13} \cdot 15H_2O$	E, A
Mallardite	$MnSO_4 \cdot 7H_2O$	E, A
Melanterite	$FeSO_4 \cdot 7H_2O$	E, A
Mercallite	$KHSO_4$	A
Mirabilite	$Na_2SO_4 \cdot 10H_2O$	E, A
Pentahydrite	$MgSO_4 \cdot 5H_2O$	E, A
Picromerite	$MgK_2(SO_4)_2 \cdot 6H_2O$	E, A
Polyhalite	$K_2Ca_2Mg(SO_4)_4 \cdot 2H_2O$	A
Potassium alum	$KAl(SO_4)_2 \cdot 12H_2O$	E, A
Quenstedite	$FeSO_4 \cdot 10H_2O$	E, A
Sanderite	$MgSO_4 \cdot 2H_2O$	E, A
Siderotil	$FeSO_4 \cdot 4H_2O$	A
Starkeyite	$MgSO_4 \cdot 4H_2O$	E, A
Sulfur	S	E

Table I. Minerals in Quaternary lacustrine sediments (continued).

Mineral Name	Composition	Occurrence[1]
	Sulfate Minerals (continued)	
Syngenite	$K_2Ca(SO_4)_2 \cdot 2H_2O$	A
Szomolnokite	$FeSO_4 \cdot H_2O$	E, A
Thenardite	Na_2SO_4	E, A
Vanthoffite	$Na_6Mg(SO_4)_4$	A
Wattevilleite	$Na_2Ca(SO_4)_2 \cdot 4H_2O$	A
Carbonate-Sulfate, Carbonate-Sulfate-Chloride and Carbonate-Phosphate Minerals		
Ardealite	$CaMgCO_3PO_4$	E, A
Bonshtedite	$Na_3Fe(PO_4)(CO_3)$	E, A
Bradleyite	$Na_3Mg(PO_4)(CO_3)$	E, A
Burkeite	$Na_4(SO_4)CO_3$	E, A
Collophanite	$Ca_{10}(PO_4)_6CO_3 \cdot H_2O$	A
Galeite	$Na_2SO_4 \cdot Na(F, Cl)$	A
Hanksite	$KNa_{22}(CO_3)_2(SO_4)_9Cl$	E, A
Kainite	$4MgSO_4 \cdot 4KCl \cdot 5H_2O$	A
Northupite	$Na_2Mg(CO_3)_2 \cdot NaCl$	A
Rapidcreekite	$Ca_2(CO_3)SO_4 \cdot 4H_2O$	E, A
Schairerite	$Na_2SO_4 \cdot Na(F, Cl)$	A
Sulfohalite	$2Na_2SO_4 \cdot NaCl \cdot 4H_2O$	A
Tychite	$Na_6Mg_2SO_4(CO_3)$	E, A
	Chloride and Iodate Minerals	
Antarcticite	$CaCl_2 \cdot 6H_2O$	E, A
Bischofite	$MgCl_2 \cdot 6H_2O$	E, A
Bruggenite	$Ca(IO_3)_2 \cdot H_2O$	E, A
Carnallite	$KMgCl_{13} \cdot 6H_2O$	E, A
Douglasite	$KFeCl_4 \cdot 2H_2O$	A
Halite	NaCl	E, A
Hydrohalite	$NaCl \cdot 2H_2O$	E
Lautarite	$Ca(IO_3)_2$	E, A
Rinneite	$K_3NaFeCl_6$	E, A
Sylvite	KCl	A
Tachyhydrite	$CaCl_2 \cdot 2MgCl \cdot 2H_2O$	A
Teepleite	$Na_2B(OH)_4Cl$	A
	Nitrate and Borate Minerals	
Ameghinite	$NaB_3O_3(OH)_4$	A
Binorite	$Ca_2B_{14}O_{23} \cdot 8H_2O$	E, A
Borax	$Na_2B_4O_7 \cdot 10H_20$	A
Carboborite	$MgCa(CO_3)_2 \cdot B(OH)_4 \cdot 4H_2O$	E, A
Colemanite	$Ca_2B_6O_{11} \cdot 5H_2O$	E, A
Darapskite	$Na_3SO_4NO_3 \cdot H_2O$	E, A
Howlite	$Ca_2SiB_5O_9 \cdot (OH)_5$	E, A
Humberstonite	$K_3Na_7Mg_2(SO_4)_6(NO_3)_2 \cdot 6H_2O$	E, A
Hungchaoite	$MgB_4O_5(OH)_4 \cdot 8H_2O$	E, A
Hydroboracite	$CaMgB_6O_{11} \cdot 6H_2O$	E, A

Table I. Minerals in Quaternary lacustrine sediments (continued).

Mineral Name	Composition	Occurrence[1]
	Nitrate and Borate Minerals (continued)	
Inderborite	$CaMgB_6O_{11} \cdot H_2O$	A
Inderite	$Mg_2B_6O_{10} \cdot 15H_2O$	E, A
Inyoite	$Ca_2B_6O_6(OH)_{10} \cdot 8H_2O$	E, A
Kaliborite	$HKMg_2B_{12}O_{16}(OH)_{10} \cdot 4H_2O$	E, A
Kernite	$Na_2B_4O_7 \cdot 4H_2O$	E, A
Kurnakovite	$MgB_6O_{19} \cdot 15H_2O$	E, A
Macallisterite	$Mg_2B_6O_7(OH)_6 \cdot 9H_2O$	E, A
Meyerhofferite	$Ca_2B_6O_{11} \cdot 7H_2O$	E, A
Niter	KNO_3	E, A
Nitrobarite	$Ba(NO_3)_2$	E, A
Nobleite	$CaB_6O_{10} \cdot 4H_2O$	E, A
Pinnoite	$MgB_2O_4 \cdot 3H_2O$	E, A
Priceite	$CaB_{10}O_{19} \cdot 7H_2O$	E, A
Proberite	$NaCaB_5O_9 \cdot 5H_2O$	E, A
Santite	$KB_5O_6(OH)_4 \cdot 2H_2O$	A
Sborgite	$NaB_5O_6(OH)_4 \cdot 3H_2O$	A
Soda Niter	$NaNO_3$	E, A
Tincalconite	$Na_2B_4O_7 \cdot 2H_2O$	A
Ulexite	$NaCaB_5O_9 \cdot 8H_2O$	E, A
	Oxide, Fluoride, and Chromate Minerals	
Anatase	TiO_2	D, A
Birnessite	$(Na, Ca)Mn_7O_{14} \cdot 3H_2O$	D, A
Boehmite	$AlOOH$	D
Corundum	Al_2O_3	D
Diaspore	$AlOOH$	D
Dietzeite	$Ca_2(IO_3)2CrO_4$	E, A
Fluorite	CaF_2	A
Geothite	$FeOOH$	D, E, A
Gibbsite	$Al(OH)_3$	D
Hematite	Fe_2O_3	D, A
Ilmenite	$FeTiO_3$	D
Jacobsite	$MnFe_2O_4$	D
Lepidocrocite	$FeOOH$	D, A
Lopezite	$K_2Cr_2O_7$	E, A
Psilomelane	$(Ba, K)(MnO_2)_{2.5} \cdot H_2O$	A
Maghemite	Fe_3O_4	D
Magnetite	Fe_3O_4	D
Pyrolusite	MnO_2	A
Rancieite	$(Ca, Mn)Mn_4O_9 \cdot 3H_2O$	E
Rutile	TiO_2	D
Tarapacaite	K_2CrO_4	E, A
Todorokite	$(Na, Ca, K, Ba, Mn)_2Mn_5O_{12} \cdot 3H_2O$	D, A
Ulvöspinel	$TiFe_2O_4$	D

Table I. Minerals in Quaternary lacustrine sediments (continued).

Mineral Name	Composition	Occurrence[1]
	Non-Clay Silicate Minerals	
Adularia	$KAlSi_3O_8$	A
Amphiboles	$(Na, Ca, K)_2(Mg, Fe, Ti, Al, Li, Mn)_3(Si, Al)_8O_{22}(OH, F)_2$[2]	D
Analcime	$NaAlSi_2O_6 \cdot 2H_2O$	A
Cristobalite	SiO_2	D
Clinoptolite	$(Na, K, Ca)_2Al_3(Al, Si)_2Si_{12}O_{36} \cdot 12H_2O$	A
Erionite	$(K_2Ca, Na_2)_2Al_4Si_{14}O_{36} \cdot 15H_2O$[2]	A
Kanemite	$NaHSi_2O_4(OH)_2 \cdot 2H_2O$	E
Kenyaite	$Na_2Si_{22}O_{41}(OH)_8 \cdot 6H_2O$	E
K-Feldspars	$KAlSi_3O_8$[2]	D, A
Magadiite	$NaSi_7O_{13}(OH)_3 \cdot 3H_2O$	E
Makatite	$Na_2Si_4O_8(OH)_2 \cdot 4H_2O$	E
Micas	$K(Mg, Fe, Al)_3AlSi_3O_{10}(OH)$[2]	D
Moganite	SiO_2	A
Mordenite	$(Ca, Na_2, K_2)Al_2Si_{10}O_{24} \cdot 7H_2O$	A
Natrolite	$Na_2Al_2Si_2O_6 \cdot 2H_2O$	A
Olivenes	$(Mg, Fe)_2SiO_4$[2]	D
Opal	$SiO_2 \cdot nH_2O$	D, E, A
Phillipsite	$KCa(Al_3Si_5O_{16}) \cdot 6H_2O$	A
Plagioclase	$(Na, Ca)Al(Al, Si)Si_2O_8$[2]	D
Pyroxenes	$(Ca, Mg, Fe)_2Si_2O_6$[2]	D
Quartz	SiO_2	D
Searlesite	$NaBSi_2O_6 \cdot H_2O$	A
Sepiolite	$Mg_4Si_6O_{15}(OH)_2 \cdot 6H_2O$	E
Thomsonite	$NaCa_2Al_5Si_5O_{20} \cdot 6H_2O$	A
	Layered Silicate Minerals	
Chlorite	$Mg_5Al_2Si_3O_{10}(OH)_8$	D
Illite	$(K, Al, Mg, Fe)_2(AlSi)_4O_{10}(OH)_2H_2O$[2]	D
Kaolinite	$Al_2Si_2O_5(OH)_4$	D, A
Mixed-layer Clays	Variable[2]	D, E, A
Palygorskite	$(Mg, Al)_2Si_4O_{10}(OH) \cdot 4H_2O$	D, A
Smectite	$(Na, Ca)_{0.33}(Al, Mg)_2Si_4O_{10}(OH)_2 \cdot nH_2O$[2]	D, A
Vermiculite	$(Mg, Fe, Al)_3(Al, Si)_4O_{10}(OH)_2 \cdot 4H_2O$	D, A
	Sulfides	
Griegite	Fe_3S_4	A
Mackinawite	FeS	E, A
Marcasite	FeS_2	D, A
Pyrite	FeS_2	D, E, A
Pyrrhotite	FeS	D, A
Sphalerite	ZnS	E
Wurtzite	ZnS	A

[1] D = detrital; E = endogenic; A = authigenic.
[2] Formula represents a series or group of minerals
Italics indicate minerals are common in lake sediments.

many different techniques and methods. Some of these analytical methods are traditional and are based on physical and chemical principles that have been well known for nearly 200 years; other techniques are rapidly evolving and dependant largely on powerful new instrumentation. Although this chapter will emphasize only two of the vast arsenal of techniques, it is appropriate to provide a short description of some of the other analytical tools, instruments, and techniques that can be brought to bear upon the problems of identifying and quantifying minerals in a lacustrine deposit.

Thermal analysis systems are a group of methods designed to evaluate the mineral components in a sample by measuring a key physical property, a change in phase, or a reaction product as a function of temperature as the sample is being incrementally heated. One of the most common of these is differential thermal analysis (DTA). In DTA studies, the difference in temperature (ΔT) between the sample and a thermally inert reference material is recorded as the components are being heated to ~1000°C. This ΔT signal is controlled by the nature of the endothermic or exothermic reactions taking place in the sample, which, in turn, are a function of the mineralogical composition (Karathanasis & Harris, 1994; Lewis & McConchie, 1994, MacKenzie, 1982). Similarly, thermogravimetric techniques (TG) monitor the change in mass of the sample over the temperature range. The changes in mass are due to reactions, such as dehydration (loss of H_2O), loss of carbon dioxide, oxidation of iron or manganese, or oxidation of sulfides, that can be related to specific temperatures. For example, a very simple type of thermogravimetric analysis, loss on ignition (LOI) between 550°C and ~ 1000°C, is commonly used to approximate the total carbonate mineral content in a non-sulfidic lake sediment sample (Dean, 1974; Heiri et al., 2001). The major advantages of thermal analysis systems are that the required equipment is relatively inexpensive, sample preparation and analyses are relatively fast and simple, and the techniques can be used to examine both crystalline as well as non-crystalline material in the sample.

Mineralogical analysis by light microscopy, discussed later in this chapter, is often supplemented by various luminescence petrographic techniques. Chief among these in sedimentary studies are cathodoluminescence (CL), caused by an incident beam of electrons hitting the minerals, and photoluminescence (PL), caused by visible or ultraviolet radiation. Although not a mineralogical analysis technique *per se,* luminescence microscopy and spectroscopy can supply very important fabric, textural, and element compositional information that aids in the understanding of the genesis and history of the sediment (see, for example, Barker & Copp, 1991). Likewise, mineral identification of individual sedimentary particles is frequently aided by the use of a scanning electron microscope (SEM; Trewin, 1988; Welton, 1984; Smart & Tovey, 1982) and transmission electron microscopy (TEM; Gilkes, 1994) and, when used in conjunction with light microscopy and/or XRD, can be very powerful analytical tools for sediment mineralogy.

Elemental analyses, involving an impressive array of nondestructive spectroscopic methods or decomposition of the material and analyses by AAS (atomic absorption spectrometry) or ICP-AES (inductively coupled plasma atomic emission spectrometry), form a very important complement to mineralogical analyses as outlined by Boyle (this volume), Korsman et al. (this volume), Amonette & Sanders (1994), Sawhney & Stilwell (1994), Hawthorne (1988), Fairchild et al. (1988), and Stone (1982). However, these elemental techniques are not intended to provide a qualitative or quantitative assessment of the mineralogy of a deposit.

X-ray diffraction

Introduction

X-ray diffractometry (XRD) is the single most important and widely used method for mineralogical assessment of lake sediments. Its usefulness in paleolimnology stems from the fact that most offshore lacustrine deposits are so fine-grained that optical mineralogy methods cannot be routinely applied. In addition, the XRD method offers a number of other significant advantages over other techniques. The method is rapid and relatively inexpensive (on a per-sample basis). Basic XRD instrumentation, although not inexpensive, is readily available in most university earth science or soil science departments, and modern equipment operation can be undertaken with a minimum of training. Similarly, sample preparation, although tedius, is relatively straightforward. Finally, XRD studies provide not only qualitative mineralogical information (i.e., which minerals are present in a sample), but also can be used to quantitatively evaluate the material as well as derive a wealth of other information, such as the degree of crystal disorder in minerals, the nature and extent of isomorphous substitution, crystallite size, and various crystal structure characteristics. However, an important disadvantage of the XRD method is that it tells the investigator nothing about the textural relationships, fabric, or other important genetic and diagenetic parameters, which can be very important in helping to understand the lacustrine processes responsible for deposition and alteration of the sediment. Thus, thin section (TS) petrography or other petrographic approaches, such as SEM, are often used as an adjunct to XRD. Finally, it must be remembered that the X-ray diffraction technique is applicable only to crystalline material; lake sediments sometimes contain large proportions of amorphous inorganic matter which cannot be routinely evaluated by XRD.

Safety

All modern X-ray diffraction equipment features built-in safeguards that minimize the operator's risk of exposure to radiation under normal working conditions. However, the use of this equipment *can* be dangerous because of both the nature of the radiation itself and the high voltage used by the equipment to generate the X-rays. X-radiation can kill; even very brief exposure to the direct X-ray beam can cause permanent skin damage. Because the effect of exposure to shortwave radiation of any form is cumulative, extreme care must be taken to avoid all exposure.

Clearly, the various manufacturer-installed safety switches and devices must not be tampered with. Never look into the shutter of the X-ray tube or even at the sample when the equipment is operating. Never attempt to reach inside the X-ray generator or to investigate problems with the electronic circuit panel. As pointed out by Moore & Reynolds (1997) and Klug & Alexander (1974), two of the standard procedural handbooks for XRD, many of the early workers with X-rays were severely injured or died from radiation exposure. Protective devices and failsafe equipment designs cannot insure complete elimination of risk of exposure, particularly if specified routines are not followed or if untrained personnel try to use the equipment.

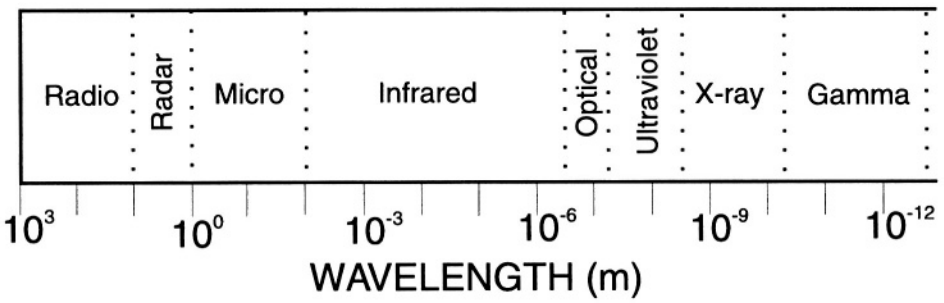


Figure 1. Electromagnetic radiation spectrum showing the position of X-radiation.

History

X-rays, or X-radiation, is that part of the electromagnetic (EMR) spectrum that lies between the low-energy, high wavelength ultraviolet radiation and the high-energy, low wavelength gamma rays (Fig. 1). X-rays were serendipitously discovered in the latter part of the 19th century by W. C. Röntgen (see Moore & Reynolds, 1997, for a more complete overview of the discovery and early experimentation with X-rays). Soon after Röntgen's discovery, research into the diffraction of X-rays by crystalline material was carried out in Europe by W. L. Bragg, L. H. Bragg, and M. T. F. von Laue (as well as several other physicists working outside of Europe). It was soon realized that the atoms in a crystal can be considered as planes that are arranged in regular, orderly, three-dimensional, repeating patterns. The fact that these regular arrangements of planes (or rows of atoms) have spacings (refereed to as '*d* spacing' or lattice spacing) of approximately the same dimensions ($\sim 10^{-8}$ cm or 1 Å) as the wavelength of X-rays meant that the diffraction phenomenon (i.e., the in-phase scattering of radiation from an incident beam of radiation to produce a secondary beam) could be viewed as simple multiple reflections of radiation by the planes of atoms. This permitted researchers to formulate a simple equation that relates the angle of incidence, the specific wavelength of the incident radiation, and the spacing between the layers. This equation is commonly referred to as Bragg's Law:

$$n\lambda = 2d \sin\theta, \tag{1}$$

where n is an integer; λ is the wavelength of the incident X-radiation; d is the lattice spacing or the distance between two adjacent planes of atoms; and θ is the angle between the incident radiation and the atomic plane, sometimes referred to as the critical angle or Bragg's angle (Fig. 2). Although θ is very difficult to measure, it can be geometrically shown that the angle between the diffracted beam of radiation and the incident radiation is 2θ, a value that can be easily measured. Thus, the diffraction pattern of a crystalline substance under an incident monochromatic (i.e., single wavelength) X-ray beam is a fundamental and unique physical property of that substance, thereby permitting easy identification irrespective of the size, morphology, or optical characteristics of the material.

With the first publication of these basic principles in 1913 (for which the Braggs shared the 1915 Nobel Prize) mineralogical and crystallographic research entered a new phase of very rapid development and explosive expansion of the literature. By the 1930s X-ray

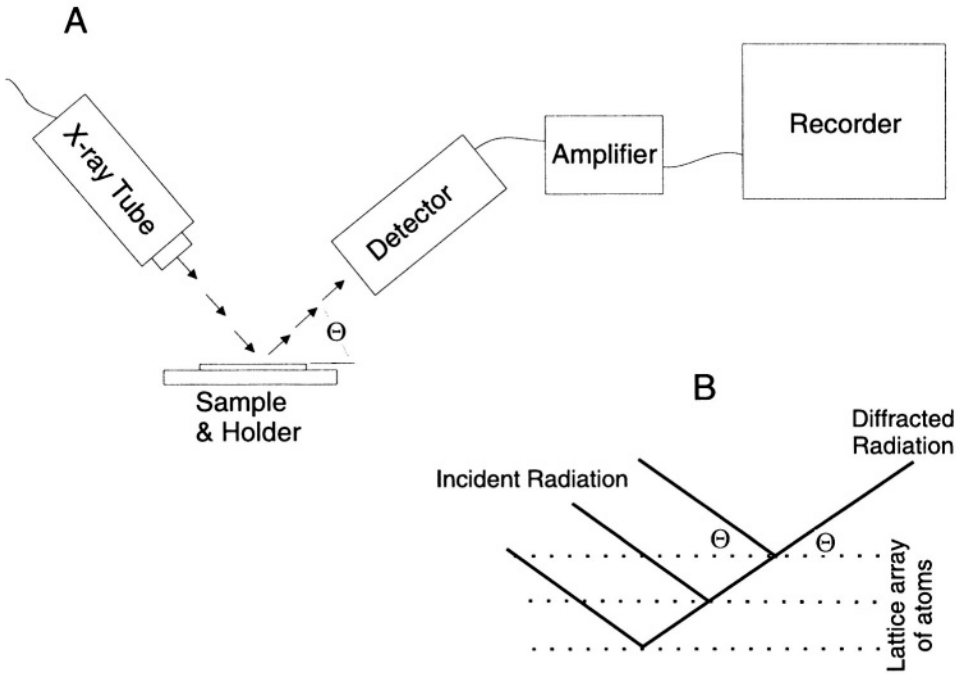


Figure 2. (a) Schematic diagram showing the geometry of powder X-ray diffraction analysis. A constant beam of monochromatic X-radiation is generated by the X-ray tube and directed at a holder containing a thin film of finely powdered sample. As the sample rotates through an angle of 2θ, the minerals in the sample diffract the incident radiation when Bragg's critical angle (θ) is achieved. The diffracted X-rays are detected at a receiver and recorded on a strip chart or microprocessor. (b) Sketch showing the diffraction of incident X-radiation at Bragg's critical angle (θ) which corresponds to the spacing between the lattice planes of the mineral.

diffraction formed the cornerstone for nearly all routine identification and quantification work on the minerals in fine grained sediments (see the reviews of the history of clay mineralogy in Moore & Reynolds, 1997; Grim, 1988; Brown & Brindley, 1980; Millot, 1970). Post-war instrumental advances resulted in the development of various new spectroscopic techniques that complement the traditional XRD method (e.g., atomic resonance spectroscopy, vibrational spectroscopy, magnetic resonance, and various electronic resonances; Calas & Hawthorne, 1988). However, X-ray diffractometry remains the premier mineral analysis tool in paleolimnology and many areas of sedimentology and soil science. Over 95% of the papers published in *Journal of Paleolimnology, Journal of Sedimentary Research, Sedimentology, Sedimentary Geology* and *The Holocene* during the past decade that report the mineralogy of lake sediments have used this method.

Principles of operation & interpretation

The basic XRD system consists of an X-ray generator, a device to hold and rotate the sample (goniometer or diffractometer), and a detector (Fig. 2). Many textbooks and laboratory

manuals provide details of this instrumentation and theory of operation and interpretation (e.g., Marfunin, 1995; Bish & Post, 1989; Jones, 1987; Cullity, 1978; Zussman, 1977; Klug & Alexander, 1974; Azároff, 1968). In normal commercially available equipment, X-rays are produced by the bombardment of a metal target (often copper, but can also be Cr, Fe, Co, Mo, or Ag) by a stream of high energy electrons. This bombardment produces radiation in the X-ray region of the EMR spectrum having several characteristic peaks (or "lines") of varying intensity corresponding to the position of the orbital electrons that are being rearranged by the bombardment (i.e., electrons displaced from the K, L, M, or N shell orbits all have different energy levels and thus produce different X-ray lines). In order to achieve monochromatic radiation, a series of filters (metal foils) are applied to remove selected radiation from the spectrum.

The filtered, monochromatic X-ray beam (with $\lambda = 1.5418$ Å for Cu-generated radiation) is then directed at the sample which has been placed in a holder that rotates. As the atomic planes in the minerals in the rotating sample attain the appropriate critical angle with respect to the incident beam, they will diffract the X-rays according to Bragg's Law. Early vintage XRD equipment recorded the diffracted X-rays on photographic film (Debye-Sherrer photographs), which then had to be accurately measured and manually converted to θ and, ultimately, to d spacing information. Most modern equipment now uses an electronic detector and counter, with the intensity of the diffracted rays recorded on a strip chart (diffractometer trace or diffractogram) and/or a digital microprocessor (Jenkins, 1989a). Because the X-ray diffractometer, including the mounted sample, is slowly rotated though a given number of $°2\theta$ and the strip chart is advanced at a speed that is synchronized with the detector, the x-axis on the chart is calibrated in $°2\theta$. Thus, it is very easy to identify the angular position, intensity, and shape of the diffraction lines.

The basis of interpreting the resulting diffractogram is that each mineral in the sample will produce a unique set of distinctive reflections, or peaks, relating to the set of lattice planes with the mineral's characteristic d spacing. Since all crystalline materials possess a unique pattern of X-ray diffraction peaks, mineral identification is done simply by comparison of the peaks on the diffractogram with patterns of known pure material. Standard patterns of some 50,000 different minerals and crystalline materials have been compiled by the Joint Committee on Powder Diffraction Standards (JCPDS) and data summaries are published in regularly-updated monographs. In addition, various charts and tables have been prepared that allow easy comparison of many of the more common minerals found in sediments and sedimentary rocks (e.g., Hardy & Tucker, 1988; Lindholm, 1987; Brown & Brindley, 1980; Chen, 1977; Griffin, 1971). Jenkins (1989b), Cook et al. (1975), Klug & Alexander (1974), and Griffin (1971) present detailed step-by-step summaries of the interpretation procedure for non-clay mineral diffractograms. Because identification and quantification of clay minerals is considerably different than the relatively simple techniques outlined above, a more complete summary of the clay mineral methodology will be outlined below. In addition, Moore & Reynolds (1997), Thorez (1975), and Carroll (1970) offer detailed guidelines and procedures for interpreting clay mineral XRD patterns. Finally, the JCPDS Powder Diffraction File (PDF) is also commercially available in digital form for use on various computer platforms. Acquisition of this or similar datasets (see Smith, 1989) allows the researcher to very quickly perform searches and to identify the non-clay mineral components in a complex mixture, although even this

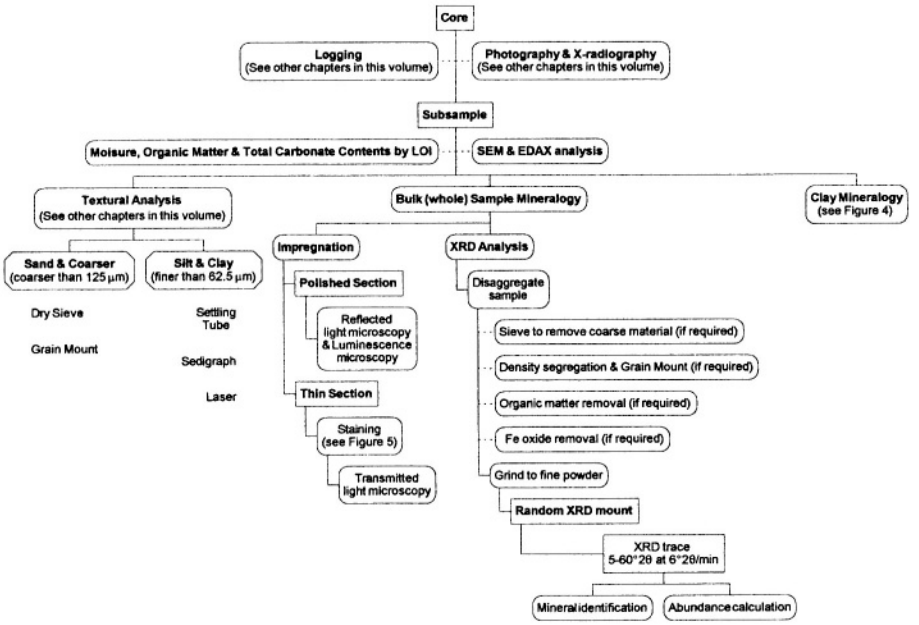


Figure 3. Flowchart showing the usual routes used at University of Manitoba for handling lake sediment samples for mineralogical analyses and other analyses. See Figure 4 for details on the clay mineral (oriented mount) analysis stream.

computerized procedure becomes increasingly more difficult as the number of minerals increases.

Sample preparation and analysis

Because of the geometric implications concerning incident and reflected radiation, the technique of sample preparation and mounting for XRD analysis is extremely critical. There is a large amount of literature on this topic but, unfortunately, there is no standard, all-purpose preparation/mounting technique used in sedimentary mineralogy, nor is there a uniform procedure of pretreatment of the samples. Moore & Reynolds (1997), Bish & Reynolds (1989), Hardy & Tucker (1988), Brown & Brindley (1980), Allman & Lawrence (1972), and Gibbs (1971) all provide excellent overviews of many of the techniques and discuss the various advantages and disadvantages of each; these references are good starting points for new investigators. Overall, there are two distinct but complementary approaches: (i) preparation and analysis of unoriented mounts in which the grains and particles making up the XRD slide assume a non-preferred (random) orientation, and (ii) analysis of mounts in which the grains have achieved a preferred orientation. Unoriented mounts are usually used for bulk (whole sediment) analysis and oriented mounts are applied to the investigation of clay minerals. Figures 3 and 4 summarize the handling of samples for XRD analysis used in my laboratory.

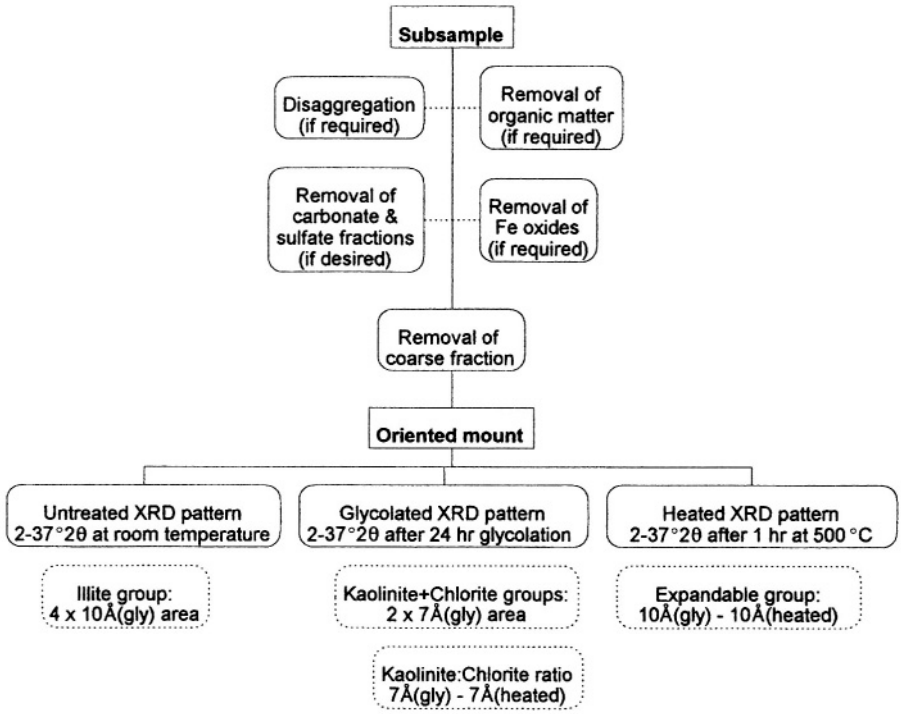


Figure 4. Flowchart showing the usual route of sediment handling for routine clay mineral analysis of lake sediments (continued from Figure 3).

Pretreatment

The best XRD results are obtained from samples that are uniformly fine grained (finer than about 10 μm), contain little or no organic matter or non-crystalline material, and are mounted in such a way as to provide a smooth, even, parallel surface upon which the X-rays can reflect. Since most lacustrine sediments are poorly sorted, organic-rich, and often contain amorphous Fe-oxides and siliceous material, at least minimal pretreatment is usually necessary. However, it must be realized that *all* pretreatment procedures have the potential of significantly affecting the mineralogy of the sample. As pointed out by Moore & Reynolds (1997) and Brown & Brindley (1980), it is advisable to do as little as possible to the sample before X-ray analysis.

Dried samples that were originally unconsolidated can be disaggregated by allowing them to sit overnight in distilled water followed by ultrasonic dispersal. Cemented or firmly aggregated samples, and material that is coarse grained or poorly sorted will need to be crushed to a uniform particle size. Moore & Reynolds (1997) and Bish & Reynolds (1989) recommend gentle crushing by impact in an agate mortar followed by wet grinding (using alcohol or acetone as a liquid lubricant) until a fine and uniform powder size is achieved. Iron and porcelain mortars should be avoided because they result in significant contamination. Most authorities in the past have cautioned against the use of automated grinders, however

Bish (1994) and Hardy & Tucker (1988) note several commercially available automated grinders with which they have achieved good results. In some cases the investigator may be specifically interested in the mineralogical assemblage of a certain size fraction, which requires either sieving or centrifugation. Other situations may call for removal of certain fractions of the sample, such as the carbonate traction (Jackson, 1969; Ostrum, 1961), the sulfate fraction (Bodine & Fernalld, 1973), or water soluble salts (Ingram, 1971).

Moderate to high amounts of organic matter and iron oxides in the sample present significant problems because they usually produce a high background on the diffractogram that can mask peaks. Unfortunately, removal of these components is difficult and, because of the strong chemicals often required, can adversely affect the mineral assemblage. The most common method for removal of Fe oxides is treatment with citrate-bicarbonate-dithionite (CBD; Jackson, 1969), but this also removes calcite and phosphate minerals and can affect the X-ray response from mixed-layer clay minerals. Organics are usually removed from the sample by treatment with hydrogen peroxide (Jones & Bowser, 1978), commercial bleach (sodium hypochlorite—NaOCl; Anderson,1963), sodium pyrophosphate ($Na_4P_2O_7$; Thomas, 1969; McKeague, 1967) but these treatments affect carbonates, sulfides and sulfate minerals in the sample. Relatively low temperature ashing (~100°C) has also been suggested (Moore & Reynolds, 1997; Gluskoter, 1965) but not yet applied to lake sediment studies.

Whole sample analysis

Once a finely ground, homogenous sample has been prepared, it is necessary to mount the material in a holder or on a slide which can then be X-rayed. Once again, there are a multitude of methods and techniques that have been suggested for this task (see, for example, overviews in Bish & Reynolds, 1989; Smith & Barrett, 1979; Gibbs, 1971). Hardy & Tucker (1988) and Klug & Alexander (1974) describe a commonly used cavity type of sample holder that is made from aluminum. The dry powder is gently packed into a well or cavity in a thin (2 mm thick) aluminum holder and the excess scraped off to produce a smooth surface to be irradiated. Because even light pressure on the surface of the mount can produce an undesirable preferred orientation of the particles, some researchers recommend back loading or side loading techniques (see Tucker & Hardy, 1988; Brown & Brindley, 1980). Alternatively, the powder can be mixed with a small amount of volatile liquid, such as alcohol, and simply smeared on to the surface of a glass petrographic slide. Rapid evaporation of the alcohol while mixing the sample on the slide presumably will not allow the particles to achieve a preferred orientation. Each of these methods, as well as several more elaborate techniques, such as the addition of amorphous binders, spray drying, and embedding in plastic, have been shown to result in satisfactory XRD data. However, it must be accepted that complete random orientation of the material is very difficult to accomplish.

As important as striving for random orientation is, close attention must also be given to the amount, thickness and coverage of the sample mount on the slide or holder. Bish (1994), Hughes et al. (1994), and Bish & Reynolds (1989) maintain that one of the most common sample mounting problems is the incomplete or insufficient coverage of the slide. The irradiated area on a slide or holder increases significantly with decreasing diffraction angle. For example, the length of exposed area at diffraction angles above about 20°2θ is 10 to 20mm; this increases to more than 50mm at angles less than 10°2θ. Thus, it is

important that the sample occupies an area on the slide or holder that is at least as large as the spread of the incident beam at the lowest angle used. Using sample coverage areas that are too small results in increased backgrounds (if a glass slide is used) or spurious peaks from the holder.

Sample thickness is also a consideration and can be a major source of error (Jenkins, 1989b). The XRD technique assumes infinite sample thickness, but 90% of the reflection pattern is generated from the upper 50 μm of the powder and ~50% is from the upper 10 μm. Consequently, a sample mount that is too thin will result in X-ray interaction with the underlying glass or holder material, whereas excessively thick mounts can cause a systematic displacement of the X-ray peaks.

As indicated above, unoriented mounts are routinely used for all non-clay mineral XRD analyses. For whole sample (bulk) analysis, the sample is generally irradiated from 5°2θ to about 60°2θ at a relatively fast scanning rate (6°2θ per minute is used in my laboratory for all bulk XRD analysis). If the investigator is interested in only certain components of the sediment, it is common practice to irradiate the sample at a slower rate between a smaller °2θ range. For example, if one is interested in the composition and crystallographic characteristics of the calcite-magnesian calcite-protodolomite-dolomite-magnesite series in a carbonate lacustrine sequence, higher precision XRD data might be collected from 24°2θ to 34°2θ at a rate of 0.6°2θ per minute. Most modern XRD equipment has the ability to preset a variety of programs containing the various operational parameters, such as scan speed, starting angle, number of degrees scanned, and step scanning, and also to collect both peak height (in terms of counts per second, cps) and peak areas.

Clay mineral analysis

Preparation of oriented powder mounts and the processing and identification of clay minerals from the resulting diffractograms can be one of the most complex and difficult tasks facing the XRD investigator. Because clay mineral crystals are usually very small, they do not give strong diffraction peaks relative to other non-clay minerals in a normal unoriented mount. Simply stated, there are too few atoms present in any one clay mineral plane to generate a usable diffraction intensity. However, clay minerals are also usually platy (i.e., one dimension very small relative to the other two). This morphological property can be used to advantage in XRD analysis by endeavoring to get X-ray diffractions from the large, flat surfaces of the minerals (referred to as basal reflections). This is done by attempting to maximize the preferred orientation of the material in the sample mount. By mounting the sample such that all the clay particles lie on top of one another, the diffraction effect from the platy minerals is greatly enhanced, while at the same time any reflections from components not parallel to the platy material are almost completely lost. In effect, the X-ray beam is seeing only the atomic planes of minerals that are parallel to the direction of orientation. The drawback to the use of oriented mounts is that the investigator cannot take advantage of the extensive powder diffraction data summaries and digital files, which are so valuable for non-clay mineral identification.

As with the preparation of unoriented mounts, there have been many methods proposed to induce orientation in the mount (Table II). The relative merits of these techniques will not be discussed here, but the reader is referred to Moore & Reynolds (1997), Hughes & Warren (1989), and Hardy & Tucker (1988) for up-to-date summaries of the most commonly used methods.

Table II. Summary of oriented mount (clay mineral) XRD sample preparation methods.

Method		References	Description	Advantages	Disadvantages
Smear		Bradley et al. (1937) Barshad (1960) Theisen & Harward (1962) Gibbs (1965) Tien (1974)	Thick clay paste is spread over surface of glass slide using spatula	Fast; simple; requires no special equipment; good precision, accuracy and peak intensity; sample is completely homogenous (no segregation)	Moderately skill-intensive (requires some practice to make even, thin smear); wet paste must be at proper consistency; poor preferred orientation
Pipette-on-slide	Air dry	Nagelschmidt (1941) Brown (1953) Jackson (1956)	Aqueous clay slurry is transferred by pipette to glass slide and dried at room temperature	Very commonly used; fast; simple; requires no special equipment; best development of preferred orientation	Allows size segregation of grains; often film is too thin
	90°C dry	Moore & Reynolds (1997)	As above except dried at 90°C	As above; more rapid drying results in less chance of size segregation	Potential mineral alteration due to elevated temperature
	Volatile medium	Last (1974)	Alcohol-based clay slurry is transferred to glass slide and dried at room temperature	As above; more rapid drying results in less chance of size segregation	Potential mineral alteration due to reaction with alcohol

Table II. Summary of oriented mount (clay mineral) XRD sample preparation methods (continued).

Method	References	Description	Advantages	Disadvantages
Powder-press (Pressure)	Mitchell (1953) Rex & Chown (1960) Cody & Thompson (1976) Gibbs (1971)	Dry powder is placed in Al holder and high-pressure piston action used to pack sediment	Fast; good precision, accuracy and peak intensity	Requires special holder and piston; holder difficult to subject to heat treatment; moderately skill-intensive
Suction-on-ceramic tile	Kinter & Diamond (1956) Rich (1969)	Aqueous clay slurry is placed on porous ceramic tile; liquid is drawn off by vacuum from below	Good precision, accuracy and peak intensity	Requires vacuum, special holder and apparatus, and non-standard ceramic plates/tiles that can be difficult to purchase or make
Centrifuge-on-ceramic tile	Gibbs (1965)	Aqueous clay slurry is placed on porous tile; liquid is removed by centrifugation	Best peak intensity; best preferred orientation; excellent uniform coverage of irradiated surface	Requires special holder and centrifuge apparatus; uses non-standard ceramic plates/tiles that can be difficult to purchase or make; size segregation; highly skill-intensive; difficult to master; lengthy preparation
Filter peel	Drever (1973)	Aqueous clay slurry is filtered through 0.45 μm filter and transferred to a glass slide	Best combination of speed, preferred orientation, and minimal size segregation	Requires special filtering apparatus and filter; costly filters; moderately skill-intensive

In general, preparing a clay mineral mount with good preferred orientation is not difficult because of the platy morphology of most clay minerals. However, a major problem arises in that the methods which produce the best preferred orientation also result in a size-segregated clay film. This size segregation is also often a mineralogical segregation because smectite (montmorillonite) particles characteristically have much smaller sizes than the other major clay mineral groups. Thus, in any technique in which the particles are allowed to settle (such as the pipette-on-slide and centrifuge-on-ceramic tile methods), there will be relative enrichment of smectite near the top of the mount and proportionately less of the other clay minerals (Stokke & Carson, 1973). Since most of the X-ray diffraction response is generated in the upper 5 to 10 μm of the clay film on the slide, quantitative results from these size/mineral segregated slides will be in error even though there may be excellent preferred orientation of the grains.

Gibbs (1965; see also Gibbs, 1971, 1968) undertook a comprehensive quantitative comparison of the major methods in use up to the early 1960s, and concluded that only a few of them (i.e., smear-on-slide and suction-on-ceramic tile methods) gave acceptable results. Stokke & Carson (1973) echo this sentiment. In contrast, others have maintained there is little or no systematic difference between the various methods (see Theisen & Harward, 1962), or argue that techniques employing settling show excellent reproducibility and the quantitative data, if not accurate, are, nonetheless, precise and do show the correct trends in mineral assemblage distributions. Most recently, Moore & Reynolds (1997) indicate that the filter peel technique of Drever (1973) probably represents the optimum compromise between speed of preparation, required operator skill, and development of non-segregated preferred orientation. Hughes et al. (1994) recognize that the choice of method depends not only on the degree of orientation and segregation, but also on the nature of the material and the purpose of study. They prefer to adopt the fastest method available that satisfies the accuracy requirement for the particular problem. Finally, Bish & Reynolds (1989) likewise recognize the factors of operator expertise, time, and purpose of study, and propose three basic levels of investigation coinciding with different methodologies: (i) reconnaissance and general qualitative clay mineralogy, in which the pipette-on-slide method is used; (ii) quantitative analysis using the filter peel method; and (iii) crystal structure analysis with samples prepared by the labor-intensive and instrument-dependent centrifuge-on-ceramic tile method.

Identification of clay minerals from oriented XRD patterns is often a perplexing task for a new researcher in the field. Nearly all of the important clay minerals have peaks that occur at relatively low diffraction angles (~2–17Å) and, in striking contrast to non-clay minerals, have broad reflections. These broad basal reflections are due to the thin nature of the crystals and the fact that many clays are characterized by disordered crystal structures and variations within the atomic layer stacking. Consequently, the XRD peaks are often overlapping and frequently one mineral's reflection can completely mask the reflections from another. This dilemma is resolved by exploiting another important property of clay minerals: swelling. Some clay types change their crystal lattice dimensions by incorporating various other molecules, thereby expanding or contracting the *d* spacing which gives rise to the XRD response. Thus, through artificially manipulating the composition of the clays by inserting or removing different molecules, the specific minerals in a mixture can be identified. The two most common molecules used in routine clay mineral XRD work are water and ethylene glycol.

Table III summarizes the responses of the main clay mineral groups to various treatments and Figure 4 provides a generalized analytical procedure. These procedures outlined below are applicable for routine recognition and quantification of the major clay mineral groups. Within most of the groups there are various subgroups and species that require more elaborate XRD and chemical techniques not covered in this chapter. Brindley & Brown (1980) and Thorez (1975) are excellent references that supply details about these more advanced techniques.

It should be emphasized that the researcher must decide before starting the analytical procedure what size fraction and/or mineral fraction is to be analyzed. *Clay sized material* is defined as any sediment finer than 2.0 μm (or sometimes 3.9 μm; see Last, this volume) whereas *clay mineral material* is defined as generally crystalline layer-lattice silicates (phyllosilicates). Many non-clay minerals can be present within the clay sized fraction and, conversely, clay minerals can often be present in the coarser-than-clay sized material of the lacustrine sediment. There are different approaches for each of these components. The following summarizes a general procedure for identification and quantification of clay minerals within the clay sized fraction.

Samples are normally prepared and analyzed in batches. Twenty-four samples per batch is convenient for the facilities in my laboratory, but this number must be determined individually according to equipment type and availability. The following comments are relative to mineralogical analyses conducted on a Philips Automated Powder Diffraction System PW1710 using monochromated CuKα radiation with Ni filtering generated at 40 k V and 40 mA. Recommended scanning speed for clay mineral work is 0.6°2θ per minute and at 200 counts per second (cps), although these may vary as a function of material analyzed and instrumentation. Other equipment settings are automatic variable divergence detector slit, 1 second measurement constant, and 0.01°2θ step size.

1. Disaggregation and crushing: If the sample is dry, disaggregate it with fingers or a wooden mallet and crush it to a fine powder using an agate mortar. Alternatively, a standard Waring-type blender may be used if available. Sieve the material through a 4ϕ (62.5 μm) sieve. If the sample is wet and uniformly fine grained, it may not be necessary to sieve, so go directly to step 2. It is not necessary to weigh the sample or make volume determinations, and it is undesirable to dry the sample. The amount of sample used depends largely on: (i) amount of clay sized material and clay mineral matter in the sample; (ii) amount of organic matter, amorphous material, and other non-clay materials in the sediment; and (iii) number of slides to be made (see step 7). It is normal to have done loss-on-ignition (see Boyle, this volume), particle size analysis (see Last, this volume), and bulk mineralogy on the sample before doing clay mineralogy in order to better anticipate the pretreatment that may be required. Generally the optimum size for normal Holocene clastic-rich lacustrine sediment of moderate to low organic content is about 1 cm^3.

2. Removal of salts and organic matter: If the material is from a salt lake, it is advisable to wash repeatedly in distilled water to dissolve and remove as much of the saline components as possible. For most modern and Holocene offshore lake sediment, removal of organic matter is necessary. This is most efficiently accomplished by repeated treatment with 30% hydrogen peroxide (H_2O_2). If the sample has relatively little organic matter, 10% H_2O_2 can be used. In either case, the hydrogen peroxide should be added slowly to the sample in sufficient quantity to cover the powder. The treatment must take place in a fume hood with the operator wearing appropriate safety shield, gloves and attire. Highly organic-rich

Table III. Response of major clay mineral groups to glycolation and heating (compiled from Brown & Brindley, 1980; Thorez, 1975; and Carroll, 1970)

Mineral group	***d* spacing from an oriented mount with °2θ (copper Kα radiation) in brackets**	**Effect of glycolation**	**Effect of heating**	
			500–550°C	higher temp
Kaolinite	7.15 Å (12.6°2θ)	no change	disappears	
Chlorite	14 Å (6.3°2θ)	no change	no change	disappears at ~800°C
Swelling chlorite	14 Å (6.3°2θ)	16 Å (5.5°2θ)	14 Å (6.3°2θ)	
Smectite	12.5–15 Å (7.4–5.9°2θ)	17 Å (5.2°2θ)	10 Å (8.8°2θ)	disappears at >700°C
Illite	10 Å (8.8°2θ)	no change	no change	disappears at >800°C
Vermiculite	14 Å (6.3°2θ)	no change	10 Å (8.8°2θ)	disappears at >700°C
Palygorskite (attapulgite)	10.5 Å (8.4°2θ)	no change	9.2 Å (9.6°2θ)	disappears at ~700°C
Sepiolite	12.2 Å (7.2°2θ)	no change	10.4 Å (8.5°2θ)	disappears at ~700°C

samples can react violently. After sitting overnight, check for completion of reaction by adding a few more ml of H_2O_2 and repeat the treatment as necessary.

3. Ultrasonic disaggregation: Add a sufficient amount of dispersant solution (10% sodium hexametaphosphate solution, or Calgon, is most commonly used; see Lewis & McConchie, 1994, for a list of others) to bring the volume to about 50–100 ml (depending on the size of the centrifuge to be used) and put the sample into an ultrasonic bath for 10 to 30 minutes.

4. Centrifugation: Immediately after ultrasonic treatment, fill a centrifuge tube with the slurry and centrifuge at 1200 rpm (revolutions per minute) for 70 seconds. This will sediment all material coarser than 2 μm (see Moore & Reynolds, 1997, and Jackson, 1969, for other rpm/time combinations). Adjust the centrifuge speed and time according to Jackson (1969) to obtain different size fractions as necessary.

5. Vacuum filtration: Carefully pour the liquid with the suspended clay particles into a vacuum filter apparatus (such as provided by the Millipore Corporation; see Moore & Reynolds, 1997) and filter through a 0.45 μm glass filter. Normal samples usually take about 5 to 15 minutes, but for very clay-rich or clay-lean samples, it may be necessary to adjust the volume of liquid in order to get an acceptable amount on the filter.

6. Peel transfer: Once the slurry has been filtered, carefully separate the vacuum apparatus, take off the filter, and transfer the clay film from the filter to a standard glass petrographic slide. This is usually the most difficult task of the preparation procedure and requires considerable practice. Refer to Reynolds & Moore (1997) and Drever (1973) for hints and guidelines on making successful peel transfers.

7. Multiple slides: Normally it is sufficient to make only one oriented mount. However, depending on the number of personnel in the laboratory and the timing of access to XRD equipment, it may be efficient to make several slides of the same sample, with the different slides being processed and irradiated with different treatments (i.e., one slide heated, another slide glycolated, a third slide untreated). Let the slide(s) dry at room temperature. Many of the expandable lattice clays react rapidly to ambient humidity conditions, so if the laboratory normally experiences fluctuations in relative humidity, place the slide in a desiccator until irradiated.

8. Untreated XRD scan: Irradiate the dry, untreated slide from 2°2θ to 37°2θ using a slow scanning speed (0.6°2θ per minute) and appropriate cps setting to generate a diffractogram that clearly shows the peaks. This will require some trial and error.

9. Glycolated XRD scan: Place the slide in a bell jar or desiccator containing ethylene glycol for at least 24 hours. Irradiate the glycolated slide using the same instrument settings as above. If the samples are being prepared in batches, glycolated slides that are awaiting XRD should be stored in the glycolator to avoid evaporation and collapse of the expanded structure.

10. Heated XRD scan: Place the slide in a muffle furnace and heat at 500–550°C for one hour. Allow to cool and irradiate the heated slide using the same instrument settings as above. If the samples are being prepared in batches, heated slides that are awaiting XRD should be stored in a desiccator to avoid rehydration.

11. Interpretation: The following qualitative and semi-quantitative evaluation is useful for routine clay mineral analysis and has been adopted and modified from many literature sources. Use Brown & Brindley (1980) and Thorez (1975) to refine the analyses if more detail is required.

Illite is a poorly defined term referring to a group of mica-like clay minerals of indefinite structure (Grim, 1968).The illite group is defined on the diffractograms by a sharp peak at ~10Å (8.8°2θ) that is not affected by glycolation or heating. Broad secondary peaks at 5 Å (17.7°2θ) and 3.3 Å (26.7°2θ) can also be used if the sample is low in quartz. The expandable clay mineral group, which includes smectite, vermiculite, expanding chlorites and various mixed-layer species, is identified on the basis of its expanding lattice. When dry it has a *d* spacing of about 12.5Å (7.05°2θ). After glycolation, the material expands to a peak at about 17 Å (5.19°2θ). The position of this peak is variable depending on the exact composition of the expandable lattice material. However, heating will cause a shift in the peak position from 17 Å to 10Å. The shapes of these peaks on the glycolated and heated traces can be used to qualitatively determine the presence and type of mixed-layer clays in the overall expandable group as outlined by Thorez (1975). Similarly, the degree of crystallinity of the material making up the expandable lattice group can be approximated by examining the ratio of the height of the 17 Å peak on the glycolated trace to the 'depth' of the valley on the low angle side of the peak (peak:valley ratio; Biscaye, 1965). The closer this ratio is to one, the better the crystallinity of the material. The kaolinite and chlorite groups are identified by their combined, overlapping reflection at 7 Å (12.4°2θ) from the glycolated slide. These two components are separated on the basis of the relative difference in peak areas of the 7 Å peak after glycolation and heating. Kaolinite becomes amorphous after heating, thus the difference in areas (i.e., glycolated minus heated) of the 7 Å peaks will give the proportion of the two minerals. The presence or absence of chlorite can also be confirmed by the 14 Å (6.3°2θ) and 3.5 Å (25.2°2θ) peaks (see Biscaye, 1964).

12. Calculation procedures: Semi-quantitative calculations of the relative abundances of the major clay mineral groups are made using the weighted peak area method of Johns et al. (1954):

$$\% \text{ expandable layer clay mineral group} = \left[\frac{X}{(X+Y+Z)}\right] \cdot 100, \tag{2}$$

$$\% \text{ kaolinite + chlorite mineral groups} = \left[\frac{Y}{(X+Y+Z)}\right] \cdot 100, \tag{3}$$

$$\% \text{ illite mineral group} = \left[\frac{Z}{(X+Y+Z)}\right] \cdot 100, \tag{4}$$

where

$$X = (\text{area of } 10\,\text{Å peak on glycolated trace}) - (\text{area of } 10\,\text{Å on heated trace}), \tag{5}$$

$$Y = 2 \cdot (\text{area of } 7\,\text{Å peak on glycolated trace}), \tag{6}$$

$$Z = 4 \cdot (\text{area of } 10\,\text{Å peak on glycolated trace}). \tag{7}$$

If it is desirable to separate the percentage of kaolinite and chlorite groups, this can be done by determining the ratio of peak intensities of the 3.5 Å couplet as outline by Biscaye (1965) or by using the difference in peak areas of the 7 Å peak from the glycolated and heated traces.

The above semi-quantitative method is in common use in much of western Canada and north-central United States, but there are numerous other weighting schemes available that are just as commonly used. For example, Schultz (1964) uses a weighting factor of

4.5 on the illite (10Å) peak and 0.25 for the kaolinite + chlorite (7 Å) peak; Hathaway & Carroll suggest using a factor of 5 on the 7 Å intensity; Pierce & Siegal (1969) propose factors of 3 for the 10Å and 2 for the 7 Å peaks. In addition, other semi-quantitative methods have been proposed (e.g., Moore & Reynolds, 1997; Bish, 1994; Hughes et al., 1994; Carroll, 1970) that use internal or external standards in a manner similar to the techniques used for unoriented samples (see below). However, the lack of pure clay mineral standards and significant variations in XRD patterns caused by changes in hydration state, mounting technique and degree of preferred orientation, and mineral crystallinity curtail the application of this standards approach. Finally, as emphasized by Hardy & Tucker (1988) all of these semi-quantitative methods suffer from the disadvantage that the mineral quantities are normalized to 100%. In other words, a change or error in one mineral abundance affects all the others.

Quantification Issues

Raw X-ray diffraction data, either digital or acquired on a strip recorder, are used make mineral identifications as summarized above. Whole sample data collected from random powder mounts are compared to patterns of known minerals either manually or using a computer search-match program such as μPDSM (Marquart, 1986). Because each component in a mixture of crystalline materials produces its own characteristic pattern that is independent of others, the identification process becomes one of simply unscrambling the superposed patterns.

Frequently, these qualitative results are summarized in publications with semi-quantitative qualifiers, such as "abundant", "minor", and "trace" on the basis of the relative intensities of the peaks. Intuitively, one would expect the intensity of the diffraction peak from a particular mineral to be simply related to that mineral's abundance. However, it has long been recognized that this relationship is not straightforward. In a mixture of minerals, the peak geometry is affected by not only the relative and absolute abundance of the particular mineral and its crystallinity, but also by the X-ray absorption characteristics (termed the mass absorption coefficient) and particle size of the other minerals, and the amount of amorphous material in the sample. The end result is that the intensity relations among peaks for a multicomponent mixture can be very complicated.

Many methods have been developed to quantitatively assess the mineralogy of a sample based on X-ray diffraction data from a random mount (see overviews in Reynolds & Moore, 1997; Bish, 1994; Snyder & Bish, 1989; Bish & Chipera, 1988; Brindley, 1980), however, only a few of these are in common use in sedimentary and paleolimnological research. One of the most often used approaches, the internal standard calibration method, is to derive peak intensity weightings for each mineral based on a series of separate calibration XRD responses from mixtures of known quantities of the minerals (e.g., Cook et al., 1975; Klug & Alexander, 1974; Schultz, 1964). The calibration standards are done using minerals found within the same geologic province and, as much as possible, having similar crystallinity and size characteristics as the material in the unknown sample. Because quartz is ubiquitous in most lacustrine bulk sediment samples, it is common practice to use 50:50 ratios of each mineral and quartz for the calibration standards, although more mixtures of different ratios (e.g., 25:75, 50:50, 75:25) will clearly lead to better statistical relationships as the minerals in the unknown deviate from a 50 : 50 mixture (Fisher & Underwood, 1995). As pointed

out by Cook et al. (1975), the resulting values need to be normalized to 100% and are, thus, estimates of relative percentages.

A technique similar to the internal standard calibration method involves adding a known amount of an easily recognized foreign material that would likely not otherwise be in the sample, such as corundum (Al_2O_3) or fluorite (CaF_2). The abundance weighting factors for each mineral are then determined on the basis of a series of calibration mixtures with this spiked external standard (Fisher & Underwood, 1995; Heath & Pisias, 1979; Moore, 1968; Lennox, 1957). The external standard method is particularly useful for situations in which quartz or another internal standard cannot be used because of absence or low abundance.

The disadvantage of these internal and external standard calibration techniques is that determination of the weighting factors is quite tedious and must be re-done for each geographic and/or geological region in which the researcher is working. In an effort to improve this quantification method and make it more universally applicable, Chung (1974a, 1974b) proposed a simpler technique referred to as the matrix flushing method. As mentioned above, the XRD peak intensity is related to the abundance of a mineral in a complex manner. Klug & Alexander (1974) show that the intensity of diffracted X-rays of a mineral in a mixture (I_i) is a function of that mineral's concentration (W_i) and density (σ_i), the average mass attenuation coefficient of the mixture and of the mineral (i.e., attenuation coefficients; μ^* and μ_i) and a constant (K_i) that depends on the geometry of the diffractometer, wavelength of the incident radiation, and various crystal structure indices, according to:

$$I_i = K_i \cdot \frac{(W_i/\sigma_i)}{\Sigma(\mu_i \cdot W_i)} \tag{8}$$

or

$$I_i = K_i \cdot \frac{(W_i/\sigma_i)}{\mu^*}. \tag{9}$$

Unfortunately, most μ_i values have not been measured and μ^* is unknown for any given mixture. Hence, W_i cannot be calculated from I_i. However, as first pointed out by Chung (1974a), the matrix absorption effect can be eliminated by calculating a ratio:

$$\frac{I_i}{I_s} = W_i \cdot \left(\frac{\mu_i}{\mu^*}\right), \tag{10}$$

where I_s is the intensity of an internal standard. The JCPDS powder diffraction file (PDF) already publishes I_i/I_s values for each mineral using synthetic corundum as the standard (i.e., I_i/I_c). So the two unknown mass attenuation coefficients (matrix effect) cancel in the ratio and the weight fraction of the mineral becomes:

$$W_i = \left[\frac{W_c}{(I_i/I_c)}\right] \cdot \left[\frac{I_i}{I_c}\right], \tag{11}$$

where W_c is the concentration of the corundum standard. Once all the minerals in the sample have been identified, W_c also cancels and the equation simplifies to:

$$W_i = \left[\left(\frac{(I_i/I_c)}{I_i}\right) \cdot \left(\frac{\Sigma I_x}{(I_x/I_c)}\right)\right]^{-1}, \tag{12}$$

where I_x is the peak intensity for each mineral in the mixture (Chung, 1974b).

As emphasized by Bish (1994) and Snyder & Bish (1989), Chung's matrix flushing method cannot be used if there are any unidentified mineral phases in the mixture. Furthermore, the technique assumes that all the material in the sample has the same degree of crystallinity, the same chemical composition, and the same mass absorption characteristics as the PDF reference material, and that sample preparation and degree of random orientation are compatible with that of the JCPDS samples. These can be significant factors that prohibit routine use of the matrix flushing technique, particularly when dealing with minerals that exhibit extensive solid solution (e.g., many carbonate and sulfate minerals) and various levels of ordering (e.g., calcite, dolomite, magnesite). Despite these caveats, the technique does have the significant advantage of eliminating the need for calibration curves in that all qualitative and quantitative data on a sample can be acquired from a single XRD scan.

Light microscopy

Introduction

Optical microscopic methods are among the oldest and most straightforward techniques to analyze the minerals in a sediment or rock sample. The primary tool, a petrographic microscope, allows easy and rapid identification of any minerals through which light can pass. The petrographic microscope is similar to an ordinary compound microscope except that it has a revolving, graduated circular stage, a light polarizing device below the stage, and another polarizer above the objective lens. Thus, light from a substage source is polarized before it reaches the sample and the operator can view the sample in either plane-polarized light (PPL) or crossed-polarized light (CPL). In addition, a supplementary lens that can be used for detecting and viewing interference figures, a Bertrand lens, can be inserted in the microscope tube between the upper polarizer and the eyepiece.

With this basic equipment an investigator can identify and quantify mineral components in a thin section (TS) or grain mount by systematic examination of key optical properties (e.g., refractive index, birefringence, optic angle and sign) and morphological and physical characteristics (Table IV). Although the mineral suite of a lake deposit can be complex as noted above, there are many well-illustrated publications available to assist investigators who have relatively little formal petrographic training (e.g., Adams & MacKenzie, 1998; MacKenzie & Adams, 1993; Adams et al., 1987; Lindholm, 1987;Matzko, 1984; Scholle, 1979; 1978)

Sample preparation

Because most Quaternary lake sediment samples are only poorly consolidated at best, vacuum embedding in a polyester resin or impregnation in epoxy is usually necessary before thin sections can be prepared. Details of these procedures and descriptions of the equipment required are given in Miller (1988a), Cady et al. (1986), Murphy (1986), Jim (1985), Ashley (1973), Innes & Pluth (1970), and Bouma (1968). Because of their low permeability and high water content, fine grained sediments are particularly difficult to work with and impregnation techniques often require lengthy diffusion and curing times (Allman & Lawrence, 1972; Stanley, 1971). In addition to artificially cementing single

Table IV. Checklist for rapid systematic petrographic microscopic examination of thin sections (modified from Milner, 1962a, and Walstrom, 1960).

With transmitted light:
Transparency, translucency or opacity
Colour
Crystal habit; presence or absence of crystal faces; evidence of crystallization
Shape and size
Cleavage, partings, fractures
Surface features: degree of pitting, intergrowths, overgrowths, abrasion
Inclusions
Refractive index
With transmitted plane-polarized light:
Pleochroism: presence or absence; weak or strong; colour
With transmitted crossed-polarized light:
Isotropic or anisotropic
Birefringence
Extinction: straight or oblique; if oblique: angle
Interference colours and order
With transmitted crossed-polarized light and Bertrand lens:
Interference figure: uniaxial or biaxial
Optic sign
Optic axial angle
Dispersion of optic axes

samples, it is also common to embed entire cores or sections of cores in resin (Kemp et al, this volume; Pike & Kemp, 1996; Stanley, 1971; Bouma, 1968), from which multiple thin sections can be cut and examined not only for mineralogy but also sedimentary structures, textures and fabrics. In the case of relatively coarse unconsolidated material in which the fabric of the sediment is not of interest or if the investigator is examining size or density fractionated components of a deposit, it is advantageous to mount loose grains (Müller, 1967; Tickell, 1965). A full treatment of these preparation techniques is given in Lewis & McConchie (1994), Lewis (1984) and Stanley (1971).

Once the lake sediment sample has been impregnated (if necessary) or a grain mount prepared and an adequate thin section cut, it is common to apply various stains to assist the investigator in recognizing certain minerals. Chemical stains, often used in conjunction with acid etching, are available for a variety of commonly occurring sedimentary minerals, as reviewed in Lewis & McConchie (1994), Miller (1988a), Hutchinson (1974), Allman & Lawrence (1972), Friedman (1971), and Reid (1969) (see Fig. 5). For example, calcite and dolomite, two very common carbonate minerals in lake sediments, can be difficult to distinguish on the basis of their optical properties alone. However, application of a solution of Alizarin red S will preferentially stain the calcite red and leave the dolomite unaltered. Similar chemical stains exist for aragonite, ferroan calcite and dolomite, Mg-calcite, magnesite, gypsum, plagioclase, K-feldspars, kaolinite, illite, and smectite.

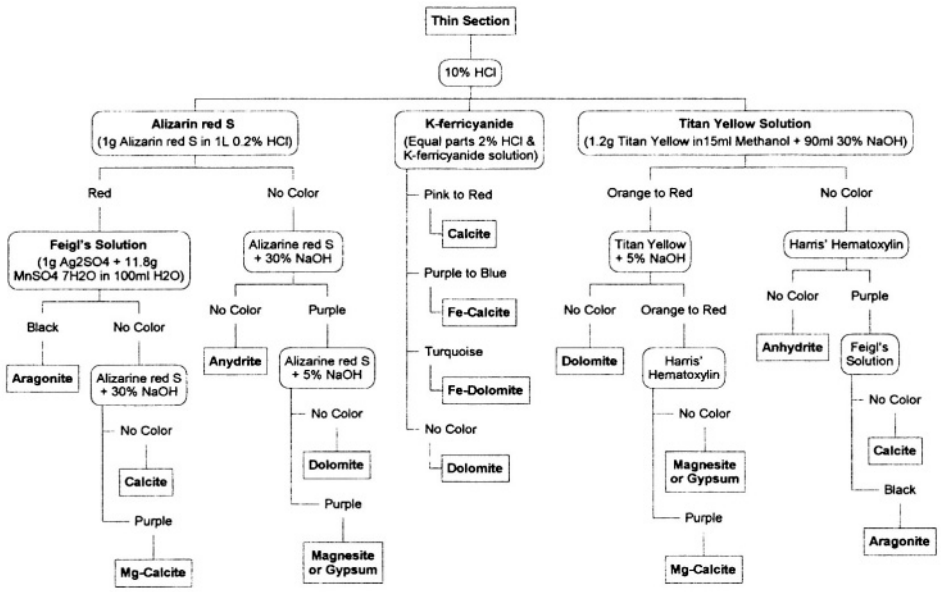


Figure 5. Thin section staining.

Reflected light and luminescence microscopy

The use of reflected light microscopy is relatively rare in paleolimnological studies because most microscopic investigations to date have concentrated on nonopaque minerals. However, there are a number of potentially important avenues of investigation that can be exploited through the application of reflected light techniques. Although not strictly a mineralogical investigation, the petrology of organic matter in sediments depends mainly on the use of reflected light microscopy (see Bustin et al., 1983; Staplin et al., 1982; Brooks, 1981; Cook & Kantsler, 1980; Durand, 1980). Study of the heavy mineral fraction (i.e., minerals with specific gravity of greater than 2.85) of sands and sandstones, which is usually dominated by opaque minerals, has provided basin analysts with considerable insight into the provenance, weathering and dispersal characteristics, and tectonic history of sedimentary deposits (e.g., Basu & Molinaroli, 1989; Pettijohn et al., 1987; Pettijohn. 1975; van Andel & Pool, 1960). Friedman et al. (1992), Peckett (1992), Lindholm (1987) and Milner (1962b) provide details on the sample preparation techniques and optical characteristics of these opaque detrital components.

The use of luminescence to supplement transmitted and reflected light microscopy has now become routine in TS petrographic work. Luminescence refers to the emission of light from a solid in response to bombardment by some form of energy. For example, ultraviolet (UV) luminescence, which occurs when a substance absorbs either visible or ultraviolet light, has been used in organic petrological studies for many years (Cook, 1980; Alpern, 1980) and holds considerable promise in helping understand complex carbonate mineral fabrics and cement neoformation (Dravis & Yurewicz, 1985). Cathodoluminescence (CL)

results from excitation by electrons and has a wide variety of applications in sedimentary petrography as reviewed by Lewis & McConchie (1994), Barker & Kopp (1991), Marshall (1988), and Walker (1985). Although the CL technique has only recently been applied to paleolimnological investigations (e.g., Mather, 1999; Nobel et al., 1996; Mazzoleni et al., 1995) and much still remains to be done in terms of understanding the actual causes of CL in minerals, Miller (1988b) maintains that it is one of the most important developments in sedimentary petrography since the 1960's.

Quantification issues

A major concern for all TS based petrographic and mineralogical research is quantification. Once the minerals have been identified, it is desirable to estimate the proportions of each component. Various percentage estimation comparison charts are available that allow the investigator to very rapidly assess approximate proportions of readily identifiable grains with reasonable precision (e.g., Drees & Ransom, 1994; Harwood, 1988; Folk et al., 1970; Terry & Chilingar, 1955). However, usually more quantitative approaches are applied. The traditional methods involve either (i) making repeated linear traverses across the slide and enumerating the mineralogy of all individual grains encountered at the cross-hairs (line method), giving a number frequency estimate; (ii) tabulating the mineralogy of all the grains encountered in a given area of the slide (ribbon or area method), which provides an estimate of the number percent; or (iii) counting all the individuals intersected at equadistant points on a grid (grid or Glagolev-Chayes method), giving an estimate of the area percent (Galehouse, 1971). These techniques work well with coarse grained and well sorted sediments but become less reliable as the proportion of finer particles (silt and clay) increases, as the particle shapes become less equant, and as the sorting decreases (Drees & Ransom, 1994; Solomon, 1963; Chayes, 1956a, b).

In order to achieve reasonable statistical significance, most authorities recommend counting about 300 to 500 points or grains on a slide. The probable error of the resulting percent of individual components (at 95% confidence) can be calculated by:

$$E = 2 \cdot \left[\frac{(P \cdot (100 - P))}{N} \right]^{0.5} \tag{13}$$

where E is the probable error in percent; N is the total number of points or grains counted; and P is the percentage of the particular component (Galehouse, 1971). For example, if 100 grains are counted and 10 of them are dolomite, then the chances are 19 out of 20 that the real percentage of dolomite in the sample is 10 ± 6% or between 4% and 16%, whereas if 500 grains were counted and 50 of them were dolomite, the real percentage (at 95% confidence) would be between 7.3% and 12.7%.

Point counting has been the standard procedure for mineral quantification in TS based petrography for most of the 20th century. Although various supplementary devices, such as both manual and automated graduated mechanical stages, integrated eyepieces, and automated counters, greatly facilitate the speed with which a petrographer can analyze a thin section (Galehouse, 1971; Griffiths, 1967), it was not until the widespread use of personal computers and the availability of inexpensive image analysis (IA) software packages that speed, accuracy, and precision increased significantly (Russ, 1990; Petruk, 1989; Meek

& Elder; 1977). Russ (1999), Drees & Ransom (1994) and Jones (1987; 1977) discuss the theory, equipment, and application of IA systems in petrographic and mineralogical analysis. These new computer assisted techniques are much faster than manual methods and produce more accurate and unbiased results, particularly in sediments with relatively simple mineralogies. However, the analytical systems still depend heavily on the expertise of the investigator to properly recognize and differentiate the mineral species and to assign the minerals to specific computer-measured classes (Drees & Ransom, 1994; Amstutz & Giger, 1971). The petrographer must also compensate for slight variations in slide thickness and other artefacts, such as air bubbles and scratches within the petrographic slide.

Advantages and disadvantages

Optical microscopy has been the mainstay of sedimentary petrographers and mineralogists since Sorby published the first sediment thin section descriptions in the mid-nineteenth century (Sorby, 1851). Although many refinements have been adopted, the basic techniques of mineral identification and quantification have changed little in the past seventy-five years. The chief advantages of optical microscopy are that it requires relatively little equipment, and that the investigator can not only decipher the minerals present and their relative abundances but also examine the fabric, microstructures, size, and surface features of the particles, thereby providing an enhanced understanding of the genesis and diagenesis of the sedimentary deposit.

However, there are also many shortcomings inherent in routine application of optical microscopy to paleolimnology. Sediments in general and Quaternary lacustrine deposits, in particular, often have a much greater mineral diversity than do igneous and metamorphic rocks or other sedimentary deposits. This great diversity can make TS examination of lacustrine sediment an arduous task for a new inexperienced researcher. Paleoenvironmentally important minerals that may occur in relatively small proportions can be easily overlooked or misidentified. Many commonly occurring minerals in lake sediments have similar optical properties and, because paleolimnologists are often dealing with detrital particles, crystal habit cannot be used to help distinguish them. Fine grained sediments, which dominate the offshore stratigraphic records of most lakes, are difficult to prepare and examine optically; medium to fine silt and clay-sized material (i.e., sediment finer than $\sim 30\,\mu m$) is almost impossible to resolve in routine petrographic analysis of normal thin sections. Quantification of the mineral assemblage of poorly sorted sediments presents many practical and interpretive problems. Although recent application of computer-assisted IA techniques have significantly improved the speed and reproducibility of mineral quantification, thin section analysis still represents a relatively large investment of time by a well trained and experienced professional.

Future developments

Because knowledge of the mineralogical composition of a lacustrine deposit is fundamental to understanding the history of the lake and the evolution of the lake's drainage basin and water systems, paleolimnologists will continue to have a strong interest in the nature and amount of inorganic crystalline materials making up their samples. The minerals (together

with texture and structures) are the basic components of a sedimentary deposit that need to be examined and quantified if only to properly describe the material. The generally fine particle size of the sediment with which most paleolimnologists work dictates that X-ray diffraction will probably remain the method of choice for both qualitative and quantitative analyses. However, as we continue to explore the more ancient lacustrine stratigraphic records of the world (e.g., Gierlowski-Kordesch & Kelts, 1994, 2000), and, in particular, as the economic potential of these pre-Quaternary lakes is realized (Katz, 2001), optical microscopy, combined with other petrographic and spectroscopic tools will increase in prominence.

Both optical microscopy and XRD are traditional methods for sedimentary petrographers. Both sets of techniques have been refined greatly over the past half century such that application of the methods is now routine and straightforward. Like many methods involving quantification, the quantitative assessment of minerals in a sample is, at present a rather tedious and labor intensive pursuit, and subject to a number of technical and practical problems. These quantification techniques will likely benefit from continued advances in image analysis methods (for TS petrography) and more streamlined numerical and computerized XRD data handling techniques (e.g., full-pattern fitting methods; Bish, 1994). Although new geochemical techniques and instruments will continue to fuel advances in our understanding of lake sediments from an elemental and molecular perspective, XRD and optical methods will remain at the forefront of mineralogical research and analysis for some time.

However, the most important advances to be made over the next decade involve not so much how paleolimnologists identify and quantify the minerals, but rather how conceptually these data are applied to helping understand the history of the lake. Tremendous advances in our understanding of the genesis and diagenesis of minerals in lakes have been made in the last decade or so of the 20th century and this will no doubt continue well into the new millennium. With this enhanced understanding of how and why a mineral forms and changes comes the potential for quantitative assessment of the history of the lake. Many aspects of paleolimnology are already impressively quantitative. One only has to read Stoermer & Smol (1999) or Birks (1998) to appreciate the rich detail and wealth of quantitative information with which the biological side of paleolimnology can decipher lake histories. The transition from descriptive to quantitative interpretation has been somewhat slower within the mineralogical realm, but important recent advances have been made and there is every indication that this will continue into the future.

Summary

This chapter has emphasized two of the most commonly used methods of mineralogical assessment of lake sediments: X-ray diffraction and optical petrography. The choice of methods is largely controlled by the nature of the sediment and the objective of the research. Optical mineralogy can provide the investigator with not only qualitative and quantitative mineralogical data but also key petrographic information, such as depositional and diagenetic fabrics and textures. However, direct petrographic examination of fine grained sediments is very difficult. X-ray diffraction techniques, in contrast, provide a relatively fast and inexpensive means of quantitatively assessing the mineral assemblage of fine

grained deposits, which are often the target for paleolimnologists, but supply no clues as to the origin or alteration of the minerals present.

Bulk or whole sample mineralogy is done by collecting X-ray diffraction data from a random powder mount. Pretreatment procedures must be kept to a minimum but the sediment to be X-rayed must be reduced to a fine powder that is relatively free of organic matter and amorphous material. The powder must be applied to the holder or slide in such a way as to present a smooth, even, parallel surface upon which the incident X-ray beam can interact. Clay minerals represent a special problem because they are so small and usually do not exhibit a usable XRD response from a random powder mount. Consequently, clays are best analyzed by preparing and irradiating a powder mount in which the particles have achieved maximum preferred orientation. However, various technical problems arise due to inherent particle size and mineral segregation when attempting to prepare oriented mounts. These problems have resulted in a wide variety of different mounting techniques in use. Quantification techniques for XRD data are complicated because the intensity of the peaks on the diffraction pattern is not directly related to the abundance of the mineral in a mixture. Thus, a system of standards and calibration mixtures must be prepared. Alternatively, if all the minerals in a sample are known and the researcher is confident that the crystallinity and stoichiometry of the minerals in the sample is similar to that used by published reference standards, then a matrix flushing method may be used which greatly simplifies the quantification process.

Optical mineralogy is a straightforward microscopic technique in which the optical characteristics of the grains are used to identify the minerals. Various supplementary devices and techniques, such as use of luminescence characteristics and staining for specific minerals, can greatly assist the petrographer in identification of the minerals present in a thin section. Like XRD, quantification techniques, if done to achieve a statistically valid estimate of the mineral assemblage, are time consuming and labor intensive.

Acknowledgments

I greatly appreciate all the help my students and laboratory technicians at the University of Manitoba have provided while writing this chapter. In nearly every way, these people who spend their days preparing samples and doing the analyses are the real experts. I gratefully acknowledge the helpful comments on this manuscript and, in particular, the many discussions on lake sediment mineralogy provided by Drs. Neil Ball, Mark Cooper, Jenny Deliqiat, Pierre Francus, John P. Smol, James T. Teller, Anke Tugulea, Bob Vance, and Jeff Young.

References

Abell, P. I. & J. P. McClory, 1986. Sedimentary carbonates as isotopic marker horizons at Lake Turkana, Kenya. In Frostick, L. E., R. W. Renaut, I. Reid & J. J. Tiercelin (eds.) Sedimentation in the African Rifts, Geol. Soc. Spec. Pub. No. 25: 153–159.

Adams, A. E. & W. S. MacKenzie, 1998. A Colour Atlas of Carbonate Sediments and Rocks Under the Microscope. John Wiley & Sons, Toronto, 192 pp.

Adams, A. E., W. S. MacKenzie & C. Guilford, 1984. Atlas of Sedimentary Rocks Under the Microscope. Longman Scientific & Technical, Essex, England, 104 pp.

Allman, M. & D. F. Lawrence, 1972. Geological Laboratory Techniques. Arco Publishing Company, Inc., New York, 335 pp.

Alpern, B., 1980. Pétrographie du kérogène. In Durand, B. (ed.) Kerogen, Insoluble Organic Matter from Sedimentary Rocks. Editions Technip, Paris: 339–383.

Amstutz, G. C. & H. Giger, 1971. Stereological methods applied to mineralogy, petrology, mineral deposits and ceramics. J. Micros. 95: 145–164.

Amonette, J. E. & R. W. Sanders, 1994. Nondestructive techniques for bulk elemental analysis. In Amonette, J. E. & L. W. Zelanzny (eds.) Quantitative Methods in Soil Mineralogy. Soil Science Society of America, Inc., Madison, Wisconsin: 1–48.

Anderson, J. U., 1963. An improved pretreatment for mineralogical analysis of samples containing organic matter. Clays Clay Min. 10: 380–388.

Azároff, L. V, 1968. Elements of X-ray Crystallography. McGraw-Hill, New York, 610 pp.

Ashley, G. M., 1973. Impregnation of fine-grained sediments with a polyester resin: a modification of Altemuller's method. J. Sed. Petrol. 43: 298–301.

Barker, C. E. & O. C. Kopp (eds.), 1991. Luminescence Microscopy and Spectroscopy: Qualitative and Quantitative Applications. SEPM Short Course 25, Tulsa, Oklahoma, 195 pp.

Barshad, I., 1960. X-ray analysis of soil colloids by a modified salted paste method. In Ingerson, E. (ed.) Seventh National Conf. Clays & Clay Minerals, Pergamon Press, London: 350–364.

Basu, A. & E. Molinaroli, 1989. Provenance characteristics of detrital opaque Fe-Ti oxide minerals. J. Sed. Petrol. 59: 922–924.

Bengtsson, L. & M. Enell, 1986. Chemical analysis. In Berglund, B. E. (ed.) Handbook of Holocene Palaeoecology and Palaeohydrology. John Wiley & Sons Ltd., New York: 423–451.

Birks, H. J. B., 1998. Numerical tools in palaeolimnology — progress, potenialities, and problems. J. Paleolim. 20: 307–332.

Biscaye, P. E., 1965. Mineralogy and sedimentation of Recent deep sea clays in the Atlantic Ocean and adjacent seas and oceans. Geol. Soc. Amer. Bull. 76: 803–832.

Biscaye, P. E., 1964. Distinction between kaolinite and chlorite in Recent sediments by X-ray diffraction. Amer. Mineral. 49: 1281–1289.

Bish, D. L., 1994. Quantitative X-Ray diffraction analysis of soils. In Amonette, J. E. & L. W. Zelanzny (eds.) Quantitative Methods in Soil Mineralogy. Soil Science Society of America, Inc., Madison, Wisconsin: 267–295.

Bish, D. L. & J. E. Post (eds.), 1989. Modern Powder Diffraction. Mineralogical Society of America, Reviews in Mineralogy, Volume 20, 369 pp.

Bish, D. L. & R. C. Reynolds, 1989. Sample preparation for X-ray diffraction. In Bish, D. L. & J. E. Post (eds.) Modern Powder Diffraction. Mineralogical Society of America, Reviews in Mineralogy, Volume 20: 73–100.

Bish, D. L. & S. J. Chipera, 1988. Problems and solutions in quantitative analysis of complex mixtures by x-ray powder diffraction. Adv. X-ray Anal. 31: 295–308.

Boggs, S., 1992. Petrology of Sedimentary Rocks. Macmillan Publishing Company, New York, 707 pp.

Blatt, H., 1992. Sedimentary Petrology (2nd edition). W. H. Freeman and Company, New York, 514 pp.

Bodine, M. W. & T. H. Fernalld, 1973. EDTA dissolution of gypsum, anhydrite, and Ca-Mg carbonates. J. Sed. Petrol. 43: 1152–1156.

Bouma, A. G., 1969. Methods for the Study of Sedimentary Structures. Wiley, New York, 654 pp.

Bradley, W. F., R. E. Grim & G. L. Clark, 1937. A study of the behavior of montmorillonite upon wetting. Z. Kristallogr. 97: 216–222.

Braitsch, O., 1971. Salt Deposits, Their Origin and Composition. Springer-Verlag, New York, 297 pp.

Brindley, G. W., 1980. Quantitative X-ray mineral analysis of clays. In Brindley, G. W. & G. Brown (eds.) Crystal Structures of Clay Minerals and Their X-ray Identification. Mineralogical Society Monograph No. 5, London: 411–438.

Brooks, J. (ed.), 1981. Organic Maturation Studies and Fossil Fuel Exploration. Academic Press, New York, 441 pp.

Brown, G., 1953. A semi-micro method for preparation of clays for X-ray study. J. Soil. Sci. 4: 229–232.

Brown, G. & G. W. Brindley, 1980. X-ray diffraction procedures for clay mineral identification. In Brindley, G. W. & G. Brown (eds.) Crystal Structures of Clay Minerals and Their X-ray Identification. Mineralogical Society Monograph No. 5, London: 305–359.

Bustin, R. M., A. R. Cameron, D. A. Grieve & W. D. Kalkreuth, 1985. Coal Petrology, Its Principles, Methods, and Applications. Geol. Assoc. Can. Short Course Notes Volume 3, Victoria, B.C., 229 pp.

Cady, J. G., L. P. Wilding & L. R. Drees, 1986. Petrographic microscopic techniques. In Klute, A. (ed.) Methods of Soil Analysis. Part 1 (2nd edition), Agron. Monograph 9, Soil Sci. Soc. Amer., Madison, Wisconsin: 185–218.

Calas, G. & F. C. Hawthorne, 1988. Introduction to spectroscopic methods. In Hawthorne, F. C. (ed.) Spectroscopic Methods in Mineralogy and Geology. Mineralogical Society of America, Reviews in Mineralogy, Volume 18: 1–9.

Campbell, I. D., W. M. Last, C. Campbell, S. Clare & J. H. McAndrews, 2000. The late Holocene paleohydrology of Pine Lake, Alberta: a comparison of proxy types. J. Paleolim. 25: 427–441.

Carozzi, A. V, 1993. Sedimentary Petrology. Prentice Hall, New Jersey, 263 pp.

Carroll, D., 1970. Clay Minerals: A Guide to Their X-ray Identification. Geol. Soc. Amer Spec. Paper 126, 80 pp.

Carver, R. E. (ed.), 1971. Procedures in Sedimentary Petrology. Wiley-Interscience, New York, 653 pp.

Chayes, F., 1956a. Petrographic Modal Analysis. John Wiley & Sons, New York, 113 pp.

Chayes, F., 1956b. The Holmes effect and the lower limit of modal analysis, Min. Mag. 31: 276–281.

Chen, P.-Y., 1977. Table of Key Lines in X-ray Powder Diffraction Patterns of Minerals in Clays and Associated Rocks. Indiana Geological Survey Occasional Paper 21, 68 pp.

Chung, F. H., 1974a. Quantitative interpretation of X-ray diffraction patterns of mixtures. I. Matrix-flushing method for quantitative multicomponent analysis. J. Applied Crystall. 7: 519–525.

Chung, F. H., 1974b. Quantitative interpretation of X-ray diffraction patterns of mixtures. II.Adiabatic principle of X-ray diffraction analysis of mixtures. J. Applied Crystall. 7: 526–531.

Cody, R. D. & G. L. Thompson, 1976. Quantitative X-ray diffraction analyses of clays using an orienting internal standard and pressed disc of bulk shale samples. Clays Clay Mineral. 24: 224–231.

Cook, A. C., 1980. Optical techniques for the examination of organic matter in oil shales. In Cook, A. C. & A. J. Kantsler (eds.) Oil Shale Petrology Workshop. Keiraville Kopiers, Wollongong, Australia: 1–16.

Cook, A. C. & A. J. Kantsler (eds.), 1980. Oil Shale Petrology Workshop. Keiraville Kopiers, Wollongong, Australia, 100 pp.

Cook, H. E., P. D. Johnson, J. C. Matti & I. Zemmels, 1975. Methods of sample preparation and X-ray diffraction analysis, X-ray Mineralogy Laboratory, Deep Sea Drilling Project, University of California, Riverside. In Hayes, D. E. & L. A. Frakes (eds.) Initial Reports. DSDP 28, Washington: 999–1007.

Coshell, L., M. R. Rosen & K. J. McNamara, 1998. Hydromagnesite replacement of biomineralized aragonite in a new location of Holocene stromatolites, Lake Walyungup, Western Australia. Sedimentology 45: 1005–1018.

Cullity, B. D., 1978. Elements of X-Ray Diffraction. Addison Wesley Publishing Co., New York, 555 pp.

Dean, W. E., 1997. Rates, timing, and cyclicity of Holocene eolian activity in north-central United States: evidence from varved lake sediments. Geology 25: 331–334.

Dean, W. E., 1993. Physical properties, mineralogy, and geochemistry of Holocene varved sediments from Elk Lake, Minnesota. In Bradbury, J. P. & W. E. Dean (eds.) Elk Lake Minnesota: Evidence for Rapid Climate Change in the North-Central United States. Geol. Soc. Amer. Spec. Paper 276: 97–113.

Dean, W. E., 1981. Carbonate minerals and organic matter in sediments of modern north temperate hard-water lakes. In Ethridge, F. G. & R. M. Flores (eds.) Recent and Ancient Nonmarine Depositional Environments: Models for Exploration. SEPM Spec. Pub. No. 31: 213–231.

Dean, W. E., 1974. Determination of carbonate and organic matter in calcareous sediments and sedimentary rocks by loss on ignition; comparison with other methods. J. Sed. Petrol. 44: 242–248.

Dean, W. E. & T. D. Fouch, 1983. Chapter 2: Lacustrine. In Scholle, P. A., D. G. Bebout & C. H. Moore (eds.) Carbonate Depositional Environments. Amer. Assoc. Petrol. Geol. Memoir 33: 98–130.

Dean, W. E. & R. O. Megard, 1993. Environment of deposition of $CaCO_3$ in Elk Lake, Minnesota. In Bradbury, J. P. & W. E. Dean (eds.) Elk Lake Minnesota: Evidence for Rapid Climate Change in the North-Central United States. Geol. Soc. Amer. Spec. Paper 276: 97–113.

Dean, W. E. & A. Schwalb, 2000. Holocene environmental and climatic change in the Northern Great Plains as recorded in the geochemistry of sediments in Pickerel Lake, South Dakota. Quat. Intern. 67:5–20.

Dravis, J. J. & D. A. Yurewicz, 1985. Enhanced carbonate petrography using fluorescence microscopy. J. Sed. Petrol. 55: 795–804.

Drees, L. R. & M. D. Ransom, 1998. Light microscopic techniques in quantitative soil mineralogy. In Amonette, J. E. & L. W. Zelanzny (eds.) Quantitative Methods in Soil Mineralogy. Soil Science Society of America, Inc., Madison, Wisconsin: 137–176.

Drever, J. I., 1997. The Geochemistry of Natural Waters: Surface and Groundwater Environments. Prentice-Hall, Inc., New Jersey, 436 pp.

Drever, J. I., 1973. The preparation of oriented clay mineral specimens for X-ray diffraction analysis by filter-membrane peel technique. Amer. Mineral. 58: 553–554.

Durand, B. (ed.), 1980. Kerogen, Insoluble Organic Matter from Sedimentary Rocks. Editions Technip, Paris, 519 pp.

Ehlers, E. G., 1987. Optical Mineralogy, Volume 1: Theory and Techniques. Blackwell Scientific Publications, Oxford, UK, 158 pp.

Engstrom, D. R. & H. E. Wright, 1984. Chemical stratigraphy of lake sediments as a record of environmental change. In Haworth, E. Y. & J. W. G. Lund (eds.) Lake Sediments and Environmental History. University of Minnesota Press, Minneapolis: 1–68.

Eugster, H. P. & K. Kelts, 1983. Lacustrine chemical sediments. In Goudie, A. S. & K. Pye (eds.) Chemical Sediments and Geomorphology: Precipitates and Residua in the Near-surface Environment. Academic Press, New York: 321–368.

Eugster, H. P. & L. A. Hardie, 1978. Saline lakes. In Lerman, A. (ed.) Lakes: Chemistry, Geology, Physics. Springer-Verlag, New York: 237–293.

Evans, M. S., 1993. Paleolimnological studies of saline lakes. J. Paleolim. 8: 97–102.

Fairchild, I., G. Hendry, M. Quest. & M. Tucker, 1988. Chemical analysis of sedimentary rocks. In Tucker, M. (ed.) Techniques in Sedimentology. Blackwell Scientific Publications, Oxford: 274–386.

Fisher, A. T. & M. B. Underwood, 1995. Calibration of an X-ray diffraction method to determine relative mineral abundances in bulk powders using matrix singular value decomposition: a test from the Barbados accretionary complex. In Proceedings Ocean Drilling Program, Initial Reports 156: 29–37.

Folk, R. L., 1980. Petrology of Sedimentary Rocks. Hemphill Publishing Company, Austin, 182 pp.

Folk, R. L., P. B. Andrews & D. W. Lewis, 1970. Detrital sedimentary rock classification and nomenclature for use in New Zealand. N. Z. J. Geol. Geophys. 13: 937–968.

Friedman, G. M., 1971. Staining. In Carver, R. E. (ed.) Procedures in Sedimentary Petrology, Wiley-Interscience, New York: 511–530.

Friedman, G. M., J. E. Sanders, & D. C. Kopaska-Merkel, 1992. Principles of Sedimentary Deposits. Macmillan Publishing Company, New York, 717 pp.

Garrels, R. M. & F. T. MacKenzie, 1971. Evolution of Sedimentary Rocks. Norton & Company, New York, 397 pp.

Gell, P. A., P. A. Barker, P. De Deckker, W. M. Last & L. Jelicic, 1994. The Holocene history of West Basin Lake, Victoria, Australia; chemical changes based on fossil biota and sediment mineralogy. J. Paleolim. 12: 235–258.

Gibbs, R. J., 1971. X-ray diffraction mounts. In Carver, R. E. (ed.) Procedures in Sedimentary Petrology. Wiley-Interscience, New York: 531–539.

Gibbs, R. J., 1968. Clay mineral mounting techniques for x-ray diffraction analysis: a discussion. J. Sed. Petrol. 38: 242–243.

Gibbs, R. J., 1965. Error due to segregation in quantitative clay mineral X-ray diffraction mounting techniques. Am. Mineral. 50: 741–751.

Gierlowski-Kordesch, E. & K. Kelts (eds.), 2000. Lake Basins Through Space and Time, Amer. Assoc. Petrol. Geol. Studies in Geology No. 46, 648 pp.

Gierlowski-Kordesch, E. & K. Kelts (eds.), 1994. Global Geological Record of Lake Basins, Volume 1. Cambridge University Press, New York, 425 pp.

Gilkes, R. J., 1994. Transmission electron microscope analysis of soil materials. In Amonette, J. E. & L. W. Zelanzny (eds.) Quantitative Methods in Soil Mineralogy. Soil Science Society of America, Inc., Madison, Wisconsin: 177–204.

Gluskoter, H. J., 1965. Electronic low-temperature ashing of bituminous coal. Fuel 44: 285–291.

Greensmith, J. T, 1979. Petrology of Sedimentary Rocks. Allen & Unwin, Boston, 241 pp.

Griffin, J. M., 1971. Interpretation of X-ray data. In Carver, R. E. (ed.) Procedures in Sedimentary Petrology. Wiley-Interscience, New York: 541–569.

Griffiths, J. C., 1967. Scientific Methods in Analysis of Sediments. McGraw-Hill, New York, 508 pp.

Grim, R. E., 1988. The history of the development of clay mineralogy. Clays and Clay Minerals 36: 97–101.

Grim, R. E., 1968. Clay Mineralogy (2nd edition). McGraw-Hill, New York, 579 pp.

Håkanson, L. & M. Jansson, 1983. Principles of Lake Sedimentology. Springer-Verlag, New York, 316 pp.

Hammer, U. T., 1986. Saline Lake Ecosystems of the World. Dr W. Junk Publishers, Dordrecht, The Netherlands, 616 pp.

Hardie, L. A., J. P. Smoot & H. P. Eugster, 1978. In Matter, A. & M. E. Tucker (eds.) Modern and Ancient Lake Sediments. International Association of Sedimentologists Special Publication No. 2, Blackwell Scientific Publications, Oxford: 7–42.

Hardy, R. & M. Tucker, 1988. X-ray powder diffraction of sediments. In Tucker, M. (ed.) Techniques in Sedimentology, Blackwell Scientific Publications, Oxford: 191–228.

Harwood, G., 1988. Microscopic techniques: II. Principles of sedimentary petrography. In Tucker, M. (ed.) Techniques in Sedimentology. Blackwell Scientific Publications, Oxford: 108–173.

Haskell, B. J., S. C. Fritz & D. R. Engstrom, 1996. Late Quaternary paleohydrology in the North American Great Plains inferred from the geochemistry of endogenic carbonate and fossil ostracodes from Devils Lake, North Dakota. Palaeogeogr., Palaeoclim., Palaeoecol. 124: 179–193.

Hawthorne, F. C. (ed.), 1988. Spectroscopic Methods in Mineralogy and Geology, Mineralogical Society of America, Reviews in Mineralogy, Volume 18, 695 pp.

Heath, G. R. & N. G. Pisias, A method for the quantitative estimation of clay minerals in North Pacific deep-sea sediments. Clays Clay Mineral. 27: 175–184.

Heiri, O., A. F. Lotter & G. Lemcke, 2000. Loss on ignition as a method for estimating organic and carbonate contents in sediments: reproducibility and comparability of results. J. Paleolim. 25: 101–110.

Henderson, P. & W. M. Last, 1998. Holocene sedimentation in Lake Winnipeg, Manitoba. Canada. J. Paleolim. 19: 265–284.

Hughes, R. E. & R. Warren. 1989. Evaluation of the economic usefulness of earth materials by x-ray diffraction. In Hughes, R. E. & J. C. Bradbury (eds.) Proc. 23rd Forum Geology of Industrial Minerals. Illinois State Geol. Surv. Mineral Notes 102: 57–57.

Hughes, R. E., D. M. Moore & H. D. Glass, 1994. Qualitative and quantitative analysis of clay minerals in soils. In Amonette, J. E. & L. W. Zelanzny (eds.) Quantitative Methods in Soil Mineralogy. Soil Science Society of America, Inc.. Madison, Wisconsin: 330–359.

Hutchison, C. S., 1974. Laboratory Handbook of Petrology Techniques. John Wiley & Sons, New York.

Ingram, R. L., 1971. Sieve analysis. In Carver, R. E. (ed.) Procedures in Sedimentary Petrology. Wiley-Interscience, New York: 49–67.

Innes, R. P. & D. J. Pluth, 1970. Thin section preparation using epoxy impregnation for petrographic and electron microprobe analysis. Soil Sci. Soc. Am. Proc. 34: 483–485.

Jackson, M. L., 1969. Soil Chemical Analysis — Advanced Course (2nd edition). published by the author. Madison, Wisconsin, 895 pp.

Jenkins, R., 1989a. Instrumentation. In Bish, D. L. & J. E. Post (eds.) Modern Powder Diffraction. Mineralogical Society of America. Reviews in Mineralogy, Volume 20: 19–45.

Jenkins, R., 1989b. Experimental procedure. In Bish, D. L. & J. E. Post (eds.) Modern Powder Diffraction. Mineralogical Society of America, Reviews in Mineralogy, Volume 20: 47–71.

Jim, C. Y., 1985. Impregnation of moist and dry unconsolidated clay samples using Spurr resin for microstructural studies. J. Sed. Petrol. 55: 597–599.

Johns. W. D., R. E. Grim & W. F. Bradley, 1954. Quantitative estimations of clay minerals by diffraction methods. J. Sed. Petrol. 24: 242–252.

Jones, B. F, 1986. Clay mineral diagenesis in lacustrine sediments. In Mumpton, F. A. (ed.) Studies in Diagenesis. U. S. Geol. Survey Bull. 1578: 291–300.

Jones, B. F. &C. J. Bowser, 1978. The mineralogy and related chemistry of lake sediments. In Lerman, A. (ed.) Lakes: Chemistry, Geology, Physics. Springer-Verlag, New York: 179–235.

Jones, M. P., 1987. Applied Mineralogy, A Quantitative Approach. Graham & Trotman, London. 259 pp.

Jones, M. P., 1977. Automatic image analysis. In Zussman, J. (ed.) Physical Methods in Determinative Mineralogy. Academic Press, New York: 167–199.

Karathanasis, A. D. & W. G. Harris, 1994. Quantitative thermal analysis of soil materials. In Amonette, J. E. & L. W. Zelanzny (eds.) Quantitative Methods in Soil Mineralogy. Soil Science Society of America, Inc., Madison, Wisconsin: 360–411.

Katz, B. J., 2001. Lacustrine basin hydrocarbon exploration — current thoughts. J. Paleolim. in press.

Kelts, K. & K. J. Hsü, 1978. Freshwater carbonate sedimentation. In Lerman, A. (ed.) Lakes: Chemistry, Geology, Physics. Springer-Verlag, New York: 295–323.

Kinter, E. B. & S. Diamond, 1956. A new method for preparation and treatment of oriented-aggregate specimens of soil clays for X-ray diffraction analysis. Soil Sci. 81: 111–120.

Klug, H. P. & L. E. Alexander, 1974. X-ray Diffraction Procedures for Polycrystalline and Amorphous Materials (2nd edition). John Wiley & Sons, New York, 965 pp.

Last, W. M., 1974. Clay mineralogy and stratigraphy of offshore Lake Agassiz sediments in southern Manitoba. M.Sc. thesis, University of Manitoba, Winnipeg, Canada, 183 pp.

Last, W. M. & P. De Deckker, 1992, Paleohydrology and paleochemistry of Lake Beeac — a saline playa in southern Australia. In Roberts, R. D. & M. L. Bothwell (eds.) Aquatic Ecosystems in Semi-Arid Regions, N.H.R.I. Symposium Series 7, Environment Canada, Saskatoon: 63–74.

Last, W. M. & P. De Deckker, 1990. Modern and Holocene sedimentology of two volcanic maar lakes, southern Australia. Sedimentology 37: 967–981.

Last, W. M. & D. J. Sauchyn, 1993. Mineralogy and lithostratigraphy of Harris Lake, southwestern Saskatchewan, Canada. J. Paleolim. 9: 23–39.

Last, W. M. & T. H. Schweyen, 1985. Holocene history of Waldsea Lake, Saskatchewan, Canada. Quat. Res. 24: 219–234.

Last, W. M. & R. E. Vance, 2001. The Holocene history of Oro Lake, one of western Canada's longest continuous lacustrine records. Sed. Geol., in press.

Last, W. M., J. T. Teller & R. M. Forester, 1994. Paleohydrology and paleochemistry of Lake Manitoba, Canada: the isotope and ostracode records. J. Paleolim. 12: 269–283.

Lennox, D. H., 1957. Monochromatic diffraction-absorption technique for direct quantitative X-ray analysis. Anal. Chem. 29: 767–772.

Lewis, D. W., 1984. Practical Sedimentology. Hutchinson Ross Publishing Company, New York, 227 pp.

Lewis, D. W. & D. M. McConchie, 1994. Analytical Sedimentology. Chapman & Hall, New York, 197 pp.

Lindholm, R., 1987. A Practical Approach to Sedimentology. Allan and Unwin, Inc., Winchester, Mass., 276 pp.

MacKenzie, R. C., 1982. Thermoanalytical methods in clay studies. In Fripiat, J. (ed.) Advanced Techniques for Clay Mineral Analysis, Elsevier, New York: 5–29.

MacKenzie, W. S. & A. E. Adams, 1993. A Colour Atlas of Rocks & Minerals in Thin Section. John Wiley & Sons, Toronto, 192 pp.

Mackereth, F. J. H., 1966. Some chemical observations on post-glacial lake sediments. Phil. Trans. R. Soc. B. 250: 165–213.

Marfunin, A. S. (ed.), 1995. Advanced Mineralogy, Volume 2, Methods and Instrumentations: Results and Recent Developments. Springer-Verlag, New York, 441 pp.

Marshall, D. J., 1988. Cathodoluminescence of Geological Materials. Unwin, London, 146 pp.

Marquart, R. G., 1986. μPDSM: mainframe search/match on an IBM PC. Powder Diffract. 1: 34–36.

Mathers, K. H., 1999. The Concentration and Distribution of Trace Elements in Otoliths Collected from Fish from Eden Lake, Northern Manitoba: A Link Between the Lacustrine Fauna and Regional Geochemistry. M.Sc. Thesis, University of Manitoba, Winnipeg, 275 pp.

Matzko, J. J., 1984. Microscopic Determination of the Nonopaque Minerals. U. S. Geol. Survey Bulletin 1627, 453 pp.

Mazzoleni, A. G., Y. Bone & V. A. Gostin, 1995. Cathodoluminescence of aragonitic gastropods and cement in Old Man Lake thrombolites, southeastern South Australia. Aust. J. Earth Sci. 42: 497–500.

McKeague, J. A., 1967. An evaluation of 0.1 M phyrophosphate and phrophosphate-dithionite in comparison with oxalate as extractants of the accumulation products in podzols and some other soils. Can. J. Soil Sci 47: 95–99.

Meek, G. A. & H. Y. Elder (eds.), 1977. Analytical and Quantitative Methods in Microscopy. Cambridge University Press, New York, 245 pp.

Menking, K. M., 1997. Climatic signals in clay mineralogy and grain-size variations in Owens Lake core OL-92, southeast California. In Smith, G. I. & J. L. Bischoff (eds.) An 800,000- year Paleoclimatic Record from Core OL-92, Owens Lake, Southeast California. Geol. Soc. Amer. Spec. Paper 317: 37–48.

Miller, J. 1988a. Microscopical techniques: I. Slices, slides, stains and peels. In Tucker, M. E. (ed.) Techniques in Sedimentology. Blackwell Scientific Publications, Oxford: 86–107.

Miller, J., 1988b. Cathodoluminescence microscopy. In Tucker, M. E. (ed.) Techniques in Sedimentology. Blackwell Scientific Publications, Oxford: 174–190.

Milner, H. B., 1978. Sedimentary petrography. In Fairbridge, R. W. & J. Bourgeois (eds.) The Encyclopedia of Sedimentology. Dowden, Hutchinson & Ross, Inc., Stroudsburg, Pennsylvania: 667–671.

Milner, H. B., 1962a. Sedimentary Petrography, Volume I, Methods in Sedimentary Petrography. MacMillan Company. New York, 643 pp.

Milner, H. B., 1962b. Sedimentary Petrography, Volume II, Principles and Applications. MacMillan Company, New York, 715 pp.

Millot, G., 1970. Geology of Clays. Springer-Verlag, New York, 425 pp.

Mitchell. W. A., 1953. Oriented-aggregate specimens of clay for X-ray analysis made by pressure. Clay Mineral. Bull. 2: 76–78.

Moore, C. A., 1968. Quantitative analysis of naturally occurring multicomponent mineral systems by X-ray diffraction. Clays Clay Min. 33: 107–117.

Moore, D. M. & Reynolds, R. C., 1997. X-ray Diffraction and the Identification and Analysis of Clay Minerals (2nd edition). Oxford University Press, Oxford, 378 pp.

Müller, G., 1967. Methods in Sedimentary Petrography. Hafner Publishing Company, New York, 281 pp.

Müller, G., G. Irion & U. Förstner, 1972. Formation and diagenesis of inorganic Ca-Mg carbonates in the lacustrine environment. Naturwissenschaften 59: 158–164.

Müller, G. & F. Wagner, 1978. Holocene carbonate evolution in Lake Balaton (Hungary): a response to climate and impact of man. In Matter, A. & M. E. Tucker (eds.) Modern and Ancient Lake Sediments. Intern. Assoc. Sed. Spec. Pub. No. 2, Blackwell Scientific Publications, Oxford: 55–80.

Murphy, C. P., 1986. Thin Section Preparation of Soils and Sediments. AB Academic Publishers, Berkhamstead, UK, 149 pp.

Nagelschmidt, G., 1941. Identification of clays by aggregate diffraction diagrams. J. Sci. Instrum. 18: 100–101.

Nobel, J. P. A., A. H. Chowdhury & H. Yu, 1996. Fluvial/lacustrine diagenesis; significance for hydrocarbon production and entrapment in the Carboniferous Albert Formation, Moncton Basin. Amer. Assoc. Petrol. Annual Meeting Abstracts Volume: 106.

Olsen, P. E., 1990. Tectonic, climatic, and biotic modulation of lacustrine ecosystems — examples from Newark Supergroup of Eastern North America. In Katz, B. J. (ed.) Lacustrine Basin Exploration, Case Studies and Modern Analogs. AAPG Memoir 50, Tulsa, Ok: 209–224.

Ordonez, S. & M. dc L. es Garcia del Cura, 1994. Deposition and diagenesis of sodium-calcium sulfate salts in the Tertiary saline lakes of the Madrid Basin, Spain. In Renaut, R. W. & W. M. Last (eds.) Sedimentology and Geochemistry of Modern and Ancient Saline Lakes. SEPM Spec. Pub. No. 50: 229–238.

Ostrum, M. E., 1961. Separation of clay minerals from carbonate rocks by using acid. J. Sed. Petrol. 31: 235–258.

Parry, W. T. & C. C. Reeves, 1968. Clay mineralogy of pluvial lake sediments, southern High Plains, Texas. J. Sed. Petrol. 38: 516–529.

Peckett, A., 1992. The Colours of Opaque Minerals. John Wiley & Sons, Toronto, 471 pp.

Petruk, W. (ed.), 1989. Image Analysis Applied to Mineral and Earth Sciences. Min. Assoc. Can. Short Course 16, 189 pp.

Pettijohn, F. J., 1975. Sedimentary Rocks (3rd edition). Harper & Row, New York, 628 pp.

Pettijohn, F. J., P. E. Potter & R. Siever, 1987. Sand and Sandstone (2nd edition). Springer-Verlag, New York, 553 pp.

Phillips, W. R. & D. T. Griffen, 1981. Optical Mineralogy — The Nonopaque Minerals. W. A, Freeman and Company, San Francisco, 677 pp.

Pienitz, R., J. P. Smol, W. M. Last, P. R. Leavitt & B. F. Cumming, 2000. Multi-proxy Holocene palaeoclimatic record from a saline lake in the Canadian Subarctic. The Holocene 10: 673–86.

Pike, J. & A. E. S. Kemp, 1996. Preparation and analysis techniques for studies of laminated sediments. In Kemp, A. E. S. (ed.) Palaeoclimatology and Palaeoceanography from Laminated Sediments, Geological Society Special Publication No. 116: 37–48.

Potter, P. E., J. B. Maynard & W. A. Pryor, 1980. Sedimentology of Shale. Springer-Verlag, New York, 306 pp.

Prothero, D. R. & F. Schwab. 1996. Sedimentary Geology. W. H. Freeman and Company, New York, 575 pp.

Reeves, C. C., 1968. Introduction to Paleolimnology. Elsevier Publishing Company, New York, 268 pp.

Reid, W. P., 1969. Mineral Staining Tests. Colorado School of Mines, Mineral Industries Bulletin 12: 1–20.

Renaut, R. W., J. J. Tiercelin & R. B. Owen, 1986. Mineral precipitation and diagenesis in the sediments of Lake Begoria basin, Kenya Rift Valley. In Frostick, L. E., R. W. Renaut, I. Reid & J. J. Tiercelin (eds.) Sedimentation in the African Rifts. Geol. Soc. Spec. Pub. No. 25: 159–175.

Rex, R. W. & R. G. Chown, 1960. Planchet press and accessories for mounting X-ray powder diffraction samples. Amer. Mineral. 45: 1280–1282.

Rich, C. I., 1969. Suction apparatus for mounting clay specimens on ceramic tiles for X-ray diffraction. Soil Sci. Amer. Proc. 33: 815–816.

Rodríguez-Clemente, R. & Y. Tardy (eds.) Geochemistry and Mineral Formation in the Earth Surface. Consejo Superior de Investigaciones Cientificas, Centre National de la Recherche Scientifique, Madrid, 893 pp.

Rollinson, H. R., 1995. Using Geochemical Data: Evaluation, Presentation, Interpretation. Longman Group, Singapore, 352 pp.

Rosen, M. R., D. E. Miser & J. K. Warren, 1988. Sedimentology, mineralogy and isotopic analysis of Pellet Lake, Coorong Region, South Australia. Sedimentology 35: 105–122.

Russ, J. C., 1990. Computer-assisted Microscopy: The Measurement and Analysis of Images. Plenum Press, New York.

Salvany, J. M. & F. Ortí, 1994. Miocene glauberite deposits of Alcanadre, Ebro Basin, Spain: sedimentary and diagenctic processes. In Renaut, R. W. & W. M. Last (eds.) Sedimentology and Geochemistry of Modern and Ancient Saline Lakes. SEPM Spec. Pub. No. 50: 203–215.

Sawhney, B. L. & D. E. Stilwell, 1994. Dissolution and elemental analysis of minerals, soils, and environmental samples. In Amonette, J. E. & L. W. Zelanzny (eds.) Quantitative Methods in Soil Mineralogy. Soil Science Society of America, Inc., Madison, Wisconsin: 49–82.

Scholle, P. A., 1979. A Color Illustrated Guide to Constituents, Textures, Cements, and Porosities of Sandstones and Associated Rocks. Amer. Assoc. Petrol. Geol. Memoir 28, Tulsa, 201 pp.

Scholle, P. A., 1978. A Color Illustrated Guide to Carbonate Rock Constituents, Textures, Cements, and Porosities. Amer. Assoc. Petrol. Geol. Memoir 27, Tulsa, 241 pp.

Schultz, L. G., 1964. Quantitative Interpretation of Mineralogical Composition from X-ray and Chemical Data for the Pierre Shale. U. S. Geol. Surv. Prof. Paper 391-C, 31 pp.

Schütt, B., 1998a. Reconstruction of palaeoenvironmental conditions by investigation of Holocene playa sediments in the Ebro Basin, Spain: preliminary results. Geomorphology 23: 273–283.

Schütt, B., 1998b. Reconstruction of Holocene paleoenvironments in the endorheic basin of Laguna de Gallocanta, central Spain by investigation of mineralogical and geochemical characters from lacustrine sediments. J. Paleolim. 20: 217–234.

Shang, Y. & W. M. Last, 1999. Mineralogy, lithostratigraphy and inferred geochemical history of North Ingebright Lake, Saskatchewan, Canada. In Lemmen, D. S. & R. E. Vance, R. E. (eds.) Holocene Climate and Environmental Change in the Palliser Triangle: A Geoscientific Context for Evaluating the Impacts of Climate Change on the Southern Canadian Prairies, Geol. Survey Can. Bull. 534: 95–110.

Smart, P. & N. K. Tovey, 1982. Electron Microscopy of Soils and Sediments: Techniques. Clarendon Press, Oxford, 264 pp.

Smith, D. K., 1989. Computer Analysis of Diffraction Data. In Bish, D. L. & J. E. Post (eds.) Modern Powder Diffraction. Mineralogical Society of America, Reviews in Mineralogy, Volume 20: 183–216.

Smith, D. K. & C. S. Barrett, 1979. Special handling problems in X-ray diffractometry. Adv. X-ray Anal. 22: 1–12.

Smith, G. I., 1979. Subsurface Stratigraphy and Geochemistry of Late Quaternary Evaporites, Searles Lake, California. U.S. Geol. Survey Prof. Paper 1043, 130 pp.

Smith. G. I. & I. Friedman, 1986. Seasonal diagenetic changes in salts of Owens Lake, California, 1970–77. In Mumpton, F. A. (ed.) Studies in Diagenesis. U. S. Geol. Survey Bull. 1578: 21–29.

Smoot, J. P. & T. K. Lowenstein. 1991. Depositional environments of non-marine evaporites. In Melvin, J. L. (ed.) Evaporites, Petroleum and Mineral Resources. Elsevier, New York: 189–348.

Snyder, R. L. & D. L. Bish, 1989. Quantitative analysis. In Bish, D. L. & J. E. Post (eds.) Modern Powder Diffraction. Mineralogical Society of America, Reviews in Mineralogy, Volume 20: 101–144.

Solomon, M., 1963. Counting and sampling errors in modal analysis. J. Petrol. 4: 367–382.

Sonnenfeld, P., 1984. Brines and Evaporites. Academic Press. New York, 613 pp.

Sonnenfeld, P. & J. P. Perthuisot, 1989. Brines and Evaporites. Amer. Geophys. Union, Short Course in Geology Vol. 3, Washington, 126 pp.

Sorby, H. C., 1851. On the microscopical structure of the Calcareous Grit of the Yorkshire coast. Q. J. Geol. Soc. Lond. 7: 1–6.

Spencer, R. J. & T. K. Lowenstein, 1990. Evaporites. In McIlreath, I. A. & D. W. Morrow (eds.) Diagenesis. Geoscience Canada Reprint Series 4: 141–164.

Stanley, D. J., 1971. Sample impregnation. In Carver, R. E. (ed.) Procedures in Sedimentary Petrology. Wiley-Interscience, New York: 183–216.

Staplin, F. L., W. D. Dow, C. W. D. Milner, D. I. O'Connor, S. A. J. Pocock, P. van Gijzel, D. H. Welte & M. A. Yukler (eds.), 1982. How to Assess Maturation and Paleotemperatures. SEPM Short Course 7, Tulsa, 279 pp.

Stoermer, E. F. & J. P. Smol (eds.), 1999. The Diatoms: Applications for the Environmental and Earth Sciences. Cambridge University Press, Cambridge, UK, 469 pp.

Stokke, P. R. & B. Carson, 1973. Variation in clay mineral X-ray diffraction results with the quantity of sample mounted. J. Sed. Petrol. 43: 957–064.

Stone, W. E. E., 1982. The use of NMR in the study of clay minerals. In Fripiat, J. (ed.) Advanced Techniques for Clay Mineral Analysis. Elsevier. New York: 77–112.

Teller, J. T., 1976. Lake Agassiz deposits in the main offshore basin of southern Manitoba. Can. J. Earth Sci. 13: 27–43.

Teller, J. T. & W. M. Last,1981. Late Quaternary history of Lake Manitoba, Canada. Quat. Res. 16: 97–116.

Teller, J. T. & W. M. Last, 1981. The Claryville Clay — A record of early glaciation in the Cincinnati region. Paleogeogr., Paleoclim., Paleoecol. 33: 347–367.

Talbot, M. R. & P. A. Allen, 1996. Lakes. In Reading, H. G. (ed.) Sedimentary Environments: Processes, Facies and Stratigraphy (3rd edition). Blackwell Science, London: 83–124.

Talbot, M. R. & K. Kelts, 1986. Primary and diagenetic carbonates in the anoxic sediments of Lake Bosumtwi, Ghana. Geology 14: 912–916.

Terry, R. D. & G. V. Chilingar, 1955. Summary of "Concerning some additional aids in studying sedimentary formations," by M. S. Shvetsov. J. Sed. Petrol. 25: 229–234.

Theisen, A. A. & M. E. Harward, 1962. A paste method for preparation of slides for clay mineral identification by X-ray diffraction. Soil. Sci. Soc Amer. Proc. 26: 90–91.

Thomas, R. L., 1969. A note on the relationship of grain size, clay content, quartz and organic carbon in some Lake Erie and Lake Ontario sediments. J. Sed. Petrol. 42: 66–84.

Thorez, J., 1975. Phyllosilicates and Clay Minerals. Editions G. Lelotte, Dison Belgium, 579 pp.

Tien, P.-L., 1974. A simple device for smearing clay-on-glass slides for quantitative X-ray diffraction studies. Clays & Clay Minerals 22: 367–368.

Trewin, N., 1988. Use of the scanning electron microscope in sedimentology. In Tucker, M. (ed.) Techniques in Sedimentology. Blackwell Scientific Publications, Oxford: 229–273.

Tucker, M. E., 1991. Sedimentary Petrology, An Introduction to the Origin of Sedimentary Rocks. Blackwell Scientific Publications, London, 260 pp.

Tucker, M. E. (ed.), 1988. Techniques in Sedimentology. Blackwell Scientific Publications, Oxford, 408 pp.

Tucker, M. E. & V. P. Wright, 1990. Carbonate Sedimentology. Blackwell Scientific Publications, Oxford, 482 pp.

Valero-Garcés, B. L. & K. R. Kelts, 1995. A sedimentary facies model for perennial and meromictic saline lakes: Holocene Medicine Lake basin, South Dakota, USA. J. Paleolim 15: 123–149.

Valero-Garcés, B. L., K. R. Laird, S. C. Fritz, K. Kelts, E. Ito & E. C. Grimm, 1997. Holocene climate in the Northern Great Plains inferred from sediment stratigraphy, stable isotopes, carbonate geochemistry, diatoms, and pollen at Moon Lake. North Dakota., Quat. Res. 48: 359–369.

Van Andel, T H. & D. M. Poole, 1960. Sources of Recent sediments in the northern Gulf of Mexico. J. Sed. Petrol. 30: 91–122.

Van Stempvoort, D. R., T. W. D. Edwards, M. S. Evans & W. M. Last, 1993. Paleohydrology and paleoclimate records in a saline prairie lake core: mineral, isotope and organic indicators. J. Paleolim. 8: 135–147.

von der Borch, C. C. & D. Lock, 1979. Geological significance of Coorong dolomites. Sedimentology 26: 813–824.

Walker, G., 1985. Mineralogical applications in luminescence techniques. In Berry, F. J. & D. J. Vaughan (eds.) Chemical Bonding and Spectroscopy in Mineral Chemistry. Chapman and Hall, London: 103–140.

Walstrom, E. E., 1960. Optical Crystallography with Particular Reference to the Use and Theory of the Polarizing Microscope (3rd edition). John Wiley & Sons, New York, 356 pp.

Warren, J. K., 1989. Evaporite Sedimentology. Prentice Hall, Englewood Cliffs, New Jersey, 283 pp.

Wasson, R. J., G. I. Smith & D. P. Agrawal, 1984. Late Quaternary sediments, minerals, and inferred geochemical history of Didwana Lake, Thar Desert, India. Palaeogr, Palaeoclim., Palaeoecol. 46: 345–372.

Watson, A., 1983a. Gypsum crusts. In Goudie, A. S. & K. Pye (eds.) Chemical Sediments and Geomorphology: Precipitates and Residua in the Near-surface Environment. Academic Press, New York: 133–162.

Watson, A., 1983b. Evaporite sedimentation in non-marine environments. In Goudie, A. S. & K. Pye (eds.) Chemical Sediments and Geomorphology: Precipitates and Residua in the Near-surface Environment. Academic Press, New York: 163–186.

Webster, D. M. & B. Jones, 1994. Paleoenvironmental implications of lacustrine clay minerals from the Double Lakes Formation, southern High Plains, Texas. In Renaut, R. W. & W. M. Last (eds.) Sedimentology and Geochemistry of Modern and Ancient Saline Lakes. SEPM Spec. Pub. No. 50: 159–172.

Welton, J. E., 1984. SEM Petrology Atlas. Amer. Assoc. Petrol. Geol. Methods in Exploration Series, No. 4. Tulsa, Oklahoma, 237 pp.

Wright, D. T., 1999. The role of sulphate-reducing bacteria and cyanobacteria in dolomite formation in distal ephemeral lakes of the Coorong region, South Australia. Sed. Geol. 126: 147–157.

Yuretich, R. F., 1986. Controls on the composition of modern sediments, Lake Turkana, Kenya. In Frostick, L. E., R. W. Renaut, I. Reid & J. J. Tiercelin (eds.) Sedimentation in the African Rifts. Geol. Soc. Spec. Pub. No. 25: 141–152.

Ziqiang, Q. & X. Zhiqiang, 1985. Borate minerals in salt lake deposits at Chaidamu Basin, China. In Schreiber, B. C. & H. L. Harner (eds.) Sixth International Symposium on Salt. The Salt Institute, Alexandria, Va., vol. 1: 185–192.

Zussman, J. (ed.), 1977. Physical Methods in Determinative Mineralogy. Academic Press, London, 720 pp.

7. FLUID INCLUSIONS IN PALEOLIMNOLOGICAL STUDIES OF CHEMICAL SEDIMENTS

TIM LOWENSTEIN (lowenst@Binghamton.edu)
SEAN T. BRENNAN
Department of Geological Sciences
& Environmental Studies
State University of New York
at Binghamton, Binghamton
NY 13902, USA

Keywords: fluid inclusions, evaporites, halite, gypsum, paleoclimate, analytical techniques, ESEM-EDS, SEM-EDS, stable isotopes, ICP-MS.

Introduction

Fluid inclusions are fluid-filled vacuoles within crystals. Fluid inclusions occur in minerals formed in a wide variety of geologic settings including lacustrine environments. Although the first recorded observations of fluid inclusions were made over a century ago (Sorby, 1858), only in the last ten years have paleolimnologists begun to exploit fluid inclusions in ancient lake deposits (Attia et al., 1995; Benison & Goldstein, 1999; Benison et al, 1998; Li et al, 1996; Lowenstein & Spencer, 1990; Lowenstein et al, 1998; Lowenstein et al, 1994; Roberts & Spencer, 1995; Roberts et al, 1997; Yang et al, 1995a, 1995b). Fluid inclusions can be formed either during or after crystal growth, and they may remain in an undamaged state as closed systems, in equilibrium with their surrounding host mineral, for millions of years. Fluid inclusions trapped during crystal growth are named primary inclusions. As a crystal precipitates in water there are surface irregularities or imperfections produced by differences in the growth rate of the crystal surface or by etching of the crystal surface (Fig. 1). These imperfections are enclosed during the growth of the crystal surface trapping the ambient water. Chemical sediments formed in lacustrine environments may contain abundant primary fluid inclusions that are important in paleolimnological studies because these aqueous inclusions record the temperatures at which the crystals formed and the chemical compositions of the ambient waters from which the lacustrine minerals precipitated. Secondary fluid inclusions are formed following crystal growth by healing of fluid-filled microfractures (Roedder, 1984; Goldstein & Reynolds, 1994). Secondary fluid inclusions provide information on deformation processes or burial conditions and are therefore of subordinate importance in paleolimnologic studies.

Fluid inclusions in lake deposits occur in chemical sediments (carbonates, sulfates, chlorides) which most commonly form in arid, closed-basin settings. Chemical sediments



W. M. Last & J. P. Smol (eds.), 2001. *Tracking Environmental Change Using Lake Sediments. Volume 2: Physical and Geochemical Methods.* Kluwer Academic Publishers, Dordrecht, The Netherlands.

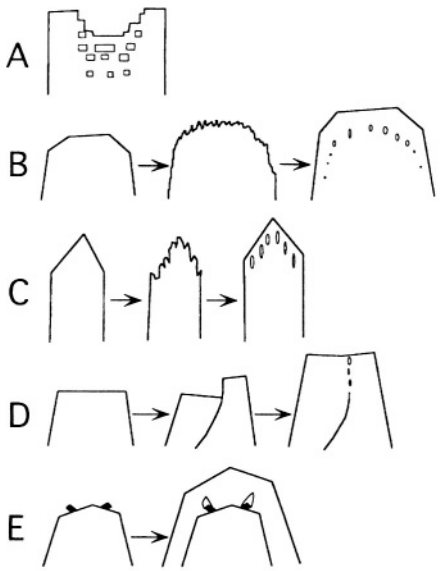


Figure 1. Sketches illustrating trapping of primary fluid inclusions. A. Relatively slow growth of crystal face center produces imperfections that are closed-off as fluid inclusions during later crystal growth. B. Rapid crystal growth may produce surface irregularities that trap fluid during subsequent crystal growth. C. Dissolutional etching of crystal surface may produce an irregular surface along which fluid inclusions may be trapped following renewed crystal growth. D. Crack imperfections may heal and trap fluid inclusions. E. Foreign materials on crystal growth surfaces, such as minerals and organic particles, may interfere with crystal growth, and form cavities that become fluid inclusions following crystal growth. (From Goldstein & Reynolds, 1994, Fig. 2.3, p. 7).

typically form in interior closed-basin drainage systems with climates that have evaporation rates sufficient to concentrate inflow waters. There are many such locations throughout the world including the U.S. Basin and Range, the Great Plains of western Canada, the central Andes of South America, western and southern Australia, and vast areas of central Asia and northern Africa. Chemical sediments, in turn, must be composed of relatively large crystals (>~1 mm) in order to clearly observe fluid inclusions under a petrographic microscope. In addition, the fluid inclusions must be large enough (at least $\sim$ 1 μm) in order to use them for the various analyses described below. Such crystal size and fluid inclusion size requirements limit the types of lacustrine sediments that may be used for fluid inclusion studies. Although carbonate minerals are by far the most common lacustrine chemical sediments, the normally small size of calcite crystals and other carbonate minerals within lacustrine settings have so far precluded fluid inclusion studies. Virtually all studies of fluid inclusions in lake sediments have been done on gypsum and halite. Minerals that meet the crystal size requirements for fluid inclusion research, but which have not yet been studied include sulfate minerals (bloedite-$Na_2SO_4 \cdot MgSO_4 \cdot 4H_2O$, epsomite-$MgSO_4 \cdot 7H_2O$, mirabilite-$Na_2SO_4 \cdot 10H_2O$) and sylvite (KC1).

Aqueous fluid inclusions in lacustrine minerals are potential indicators of paleotemperatures, paleochemistries, and paleoenvironments. Recent studies of fluid inclusions have

determined the temperatures of crystal growth in ancient saline lakes and the major and minor element and isotopic composition of paleolake waters (Attia et al., 1995; Benison & Goldstein, 1999; Benison et al, 1998; Li et al, 1996; Lowenstein & Spencer, 1990; Lowenstein et al, 1998; Lowenstein et al, 1994; Roberts & Spencer, 1995; Roberts et al, 1997; Yang et al, 1995a, 1995b). This chapter is a progress report on the techniques being developed for research on fluid inclusions in lake deposits.

Distinguishing primary from secondary features in chemical sediments

Before beginning any study of fluid inclusions in lake sediments, it is necessary to distinguish the minerals, textures, and structures of sedimentary origin from those formed during burial alteration processes. Many of these features are best observed in large format thin sections using a low magnification binocular microscope. Thin sections should be specially prepared without heating or dissolving samples. Although soluble chemical sediments can be cut and polished with ordinary trim saws and thin sectioning equipment using non-aqueous lubricants, diamond wire saws (Laser Technology West Limited, Colorado Springs, Colorado, USA) are relatively inexpensive and ideal for cutting flat thin section surfaces without heating or damaging delicate samples.

Hardie et al. (1985, p. 12) separated chemical sediments (minerals, mineral assemblages, textures, fabrics) by their timing of formation into three types: 1. Syndepositional, defined as "formed at the time of deposition of a sedimentation unit or deposited in its existing form", 2. Post-depositional (but pre-burial), defined as "formed diagenetically soon after deposition by processes controlled by the existing depositional environment", and 3. Post-burial defined as "formed by late diagenetic or metamorphic-metasomatic processes controlled by the subsurface burial environment". Syndepositional minerals are the only type that might contain paleoenvironmental information and therefore should be the focus of any paleolacustrine fluid-inclusion study. There are several types of sedimentary structures that can be used to identify syndepositional chemical sediments. Detrital framework textures, especially the settle-out accumulations of surface nucleated gypsum plates and for halite, pyramidal hopper crystals, linked rafts, and cubes (collectively termed "cumulates"), are well documented in modern and ancient evaporite deposits (Fig. 2) (Neev & Emery, 1967; Last, 1984; Lowenstein & Hardie, 1985; Smoot & Lowenstein, 1991; Li et al., 1996; Schubel & Lowenstein, 1997). These crystals accumulate at the bottom of a lake in layers of loosely packed crystals. Mechanical sedimentary structures can be formed by loose grains of chemical precipitates (i.e., ripple marks and cross stratification composed of gypsum, mirabilite, and halite; Neev & Emery, 1967; Last, 1984; Hardie et al., 1985). Even more common in lacustrine evaporite deposits are crystalline framework crusts, formed by in situ open space growth on the floors of saline lakes. Characteristic features of bottom-growth crystalline frameworks include vertically-oriented, vertically-elongated, upward-widening crystals formed on a common substrate (Fig. 3). Vertically-oriented gypsum crystals, termed selenite (Hardie & Eugster, 1971; Warren, 1982; Attia et al., 1995) and vertical halite "chevrons", along with crusts composed of trona (Eugster, 1970, 1980), mirabilite, epsomite and bloedite (Last, 1984), have been widely reported from modern and ancient closed-basin lake deposits. Lacustrine crystalline frameworks in particular are important to fluid inclusion studies because the constituent crystals are commonly large (several millimeters to several centimeters) with abundant fluid inclusions.

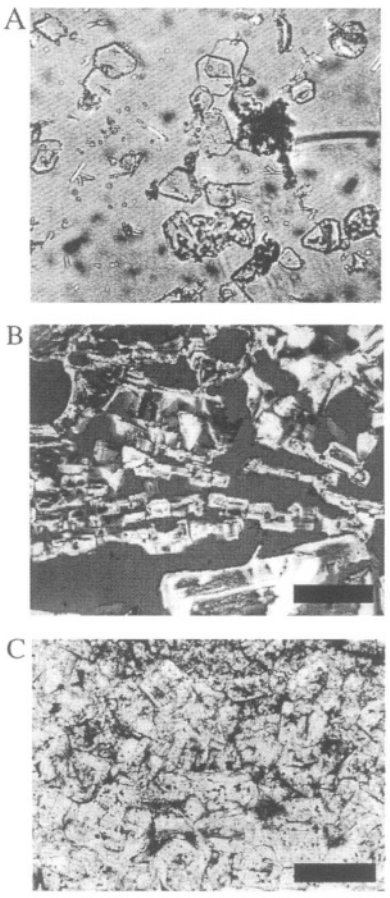


Figure 2. A. Photomicrograph of cumulate crystals of gypsum (25 × 35 μm flat hexagonal plates) and tiny aragonite needles collected in a sediment trap at a depth of 68 m, Dead Sea, Jordan and Israel. (From Neev & Emery, 1967, Fig. 46, p. 89). B. Thin section photograph of a cross-section of a halite surface crust, Salina Omotepec, Baja California, Mexico, showing cumulate halite crystals as flattened rectangular- and square-shaped plates and laterally-linked rafts. These crystals nucleated and grew at the surface and then sank to form a horizontally-oriented, grain supported framework. Halite crystals are clouded with fluid inclusion bands. Dark gray areas are void spaces. Scale bar is 2 mm. (From Lowenstein & Hardie, 1985, Fig. 11, p. 635). C. Thin section photograph of randomly-oriented cumulate halite cubes, Permian Salado Formation, New Mexico. Dark clots and bands in the cores of halite cubes are fluid inclusions. Scale bar is 2.5 mm. (From Hardie et al., 1985, Fig. 2, p. 15).

Layered chemical sediments may contain a variety of dissolution features produced by contact with undersaturated waters such as rounded or truncated crystal surfaces, rounded dissolution cavities, and vertically-oriented dissolution pipes (Fig. 3D and 3E). The frequency and nature of these syndepositional dissolution features may be used to distinguish perennial saline lake deposits from saline pan (ephemeral lake) sediments (Li et al., 1996; Schubel & Lowenstein, 1997). In very shallow water (centimeters deep) to subaerially-exposed environments, layered halite crusts have little to no protection from incoming

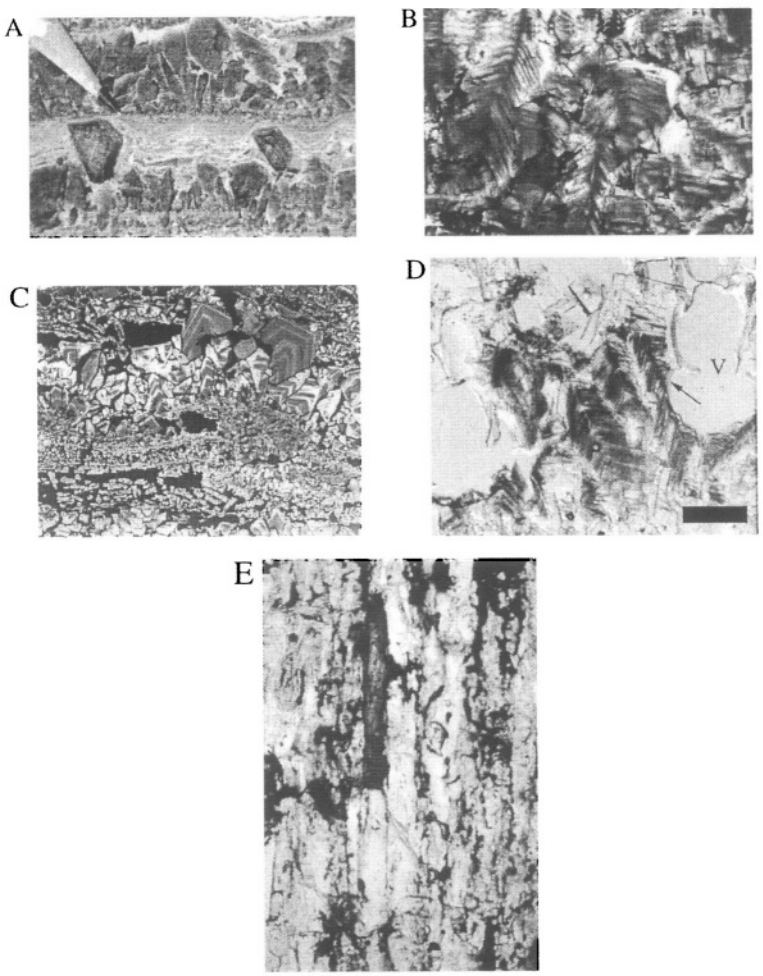


Figure 3. A. Vertically-oriented gypsum "selenite" interbedded with laminated gypsum from the Upper Miocene Solfifera Series, Sicily. Pencil for scale. (From Hardie & Eugster, 1971, Fig. 21, p. 212). B Thin section photograph showing competitively-grown halite chevrons with fluid inclusion bands, typical of halite formed at the bottom of a shallow saline lake. Dark banded parts of chevrons contain a multitude of tiny fluid inclusions, trapped during crystal growth. Death Valley, California, borehole core, depth of 83 m. Horizontal field of view is 20 mm. C. Thin section photograph of modern halite crust, Salina Omotepec, Baja California, Mexico showing alternating layers of coarsely crystalline vertically oriented chevrons that grew upward from the saline lake bottom and fine-grained cumulates of halite (sunken rafts, plates, hopper cubes). Note fluid inclusion bands in halite chevrons that can be traced stratigraphically across crystal boundaries from one crystal to the next. Dark gray areas are void spaces. Chevron crystals are 10 to 20 mm in size (From Lowenstein & Hardie, 1985, Fig. 12, p. 635). D. Thin section photograph of halite crust, Salina Omotepec, Baja California, Mexico, showing fluid inclusion-banded chevron halite partly truncated by dissolution cavities (arrow). V indicates dissolution void. Scale bar is 2 mm (From Lowenstein & Hardie, 1985, Fig. 2, p. 631). E. Thin section photograph of saline pan halite with vertical dissolution pipes, Death Valley, California, borehole core, depth of 40.5 m. Vertical pipes are lined with mud (dark) along walls and cemented with clear halite. Virtually no primary chevron halite framework is preserved because of the pervasive syndepositional recycling of surface crusts that occurs in normally subaerially-exposed saline pan environments. Horizontal field of view is 5 mm. (From Li et al., 1996, Fig. 10, p. 193)

dilute surface waters. These dilute waters produce unique dissolution surfaces and cavities leaving only sparse "patchy" preservation of primary mineral textures (Fig. 3D and 3E). In contrast, the dense brine of perennial saline lakes acts as a protective barrier between the primary sedimentary minerals of the lake bottom and the incoming dilute surface waters. Crystalline frameworks, cumulates and other chemical sediments that exhibit little to no evidence of syndepositional dissolution are characteristic of these perennial lake systems (Fig. 3A and 3B).

Salts precipitate from saline groundwaters in evaporative environments either as cements or displacively grown crystals. The cements are typically crystal overgrowths or cavity fillings and the displacively-grown minerals are typically large euhedral crystals, nodules or fine crystals. It is commonly difficult to interpret from petrographic study whether these diagenetically-formed saline minerals are syndepositional and formed by processes controlled by the surface environment or secondary and deeper burial in origin. A more complete description of these features, as well as criteria for recognizing post-burial alteration (features that deform, disrupt, or completely destroy depositional textures and fabrics) is given in Hardie et al. (1985) and Smoot & Lowenstein (1991).

Fluid inclusions in ancient chemical sediments

Fluid inclusions in primary gypsum crystals have been described by Sabouraud-Rosset (1969, 1972, 1974, 1976), Attia et al. (1995), and Petrichenko et al. (1997). Thin sections or cleavage fragments (especially the perfect {010} cleavage plane) may be used for preliminary petrographic studies of fluid inclusions in gypsum. Primary aqueous inclusions are single phase (water) and arranged in rows parallel to the growth direction of the host gypsum crystal. Inclusions are commonly tapered in the direction of crystal growth; inclusions in two dimensions are triangular, five-sided, horn-shaped, trapezoidal, or negative crystals (Fig. 4). Primary fluid inclusions in bottom-growth gypsum are located along crystal growth bands and are commonly found in association with parallel zones of solid inclusions such as clay, carbonate, microorganisms (coccoid cyanobacteria, charophytes) (Fig. 4A), and unidentified organic matter (Attia et al., 1995; Petrichenko et al., 1997). Secondary fluid inclusions in gypsum commonly occur parallel to the {011} and {010} cleavage planes and typically are tabular-shaped, single-phase, and up to several tens of microns in size (Fig. 4D) (Attia et al., 1995).

Fluid inclusions in primary halite crystals are abundant and have been described and illustrated by numerous researchers (Roedder & Belkin, 1979; Roedder, 1984; Lowenstein & Hardie, 1985; Lowenstein & Spencer, 1990; Goldstein & Reynolds, 1994; Roberts & Spencer, 1995; Kovalevich et al., 1998; Benison & Goldstein, 1999, to name a few). Primary fluid inclusions occur in halite chevrons and in sunken rafts, cubes and plates most commonly as single phase (aqueous) negative cubes, $< 1\ \mu m$ to $\sim 100\ \mu m$ in size, and rarely up to $1000\ \mu m$ or larger (Fig. 5). Less common are two-phase, liquid-solid or liquid-vapor inclusions. Solid crystals in fluid inclusions may be accidentally trapped during crystal growth or may have formed by precipitation inside inclusions as daughter crystals. Fluid inclusions in halite may occur as dense clouds in quantities up to $10^{10}\ cm^{-3}$ (Roedder, 1984). Commonly, zones $\sim 100\ \mu m$ to $\sim 1000\ \mu m$ in thickness containing abundant fluid inclusions alternate sharply with inclusion-poor zones of comparable thickness. This type of inclusion banding, common in laboratory-grown halite and in halite from modern

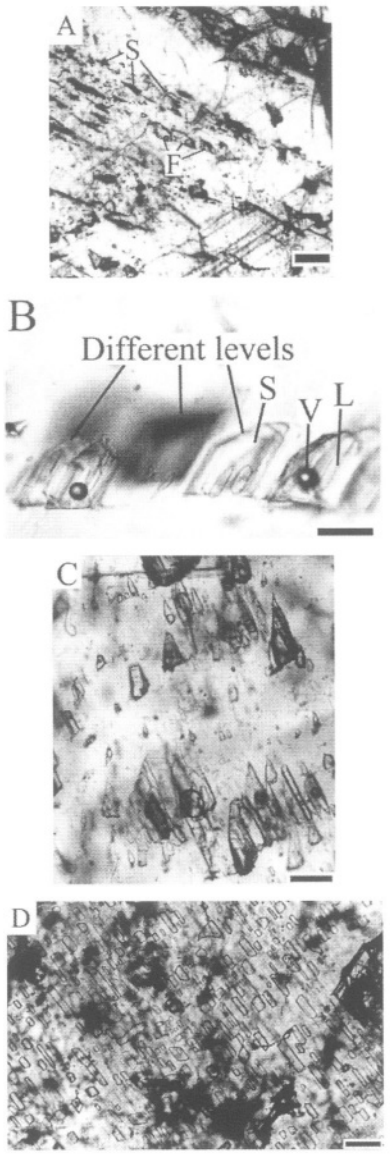


Figure 4. Fluid inclusions in vertically-oriented gypsum selenite crystals, Middle Miocene, Gulf of Suez, Egypt. A. Thin section photograph showing solid inclusions (s) and fluid inclusions (f) arranged in planes parallel to the growth direction of the gypsum crystal. Vapor bubbles in fluid inclusions were produced artificially during freezing. Scale bar is 60 μm. (From Attia et al., 1995, Fig. 6, p. 617). B. Primary fluid inclusions in gypsum, all formed along a common surface. V = vapor bubble produced artificially during freezing, L = liquid water, S = single phase aqueous inclusion. Scale bar is 20 μm. C. Primary fluid inclusions in rows parallel to growth zones of the host gypsum crystal. Fluid inclusions taper in the direction of crystal growth. Vapor bubbles in fluid inclusions were produced artificially during freezing. Scale bar is 20 μm. D. Plane of tabular single phase secondary aqueous inclusions along a cleavage plane. Scale bar is 30 μm. (B, C, and D from Attia et al., 1995, Fig. 8, p 621).

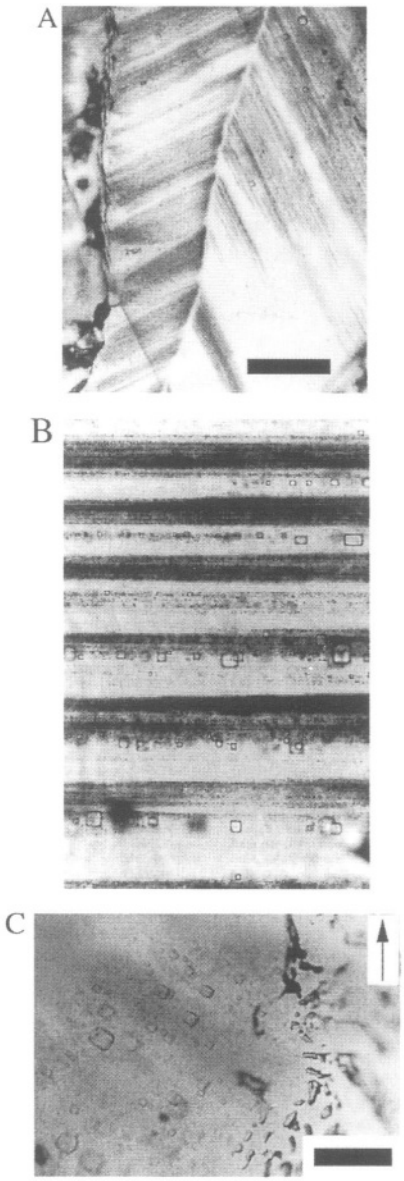


Figure 5. Thin section photographs of fluid inclusions in halite. A. Vertically oriented chevron. Dark bands rich in fluid inclusions alternate with lighter bands containing fewer fluid inclusions. Sample from Permian Salado Formation, New Mexico. Scale bar is 1 mm. (From Lowenstein & Spencer, 1990, Fig. 1, p. 4). B. Fluid inclusion bands from the Death Valley borehole core, 170.4 m, showing regular alternation of fluid inclusion-rich and fluid inclusion-poor bands. Horizontal field of view is 1 mm. (From Roberts et al., 1997, Fig. 7, p. 112). C. Primary inclusions along chevron band truncated by curved plane of irregularly-shaped secondary fluid inclusions. (From Benison & Goldstein, 1999, Fig. 9, p. 118).

saline lakes, forms by variations in crystallization rates. Such fluctuations in crystal growth rates have been interpreted to represent diurnal or seasonal changes in evaporation rates. Within cloudy fluid inclusion rich bands, there may be smaller scale sub-bands, called "high frequency" bands described by Benison & Goldstein (1999). Secondary fluid inclusions in halite are recognized by their commonly irregular shapes and their occurrence along curved healed microfractures (Fig. 5C).

Although carbonate minerals are ubiquitous in fresh-, brackish-, and saline-lake deposits, they tend to be very finely crystalline calcite mud, too fine for fluid inclusion studies (Kelts & Hsu, 1978). Large bottom-grown carbonate crystals are uncommon in ancient lake sediments. However large pseudomorphs of the cold-water carbonate mineral ikaite ($CaCO_3 \cdot 6H_2O$) as well as radial dendritic and bladed calcite crystals have been identified in ancient lacustrine carbonates, particularly tufas (Shearman et al., 1989; Bischoff et al., 1993; Demicco & Hardie, 1994). Calcite crystals in cave deposits are often sufficiently large for observation of fluid inclusions and have been used for paleoclimate studies by Winograd et al. (1985). Relatively large carbonate crystals (> 1 mm), such as megascopic botryoidal aragonite cements, also precipitate in open water marine settings (James & Choquette, 1990). Primary fluid inclusions containing seawater have been identified in ancient marine calcite cements, particularly those filling neptunian dikes (Johnson & Goldstein, 1993; Ward et. al., 1993). The density of fluid inclusions is much lower in carbonates compared to halite and gypsum, so identification of primary inclusions may be more problematic. Primary inclusions are typically found outlining "growth-zone" boundaries as thin cloudy zones of fluid inclusions which outline a euhedral crystal termination (Fig. 6). There are a variety of other types of primary inclusions in carbonate, described in detail by Goldstein & Reynolds (1994). Fluid inclusions in lacustrine carbonate minerals need not be negative crystal shapes to be primary, but they must be single-phase aqueous inclusions. Liquid-vapor two-phase fluid inclusions in primary calcite should be viewed with caution because the inclusions may have been altered after entrapment due to cracking or thermal stretching of the fluid, or they may have trapped gas.

Fluid inclusion liquid-vapor homogenization temperatures: paleolake temperatures

A relatively new method has been developed using measurements of homogenization temperatures of fluid inclusions in primary halite crystals for interpretation of lake water paleotemperatures (Roberts & Spencer, 1995). Fluid inclusions in sedimentary and diagenetic minerals are most commonly trapped as a single phase (water) during crystal growth. Fluid inclusions in crystals formed at temperatures higher than about 50 °C undergo phase separation into a liquid and vapor upon cooling to room temperature due to differential contraction between the host mineral and the trapped fluid (Roedder & Bodnar, 1980; Goldstein & Reynolds, 1994). This process may be reversed in the laboratory by heating fluid inclusions until the vapor shrinks and finally disappears. This process has been termed homogenization. The temperature at which a two phase inclusion becomes one homogeneous fluid is referred to as the homogenization temperature (Th). Theoretically, fluid inclusions are excellent geothermometers; homogenization temperatures have been used extensively to study crystal growth temperatures of minerals in sedimentary rocks

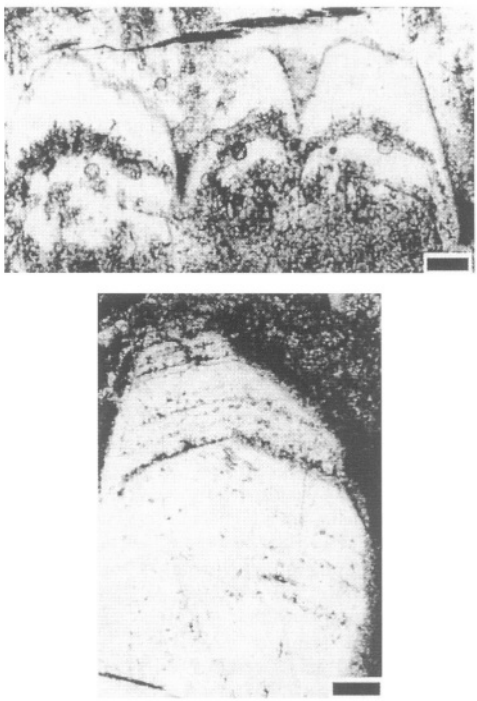


Figure 6. Thin section photographs of fluid inclusions in calcite. Primary fluid inclusions (dark) occur along well-defined calcite crystal growth zones. Scale bars are 100 μm. (From Goldstein & Reynolds, 1994, Fig. 2.5, p. 10).

including quartz, calcite, dolomite, flourite and sphalerite (Roedder, 1984; Shepherd et al., 1985; Goldstein & Reynolds, 1994).

Fluid inclusions in lacustrine halites present special difficulties in homogenization studies because of the ease with this mineral may be deformed. Anomalously high homogenization temperatures in halites, well above the temperatures expected of surface waters, have been reported (for example, Roedder & Belkin, 1979). These high homogenization temperatures may be due to permanent deformation ("thermal stretching") of inclusions or leakage of fluids after crystallization, during burial or during sample preparation. In addition, high homogenization temperatures will be obtained from fluid inclusions that contain trapped gas. Clearly, fluid inclusion homogenization studies in lacustrine halites require extraordinary care in sample selection and preparation.

Roberts & Spencer (1995) avoided problems of stretching or leaking of inclusions and possible trapping of gases in inclusions by selecting halite crystals with one-phase (aqueous) inclusions at room temperature. Halite crystals were examined petrographically to confirm their primary origin and to establish the primary origin of the aqueous inclusions. These aqueous inclusions, formed at temperatures below 50 °C, were cooled in a laboratory freezer at – 15 °C to nucleate vapor bubbles by the "cooling nucleation method" (Roberts & Spencer, 1995). Variations of this method have been used on halites from a 186-m-long core

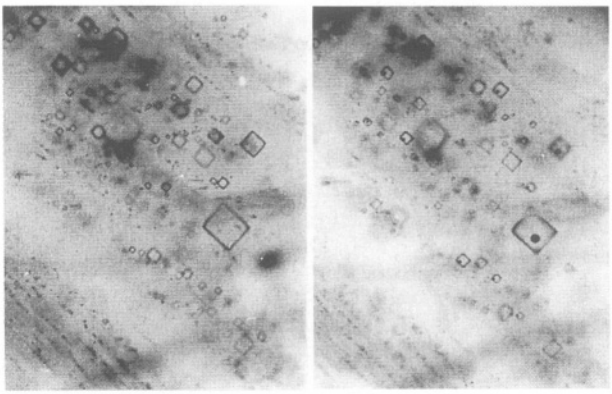


Figure 7. Photograph of fluid inclusions in a halite cleavage fragment before (left) and after (right) using the cooling nucleation method. Vapor bubbles in fluid inclusions were nucleated in a freezer at ~ −20 °C. Vapor bubbles disappeared after heating to 30 °C on the fluid inclusion heating-freezing stage. Largest fluid inclusion visible is 30 μm in size. (From Lowenstein et al., 1998, Fig. 2, p. 227)

(200,000 years old) from Death Valley, California (Roberts & Spencer, 1995; Roberts et al., 1997; Lowenstein et al., 1998), and from Permian halite, Nippewalla Group, Kansas (Benison & Goldstein, 1999). In these studies, halite cleavage fragments, several millimeters across and < 1 millimeter thick, were glued to microscope cover glasses, placed into air-tight containers along with desiccant to avoid condensation on crystal surfaces at low temperatures, and cooled in a freezer (−10 °C to − 20 °C) for several days or longer in order to nucleate vapor bubbles (Fig. 7). At those temperatures, halite-saturated brines in fluid inclusions did not freeze, which would cause stretching of inclusions because the volume of ice is greater than water. Samples were then placed in a portable cooler and quickly transferred from the freezer to a pre-cooled heating-freezing stage mounted to a petrographic microscope.

Crystals of halite, after placement into the pre-cooled heating/freezing stage, were heated slowly, at rates of less than 1 °*C* per minute, and fluid inclusion homogenization temperatures were recorded until all fluid inclusions studied in the cleaved halite crystal homogenized, which nearly always occurred at temperatures below 40 °C. Details on the mechanics of homogenization temperature measurements, including the important "cycling" technique are carefully described by Goldstein & Reynolds (1994, p. 92–95).

Homogenization temperatures, if measured from primary fluid inclusions in primary halite, record the water temperatures of the saline lakes in which crystal growth occurred. The method is of great interest for paleoclimate studies because homogenization temperatures are actual paleo-water temperatures and they are relatively easy to measure. The results from modern, Pleistocene, and Permian halites, summarized below, are encouraging. All of the results represent "snapshots" of water temperatures during crystal growth, which record paleo-weather conditions. Homogenization temperatures from primary fluid inclusions must be used with caution for paleoclimate interpretations because they depend on factors such as brine depths, periodic or seasonal halite precipitation, and the time of day of halite crystallization. Variations in homogenization temperatures due to these

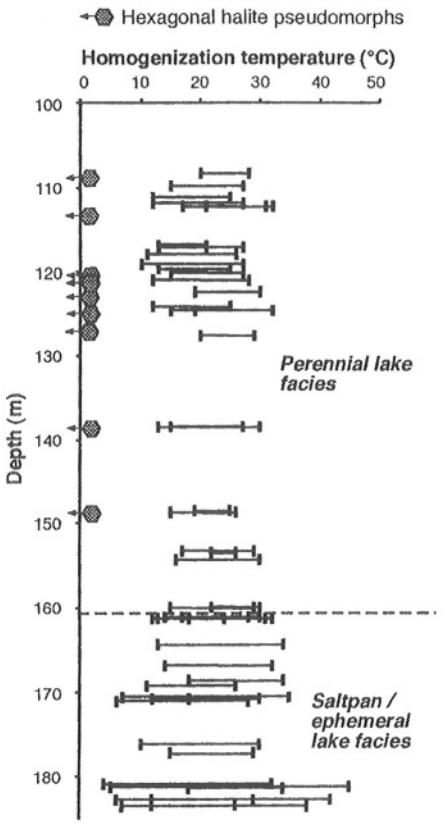


Figure 8. Fluid inclusion homogenization temperatures from the Death Valley salt core, depths of 186 m to 109 m (~ 192 ka to 120 ka). Ranges of fluid inclusion homogenization temperatures for different stratigraphic intervals are plotted. Note that the range of homogenization temperatures in the salt pan facies is higher than in the perennial lake facies. (From Roberts et al., 1997, Fig. 14, p. 119).

factors may be minimized by comparing halite samples deposited in similar depositional environments (i.e., only compare perennial lake deposits to perennial lake deposits) and by measuring large numbers (hundreds) of fluid inclusions from a given stratigraphic interval. For example, the hundreds of measurements taken from halite samples from the perennial-saline-lake-interval in the Death Valley core (186 ka to 120 ka) gave homogenization temperatures between 10°C and 32 °C, indicating temperatures 10°C to 15 °C lower than modern temperatures in Death Valley during that period (Fig. 8) (Roberts & Spencer, 1995; Roberts et al., 1997).

All the studies cited used the FLUID INC. adapted U.S.G.S. Gas-Flow Heating/Freezing stage, but other commercially available heating/freezing systems work equally well. There are three types of heating/freezing stages used for microthermometric analysis of fluid inclusions: Chaixmeca, Linkham, and the FLUID INC./U.S.G.S. type. These heating

freezing systems are discussed in more detail elsewhere (Roedder, 1984, Shepherd et al., 1985, p. 78–92). The Chaixmeca and Linkham stages are heated and cooled by thermal conduction through metal to the sample chamber. The temperature of the FLUID INC./U.S.G.S. type stage is controlled by pre-heated or pre-cooled gas flowing through the sample chamber and across the sample.

In order to use fluid inclusions from lacustrine halites for detailed paleoclimate interpretations, it is important to have air temperature and water temperature records from the study area. The modern records serve as the reference against which fluid inclusion homogenization temperatures are compared. Information on the temperatures of saline lakes in Africa and Canada may be found in Hammer (1986). Other sources of saline lake temperatures are Carpelan (1958) for the Salton Sea, California, Eubank & Brough (1980) for Great Salt Lake, Utah; Smith et al. (1987) for Owens Lake, California, Gavrieli et al. (1989) for the Dead Sea, Israel and Jordan, and Casas et al. (1992) for Qaidam Basin, Qinghai Province, China.

Halite crystals precipitated as a 3 cm-thick crust in Badwater salt pan, Death Valley, California, in April, 1993, were used to test the cooling nucleation method (Roberts & Spencer, 1995; Lowenstein et al., 1998). Homogenization temperatures from fluid inclusions in this halite crust mostly fell within the range of water temperatures measured during growth of the halite (16 °C to 34 °C), and also closely matched average late April to early May air temperatures in Death Valley (Fig. 9). Some fluid inclusion homogenization temperatures from the 1993 halite crust were below 16 °C, which could be partly explained by lower brine temperatures in the evening hours when no measurements were taken. Fluid inclusions with anomalously low homogenization temperatures were interpreted by Lowenstein et al. (1998) to have been damaged (partially collapsed) during the cooling/vapor nucleation process (Lowenstein et al., 1998). Roberts & Spencer (1995) and Roberts et al. (1997) did not find the low-temperature fluid inclusion homogenization temperatures from the Death Valley samples reported by Lowenstein et al (1998).

Roberts & Spencer (1995), Roberts et al. (1997), and Lowenstein et al. (1998) reported homogenization temperatures in halites from the 200,000 year-old sediments in the Death Valley paleoclimate core. Homogenization temperatures measured from single fluid inclusion bands in ancient crystals of saline pan halite varied by 6 to 16 °C, which are similar to modern diurnal water temperature variations in Death Valley (Roberts et al., 1997). Fluid inclusions from ancient perennial lake halites normally had smaller homogenization temperature variations within fluid inclusion bands, consistent with precipitation from a larger water body with less diurnal variation in temperature (Roberts & Spencer, 1995, Benison & Goldstein, 1999). Fluid inclusions in "high frequency" growth bands, which are thin bands within the thicker, cloudy chevron bands, had homogenization temperatures that varied by no more than 8 °C; homogenization temperatures showed a maximum range of 26 °C from the bottom to the top of thicker chevron growth bands (Benison & Goldstein, 1999).

Lowenstein et al. (1998) presented data on maximum fluid inclusion temperatures for the Death Valley core (Fig. 10). By selecting only the highest fluid inclusion homogenization temperatures from a given stratigraphic interval, problems of possible anomalously low homogenization temperatures due to damaged fluid inclusions were avoided. This approach ensures against damaged fluid inclusions but eliminates potentially important paleoclimate information that can be obtained from the full range of fluid inclusion homogenization temperatures.

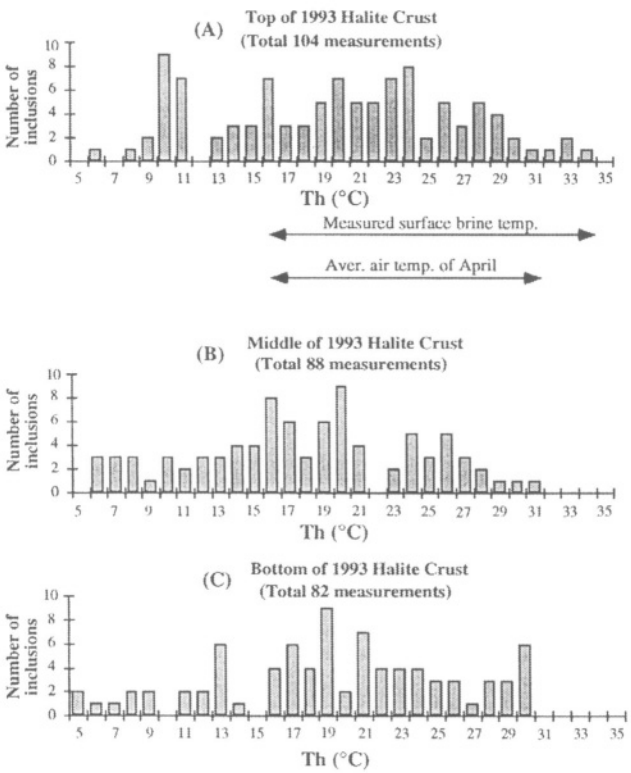


Figure 9. Histograms of homogenization temperatures from fluid inclusions in the halite crust crystallized in Death Valley, California, in late April 1993. Horizontal lines near the top indicate the measured brine temperatures during halite precipitation and the average air temperatures in Death Valley in April. Homogenization temperatures are 4 °C to 34 °C. Maximum homogenization temperatures are the same as maximum brine temperatures measured during halite precipitation and very similar to average maximum air temperatures in Death Valley from late April to early May. The increase in homogenization temperatures from the bottom (C) to the top (A) of the halite crust is compatible with the increase in air and water temperatures during April. (From Lowenstein et al., 1998, Fig. 4, p. 232).

Fluid inclusion freezing-melting behavior: paleolake chemical compositions

Low temperature microthermometry (freezing-melting behavior) of primary aqueous fluid inclusions in lacustrine minerals can provide important information on the chemical composition of ancient lake waters. Such information can be used to interpret paleolake salinities and semi-quantitative major-ion chemistry. The method involves freezing aqueous inclusions and observing the temperatures at which the various frozen phases melt and disappear upon warming. Most lake waters are multicomponent systems and therefore fluid inclusions formed from such waters display quite complex freezing-melting behavior. Although many studies have attempted to fully quantify the freezing melting behavior of complex aqueous inclusions (Davis et al., 1990; others summarized in Goldstein & Reynolds, 1994), new methods developed in the last fifteen years for directly determining the major element

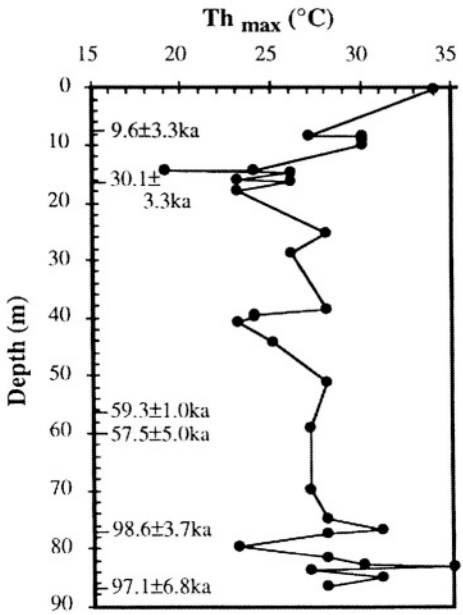


Figure 10. Maximum homogenization temperatures of fluid inclusions in halite (Th_{max}) versus depth from the top 90 m of the Death Valley core (100 ka–0 ka, with uranium series dates shown on left) The plot represents a total of 2,328 homogenization temperature measurements Lacustrine halites, deposited in a perennial saline lake, 35 ka to 10 ka, have exceptionally low maximum homogenization temperatures which suggests brine temperatures 4 °C to 15 °C below modern late April temperatures (From Lowenstein et al., 1998, Fig. 8, p. 239).

chemistry of aqueous fluid inclusions are replacing the freezing-melting approach (see below). Nevertheless, there are three significant low temperature measurements which can commonly be made using fluid inclusions in lacustrine minerals: first melting "eutectic" temperature, final melting temperature of ice, and final melting temperature of hydrohalite ($NaCl \cdot 2H_20$). The general principles of low temperature phase equilibria and the techniques involved in microthermometry are given in detail in Goldstein & Reynolds (1994, p. 95–121), and should be consulted as an essential reference. This section will review applications of low temperature microthermometry in paleolake studies.

The freezing-melting behavior of primary fluid inclusions in subaqueous gypsum crystals has been studied by Sabouraud-Rosset (1969, 1972, 1976), Attia et al. (1995), and Petrichenko et al. (1997). The methods employed by Attia et al (1995) to study fluid inclusions from primary vertically-oriented gypsum crystals from the Gulf of Suez, Egypt (Middle Miocene) provides a good overview about how these analyses can be used in paleoclimatology studies. Prior to attempting freezing-melting analyses, vapor bubbles were artificially produced in originally single-phase primary fluid inclusions by freezing the sample at –90 °C in a heating-freezing stage. It is necessary to cool the sample down to this low temperature, which is well below the final ice-melting temperature, due to extreme cooling required for crystal nucleation. The volume increase upon freezing caused the inclusion to stretch permanently, leading to the formation of a vapor bubble that persisted

at room temperature and during all subsequent freezing-melting runs. Vapor bubbles formed artificially in this manner ensure that all melting temperatures observed occurred at low pressures. Fluid inclusions frozen without vapor bubbles have high internal pressures which influences melting temperatures (see Goldstein & Reynolds, 1994 p. 99–101). In general, all freezing-melting work on single-phase fluid inclusions in lacustrine minerals will require this preliminary stretching step. The two-phase fluid inclusions were then frozen and subsequently heated at rates of 1–2°C per minute. During this heating phase the melting temperatures of the solid phases formed during freezing were observed. Slower heating rates of < 1 °C per minute were used near the temperatures at which phases disappeared.

Attia et al. (1995) observed the temperatures of first melting and the final melting temperature of ice in inclusions in primary gypsum (Fig. 11). Most primary fluid inclusions in gypsum froze between –40 °C and –60 °C; freezing was indicated by the irregular shape of the vapor bubble, and by the granular or glassy texture of the frozen inclusion. First melting of frozen inclusions was recognized between –42 °C and –21 °C by the increased transparency of the inclusion or the slight shifting of the vapor bubble. Typically, it is difficult to accurately determine the first melting temperature of fluid inclusions because of the subtle textural changes that occur. Ice, on the other hand, with its large volume, low birefringence, and low relief is readily identified in fluid inclusions (Fig. 11 B and 11C) (Roedder, 1984; Goldstein & Reynolds, 1994). During heating to temperatures above first melting, ice crystals generally increased in size, became fewer in number, and appeared rounded (Fig. 11B). Near the final ice melting temperature, the vapor bubble became larger (Fig. 11C). The final melting temperature of ice recorded by Attia et al (1995) ranged from –13.0 °C to –1.0 °C.

Eutectic first melting of fluid inclusions involves the melting and disappearance of a hydrated frozen salt in the inclusion. Theoretically, different salt systems have different first melting (eutectic) temperatures (Davis et al., 1990; others summarized in Goldstein & Reynolds, 1994). Therefore, identification of first melting temperature can provide information on the types of salts in solution. For example, first melting in the $NaCl\text{-}H_2O$ system occurs at –21.2°C whereas first melting in the $NaCl\text{-}CaCl_2\text{-}MgCl_2\text{-}H_2O$ system occurs at –57 °C. Two problems limit the use of first melting temperature data: 1. The difficulty of actually observing first melting, and 2. Metastable salt hydrates that may have formed during the freezing process influencing the eutectic temperature (Davis et al., 1990).

Final melting temperatures of ice are usually much more useful data because they can be used to calculate the salinity of fluid inclusions. With no knowledge of the major ion chemistry of fluid inclusions, we can assume a simple $NaCl\text{-}H_2O$ system and calculate the salinity of fluid inclusions from the equation (Goldstein & Reynolds, 1994):

$$\text{Salinity (wt \%)} = 1.78\,\theta - 0.0442\,\theta^2 + 0.000557\,\theta^3, \quad (1)$$

where θ is the freezing point depression of ice, in °C, below 0.0 °C.

Final melting temperatures of ice had a narrow range (<1 °C) along single gypsum crystal growth bands studied by Attia et al. (1995), indicating growth and trapping of fluid inclusions under uniform conditions. Final melting temperatures of ice from one growth band to another in a single crystal varied by up to 11.6°C, which indicates large changes in salinity during crystal growth, compatible with crystallization in a shallow water environment (Fig. 12). Gypsum crystals formed at the bottom of a deeper water setting, in contrast, would normally trap fluid inclusions with similar final melting temperatures of

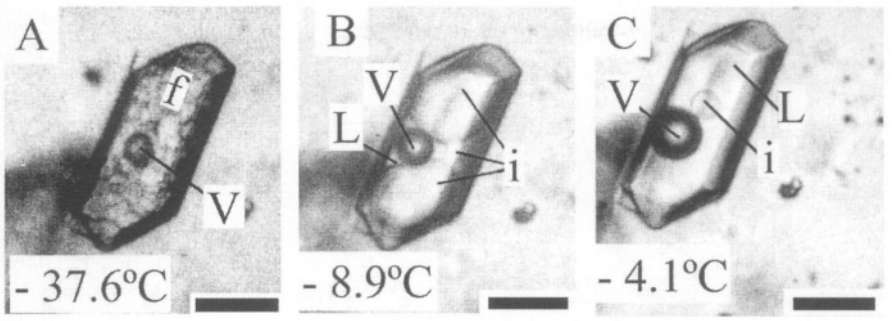


Figure 11. Melting behavior of frozen primary inclusion, 60 μm by 25 μm in size, in primary gypsum. At −37.6 °C (A), the inclusion contains frozen solids (f) composed of ice and salt hydrates which have deformed the spherical vapor bubble (v). At −8.9 °C (B), much melting has occurred and the vapor now has a spherical shape; the only solid phase left is rounded crystals of ice (i) Near the final ice melting temperature, −4.1 °C (C), the vapor bubble has grown in size as ice melted and only one small ice crystal remains. If the fluid inclusion heating-freezing stage is cooled just before the point of final ice melting temperature, ice crystals with euhedral terminations will grow back. Heating the sample will once again melt the ice and the final ice melting temperature can be approached a second time. This heating- cooling technique, called "cycling" by Goldstein & Reynolds (1994), allows the observer to accurately measure the final melting temperature of the ice. Once the ice has completely melted, cooling the sample will no longer produce growth of ice because of the supercooling required for crystal nucleation. Temperatures below −40 °C are needed to refreeze the inclusion. (From Attia et al., 1995, Fig. 10, p. 622).

ice because the large water body would probably not undergo large changes in chemical composition during crystallization of a crystal of gypsum.

The final melting temperatures of ice in fluid inclusions were also used by Attia et al.(1995) to constrain the chemical composition of the parent waters from which the primary gypsum precipitated. The range of ice melting temperatures (–1 °C to –13 °C) was compared to the final melting temperature of ice in: freshwater saturated with gypsum (~ 0°C), normal seawater (–1.9°C) and seawater evaporated to the point of gypsum saturation (–7.0 °C to –8.0 °C). These final melting temperatures of ice were equated to the various water chemistries described above using a computerized aqueous solution model at low temperatures (Spencer et al., 1990). Attia et al. (1995) concluded from final ice melting temperatures above – 1.9 °C that some of the gypsum studied formed from relatively dilute, nonmarine inflow waters. Petrichenko et al. (1997) also concluded that the Middle Miocene gypsum they studied from Ukraine contained primary aqueous inclusions not saline enough to be evaporated seawater. The final melting temperatures of ice in these deposits showed complex variations and commonly had final ice melting temperatures above – 1.9 °C.

Another application of low temperature microthermometry was done by Casas et al. (1992) and Lowenstein et al. (1994) on lacustrine halites from the Qaidam Basin, western China. Fluid inclusions in halite have high salinities, 26.3% for the pure $NaCl$-H_2O binary system and >26.3% for more complex salt systems such as $NaCl$-KCl-$MgCl_2$-$CaCl_2$-H_2O. In these complex saline systems, the final phase to melt is hydrohalite ($NaCl \cdot 2H_2O$). In the pure $NaCl$-H_2O system, the final melting temperature of hydrohalite is +0.1 °C; the addition of other salts (KC1, $CaCl_2$, and $MgCl_2$) causes a depression of the final melting

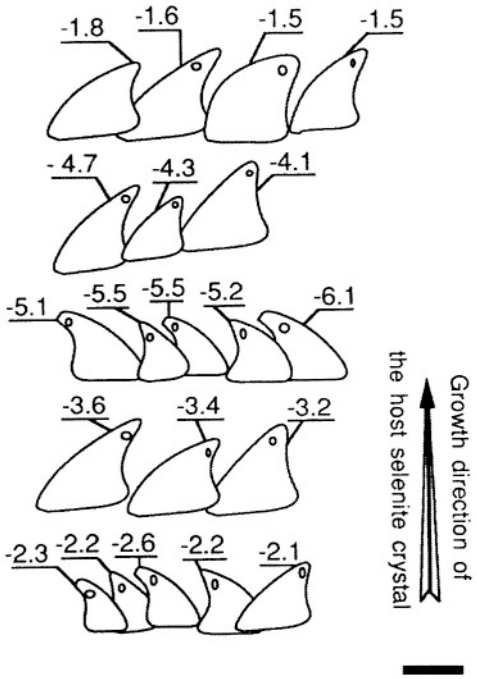


Figure 12. Sketch to scale of the final melting temperatures of ice in primary fluid inclusions along growth bands in one selenite crystal, Middle Miocene, Gulf of Suez, Egypt. Note the similar final melting temperatures of ice along individual fluid inclusion bands but the large range of ice melting temperatures recorded during the growth of the entire crystal. Scale bar is 30 μm. (From Attia et al., 1995, Fig. 12, p. 624).

temperature of hydrohalite (Davis et al., 1990). These principles can allow the final melting temperature of hydrohalite to be used as a concentration gauge in much the same way as the final melting temperature of ice is used.

Fluid inclusions in halite from two 43-m-long borehole cores from the Qaidam Basin were used to document saline lake salinities over the past 54 kyr. Primary single-phase aqueous inclusions came from chevron and cumulate halites crystallized at the brine bottom and at the air-brine interface, respectively. Aqueous inclusions in cleavage fragments of halite were initially "stretched" in the same manner as the gypsum samples described above, in order to nucleate a vapor phase. The two-phase fluid inclusions were then frozen and then slowly heated at the rate of 2 °C to 3 °C per minute. When the solid phases began to melt, the heating rate was slowed down considerably, in order to document as precisely as possible the first and final melting temperatures. Most fluid inclusions froze during cooling or during heating between –100 and – 70 °C. The frozen inclusions had a cryptocrystalline glassy texture or a coarser, granular mass of submicron size crystals. These frozen fluid inclusions displayed complex melting behaviors. The final melting temperature of hydrohalite, however, was easily observed and compared to the phase equilibrium relations reported by Spencer et al. (1990) and Davis et al. (1990). The final melting temperature

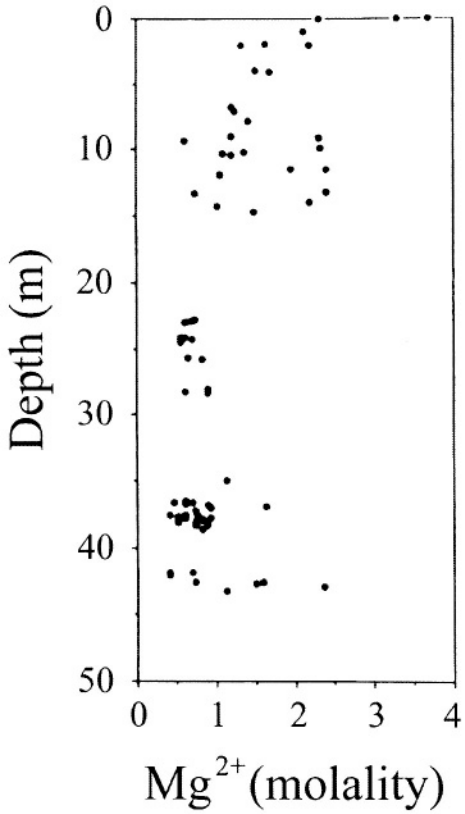


Figure 13. Plot of fluid inclusion salinities, using the molalities of Mg^{2+}, determined from the final melting temperature of hydrohalite in fluid inclusions, as a relative brine concentration indicator. The plot shows salinity versus depth for a 42-m-long core (54 kyr) from the Qaidam Basin, Qinghai Province, western China. The most concentrated brines occur near the top of the core, suggesting that the Holocene had the driest climate over the past 54 kyr in this region of western China. (From Casas et al., 1992, Fig. 14, p. 894).

was used to calculate the a_{H_2O} as well as the molality of Mg (m_{Mg}) in the paleolake waters because it was known that the brines in this basin were dominated by Mg-Na-Cl (Lowenstein et al., 1994). The a_{H_2O} and m_{Mg} were used, in turn, to determine the periods over the past 54 kyr when the Qaidam Basin contained hypersaline brines (Fig. 13). These extremely arid periods were also the times when precipitation of economically valuable potash minerals occurred.

Stable isotopes (δD, $\delta^{18}O$) from fluid inclusion waters

Fluid inclusions in lacustrine minerals may carry information on the stable isotopic composition of surface waters, which can potentially be used for paleoclimate interpretations. A technique has been developed that involves extraction and analysis of microliter quantities

of water from fluid inclusions in halite (Yang, 1993; Yang et al, 1995a, 1995b). This technique has been used on ancient halites in borehole cores from the Qaidam Basin, western China (up to 50 kyr old), and from Death Valley, California (up to 200 kyr old) (Lowenstein et al., 1994; Yang et al., 1995a. 1995b; Roberts et al., 1997). The well-known relationship between temperature and fractionation of hydrogen and oxygen isotopes in the water cycle may be used for paleoclimate interpretations (Faure, 1998). The isotopic composition of fluid inclusions in halite is a function of the isotopic composition of dilute inflow waters and their degree of evaporation. Dilute inflow waters in most arid closed basins are mixtures of surface runoff from precipitation and spring inflows from various subsurface sources. The isotopic composition of precipitation, in turn, is produced by complex processes of fractionation during evaporation of seawater, transport of air masses inland, and precipitation as rain and snow. Changes in the isotopic composition of fluid inclusion waters in halite from a borehole core may reflect changes in temperature of precipitation, atmospheric circulation patterns, sources of moisture, or seasonality of precipitation, all of which may have paleoclimate significance.

The technique developed for extraction and analysis of hydrogen and oxygen isotopes in fluid inclusions in halite is a modification of the vacuum volatilization method (Knauth & Kumar, 1981; Knauth & Beeunas, 1986). Halite crystals (300 to 600 mg), hand picked for primary fluid inclusions, were placed in a glass tube following cleaning in acetone and alcohol (details of the method are given in Yang, 1993; Yang et al., 1995a). The glass tube was heated under vacuum to ~ 950 °C at which point the halite melted and the inclusion waters were released (4 to 10 microliters). One split of the fluid inclusion water was reacted with zinc to produce H_2, which was analyzed by isotope ratio mass spectrometry. A second split of fluid inclusion water, for oxygen isotope analysis, was reacted with guanidine hydrochloride to produce CO_2, which was then analyzed on the mass spectrometer.

Fluid inclusions in primary halite from a 42-m-long (50 kyr) core, Qaidam Basin, western China, were analyzed for stable isotopes. δD and $\delta^{18}O$ values of fluid inclusions from 33 stratigraphic intervals were compared to the isotopic composition of modern surface waters in the Qaidam Basin. The major source of water to the study area is the Golmud River, which is fed by melting of snow in the surrounding mountains. The Golmud River waters are meteoric in origin and plot on the well-known plot of δD vs. $\delta^{18}O$, the meteoric water line (MWL). Evaporated saline waters from the Qaidam Basin fall off the meteoric water line along a linear trend whose slope is defined by the humidity (Fig. 14). This evaporation path begins with the Golmud River isotopic composition on the MWL and branches off from the MWL with increasing evaporation (Yang et al. 1995b). Fluid inclusions from modern halite in the Qaidam Basin and from most of the 42-m-long core fall along the modern evaporation trend. However, fluid inclusions from six intervals between 6.9 and 12.2m (13 to 18.5 ka) fall well below the modern evaporation path (Fig. 14). The very low values of δD and $\delta^{18}O$ were interpreted to reflect regionally cooler climate during the end of the last glacial period. These types of trends in fluid inclusion stable isotopes have great potential for documenting glacial-interglacial climate signals. The same technique was used to measure δD and $\delta^{18}O$ in 21 samples from different stratigraphic intervals in the 186-m-long core from Death Valley, California (Roberts et al., 1997). The δD and $\delta^{18}O$ values for these paleo-waters may be controlled by the same types of factors that affects the modern waters (Friedman et al., 1992), including: 1. The influence of various storm paths

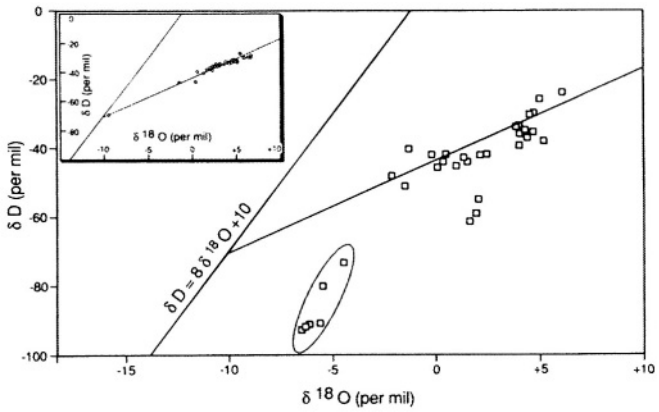


Figure 14. Stable isotope compositions of fluid inclusions in primary halites from 33 stratigraphic intervals in a 42-m-long salt core (54 kyr) from the Qaidam Basin, Qinghai Province, western China. The inset shows data from 31 analyses of: modern Golmud River water (circle close to the meteoric water line, MWL, $\delta D = 8\delta^{18}O + 10$), modern lake brines, and modern salt flat brines that define an evaporation path ($\delta D = 2.6\delta^{18}O - 43.5$) that branches off from the MWL. Yang et al. (1995a, 1995b) have shown that fluid inclusions in modern halite plot along the evaporation path which indicates that halite crystals trap fluid inclusions with the same isotopic composition as the waters from which they crystallized. Most fluid inclusions in ancient halite crystals in the Qaidam Basin core also lie near the modern evaporation path. Six fluid inclusions (circled) from depths of 6.9 m to 12.2 m (13 ka to 18.5 ka) with exceptionally low isotopic values fall well below the modern evaporation path, which are interpreted to reflect regionally cooler climate during this period. (From Lowenstein et al., 1994, Fig. 5, p. 28).

such as storms which initiate in the Pacific Ocean versus the Gulf of Mexico, 2. Variations in temperature due to either climatic changes or seasonal variations in halite precipitation, and 3. Temporal variations in inflow water sources.

Major element chemistry of fluid inclusions: paleolake water compositions

The chemistry of single fluid inclusions can be determined with certain microanalytical chemical techniques. The chemistry of fluid inclusions can be used to document the types of waters at the Earth's surface in the past and to interpret what controlled the chemistry of those waters through time. To date, little attention has been given to chemical analysis of fluid inclusions in lacustrine minerals. However, given the great developments in the last ten years in chemical analysis of individual fluid inclusions, the following techniques could be applied to some lacustrine minerals.

There are several techniques that are capable of analyzing a single fluid inclusion; unfortunately, most methods involve the destruction of the fluid inclusion. The most common methods used in the past decade are: fluid inclusion extraction/IC (ion chromatography) (Lazar & Holland, 1988), laser ablation ICP-MS (inductively coupled plasma-mass spectrometry) (Shepherd & Chenery, 1995), SEM-EDS (scanning electron microscopy with an attached energy dispersive spectrometer) (Ayora & Fontarnau, 1990), ESEM-EDS (environmental scanning electron microscopy with an attached energy dispersive spectrometer) (Timofeeff et al., 2000), and laser Raman microspectroscopy (Rosasco & Roedder, 1979;

Pasteris et al., 1988; Dubessy et al., 1989). These methods all have strengths and weaknesses, and the most effective of these methods depends on the specific scientific question under investigation.

Extraction from single aqueous inclusions was originally attempted by Holser (1963, 1979a, b). These early studies relied on very large inclusions in halite (2 mm to 15 mm), which were likely formed during recrystallization. Petrichenko (1973) pioneered a method which involved the micro-extraction of much smaller inclusions (as small as 40 μm but ideally $>100\ \mu$m) in halite. A thin jet of water is used to dissolve a path to within tens of microns of an inclusion. The halite is dried, and then the inclusion wall is pierced with a needle, and the fluid is extracted with a tapered capillary tube. A reagent is added to the capillary and the tube is sealed and centrifuged. The volume of the precipitate formed by reaction of the inclusion water with the reagent is compared to that formed from prepared standards. This method can be used to determine the concentrations of K, Mg, Ca, and SO_4 but not the concentration of sodium or chloride in the fluid inclusions. The uncertainty of this method is on the order of 20%.

Lazar & Holland (1988) used a similar micro-extraction technique with much more success. A tungsten microdrill is used to bore through halite samples and pierce inclusion walls. When the inclusion wall is breached, the fluid is extracted using a specially constructed micropipette assembly. After extraction, the length of the micropipette containing the inclusion fluid is measured and, as the diameter of the micropipette is known, the volume of fluid can be calculated. The fluid is then run through an ion chromatograph in order to measure the concentration of the major cations and anions (Na, K, Mg, Ca, Cl and SO_4). The analytical error of this technique is much lower than Petrichenko's (1973) method; for major ions it is ±4%. Some minor ions can also be measured with this technique, but with higher uncertainties than for major ions, ±6% for bromide and ±10% for lithium. This fluid inclusion extraction method requires inclusions that are $\sim 200\ \mu$m or larger, which is potentially problematic because it is difficult to determine if inclusions this large are primary or secondary in origin. Therefore the fluids being measured could be surface waters or diagenetic fluids. This method has been used to analyze inclusions from Silurian halite (Das et al., 1990), Permian halite (Horita et al., 1991), and Devonian halite (Horita et al., 1996).

Shepherd & Chenery (1995) pioneered the laser ablation ICP-MS (inductively coupled plasma-mass spectrometry) method of analyzing individual fluid inclusions. An UV laser ablation microprobe is used to drill a hole into a mineral, to reach an inclusion up to 60 μm below the sample surface. For the laser ablation procedure the sample is placed in a modified thermal vacuum cell. The elevated temperature in the ablation cell raises the internal vapor pressure of the inclusion, which causes instantaneous rupture and highly efficient fluid expulsion as the beam breaches the inclusion wall. The vacuum pulls the vaporized fluid into the ICP-MS, where it is analyzed for major and minor ion concentrations. The advantages of the ICP-MS method are the small spot size of the laser ($<2\ \mu$m), allows analysis of small inclusions ($>10\ \mu$m) in a variety of minerals (halite, calcite, quartz, and others). A wide range of ions can be analyzed simultaneously, including low concentrations of minor ions. With multicollector ICP-MS, it will be possible to analyze strontium isotopes and other stable isotopes ($\delta^{13}C$, $\delta^{18}O$, $\delta^{34}S$) in fluid inclusions. Laser ablation ICP-MS is not as precise as other methods (~ 30%) and the results can only be reported as ionic ratios as the volume of an inclusion cannot be determined prior to analysis. However, if the concentration

of one ion is known, then the results can be converted from ratios to absolute concentrations. This method has been used on halite from the Triassic (Shepherd & Chenery, 1995), and from the Eocene, Miocene, Neogene and modern (Shepherd et al., 1998).

The SEM-EDS (scanning electron microscopy with an attached energy dispersive spectrometer) technique pioneered by Ayora & Fontarnau (1990) is able to produce precise measurements of small ($\geq 15\ \mu m$) individual fluid inclusions. This method involves placing a small cleavage chip or mineral slice (typically 1 × 1 × 4 mm) into a brass holder, and freezing the sample in supercooled liquid nitrogen. When the mineral sample is frozen, it is placed into a cryostage, where it is cleaved using a manipulator knife. The cleaving of the mineral exposes frozen fluid inclusions for analysis. The exposed surface is coated with carbon, and the mineral is placed in the SEM chamber. When primary inclusions of sufficient size ($\geq 15\ \mu m$) are located, they are analyzed with an attached electron microbeam. With this method, several analyses of major ions can be rapidly gathered from small inclusions with high precision (<10%). There are difficulties with this procedure, the most glaring one being that the researcher cannot pre-select the inclusion to be analyzed. Samples with high inclusion densities should be used, in order to increase the chances of exposing frozen inclusions during the cleaving process. Fortunately, halite tends to have abundant primary fluid inclusions, so it is typically not a problem finding suitable fluid inclusions in halite with this method. Another problem is the sensitivity of the instrument. The detection limits for the SEM-EDS are typically on the order of 0.1 to 1 wt %. This method has been used to study marine halites (Ayora et al., 1994a, 1994b; Garcia-Veigas et al., 1995; Fanlo & Ayora, 1998; Shepherd et al., 1998), and could potentially be used for other minerals in lacustrine deposits.

The ESEM-EDS (environmental scanning electron microscopy with an attached energy dispersive spectrometer) method of Timofeeff et al. (2000) is very similar to the SEM-EDS method of Ayora & Fontarnau (1990). The major difference is the instrument used for analysis. The ESEM allows for analyses of a sample in a low-pressure environment, as opposed to the high vacuum necessary in a conventional SEM. The environment used in the ESEM for this method is nitrogen gas, typically at 1.3 torr. A carbon coating is needed for samples to be viewed in an SEM in order to absorb the charge buildup due to the electron beam. However, in the ESEM, the ambient environment absorbs the charge, which allows for analyzing uncoated samples. The lack of the carbon coating allows one to directly observe the texture of the inclusion surface prior to analysis. One problem associated with the ESEM technique is that electrons from the electron beam collide with the ambient gas molecules in the environmental chamber. These collisions cause the electrons to be deflected which leads to a phenomenon termed the "skin effect", so named because the beam is slightly defocused, and resembles the flared shape of a skin rather than a beam of uniform size. The skirt effect is minimized as much as possible by operating at low ambient pressures. Multiple analyses are conducted on each sample (five per frozen aqueous inclusion), and averaged. Due to the skirt effect, this method cannot be used on inclusions smaller than 30 μm because the skirt of the beam will strike some of the halite matrix causing the sodium and chloride concentrations to be too high. To correct this problem, the analyses are run through a computerized specific ion interaction equilibrium program (Harvie et al., 1984) using the measured concentrations of major ions (Mg, K, Ca, SO_4), at halite saturation. With these inputs, the equilibrium program can calculate the unique concentration of sodium and chloride for the brine in an individual inclusion. The precision

of the ESEM-EDS method is typically between 3% and 16% and the accuracy is typically 3% to 10%. The detection limits of the method are 0.1 wt % for all of the major ions except sodium, which is 0.5 wt %.

Laser Raman microspectroscopy is unique among these techniques in that it is non-destructive. This method was first attempted on fluid inclusions by Rosasco & Roedder (1979), and has been used by several researchers on a variety of fluid inclusions. This method involves focusing a non-destructive laser microprobe on a single fluid inclusion. A very small portion of the energy from the laser excites covalent bonds, causing vibrations due to stretching or bending of the bond. Therefore, only covalently bonded species can be identified such as sulfate, or bicarbonate. This method has been used to determine the pH of fluid inclusions in Permian lacustrine halite from Kansas (Benison et al., 1998).

Summary

Primary fluid inclusions in evaporites are data recorders that preserve information about the conditions of a lake at the time the inclusions were entrapped. Simple petrography of evaporitic minerals and their growth bands delineated by primary fluid inclusions can be used to determine the depositional environment and relative lake depth. Fluid inclusion homogenization temperatures yield information about paleo-lake temperatures which, in some cases, can be used as a proxy for paleo-air temperatures. Observations of freezing-melting behavior can be used to determine several things about the brine: the salinity, the source (oceanic versus meteoric), and qualitative information about the major ionic composition. Stable isotopic analyses (δD, δ^{18}O) of the inclusions allow for comparison of how temperatures may have been different in the past. There are several techniques for analyzing the chemistry of the fluid inclusions. The most precise quantitative analyses come from either SEM-EDS or ESEM-EDS analyses, which yield accurate analyses for ions with concentrations over 0.1 wt %. The extraction-IC technique also produces very good data. Laser ablation ICP-MS allows for the analysis of very low concentrations of many ions, and is excellent for determining what minor and trace metal ions are present in the fluid. Laser Raman microspectroscopy can be used to determine what covalent bonded complexes, and their relative abundance, are present in the fluid, and this technique does not destroy the inclusion.

Fluid inclusions, if treated properly, can yield large amounts of data specific to a single paleo-lake of any age, from the Holocene to the Precambrian, that potentially has regional and global implications.

Acknowledgements

We dedicate this chapter to present and former Binghamton University students for their contributions to the understanding of Earth's ancient waters through their studies of fluid inclusions: Osama Attia, Kathy Benison, Andy Bobst, Chris Brown, Enrique Casas, Andrea Cicero, Dan Davis, Jeff Hanna, Matthew C. Hein, Laura Howe, Douglas Jennings, Eric Johnson, Jianren Li, Kathy Schubel, Michael Timofeeff, Denise Waite, and Qingjun Yao.

References

Attia, O. E., T. K. Lowenstein & A. M. A. Wali, 1995. Middle Miocene gypsum. Gulf of Suez: marine or nonmarine? J. Sed. Res. A65: 614–626.

Ayora, C. & R. Fontarnau, 1990. X-ray microanalysis of frozen fluid inclusions. Chem. Geol. 89: 135–148.

Ayora, C., J. Garcia-Veigas & J.-J. Pueyo, 1994a. X-Ray microanalysis of fluid inclusions and its application to the geochemical modeling of evaporite basins. Geoch. Cosmoch. Acta. 58: 43–55.

Ayora, C., J. Garcia-Veigas & J.-J. Pueyo, 1994b. The chemical and hydrological evolution of an ancient potash-forming evaporite basin in Spain as constrained by mineral sequence, fluid inclusion composition, and numerical simulation. Geoch. Cosmoch. Acta. 58: 3379–3394.

Benison, K. C. & R. H. Goldstein, 1999. Permian paleoclimate data from fluid inclusions in halite. Chem. Geol. 154: 113–132.

Benison, K. C., R. H. Goldstein, B. Wopenka, R. C. Burruss & J. D. Pasteris, 1998. Extremely acid Permian lakes and ground waters in North America. Nature 392: 911–914.

Bischoff, J. L., J. A. Fitzpatrick & R. J. Rosenbauer, 1993. The solubility and stabilization of ikaite ($CaCO_3 \cdot 6H_20$) from 0° to 25 °C: Environmental and paleoclimatic implications for thinolitic tufa. J. Geol. 101: 21–33.

Casas, E., T. K. Lowenstein, R. J. Spencer & P. Zhang, 1992. Carnallite mineralization in the nonmarine Qaidam basin, China: Evidence for the early diagenetic origin of potash evaporites. J. Sed. Pet. 62: 881–898.

Carpelan, L. H., 1958. The Salton Sea, physical and chemical characteristics. Limnol. Oceanogr. 3: 373–386.

Das, N., J. Horita & H. D. Holland, 1990. Chemistry of fluid inclusions in halite from the Salina Group of the Michigan Basin: Implications for Late Silurian seawater and the origin of sedimentary brines. Geoch. Cosmoch. Acta. 54: 319–327.

Davis, D. W., T. K. Lowenstein & R. J. Spencer, 1990. Melting behavior of fluid inclusions in laboratory-grown halite crystals in the systems $NaCl\text{-}H_2O$, $NaCl\text{-}KCl\text{-}H_2O$, $NaCl\text{-}MgCl_2\text{-}H_2O$, and $NaCl\text{-}CaCl_2\text{-}H_2O$. Geoch. Cosmoch. Acta. 54: 591–601.

Demicco, R. V. & L. A. Hardie, 1994. Sedimentary Structures and Early Diagenetic Features of Shallow Marine Carbonate Deposits. Society of Sedimentary Geology Atlas Series No. 1, Tulsa, Oklahoma, 265 pp.

Dubessy, J., B. Poty & C. Ramboz, 1989. Advances in C-O-H-N-S fluid geochemistry based on micro-Raman spectrometric analysis of fluid inclusions. Eur. J. Mineral 1: 517–534.

Eubank, M. E. & R. C. Brough, 1980. The Great Salt Lake and its influence on the weather. In Gwynn, J. W. (ed.) Great Salt Lake — A Scientific, Historical and Economic Overview. Utah Geological and Mineral Survey, Bull. 116: 279–283.

Eugster, H. P., 1970. Chemistry and origin of the brines of Lake Magadi, Kenya. Mineral. Soc. Am., Spec. Paper 3: 215–235.

Eugster, H. P., 1980. Lake Magadi, Kenya, and its precursors. In Nissenbaum, A. (ed.) Hypersaline Brines and Evaporitic Environments (Developments in Sedimentology 28). Elsevier, Amsterdam: 195–232.

Fanlo, I. & C. Ayora, 1998. The evolution of the Lorraine evaporite basin: implications for the chemical and isotope composition of the Triassic ocean. Chem. Geol. 146: 135–154.

Faure, G., 1998. Principles and Applications of Geochemistry. Prentice Hall, Upper Saddle River (N.J.), 600 pp.

Friedman, I., G. I. Smith, J. D. Gleason, A. Warden & J. M. Harris, 1992. Stable isotope composition of waters in southeastern California 1. Modern precipitation. J. Geophys. Res. 97: 5795–5812.

Garcia-Veigas, J., F. Orti, L. Rosell, C. Ayora, J.-M. Rouchy & S. Lugli, 1995. The Messinian Salt of

the Mediterranean: Geochemical Study of the Salt from the Central Sicily Basin and Comparison with the Lorca Basin (Spain). Bulletin Societe Geologie France 166, 699–710.

Gavrieli, I., A. Starinsky & A. Bein, 1989. The solubility of halite as a function of temperature in the highly saline Dead Sea brine system. Limnol. Oceanogr. 34: 1224–1234.

Goldstein, R. H. & T. J. Reynolds, 1994. Systematics of Fluid Inclusions in Diagenetic Minerals. SEPM Short Course 31, 199.

Hammer, U. T., 1986. Saline Lake Ecosystems of the World. Dr. W. Junk Publishers, Dordrecht, 616 pp.

Hardie, L. A. & H. P. Eugster, 1971. The depositional environment of marine evaporites: a case for shallow, clastic accumulation. Sedimentology 16: 187–220.

Hardie, L. A., T. K. Lowenstein & R. J. Spencer, 1985. The problem of distinguishing between primary and secondary features in evaporites. In Schreiber, B. C. & H. L. Harner (eds.) Sixth International Symposium on Salt. The Salt Institute, Alexandria, Virginia: 11–38.

Harvie, C. E., N. Møller & J. H. Weare, 1984. The prediction of mineral solubilities in natural waters: the $Na\text{-}K\text{-}Mg\text{-}Ca\text{-}H\text{-}Cl\text{-}SO_4\text{-}OH\text{-}HCO_3\text{-}CO_3\text{-}H_2O$ system to high ionic strengths at 25 °C. Geoch. Cosmoch. Acta. 48: 723–751.

Holser, W. T., 1963. Chemistry of brine inclusions in Permian salt from Hutchinson, Kansas. Symposium on Salt, v. 1. Northern Ohio Geological Society, Cleveland, Ohio: 86–95.

Holser, W. T., 1979a. Trace elements and isotopes in evaporites. In Burns, R. G. (ed.) Marine Minerals. Mineralogical Society of America, Reviews in Mineralogy, v. 6, Washington (D.C.): 295–346.

Holser, W. T., 1979b. Mineralogy of evaporites. In Burns, R. G. (ed.) Marine Minerals. Mineralogical Society of America, Reviews in Mineralogy, v. 6. Washington (D.C.): 211–294.

Horita, J., T. J. Friedman, B. Lazar & H. D. Holland, 1991. The composition of Permian seawater. Geoch. Cosmoch. Acta. 55: 417–432.

Horita, J., A. Weinberg, N. Das & H. D. Holland, 1996. Brine inclusions in halite and the origin of the Middle Devonian Prairie evaporites of Western Canada. J. Sed. Res. 66: 956–964.

James, N. P. & P. W. Choquette, 1990. Limestones — The Sea Floor Diagenetic Environment. Geoscience Canada Reprint Series 4. Geological Association of Canada, St. Johns, Newfoundland: 13–34.

Johnson, W. J. & R. H. Goldstein, 1993. Cambrian sea water preserved as inclusions in marine low-magnesium calcite cement. Nature 362: 335–337.

Kelts, K. & K. J. Hsu, 1978. Freshwater carbonate sedimentation. In Lerman, A. (ed.) Lakes — Chemistry, Geology, Physics. Springer-Verlag, New York: 295–323.

Knauth, L. P. & M. B. Kumar, 1981. Trace water content of salt in Louisiana salt domes. Science 213: 1005–1007.

Knauth, L. P. & M. A. Beeunas, 1986. Isotope geochemistry of fluid inclusions in Permian halite with implications for the isotopic history of ocean water and the origin of saline formation waters. Geoch. Cosmoch. Acta. 50: 419–433.

Kovalevich, V. M., T. M. Peryt & O. I. Petrichenko, 1998. Secular variation in seawater chemistry during the Phanerozoic as indicated by brine inclusions in halite. Jour. Geol. 106: 695–712.

Last, W. M., 1984. Sedimentology of playa lakes of the northern Great Plains. Can. J. Earth Sci. 21: 107–125.

Lazar, B. & H. D. Holland, 1988. The analysis of fluid inclusions in halite. Geoch. Cosmoch. Acta. 52: 485–490.

Li, J., T. K. Lowenstein, C. B. Brown. T.-L. Ku & S. Luo, 1996. A 100 ka record of water tables and paleoclimates from salt cores, Death Valley, California. Palaeogeogr., Palaeoclim., Palaeoecol. 123: 179–203.

Lowenstein, T. K. & L. A. Hardie, 1985. Criteria for the recognition of salt-pan evaporites. Sedimentology 32: 627–644.

Lowenstein, T. K. & R. J. Spencer, 1990. Syndepositional origin of potash evaporites: petrographic and fluid inclusion evidence. Am. J. Sci. 290: 1–42.

Lowenstein, T. K., J. Li & C. B. Brown, 1998. Paleotemperatures from fluid inclusions in halite: Method verification and a 100,000 year paleotemperature record. Death Valley, California. Chem. Geol. 150: 223–245.

Lowenstein, T. K., R. J. Spencer, W. Yang, E. Casas, P. Zhang, B. Zhang, H. Fan & H. R. Krouse, 1994. Major-element and stable-isotope geochemistry of fluid inclusions in halite, Qaidam Basin, western China: Implications for late Pleistocene/Holocene brine evolution and paleoclimates. In Rosen, M. R. (ed.) Paleoclimate and Basin Evolution of Playa Systems. Geol. Soc. Am. Special Paper 289, Boulder, Colorado: 19–32.

Moissette, A., T. J. Shepherd & S. R. Chenery, 1996. Calibration strategies for the elemental analysis of individual aqueous fluid inclusions by laser ablation-ICP-MS. Journal of Anal. Atom. Spec. 11: 177–186.

Neev. D. & K. O. Emery, 1967. The Dead Sea: Depositional Processes and Environments of Evaporites. Israel Geol. Surv. Bull. 41, 147 pp.

Pasteris, J. D., B. Wopenka & J. C. Seitz, 1988. Practical aspects of quantitative laser Raman microprobe spcctroscopy for the study of fluid inclusions. Geoch. Cosmoch. Acta. 52: 979–988.

Petrichenko, O. I., 1973. Methods of Study of Inclusions in Minerals of Saline Deposits. Naukova dumka, Kiev, p. 98 (in Ukrainian; transl. In Fluid Inclusion Research Proc. COFFI, 12 214–274, 1979).

Petrichenko, O. I., T. M. Peryt & A. V. Poberegsky, 1997. Peculiarities of gypsum sedimentation in the Middle Miocene Badenian evaporite basin of Carpathian Foredeep. Slovak Geol. Mag. 3: 91–104.

Roberts, S. M. & R. J. Spencer, 1995. Paleotemperatures preserved in fluid inclusions in halite. Geoch. Cosmoch. Acta. 59: 3929–3942.

Roberts, S. M., R. J. Spencer & T. K. Lowenstein, 1994. Late Pleistocene saline lacustrine sediments, Badwater Basin. Death Valley, California. In Lomando. A. J., B. C. Schreiber & P. M. Harris (eds.) Lacustrine Reservoirs and Depositional Systems. Society for Sedimentary Geology Core Workshop 19: 61–103.

Roberts, S. M., R. J. Spencer, W. Yang & H. R. Krouse, 1997. Deciphering some unique paleotemperature indicators in halite-bearing saline lake deposits from Death Valley, California, USA. J. Paleolim. 17: 101–130.

Roedder, E., 1984. Fluid inclusions. In Ribbe, P. H. (ed.) Mineralogical Society of America, Reviews in Mineralogy, v. 12. Washington (D.C.): 644.

Roedder, E. & H. E. Belkin, 1979. Application of Studies of fluid inclusions in Permian Salado salt. New Mexico, to problems of siting the Waste Isolation Pilot Plant. In McCarthy, G. J. (ed.) Scientific Basis for Nuclear Waste Management. Plenum Publishing Corp., New York: 313–321.

Roedder, E. & R. J. Bodnar, 1980. Geologic pressure determination from fluid inclusion studies. Ann. Rev. Earth Planet. Sci. 8: 263–301.

Rosasco, G. J. & E. Roedder. 1979. Application of a new Raman microprobe spectrometer to non-destructive analysis of sulfate and other ions in individual phases in fluid inclusions in minerals. Geoch. Cosmoch. Acta. 43: 1907–1915.

Sabouraud-Rosset, C., 1969. Characteres morphologiques des cavites primaires des monocristaux. sur l' example du gypse de synthese. Academie des Sciences (Paris), Comptes Rendus 268 Serie D: 749–751.

Sabouraud-Rosset, C., 1972. Microcryoscopie des inclusions liquides du gypse et salinite des milieux generateurs. Revue de Geographie Physique et de Geologie Dynamique 14: 133–144.

Sabouraud-Rosset, C., 1974. Determination par activation neutronique des rapports Cl/Br des inclusions fluides de divers gypses. Correlation avec les donnees de la microcryoscopie et interpretations genetiques. Sedimentology 21: 415–431.

Sabouraud-Rosset, C., 1976. Les conditions de genese de certaines formes de cavites intracristallines eclairces par la methode experimentale. Bull. Soc. France Mineral. Cristallogr. 99: 74–77.

Schubel, K. A. & T. K. Lowenstein, 1997. Criteria for the recognition of shallow-perennial-saline-lake halites based on Recent sediments from the Qaidam Basin, western China. J. Sed. Res. 67: 74–87.

Shearman, D. J., A. McGugan, C. Stein & A. J. Smith, 1989. Ikaite, $CaCO_3 \cdot 6H_2O$. precursor of the thinolites in the Quaternary tufas and tufa mounds of the Lahontan and Mono Lake Basins, western United States. Geological Society of America Bulletin. 101: 913–917.

Shepherd, T. J., A. H. Rankin & D. H. M. Alderton, 1985. A Practical Guide to Fluid Inclusion Studies. Blackie & Son Ltd., Glasgow, 239 pp.

Shepherd, T. J. & S. R. Chenery, 1995. Laser ablation ICP-MS elemental analysis of individual fluid inclusions: An evaluation study. Geoch. Cosmoch. Acta. 59: 3997–4007.

Shepherd, T. J., S. R. Chenery & A. Moissette, 1995. Optimization of Laser Ablation-ICP-MS for the Chemical Analysis of Fluid Inclusions in Evaporite Minerals. Abstract EUG 8, Strasbourg 1995, Terra Nova 7, 344.

Shepherd, T. J., C. Ayora, D. I. Cendon, S. R. Chenery & A. Moissette, 1998. Quantitative solute analysis of single fluid inclusions in halite by LA-ICP-MS and cryo-SEM-EDS: complementary microbeam techniques. European Journal of Mineralogy 10: 1097–1108.

Smith, G. I., I. Friedman & R. J. McLaughlin, 1987. Studies of Quaternary saline lakes: III. mineral, chemical, and isotopic evidence of salt solution and crystallization processes in Owens Lake, CA., 1969–1971. Geoch. Cosmoch. Acta. 51: 811–827.

Smoot, J. P. & T. K. Lowenstein, 1991. Depositional environments of non-marine evaporites. In Melvin, J. L. (ed.) Evaporites, Petroleum and Mineral Resources. Developments in Sedimentology 50. Elsevier Science Publishers B.V., Amsterdam, Holland: 189–347.

Sorby, H. C., 1858. On the microscopical structure of crystals indicating the origin of rocks and minerals. Geological Society of London Journal 14: 453–500.

Spencer, R. J., N. Moller & J. H. Weare, 1990. The prediction of mineral solubilities in natural waters. A chemical equilibrium model for the $Na\text{-}K\text{-}Ca\text{-}Mg\text{-}Cl\text{-}SO_4\text{-}H_2O$ system at temperatures below 25 °C. Geoch. Cosmoch. Acta 54: 575–590.

Timofeeff, M. N., T. K. Lowenstein & W. H. Blackburn, 2000. ESEM-EDS: An Improved technique for major chemical analysis of fluid inclusions. Chem. Geol. 164: 171–182.

Ward, W. B., A. Cox, M. H. Kwong, W. J. Meyers & J. L. Banner, 1993. Upper Devonian seawater samples encased in calcite cements: single-phase fluid-inclusion salinities and cement compositions, Devonian reef complexes, Canning Basin, Western Australia. AAPG 1993 Annual Meeting Program: 197–198.

Warren, J. K., 1982. The hydrological setting, occurrence and significance of gypsum in Late Quaternary salt lakes in South Australia. Sedimentology 29: 609–637.

Winograd, I., B. J. Szabo, T. B. Coplen, A. C. Riggs & P. T. Kolesar, 1985. Two-million-year record of deuterium depiction in Great Basin ground waters. Science 227: 519–522.

Yang, W., 1993. Improved techniques for stable isotope analyses of microlitre quantities of water and applications to paleoclimate and diagenesis using fluid inclusions in halite and dolomite. Ph.D. thesis. University of Calgary, Alberta, 151 pp.

Yang, W., R. J. Spencer, H. R. Krouse & T. K. Lowenstein, 1995a. Stable hydrogen and oxygen isotope techniques for studying arid basin hydrology. In Tracer Technologies for Hydrological Systems (Proceedings of a Boulder Symposium, July 1995) IAHS Publ. 229: 305–310.

Yang, W, R. J. Spencer, H. R. Krouse, T. K. Lowenstein & E. Casas, 1995b. Stable isotopes of lake and fluid inclusion brines, Dabusun Lake, Qaidam Basin, western China: Hydrology and paleoclimatology in arid environments. Palaeogeogr. Palaeoclim. Palaeoecol. 117: 279–290.

8. APPLICATION OF MINERAL MAGNETIC TECHNIQUES TO PALEOLIMNOLOGY

PER SANDGREN (Per.Sandgren@geol.lu.se)
IAN SNOWBALL (Ian.Snowball@geol.lu.se)
Department of Quaternary Geology
Tornavägen 13
SE-223 63 Lund
Sweden

Keywords: magnetic susceptibility, magnetic remanence, iron oxides, iron sulphides, dissolution, authigenesis

Introduction

This chapter provides an introduction to the application of mineral magnetic methods to studies of lake-sediments. It is not detailed; but instead contains a substantial number of references to textbooks and articles that fully explain routine and advanced methodologies and their modes of application.

Why measure the magnetic properties of mud deposited on the bottoms of lakes? This question, often asked by the non-specialist, is by no means easy to answer. Two answers can be given. The first is that, under specific sedimentary conditions, lake-sediments preserve a record of variations in the direction and strength of Earth's geomagnetic field (which is an answer that typically causes a deluge of more questions). The second answer is that the type, concentration and grain-size of magnetic minerals found in lake-sediments vary according to a variety of processes operating in response to changes in climate, human activity and limnology. Examination of ancient sediments, using the paradigm that "the present is the key to the past," enables inferences to be made about past environments.

As will be discussed in this chapter, all materials can be classified according to their behaviour during (and after) exposure to an external magnetic field. This behaviour can be qualified and quantified, which enables mineral magnetic measurements to be discriminatory and diagnostic. By applying a range of increasing or decreasing positive and negative magnetic fields to a sample (and also at variable temperatures and pressures, or energy levels), it is possible to obtain information about the overall composition of the "magnetic assemblage", including concentration, mineralogy and magnetic grain-size.

Freshwater lakes often have well-defined catchments (or watersheds) and receive sediment from many sources, most of which have unique or well-defined magnetic characteristics (which must also be measured as part of a comprehensive magnetic study of lake-sediments). The majority of magnetic minerals found in lake-sediments are derived by catchment erosion and originate from bedrock, subsoil, and topsoil in the lake's drainage



W. M. Last & J. P. Smol (eds.), 2001. *Tracking Environmental Change Using Lake Sediments. Volume 2: Physical and Geochemical Methods.* Kluwer Academic Publishers. Dordrecht, The Netherlands

basin. They are transported as suspended load and/or bedload in rivers and streams, or possibly by overland flow and eventually deposited as sediment. Atmospheric sources of magnetic minerals in lake-sediments include aerosols emitted from volcanoes, dust transported by storms and particles produced by anthropogenic activities (such as fossil fuel combustion). In many sedimentary environments, it is assumed that the detrital magnetic assemblage remains unaltered after deposition. However, *in-situ* post-depositional diagenetic processes may lead to the destruction (dissolution) of magnetic phases or the production of new magnetic minerals (authigenesis). Dearing (1999) provides an in-depth review of processes that determine the origins and transformations of magnetic minerals in lakes and their catchments.

A brief history of the application of mineral magnetic measurements to lake sediments

It was known by the Swede Gustav Ising in the 1920's (Ising, 1943) that varved clays deposited in ancient ice-lakes carried a stable natural remanent magnetisation (NRM), and hence a potential record of temporal changes in the direction and intensity of Earth's geomagnetic field. His pioneering study led to many (and often unsuccessful) attempts to reconstruct changes in the Earth's geomagnetic field through studies of the NRM carried in varved clays (e.g., McNish & Johnson, 1938; Granar, 1958). In the context of future studies of environmental change, one of Isings' most important observations was that the spring layer of the varves contained a higher concentration of magnetite than the other seasonal layers. It was believed that this grading was caused by the preferential deposition of relatively heavy minerals (e.g., magnetite) during the intense spring meltwater floods. As will be discussed later, this relationship does not necessarily hold true for lake-sediments with a considerably higher organic carbon content, and for reasons that Gustav Ising could not possibly have contemplated in the 1920's.

The current applications of mineral magnetic techniques to lake-sediments originated through the work of primarily three people in the 1960–1980's. In the late 1960's John Mackereth discovered that unconsolidated organic-rich sediments deposited in Lake Windermere also carried a stable NRM, and that it should be possible to establish regional palaeomagnetic secular variation (PSV) master curves, which could be used for relative dating and correlation (Mackereth, 1971). Mackereth's work was continued by Roy Thompson in the early 1970's, who successfully applied the palaeomagnetic technique to several localities in northern Europe (Thompson, 1973). At approximately the same time, Frank Oldfield (Oldfield, 1977) was comprehensively exploring the use of lakes and their drainage basins as units of ecological study. During an environmental study of relatively recent sediments deposited in Lough Neagh, Northern Ireland by Thompson et al. (1975), it was discovered that down-core magnetic susceptibility peaks were linked to periods of deforestation and the subsequent erosion of mineral soils. These magnetic susceptibility peaks could be traced from core to core, enabling correlation, and the variations in the amplitude of the magnetic susceptibility record could be used as a proxy-indicator of the intensity of erosion. This observation opened the "flood-gates" for a variety of projects designed to qualify and quantify the source of the magnetic signal identified in lake-sediments and peat bogs. These projects have included studies of atmospheric particles, the relationships between particle-size distribution and magnetic properties, and the transformation and production

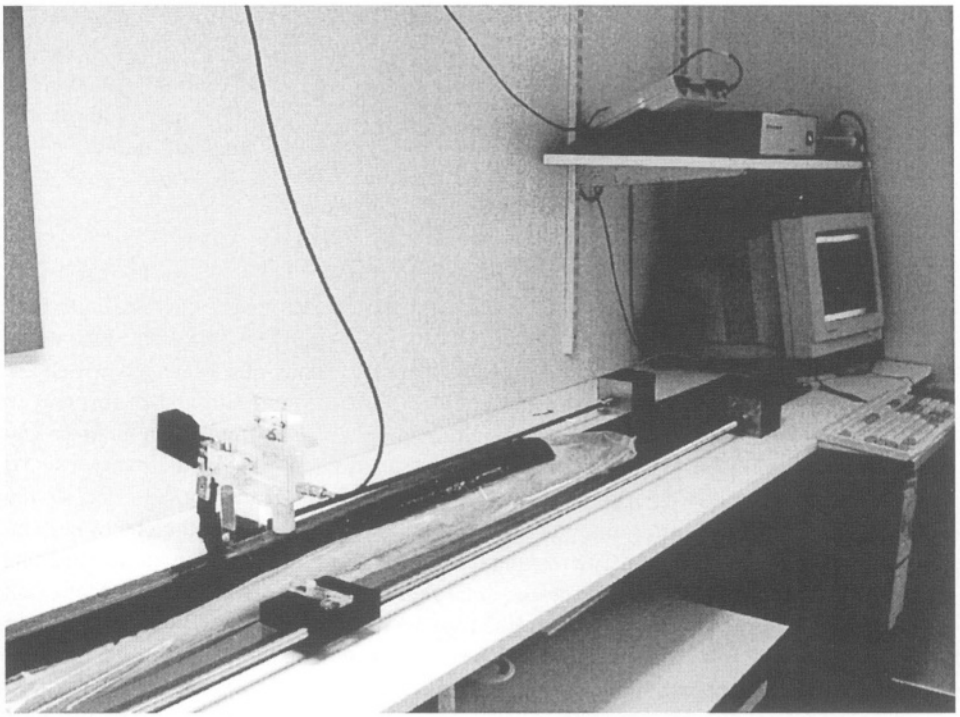


Plate 1. Measuring the long-core surface scanning magnetic susceptibility of a 1.5 m long varved-lake sediment sequence (using a Bartington Instruments Ltd MS2E1 sensor and a Lund University, Department of Quaternary Geology, TAMISCAN-TS1 automatic conveyor).

of magnetic minerals through pedogenesis, diagenesis, authigenesis and dissolution. Intimately linked to the expansion in the application of mineral magnetic techniques was the development of analytical equipment and improved computing power (see plate 1). A modern mineral magnetic/palaeomagnetic laboratory is not a cheap investment and requires knowledge of solid-state physics and electromagnetism, cryo-technology and computer science.

Although the majority of sediments investigated have displayed a positive relationship between the concentration of allochthonous mineral matter and concentration dependent magnetic parameters (e.g., Thompson et al., 1975; Dearing, 1991; Dearing & Flower, 1982), three discoveries demonstrated that this relationship is not universal. First was the finding that detrital (titano)magnetite could be dissolved by post-depositional reductive diagenesis (dissolution) (Hilton & Lishman, 1985; Andersen & Rippey, 1988; Snowball, 1993). Second was the discovery of bacteria living in sediments and soils that produce fine-grained magnetite as part of their internal metabolism, primarily for navigational purposes (Blakemore, 1975). Third was the discovery that relatively high concentrations of authigenic magnetic iron sulphides could form in specific geochemical environments (Snowball & Thompson, 1988; Snowball, 1991; Roberts et al., 1996). All three discoveries testify to the intimate link between the production, deposition and subsequent decomposition of

organic matter and the magnetic properties of lake sediments. Considering Gustav Isings original observations on clastic varves, it is somewhat ironic that recent studies of varved lake-sediments in Sweden and Finland (Snowball & Saarinen, pers. com.) indicate that the highest concentration of magnetite is found in the organic rich summer and winter layers of the varves, where bacterial thrive and produce their magnetite "magnetosomes".

Magnetic properties

It is well known that a permanent hand magnet attracts ferromagnetic materials, e.g., metallic iron. However, this positive attraction, which can easily be observed without any instrumentation, is only one of several types of magnetic behaviour. Materials which are generally considered to be non-magnetic (such as plastic, wood and chalk) respond to applied magnetic fields in a specific manner, although relatively strong magnetic fields and sensitive measuring instruments (magnetometers) are required to detect their response. At the sub-atomic level a magnetic moment is produced due to the combined effect of the orbital spin of the electrons around the nucleus and the spin motion of the electron about its own axis of rotation (Fig. 1). The resultant of all the orbital and spin magnetic moments of the electrons in an atom leads to a magnetic dipole moment and the total effect of all magnetic moments at the atomic level influences the magnetic properties of a material. In electron shells with a paired number of electrons, the magnetic dipole effects cancel each other out and the net magnetic moment is zero.

Diamagnetism

The diamagnetic behaviour is fundamental to all substances. It is extremely weak and negative (in relation to the applied field) and is often masked by other forms of magnetism if they are present. Diamagnetic substances have paired electrons in the electron shells of the constituent atoms. In the presence of an applied field, the electron orbits become aligned anti-parallel to the external field, which results in a net negative magnetic moment. When the magnetic field is removed, the net negative magnetisation is lost. Diamagnetism is independent of temperature. Many common natural minerals such as quartz, feldspar, calcite and also water exhibit diamagnetic behaviour.

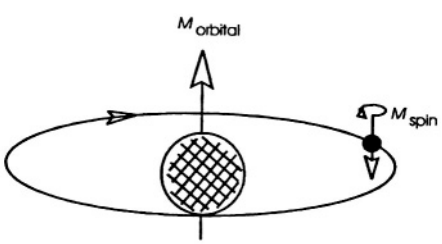


Figure 1. Magnetism of an atom. The magnetisation arises from the spin of an electron about its axis and from the orbital motion of the electrons about its nucleus (from Tarling 1971).

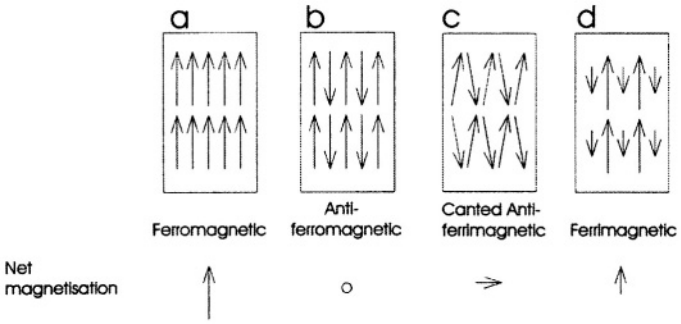


Figure 2. Schematic representation of the distribution of magnetisation vectors in ferromagnetic materials, (a) ferromagnetic, (b) antiferromagnetic, (c) canted antiferromagnetic, (d) ferrimagnetic (after McElhinny 1973).

Paramagnetism

Paramagnetism results from the alignment of atoms with unpaired electrons so that a weak positive net magnetic moment is produced (from both the electron spin and orbital spin) parallel to the applied field. Because of dominating thermal effects, the magnetisation is lost when the external magnetic field is removed. In the presence of an applied magnetic field the paramagnetic materials are, as opposed to diamagnetic materials, attracted to the field. The paramagnetic effect is generally one or two orders of magnitude greater than the diamagnetic effect, although it is considerably weaker compared to the magnetic moment of ferromagnets. Paramagnetism is dependent on temperature and is exhibited by many natural iron-bearing mineral (e.g., olivine, pyroxene, garnet, biotite and carbonates containing iron and manganese).

Ferromagnetism

Ferromagnetic substances have atoms in which unpaired electrons are closely and regularly spaced. This arrangement leads to a strong interaction (coupling) between unpaired electron spins, which produces a permanent magnetisation (called a spontaneous magnetisation) to exist, even in the absence of a magnetic field. Four different ferromagnetic behaviours can be defined as a result of their atomic and crystal lattice structures. Iron, cobalt, nickel and their alloys exhibit true *ferromagnetism.* In such substances a parallel coupling of all unpaired electrons leads to an extremely strong spontaneous magnetisation (Fig. 2a). This strong magnetisation is lost above a critical temperature, called the Curie/Neél temperature, which has a specific value for each different ferromagnetic material. Ferromagnets exhibit paramagnetic behaviour above their Curie temperature. The net magnetic moment of ferromagnetic materials is several orders of magnitude greater than that of diamagnetic and paramagnetic materials. It is for this reason that ferro/ferrimagnetic minerals (such as magnetite) dominate the magnetic properties of lake-sediments, even if present in low concentrations.

Anti-ferromagnetism and canted anti-ferromagnets

Anti-ferromagnetic substances have two anti-parallel sub-lattices with identical magnetic moments, which creates a zero net spontaneous magnetisation (Fig. 2b). If for some reason the sub-lattices are not perfectly anti-parallel (or canted) the basic anti-ferromagnetic arrangement will be modified and there will be a small spontaneous net magnetisation (Fig. 2c). This type of magnetic behaviour is called canted anti-ferromagnetism. Haematitie and goethite are two common canted anti-ferromagnetic minerals.

Ferrimagnetism

Ferrimagnetic materials also contain alternating layers of crystal lattices that are magnetised in opposite directions. However, the coupling occurs via an intermediate oxygen atom. Neighbouring sub-lattices are thus of unequal magnetic moment and a net spontaneous magnetic moment can exist below the materials Curie temperature (Fig. 2d). Above the Curie temperature the ferrimagnets behave like paramagnets. Magnetite is the most common natural ferrimagnet. Ferrimagnetic minerals dominate the magnetic properties of most natural magnetic assemblages. Although ores of elemental iron, cobalt and nickel exist, these are generally oxidised upon exposure to Earth's oxygen-rich atmosphere (producing oxides that may be ferrimagnetic, such as magnetite) or reduced in sulphur-rich anaerobic environments as part of organic matter decomposition (producing sulphides that may be ferrimagnetic, such as greigite).

Magnetic hysteresis

Hysteresis is a common physical phenomenon and also applies to magnetic properties. The relationships between an applied field (H or B) and the intensity of magnetisation (M) induced in a sample can be used to magnetically characterise the sample, according to the previously described behaviours. Graphical presentations of these fundamental measurements are commonly called magnetic hysteresis curves. Most (but not all) parameters used in magnetic analyses can be deduced from a hysteresis curve. A hysteresis curve demonstrating how M changes in response to increasing forward (positive) and decreasing (negative) magnetic fields (along $+H$ and $-H$) is shown in Figure 3.

A magnetic hysteresis curve of the type described above requires both '*in-field' and 'out-of-field'* measurements of *M,* but this type of combined analyses requires relatively sophisticated equipment. Most mineral magnetic laboratories in Earth science departments are equipped with magnetometers that measure the (almost) permanent (remanent) magnetisation induced in a sample after it has been exposed to Earth's magnetic field or an artificial magnetic field. A general exception is the measurement of initial magnetic susceptibility (which applies a very weak magnetic field during measurement). For a wide range of positive magnetic fields, a paramagnetic sample will acquire a positive magnetisation (Fig. 4), while a diamagnetic sample will acquire a negative magnetisation (Fig. 4). Diamagnetic and paramagnetic materials lose their magnetisation (M) when removed from the magnetic field (H) and therefore exhibit no magnetic hysteresis. The slope of the line ($\Delta M/\Delta H$ and $-\Delta M\Delta H$) is called the initial magnetic susceptibility (κ), generally defined as per unit

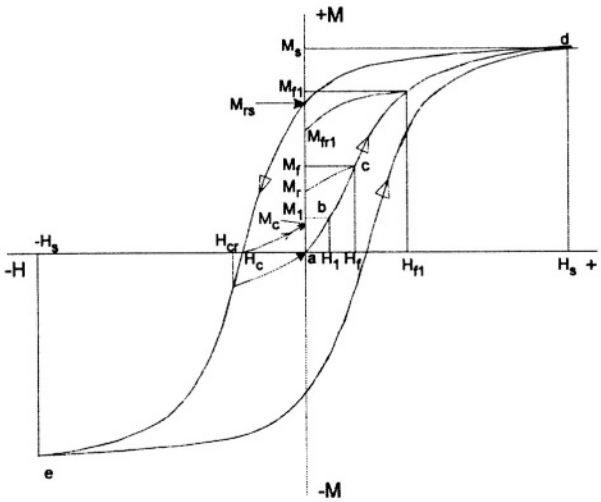


Figure 3. Hysteresis loop for ferromagnetic materials. See main text for a full description.

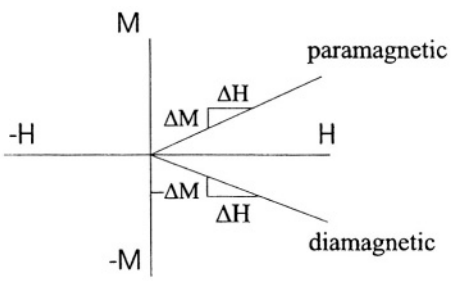


Figure 4. M-H plots for diamagnetic and paramagnetic materials.

volume of material. Mass specific susceptibility (χ) is obtained by dividing κ by the mass of the material.

Ferro/ferrimagnetic substances possessing a spontaneous magnetisation show a more complicated response to applied magnetic fields and they exhibit true magnetic hysteresis. In this chapter we restrict our description of true magnetic hysteresis to samples containing many ferro/ferrimagnetic particles randomly distributed within a non-magnetic matrix, which is a situation similar to many natural magnetic assemblages.

A sample that has not been exposed to a magnetic field *(H)* has no magnetisation (the random orientation of many magnetic particles leads to a net zero magnetisation). In the magnetic hysteresis plot, this magnetisation is represented by point *a* (Fig. 3). If the sample is exposed to a very weak magnetic field (H_1) this will result in a magnetisation (M_1), represented by point *b*. The slope of the line segment *a-b* is called the initial low magnetic

susceptibility. When the sample is removed from the field H_1 the magnetisation M_1 returns to zero, i.e. the procedure is reversible or anhysteretic. When the sample is exposed to a higher magnetic field H_f ($H_f > H_1$), it will acquire a magnetisation, represented by point *c,* corresponding to M_f (in-field magnetisation) *(c* in Fig. 3). Important changes will take place in the magnetic behaviour when it is removed from the field (M_f). The magnetisation will not return to zero but will drop to M_r, following the path c-M_r. This point represents the remanent magnetisation (M_r) (out-of field magnetisation) corresponding to the field H_f. Magnetisation at a higher field e.g., H_{f1} corresponds to a (in-field) magnetisation of M_{f1} and a remanent magnetisation of M_{fr1}. Application of gradually stronger magnetic fields will cause the magnetisation of the sample to increase. However, eventually the slope of the curve will gradually attenuate and at a certain point (H_s) the sample magnetisation will not increase in response to the application of stronger magnetic field. In other words, the sample has reached saturation (M_s). The sample has magnetically become saturated corresponding to a saturated (in-field) magnetisation (M_s) and a saturated (out-of-field) remanent magnetisation (M_{rs}). If the sample now is applied to a series of increasing fields in the reverse direction ($-H$), the magnetisation will again gradually decrease. At a specific value of H (H_c) the magnetisation is reduced to zero. This reverse field H_c is called the 'coercivity' or the 'coercive force', although the sample still has a positive remanent magnetisation corresponding to Mc. An even higher reversed field is required to reduce the remanent magnetisation to zero. This field is called the coercivity of remanence and is represented by the field at $(H)_{CR}$. Progressive magnetisation in increasingly higher reversed fields continue until a point of negative magnetic saturation is reached. When the field again is increased to 0 and then progressively increased in forward direction the M-H plot will follow the lower curve on Figure 3 from e to d. The hysteresis loop can now be repeated by applying increasing and decreasing fields between H_S and $-H_S$.

Anhysteretic remanent magnetisation (ARM)

The common iron minerals have imperfections, which cause the hysteresis properties discussed above. An anhysteretic (free of hysteresis) magnetisation can be achieved in such materials by applying an alternating field (AF) of gradually decreasing amplitude in the presence of a direct current bias field (which we will call the DC bias field). As the AF is reduced, the hysteresis is progressively removed and the magnetisation of the material gradually converges on the anhysteretic value for the prevailing DC bias field intensity. ARM is related to magnetic grain size (e.g., King et al. 1982; Maher, 1988). Measurement of this parameter is now routine at most laboratories.

Sample collection and preparation

Collection of lake sediment cores for magnetic analyses

A number of various coring techniques are used to collect lake-sediments (Glew et al., volume 1). The choice of coring technique has to be made with respect to a number of factors like water depth, sediment thickness, type of material, compaction of sediment, etc. With respect to palaeomagnetic measurements (i.e. measurements of the natural remanent

magnetisation, NRM) it is critical that physical disturbance of the sediment sequence is minimal and that the orientation of the core is known, or that at least the core penetrates vertically and does not twist or bend during operation. Ideally the core barrel should be made from a "non-magnetic" material (e.g., plastic) and penetrate the sediment slowly and smoothly. Recovered cores should also be kept well away from any generators of relatively strong magnetic fields (for example electric motors). With regards to mineral magnetic measurements (i.e. those pertaining to magnetic mineral concentration and type), it is critical that the sediments are kept free of contamination (rusty metal corers are to be avoided). With the Russian peat corer (Jowsey, 1966), cores 1 m long can be typically collected. The internal diameter of the u-shaped chamber (made of a clean metal, preferably aluminium or stainless steel) generally ranges between 5 and 10 cm. After the core collection, the material is transferred to u-shaped plastic liners and sealed in plastic film. With piston-corers (e.g., Livingstone corer and Mackereth corer) continuous, generally up to 10m long sequences, can be retrieved in airtight plastic tubes. These must be sealed and preferably kept in cold storage until split into two halves and sub-sampled. Long-time storage and subsequent oxidation can significantly affect the mineral magnetic properties of sediment deposited under both anaerobic and aerobic conditions. Ferrimagnetic iron oxides and iron sulphides are known to alter to less (non-) magnetic minerals during storage (Hilton & Lishman, 1985; Snowball & Thompson, 1988; Oldfield et al. 1992). To avoid significant storage alteration, sediments have been embedded in epoxy resin (e.g., Snowball et al. 1999) or stored in an inert gas atmosphere (Hawthorne & McKenzie 1993).

Sub-sampling of sediment cores for routine mineral magnetic analyses

'Routine' or 'standard' mineral magnetic analyses include measurements of magnetic susceptibility and a range of remanence measurements, i.e. a sample is magnetised and the remanent magnetisation is measured after the exposure to a magnetic field. The main advantages of these routine analyses over many other analytical techniques are that they are fast, cheap (once one has the instrument) and non-destructive. After the magnetic measurements are complete the samples can be used for a range of additional analyses (e.g., geochemistry, palynology, grain-size distribution, mineralogy).

To avoid spurious results due to magnetic mineral alterations, it is strongly recommended to perform the magnetic analyses on fresh sediments that have been stored in a cold room and/or an inert atmosphere (which can include sealed core tubes). Properly sealed cores can be stored in a cold room for many years, even decades. Alternatively the samples could be freeze-dried, a procedure which seems to reduce the alteration of magnetic properties (of course this is unsuitable for NRM measurements). A standard practice is to use hollow plastic cubes that are gently pushed into the cleaned sediment surface. The entire sediment section can be analysed. A useful size is 2 x 2 x 2 cm, an easily obtainable size that can be accepted by the majority of instruments used for standard mineral magnetic measurements. However, sediment slices at any desired thickness can be cut out from the fresh sediment with a non-magnetic knife, depending on the aim of the investigation and the desired resolution, and transferred to a plastic container.

The disadvantage of analysing many fresh lake-sediments is that water dilutes the concentration of magnetic minerals (and also contributes a negative initial magnetic susceptibility). The concentration per unit volume can be very low in the case of organic

rich sediments or if weakly magnetic bedrock types dominate in the lake catchment. It may therefore be necessary to concentrate the magnetic minerals by removing the water through oven or freeze-drying. Unconsolidated sediment with a high water content (generally the uppermost sediment) may not be suitable to measure in a "moist" state as some analyses (see below) require that the sediment grains remain fixed relative to the sample holder and magnetometer during measurement. However, the problem of low magnetic concentration (and hence low magnetic remanent intensity) can be minimised by using very sensitive magnetic magnetometers that are available on the market. After the analyses, the samples are freeze-dried or oven-dried at 40–50 °C and weighed to allow calculation of mass specific magnetic parameters. If the samples are magnetically very weak the containers have to be weighed individually before the sub-sampling procedure, otherwise an average weight of 10 or 20 containers can subtracted from each sub-sample.

Collection and preparation of catchment samples

To determine possible sources of lake-sediment it is recommended (if not obligatory) to analyse the mineral magnetic properties of a range of representative samples collected from the lake catchment. Catchment samples from outcrops, soil profiles, from bedload or suspended river material etc. can be collected and stored in plastic containers. Bulk samples are transferred to the standard size of plastic containers used for the lake-sediment magnetic analyses. It is well known that the chemical and mineralogical properties of sediments vary according to their particle-size distribution, and thus it is useful to perform magnetic analyses on a particle-size basis. This procedure requires that the catchment samples also be split into a range of particle-size classes. Wet sieving can be used to separate the sand fractions and the finer particle size classes can be achieved through gravity settling based on Stoke's Law. Sub-samples can be obtained by various methods like decantation (e.g., Walden et al. 1987, 1992), pipette (e.g., Yu & Oldfield 1993) or controlled centrifuging (Peters 1995). To avoid alteration of the magnetic properties, it is recommended to perform the analyses of the sub-samples before drying.

It must be stressed that comparisons to the lake-sediment record are not straightforward. The separation procedure of the smaller particle size classes is not perfect, as shown by Walden & Slattery (1993). In addition, smaller magnetic grains will settle at the same rate as relatively larger quartz grains because the iron oxides have a higher density. Attempts to digest the organic fraction through treatment with hydrogen peroxide (H_2O_2) can lead to both the destruction and production of magnetic phases (Snowball pers. comm.).

Sample preparation for advanced magnetic analyses

The standard size of cube that is utilised for 'routine' magnetic analyses can be unsuitable for more advanced magnetic analyses, which often require smaller samples. Reduction of sample size can lead to representation problems and it is critical that samples are homogenised before they are sub-sampled. However, care must be taken not to mechanically grind samples to the point that the magnetic-grain size distribution changes, which would alter the magnetic properties of the sub-sample compared to the parent sample.

Certain advanced techniques offer the advantage of higher temporal resolution. Magnetic hysteresis measurements require that the sample remain fixed with respect to the sample holder. Chips of oven-dried (<50 °C) inorganic sediments may be suitable if they turn solid. Otherwise stabilisation in epoxy resin of more organic sediment is a suitable method if the samples are cured at a low temperature. A temporal resolution of 4–5 years per sample was obtained in a magnetic hysteresis study of a 9,000 year varved lake sediment in Sweden (Snowball et al. 1999). Seasonal resolution has been obtained for the uppermost 20 years of a Finnish varved lake-sediment (Saarinen & Snowball, pers. comm.). The samples measured in these two studies were obtained by embedding the sediments with a low viscosity epoxy resin (Lameroux, 1994) prior to cutting and polishing samples of the required size (c. 2 mm).

Temperature dependent magnetic susceptibility measurements (see below) may also require a dry sample: water will either freeze or boil and these effects should be avoided by using dried samples. High (>room temperature) temperature magnetic measurements (of magnetic susceptibility or magnetisation) of lake-sediments and soils can be complicated by the oxidation and eventual combustion of organic matter, which produces uncontrollable flash temperatures. Such problems can be avoided by concentrating (or separating) the magnetic minerals from the "non-magnetic" matrix. Magnetic separation techniques are comprehensively reviewed by Hounslow & Maher (1999) and will not be discussed further here. Magnetic separates can be subject to electron microscopy (SEM or TEM) which can provide independent information about magnetic grain-size, mineralogy and origin.

Sequence of measurements

As the magnetic properties of the sub-samples can be irreversibly altered by some of the magnetic analyses discussed above, it is important to perform the analyses in a certain sequence, as illustrated in Figure 5.

Before the sediment is destroyed by the sub-sampling procedure, whole-core susceptibility scanning of cores is recommended (see below). The scanning will give a quick overview of the magnetic stratigraphy. If the total sediment succession consists of a number of shorter, overlapping core-segments, this procedure will provide an objective and quantifiable method of core correlation. This procedure is especially useful as many Holocene lake-sediment sequences consist of brownish/blackish gyttja that lack visual stratigraphic marker horizons. It is also a rapid way to perform intra-basin correlation if a suite of spatially separated cores has been collected at various places in a lake (e.g., Sandgren et al. 1990).

Routine analyses of all sub-samples should at least include the following sequence. Magnetic susceptibility measurements should be carried out first: at least low frequency magnetic susceptibility (χ_{lf}) and if possible the high frequency magnetic susceptibility (χ_{hf}). Dual frequency magnetic susceptibility measurements can be used to determine the frequency dependency of magnetic susceptibility. Remanence measurements should be carried out after magnetic susceptibility. ARM measurements must be conducted before the sample is exposed to strong magnetic fields. Determination of saturation isothermal remanent magnetisation (SIRM) requires the progressive application of magnetic fields of increasing intensity (forward-fields). Alternatively, or as a complement, the samples can first be saturated (if the saturation field is known) and subject to a set of reversed magnetic-fields (back-fields) of increasing intensity.

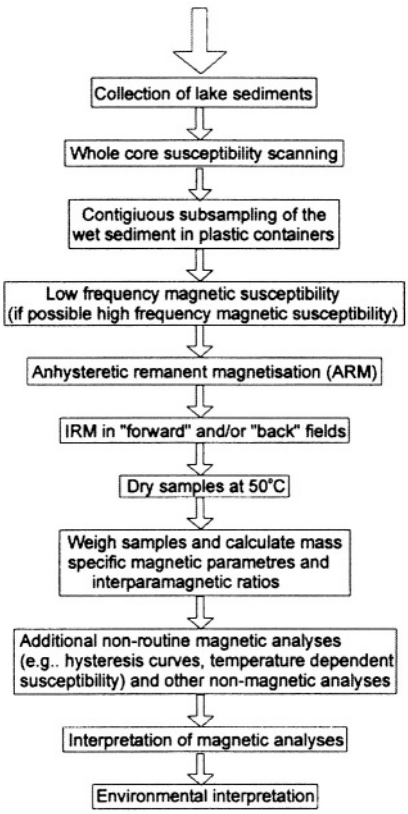


Figure 5. Suggested sequence of routine magnetic analyses of lake-sediment.

Magnetic susceptibility

Low field or initial magnetic susceptibility is a measure of how easily a material can be magnetised (Thompson & Oldfield 1986). It is perhaps the most common magnetic parameter and is very simple to measure. Samples are measured at room temperature *in* a low magnetic field (generally 0.1 milliTesla-mT). Mass specific susceptibility (χ) is obtained by dividing the volume susceptibility (κ) by the dry sample weight. The most common method is to measure initial susceptibility using a balanced alternating current (AC) bridge circuit. There are various systems available on the market that range from less sensitive (at least with respect to lake sediments that often have a high organic/water content) to very sensitive. With the more sensitive instruments, it is possible to determine the diamagnetic contribution to the susceptibility from the plastic holder and plastic container. Especially in the case of magnetically weak sediments, it is important to correct for this. As magnetic susceptibility is an in-field measurement, it is a measure of the net contribution of all the materials in the samples. If ferrimagnetic minerals are present in very low concentrations the concentration of diamagnetic, paramagnetic and also canted antiferromagnets can contribute to the result.

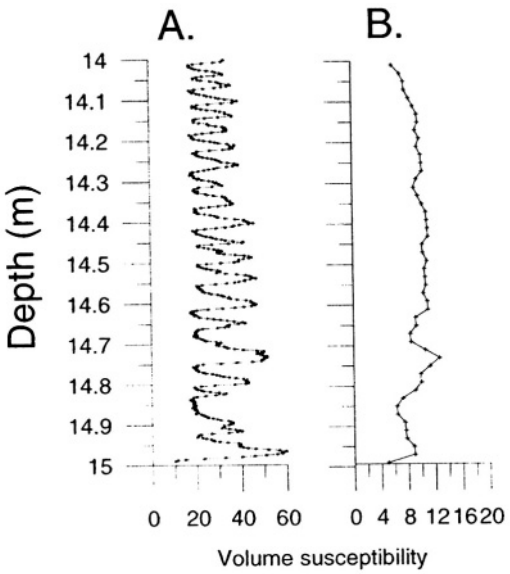


Figure 6. Initial magnetic susceptibility measurements of a varved sequence from Estonia, using (A) a Bartington Instruments MS2E1 surface scanning sensor attached to a TAMISCAN automatic conveyor system and (B) a Bartington Instruments whole core loop sensor, MS2C.

The generally very small effects of grain interactions can lead to a measured value of magnetic susceptibility that is lower than the true or intrinsic susceptibility. However, this effect is normally ignored in mineral magnetic studies where the magnetic grains are normally assumed to be dispersed and randomly orientated within the bulk sediment matrix.

Whole core magnetic susceptibility scanning

For measurements of whole core magnetic susceptibility, a ring or loop sensor can be used (preferably in conjunction with an automated sample logger). An advantage of this method is that core tubes do not have to be opened and cores can be logged and stored for many years before further sub-sampling. However, for most lake-sediments with a high organic and water content, the sensitivity level of the loop sensors is too low and the stratigraphic resolution is about 5 cm. Alternatively, the surfaces of opened cores can be scanned using recently developed surface sensors. These sensors have a stratigraphic resolution of c. 4 mm and measurements can be repeated with a high-degree of accuracy. Figure 6 shows a comparison between magnetic susceptibility measurements of varved clay from Estonia that was undertaken with a loop sensor and a surface scanning sensor (shown in plate 1). As seen from Figure 6 the surface scanning sensor picks out the individual silty summer varves (high magnetic mineral concentration) and the more fine grained winter varves (low magnetic concentration) whereas the loop sensor only gives a more general trend.

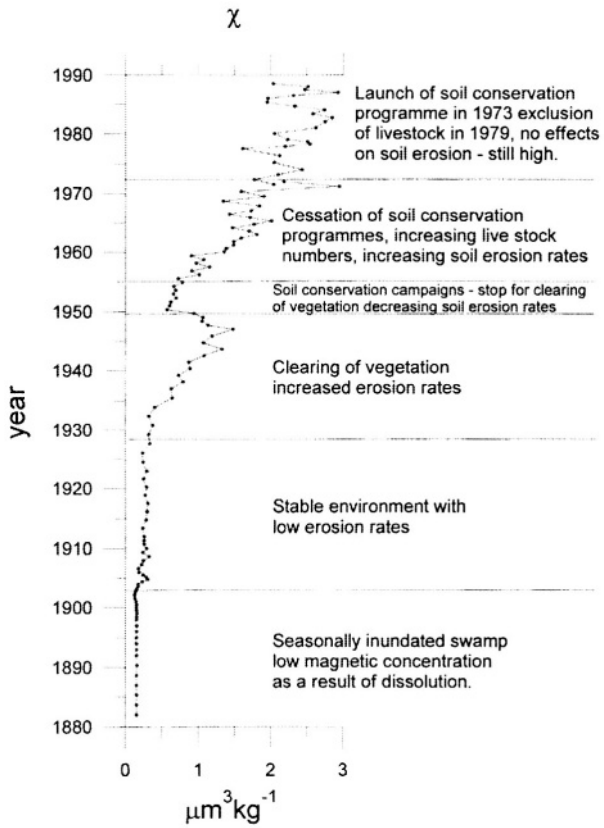


Figure 7. Initial magnetic susceptibility from Lake Haubi in central Tanzania reflecting periods of gradually in increasing erosion throughout the 20th century (from Eriksson & Sandgren 1999).

Low field initial magnetic susceptibility

Measurement of magnetic susceptibility at room temperature is relatively rapid, and with a suitable susceptibility meter a hundred samples can easily be processed in an hour. Figure 7 is an example of the downcore variations of initial magnetic susceptibility in a core from Lake Haubi in Tanzania in Africa reflecting soil erosion during the 20th century (Eriksson and Sandgren 1999). The clearing of vegetation e.g., that started in 1928 resulted in increased erosion bringing more minerogenic particles (and magnetic minerals) into the lake, which is reflected by increased values of magnetic susceptibility.

Frequency dependent magnetic susceptibility

With certain magnetic susceptibility meters more than one frequency field (of the same low magnetic intensity) can be applied. Use of (at least) two frequencies enables the

frequency dependency of susceptibility to be determined. It is possible to calculate the frequency dependent magnetic susceptibility in either absolute values or as a percentage of the low frequency magnetic susceptibility. Measurements at the two frequencies are generally used to detect the presence of ultrafine ($<0.03\ \mu m$) superparamagnetic grains. It must be considered that the absolute frequency dependency detected must also lie within the sensitivity of the equipment used. This problem can, to some extent, be overcome by analysing dried samples, which enables more sediment per unit volume to be packed into sample holders. The measurements can be repeated several times to improve the statistical reliability if the samples are very weak.

Anisotropy of magnetic susceptibility

The anisotropy of magnetic susceptibility (AMS) is measured to determine the fabric properties of the sample. It yields information on the degree of orientation of magnetic grains in the sample and/or the surrounding matrix. Unconsolidated sediments must be undisturbed for this type of measurement. Undisturbed samples have either to be impregnated in resin or measured in naturally moist conditions. Very sensitive instruments are required, as it is necessary to measure very small differences in susceptibility (similar to frequency dependency). Measurement of the anisotropy of magnetic susceptibility is not generally carried out in mineral magnetic studies of lake-sediments, although it is useful for determining the reliability of palaeomagnetic directions (which can be influenced by gravitational forces acting on elongated particles).

Temperature dependent susceptibility

Temperature dependent magnetic susceptibility is a measurement of low field susceptibility in a single sample across a range of temperatures, from liquid helium (–269 °C) or liquid nitrogen (–196°C) temperatures to c. normally 700°C (which will surpass the Curie temperature of haematite). Temperature dependent magnetic susceptibility is not normally carried out as a routine measurement, but it can be applied to representative samples from various stratigraphical horizons and give information about mineral type and grain-size. Only a relatively small sample is required, which has been dried at 105 °C. In some lake-sediments the paramagnetic minerals will dominate the result and suppress the signal from the ferromagnetic minerals. Extremely advanced equipment can measure magnetic susceptibility at varying temperatures, frequencies and applied fields. Software provided by the manufactures of equipment can distinguish between ferrimagnetic and diamagnetic/paramagnetic contributions to temperature dependent magnetic susceptibility.

Remanence measurements

In the magnetic remanence experiments the samples are exposed to a combination of much stronger specific magnetic fields than those that are applied in magnetic susceptibility analyses. After exposure to each successive magnetic field, the remanent magnetisation is measured. When the magnetisation is measured 'out of the field', only substances that are

capable of holding a magnetic remanence will contribute to the signal, i.e. paramagnetic and diamagnetic substances will not influence the result, as opposed to susceptibility measurements. The magnetisation procedure gradually alters the magnetic intensity of the sample.

Anhysteretic remanent magnetisation (ARM)

Measurements of ARM have over the last years become routine in mineral magnetic analyses. An ARM is induced by applying an AF of gradually decreasing amplitude in the presence of a constant DC bias field. As the AF is cycled, the hysteresis is progressively removed and the magnetisation of the material converges on the anhysteretic value for the prevailing DC bias field. ARM measurements can be interpreted in terms of magnetite grain size variation (e.g., King et al. 1982; Maher 1988). Some magnetometers specifically designed for geological purposes contain automatic systems for AF demagnetisation and ARM induction.

Isothermal remanent magnetisation (IRM)

Electromagnets or pulse magnetic chargers can be used to generate quite strong magnetic fields (compared to the DC bias fields used in ARM induction). The disadvantage of electromagnets is that the pole pieces generate stray fields even when the electric current is turned off, which reduces the efficiency of the analyses. Pulse magnetic chargers use a capacitor bank to produce a high voltage discharge through a coil, which generates a magnetic field for a fraction of a second along the axis of the coil. There are a number of commercial companies selling pulse magnetic chargers. For mineral magnetic measurements a maximum field of 1 T is a minimum requirement, although fields up to 7 T can be obtained without considerably more investment. A combination of two units, one for fields <0.1 T and one for higher fields is often the best solution.

The magnetic remanence induced in a sample in the way described above is known as the Isothermal Remanent Magnetisation (IRM). A particular field that has been used can be denoted $IRM_{20\,mT}$, $IRM_{400\,mT}$, $IRM_{1\,T}$ etc. for specific forward fields and $IRM_{-20\,mT}$, $IRM_{-400\,mT}$ etc. to denote that negative fields have been used. The $IRM_{1\,T}$ is generally called SIRM (Saturation Isothermal Remanent Magnetisation) which refer to that the sample has been magnetised in a strong magnetic field of 1 T enough to saturate magnetite. In most articles and texts the acronym (S)IRM refers to measurements carried out at room temperature measurements.

When the sample becomes magnetised, a magnetisation will remain generally parallel (or very close to) to the induced magnetic field. A magnetometer is required to measure the strength of the magnetisation. There are a number of different types available on the market. Superconducting quantum interference devices (SQUIDs) are the most sensitive and stable detectors, but currently require liquid helium or liquid nitrogen to cool the detectors to a superconducting temperature. Spinner magnetometers that use Fluxgate detectors or coils to detect magnetisations are less sensitive, but they are normally quite suitable for routine analyses.

Gyro & rotational remanent magnetisations (GRM/RRM)

Stable-single-domain grains of magnetite and greigite have the ability to acquire a gyro remanent magnetisation (see Stephenson 1980a, 1980b; Snowball 1997a). A GRM can be acquired by a static sample when it is subject to AF demagnetisation. The GRM is acquired in a plane perpendicular to the applied AF, and rotation of the sample around an axis perpendicular to the applied AF causes the GRM to be acquired along the rotation axis (which is denoted as an RRM). Potter & Stephenson (1986) and Snowball (1997b) show how measurements of GRM, RRM and ARM can be used as a magneto-granulometric tool. Although these methods have not been extensively used in mineral magnetic studies, the potential exists to use GRM and RRM to selectively detect the presence, and measure the concentration, of stable-single domain bacterial magnetosomes (magnetite and greigite) in samples which have relatively high concentrations of coarser grained detrital magnetic minerals (which do not acquire GRM).

Hysteresis curves

The construction of complete hysteresis curves (Fig. 3) through a series of magnetic fields requires access to high-precision instruments. The more advanced is the alternating gradient magnetometer, which measures smaller samples at a faster rate than most vibrating sample magnetometers or magnetic balances. Attachments for temperature dependent measurements are also available. Based on a magnetic hysteresis curve, many more parameters are available than with just susceptibility and remanence measurements alone. It is, for example, possible to calculate the non-ferromagnetic contribution to magnetic susceptibility, which may have its own specific environmental interpretation (see Fig. 8).

Summary

Since the 1950's, when palaeomagnetism came to a fore because of its contribution to studies of plate tectonics, the employment of magnetic measurements in Earth sciences has expanded rapidly and studies of lake-sediments have benefited from (and contributed to) this development. Applications of mineral (rock) magnetism to studies of paleolimnology are diverse and range from investigations of temporal and spatial variations in the direction and intensity of Earth's magnetic field to the study of single magnetotactic bacteria. The rapidity of the measurement techniques, the minimal need for sample preparation and the generally non-destructive nature of the methods are major advantages compared to other more time-consuming techniques that require considerable sample preparation.

Modern paleolimnological studies are frequently multidisciplinary, and mineral (rock) magnetism can provide a first glimpse of variations in sediment properties. However, although the method can be used for simple stratigraphic core correlation, there is a trend (as displayed by many other proxy-climate/environmental methods) towards the quantification and calibration of mineral magnetic parameters in terms of climate parameters and other indices of environmental climate change (e.g., Maher & Thompson 1995). The relatively recent observation that biogeochemical processes can cause major post-depositional changes in the magnetic properties of lake-sediments has opened up new avenues of research.

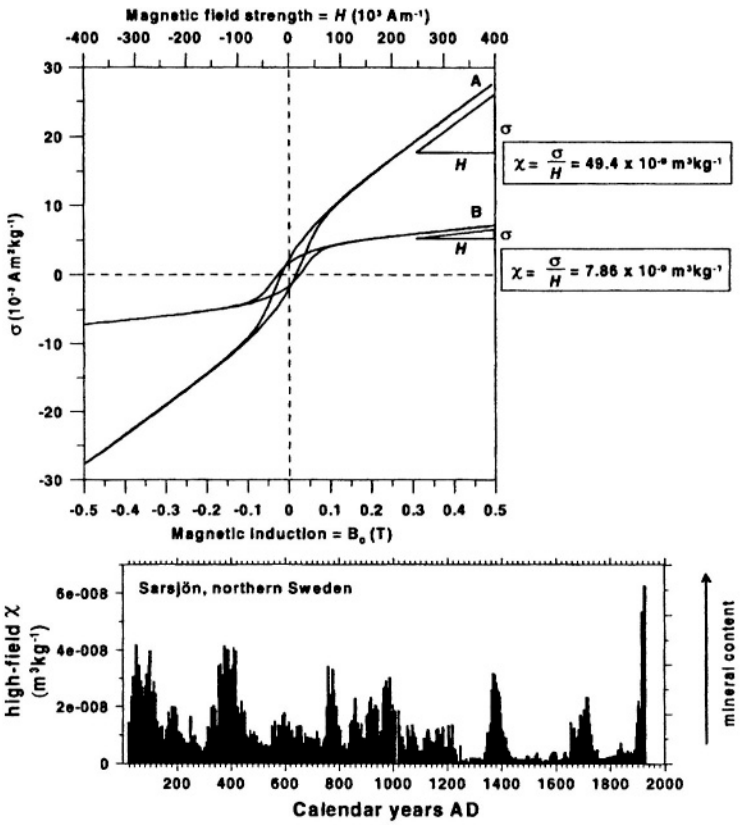


Figure 8. An example of the calculation of high-field magnetic susceptibility from two magnetic hysteresis loops (a). Both loops have a wide open middle section, characteristic of single-domain-magnetite (in this case bacterial magnetite), and high-field magnetic susceptibilities dominated by paramagnetic minerals. Sample A has a much higher concentration of detrital paramagnetic minerals than sample *B*. Such measurements were used to construct a high resolution record of mineral matter content of a varved lake-sediment in northern Sweden, based on the high-field paramagnetic susceptibility. The most recent 2,000 years of this high-field magnetic susceptibility record is shown in (b). Data adapted from Snowball et al. (1999).

The basic concepts of mineral magnetic techniques and magnetic measurements were first presented by Thompson & Oldfield (1986). This benchmark text book can still be recommended as an introduction to the subject. The second part of this book contains the application of mineral magnetism not only to lake-sediments but also to a range of environmental systems. Two other recently published books can be recommended as further reading. The first, "Environmental magnetism — a practical guide" (Walden et al. 1999), is an excellent introduction to undergraduate students, postgraduate students and others who want to get to grips with the technical aspects of magnetic analyses. The second book, Maher & Thompson (1999) "Quaternary Climates, Environments and Magnetism," presents reviews of the major developments in environmental magnetism (with a focus

on the Quaternary era) since 1986. This book contains an excellent chapter by Dearing (1999) which is dedicated to "Holocene environmental change from magnetic proxies in lake sediments." Finally, it must be stated that despite all of the possible palaeoclimatic and environmental applications of mineral magnetism, one must not forget to devote some time to understanding the fundamental principles of magnetism and its relation to mineral/rock magnetic studies. For this reason the book "Rock Magnetism: Fundamentals and Frontiers" (Dunlop & Özdemir, 1997) can be recommended.

References

Anderson, N. J. & B. Rippey, 1988. Diagenesis of magnetic minerals in the recent sediments of a eutrophic lake. Limnol. Oceanogr. 33: 1476–1492.

Blakemore, R. P., 1975. Magnetotactic bacteria. Science 190: 277–379.

Dearing, J. A., 1991. Erosion and land use. In Berglund, B. E. (ed.) The cultural landscape during 6000 years in Southern Sweden. Ecol. Bull. 41: 283–292.

Dearing, J. A., 1999. Holocene environmental change from magnetic proxies in lake sediments. In Maher, B. A. & R. Thompson (eds.) Quaternary Climates, Environments and Magnetism. Cambridge University Press: 231–278.

Dearing, J. A. & R. J. Flower, 1982. The magnetic susceptibility of sedimenting material trapped in Lough Neagh, Northern Ireland, and its erosional significance. Limnol. Oceanogr. 27: 969–975.

Dunlop, D. J. & Ö. Özdemir, 1997. Rock Magnetism: Fundamentals and Frontiers. Cambridge University Press, UK, 573 pp.

Eriksson, M. G. & P. Sandgren, 1999. Mineral magnetic analyses of sediment cores recording recent soil erosion history in central Tanzania. Palaeogr. Palaeoclim. Palaeoecol. 152. 365–383.

Granar, L., 1958. Magnetic measurements on Swedish varved sediments. Ark. f. Geofys. 3: 1–40.

Hawthorne, T. B. & J. A. McKenzie, 1993. Biogenic magnetite: authigenesis and diagenesis with changing redox conditions in Lake Greifen, Switzerland. In Aássaoui, D. M., N. F. Hurley & B. H. Lidz (eds.) Applications of Paleomagnetism to Sedimentary Geology. Society of Sedimentary Geology, special publication no. 49: 3–15.

Hilton, J. & J. P. Lishman, 1985. The effects of redox changes on the magnetic susceptibility of sediments from a seasonally anoxic lake. Limnol. Oceanogr. 30: 907–909.

Hounslow, M. & B. Maher, 1999. Laboratory procedures for use in source identification, classification and modelling of natural environmental materials. In Walden, J., F. Oldfield & J. Smith (eds.) Environmental Magnetism — a practical guide. Quaternary Research Association. Technical Guide 6: 139–184.

Ising, G., 1943. On the magnetic properties of varved clay. Ark. Mat. Astron. Fys. 29(5): 1–37.

Jowsey, P. C., 1966. An improved peat sampler. New Phytol. 65: 242–245.

King, J., S. K. Banarjee, J. Marvin & Ö. Özdemir, 1982. A comparison of different magnetic methods for determining the relative grain size of magnetite in natural materials: some results from lake sediments. Earth Planet. Sci. Lett. 59: 404–419.

Maher, B. A., 1988. Magnetic properties of some synthetic sub-micron magnetites. Geophysical Journal of the Royal Astronomical Society 94: 83–96.

Maher, B. A. & R. Thompson, 1995. Paleorainfall reconstructions from pedogenic magnetic susceptibility variations in the Chines loess and paleosols. Quat. Res. 44. 383–391.

Maher, B. A. & R. Thompson (eds.), 1999. Quaternary Climates, Environments and Magnetism. Cambridge University Press, Cambridge, 390 pp.

Mackereth, F. J. H., 1971. On the variation in direction of the horizontal component of remnant magnetisation in lake sediments. Earth Planet. Sci. Lett. 12: 332–338.

McNish, A. G. & E. A. Johnson, 1938. Magnetization of unmetamorphosed varves and marine sediments. Terr. Mag. 43: 401–107.

Oldfield, F., 1977. Lakes and their drainage basins as units of sediment-based ecological study. Prog. Phys. Geog. 3: 460–504.

Oldfield, F., I. Darnley, G. Yates, D. E. France & J. Hilton, 1992. Storage diagenesis versus sulphide authigenesis: possible implications in environmental magnetism. J. Paleolimn. 7: 179–189.

Peters, C., 1995. Unravelling Magnetic Mixtures in Sediments. Soils and Rocks. Unpublished Ph.D. thesis. University of Edingburh.

Potter, D. K. & A. Stephenson. 1986. The detection of line particles of magnetite using anhysteretic and rotational remanent magnetisations. Geophys. J. R. Astron. Soc. 87: 569–582.

Roberts, A. P., R. L. Reynolds, K. L. Verosub & D. P. Adam, 1996. Environmental magnetic implications of greigite (Fe_3S_4) formation in a 3 My lake sediment record from Butte Valley, Northern California, US. Geophys. Res. Lett. 23: 2859–2862.

Sandgren, P., J. Risberg & R. Thompson, 1990. Magnetic susceptibility in sediment records of Lake Ådran. Eastern Sweden, correlation among cores and interpretation. J Paleolimn. 3: 129–141.

Snowball, I. F., 1991. Magnetic hysteresis properties of greigite (Fe_3S_4) and a new occurrence in Holocene sediments from Swedish Lappland. Phys. Earth Planet. Int. 68: 32–40.

Snowball, I. F, 1993. Geochemical control of magnetite dissolution in subarctic lake sediments and the implications for environmental magnetism. J. Quat. Sci. 8: 339–346.

Snowball, I. F. 1997a. Gyroremanent magnetization (GRM) and the magnetic properties of greigite bearing clays in southern Sweden. Geophys. J. Int. 129: 624–636

Snowball, I. F., 1997b. The detection of single-domain greigite (Fe_3S_4) using rotational remanent magnetization (RRM) and the effective gyro held (Bg): mineral magnetic and palaeomagnetic applications. Geophys. J. Int. 130: 704–716.

Snowball I. F & R. Thompson, 1988. The occurrence of greigite in sediments from Loch Lomond. J. Quat. Sci. 3: 121–125.

Snowball, I. F., P. Sandgren & G. Petterson, 1999. The mineral magnetic properties of an annually laminated Holocene lake sediment sequence in northern Sweden. The Holocene 9. 353–362.

Stephenson, A., 1980a A gyroremanent magnetisation in anisotropic magnetic material. Nature 284: 49–51.

Stephenson, A., 1980b. Gyromagnetism and the remanence acquired by a rotating rock in an alternating field. Nature 284: 48–49.

Tarling, D. H., 1971. Principles and Applications of Palaeomagnetism. Chapman and Hall, London, 95–113.

Thompson, R., 1973. Palaeolimnology and palaeomagnetism. Nature 242: 182–184.

Thompson, R. & F. Oldfield, 1986. Environmental Magnetism. George Allen and Unwin, London, 227 pp.

Thompson, R., R. W. Batterbee, P. E. O'Sullivan & F. Oldfield, 1975. Magnetic susceptibility of lake sediments. Limnol. Oceanogr. 20: 687–698.

Walden, J., F. Oldfield &. J. Smith (eds.), 1999. Environmental Magnetism: a Practical. Guide. Quaternary Research Association, Technical Guide No. 6. Quaternary Research Association, London.

Walden, J., J. P. Smith & R. V. Dackombe, 1987. The use of mineral magnetic analyses in the study of glacial diamicts: a pilot study. J. Quat. Sci. 2: 73–80.

Walden, J., J. P. Smith & R. V. Dackombe, 1992. Mineral magnetic analyses as a means of lithostratigraphic correlation and provenance indication of glacial diamicts: intra- and inter-unit variation. J. Quat. Sci. 7: 257–270.

Walden, J. & M. C. Slattery, 1993. Verification of a simple gravity technique for separation of particle size fractions suitable for mineral magnetic analysis. Earth Surf. Proc. Landforms. 18: 829–833.

Yu, L. & F. Oldfield, 1993. Quantitative sediment source ascription using magnetic measurements in a reservoir catchment system near Nijar, S.E. Spain. Earth surf. Proc. Landforms 18: 441–454.

9. SEDIMENT ORGANIC MATTER

PHILIP A. MEYERS (pameyers@umich.edu)
Department of Geological Sciences
The University of Michigan
Ann Arbor, MI 48109-1063
USA

JANE L. TERANES (jteranes@ucsd.edu)
Geosciences Research Division
Scripps Institution of Oceanography
University of California San Diego
La Jolla, CA 92093-0244
USA

Keywords: $\delta^{13}C_{org}$ values, $\delta^{15}N$ values, C_{org}/N_{total} ratios, compound-specific isotope ratios, lignin phenols, biomarker hydrocarbons, Rock-Eval pyrolysis, paleolimnology.

Introduction

The organic matter content of lake sediments provides a variety of indicators, or proxies, that can be used to reconstruct paleoenvironments of lakes and their watersheds and to infer histories of regional climate changes. Organic matter constitutes a minor but important fraction of lake sediments. It originates from the complex mixture of lipids, carbohydrates, proteins, and other organic matter components produced by organisms that have lived in and around the lake (e.g., Meyers, 1997; Rullkötter, 2000). As an accumulation of "geochemical fossils", the organic matter content of lake sediments provides information that is important to interpretations of both natural and human-induced changes in local and regional ecosystems.

Some reconstructions of regional and continental paleoclimates that are based on organic matter contents of sediments of lakes from different parts of the world are summarized by Meyers & Ishiwatari (1993), Meyers (1997), Dean (1999), and Meyers & Lallier-Verges (1999). Determinations of the amounts and the origins of the organic matter in sedimentary records are essential components of paleolimnologic investigations. The purpose of this chapter is to describe and critique some of the elemental, isotopic, and molecular methods that are available to make these determinations.



W. M. Last & J. P. Smol (eds.), 2001. *Tracking Environmental Change Using Lake Sediments. Volume 2: Physical and Geochemical Methods.* Kluwer Academic Publishers, Dordrecht, The Netherlands.

Paleolimnological proxies

The primary source of organic matter to lake sediments is from plants in and around the lake. Plants can be divided into two geochemically distinctive groups on the basis of their biochemical compositions: (1) non-vascular plants that contain little or no carbon-rich cellulose and lignin, such as phytoplankton, and (2) vascular plants that contain large proportions of these fibrous tissues, such as grasses, shrubs, and trees on land and macrophytes in lakes. The organic matter derived from these two broad groupings of plants retains these source distinctions. However, accumulations of sedimentary organic matter in lake sediments reflect not only the types and amounts of original materials but also the extent of alteration and degradation of the starting material. Lake systems are diverse, and the sources and alterations of organic matter are geographically and temporally variable. Nonetheless, useful generalizations about the geochemical characteristics of organic matter having different origins and histories can be made. We describe some of these parameters in this chapter.

General analytical considerations

Most of the analytical methods that are used to measure organic matter paleoenvironmental proxies are relatively routine, but the procedures are typically not completely uniform among their practitioners. Instead, different groups have developed their individual protocols that are specialized to the instruments available to them, the number of analyses demanded from these instruments and their operators, and the kinds of paleolimnologic questions that are being asked. Because the procedures that are employed to obtain the organic matter parameters are rarely identical, use of sediment standards that have accepted compositions is important to compare analytical results from different laboratories.

Samples of lake sediment are commonly dried before analyses of their organic matter contents. Freeze-drying is the generally preferred means for preparing sediment samples for analysis because either air-drying or oven-drying may result in loss of volatile organic matter components, which can bias elemental and isotopic compositions. Furthermore, molecular compositions of sediment organic matter can be altered by oxidation of sensitive components during either air-drying or oven-drying. However, non-recent (> 100 years) sediment is less likely to contain the kinds of components that are sensitive to drying in air or in an oven, making this procedure less risky for studies involving such sediments.

Organic carbon concentration

Environmental significance

The concentration of total organic carbon (TOC) is a fundamental parameter for describing the abundance of organic matter in sediments. Weight loss on ignition (LOI) is also sometimes used to estimate how much organic matter is present in sediments (Dean, 1974). Typical organic matter contains approximately 50% carbon, so LOI values are equivalent to about twice the TOC values. Because variable amounts of volatile non-carbon sediment components can sometimes increase LOI values and lead to inflated organic matter

concentrations, measurement of the TOC concentrations is generally preferred over LOI determinations to approximate how much organic matter is present.

Analytical methods

The amount of organic carbon in sediment samples is usually determined by some version of two fundamentally different procedures — either as the difference between the total carbon and the carbonate carbon concentrations or as the concentration of carbon remaining after carbonate carbon has been removed.

In the by-difference procedure, the total carbon concentration is measured using an elemental analyzer that combusts a subsample of the dried sediment at a high temperature (850 °C to 1100 °C) in an oxidizing atmosphere and then separates the gaseous products by chromatography (e.g., Verardo et al., 1990). The carbonate carbon concentration is measured on a second subsample, either using a coulometric inorganic carbon analyzer (e.g., Huffman, 1977; Engleman et al., 1985) or as the volume of CO_2 released by acidification of the sediment (e.g., Müller & Gastner, 1971).

In the direct-determination procedure, carbonate carbon is first removed from the sediment subsample by treatment with dilute (3N) hydrochloric or phosphoric acid, washing and drying the carbonate-free residue, and then measuring the carbon content of the residue with an elemental analyzer. An alternative direct-determination procedure employs acid vapors to remove inorganic carbon (Yamamuro & Kayanne, 1995). A related procedure employs direct reaction with HCl that is added to the sediment sample while it is in the tin boat that is used in the elemental analyzer. After reaction for 24 hours, the acid is evaporated prior to carbon analysis. Yet another alternative direct-determination method involves measuring the amount of CO_2 released from carbonate-free sediment subsamples during off-line oxidation of the residual carbon in preparation for carbon isotope analysis. Off-line preparation lines for isotopic analyses can be manometrically calibrated to yield this measurement. Regardless of the procedure, TOC concentrations of lake sediments are usually expressed on a whole-sediment basis.

Meyers & Silliman (1996) compared the by-difference and basic direct-determination TOC procedures using sediments from the North Atlantic Ocean. The direct-determination procedure is more reliable at TOC concentrations <0.1%, but agreement between the two procedures is good above this value. Because lake sediments generally contain much more than 0.1% TOC, results from the two approaches are probably not significantly different for most lake sediments. Very young sediments, however, are likely to contain low-molecular-weight organic matter components that might be lost during the washing step that follows carbonate carbon removal in the direct-determination method. Investigators should consider this possibility before selecting the procedure that will be used for their TOC determinations.

Interpretation

TOC concentration is a bulk value that represents the fraction of organic matter that escaped remineralization during sedimentation. TOC concentrations are influenced by both initial production of biomass and subsequent degree of degradation, so they integrate the different origins of organic matter, delivery routes, depositional processes, and amount of preservation. It is common for sediment TOC concentrations to vary substantially from place to place within a lake (Table I) because these multiple factors interact in sometimes complicated ways. However, it is also often possible to separate the effects of these factors. For example,

Table I. Relations of organic carbon concentrations, organic matter atomic C/N ratios, and $\delta^{13}C$ values (‰ PDB) in surface sediments with distance from shore in Lake Victoria, East Africa (Talbot & Laerdal, 2000), and with water depth in Pyramid Lake, Nevada (Tenzer et al., 1997).

Sediment Sample Location	TOC (%)	C/N (atomic)	$\delta^{13}C_{org}$ (‰)
Lake Victoria			
swampy margin	35.9	16.4	−20.6
100 m offshore	38.6	17.5	−20.5
200 m offshore	31.2	12.3	−20.5
300 m offshore	27.6	16.1	−20.6
400 m offshore	12.1	11.6	−19.6
Pyramid Lake			
20 m depth	0.6	6.7	−24.9
30 m depth	0.9	9.4	−24.9
40 m depth	1.3	7.4	−24.5
50 m depth	1.6	10.8	−26.4
60 m depth	2.2	9.8	−26.1
70 m depth	2.9	9.3	−27.9
90 m depth	3.5	9.1	−27.5
100 m depth	3.6	8.7	−27.8

Tenzer et al. (1997) were able to distinguish between in-lake and land sources of organic matter and to describe the impacts of hydraulic sorting on the organic matter contents of surficial sediment during sediment focusing in Pyramid Lake, Nevada. Contributions of land-derived material to sediment organic matter become minor beyond a few hundred meters from shore in this large, mesotrophic lake.

TOC concentrations are expressed in weight/weight ratios and are therefore influenced by other sediment components. TOC can be both diluted by addition of clastic sediment particles and concentrated by dissolution of carbonate minerals in sediment (e.g., Dean, 1999). TOC concentrations commonly increase as sediment grain size decreases (e.g., Thompson & Eglinton, 1978). A consequence is that concentrations can become larger in deeper parts of lake basins where fine-grained sediments slowly settle than in shallower parts where coarser sediments rapidly accumulate (Table I). For these reasons, mass accumulation rates (MARs) of organic carbon are more useful measures of delivery and preservation of organic matter than TOC percentages. MARs are expressed as mass of TOC per unit of lake bottom area per unit of time, typically $mg\ cm^{-2}\ y^{-1}$. Reliable sediment dating is obviously important to calculating meaningful MAR values.

Organic carbon MARs are especially useful to paleolimnology for identification of changes in delivery rates of organic matter to lake sediments (cf., Meyers & Lallier-Verges, 1999). Often the proportions of lake-derived and land-derived organic matter can be estimated by determinations described later in this chapter, allowing calculation of separate

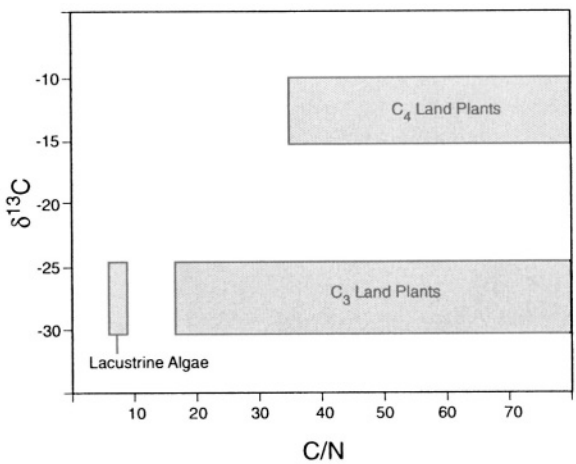


Figure 1. Representative elemental and carbon isotopic compositions of organic matter from lacustrine algae, C_3 land plants, and C_4 land plants that use CO_2 as their source of carbon during photosynthesis. Deviations from these generalized patterns occur and can provide paleolimnologic information. Atomic C/N ratios and organic $\delta^{13}C$ values for individual plant samples in the general groupings are given in Table I.

MARs for autochthonous and allochthonous organic carbon (e.g., Sifeddine et al., 1996). Increases and decreases in primary productivity that result from paleoenvironmental changes can also be inferred from organic carbon MAR records. However, post-burial degradation of organic matter can diminish the apparent accumulation rates of TOC in lake bottoms. In sediments with oxic pore-waters, post-burial diagenesis will continue to decrease the mass of TOC until burial below the oxic-anoxic interface. For example, Hodell & Schelske (1998) compared the concentration of organic carbon in two sediment cores that were collected six years apart from the same location in Lake Ontario. They concluded that microbial processing created a 20% decrease in the mass of organic matter that had remained buried in the lake bottom for the six years.

C/N *ratios of organic matter*

Environmental significance

The amounts of sedimentary organic matter that originate from aquatic as opposed to land sources can be distinguished by the characteristic C/N ratio compositions of algae and vascular plants (Fig. 1). Some examples of the C/N atomic values of plants that contribute organic matter to lake sediments and of the resulting C/N ratios in lake sediments are given in Table II. Fresh organic matter from phytoplankton has C/N values that are commonly between 4 and 10, whereas vascular land plants, which are cellulose-rich and protein-poor, create organic matter that usually has C/N ratios of 20 and greater.

Analytical methods

Carbon and nitrogen weight percentages of sediment samples are typically determined simultaneously with an elemental analyzer. The weight percentages are used to calculate

Table II. Representative atomic C/N ratios and organic $\delta^{13}C$ values (‰ PDB) of different types of primary organic matter sources to sediments of lakes and examples of the C/N and $\delta^{13}C$ signatures of bulk organic matter in modern lake sediments.

Organic Matter Source	Location	C/N (atomic)	$\delta^{13}C$ (‰)	Reference
C_3 Vascular Plants				
willow leaves	Walker Lake, Nevada	38	−26.7	Meyers (1990)
poplar leaves	Walker Lake, Nevada	62	−27.9	Meyers (1990)
cottonwood leaves	Grosse Ile, Michigan	31	−30.5	Meyers & Lallier-Verges (1999)
yellow poplar leaves	Ann Arbor, Michigan	33	−29.1	Meyers & Lallier-Verges (1999)
white oak leaves	Ann Arbor, Michigan	22	−29.0	Meyers & Lallier-Verges (1999)
red oak leaves	Ann Arbor, Michigan	29	−29.8	Meyers & Lallier-Verges (1999)
American beech leaves	Grosse Ile, Michigan	17	−28.3	Meyers & Lallier-Verges (1999)
European beech leaves	Ann Arbor, Michigan	17	−30.2	Meyers & Lallier-Verges (1999)
pinyon pine needles	Walker Lake, Nevada	42	−24.8	Meyers (1990)
white spruce needles	Ann Arbor, Michigan	42	−25.1	Meyers et al. (1995)
white spruce bark	Ann Arbor, Michigan	57	−23.5	Meyers et al. (1995)
white spruce wood	Ann Arbor, Michigan	163	−23.1	Meyers et al. (1995)
white pine needles	Ann Arbor, Michigan	42	−25.2	Meyers & Lallier-Verges (1999)
red pine needles	Ann Arbor, Michigan	39	−27.1	Meyers & Lallier-Verges (1999)
palm fronds	Lake Bosumtwi, Ghana	91	−25.5	Talbot & Johanessen (1992)
Sphagnum	Newfoundland Canada	9	−27.5	Macko et al. (1991)
C_4 Vascular Plants				
salt grass	Walker Lake, Nevada	160	−14.1	Meyers (1990)
tumbleweed	Walker Lake, Nevada	68	−12.5	Meyers (1990)
blood grass	Lake Bosumtwi, Ghana	42	−11.1	Talbot & Johanessen (1992)
wild millet	Lake Bosumtwi, Ghana	156	−10.8	Talbot & Johanessen (1992)
Soil Organic Matter				
Lake Baikal watershed	Siberia, Russia	20	−23.4	Prokopenko et al. (1993)
Willamette valley	Oregon, USA	13	−26.2	Prahl et al. (1994)
peat bog	Washington, USA	17	−28.7	Ertel and Hedges (1984)
Lake Algae				
mixed plankton	Lake Baikal, Russia	9	−30.9	Prokopenko et al. (1993)
mixed plankton	Walker Lake, Nevada	8	−28.8	Meyers (1990)
mixed plankton	Pyramid Lake, Nevada	6	−28.3	Meyers (1994)
mixed plankton	Lake Michigan	7	−26.8	Meyers (1994)
mixed plankton	Lake Biwa, Japan	7	−27.5	Nakai & Koyama (1987)
Lake Surface Sediments				
Lake Biwa	Honshu, Japan	6	−25.3	Meyers & Horie (1993)
Lake Ontario	North America	8	−26.2	Hodell & Schelske (1998)
Lake Michigan	North America	8	−26.3	Rea et al. (1980)
Walker Lake	Nevada, USA	8	−24.2	Meyers (1990)
Baldeggersee	Switzerland	8	−33.1	Teranes & Bernasconi (unpub.)
Lake Baikal	Russia, Siberia	11	−29.9	Qiu et al. (1993)
Lake Bosumtwi	Ghana, Africa	14	−26.4	Talbot & Johannessen (1992)

C/N mass ratios, which can be multiplied by 1.167 (the ratio of atomic weights of nitrogen and carbon) to yield C/N atomic ratios. Both weight and mass ratio values appear in published reports; readers need to make note of which type of C/N ratio is being employed if they compare results from different reports. Atomic C/N values are used in this contribution because they reflect biochemical stoichiometry.

C/N ratios sometimes give misleading indications of bulk organic matter origin. The most typical problem arises because most analysts measure the carbon and nitrogen contents that remain in sediment samples after removal of carbonate carbon and thereby obtain a residual nitrogen value that combines both organic nitrogen and inorganic nitrogen. In most sediments, inorganic nitrogen concentrations are small compared to those of organic nitrogen, and this analytical approach yields C/N ratios that faithfully represent organic matter origins. In sediments having low organic matter concentrations ($C_{org} < 0.3\%$), however, the proportion of inorganic nitrogen can sometimes be a large fraction of the residual nitrogen, and C/N ratios based on residual nitrogen could be artificially depressed. Because most lake sediments contain 1% or more TOC, C/N values are normally reliable indicators of organic matter sources in paleolimnologic studies.

Interpretation

Lakes for which the contribution of organic matter from vascular plants is small relative to water-column production, exemplified by Walker Lake (Nevada) and Lake Michigan, have lower C/N ratios in their sediments than lakes receiving important amounts of vascular plant debris, such as Mangrove Lake (Bermuda) and Lake Bosumtwi (Ghana) (Table II). Ratios of 13–14 for surface sediments of the latter two lakes suggest a subequal mixture of algal and vascular plant contributions, which is expected for most lakes. Decreases in the land-derived proportion of sediment organic matter with increasing distance from shore in Lake Victoria, East Africa, are evident in smaller C/N values (Table I).

Partial degradation of organic matter during early diagenesis can modify elemental compositions and hence C/N ratios of organic matter in sediments. C/N ratios of fresh wood samples, for example, are generally higher than those of wood that has been buried in sediments (Meyers et al., 1995). This change reflects selective degradation of carbon-rich sugars and lipids in the buried wood. In contrast, the C/N ratio of organic matter derived from algae can increase during sinking and early sedimentation as nitrogen-rich proteins are selectively degraded. This trend is sometimes observed in lakes having high productivity, such as eutrophic Aydat Lake in France, where a downcore increase in C/N values throughout the upper 40cm of sediment (Sarazin et al., 1992) indicates active microbial denitrification of organic matter.

Changes in the elemental composition of sedimentary organic matter are not commonly large enough, however, to erase the large C/N differences (Table II, Fig. 1) between the organic matter derived from land plants and algae. For example, vascular plant debris isolated from a coastal marine sediment having a bulk C/N of 15 retains the C/N values between 30 and 40 that are characteristic of cellulosic plants (Ertel & Hedges, 1985). Elevated C/N values consequently identify delivery of land-plant organic matter to lake sediments, as seen in Lake Victoria (Table I). Similarly, Kaushal & Binford (1999) document an increase in C/N ratios from 16 to 25 that corresponds with deforestation of the watershed of Lake Pleasant, Massachusetts. This environmental change occurred around 1780 and evidently enhanced delivery of both land-plant organic matter and sediment to the lake,

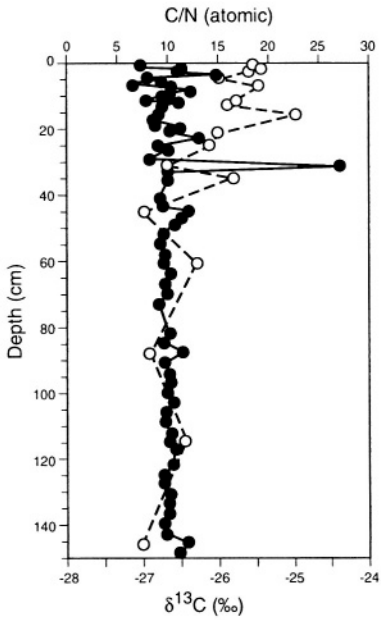


Figure 2. Evidence for changes in organic matter delivery from changes in organic C/total N values (solid symbols) and organic $\delta^{13}C$ values (open symbols) in sediment from Seneca Lake, New York (Meyers, unpublished). C/N values indicate dominance of lake-derived organic matter in sediments, except at core depths of 8 and 32 cm where elevated values record delivery of land-plant organic matter, presumably from periods of extreme precipitation. Less negative organic $\delta^{13}C$ values in upper 35 cm of sediment record reflect eutrophication that has occurred in this watershed since ~1825 as a consequence of agriculture and human population growth.

inasmuch as sedimentation rates also increased and diluted TOC concentrations. In a related example, episodes of magnified wash-in of land-derived organic matter to Seneca Lake, New York, are indicated by two spikes in the C/N values of its sediments (Fig. 2). These episodes evidently represent short periods of wet weather. Small variations in C/N values in the upper 20cm of the sediment column suggest environmental destabilization of this watershed since introduction of European agriculture in the early 1800's.

Organic carbon isotope ratios

Environmental significance

The carbon isotopic composition of organic matter in lake sediments is important to assessing organic matter sources, for reconstructing past productivity rates, and for identifying changes in the availability of nutrients in surface waters. Increases in the accumulation rates of organic matter and its $^{13}C/^{12}C$ ratio have been widely used as an indicator of enhanced aquatic productivity in lakes (e.g., Hollander & McKenzie, 1991; Hollander et al., 1992; Hodell & Schelske, 1998; Brenner et al., 1999). Phytoplankton (C_3 algae) preferentially utilize ^{12}C to produce organic matter that averages 20‰ lighter than the $^{13}C/^{12}C$ ratio of their dissolved inorganic carbon (DIC) source (cf., O'Leary, 1988; Wolfe et al., this volume).

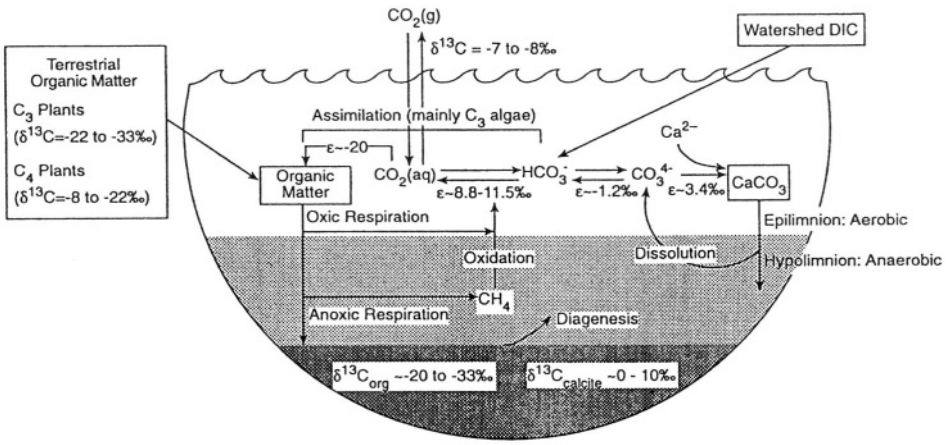


Figure 3. Idealized carbon isotope cycle in a small stratified lake. The isotopic composition of organic matter buried in sediments is determined by the proportions of different terrestrial and lacustrine organic matter, the carbon isotopic composition of dissolved inorganic carbon (DIC), and the rates of primary production and respiration within the water column. Isotope enrichment factors (ε), listed here as the difference between the product and the substrate, vary with the form of DIC that lake algae assimilate (e.g., $CO_{2(aq)}$ or HCO_3^-). Inorganic carbonate ($CaCO_3$) typically forms in isotopic equilibrium with the dissolved inorganic carbon pool and, as such, is indirectly affected by organic matter sources and primary production and respiration rates.

Sedimentation of algal organic matter consequently removes ^{12}C from surface-water DIC reservoirs (Fig. 3). As supplies of DIC become depleted, the $\delta^{13}C$ values of the remaining inorganic carbon increase and produce a subsequent increase in the $\delta^{13}C$ values of newly produced organic matter. Increased or decreased productivity therefore yields a respective increase or decrease in the $\delta^{13}C$ of organic matter that is produced in the lake and is available for sedimentation.

The rate of carbon uptake during algal productivity and the DIC isotopic composition are usually the principal determinants of sediment $\delta^{13}C$ values. However, changes in pH, temperature, nutrient limitation, and growth rate are also known to affect the $\delta^{13}C$ of organic matter produced by phytoplankton (Takahashi et al., 1990; Fogel & Cifuentes, 1993; Laws et al., 1995; Wolfe et al., this volume). One or more of these secondary factors can become important in specialized situations and thereby give additional paleoenvironmental significance to the carbon isotopic composition of organic matter.

Analytical methods

The traditional method to determine the $^{13}C/^{12}C$ ratio of sediment organic matter is by oxidation of carbonate-free samples in an "off-line" procedure that employs a vacuum transfer system to produce and isolate the CO_2 needed for isotopic analysis (cf., Boutton, 1991). Removal of carbonate carbon is accomplished by one of the methods discussed under "Organic carbon concentration" (this chapter). The CO_2 is produced by reaction of the residual organic carbon with an oxidant such as CuO in an evacuated and sealed Pyrex tube at 600°C; quartz tubes can be heated to 800°C to insure more complete oxidation.

The $^{13}C/^{12}C$ ratio of the CO_2 is measured with an isotope ratio mass spectrometer (IRMS). Although quite reproducible and reliable, this method is also time-consuming and tedious.

Development of Continuous Flow-Isotope Ratio Mass Spectrometers (CF-IRMS) has dramatically facilitated measurement of the $^{13}C/^{12}C$ ratio of sediment organic matter. CF-IRMS consists of an IRMS coupled on-line to a device that produces the CO_2 to be analyzed. In the case of sediment organic matter, the on-line connection is to an elemental analyzer. The coupled elemental analyzer-IRMS has greatly simplified isotopic measurements; key improvements over conventional off-line preparations include significant reduction of sample size and analysis time. Some loss in precision occurs, although the reproducibility of $\delta^{13}C$ values is commonly ±0. 1‰.

Interpretation

Lake-derived organic matter that is produced by phytoplankton (C_3 algae) using dissolved CO_2 in isotopic equilibrium with the atmosphere is usually isotopically indistinguishable from organic matter produced by C_3 plants in the surrounding watershed (Table II). Algal organic matter nonetheless usually has a distinctly different carbon isotopic composition than material produced by C_4 plants growing either on land or the lake bottom (Fig. 1). However, this generalization about carbon isotopic source signatures erodes when the availability of dissolved atmospheric CO_2 ($\delta^{13}C = -7‰$) is limited and algae begin to use dissolved HCO_3^- ($\delta^{13}C = 1‰$) as their source of carbon (Fig. 3). Situations where HCO_3^- becomes important include periods of high photosynthetic uptake of dissolved inorganic carbon during which the availability of CO_2 becomes diminished (Keeley & Sandquist, 1992; Hollander & McKenzie, 1991; Bernasconi et al., 1997) and in waters where the ratio of HCO_3^- to CO_2 is kept elevated by an alkaline pH (e.g., Hassan et al., 1997). In such cases, $\delta^{13}C$ values of algal organic matter can increase to reach as high as –9‰, which is in the range of C_4 plants. In other cases, delivery of isotopically light DIC from land run-off ($\delta^{13}C \cong -12‰$) can result in isotopically light algal organic matter ($\delta^{13}C \cong -32‰$). The possibility of these excursions in isotopic source signatures is a potent reminder that multiple indicators of organic matter origin should be employed in paleolimnologic studies.

Post-burial diagenesis of organic matter may alter its bulk $\delta^{13}C$ value (Herezeg, 1988) and thereby obscure its paleolimnological information. Sediment organic matter consists of a mixture of different compounds that have different isotopic compositions; some of these components degrade more readily than others. However, comparison of organic matter $\delta^{13}C$ values in two sediment cores that were collected six years apart from the same location in Lake Ontario demonstrate that this diagenetic effect is minimal (Hodell & Schelske, 1998). Microbial activity diminished the concentration of organic matter by nearly 20% during the six additional years that sediments resided in the lake bottom, but it did not significantly alter its bulk $\delta^{13}C$ value.

The $\delta^{13}C$ values of sediment organic matter are proxies for paleoenvironmental changes in lake watersheds as well as in the lakes themselves. Increased delivery of nitrates and phosphates derived from soil erosion, agricultural fertilizers, or domestic sewage enhances algal productivity, which draws down the supply of DIC in the epilimnion, which in turn decreases algal discrimination in favor of ^{12}C and yields less negative $\delta^{13}C$ values in algal organic matter (Hollander & McKenzie, 1991; Keeley & Sandquist, 1992; Bernasconi et al., 1997; Brenner et al., 1999). The history of anthropogenic additions of nutrients to Seneca Lake, New York, is recorded in an isotopic shift in the upper 20 cm of the sediment

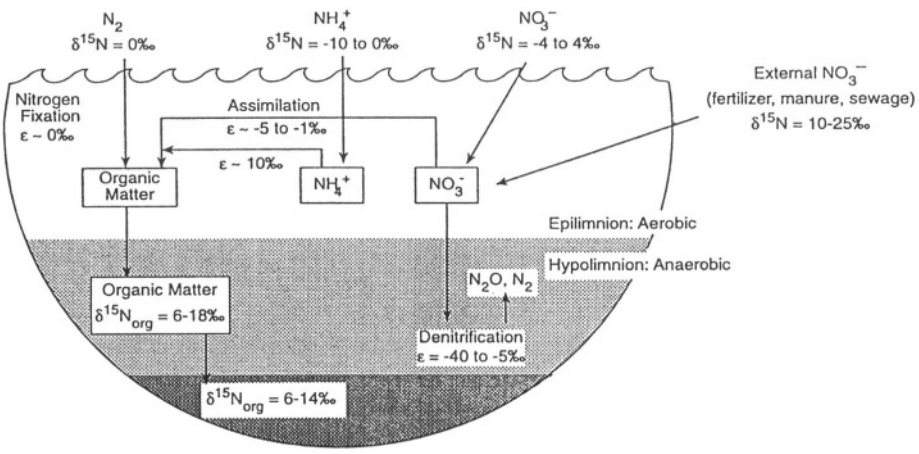


Figure 4. Idealized nitrogen isotope cycle in a small stratified lake. The isotopic composition of organic matter buried in sediment is determined by sources of nitrogen, rates of primary production and respiration, and the types of denitrification processes. Isotopic values for external sources of atmospheric and combined forms of nitrogen are from Kendall (1998). Isotope enrichment factors (ε) are from Fogel & Cifuentes (1993) and vary with the form of inorganic nitrogen that lake algae assimilate. Note that nitrogen isotopes are not fractionated by algal fixation of atmospheric N_2 and that the importance of nitrogen fixation can vary greatly from lake to lake.

record (Fig. 2) to less negative $\delta^{13}C$ values. The watershed of this lake changed from an undisturbed forest to clear-cut farm fields shortly after the completion of the Erie Canal in 1825. This environmental change released soil nutrients into the lake. Subsequent growth of human and livestock populations further increased nutrient deliveries to the lake system and led to increasingly smaller algal discrimination in favor of ^{12}C. These changes in watershed conditions are mirrored in the progressively less negative $\delta^{13}C$ values of organic matter in the younger lake sediments (Fig. 2).

Nitrogen isotope ratios

Environmental significance

Although not as widely used as a paleolimnological proxy as carbon isotopic determinations, the nitrogen isotopic composition of sediment organic matter can similarly help to distinguish the sources of this material to lakes and to reconstruct past productivity rates. This proxy is particularly useful in identifying changes in the past availability of nitrogen to aquatic primary producers. However, the dynamics of nitrogen biogeochemical cycling are more complicated that those of carbon (Fig. 4), thereby making interpretations of sedimentary $\delta^{15}N$ records more difficult (Fogel & Cifuentes, 1993; Bernasconi et al., 1997; Hodell & Schelske, 1998; Brenner et al., 1999; Talbot, this volume).

Application of $\delta^{15}N$ values to identify organic matter sources is founded on the difference between the $^{15}N/^{14}N$ ratios of the inorganic nitrogen reservoirs available to plants in water and those on land. The $\delta^{15}N$ value of dissolved NO_3^-, which is the most common

form of dissolved inorganic nitrogen (DIN) used by algae, is typically larger than that of atmospheric N_2, which is the form used by land plants. The generally expected $\delta^{15}N$ value of NO_3^- is between +7‰ to + 10‰, whereas that of atmospheric nitrogen is about 0‰ (cf., Peters et al., 1978). The isotopic difference between these two sources of nitrogen is roughly preserved in the $\delta^{15}N$ values of organic matter from coastal marine plankton (+8.5‰) and from C_3 land plants (+0.5‰) (Peterson & Howarth, 1987).

Complications in the use of $\delta^{15}N$ values for paleoenvironmental reconstructions arise in several ways. One is that algal utilization of the DIN available lake waters typically increases nitrate $\delta^{15}N$ values. Algae commonly discriminate in favor of ^{14}N over ^{15}N, with the result that their organic matter has a somewhat lower $\delta^{15}N$ value than the total NO_3^- (e.g., Fogel & Cifuentes, 1993, and references therein; Fig. 4). As nitrate is removed from surface waters, its $\delta^{15}N$ value progressively increases to create an increase in the $\delta^{15}N$ of organic matter that is produced from the remaining supply (Altabet & François, 1993; 1994). Another complication is that phosphorus — not nitrogen — commonly limits primary production in lakes. If phosphorus becomes depleted when only a small fraction of the available nitrate has been consumed, the nitrogen isotopic composition of the DIN is never significantly altered. Under these conditions, the $\delta^{15}N$ values of algal organic matter will reflect an unchanging $\delta^{15}N$ signal, and variations in phytoplankton productivity will not be readily discerned from the $\delta^{15}N$ values of sedimented organic matter.

In addition, factors other than primary productivity can influence the nitrogen isotopic composition of organic matter produced within a lake. For example, water column denitrification in anoxic basins will considerably enrich the residual DIN in ^{15}N (Fig. 4). Shifts in phytoplankton species composition or addition of heterotrophs can also influence the $\delta^{15}N$ of sedimenting organic matter. An increase in abundance of nitrogen-fixing cyanobacteria, which directly fix atmospheric N_2, would decrease $\delta^{15}N$ values in sedimented organic matter (Fogel & Cifuentes, 1993). In contrast, addition of heterotrophic organic matter will increase the $\delta^{15}N$ of organic matter because $\delta^{15}N$ increases by 3–4‰ with each trophic transfer (Deniro & Epstein, 1981; Minagawa & Wada, 1984; Peterson & Fry, 1987).

The multiple factors involved with the dynamics of nitrogen recycling and biological isotopic discrimination during uptake of nitrogen introduce considerable variability into the numbers generalized in Figure 4 (Fogel & Cifuentes, 1993; Bernasconi et al., 1997; Hodell & Schelske, 1998). Although the variability makes interpretations of $\delta^{15}N$ values challenging, it also provides opportunities to assess the impacts of a wide range of paleoenvironmental changes in lake sedimentary records.

Analytical methods

The traditional method to determine the $^{15}N/^{14}N$ ratios of sediment organic matter is by oxidation of sediment samples in an "off-line" procedure that employs a vacuum transfer system to produce and isolate the gas needed for isotopic analysis (cf., Kendall & Grim, 1990). NO_x is first produced by oxidation of the sediment organic matter in an evacuated and sealed Pyrex tube at 600 °C. Quartz tubes can be heated to 800 °C to insure more complete oxidation. The mixture of nitrogen oxides is reduced to a single gas, N_2, prior to measurement of its $^{15}N/^{14}N$ ratio with an isotope ratio mass spectrometer (IRMS). Seemingly minor leakages of air into the vacuum system must be avoided, because they will result in major amounts of N_2 contamination. Although quite reproducible and accurate, this method is also laborious.

As described earlier for carbon isotopic determinations, development of Continuous Flow-Isotope Ratio Mass Spectrometry (CF-IRMS) has greatly simplified nitrogen isotopic measurements of organic matter by significantly reducing both sample size and analytical time. CF-IRMS consists of an IRMS coupled on-line to a device that produces the N_2 gas to be analyzed. In the case of sediment organic matter, the on-line connection is to an elemental analyzer. Some loss in analytical precision compared to the off-line method occurs, although the reproducibility of $\delta^{15}N$ values remains good (±0.2‰).

A attractive feature of the elemental analyzer CF-IRMS combination is that it can provide simultaneous determinations of the concentrations and isotopic ratios of both the carbon and nitrogen in a single sample. However, best CF-IRMS results are obtained when optimizing for either carbon or nitrogen. This limitation occurs because carbon atoms typically outnumber nitrogen atoms by 10 : 1 in typical organic matter, making a dilution step necessary to decrease the amount of CO_2 gas relative to N_2 before introducing the gases into the mass spectrometer. Another possible problem can be created by the carbonate-dissolution step that is required to remove carbonate-carbon prior to carbon isotopic measurement of organic matter. The risk of biasing of organic $\delta^{13}C$ values by the dissolution procedure ("Organic carbon isotope ratios" section, this chapter) appears to be greater for $\delta^{15}N$ values, especially in young, organic-carbon-rich lake sediments.

Teranes & Bernasconi (unpublished) have explored the risk of biasing of sediment $\delta^{15}N$ values during carbonate dissolution with a core of varved sediment from Baldeggersee, a small eutrophic lake located in central Switzerland. The alternating light and dark layers represent seasonal laminations. Primary production and calcite precipitation during the spring and summer create the thick, light-colored, carbonate-rich (60–80%) sediment layers. Increased sedimentation of organic matter and diminished calcite concentrations (30–50%) in autumn produce the thinner, dark laminations. Nitrogen concentrations increase (Fig. 5A) as a result of increasing eutrophication of the lake beginning around 1900 (Teranes & Bernasconi, 2000). Organic $\delta^{15}N$ values were measured on duplicate subsamples of light and dark sediments after preparation by two procedures: (1) reaction with weak (1N) HCl followed by rinsing with copious amounts of distilled water and drying, and (2) simply drying the intact, carbonate-containing sediment. The $\delta^{15}N$ values of acid-washed sediment and the non-treated sediment differ (Fig. 5B). Acid-washing lowers $\delta^{15}N$ values by as much as 8‰ in the post-1950 sediments, which have not experienced much post-burial diagenesis. In contrast, $\delta^{15}N$ values increase as a result of acid-washing in pre-1950 sediments (Fig. 5B). The extent of nitrogen biasing is similar in both the light and dark layers, indicating that presence of calcite is not as important as is the reactivity of the organic matter. This experiment illustrates that isotopic analysis of carbonate-containing lake sediments is best done by two steps: (1) determining $\delta^{15}N$ values from untreated sediment and (2) determining $\delta^{13}C$ values after carbonate removal.

Interpretation

The $^{15}N/^{14}N$ ratio of sedimentary organic matter is used widely to complement $\delta^{13}C$ values in marine paleoproductivity studies (Calvert et al., 1992; François et al., 1992) and to a lesser extent in paleolimnology. Gu et al. (1996) suggest a weak positive correlation between $\delta^{15}N$ values in lacustrine plankton and phosphate levels, growth rate, and primary productivity in Florida lakes. Teranes & Bernasconi (2000) document an inverse relationship between surface water nitrate concentration and the $\delta^{15}N$ of sedimenting organic matter in sediment

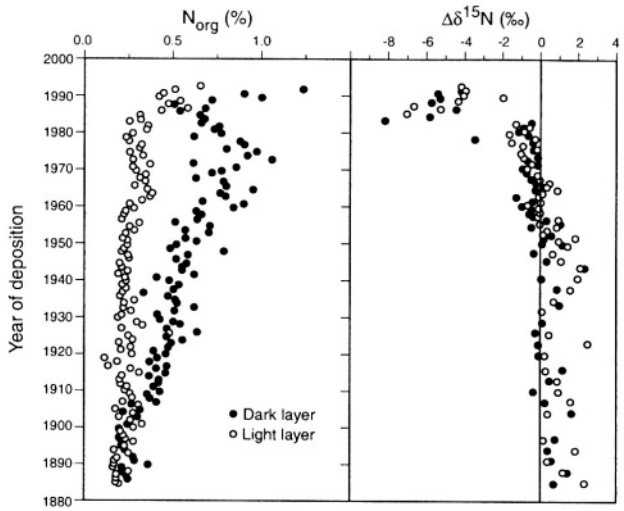


Figure 5. Comparison of nitrogen concentrations in light and dark layers of varved Baldeggersee (Switzerland) sediment (A) and effects of acid washing of sediment to remove carbonate on sediment nitrogen isotopic composition (B). Dark layers are richer in organic nitrogen than light layers. The isotopic difference between the acid-washed and untreated sediment is greatest in the upper part of the sedimentary sequence ($\Delta\delta^{15}N = \delta^{15}N_{washed} - \delta^{15}N_{untreated}$). Acid-washing, especially of young sediments, evidently can remove nitrogen-containing components of organic matter that have isotopically heavy compositions. Teranes & Bernasconi (unpublished).

trap data in Baldeggersee, Switzerland; increases in productivity are accompanied by higher $\delta^{15}N$ values. Talbot & Laerdal (2000) document larger $\delta^{15}N$ values in organic matter from Lake Victoria, East Africa, during a period of wetter climate around 15.2 ka. They attribute the $\delta^{15}N$ increase to utilization of a greater proportion of the DIN as a consequence of productivity being dramatically enhanced by release of phosphorus from flooded soils around the lake.

Factors other than primary productivity can also strongly influence the nitrogen isotopic composition of lacustrine organic matter. Changes in nitrogen cycling that accompany anthropogenic eutrophication of lakes can mimic the isotopic shifts caused by higher productivity. For example, an increase in $\delta^{15}N$ values can record deliveries of isotopically heavy nitrate ($\delta^{15}N = 10$ to 25‰) from farm runoff and human sewage (Teranes & Bernasconi, 2000). Alternatively, it can indicate increasing water column denitrification under anoxic conditions. A 6‰ increase in organic matter $\delta^{15}N$ values in Lake Ontario sediments since 1840 is interpreted to indicate increased denitrification because of longer periods of seasonal bottom-water anoxia as lake productivity has increased (Hodell & Schelske, 1998).

Changes in phytoplankton assemblages, addition of heterotrophs, and presence of nitrogen fixers can also influence the $\delta^{15}N$ of organic matter in lake sediments. A 6‰ difference in $\delta^{15}N$ values exists between organic matter settling in Lake Ontario in the summer and in the winter (Hodell & Schelske, 1998). The difference is attributed to the dominance of isotopically light phytodetritus during the summer and isotopically heavy organic matter from heterotrophic or detrital sources during the winter. Shifts to low (–1 to 3‰) $\delta^{15}N$

values in sediments deposited in Florida lakes since the early 1900s record increases in the contributions of nitrogen-fixing cyanobacteria to organic matter production as eutrophication of these lakes increased (Brenner et al., 1999). Low $\delta^{15}N$ values (~3‰) in Lake Victoria sediments suggest that nitrogen fixation has been an important process in this lake throughout the Holocene (Talbot & Laerdal, 2000).

Oxygen and hydrogen isotope compositions

Environmental significance

The $^{18}O/^{16}O$ and D/H ratios in water, ice, and minerals like calcite and apatite are commonly employed as paleoprecipitation proxies in paleoclimate reconstructions. Despite their great potential in providing paleolimnologic information, the oxygen and hydrogen isotopic compositions of organic matter have rarely been determined in sedimentary records, largely because of practical difficulties in their analysis. Applications of $^{18}O/^{16}O$ ratios have been discouraged because the contribution of oxygen from the oxygen-rich compounds that are usually used to convert organic matter to CO_2 prior to isotopic analysis severely complicates interpretation of the analytical results. D/H ratios of sedimentary organic matter have similarly not been widely applied, but largely because not many laboratories are skilled in their analysis. Nonetheless, they have considerable promise in paleolimnology.

Analytical methods and interpretations

Some investigators have found ways to circumvent the challenges that have discouraged determinations of the $\delta^{18}O$ values of sediment organic matter (cf., Wolfe et al., this volume). For example, Beuning et al. (1997) isolated aquatic cellulose from the sediments of Lake Victoria, which they then pyrolyzed with a nickel catalyst to produce CO_2 that preserved the original $^{18}O/^{16}O$ ratios of organic matter produced within the waters of this lake. The cellulose $\delta^{18}O$ values yield a reconstruction of the hydrologic balance of Lake Victoria over the past 13 ky that reflects a combination of changes in precipitation over East Africa caused by orbital precession and a change in residence time of water in the lake caused by downcutting of its outlet.

Aucour et al. (1993) isolated the cellulose fraction of organic matter from the Kashiri peat bog on the Burundi highlands of Equatorial Africa and used both its $\delta^{18}O$ and $\delta^{13}C$ values to recreate the history of climate change over the past 30 ky. They employed pyrolysis with mercuric chloride to obtain the CO_2 for determination of the original $^{18}O/^{16}O$ ratios of the emergent plants that produced the peat. Pollen analyses were combined with the two isotopic parameters to show that the proportions of C_3 and C_4 plants shifted in the bog between full-glacial, end-glacial, and post-glacial times and that the origins of the airmasses delivering moisture to this region changed. Dominance of C_4 plants between 30 ka and 15 ka was accompanied by cooler and drier climate. C_3 plants became more important after 15 ka on the basis of the isotopic evidence but not from the pollen contents. After 7 ka, both pollen and isotopic proxies show the dominance of C_3 plants that exists today.

Hydrogen isotopic compositions of organic matter are especially sensitive to paleoenvironmental changes. Fractionation of hydrogen isotopes by land plants is affected by ambient temperatures, origin and availability of water, and plant growth rates (Fogel & Cifuentes, 1993; White et al., 1994), making interpretation of δD values of land-derived

organic matter complicated. In contrast, the δD values of the aquatic organic matter that is buried in lake sediments reflect principally the origin of lake water and therefore provide a relatively straightforward hydrologic history of the lake. The difference arises because water is unlimited to lake algae and temperature changes are small in lakes relative to on land. Interpretation of the δD record of organic matter in lake sediments is based on the demonstrable relation between the δD value of water in which lake algae lived and the δD of the non-exchangeable, carbon-bound hydrogen in the algal cell walls. D/H ratios are then interpreted in terms of past precipitation/evaporation balances and air mass trajectories.

This strategy has been employed by Krishnamurthy et al. (1995) to reconstruct the history of post-glacial paleoclimate changes provided by organic matter in the sediments of Austin Lake, Michigan. Their analyses involved an exhaustive extraction procedure to remove clay minerals, which contain hydrogen, and oxygen- and nitrogen-bearing organic matter components, which contain hydrogen atoms that might have been exchanged with sediment pore water after deposition and thereby had become unreliable proxies of the water balance in this groundwater lake. The Austin Lake δD values separate into four time intervals that represent changes in Holocene climate. Especially prominent among the intervals is the period between 9 ka to 2 ka, during which δD values increase to ca. –75‰ from an earlier average of –110‰. The δD increase may reflect evaporative distillation of isotopically light water from the lake in response to the mid-Holocene Hypsithermal time of warm, dry climate that has been recorded in lake sediments throughout the Great Plains and Rocky Mountain regions of North America (Dean et al., 1996), or it may reflect an increase in the importance of air masses carrying isotopically heavy moisture from the Gulf of Mexico to the Great Lakes region.

Biomarker hydrocarbon molecules

Environmental significance

Biological marker (biomarker) molecules are compounds that have distinctive biotic sources and that retain their identity after burial in sediments, even after partial alteration. Most biomarkers are lipids, which are hydrocarbons and hydrocarbon-like molecules. Because of their low susceptibility to microbial degradation compared to other types of organic matter, saturated hydrocarbons — those having only carbon-carbon single bonds — can record many aspects of the depositional history of organic matter sources in lake sediments. A number of detailed reviews of the biomarker contents of lake sediments exist (e.g., Barnes & Barnes, 1978; Cranwell, 1982; Johns, 1986; Müller, 1987; Meyers & Ishiwatari, 1993).

The two principal sources of biotic hydrocarbons to lake sediments are algae that live within a lake and plants that live around it. Because these sources produce distinctively different suites of hydrocarbons, their characteristic molecules serve as proxies for changes in delivery of organic matter. The hydrocarbon compositions of many aquatic algae and photosynthetic bacteria are dominated by the C_{17} *n*-alkane (e.g., Blumer et al., 1971; Giger et al., 1980; Cranwell et al., 1987), and the abundances of this and related compounds reflect lacustrine paleoproductivity rates. Vascular plants on land or along the edges of lakes contain large proportions of C_{27}, C_{29}, and C_{31} *n*-alkanes in their epicuticular waxy coatings (e.g., Eglinton & Hamilton, 1963, 1967; Cranwell, 1973; Cranwell et al., 1987;

Rieley et al., 1991). Abundances of these waxy hydrocarbons reflect the amount of organic matter transported to lakes from the surrounding land.

Analytical methods

The procedures used by different laboratories to extract, isolate, and analyze the biomarker hydrocarbon contents of sediments are rarely identical, but they differ largely only in their details. The general analytical scheme in which the fundamental elements common to the different procedures has been nicely summarized by Rullkötter (2000). For their analysis, hydrocarbons first need to be separated from sediments by extraction into an organic solvent. The most common solvent that is used for dried sediment samples is dichloromethane, although other solvents or mixtures of solvents are also employed. A risk involved with the common practice of first drying the sediments is that some organic compounds may become irreversibly associated with minerals and will not be released by subsequent solvent extraction. Moreover, freeze-drying of sediment samples can sometimes create a more serious problem — contamination of the natural hydrocarbon composition with pump oil vapors (Barwise et al., 1996) — unless suitable filters are employed. For these reasons, extraction of wet sediment samples is sometimes preferred. In these cases, solvents like methanol or acetone that can remove the sediment porewater are used first and then followed by mixtures of these hydrophilic solvents with non-polar solvents such as dichloromethane.

Actual extraction procedures cover a wide range. Simple shaking of the sediment with solvents can be effective for small samples of less than a few grams. More commonly, procedures such as Soxhlet refluxing, microwave extraction, or ultrasonication are used because of their greater efficiencies in extracting hydrocarbon-containing material. The typical amount of solvent-extractable material in lake sediments is only a few percent of the total organic matter, and much of the soluble material consists of non-hydrocarbon lipids such as fatty acids, alcohols, and pigments. Hydrocarbons usually need to be separated from these other lipids by liquid chromatography before subsequent analysis. Column chromatography, thin-layer chromatography, medium-pressure liquid chromatography, and high-pressure liquid chromatography are all used, depending on the sample quantity and the separation efficiency required.

The separated hydrocarbon fraction is then analyzed by capillary column gas chromatography, which simultaneously separates the mixture of hydrocarbons into its components and measures how much of each compound is present. Individual *n*-alkanes can usually be identified by their relative retention times in gas chromatograms, although sometimes branched hydrocarbon molecules will share the same retention time as an *n*-alkane. For this reason, positive identification of biomarker hydrocarbons require the combination of gas chromatography and mass spectrometry using verified mass spectra.

Interpretation

The hydrocarbon fraction of organic matter in lake sediments is generally a robust recorder of environmental changes because these compounds have long residence times in lake sediments. It is important to remember, however, that hydrocarbons normally constitute a very small fraction of the total organic matter in both biota and in sediments. In addition, diagenetic losses of the non-hydrocarbon components of the total organic matter can

exaggerate the importance of sources implied by biomarker hydrocarbons. Use of multiple source proxies is recommended.

Hydrocarbons from petroleum contamination have augmented biotic hydrocarbons since the late 1800s in sediments of lakes near urban areas (Wakeham, 1977a, I977b; Meyers, 1987; Bourbonniere & Meyers, 1996). Petroleum hydrocarbons can be distinguished from biological hydrocarbons by two distinctive characteristics: (1) absence of the characteristic odd-carbon chain-length dominance of biological hydrocarbons, and (2) presence of a more diverse range of molecular structures than is found in biological hydrocarbon mixtures (e.g., Meyers & Takeuchi, 1981). This latter characteristic results in a mixture of hydrocarbon compounds that cannot be separated by even high resolution capillary gas chromatography, giving rise to the term "unresolved complex mixture" or UCM.

Wakeham (1976) provides a classic illustration of the temporal and geographic differences in delivery of hydrocarbons to lake sediments. Sediments of Lake Quinalt, which is surrounded by a forested and virtually pristine watershed on the Olympic Peninsula of Washington, contain low concentrations of hydrocarbons that are dominated by the C_{27} *n*-alkane diagnostic of tree waxes (Fig. 6). No significant difference exists in the *n*-alkane contents of sediments deposited in the early 1800's and in the mid-1970's. In contrast, modern sediments of Lake Washington, which is surrounded by the city of Seattle and its suburbs, have hydrocarbon contents dominated by the unresolved complex mixture (UCM) indicative of petroleum residues (Fig. 6). Furthermore, the contribution of short-chain-length *n*-alkanes derived from algae is equal to the land-plant *n*-alkane contributions, suggesting eutrophication of the waters of Lake Washington. In progressively older sediments, the contributions of UCM and short-chain hydrocarbons diminish, until in sediments deposited in the mid-1800's the concentrations and distributions resemble those of Lake Quinalt sediments (Fig. 6). Three sources of hydrocarbons can be identified in these sediments: (1) a natural, low contribution of land-plant *n*-alkanes that is found throughout the sedimentary records of both lakes. (2) an input of petroleum residues from urban run-off, which first appears in the Lake Washington record around 1900 and becomes dominant in modern sediments, and (3) an algal contribution of C_{17} and C_{19} *n*-alkanes. which is usually small in comparison to the land-plant contributions, probably because of its selective diagenetic degradation (e.g., Meyers & Ishiwatan, 1993). The algal components become large only in the sediments of Lake Washington that were deposited starting ca. 1950, when growth of Seattle and its suburbs led to eutrophication of the lake.

Lignin oxidation products

Environmental significance

Lignins are phenolic polymers synthesized by higher plants to construct parts of their vascular and structural systems. Nearly all vascular plants grow on land, and therefore the lignin fraction of sediment organic matter largely records the contribution and preservation of land-plant materials. Lignin-containing plant debris is delivered to lakes principally by rivers and streams, although some lakes receive important amounts from shoreline flora. The proportion of land-plant organic matter in lake sediments can be estimated from the fraction of lignin that is present. Gymnosperms and angiosperms synthesize distinctive types of lignin components. As a consequence, past changes in watershed vegetation can

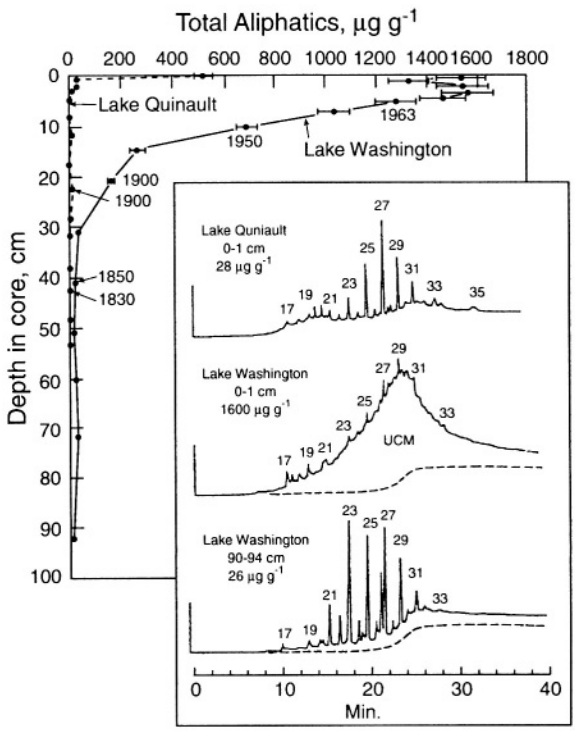


Figure 6. Concentrations of total extractable aliphatic hydrocarbons in sediment cores from Lake Washington in urban Seattle and Lake Quinault in rural Washington. Gas chromatographic traces illustrate hydrocarbon distributions in three of these core samples. Carbon numbers of *n*-alkanes are indicated on the traces; UCM represents the unresolved complex mixture of hydrocarbons underlying the individual aliphatic hydrocarbon peaks. Most of the increase in Lake Washington hydrocarbon concentrations since ca. 1900 is due to the large addition of petroleum residues, indicated by the UCM, to a low background of land plant *n*-alkanes, typified by the Lake Quinalt hydrocarbon contents. Core sediment ages shown are from ^{210}Pb dating. Adapted from Wakeham (1976).

be inferred from the kinds of lignin found in sediment records. Moreover, lignin is relatively resistant to diagenesis, making its sedimentary record longer-lived than many other forms of organic matter.

Analytical methods

Molecular analysis of lignin typically begins with an aggressive oxidation step to break down the biopolymer into various phenolic monomeric fragments. The most widely used methods are based on the cupric oxide oxidation procedure pioneered by Hedges & Parker (1976) and refined by Hedges & Mann (1979). Samples of dried sediment or plant material are placed in a pressure container with an alkaline cupric oxide solution and heated at about 170 °C for several hours in a nitrogen atmosphere. The oxidation products are extracted with an organic solvent, such as ethyl ether, and analyzed by gas chromatography.

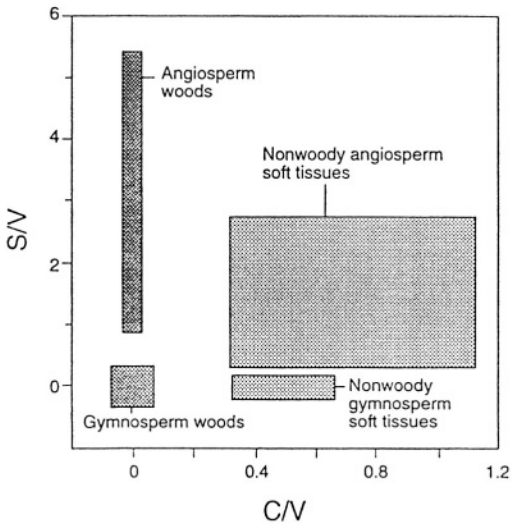


Figure 7. Lignin parameters S/V *vs* C/V with their general vascular plant source assignments indicated. Data adapted from Hedges & Mann (1979).

Interpretation

The oxidation fragments of lignin have been grouped by Hedges & Mann (1979) as a guide to identifying their plant sources (Fig. 7). A measure of the relative contributions of woody and non-woody land-plant tissues is given by the C/V (cinnamyl/vanillyl) ratio, which is the sum of p-coumaric acid plus ferulic acid concentrations divided by the sum of the three vanillyl phenols. Gymnosperm sources of land-plant residues are distinguished from angiosperm sources by the S/V (syringyl/vanillyl) ratio, which is the sum of the amounts of the three syringyl phenols divided by the sum of the vanillyl phenols. Oxidative diagenesis of lignin components can be inferred from an increase in the total phenolic acids relative to the total phenolic aldehydes, expressed as the Ad/Al ratio (Hedges et al., 1982; Ertel & Hedges, 1984).

Lignin phenols isolated from a sediment core from Lake Washington near Seattle, Washington, have been used to identify four stages in the post-glacial succession of watershed plants around this lake. In the bottom of the 11 -m core, low S/V and C/V ratios indicate an approximately equal mixture of plant tissues from woody (conifers) and nonwoody (ferns) gymnosperms (Hedges et al., 1982). Between 10 m and 8 m in the core, high S/V and C/V ratios indicate a predominance of nonwoody angiosperm tissues, probably originating from marsh or grassland sources. In contrast, pollen data suggest that pines dominated the watershed during this interval (Leopold et al., 1982). Evidently, the pine pollen records eolian transport from regions outside the watershed and not fluvial contributions of organic matter from within the local catchment, as does lignin. High S/V and low C/V ratios from 7 m to 4 m suggest large contributions of angiosperm wood, a conclusion that is consistent with the abundance of alder pollen. A decrease in the S/V ratio and a constant C/V ratio

Table III. Carbon isotopic compositions of total organic matter and the C_{31} *n*-alkane wax coatings of leaves from representative land plants using C_3, C_4, and CAM carbon-fixing pathways. From Collister et al. (1994).

Plant Species	CO_2-fixing metabolism	Total $\delta^{13}C$ (‰)	*n*-C_{31} $\delta^{13}C$ (‰)
Quercus turneri	C_3	−28.8	−35.7
Quercus rober	C_3	−30.5	−36.9
Acer campestre	C_3	−30.4	−35.0
Magnolia delabayi	C_3	−28.7	−34.3
Cyprus alternifolius	C_3	−27.6	−35.3
Saccharum officinarum	C_4	−10.7	−23.4
Miscanthuys sacchariflorum	C_4	−11.9	−18.4
Zea mays	C_4	−11.2	−20.5
Selenecereus grandiflorus	CAM	−13.0	−26.4
Tillandsia usneoides	CAM	−14.9	−29.2
Aechmeade albata	CAM	−16.2	−25.2

between 4 m to the core top indicates a gradual replacement of deciduous trees by conifers, which is also consistent with the pollen record (Hedges et al., 1982; Leopold et al., 1982).

Compound-specific isotope ratios

Environmental significance

The isotopic compositions of individual compounds isolated from the mix of molecules that constitute sediment organic matter are useful to paleolimnological studies. In particular, carbon isotope analyses of individual biomarker compounds provide a powerful source of paleoenvironmental information that complements the $\delta^{13}C$ values of bulk organic matter. The analytical combination of capillary gas chromatography (GC) interfaced with isotope ratio mass spectrometry (IRMS) offers rapid, precise, and convenient analysis of $^{13}C/^{12}C$ ratios in specific organic compounds isolated from sediment samples. Compound-specific carbon-isotope GC-IRMS has become the method of choice to determine the origin of a given organic compound, to explore the effects of diagenesis, and to reconstruct paleo-depositional settings in ways that neither bulk organic matter characterizations nor traditional biomarker analyses can individually provide. The advantages arise partly because different organisms that synthesize the same biomarker will often fractionate carbon isotopes differently, thereby aiding source identification (Table III), and partly because the $\delta^{13}C$ values of individual molecules are not affected by diagenesis as long as the carbon skeleton remains intact, thereby preserving source identification.

Determinations of the $^{15}N/^{14}N$, D/H, $^{18}O/^{16}O$, and $^{14}C/^{12}C$ ratios of selected compounds are also employed in paleoenvironmental studies. Use of these isotopic ratios are less common than those of $^{13}C/^{12}C$, yet they each convey special information about the origins of sediment organic matter, cycling of their respective nutrient element, and conditions of the past.

Analytical methods

A capillary GC system is used to separate the mixture of organic compounds that has been isolated from a sediment sample by procedures described in the sections on "Biomarker hydrocarbon molecules" and "Lignin oxidation products" in this chapter. Individual organic compounds are then swept directly from the GC into a combustion reactor where they are oxidized at ~800-900 °C to produce CO_2, NO_x, and H_2O. For carbon-isotope analysis, the gases pass through an on-line water removal system, and then the dried CO_2 flows directly into the ion source of an IRMS. The coupling of GC and IRMS yields measurements of both the types and amounts of individual organic matter components and their $\delta^{13}C$ values. Brand (1996) and Meier-Augenstein (1999) provide details of GC-IRMS techniques.

Paleoenvironmental applications also exist for compound-specific $\delta^{15}N$ values of organic matter from lake sediments. As noted in the "Nitrogen isotope ratios" section of this chapter, $\delta^{15}N$ values are sensitive indicators of sources of nitrogen to biota and of biogeochemical cycles. This sensitivity is especially true for compound-specific $\delta^{15}N$ values. However, the analytical challenges are greater for nitrogen isotopes than for those of carbon (Brenna, 1997; Meier-Augenstein, 1999). Foremost among these is that nitrogen exists at substantially lower concentrations than carbon in organic molecules and thereby nears the limit of isotopic measurement. Also, $^{15}N/^{14}N$ ratios are measured on N_2 gas; the NO_x obtained from combustion of the GC-separated compounds must be reduced to N_2, which introduces the risk of isotopic fractionation. Finally, even small leakages of air into the coupled GC-IRMS system result in a high level of N_2 contamination. Despite these challenges, the potential rewards that are promised by determinations of $\delta^{15}N$ values of organic compounds have encouraged continued instrumental advances.

D/H ratios of biomarkers are source-specific proxies for paleoenvironmental hydrologic balances and water sources. These ratios can be determined using a high-temperature (1450 °C) pyrolysis system that converts the hydrogen in the organic compounds into H_2 gas for isotopic analysis (Burgoyne & Hayes, 1998). Specialized GC-IRMS units can provide simultaneous measurements of biomarker concentrations and their D/H ratios (Hilkert et al., 1999).

Interpretation

Compound-specific $\delta^{13}C$ values enable source assignments to be made for biomarkers that have multiple origins. For example, nearly all vascular land plants synthesize long-chain *n*-alkanes for use as waxy coatings on their leaves, flowers, and pollen. Application of *n*-alkane distributions to deciphering the changes in continental climates that would modify the types of land plants has therefore been blunted by this non-specific hydrocarbon biomarker synthesis. Plants that use different carbon-fixing pathways, however, produce *n*-alkanes that have different carbon isotopic signatures. The waxy hydrocarbons, as well as the bulk organic matter, of the leaves of C_3, C_4, and CAM plants clearly have different $\delta^{13}C$ values (Table III).

The distinction between the isotopic compositions of *n*-alkanes from land-plants having different metabolic pathways has been used by Bird et al. (1995) to trace the history of changes in the amounts of C_3 and C_4 plants in the watershed of the Johnstone River, northern Queensland, Australia. Clearing of the original forests for sugar cane production and pastures is recorded in a +3‰ shift in the $\delta^{13}C$ values of *n*-alkanes isolated from river sediments deposited since the late 1800's. A smaller shift of + 1‰ that occurs in sediments

deposited around 6 ka may record either a mid-Holocene transition to dryer climate or the onset of aboriginal slash-and-burn agriculture.

Compound-specific carbon isotope analyses have also proven useful to identifying origins of organic matter components even in cases where changes in watershed flora have not occurred. Rieley et al. (1991) compared the $\delta^{13}C$ values of individual C_{25} to C_{29} *n*-alkanes extracted from sediments of Ellesmere, England, to those from the leaves of trees overhanging the lake. Their analyses reveal that willow leaves appear to be the major source of the sedimentary *n*-alkanes. Brincat et al. (2000) similarly employed $\delta^{13}C$ values of waxy *n*-alkanes to test the hypothesis that the C_3 plants that have dominated the post-glacial flora around Lake Baikal, Siberia, succeeded a flora dominated by C_4 tundra plants during the last glacial period (Qiu et al., 1993). This interpretation is based on the 3‰ shift to more negative TOC $\delta^{13}C$ values that occurs in sediments of this lake at the end of the glacial period. In contrast to the bulk values, the leaf-wax $\delta^{13}C$ values remain between –31.0 to –31.5‰ throughout the entire sediment record, indicating that C_3 plants have remained the dominant vegetation around Lake Baikal since 20 ka.

Changes in the proportions of land-plant and aquatic organic matter delivered to the sediments of Sacred Lake, Mt. Kenya, from 40 ka to the present have been identified using biomarker $\delta^{13}C$ values (Huang et al., 1999a). Plant-wax $\delta^{13}C$ values reveal a shift from late-glacial vegetation dominated by C_4 grasses and sedges (values of –20 to – 18‰) to post-glacial vegetation dominated by C_3 plants (values of –34 to –27‰). Unsaturated hydrocarbon biomarkers that are specific to algae undergo a dramatic excursion from values of –5. 1‰ at the glacial maximum to values of – 30.3‰ in the early Holocene. The isotopic shift shows that the low pCO_2 of the last glacial maximum favored C_4 grasses and limited isotopic discrimination by freshwater algae. Refinement of this reconstruction is provided by compound-specific $\delta^{13}C$ analyses of lignin phenols isolated from the lake sediments (Huang et al., 1999b). The lignin $\delta^{13}C$ results support the hypothesis of CO_2 limitation favoring C_4 grasses and add evidence of increased aridity that enabled dominance of these plants around Sacred Lake near the termination of the last glacial period.

Xie et al. (2000) employed D/H ratios of the C_{23} *n*-alkane that is diagnostic *of Sphagnum* in a core from Bolton Fell Moss, Cumbria, England, to explore for effects of climate change on this aquatic environment. The δD values of the biomarker hydrocarbon increase to – 140‰ during two times of warmer climate around 1800 and 1960, and they decrease to – 180‰ when climate was cooler around 1870. These fluctuations reflect changes in the amounts of evaporative distillation of bog waters as air temperature increased or decreased. The hydrogen isotopic composition of the bog water utilized by the *Sphagnum* changed as the evaporation rate varied.

Organic matter pyrolysis

Environmental significance

The majority of organic matter in sediments consists of macromolecules that cannot be characterized by usual chemical analyses. Pyrolysis uses heat to break the large molecules into smaller molecules that can then be chemically identified. One type of pyrolysis that has been shown to be of real value to paleolimnology is Rock-Eval pyrolysis, which was initially developed to evaluate the hydrocarbon potential of petroleum source rocks (Espitalié et al.,

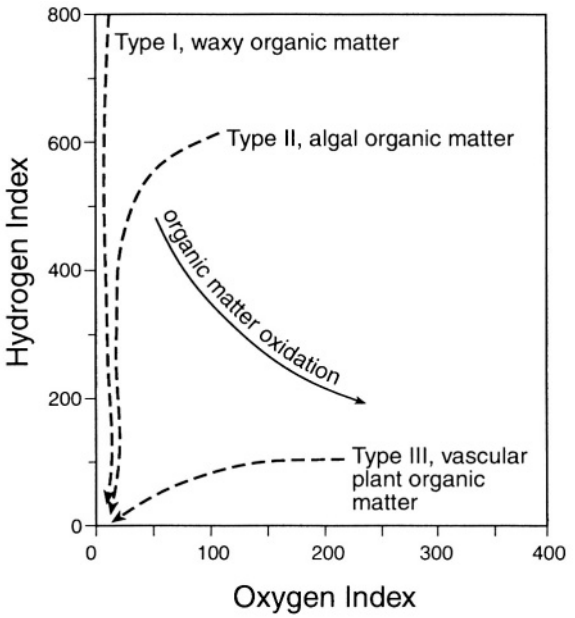


Figure 8. Rock-Eval van Krevelen-type diagrams for sedimentary organic matter. Units for hydrogen index are milligrams of hydrocarbons per gram TOC and for oxygen index are milligrams of CO_2 per gram TOC. Thermal alteration pathways of organic matter Types I, II, and III from source material to graphite are indicated by dashed lines, and the oxidation alteration pathway from hydrocarbon-rich Type I and Type II organic matter to hydrocarbon-poor material Type III is shown.

1985a). This procedure approximates elemental analyses of organic matter in ways that cannot be duplicated by actual elemental analyses.

Analytical method

Rock-Eval pyrolysis consists of the progressive heating of whole sediment samples and measurement of the amounts of hydrocarbon-like substances that escape from the sediment at different temperatures. Signals corresponding to gaseous hydrocarbons, volatile hydrocarbons, and hydrocarbon components produced due to thermal degradation of organic matter are generated during heating from 200 °C to 600 °C. The systems also calculate the amount of CO_2 created during pyrolysis. TOC is determined as the sum of residual and pyrolyzed organic carbon contents.

Interpretation

Two Rock-Eval parameters that are particularly useful to paleolimnological studies are: (1) the Hydrogen Index (HI), which represents the hydrocarbons generated from the total organic matter expressed in mg HC g^{-1} C_{org}, and (2) the Oxygen Index (OI), which roughly represents the amount of oxygen in mg CO_2 g^{-1} C_{org}. The HI values are proxies for the H/C ratios of organic matter, whereas the OI values roughly represent the O/C ratios (Espitalié et al., 1985a, 1985b). These parameters reflect the origin of the sediment organic matter (Peters, 1986) and are commonly plotted against each other in a Van Krevelen-type HI-OI

plot. HI-OI plots identify three main types of organic matter and their alteration routes during thermal maturation (Fig. 8). Type I organic matter is especially rich in hydrocarbon-producing material that is typically derived from microbial biomass or the waxy coatings of land plants. Type II organic matter is moderately rich in hydrocarbon-like material that originates from algae. Type III organic matter is poor in hydrocarbon-generating materials but rich in carbohydrates; it typifies woody plant matter. Oxidation of organic matter affects both HI values and OI values. As hydrocarbon-rich organic matter (Type I or II) is oxidized, its hydrogen content decreases while its oxygen content increases, and it takes on the HI-OI characteristics of Type III organic matter. Talbot & Livingstone (1989) provide a practical guide to interpreting Rock-Eval analyses that summarizes typical H/C ratios and HI values of the major types of organic matter delivered to lake sediments.

TOC concentrations and HI values often vary through lacustrine sedimentary sequences and indicate changes in organic deposition under different paleoenvironmental conditions (e.g., Talbot & Livingstone, 1989; Hollander et al., 1992; Ariztegui et al., 1996a; Wilkeset al., 1999; Talbot & Laerdal, 2000). A correspondence between elevated TOC and HI values is often found in some sediment intervals and implies periods of greater algal paleoproductivity. Of particular interest to paleolimnological studies, variations in the HI values of sedimentary organic matter appear to reflect changes in algal communities. Ariztegui et al. (1996b) note that sediments in Lago di Albano, Italy, that have elevated HI values correspond to periods dominated by cyanobacteria production. In contrast, sediments having lower HI values were deposited during times when diatom production was dominant.

Summary

Organic matter constitutes a minor fraction of lake sediments, yet it provides important information for paleoenvironmental reconstructions. The organic matter content of sediments is made up of the residue of former biota. The amounts and types of organic matter present in sediments consequently reflect environmental conditions that impacted ecosystems in and around a lake at different times in the past.

Plants living in the lake and in its watershed are the principal sources of the organic substances initially delivered to a lake system, and changes in the amounts and kinds of these biota reflect changes in climate and other environmental factors. Microbial reworking of organic matter components during sinking and early sedimentation markedly diminishes the total amount of organic matter while replacing many of the primary compounds with secondary ones. The magnitude and nature of the microbial activity is also influenced by environmental conditions.

Despite the generally low survival rate for most primary organic compounds, various organic matter components of lake sediments retain source information and thereby become important parts of paleolimnological and paleoclimatological records. Progressive eutrophication of lacustrine systems, changes in watershed vegetation, and the advent of agriculture are some of the paleoenvironmental aspects that can be inferred from geochemical characteristics of sediment organic matter. Bulk parameters, such as elemental and isotopic compositions, Rock-Eval pyrolysis results, and lignin oxidation products give summaries of changes in delivery of organic matter to lake sediments. Carbon/nitrogen ratios of total organic matter can reflect original proportions of aquatic and land-derived material. Carbon isotopic compositions indicate the history of productivity and carbon

recycling within the lake and provide evidence of changes in watershed vegetation that may have accompanied climate change. Nitrogen isotopic compositions record some of the dynamics of biogeochemical cycles and consequent availability of nitrogen to algae. Changes in hydrogen isotopic compositions of lake-derived organic matter reflect changes in hydrologic balances of aquatic environments. Biomarker hydrocarbon compositions indicate relative abundances of trees, shrubs, and grasses in former times.

Processes active in the lake water, in the lake catchment, and in the lake bottom impact the organic matter content of sediments, both in creating the components that collectively constitute total organic matter and in altering and degrading them. Because of the multiplicity of processes, multiple organic matter paleoenvironmental proxies should be employed. An incomplete and potentially misleading paleolimnologic reconstruction may result if only one or two proxies are used. Comparison of several independent organic geochemical proxies helps not only to improve interpretations of paleoenvironmental change but also to identify more of the processes that have participated in the changes.

Acknowledgments

We are grateful to G. Eglinton and A. Lini for reading and commenting on this chapter; their suggestions helped to make it better. We also thank S. Bernasconi for many useful discussions and especially for practical advice with the nitrogen isotope analyses carried out in the Stable Isotope Laboratory at the Swiss Federal Institute of Technology, Zurich, Switzerland. PAM appreciates the support of the Hanse-Wissenschaftskolleg, Delmenhorst, Germany, during the preparation of this contribution.

References

Altabet, M. A. & R. François, 1993. The use of nitrogen isotopic ratio for reconstruction of past changes in surface ocean nutrient utilization. In Zahn, R., T. R. Pederson, M. Kaminshi & L. Labeyrie (eds.) NATO ASI Series, Series I: Global Environmental Change Vol. 17. Carbon Cycling in the Glacial Ocean; Constraints on the Ocean's Role in Global Change; Quantitative Approaches in Paleoceanography. Springer Verlag: 281–306.

Altabet, M. A. & R. François, 1994. Sedimentary nitrogen isotopic ratio as a recorder for surface ocean nitrate utilization. Global Biogeochem. Cycles 8: 103–116.

Ariztegui, D., P. Farrimond & J. A. McKenzie, 1996a. Compositional variations in sedimentary lacustrine organic matter and their implications for high Alpine Holocene environmental changes; Lake St. Moritz, Switzerland. Org. Geochem. 24: 453–461.

Ariztegui, D., D. J. Hollander & J. A. McKenzie, 1996b. Algal dominated lacustrine organic matter can be either Type I or Type II: Evidence for biological, chemical and physical controls on organic matter quality. In Mello, M. R., L. A. F. Trindade & M. H. R. Hessel (eds.) ALAGO Special Publication: Selected Papers from 4th Latin American Congress on Organic Geochemistry. Bucaramanga, Columbia: 12–16.

Aucour, A.-M., C. Hillaire-Marcel & R. Bonnefille, 1993. A 30,000 year record of ^{13}C and ^{18}O changes in organic matter from an equatorial peatbog. In Swart, P. K., K.C. Lohmann, J. McKenzie & S. Savin (eds.) Climate Change in Continental Isotopic Records. Am. Geophys. Un. Geophys. Monogr. 78, Washington (DC): 343–351.

Barnes, M. A. & W. C. Barnes, 1978. Organic compounds in lake sediments. In Lerman, A. (ed.) Lakes-chemistry, Geology, Physics. Springer-Verlag, New York: 127–152.

Barwise, T., S. Hay & J. Thrasher, 1996. Contamination of shallow cores: A common problem. In Schumacher, D. & M. A. Abrams (eds.) Hydrocarbon Migration and its Near-surface Expression. AAPG Memoir 66, Tulsa: 359–362.

Bernasconi, S. M., A. Barbieri & M. Simona, 1997. Carbon and nitrogen isotope variations in sedimenting organic matter in Lake Lugano. Limnol. Oceanogr. 42: 1755–1765.

Beuning, K. R. M., K. Kelts, E. Ito & T. C. Johnson, 1997. Paleohydrology of Lake Victoria, East Africa, inferred from $^{18}O/^{16}O$ ratios in sediment cellulose. Geology 25: 1083–1086.

Bird, M. I., R. E. Summons, M. K. Gagan, Z. Roksandic, L. Dowling, J. Head, L. K. Fifield, R. G. Cresswell & D. P. Johnson, 1995. Terrestrial vegetation change inferred from *n*-alkane $\delta^{13}C$ analysis in the marine environment. Geochim. Cosmochim. Acta 59: 2853–2857.

Blumer, M., R. R. L. Guillard & T. Chase, 1971, Hydrocarbons of marine plankton. Mar. Biol. 8: 183–189.

Bourbonniere, R. A. & P. A. Meyers, 1996. Anthropogenic influences on hydrocarbon contents of sediments deposited in eastern Lake Ontario since 1800. Environ. Geol. 28: 22–28.

Boutton, T. W., 1991. Stable isotope ratios of natural materials: I. Sample preparation and mass spectrometric analysis. In Coleman, D. C. & B. Fry (eds.) Carbon Isotope Techniques. Academic Press, New York: 155–171.

Brand, W. A., 1996. High-precision isotope ratio monitoring techniques in mass spectrometry. J. Mass Spectr. 31:223–235.

Brenna, J. T., T. N. Corso, H. J. Tobias & R. J. Caimi, 1997. High-precision continuous-flow isotope ratio mass spectrometry. Mass Spectr. Rev. 16: 227–258.

Brenner, M., T. J. Whitmore, J. H. Curtis, D. A. Hodell & C. L. Schelske, 1999. Stable isotope ($\delta^{13}C$ and $\delta^{15}N$) signatures of sedimented organic matter as indicators of historic lake trophic state. J. Paleolimnol. 22: 205–221.

Brincat, D., K. Yamada, R. Ishiwatari, H. Uemura & H. Naraoka, 2000. Molecular-isotopic stratigraphy of long-chain *n*-alkanes in Lake Baikal Holocene and glacial age sediments. Org. Geochem. 31:287–294.

Burgoyne, T. W. & J. M. Hayes, 1998. Quantitative production of H_2 by pyrolysis of chromatographic effluents. Anal. Chem. 70: 5136–5141.

Calvert, S. E., B. Nielsen & M. R. Fontugne, 1992. Evidence from nitrogen isotope ratios for enhanced productivity during formation of eastern Mediterranean sapropels. Nature 359: 223–225.

Collister, J. W., G. Rieley, B. Stern, G. Eglinton & B. Fry, 1994. Compound-specific $\delta^{13}C$ analyses of leaf lipids from plants with differing carbon dioxide metabolisms. Org. Geochem. 21: 619–627.

Cranwell, P. A., 1973. Chain-length distribution of *n*-alkanes from lake sediments in relation to post-glacial environmental change. Freshwater Biol. 3: 259–265.

Cranwell, P. A., 1982. Lipids of aquatic sediments and sedimenting particulates. Progr. Lipid Res. 21:271–308.

Cranwell, P. A., G. Eglinton & N. Robinson, 1987. Lipids of aquatic organisms as potential contributors to lacustrine sediments - II. Org. Geochem. 11: 513–527.

Dean, W. E., 1974. Determination of carbonate and organic matter in calcareous sediments and sedimentary rocks by loss on ignition: comparison with other methods. J. Sed. Petrol. 44: 242–248.

Dean, W. E., 1999. The carbon cycle and biogeochemical dynamics in lake sediments. J. Paleolimnol. 21: 375–393.

Dean, W. E., T. S. Ahlbrandt, R. Y. Anderson & J. P. Bradbury, 1996. Regional aridity in North America during the middle Holocene. The Holocene 6: 145–155.

DeNiro, M. J. &S. Epstein, 1981. Influence of diet on the distribution of nitrogen isotopes in animals. Geochim. Cosmochim. Acta 45: 341–351.

Eglinton, G. & R. J. Hamilton, 1963. The distribution of alkanes. In Swaine, T. (ed.) Chemical Plant Taxonomy. Academic: 187–217.

Eglinton, G. & R. J. Hamilton, 1967. Leaf epicuticular waxes. Science 156: 1322–1335.

Engleman, E. E., L. L. Jackson & D. R. Norton, 1985. Determination of carbonate carbon in geological materials by coulometric titration. Chem. Geol. 53: 125–128.

Ertel, J. R. & J. I. Hedges, 1984. The lignin component of humic substances: Distribution among soil and sedimentary humic, fulvic, and base-insoluble fractions. Geochim. Cosmochim. Acta 48: 2065–2074.

Ertel, J. R. & J. I. Hedges, 1985. Sources of sedimentary humic substances: vascular plant debris. Geochim. Cosmochim. Acta 49: 2097–2107.

Espitalié, J., G. Deroo & F. Marquis, 1985a. La pyrolyse Rock Eval et ses applications. 2de partie. Revue de l'Institut Français du Pétrole 40: 755–784.

Espitalié, J., G. Deroo & F. Marquis, 1985b. La pyrolyse Rock Eval et ses applications. 3éme partie. Revue de 1'Institut Français du Pétrole 41: 73–89.

Fogel, M. L. & L. A. Cifuentes, 1993. Isotope fractionation during primary production. In Engel, M. H. & S. A. Macko (eds.) Organic Geochemistry: Principles and Applications. Plenum Press, New York: 73–98.

François, R., M. A. Altabet & L. H. Burckle, 1992. Glacial to interglacial changes in surface nitrate utilization in the Indian sector of the Southern Ocean as recorded by sediment $\delta^{15}N$. Paleoceanography 7: 589–606.

Giger, W., C. Schaffner & S. G. Wakeham, 1980. Aliphatic and olefinic hydrocarbons in recent sediments of Greifensee, Switzerland. Geochim. Cosmochim. Acta 44: 119–129.

Gu, B., C. L. Schelske & M. Brenner, 1996. Relationship between sediment and plankton isotope ratios and primary productivity in Florida Lakes. Can. J. Fish. Aquat. Sci. 53: 875–883.

Hassan, K. M., J. B. Swinehart & R. F. Spalding, 1997. Evidence for Holocene environmental change from C/N ratios and $\delta^{13}C$ and $\delta^{15}N$ values in Swan Lake sediments, western Sand Hills, Nebraska. J. Paleolimnol. 18: 121–130.

Hedges, J. I. & D. C. Mann, 1979. The characterization of plant tissues by their lignin oxidation products. Geochim. Cosmochim. Acta 43: 1803–1807.

Hedges, J. I. & P. L. Parker, 1976. Land-derived organic matter in surface sediments from the Gulf of Mexico. Geochim. Cosmochim. Acta 40: 1019–1029.

Hedges, J. I., J. R. Ertel & E. B. Leopold, 1982. Lignin geochemistry of a Late Quaternary core from Lake Washington. Geochim. Cosmochim. Acta 46: 1869–1877.

Herezeg, A., 1988. Early diagenesis of organic matter in lake sediments: A stable carbon isotope study of pore waters. Chem. Geol. 72: 199–209.

Hilkert, A. W., C. D. Douthitt, H. J. Schlüter & A. W. Brand, 1999. Isotope ratio monitoring gas chromatography/mass spetrometry of D/H by high temperature conversion isotope ratio mass spectrometry. Rapid Commun. Mass Spectrom. 13: 1226–1230.

Hodell, D. A. & C. L. Schelske, 1998. Production, sedimentation, and isotopic composition of organic matter in Lake Ontario. Limnol. Oceanogr. 43: 200–214.

Hollander, D. J. & J. A. MacKenzie, 1991. CO_2 control on carbon-isotope fractionation during aqueous photosynthesis: A paleo-pCO_2 barometer. Geology 19: 929–932.

Hollander, D. J., J. A. MacKenzie & H. L. ten Haven, 1992. A 200 year sedimentary record of progressive eutrophication in Lake Greifen (Switzerland): Implications for the origin of organic-carbon rich sediments. Geology 20: 825–828.

Huang, Y, K. H. Freeman, T. I. Eglinton & F. A. Street-Perrott, 1999b. $\delta^{13}C$ analyses of individual lignin phenols in Quaternary lake sediments: A novel proxy for deciphering past terrestrial vegetation changes. Geology 27: 471–474.

Huang, Y., F. A. Street-Perrott, R. A. Perrott, P. Metzger & G. Eglinton, 1999a. Glacial-interglacial environmental changes inferred from molecular and compound-specific $\delta^{13}C$ analyses of sediment from Sacred Lake, Mt. Kenya. Geochim. Cosmochim. Acta 63: 1383–1404.

Huffman, E. W. D., 1977. Performance of a new carbon dioxide coulometer. Microchem. J. 22: 567–573.

Johns, R. B. (ed.), 1986. Biological Markers in the Sedimentary Record. Elsevier, Amsterdam.

Kaushal, S. & M. W. Binford, 1999. Relationship between C : N ratios of lake sediments, organic matter sources, and historical deforestation of Lake Pleasant, Massachusetts, USA. J. Paleolimnol. 22: 439–442.

Keeley, J.E. & D. R. Sandquist, 1992. Carbon: freshwater plants. Plant Cell Environ. 15: 1021–1035.

Kendall, C., 1998. Tracing nitrogen sources and cycling in catchments. In Kendall, C. & J. J. McDonnell (eds.) Isotope Tracers in Catchment Hydrology. Elsevier: 519–576.

Kendall, C. & E. Grim, 1990. Combustion tube method for measurement of nitrogen isotope ratios using calcium oxide for total removal of carbon dioxide and water. Anal. Chem. 62: 526–529.

Laws, E. A., B. N. Popp, R. R. Bidigare, M. C. Kennicutt & S. A. Macko, 1995. Dependence of phytoplankton isotopic composition on growth rate and $[CO_2]_{aq}$: Theoretical considerations and experimental results. Geochim. Cosmochim. Acta 59: 1131–1138.

Leopold, E. B., R. Nickman, J. I. Hedges & J. R. Ertel, 1982. Pollen and lignin records of Late Quaternary vegetation, Lake Washington. Science 218: 1305–1307.

Krishnamurthy, R. V, K. A. Syrup, M. Baskaran & A. Long, 1995. Late glacial climate record of midwestern United States from the hydrogen isotope ratio of lake organic matter. Science 269: 1565–1567.

Macko, S. A., M. H. Engel, G. Hartley, P. Hatcher, R. Helleur, P. Jackman & J. A. Silfer, 1991. Isotopic compositions of individual carbohydrates as indicators of early diagenesis of organic matter in peat. Chem. Geol. 93: 147–161.

Meier-Augcnstein, W., 1999. Applied gas chromatography coupled to isotope ratio mass spectrometry. J. Chromatogr. 842: 351–371.

Meyers, P. A., 1987. Chronic contamination of lakes by petroleum hydrocarbons: The sedimentary record. In Vandermeulen, J. H. & S. E. Hrudy (eds.) Oil in Freshwater: Chemistry, Biology, Countermeasure Technology. Pergamon Press, New York: 149–160.

Meyers, P. A., 1990. Impacts of regional Late Quaternary climate changes on the deposition of sedimentary organic matter in Walker Lake Nevada. Palaeogeogr. Palaeoclim. Palaeoecol. 78: 229–240.

Meyers, P. A., 1994. Preservation of source identification of sedimentary organic matter during and after deposition. Chem. Geol. 144: 289–302.

Meyers. P. A., 1997. Organic geochemical proxies of paleoccanographic, paleolimnologic, and paleoclimatic processes. Org. Geochem. 27: 213–250.

Meyers, P. A. & S. Horie, 1993. An organic carbon isotopic record of glacial-postglacial change in atmospheric pCO_2 in the sediments of Lake Biwa, Japan. Palaeogeogr. Palaeoclim. Palaeoecol. 105: 171–178.

Meyers, P. A. & R. Ishiwatari, 1993. Lacustrine organic geochemistry — an overview of indicators of organic matter sources and diagenesis in lake sediments. Org. Geochem. 20: 867–900.

Meyers, P. A. & E. Lallier-Verges, 1999. Lacustrine sedimentary organic matter records of Late Quaternary paleoclimates. J. Paleolimnol. 21: 345–372.

Meyers, P. A. & J. E. Silliman, 1996. Organic matter in Pleistocene to Quaternary turbidites from Sites 897, 898, 899, and 900, Iberia Abyssal Plain. In Whitmarsh. R. B., D. S. Sawyer, A. Klaus & D. G. Masson (eds.) Proc. ODP, Init. Repts., College Station, TX (Ocean Drilling Program) 149: 305–313.

Meyers, P. A. & N. Takeuchi, 1981. Environmental changes in Saginaw Bay, Lake Huron, recorded by geolipid contents of sediments deposited since 1800. Environ. Geol. 3: 257–266.

Meyers, P. A., M. J. Leenheer & R. A. Bourboniere, 1995. Diagenesis of vascular plant organic matter components during burial in lake sediments. Aq. Geochem. 1: 35–52.

Minagawa, M. & E. Wada, 1984. The stepwise enrichment of ^{15}N along food chains: further evidence and the relation between $\delta^{15}N$ and animal age. Geochim. Cosmochim. Acta 48: 1135–1140.

Müller, H., 1987. Hydrocarbons in the freshwater environment. A literature review. Arch. Hydrobiol. Beihandl. Ergib. Limnol. 24: 1–69.

Müller, G. & M. Gastner, 1971. The "Karbonat-Bombe", a simple device for the determination of the carbonate content in sediments, soils and other materials. Neues Jb. Mineralogie 10: 466–469.

Nakai, N. & M. Koyama, 1987. Reconstruction of paleoenvironment from the view-points of the inorganic constituents, C/N ratio and carbon isotopic ratio in the 1400m core taken from Lake Biwa. In Horie, S. (ed.) History of Lake Biwa. Kyoto Univ. Contrib, Kyoto: 137–156.

O'Leary, M. H., 1988. Carbon isotopes in photosynthesis. Bioscience 38: 328–336.

Peters, K. E., 1986. Guidelines for evaluating petroleum source rock using programmed pyrolysis. AAPG Bull. 70: 318–329.

Peters, K. E., R. E. Sweeney & I. R. Kaplan, 1978. Correlation of carbon and nitrogen stable isotope ratios in sedimentary organic matter. Limnol. Oceanogr. 23: 598–604.

Peterson, B. J. & B. Fry, 1987. Stable isotopes in ecosystem studies. Ann. Rev. Ecol. System 18: 293–320.

Peterson, B. J. & R. W. Howarth, 1987. Sulfur, carbon, and nitrogen isotopes used to trace organic matter flow in the salt-marsh estuaries of Sapelo Island, Georgia. Limnol. Oceanogr. 32: 1195–1213.

Prahl, F. G., J. R. Ertel, M. A. Goñi, M. A. Sparrow & B. Eversmeyer, 1994. Terrestrial organic carbon contributions to sediments on the Washington margin. Geochim. Cosmochim. Acta 58: 3035–3048.

Prokopenko, A., D. F. Williams, P. Kavel & E. Karabanov, 1993. The organic indexes in the surface sediments of Lake Baikal water system and the processes controlling their variation. IPPCCE Newslett. 7: 49–55.

Qiu, L., D. F. Williams, A. Gvorzdkov, E. Karabanov & M. Shimaraeva, 1993. Biogenic silica accumulation and paleoproductivity in the northern basin of Lake Baikal during the Holocene. Geology 21: 25–28.

Rea, D. K., R. A. Bourbonniere & P. A. Meyers, 1980. Southern Lake Michigan sediments: Changes in accumulation rates, mineralogy, and organic content. J. Great Lakes Res. 6: 321–330.

Rieley, G., R. J. Collier, D. M. Jones & G. Eglinton, 1991. The biogeochemistry of Ellesmere Lake, UK - I: source correlation of leaf wax inputs to the sedimentary record. Org. Geochem. 17: 901–912.

Rullkötter, J., 2000. Organic matter: The driving force for early diagenesis. In Schulz, H. D. & M. Zabel (ed.) Marine Geochemistry. Springer Verlag, Berlin: 129–172.

Sarazin, G., G. Michard, I. Al Gharib & M. Bernat, 1992. Sedimentation rate and early diagenesis of particulate organic nitrogen and carbon in Aydat Lake (Puy de Dôme, France). Chem. Geol. 98: 307–316.

Sifeddine, A., P. Bertrand, E. Lallier-Verges & A. J. Patience, 1996. Lacustrine organic fluxes and palaeoclimatic variations during the last 15 ka: Lac du Bouchet (Massif Central, France). Quat. Sci. Rev. 15: 203–211.

Takahashi, K., T. Yoshioka, E. Wada & M. Sakamoto, 1990. Temporal variations in carbon isotope ratio of phytoplankton in an eutrophic lake. J. Plankton. Res. 12: 799–808.

Talbot, M. R. & T. Laerdal, 2000. The Lake Pleistocene-Holocene palaeolimnology of Lake Victoria, East Africa, based upon elemental and isotopic analyses of sedimentary organic matter. J. Paleolimnol. 23: 141–164.

Talbot, M. R. & D. A. Livingstone, 1989. Hydrogen index and carbon isotopes of lacustrine organic matter as lake level indicators. Palaeogeogr. Palaeoclim. Palaeoecol. 70: 121–137.

Talbot, M. R. & T. Johannessen, 1992. A high resolution palaeoclimatic record for the last 27,500 years in tropical West Africa from the carbon and nitrogen isotopic composition of lacustrine organic matter. Earth Planet. Sci. Lett. 110: 23–37.

Tenzer, G. E., P. A. Meyers & P. A. Knoop, 1997. Sources and distribution of organic and carbonate carbon in surface sediments of Pyramid Lake, Nevada. J. Sed. Res. 67: 887–893.

Teranes, J. L. & S. M. Bernasconi, 2000. The record of nitrate utilization and productivity limitation provided by $\delta^{15}N$ values in lake organic matter — A study of sediment trap and core sediments from Baldeggersee, Switzerland. Limnol. Oceanogr. 45: 801–813.

Thompson, S. & G. Eglinton, 1978. The fractionation of a recent sediment for organic geochemical analyses. Geochim. Cosmochim. Acta 42: 199–207.

Verardo, D. J., P. N. Froelich & A. McIntyre, 1990. Determination of organic carbon and nitrogen in marine sediments using the Carlo Erba NA 1500 analyzer. Deep-Sea Res. 37: 157–165.

Wakeham, S. G., 1976. A comparative survey of petroleum hydrocarbons in lake sediments. Mar. Poll. Bull. 7: 206–211.

Wakeham, S. G., 1977a. A characterization of the sources of petroleum hydrocarbons in Lake Washington. J. Water Poll. Cont. Fed. 49: 1680–1687.

Wakeham, S. G., 1977b. Hydrocarbon budgets for Lake Washington. Limnol. Oceanogr. 22: 952–957.

Wilkes, H., A. Ramrath & J. F. W. Negendank, 1999. Organic geochemical evidence for environmental changes since 34,000 yrs BP from Lago di Mezzano, central Italy. J. Paleolimnol. 22: 349–365.

White, J. W. C., J. R. Lawrence & W. S. Broecker, 1994. Modeling and interpreting D/H ratios in tree rings: A test case of white pine in the northeastern United States. Geochim. Cosmochim. Acta 58: 851–862.

Yamamuro, M. & H. Kayanne, 1995. Rapid direct determination of organic carbon and nitrogen in carbonate-bearing sediments with a Yanaco MT-5 CHN analyzer. Limnol. Oceanog. 40: 1001–1005.

Xie, S., C. J. Nott, L. A. Avsejs, F. Volders, D. Maddy, F. M. Chambers, A. Gledhill, J. F. Carter & R. P. Evershed, 2000. Palaeoclimate records in compound-specific δD values of a lipid biomarker in ombrotrophic peat. Org. Geochem. 31: 1053–1057.

10. PALEOLIMNOLOGICAL METHODS AND APPLICATIONS FOR PERSISTENT ORGANIC POLLUTANTS

JULES M. BLAIS (jblais@science.uottawa.ca)
Program for Environmental and Chemical Toxicology
Department of Biology, University of Ottawa
30 Marie Curie St., P.O. Box 450, Stn. A
Ottawa, Ontario KIN 6N5, Canada

DEREK C.G. MUIR (derek.muir@cciw.ca)
Environment Canada, National Water Research Institute
867 Lake shore Road, Burlington
Ontario, L7R 4A6, Canada

Keywords: persistent organic pollutants, paleolimnology, pesticides, PCB, polyaromatic hydrocarbon, organochlorine

Introduction

In 1998, the United Nations Economic Commission for Europe (UNECE) issued a Protocol on Long Range Transport for a hemispheric reduction of emissions of 16 persistent organic pollutants (POPs) (UNECE, 1998). With the exception of polyaromatic hydrocarbons, these chemicals are all halogenated organic compounds (Tables I and II) that are characterized by a high toxicity, a relative insolubility in water, and a high capacity for environmental persistence and biomagnification in foodchains. Many of these chemicals or their metabolites have been shown to affect immune and reproductive systems, and some are known for their ability to interfere with endocrine function. Perhaps the best known case is the metabolite p,p'-DDE which has been linked to egg shell thinning in birds (Longcore & Stendell, 1977) and has anti-androgen properties (USEPA, 1997a).

Their environmental persistence is due in part to the fact that the carbon-chlorine covalent bonds have a relatively high bond strength, which imparts stability and environmental persistence to these molecules (Fiedler & Lau, 1998). Once these chemicals are dispersed, they are capable of persisting for many years in the environment, with environmental half-lives often on the order of years to decades (Mackay et al., 1992, 1997). Most POPs are only sparingly soluble in water (Table I) with water solubilities ranging between 10^{-6} and $7\,g\,m^{-3}$ (Mackay et al., 1992, 1997). The fact that they are rapidly assimilated in lipids and are excreted and metabolized very slowly causes them to be biomagnified with concentrations increasing at each trophic level. In some cases, lipids from top aquatic carnivores in freshwater systems (e.g., lake trout, burbot) are more than 10^9 times more



W. M. Last & J. P. Smol (eds.), 2001. *Tracking Environmental Change Using Lake Sediments. Volume 2: Physical and Geochemical Methods*. Kluwer Academic Publishers, Dordrecht, The Netherlands.

Table I. The UNECE list of 16 persistent organic pollutants (UNECE Protocol 1998). Data are from Mackay et al. (1992; 1997). Henry's Law Constants and vapor pressures are calculated for 20 °C.

Compound	Approximate number of components[1]	Water solubility ($g\ m^{-3}$)	Henry's Law Constant ($Pa\ m^3\ mol^{-1}$)	Log Kow	Subcooled vapor pressure (Pa)
Chlorinated Pesticides					
Aldrin	1	0.02	91.2	3.01	5×10^{-3}
Dieldrin	1	0.17	1.12	5.20	5×10^{-4}
DDT	6	5.5×10^{-3}	2.36	6.19	2×10^{-5}
Endrin	1	0.23	0.033	5.20	2×10^{-5}
Chlordane	~20?	0.056	0.342	6.0	4×10^{-4}
Chlordecone (kepone)	1	3.0	0.005	5.4	5×10^{-2}
Hexachlorocyclohexanes	5	7.3	0.15	3.8	2.7×10^{-2}
Mirex	1	6.5×10^{-5}	839	6.9	1×10^{-4}
Toxaphene	~200	0.5	0.745	5.5–6.5	9×10^{-4}
Heptachlor	1	0.056	353	5.3	0.053
Industrial Products					
PCBs	209	See Table II			
Hexachlorobenzene	1	0.005	131	5.5	2×10^{-3}
Hexabromobiphenyl	42	?	?	9.1	
Byproducts					
PCDD[2]	75	0.019	3.34	6.8	2×10^{-7}
PCDF[2]	75	0.42	1.46	6.1	2×10^{-6}
Polyaromatic hydrocarbons (PAHs)	18	See Table II			

[1] Approximate number of components in technical mixtures and persistent metabolites. In the case of chlordane (see Dearth & Hites, 1991) and toxaphene (Zhu et al. 1994), the number refers to the number of hepta- to nonachloro- components reasonably well separated by high resolution GC. The list does not include enantiomers (optical isomers). For PAHs, only unsubstituted 2 to 5 ring compounds associated with combustion sources are listed.

[2] Physical properties for PCDD/F represented here by the 2, 3, 7, 8 TCDD/F congeners.

concentrated than the water as a result of bioconcentration and biomagnification processes (Kidd et al., 1995).

The 15 halogenated POPs (Table I) actually consist of more than 500 individual components ranging from mono-chlorobiphenyls and monochlorodibenzo-p-dioxins/dibenzofurans, to decachlorobiphenyls, decachlorobornanes and mirex. The above chemicals are all semi-volatile to varying degrees, which means that they may be found in gas phase and in condensed phases (water, soil, sediments) at ambient temperatures and pressures. The lower chlorinated PCBs, HCH isomers and other components with higher vapor pressures have the capacity to evaporate in warm environments and condense when they encounter cold temperatures at high latitudes (e.g., Wania & Mackay, 1993, 1996) and altitudes (Blais et al., 1998). This fractionation process has raised concerns for more remote ecosystems that may be impacted by industrial and agricultural activities in tropical and temperate latitudes, as discussed further below.

Because of the persistence and hydrophobicity of these chemicals, lake sediments can act as strong sinks, and thus are potentially useful to determine a chronological sequence of contaminant deposition. Such paleolimnological investigations are frequently used to examine changes in contaminant loading through time, as well as to identify sources and trajectories based on spatial patterns of chemical composition in sediments. Many processes

Table II. Physical-chemical properties of the polychlorinated biphenyl (PCB) homologues and some polyaromatic hydrocarbons (PAHs). Data are from Mackay et al. (1995, 1997).

PCB Homologue	Molecular weight ($g\ mole^{-1}$)	Subcooled vapor pressure (Pa)	Water solubility ($g\ m^{-3}$)	Log K_{OW}	PCB #
Monochlorobiphenyl	188.7	0.9–2.5	1.21–5.5	4.3–4.6	1–3
Dichlorobiphenyl	223.1	0.008–0.60	0.06–2.0	4.9–5.3	4–15
Trichlorobiphenyl	257.5	0.003–0.22	0.015–0.4	5.5–5.9	16–39
Tetrachlorobiphenyl	292.0	0.002	0.0043–0.010	5.6–6.5	40–81
Pentachlorobiphenyl	326.4	0.0023–0.051	0.004–0.02	6.2–6.5	82–127
Hexacholorbiphenyl	360.9	0.0007–0.012	0.0004–0.0007	6.7–7.3	128–169
Heptachlorobiphenyl	395.3	0.00025	0.000045–0.0001	6.7–7	170–193
Octachlorobiphenyl	429.8	0.0006	0.0002–0.0003	7.1	194–205
Nonachlorobiphenyl	464.2	–	0.00018–0.0012	7.2–8.2	206–208
Decachlorobiphenyl	498.7	0.00003	0.000001–0.0001	8.26	209
Polyaromatic Hydrocarbons					
Anthracene	178.2	0.0778	0.045	4.54	
Benz(a)anthracene	228.3	6.06×10^{-4}	0.011	5.91	
Benzo(a)pyrene	252.3	2.13×10^{-5}	0.0038	6.04	
Chrysene	228.3	1.07×10^{-4}	–	1.65	
Fluoranthene	202.3	8.72×10^{-3}	0.26	5.22	
Naphthalene	128.19	36.81	31	3.37	
Pyrene	202.3	0.0119	0.132	5.18	

affect the distribution of organic contaminants in sediments, and historical interpretations of sediment cores must consider these factors. In this chapter, we discuss advances in extraction and analytical methods for chlorinated contaminants, review some of the major processes that affect the fate of persistent organic pollutants, and discuss their implications for paleolimnological investigations.

Advances in extraction and quantitative analytical techniques for POPs in sediment

Reliable extraction and quantitation procedures are clearly essential for the determination of POPs in sediment. During the 1950's and '60's, it was established that methods used for extraction of pesticides from plant and animal tissue, such as Soxhlet extraction, shaking or blending of a dry sample mixture with an organic solvent, worked well for isolation of chlorinated pesticides from soils with some modifications (Saha, 1971; Chiba, 1969). The major modification was the use of polar solvents (e.g., dichloromethane DCM), or mixtures (acetone:hexane, 1:1) which were found to give better recoveries of POPs in soils than nonpolar solvents like hexane. More robust conditions (e.g., using alkaline or acid preextraction), did not improve recoveries of neutral organics such as chlorinated pesticides from soils because of co-extraction of humic and fulvic acids which created problems in subsequent isolation steps (Chiba, 1969). Also some chlorinated aliphatic pesticides (e.g., DDT) were susceptible to degradation (dehydrochlorination) under alkaline conditions.

Although early method development work was done on soils, the methodology was soon adopted for sediments (Miles & Harris, 1971). Most studies now use rather similar extraction, isolation and quantitation methodologies reflecting the maturity of the knowledge base on this topic. We will not attempt a comprehensive review of analytical methods for sediments, but instead present an overview of quality assurance, extraction, isolation and quantitation steps widely used for determination of POPs. For greater detail we recommend the reader consult well-reviewed analytical methods publications such as USEPA Methods 1613, 1668 and 3541 and ASTM (1989). Our aim is to inform scientists in the paleolimnological and related environmental organic geochemistry area of the basic steps and quality assurance criteria for the determination of POPs in sediments, and then discuss factors that affect their distribution in sediments.

Quality assurance steps in the determination of POPs

During sample collection

In general there are few standard, well-documented procedures for assuring quality control of field collection of sediments for POPs. The basic approach is to consider the possible sources of contamination during all phases of the field work from collection, transport to and from the site, and during storage. Most contamination from POPs arises from past use of PCBs in building materials and electrical devices, past use of organochlorine (OC) pesticides for pest control, and from combustion (polyaromatic hydrocarbons (PAHs), and polychlorinated dibenzo-p-dioxins and furans (PCDD/Fs). Sediment coring devices should be rinsed with solvent (acetone is useful), air-dried and stored in polyethylene bags or other sealed containers during transport. Between sites, thorough washing with water from a clean field site, followed by solvent rinsing, is satisfactory except for highly contaminated sediments. At the latter sites, additional rinsing with solvent and trace residue grade water may be required. During extrusion of cores, samples should be placed in clean, thick walled, polyethylene bags and tightly sealed, or stored in pre-cleaned glass jars with Teflon or aluminum foil lined screw caps. Polyethylene is a suitable storage medium for sediments in our experience, but may contain plasticizers (phthalates) and flame retardant chemicals. As a precaution, it may be useful to ask the analytical laboratory to pre-extract a sample of any container being considered for use by rinsing with solvent (e.g., DCM or hexane), to determine if it contains any compounds interfering with the analysis of POPs.

By definition, POPs are quite stable in sediments in the short term and therefore samples can be safely stored for periods of months to years at 0°C or lower. To date there have been no storage stability studies of POPs in sediment; however, slow dechlorination is a common degradation pathway in the environment e.g., DDT to DDD. A more pressing concern is avoiding contamination from the storage building. Buildings built prior to the mid- 1970's are likely to have ng/m^3 PCBs in air (Wallace et al., 1996) which may eventually contaminate samples that are not in well-sealed containers with low levels of contamination.

In the laboratory

For low level (i.e., low ng/g dry weight PAHs and PCBs and pg/g level PCDD/Fs), some laboratories conduct analyses for POPs in Class A clean rooms. These rooms are physically isolated from other laboratory space by special entry passages, and utilize positive pressured, carbon and HEPA filtered air. This reduces inadvertent introduction of lab air which

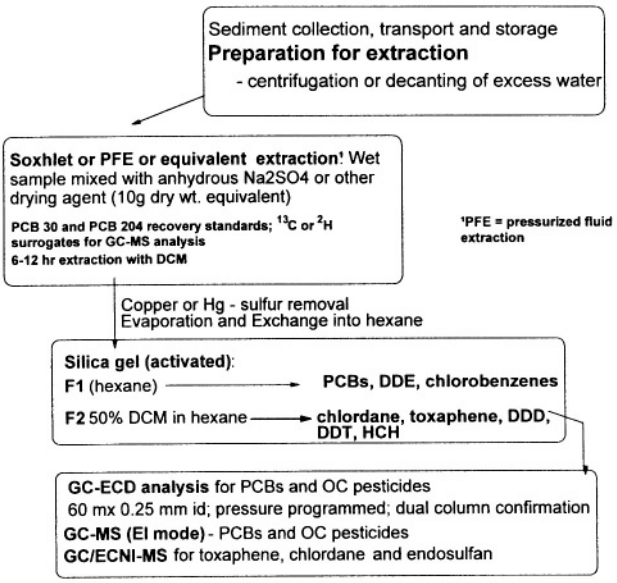


Figure 1. General procedure for analyzing POPs in sediments.

can contain elevated levels of some contaminants found in building materials (e.g., PCBs in paints, window gaskets), computer equipment (e.g., brominated diphenyl ethers), and PAHs from urban dust and fuel sources. All solvents used for extraction are glass distilled, trace residue grade. Glassware is precleaned by rinsing with solvents. Many laboratories preheat glassware in clean ovens to 300–400°C overnight to remove semivolatile contaminants. Sodium sulfate is heated at 600 °C before use.

Sample preparation and extraction steps

Extraction, isolation and quantitation steps for POPs are summarized in Figure 1. Soxhlet extraction remains the method used by most analysts for recovery of chorinated pesticides and PCBs from sediments, and the one which other techniques such as shaking with solvent, ultrasonication, microwave assisted extraction, pressurized fluid extraction (PFE) and supercritical fluid extraction, are compared.

Prior to extraction in a Soxhlet apparatus or by other related techniques such as pressurized fluid extraction (PFE), an anhydrous mixture is prepared usually by mixing wet sediment (excess water removed by decanting or low speed centrifugation) with anhydrous, precleaned sodium sulfate. Pre-drying of sediment (by freeze drying, oven or air drying) has been commonly employed but is not recommended for sediments with low levels of POPs because of possible contamination from laboratory air (Wallace et al., 1996; Alcock et al., 1994).

Analysis of clay-silt fractions rather than bulk sediments has also been recommended because these fine particle fractions usually contain most of the mass of hydrophobic

organics (Price & Birge, 1999). This is less of a problem for sediment core material, which is generally fine grained if collected from depositional zones. Furthermore, excessive handling of the sample (e.g., wet or dry sieving to isolate the fine fraction), may give rise to additional contamination as discussed above.

Surrogate recovery standards are added to each sample at the extraction step to monitor the performance of the extraction and cleanup steps. PCBs 30 and 204 are often used because they are not present in commercial PCB mixtures. For samples to be analysed by mass spectrometry, these surrogates are usually deuterated (PAHs) or ^{13}C labelled (most OC pesticides. PCDD/Fs and PCB congeners). Sample batches (6–12 samples) should include a blank (all reagents except sediment) and a certified reference material. Soxhlet extraction times vary widely but relatively long contact times i.e., >6 hrs are generally used. For OC pesticides and PCBs, most laboratories use dichloromethane or acetone:hexane. For PCDD/Fs, which are sparingly soluble in DCM, toluene is recommended as the extraction solvent for sediment either by itself or as a second extraction (Oehme et al., 1993).

Use of certified reference sediments is critical to evaluating performance of extraction and subsequent analytical steps. Sediment CRMs are available from the National Institute of Standards and Technology (NIST, Gaithersburg MD, www.Nist.gov), BCR (Brussels), Environment Canada, National Water Research Institute (www.cciw.ca) and National Research Council of Canada (Halifax). These sediments have been thoroughly analyzed for a range of POPs by independent laboratories. While surrogates added at the extraction step allow evaluation of any losses of analyte during extraction and isolation steps, they do not evaluate the recovery of naturally incorporated contaminants in sediments. This is only possible by using ^{14}C labeled chemicals incorporated in the field (Chiba, 1969; Saha, 1971) or in long term incubations of sediment where the analyte has been well equilibrated. Although relatively expensive, CRMs are useful for comparing extraction efficiencies of various solvents and techniques because results for individual analytes can be compared with the certified values. A limitation to this approach is that CRMs are usually certified only for a limited suite of individual PCB congeners or OC pesticide components.

Isolation steps

Sediment extracts usually contain co-extractive pigments, plant waxes and other related nonpolar components, as well as sulfur. If acetone has been used for extraction, it can be removed by partitioning with water and hexane (Gchswend & Hites, 1981). Sulfur removal is accomplished by stirring the crude extract with activated copper filings (prewashed with HCl and stored in hexane) or mercury. The sample extract is then concentrated to small volume using a rotary evaporator. The residual extract is exchanged into a nonpolar solvent, usually hexane or pentane, by rinsing the flask with small amounts of solvent. It is critical to have the final extract in a nonpolar solvent for chromatography steps.

Removal of co-extractive pigments is generally accomplished using silica or Florisil columns (Fig. 1). For PAHs, alumina is also used. Alumina columns may dehydrochlorinate some aliphatic organochlorines, and therefore should be avoided if halogenated compounds are being determined. Florisil is known to retain PAHs and planar halogenated aromatics such as PCDD/Fs, and so is generally not used for these analytes. Additional cleanup steps are usually employed for isolation of PCDD/F and coplanar PCBs in sediment. These

include use of KOH coated silica, sulfuric acid coated silica and carbon columns (Kjeller & Rappe, 1995; Oehme et al., 1993). Size exclusion chromatography using high performance liquid chromatography (HPLC) columns has also been used for isolation of POPs especially PAHs. A typical procedure (Fig. 1) is as follows: Florisil columns (1.2% deactivated; 100–200mm mesh) are prepared by carefully pouring preweighed Florisil into hexane filled columns (1 cm outer diameter). The column is topped with anhydrous sodium sulfate. The hexane is drained to the top of the column and sample extract is carefully added with a Pasteur pipet. The sample is rinsed into the column and then a reservoir is added, and hexane is used to elute PCBs and other very hydrophobic OCs. The hexane is followed by elution with hexane:DCM (15:85) to isolate HCH, toxaphene, chlordane related compounds, p,p'-DDT and other moderately polar OC pesticides and finally, elution with (1:1) hexane:DCM to elute dieldrin, endosulfan and heptachlor epoxide. Actual volumes of eluate will depend on length and volume of the column bed and are adjusted for each batch of absorbent. PCBs and OC pesticides are isolated and separated on silica columns with similar elution solvents. PAHs are generally separated from saturated hydrocarbons by the same type of elution scheme; first elution with hexane or pentane for the alkanes then with DCM for PAHs (Gschwend & Hites, 1981; Yunker et al., 1996).

Quantitative analysis by gas chromatography

Capillary gas chromatography coupled with a electron capture detector (ECD) and/or a mass spectrometer (MS) is universally used for analysis of the 500+ components of the 16 POPs (Table I). The only exception is for PAHs where HPLC with fluorescence detection is a practical alternative especially for unsubstituted 3 to 5 ring compounds.

A reliable supply of analytical standards is crucial for quantitative analysis of POPs. Unless the laboratory has good facilities for storage and handling of pure, crystalline standards, it is preferable to purchase analytical standards in pre-certified solutions from commercial suppliers. These standards must be stored so as to limit evaporation of solvent. Working standards are prepared, in the solvent used for gas chromatography (GC) injection, from a more concentrated solution for daily or weekly use.

Capillary GC-ECD separation of POPs is conducted with a $60\,m \times 0.25\,\mu m$ DB-5 (5% phenylmethyl silicone open tubular coated) column or with dual 30 or 60 m DB5 and DB17 columns using hydrogen or helium carrier gas. Various film thicknesses of the liquid phase on the column are available; typically 0.1 to $0.25\,\mu m$ are used. The use of dual columns allows confirmation of PCBs and OC pesticides which co-elute on one column but not on another. Pressure programming, now widely available, aids in resolution especially of higher molecular weight OCs (higher chlorinated PCBs) which have long retention times. Split-splitless injection is generally used because it is less susceptible to contamination of the injection port from co-extractive materials remaining in the isolated extracts, compared with on column injection. Automated injection systems are widely used as they give improved reproducibility compared to manual injections.

GC-MS is conducted with the same types of capillary columns using He carrier gas. Gas chromatographic conditions are usually similar to GC-ECD. There are a range of possible detection modes for POPs by GCMS and the reader is referred to recent texts on the subject (Chapman, 1995, Oehme, 1999). Electron ionization (EI) mode is used for

determination of PAHs and PCBs. This mode involves ionization, typically at 70 eV, with detection of positive ion fragments. High sensitivity is achieved for aromatic compounds which do not fragment and yield intense parent ions. Electron capture negative ionization MS detection is a softer ionization technique widely used to detect highly chlorinated compounds especially chlorinated aliphatics such as toxaphene, which fragment in EI mode. In this mode, methane or argon are used as modifying gases in the ionization source of the mass spectrometer and negative ions are detected. Quantitative analysis by GC-MS is often performed by "isotope dilution" technique in which ^{13}C or deuterated internal standards, added at the extraction step, are quantified and the amount of native compounds present in the sample is determined by a ratio to the known amount of surrogate present. This method has the advantage of adjusting automatically for losses of analyte in the workup steps. It can only be applied to analytes that are structurally identical or behave very similarly to the surrogate during extraction and isolation steps. In addition to surrogates added at the extraction step, other surrogates are usually added just prior to GC-MS (or ECD analysis) to correct for small changes in volume of the solvent in the vial used for injection into the GC. This permits use of small final volumes (e.g., 100 μL) or smaller in the case of PCDD/F analysis. Confirmation of the identity of each peak by GC-MS is based on retention time and correct ratios of 2 characteristic fragment ions using selected ion monitoring. Using high resolution MS improves the specificity of the analysis for POPs and is required in standard methods of analysis of PCDD/F and co-planar PCBs (USEPA 1613, 1668). With the higher resolving power of the high-resolution mass spectrometer (HRMS), characteristic ions are distingished at millimass resolution resulting in fewer false positives and lower detection limits.

At least 150 individual organochlorines that make up the 15 organohalogen compounds on the POPs list (Table I) can theoretically be routinely quantified by capillary GC-ECD using commercially available standards and peak integration software. A list of these compounds (with some co-eluting PCB congeners) is given in Table i. It must be stressed that it is difficult and time consuming to achieve reproducible results for all components, especially those at low concentrations. Inter-laboratory studies of PCB congeners in marine sediment have shown that the majority of experienced laboratories were within 20% of target values in cleaned up and non-cleaned up sediment extracts for 10 major PCB congeners (de Boer, 1998). Other studies have shown that good agreement between experienced labs can be obtained on far larger number of PCB congeners and OC pesticides in biological samples (Schantz et al., 1996).

Method detection limits

Detection of POPs in sediments, especially in samples from remote locations, is limited by sample size, sensitivity of the instrument, reproducibility of the injection and instrument response, and blank values. Method detection limits (MDLs) are calculated taking into account these parameters (Keith, 1991). The MDL is usually defined as the blank value for an analyte in a reagent blank (or the practical instrumental detection limit if the blank is zero) +3*Standard deviation of the analyte peak in a low concentration sample or blank (Keith, 1991). The risk of false positives or negatives becomes progressively lower the higher the result is above the MDL and is 0.1% at 6xSD above the mean blank. This latter limit is called the Reliable Detection Limit (Keith, 1991). Typically MDLs for GC-ECD for

Table III. List of persistent organochlorine (OC) compounds that can be routinely determined by GC-ECD or GC-MS in sediment sample extracts. # Cl = number of chlorine atoms.

PCBs	# Cl	PCBs	# Cl	PCBs	# Cl	Other OCs	Group
3	1	56/60	4/4	187	7	β-endosulfan	
4/10	2	91	5	183	7	1245-Cl_4benzene	CBz
7	2	84/89	5	128	6	1234-Cl_4benzene	CBz
6	2	101	5	185	7	Cl_5-benzene	CBz
8/5	2	99	5	174	7	Cl_6-benzene	CBz
19	3	83	5	177	7	α-HCH	HCH
18	3	97	5	171	7	β-HCH	HCH
17	3	87	5	156	6	γ-HCH	HCH
24/27	3	85	5	201/157	8/6	heptachlor	Chlordane
16/32	3	136	6	172/197	7/8	Cl_8-sytrene	
26	3	110	5	180	7	Chlordane-C1B	Chlordane
25	3	82	5	193	8	Chlordane-C2	Chlordane
31	3	151	6	191	8	Chlordane-C3	Chlordane
28	3	144/135	6	200	9	Chlordane-C5	Chlordane
33	3	149	6	170	8	Nonachlor-III	Chlordane
22	3	118	5	190	8	oxychlordane	Chlordane
45	4	134	6	198	8	t-chlordane	Chlordane
46	4	114	5	199	8	c-chlordane	Chlordane
52	4	131	6	196/203	8/8	t-nonachlor	Chlordane
49	4	146	6	189	8	c-nonachlor	Chlordane
47	4	153	6	208	9	hept. epoxide	Chlordane
48	4	132	6	195	8	dieldrin	
44	4	105	5	207	9	endrin	
42	4	141	6	194	8	p,p'-DDE	DDT
41/71	4	130	6	205	8	p,p'-DDD	DDT
64	4	141	6	206	9	p,p'-DDT	DDT
40	4	130/176	6/7	209	10	o,p'-DDE	DDT
74	4	179	7	**Other OCs**	**Group**	o,p'-DDD	DDT
70/76	4	137	6	Toxaphene[1]		o,p'-DDT	DDT
66	4	138	6	H6-923	Tox	mirex	
95	5	158	7	H7-1001	Tox	Tetrachloro veratrole	
		178/129	7/6	B8-1413	Tox	Pentachloroanisole	
		175	7	α-endosulfan		methoxychlor	

[1] Toxaphene is best determined by GC-ECNIMS. H6-923 and H7-1001 are hexa- and heptachlorobornanes which are major toxaphene endproducts in many sediments (see Miskimmin et al., 1995; Stern et al., 1997; Rose et al., 2001).

a 10 g dry weight sediment sample analysed at a final volume of 100 μL, range from 0.02 to 0.03 ng/g for PCB congeners and most OC pesticides assuming no blank interferences. Method detection limits of POPs by GC-MS under low resolution EI-MS conditions are generally about 10x higher than for ECD. HRGC can achieve similar or lower MDLs than GC-ECD for halogenated aromatics in EI mode and for many halogenated aliphatic POPs under ECNI conditions because of higher specificity and lower blank values.

For determination of low levels of PCBs and OC pesticides in sediment cores, a slice dated to pre-1900 (i.e. prior to manufacture of PCBs) should also be analysed as a control sample. Frequently these deep slices have low levels of PCBs due to smearing of sediments downcore as the coring tube penetrates the sediments. These sediments also control for contamination on storage, or during preparation (e.g., drying). Consideration should be given to subtracting the results (congener by congener) for the deep slice. Results are expressed on a ng/g dry weight (dw) blank corrected basis.

Recent advances in analysis for persistent organics not classified as POPs

While the 15 halogenated POPs and PAHs are best analysed by GC-ECD and GC-MS, many other organic compounds in current use have similar physical properties and can be expected to partition to sediments in aquatic systems although they may be less persistent. The nonyl phenol ethylate surfactants have been shown to be relatively persistent in sediments. Analysis by HPLC-triple quad MS permitted the ethoxylates and nonyl phenol to be determined simultaneously (Shang et al., 1999). The short and medium chain chlorinated paraffins, which are complex mixtures of C10–C17 chlorinated n-alkanes, have been determined in sediments by GC-high resolution ECNI MS (Tomy et al., 1997, Tomy & Stern, 1999) following conventional extraction and cleanup procedures (Fig. 1).

Selecting an analytical lab

Leading analytical laboratories in the field of POPs measurements in sediments and soils are certified by national or international standards organizations to recognized standards such as ISO-9000. These standards ensure that sample handling after being received by the lab, certification of personnel, record keeping, storage and use of analytical standards, method certification, performance in interlab tests, and archiving of data are consistently maintained. This is essential for work that may have regulatory and legal implications. These rigorous standards come at a price. Typically costs per sample are relatively high and in some cases there is a lack of flexibility for determining new contaminants or meeting low detection limit criteria. Research oriented work on pathways and fate of POPs does not always require this level of rigor. Good quality analyses of POPs in sediments, acceptable in peer reviewed environmental science journals, can be accomplished by using a common sense approach in which most of the quality assurance steps recommended by leading certification organizations are adopted without seeking independent certification. This is a practical alternative, especially for university based scientists and those in developing countries, who may have experienced laboratory personnel and basic equipment for analysis, but may lack funding for submitting samples to a certified lab.

Transfer processes in lakes

Conducting a comprehensive paleolimnological study of persistent organic pollutants requires an understanding of the processes that lead to the eventual burial of these chemicals in sediments. Once chemicals are released into the environment, they will enter aquatic

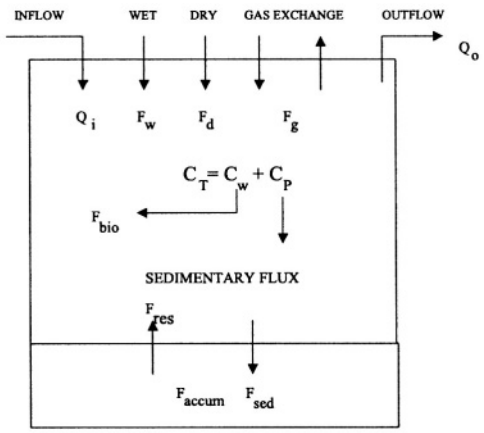


Figure 2. Schematic showing the major transfer processes of organic contaminants in lakes. Q_i and Q_o are inputs and outputs by streams, F_w, F_d, and F_g are fluxes by wet, dry and gaseous exchange, respectively. F_{bio}, F_{sed}, F_{res} and F_{accum} are fluxes by biological uptake, sedimentation, resuspension, and burial, respectively. C_T, C_w and C_p are concentrations of organic contaminants in the total, dissolved and particle associated forms. Based on Strachan & Eisenreich (1988).

environments via direct deposition on lake surfaces, and by fluvial sources. Direct deposition occurs by wet and dry deposition and by vapor exchange, each of which is shown in Figure 2. Once these compounds are in the water column, there will be an exchange between dissolved and adsorbed phases, with the latter settling to bottom sediments. Resuspension may result from bioturbation due to benthic invertebrates in surficial sediments as well as by physical resuspension by waves and water currents. Transformation by microbial metabolic processes may also result in removal of the deposited organics if the products are more water soluble. Ultimately, the distribution of organic contaminants in sediments will depend upon all of these processes.

Air-water gas exchange

Multimedia models and field data indicate that this is a dominant process for the transfer of persistent organic pollutants to lakes (e.g., Bidleman & McConnell, 1995; Mackay & Wania, 1995). Fluxes of air-water gas exchange are typically calculated using the two-film resistance model (Schwartzenbach et al., 1993). Fluxes can be in either direction and depend upon air and water concentrations, partition coefficients, and air and water resistivities.

In natural waters, the 'dissolved' concentration that is measured ($C_{w,meas}$) will contain POPs that are associated with colloids that pass through the glass fiber filter (GFF), yet are not directly involved in the process of gas exchange. We therefore adjust $C_{w,meas}$ to account for sorption to colloids. Work on the binding of POPs to dissolved organic carbon (Landrum et al., 1984, Chin et al., 1997) shows that the relation between the colloid-water partition coefficient (K_c, L kg^{-1}) and the organic carbon-water partition coefficient (K_{oc}) can be estimated simply by

$$K_c = 0.2K_{oc} \quad (1)$$

K_{oc} is estimated from the octanol-water partition coefficient (K_{ow}, Table I) using the equation of Karickhoff (1981):

$$K_{oc} = 0.41 K_{ow}. \tag{2}$$

The actual dissolved concentration (C_w) is estimated using the measured dissolved concentration $C_{w,meas}$, K_c and the concentration of DOC [(DOC), kg L^{-1}] as follows:

$$C_w = \frac{C_{w,meas}}{1 + [K_c(DOC)]}. \tag{3}$$

The flux (F_g) of organic compounds across the air-water interface (ng m^{-2} day^{-1}) is calculated with this estimate of C_w:

$$F_g = K_{ol}(C_w - C_a RT/H), \tag{4}$$

where K_{ol} is the overall mass transfer coefficient (m day^{-1}), C_a is the air (vapor) concentration of the compound (ng m^{-3}), H is Henry's Law constant (Pa m^3 mol^{-1}) R is the universal gas constant (Pa m^3 mol^{-1} K^{-1}) and T is absolute temperature (K). A negative value indicates a net flux to the water, and a positive value indicates a net flux to the air. K_{ol} is determined on the basis of air-side and water-side resistance as follows:

$$\frac{1}{K_{ol}} = \frac{1}{K_w} + \frac{RT}{HK_a}, \tag{5}$$

where K_w and K_a are the liquid and gas transfer coefficients (m day^{-1}). The air-side and water-side resistance is analogous to electrical resistance. For example, K_{ol}^{-1} (day m^{-1}) may be defined as the sum of air side resistance (R_a, day m^{-1}) and water side resistance (R_w):

$$\frac{1}{K_{ol}} = (R_a + R_w). \tag{6}$$

Air-side resistance is calculated using an empirical equation with air diffusivities (D_a, cm^2 sec^{-1}), Henry's constant (H, Pa m^3 mol^{-1}), wind speed at 10m height (U_{10}, m/sec) and RT (Schwartzenbach et al., 1993):

$$R_a = \frac{RT}{[(D_a/D_a^{H_2O})^{0.67} H(0.2U_{10} + 0.3)864]}. \tag{7}$$

Likewise, water-side resistance is calculated with water diffusivities and U_{10} as follows (Schwartzenbach et al., 1993):

$$R_w = \frac{1}{[(D_w/D_w^{O_2})^{0.57}(4 \times 10^{-5} U_{10}^2 + 4 \times 10^{-4})864]}. \tag{8}$$

Values used for $D_a^{H_2O}$ and $D_w^{O_2}$ are 0.26 cm^2/s and 2.1×10^{-5} cm^2/s, respectively. All other diffusivities are calculated using the compounds' molecular weights (M) with the following equation (Schwartzenbach et al., 1993):

$$\frac{D_x^{unknown}}{D_x^{known}} = \left(\frac{M_{known}}{M_{unknown}}\right)^{0.5}. \tag{9}$$

Table IV. Calculation of Henry's Law constants (Pa m^3 mol^{-1}) at different ambient temperatures using the format: $H(T) = H(T_{ref}) \exp[m(1/T - 1/T_{ref})]$. References are as follows: A. Kucklick et al. (1991); B. Warner et al. (1997); C. Tateya et al. (1988); D. Fendinger et al. (1989); Suntio et al. (1987); E. ten Hulsher et al. (1992); G. Murphy et al. (1987).

Compound	T_{ref}	H (T_{ref})	m	Reference
αHCH	298	0.76	−6471	A
γHCH	298	0.35	−5485	A
Dieldrin	298	0.35	−5485	B,C
DDT	296	1.2	−7868	C,D
DDD	298	0.64	−7868	C,E
HCB	293	41	−5900	F
PCB18	293	29.6	−6000	F,G
PCB44	293	18.7	−6000	F,G
PCB52	293	16.4	−6260	F
PCB101	293	17.6	−6260	F,G
PCB153	293	17	−6260	F,G
ΣPCB	293	20	−6000	E

Wind velocities are determined with an anemometer and adjusted to a 10 meter height (U_{10}) using:

$$U_z = \left[\frac{(\ln z + 8.1)}{10.4}\right] U_{10}, \tag{10}$$

where z is anemometer height and U_z is wind speed at that height (m/sec). Note that Henry's Law constants must be corrected for water temperature at time of sampling. This is accomplished a number of ways, typically using the format described in Table IV. See also reviews by Hulscher et al., (1992); Passivirta et al., (1999); and Bamford et al., (1999).

Air-water gas exchange is one of the dominant processes for the delivery of most POPs to remote areas and is strongly affected by temperature (eq. 4). For example, a drop of 8 °C in water temperature resulted in a drop in volatilization rates from 35 ng m^{-2} day^{-1} to 2 ng m^{-2} day^{-1} in the Bering and Chukchi Seas (Jantunen & Bidleman, 1996). Declining air concentrations of lindane (γHCH) in recent years has caused gas exchange in the Bering Sea to shift from a net deposition of lindane in the late 80s to a net volatilization by 1993 (Jantunen & Bidleman, 1996). Similar declines in air concentrations of PCBs have caused the Laurentian Great Lakes to become regional sources of PCBs by net volatilization from the water (Jeremiason et al., 1994). These authors showed that volatilization from the lake surface, not sedimentation to the lake bottom, was the dominant loss mechanism of PCBs in Lake Superior.

Atmospheric deposition

In theory, a water drop equilibrating with airborne pollutants in the vapor phase is inversely proportional to Henry's Law.

$$W_g = \frac{RT}{H}, \tag{11}$$

where W_g is the dimensionless gas phase scavenging efficiency, R is the universal gas constant (Pa m^3 mol^{-1} K^{-1}) and H is Henry's Law constant (Pa m^3 mol^{-1}). In practice, $W_g = C_{R,d}/C_a$, where $C_{R,d}$ is the dissolved concentration of the pollutant in rain.

The dimensionless particle phase scavenging efficiency (W_p) is defined as $C_{R,p}/C_{a,p}$ where $C_{R,p}$ is particle concentration of contaminant in rain, and $C_{a,p}$ is particle concentration of contaminant in air. W_g usually ranges from 10^3 to 10^6 and depends on particle size, particle concentration, precipitation intensity and the nature of the precipitation event (Gatz, 1975).

The total flux (ng m^{-2} day^{-1}) of chemical by wet deposition is:

$$F_w = W_g(1 - \phi)C_T P + W_p \phi C_T P, \tag{12}$$

where ϕ is the fraction of total atmospheric solute concentration on the particle phase and C_T is the total atmospheric solute concentration (vapor + particles) in ng m^{-3}, and P is precipitation (m day^{-1}). Wet deposition therefore depends on both vapor dissolution and particle scavenging by rain drops. The dominance of one process over the other depends on the gas phase and particle phase scavenging efficiencies. For example, compounds with higher H will have smaller gas phase scavenging efficiencies (eq. 6) thus vapor dissolution in water droplets would be small compared to particle scavenging by rain.

Atmospheric deposition of solutes on particles (Flux by dry deposition, F_d, ng m^{-2} day^{-1}) is estimated simply as:

$$F_d = V_d C_T \phi, \tag{13}$$

where V_d is deposition velocity (m day^{-1}). Dry deposition of many organic contaminants to lakes is generally small compared to wet deposition, with the possible exception of urban areas where aerosol concentrations (and thus ϕ) are much higher than remote locations. Wet deposition is typically a dominant delivery process to water surfaces in remote areas for many of the chemicals in Table I (Hoff et al., 1996, Jeremiasson et al., 1999). Dry deposition may be a dominant process in urban areas, however, as was recently shown in populated areas around Lake Michigan (Franz et al., 1998).

Sedimentation

The loss rate of POPs by sedimentation (F_{sed}) can be defined as follows:

$$F_{sed} = -\frac{(V_{sed}/INV_w)\phi_p}{RR}, \tag{14}$$

where V_{sed} is the mass sedimentation rate (mg m^{-2} day^{-1}), INV_w is the inventory of total suspended sediment in the water column on a volume basis (mg m^{-3}), ϕ_p is the fraction of chemical on suspended particles, and RR is the sediment recycling ratio.

The recycling ratio is the ratio of chemical concentration on settling solids relative to the chemical concentration on surficial sediments and represents the extent that the contaminants are degraded and desorbed from particles before sediment burial. Recycling ratios for polychlorinated biphenyls (PCBs) were shown to range from 5 to 2400 in Lake Superior (Baker et al., 1991) with the higher values for lower molecular weight congeners (Fig. 3). These results clearly show that the sediment core profiles are skewed relative to

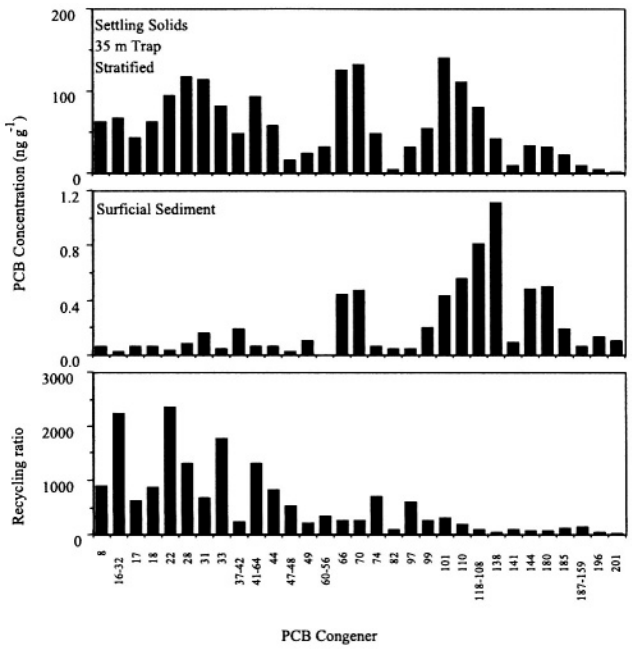


Figure 3. Congener-specific analysis of PCBs in settling solids and surficial sediments from Lake Superior. Their ratio (the recycling ratio) is plotted beneath. Data are from Baker et al. (1991).

the congener abundance of settling particles, thus the concentrations of contaminants in the sediment record are not identical to contaminants in suspension in the water column and interpretations of the data must reflect this fact. Comparing chemical composition on settling particles with that of surface sediments may allow a clearer interpretation of the core profile by identifying those compounds that resist rapid degradation or desorption from sediment.

The effect of lake trophic status

Sedimentation of phytoplankton biomass is an effective pump for contaminants to sediments. Several studies have shown that phytoplankton biomass can significantly influence POP distributions in the water column (e.g., Baker et al., 1991; Dachs et al., 1997; Dachs et al., 1999). In general, high biomass results in lower concentrations of POPs in phytoplankton (Chung et al., 1999) and water (Larsson et al., 1992) and high rates of phytoplankton biomass production result in rapid depletion of POPs in the water column (Axelman et al., 1997). This, in turn, affects air-water gas exchange (eq. 4) by altering C_w. Lake trophic status thus impacts the flux of PCBs and other POPs across the air-water interface, and thus will affect the deposition of POPs in sediments when nutrient availability and phytoplankton dynamics are altered.

In experimental fertilization studies at the Experimental Lakes Area in northwestern Ontario, Jeremiasson et al. (1999) compared rates of gas exchange, wet and dry deposition,

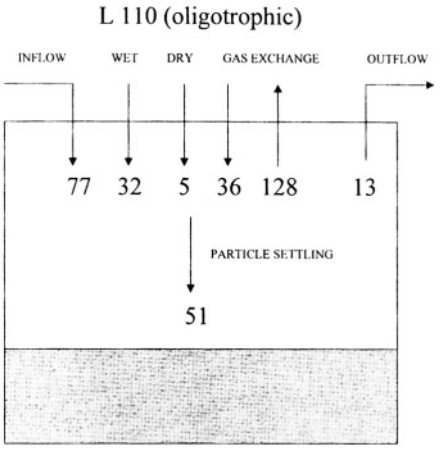


Figure 4. Rates of PCB transfer processes (mg year^{-1}) are shown for oligotrophic Lake 110 from the Experimental Lakes Area, Ontario. Data are from Jeremiasson et al. (1999).

and settling velocities of PCBs in a control lake and an experimentally fertilized lake. Figures 4 and 5 demonstrate increased sedimentation and gas absorption rates of PCBs and decreased rates of volatilization in the experimentally fertilized Lake 227. This occurred because higher plankton biomass scavenged more POPs from the water column, effectively decreasing C_w and driving up the net flux of gas absorption to the water (eq. 4). Bergland (1999) showed that the mass of PCBs in surface and subsurface sediments of 19 Swedish lakes was positively related to lake trophy as measured by total phosphorus concentrations in lake water, and concluded that higher sedimentation rates in the eutrophic lakes were responsible.

These results indicate that altering lake trophic status will alter air-water dynamics of POPs and affect the rate that these chemicals are delivered to lake sediments. However, the impact of changing lake trophic status on the rate of contaminant delivery to lake sediments is still poorly known. Reductions in emissions of PCBs and other POPs in the Great Lakes since the early 70s have coincided with declines in lake trophic status. The declines in contaminant delivery to the sediments since the 1970s are likely the result of both reduced PCB emissions, altered air-water dynamics from declining PCB concentrations (Jeremiasson et al., 1994), and lower phytoplankton abundance.

Molecular diffusion

Diffusion in sediments can cause a net downward migration of POPs with the result that their presence may appear in sediment horizons that are 'too early'. The diffusion distance can be determined by first calculating the effective porous media diffusivity (D_{eff}, cm^2/sec) as follows:

$$D_{eff} = \frac{(D_{mol}\varphi^2)}{(1 + K_p P_b/\varphi)}, \tag{15}$$

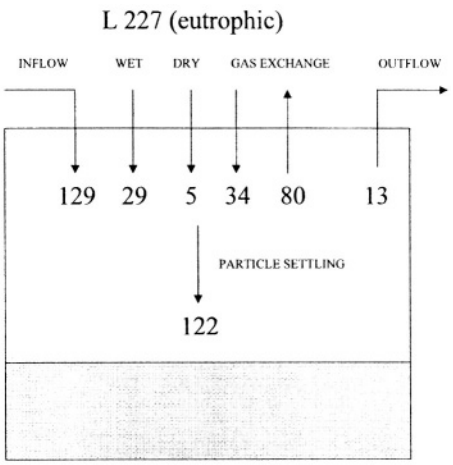


Figure 5. Rates of PCB transfer processes (mg year^{-1}) are shown for the experimentally fertilized Lake 227 from the Experimental Lakes Area, Ontario. Data are from Jeremiasson et al. (1999).

where φ is sediment porosity, φ^2 is a measure of tortuosity in porous media, K_p is the particle adsorption coefficient (cm^3/g), P_b is sediment bulk density (g cm^{-3}) and D_{mol} is the aqueous solution molecular diffusivity (cm^2 sec^{-1}). Next, the solute quantity diffused per unit area of sediment (Q/A) is calculated as follows:

$$\frac{Q}{A} = C_0 \left(\frac{D_{eff}}{\pi} \right)^{1/2}, \tag{16}$$

where C_0 is the initial concentration (mol cm^{-3}).
Penetration depth (Z, cm) can be calculated from Edgington et al. (1991):

$$Z = (4 D_{eff} t)^{1/2}, \tag{17}$$

where t = time. Since D_{eff} is inversely proportional to the sorption coefficient, compounds with low K_p or K_{oc} values such as HCH isomers, and hexa- and hepta-chlorinated toxaphene components, can be expected to have relatively high pore water diffusivities. Miskimmin et al. (1995) estimated that heptachlorobornanes had Z values of 2.7 cm after 30 years in Chatwin Lake (AB), a lake that had been treated with toxaphene in the early 1960's. This accounted for the relatively broad peak of unaltered toxaphene observed in the core both above and below the slice dated (with ^{210}Pb and ^{137}Cs) to the year of addition of the chemical. The analysis of lake and reservoir sediments known to be historically contaminated with various POPs provides additional confirmation of dating techniques, as well as a better understanding of the processes leading to loss and dispersion of the added chemicals.

Mixing depth and its effect on resolution are important considerations in the interpretation of concentration profiles of POPs in sediment (Eisenreich et al., 1989; Wong et al., 1995). The intrinsic resolution (τ), the period over which any change in input rate of a chemical species will not be detected within the sediment profile, is dependent on sediment

mixing occurring at a steady-state (Eisenreich et al., 1989). $\tau(\eta)$ *is* calculated using the equation:

$$\tau = \frac{\text{mixed depth (cm)}}{\text{sedimentation rate (cm y}^{-1})}. \quad (18)$$

Mixed depths can be inferred from the ^{210}Pb profile, or by analysis of short-lived radioisotope tracers in sediment like ^{7}Be. Wong et al. (1995) found values of τ ranging from 4 to 16yrs in Lake Ontario. The intrinsic resolution in 6 southern Yukon Lakes and in Lake Winnipeg ranged from 1 yr to 15 yr (Rawn et al., 2001). The depositional history of chemicals, such as ^{210}Pb whose input flux (or decay rate) varies over a time period greater than τ may not be preserved in sediment within the mixing zone because mixing will obscure the trend. Eisenreich et al (1989) concluded that the historical profile of POPs, which have shorter input half lives than ^{210}Pb decay, will not be destroyed.

Post-depositional transformation processes

It is important to consider post-depositional transformation processes when interpreting historical deposition patterns of POPs in sediments. Although these compounds are persistent by definition, it is possible for transformation processes to alter their abundance, particularly over the course of decades. A critical step in the degradation of chlorinated organic compounds is the cleavage of the carbon-chlorine bond. This may occur by hydrolysis, or through reductive dechlorination, which consists of a replacement of a chlorine substituent with a hydrogen atom.

In aerobic environments, several bacteria have been shown to degrade PCBs and other chlorinated organic compounds using mono- and dioxygenase systems, including *Acinobacter, Bacillus, Acetobacter* and *Pseudomonas.* However, as PCBs must be used as a carbon source, this process is thought to be minor in most natural sediments where PCB concentrations are only a few ng/g (Rochkind et al. 1986). Under anoxic conditions (redox potential <-300mV) reductive dechlorination of chlorinated organic compounds may occur. Reductive dechlorination tends to be more rapid for compounds with a high number of chlorine substituents (like PCBs, hexachlorobenzene, hexachlorocyclohexane, etc.) In the case of PCBs, it has also been shown that reductive dechlorination reduces chlorines in meta- and para substituted positions, resulting in an accumulation of ortho-substituted PCBs over time (Young & Haggblom, 1991).

Although aerobic degradation of lindane (γHCH) is thought to be negligible in sediments (Fiedler & Lau 1998), under methanogenic conditions, successive reductive dechlorination of lindane can produce monochlorobenzene and other constituents (Fiedler & Lau, 1998, and references therein). Studies carried out on anaerobic and aerobic sediments showed bio-isomerization of $\alpha \rightarrow \beta$, $\alpha \rightarrow \gamma$ and $\alpha \rightarrow \delta$HCH. β-HCH was the most persistent isomer in a field environment due to bio-isomerization of α-HCH into β-HCH and to the greater chemical stability of the latter isomer (Wu et al., 1997).

PCBs having 6 to 10 chlorines are reductively dechlorinated (Brown, 1987; Brown & Wagner, 1990; Quensen et al., 1990). Under anoxic conditions, enrichment of mono- and dichlorobiphenyls relative to tri, tetra- and penta- chlorobiphenyls was greater than in aerobic sediments indicative of reductive dechlorination in the anoxic environments (Brown, 1987). Meta- and para- substituted chlorines were removed from chlorinated

biphenyls having 3 to 6 chlorines in anaerobic incubations of lake and river sediments in the laboratory. Greater dechlorinating ability was associated with PCB contaminated sediments which suggests that there has been a selection of microorganisms capable of dechlorination. The microorganisms capable of dechlorinating PCBs may be able to use PCBs as terminal electron acceptors and/or may use the energy potentially available from dechlorination. Anaerobic degradation may lead to other "hexane extractable" products besides dechlorinated PCBs (Rhee et al., 1993).

Congener-specific analysis of PCBs in Lake Ontario cores indicated that PCB concentration profiles in sediments were affected by diffusion and degradation from reductive dechlorination below the mixing zone (Eisenreich et al., 1989; Wong et al., 1995). These processes modified, but did not destroy the historical input record, which resembled the known history of PCB releases in North America (Eisenreich et al., 1989).

Reductive dechlorination in anaerobic sediments also caused the conversion of pp' DDT to p,p'-DDD. Sediment half-lives of pp' DDT were estimated to be between 14 and 21 years in Lake Ontario sediments with 1^{st} order kinetics (Oliver et al., 1989) thus rates of degradation in sediments could be considered to interpret historical deposition. For example, the rate of reductive dechlorination of DDT in sediment cores was calculated by plotting 1n (DDT/ DDT + DDD) vs. sediment age as inferred by ^{210}Pb (Oliver et al., 1989). Muir et al. (1995) found that the proportion of DDD/DDD + DDT increased downcore in many lakes along a mid-continental transect from Northwestern Ontario to Ellesmere Island (Canadian High Arctic). The half-life for anaerobic conversion of DDT to DDD was <20 years in most lakes (assuming a constant ratio of DDD/DDT input to sediments).

Reductive dechlorination of toxaphene homologs has also be observed in Lake Ontario sediments (Howdeshell & Hites, 1996). Amounts of hexa- and heptachlorobornanes were shown to increase with increasing years of burial of the sediments. Miskimmin et al. (1995) and Stern et al., (1996) identified a hexachlorobornane, B-923 (Hx-sed), and a heptachlorobornane (B7-1001) as stable endproducts in lake sediments treated with toxaphene. The appearance of B6-923 and B7-1001 in sediments from Yukon lakes appeared to be consistent with past use patterns of toxaphene for biting fly control, while low amounts were consistent with solely atmospheric sources (Stern et al., 1998). Enantiomer ratio (ER) values for these congeners in one of the lakes treated with toxaphene showed evidence for enantio-enrichment of B7-1001 but not B6-923 (Vetter et al., 1999). This suggests that not all dechlorination is microbially mediated.

The global distillation model: A paleolimnological validation

Paleolimnological investigations of organic contaminants in sediments have demonstrated patterns of contaminant cycling on a global scale. Confirmation of the global distillation model by Wania & Mackay (1993, 1996) is one example. Recent studies have shown a tendency for semi-volatile POP chemicals to become concentrated in cold environments. Air concentrations of organic contaminants often show an annual cycle with highs in summer and lows in winter which relate closely with the slopes of their vapor pressure-temperature curves (Wania et al., 1998).

The Global Distillation Model, also called the Grasshopper Effect and the Cold-Condensation Effect, predicts a global fractionation of these chemicals will occur whereby more

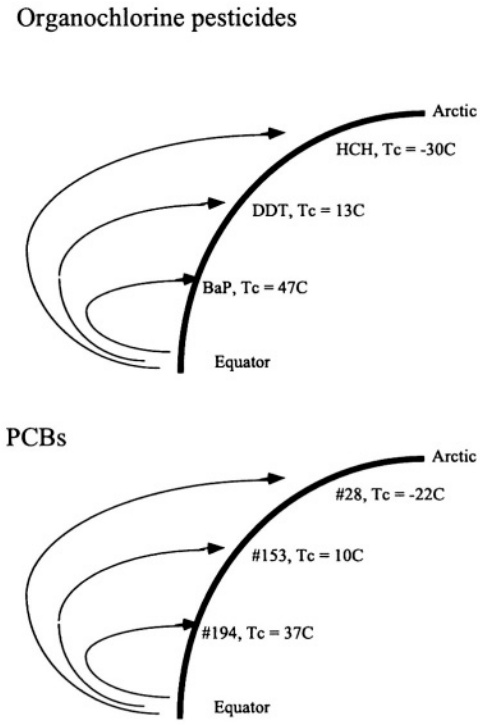


Figure 6. The global distillation effect. Semi-volatile chemicals tend to move toward cold climates as a result of their lower vapor pressures at colder temperatures. T_c is the temperature of condensation (°C) defined as the temperature at which half the total air concentration of that compound is in the vapor phase, and half is in the aerosol phase assuming that constant aerosol concentrations and other standard conditions prevail. We expect chemicals with higher volatilities and lower T_c values to be transported the furthest. Based on Wania & Mackay (1993, 1996).

volatile compounds prevail in colder environments. In general, the global distillation model predicts that compounds with higher vapor pressures and lower condensation temperatures will tend to fractionate towards colder environments (Fig. 6). This may happen as a result of (1) differential volatility at lower temperatures causing semi-volatile compounds to be retained in cold environments; (2) funneling of semi-volatile chemicals by evaporation over large tropical and temperate areas and subsequent deposition over relatively small areas in colder northern or mountain environments; and (3) greater preservation and persistence in colder environments.

This distillation effect has been shown to influence global distributions of many semi-volatile organic contaminants. Simonich & Hites (1995) showed that concentrations of the most volatile POPs in tree bark (HCH, HCB, PCA) increased significantly at higher latitudes whereas less volatile compounds (DDT, endosulfan) were not correlated with latitude, consistent with the predictions of the global distillation model (Fig. 6).

Allowing the global distillation model to run through time (Fig. 7), we expect a gradual migration of semi-volatile organic compounds toward colder regions for they are progressively evaporated from warmer environments. Although the use of chemicals like

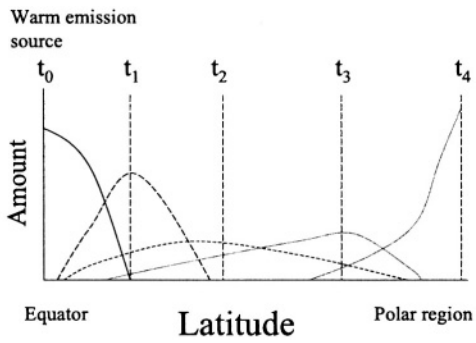


Figure 7. Model prediction of a chemical distribution following an emission pulse at the equator. The distribution peaks are shown as a progression in time with t_0 = time 0 and hypothetical times following in the order t_1 t_2 t_3 and t_4. The global distillation model predicts that relatively mobile, persistent semi-volatile chemicals will gradually migrate toward cold environments. Data are from Wania & Mackay (1996).

PCBs are banned in many countries, and are expected to continue their decline in the industrialized parts of North America and Western Europe, their gradual migration to colder northern regions can potentially cause problems to persist well into the future. With recent declines in water concentrations of persistent organochlorine pesticides in the Great Lakes, virtual elimination dates have been estimated to range between 2010 for DDT, and 2100 for hexachlorobenzene (HCB, Cortes et al., 1998). Environmental half-lives for PCBs have been estimated by Van Metre et al. (1998) at about 9 yrs in the southern United States with the current restrictions on PCB manufacture in place. However, the trend for PCB deposition in lake sediments of the far north shows at least a 20 yr lag with rates increasing to the present day (Fig. 8). These paleolimnological results support the global distillation model and suggest that the problems of contamination by chlorinated xenobiotics in the far north may persist longer than they will in southern latitudes. However, temporal trend studies with biota show declining PCBs and DDT since the 1970's in marine biota, especially from the early 1970's to mid-1980's (Addison & Smith, 1998; Braune, 1999). The terrestrial and marine systems may reflect different input pathways and time trends.

Further evidence in support of the global distillation model is shown by PCB congener-specific analysis of surface lake sediments over a full latitude gradient across Canada (Muir et al., 1996). Canadian mid-latitude sediments contained a full suite of PCB congeners from the lighter, more volatile di- and tri- chlorobiphenyl congeners (e.g., #8, 18, 28) to the relatively immobile nonachlorobiphenyl congeners (e.g., #206). A clear shift in the predominance of the lighter di- and tri-chlorobiphenyls is observed in the far north (Amituk and Hawk lakes, Fig. 9). This pattern supports the hypothesis that the heavier PCBs with higher temperatures of condensation will fall out at lower latitudes. The distribution pattern also showed a significant positive correlation between congener concentrations of PCBs 8, 18 and 28 and latitude, thus the concentrations of these specific congeners are higher in the remote north than they are in the industrialized south. This outcome is consistent with global distillation model predictions (Wania & Mackay, 1993), although differences in sediment preservation are also a potential cause for higher concentrations of some PCB

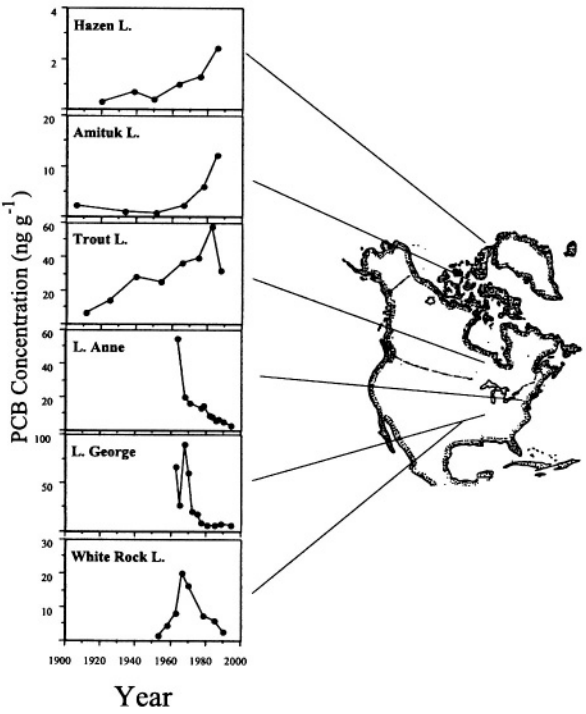


Figure 8. Sediment core profiles of PCBs across a latitude gradient of North America. PCBs were first used in the 1940s, and North America sales peaked in the late 1960s. Note how the northern sites show a lag in the onset and peak of PCB deposition consistent with the prediction in Figure 7. Data are from Muir et al. (1996) and Van Metre et al. (1998).

congeners at higher latitudes. Studies of PCB distributions over latitude gradients in Canada have also identified a shift toward lower chlorinated PCB congeners in the far north when examining burbot liver (Muir et al., 1990) and zooplankton (Koenig & Lean, 1997).

Summary

A review of current analytical methods for persistent organic pollutants (POPs) in sediments is presented, along with a summary of the major processes that govern the fate of POPs in the environment. Reliable analytical methods are essential for developing datasets on concentrations of POPs in sediment cores. Prevention of contamination during the sampling, storage, preparation and extraction of sediments is critical to the analytical work, especially for sediments from remote areas. In addition to good quality chemical residue data, an understanding of transport processes in the environment is necessary for a complete interpretation of sedimentary deposits of POPs for paleolimnological reconstructions of organic contaminant deposition. The example of long range transport of POPs to polar regions is used as a case study showing the utility of paleolimnological approaches to understand global transport processes.

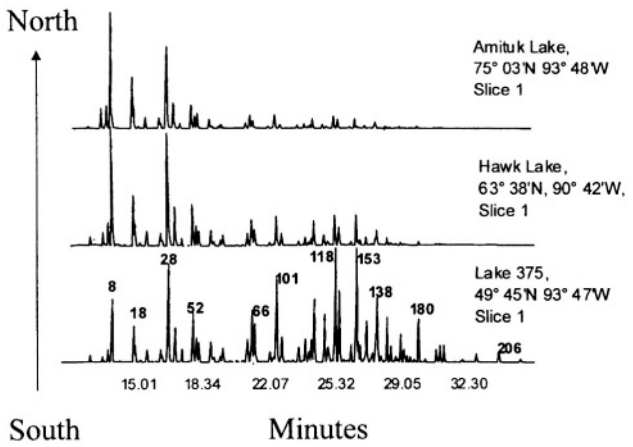


Figure 9. Chromatograms showing PCB congeners from surface sediments of lakes spanning a latitude gradient from southern Ontario to the High Arctic. Congener numbers are shown on selected peaks. Lighter, more volatile PCB congeners appear at the left and heavier, less volatile congeners are at the right. Note the increase in concentration of the more volatile PCB congeners in the Arctic, and the decline of the heavier, less volatile congeners in the north. This outcome is consistent with the Global Distillation Model (Fig. 6). Data are from Muir et al. (1996).

We conclude that lake sediments provide a valuable record of historical deposition of organic contaminants provided it is recognized that degradation, desorption and diffusion of some constituents is inevitable. We recommend a holistic approach that considers the potential for these factors by examining water column processes as well as sediment processes for core reconstructions that infer past changes in historical deposition of persistent organic contaminants. This includes an understanding of desorption/degradation prior to burial and the calculation of recycling ratios for constituents or interest. Further research will be needed to assess linkages between changes in lake trophic status and their impact on sediment burial of POPs. Recent advances in analytical techniques, such as use of HPLC-MS, will allow the approach to be extended to other persistent non-halogenated compounds (e.g., nonyl phenol ethoxylates).

Acknowledgments

Funding for this project was provided by an NSERC research grant to JMB, and an NSERC strategic grant to D. W. Schindler and M. Sharp.

References

Addison, R. F. & T. G. Smith, 1998. Trends in organochlorine residue concentrations in ringed seal (*Phoca hispida*) from Holman NWT, 1972–1991. Arctic 51: 253–261.

Alcock, R. E., C. J. Halsall, C. A. Harris, A. E. Johnston, W. A. Lead, G. Sanders & K. C. Jones, 1994. Contamination of environmental samples prepared for PCB analysis. Environ. Sci. Technol. 28: 1838–1841.

Axelman, J., D. Broman & C. Naf, 1997. Field measurements of PCB partitioning between water and planktonic organisms: Influence of growth, particle size, and solute-solvent interactions. Environ. Sci.Technol. 31: 665–669.

American Society of Testing and Materials (ASTM), 1989. Annual Book of ASTM Standards. Method D-3976-88. Philadelphia PA.: 598–600.

Bamford, H. A., D. L. Poster & J. E. Baker, 1999. Temperature dependence of Henry's Law constants of thirteen polycyclic aromatic hydrocarbons between 4C and 31C. Environ. Toxicol. Chem. 18: 1905–1912.

Baker, J. E., S. J. Eisenreich & B. J. Eadie, 1991. Sediment trap fluxes and benthic recycling of organic carbon, polycyclic aromatic hydrocarbons, and polychlorinated biphenyl congeners in Lake Superior. Environ. Sci. Technol. 25: 500–509.

Berglund, O., 1999. The influence of ecological processes on the accumulation of persistent organochlorines in aquatic ecosystems. Ph.D. thesis, University of Lund, 144 pp.

de Boer, J., 1998. Report on the Results of the UCES/IOC/OSPARCOM intercomparison programme on the determination of Chlorobiphenyl congeners in Marine Media — Step 3a. ICES Coop. Res. Rep. No 226., Int'l Coun. Explor. Sea, Copenhagen DK, 159 pp.

Bidleman, T. F. & L. L. McConnell, 1995. A review of field experiments to determine air-water gas exchenge of persistent organic pollutants. Sci. Tot. Environ. 159: 101–117

Blais, J. M., D. W. Schindler, D. C. G. Muir, L. E. Kimpe, D. B. Donald & B. Rosenberg, 1998. Accumulation of persistent organochlorine compounds in mountains of western Canada. Nature 395: 585–588.

Braune, B., 1999. Contaminants in Arctic seabird eggs. Synopsis of research under the 1998–1999 Northern Contaminants Program. Minister of Public Works and Government Services Canada: 77–80.

Brown, J. F., D. L. Bedard, M. J. Brennan, J. C. Carnahan, H. Feng & R. E. Wagner, 1987. Polychlorinated biphenyl dechlorination in aquatic sediments. Science 236: 709–712.

Brown, J. F. & R. E. Wagner, 1990. PCB movement, dechlorination and detoxication in the acushnet estuary. Environ. Toxicol. Chem. 9: 1215–1233.

Chapman, J. R., 1995. Practical Organic Mass Spectrometry: A Guide for Chemical and Biochemical Analysis, 2nd ed. John Wiley and Sons, NY, 338 pp.

Chiba, M., 1969. Factors affecting the extraction of organochlorine insecticides from soil. Residue Rev. 30: 63–114.

Chin, Y. P., G. R. Aiken & K. M. Danielsen, 1997. Binding of pyrene to aquatic humic substances: The role of molecular weight and aromaticity. Environ. Sci. Technol. 31: 1630–1635.

Chung, C-W., M. T. Morandi, T. H. Stock & M. Afshar, 1999. Evaluation of a passive sampler for volatile organic compounds at ppb concentrations, varying temperatures, and humidities with 24-hr exposures. 2. Sampler performance. Environ. Sci. Technol. 33: 3666–3671.

Cortes, D. R., I. Basu, C. W. Sweet, K. A. Brice, R. H. Hoff & R. A. Hites, 1998. Temporal trends in gas-phase concentrations of chlorinated pesticides measured at the shores of the Great Lakes. Environ. Sci. Technol. 32: 1920–1927.

Dachs, J., J. M. Bayona, C. Raoux & J. Albaigés, 1997. Spatial, vertical distribution and budget of polycyclic aromatic hydrocarbons in the western Mediterranean seawater. Environ. Sci. Technol. 31: 682–688.

Dachs, J., S.J. Eisenreich, J. E. Baker, F.-C. Ko & J. D. Jeremiasson, 1999. Coupling of phytoplankton uptake and air-water exchange of persistent organic pollutants. Environ. Sci. Technol. 33: 3653–3660.

Dearth, M. A. & R. A. Hites, 1991. Complete analysis of technical chlordane using negative ionization mass spectrometry. Environ. Sci. Technol. 25: 245–254.

Edgington, D. N., J. Van Klump, J. A. Robbins, Y. S. Kusner, V. D. Pampura & I. V. Sandimirov, 1991. Sedimentation rates, residence times and radionuclide inventories in Lake Baikal from ^{137}Cs and

^{210}Pb in sediment cores. Nature 350: 601–604.

Eisenreich, S. J., P. D. Capel, J. A. Robbins & R. Bourbonniere, 1989. Accumulation and diagenesis of chlorinated hydrocarbons in lacustrine sediments. Environ. Sci. Technol. 23: 1116–1126.

Fendinger, N. J., D. E. Glotfelty & H. P. Freeman, 1989. Comparison of two experimental techniques for determining air-water Henry's law constants. Environ. Sci. Technol. 23: 1528–1531.

Fiedler, H. & C. Lau, 1998. Transformation of chlorinated xenobiotics in the environment. In Schuurmann, G. & B. Markert (eds.) Ecotoxicology: Ecological Fundamentals, Chemical Exposure and Biological Effects. John Wiley and Sons, New York, 900 pp.

Franz, T. P., S. J. Eisenreich & T. M. Holsen, 1998. Dry deposition of particulate polychlorinated biphenyls and polyaromatic hydrocarbons to Lake Michigan. Environ. Sci. Technol. 32: 3681–3688.

Gatz., D. F., 1975. Pollutant aerosol deposition into southern Lake Michigan. Water, Air & Soil Pollut. 5: 239–251.

Gschwend, P. M. & R. A. Hites, 1981. Fluxes of polyaromatic hydrocarbons to marine and lacustrine sediments in the northeastern United States. Geochim. Cosmochim. Acta 45: 2359–2367.

Howdeshell, M. J. & R. A. Hites, 1996. Historical input and degradation of toxaphene in Lake Ontario sediment. Environ. Sci. Technol. 30: 220–227.

Jantunen, L. M. & T. Bidleman, 1996. Air-water gas exchange of hexachlorocyclohexanes (HCHs) and the enantiomers of a-HCH in arctic regions. J. Geophysical Res. 101: 28837–28846.

Jeremiason, J. D., S. J. Eisenreich, M. J. Patterson, K. G. Beaty, R. Hecky & J. J. Elser, 1999. Biogeochemical cycling of PCBs in lakes of variable trophic status: A paired lake experiment. Limnol. Oceanogr. 44: 889–902.

Jeremiason, J. D., K. C. Hornbuckle & S. J. Eisenreich, 1994. PCBs in Lake Superior, 1978–1992: Decreases in water concentrations reflect loss by volatilization. Environ. Sci. Technol. 28: 903–914.

Karickhoff, S. W., 1981. Semiempirical estimation of sorption of hydrophobic pollutants on natural sediments and soils. Chemosphere 10: 833–849.

Keith, L. H., 1991. Environmental Sampling and Analysis: A Practical Guide. Lewis Publishers. CRC Press Inc. Boca Raton, Florida.

Kidd, K. A., D. W. Schindler, D. C. G. Muir, W. L. Lockhart & R. H. Hesslein, 1995. High concentrations of toxaphene in fishes from a subarctic lake. Science 269: 240–242.

Kjeller, L-O. & C. Rappe, 1995. Time trends in levels, patterns and profiles of polychlorinated dibenzo-p-dioxins, dibenzofurans and biphenyls in a sediment cores from the Baltic proper. Environ. Sci. Technol. 29: 346–355.

Koenig, B. & D. Lean, 1997. Polychlorinated biphenyls in zooplankton. In Kidd, K. A., R. E. Hecky (and 6 others) (eds.) Interrelationships Among Climatic Variation, Climate Change and Persistent Organic Pollutant Cycling in the Americas. NWRI Contribution No. 98–128. NWRI, Burlington.

Kucklick, J. R., D. A. Hinkley & T. F. Bidleman, 1991. Determination of Henry's Law constants for hexachlorocyclohexanes in distilled water and artificial seawater as a function of temperature. Marine Chem. 34: 197–209.

Landrum, P. F., S. R. Nihart, B. J. Eadie & W. S. Gardner, 1984. Reverse phase separation method for determining pollutant binding to Aldrich humic acid and dissolved organic carbon of natural waters. Environ. Sci. Technol. 18: 187–192.

Larsson, P., L. Colvin, L. Okla & G. Meyer, 1992. Lake productivity and water chemistry as governors of the uptake of persistent pollutants in fish. Environ. Sci. Technol. 26: 346–352.

Longcore, J. R. & R. C. Stendell, 1977. Shell thinning and reproductive impairment in black ducks after cessation of DDE dosage. Arch. Environ. Contam. Toxicol. 6: 293–304.

Mackay, D., W.-Y. Shiu & K-C Ma, 1992. Illustrated Handbook of Physical-chemical Properties and Environmental Fate for Organic Chemicals. Monoaromatic Hydrocarbons, Chlorobenzenes, and PCBs. Vol. 1. Lewis Publishers, Boca Raton, 697 pp.

Mackay, D., W-Y Shiu & K-C Ma, 1997. Illustrated Handbook of Physical-chemical Properties and Environmental Fate for Organic Chemicals. Vol. 5. Pesticide Cemicals. Lewis Publishers. Boca Raton, 812 pp.

Mackay, D. & F. Wania, 1995. Transport of contaminants to the Arctic: partitioning, processes and models. Sci. Tot. Environ. 160/161: 25–38.

Miles, J. R. W. & C. R. Harris, 1971. Insecticide residues in a stream and a controlled drainage system in agricultural areas of southwestern Ontario, 1970. Pestic. Monit. J. 5: 289–294.

Miskimmin, B. M., D. C. G. Muir, D. W. Schindler, G. A. Stern & N. P. Grift, 1995. Chlorobornanes in sediments and fish thirty years after toxaphene treatment of lakes. Environ. Sci. Technol. 29: 2490–2495.

Muir, D. C. G., N. P. Grift, W. L. Lockhart, P. Wilkinson, B. N. Billeck & G. J. Brunskill, 1995. Spatial trends and historical profiles of organochlorine pesticides in Arctic lake sediments. Sci. Total Environ. 160/161: 447–457.

Muir, D. C. G., A. Omelchenko, N. P. Grift, D. A. Savoie, W. L. Lockhart, P. Wilkinson & G. T. Brunskill, 1996. Spatial trends and historical deposition of polychlorinated biphenyls in Canadian midlatitude and arctic lake sediments. Environ. Sci. Technol. 30: 3609–3617.

Murphy, T. J., M. D. Mulin & J. A. Meyer, 1987. Equilibration of polychlorinated biphenyls and toxaphene with air and water. Environ. Sci. Technol. 21: 155–162.

Oehme, M., J. Klungsøyr, A. Biseth & M. Schlabach, 1993. Quantitative determination of ppq-ppt levels of polychlorinated dibenzo-p-dioxins and dibenzofurans in sediments from the Arctic (Barents Sea) and the North Sea. Anal. Method Instrum. 1: 153–163.

Oehme, M., 1999. Practical Introduction to GC-MS Analysis with Quadrupoles. John Wiley and Sons, N.Y., 196 pp.

Oliver, B. G., M. N. Charlton & R. W. Durham, 1989. Distribution, redistribution, and geochronology of polychlorinated biphenyl congeners and other chlorinated hydrocarbons in Lake Ontario sediments. Environ. Sci. Technol. 23: 200–208.

Paasivirta, J., S. Sinkkonen, P. Mikkelson,T. Rantio & F. Wania, 1999. Estimation of vapor pressures, solubilities and Henry's law constants of selected persistent organic pollutants as functions of temperature. Chemosphere 39: 811–832.

Price, D. J. & W. J. Birge, 1999. Aquatic sediment pre-extraction preparations and the effects on Aroclor 1248 concentrations. Environ Sci Technol. 33: 1137–1140.

Quensen, J. F., S. A. Boyd & J. M. Tiedje, 1990. Dechlorination of four commercial polychlorinated biphenyl mixtures (Aroclors) by anaerobic microorganisms from sediments. Appl. Environ. Microbiol. 56: 2360–2369.

Rawn, D. F. K., D. C. G. Muir, D. A. Savoie, G. B. Rosenberg, W. L. Lockhart & P. Wilkinson, 2000. Historical deposition of PCB and organochlorine pesticides to Lake Winnipeg (Canada). J. Great Lakes Res. 26: 3–17.

Rawn, D. F. K., W. L. Lockhart, P. Wilkinson, D. A. Savoie & D. C. G. Muir, 2001. Historical Contamination of Yukon Lake Sediments by PCBs and Organochlorine Pesticides: Influence of Local Sources and Watershed Characteristics. Sci. Total Environ. 280: 17–37.

Rhee, G. Y., R. C. Sokol, C. M. Bethoney & B. Bush, 1993. A long term study of anaerobic dechlorination of PCB congeners by sediment microorganisms: Pathways and mass balance. Environ. Toxicol. Chem. 12: 1829–1834.

Rochkind, M. L., J. W. Blackburn & G. S. Sayler, 1986. Microbial decomposition of chlorinated aromatic hydrocarbons. EPA / 600 / 2–86 / 090. US Environmental Protection Agency, Cincinati, Ohio, USA.

Rose, N. L., S. Backus, H. Karlesson & D. C. G. Muir, 2001. An historical record of toxaphene and its congeners in a remote lake in western Europe. Environ. Sci. Technol. 35: 1312–1319.

Saha, J. G., 1971. Comparison of several methods for extracting chlordane residues from soil. J. Assoc. Offic. Anal. Chem. 54: 170–174.

Schantz, M. M., B. J. Porter, S. A. Wise, M. Segstro, D. C. G. Muir, S. Mössner, K. Ballschmiter & P. R. Becker, 1996. Interlaboratory comparison study for PCB congeners and chlorinated pesticides in beluga whale blubber. Chemosphere 33: 1369–1390.

Schwartzenbach, R. P., P. M. Gschwend & D. M. Imboden, 1993. Environmental Organic Chemistry. John Wiley and Sons. New York, 681 pp.

Shang, D. Y, Macdonald, R. W. & M. G. Ikonomou, 1999. Persistence of Nonylphenol Ethoxylate Surfactants and Their Primary Degradation Products in Sediments from near a Municipal Outfall in the Strait of Georgia, British Columbia, Canada. Environ. Sci. Technol. 33: 1366–1372.

Simonich, S. L. & R. A. Hites, 1995. Global distribution of persistent organochlorine compounds. Science 269: 1851–1854.

Suntio, L. R., W. Y. Shiu, D. Mackay, J. N. Sieber & D. Glotfelty, 1987. A critical review of Henry's law constants. Rev. Environ. Contam. Toxicol. 103: 1–59.

Tateya, S., S. Tanabe & R. Tatsukawa, 1988. PCBs on the globe: possible trends of future levels in the open ocean. In Schmidtke, N.W. (ed.) Toxic Contamination in Large Lakes Vol. 3: Sources, Fate and Controls of Toxic Contaminants. Lewis Publishers, Chelsea, Mich.: 237–281.

Strachan, W. M. J. & S. J. Eisenreich, 1988. Mass Balancing of Toxic Chemicals in the Great Lakes: The Role of Atmospheric Deposition. Report to the International Joint Commission. Windsor, Ontario.

Stern, G. A., M. D. Loewen, B. M. Miskimmin, D. C. G. Muir & J. D. Westmore, 1996. Characterization of Two Major Toxaphene Components in Treated Lake Sediment. Environ. Sci Technol. 30: 2251–2258.

Stern, G. A., B. Billeck, W. L. Lockhart, D. C. G. Muir, G. T. Tomy & P. Wilkinson, 1998. Chlorinated Bornanes (Toxaphene) in Yukon Lakes: Atmospheric or Non-Atmospheric Source. Organohalogen Compounds. 35: 299.

Ten Hulscher, E. M., L. E. Van der Velde & W. A. Bruggeman, 1992. Temperature dependence of Henry's Law constants for selected chlorobenzenes, polychlorinated biphenyls and polycyclic aromatic hydrocarbons. Environ. Toxicol. Chem. 11: 1595–1603.

Tomy, G. T., G. A. Stern, D. C. G. Muir, A. T. Fisk, C. D. Cymbalisty & J. B. Westmore, 1997. Quantifying C_{10}–C_{13} polychloroalkanes in environmental samples by high resolution gas chromatography/electron capture negative ion high resolution mass spectrometry. Anal. Chem. 69: 2762–2771.

Tomy, G. T. & G. A. Stern, 1999. Analysis of C14–C17 Polychloro-n-alkanes in Environmental Matrixes by Accelerated Solvent Extraction-High-Resolution Gas Chromatography/Electron Capture Negative Ion High-Resolution Mass Spectrometry, Anal. Chem. 71: 4860–4865.

United Nations Economic Commission for Europe (UNECE), 1998. Protocol To The 1979 Convention On Long-Rangc Transboundary Air Pollution On Persistent Organic Pollutants. *http://www.unece.org/env/lrtap/*

U.S. Environmental Protection Agency, 1994. Method 1613: Tetra-Through Octa-Chlorinated Dioxins And Furans by Isotope Dilution HRGC/HRMS, Update, October 1994. National Service Center for Environmental Publications, Cincinnati, OH 45242–2419 Phone Number: 800/490-91981984.

U.S. Environmental Protection Agency, 1996. Method 3541. Test methods for evaluating solid wastes, SW-846, Final Version. Office of Solid Waste and Emergency Response, Washington DC.

U.S. Environmental Protection Agency, 1997a. Special Report on Environmental Endocrine Disruption: An Effects Assessment and Analysis. EPA/630/R-96/012. Risk Assessment Form, U.S. EPA, Washington DC., 111 pp.

U.S. Environmental Protection Agency, 1997b. Toxic Polychlorinated Biphenyls by Isotope Dilution High Resolution Gas Chromatography/High Resolution Mass Spectrometry. Office of Science and Technol. Washington DC., 62 pp.

Van Metre, P. C., J. T. Wilson, E. Calendar & C. C. Fuller, 1998. Similar rates of persistent hydrophobic and particle-reactive contaminants in riverine systems. Environ. Sci. Technol. 32: 3312–3317.

Vetter, W., R. Bartha, G. Stern & G. T. Tomy, 1999. Enantioselective determination of two persistent chlorobornane congeners in sediment from a toxaphene treated Yukon lake. Environ. Toxicol. Chem. 18: 2775–2781.

Wallace, J. C., I. Basu & R. A. Hites, 1996. Sampling and analysis artifacts caused by elevated indoor air Polychlorinated biphenyl concentrations. Environ. Sci. Technol. 30: 2730–2734.

Wania, F., J-E. Haugen, Y. D. Lei & D. Mackay, 1998. Temperature dependence of atmospheric concentrations of semivolatile organic compounds. Environ. Sci. Technol. 31: 1013–1021.

Wania, F. & D. Mackay, 1993. Global fractionation and cold condensation of low volatility organochlorine compounds in polar regions. Ambio 22: 10–18.

Wania, F. & D. Mackay, 1996. Tracking the distribution of persistent organic pollutants. Environ. Sci. Technol. 30: 390A–396A.

Wong, C. S., G. Sanders, D. R. Engstrom, D. T. Long, D. L. Swackhamer & S. J. Eisenreich, 1995. Accumulation, inventory, and diagenesis of chlorinated hydrocarbons in Lake Ontario sediments. Environ. Sci. Technol. 29: 2661–2672.

Wu, W. Z., Y. Xu, K-W. Schramm & A. Kettrup, 1997. Study of sorption, biodegradation and isomerization of HCH in stimulated sediment/water system. Chemosphere 9: 1887–1894.

Young, L. Y. & M. M. Haggblom, 1991. Biodegradation of toxic and environmental pollutants. Cur. Opin. Biotechnol. 2: 429–435.

Yunker, M. B., L. R. Snowdon, R. W. MacDonald, J. N. Smith, M. G. Fowler, D. N. Skibo, F. A. McLaughlin, A. I. Danyushevskaya, V. I. Petrova & G. I. Ivanov, 1996. Polycyclic aromatic hydrocarbon composition and potential sources for sediment samples from the Beaufort and Barents Seas. Environ Sci Technol 30: 1310–1320.

Zhu, J., M. J. Mulvihil & R. J. Norstrom, 1994. Characterization of technical toxaphene using combined high-performance liquid chromatography-gas chromatography-electron capture negative ionization mass spectrometry techniques. J. Chromatogr. 669: 103–117.

11. NEAR-INFRARED SPECTROMETRY (NIRS) IN PALAEOLIMNOLOGY

TOM KORSMAN (tom.korsman@eg.umu.se)
INGEMAR RENBERG
Department of Ecology and Environmental Science
UmeåUniversity, SE-901 87 Umeå
Sweden

EIGIL DÅBAKK
Department of Ecology and Environmental Science
Umeå University, SE-901 87 Umeå
Sweden, and
Department of Organic Chemistry
Umeå University, SE-901 87 Umeå
Sweden

MATS B. NILSSON
Department of Forest Ecology
Swedish University of Agricultural Sciences
SE-901 83 Umeå
Sweden

Keywords: near-infrared spectrometry (NIRS), lake sediments, calibration models, palaeolimnological reconstruction, optimal sample selection. NIR theory, spectral filters, instrument design, sample preparation.

Introduction

The near infrared (NIR) part of the electromagnetic spectrum is commonly defined as the region spanning wavelengths from 780 nm to 2500 nm. The astronomer, William Herschel, discovered the near infrared region as early as 1800 (Herschel, 2000), but it took a long time before this part of the electromagnetic spectrum found practical use. The difficulties in interpreting the rather complex NIR signals, which usually demand multivariate modelling, was a major reason for its late introduction as an analytical technique in chemistry.

Modern near-infrared spectrometry (NIRS) commonly involves the measurement of the absorption spectrum for a sample at tight intervals along the whole NIR wavelength region, which could result in a few hundred to many thousands of absorbance-variables,



W. M. Last & J. P. Smol (eds.), 2001. *Tracking Environmental Change Using Lake Sediments. Volume 2: Physical and Geochemical Methods.* Kluwer Academic Publishers, Dordrecht, The Netherlands.

depending on instrument technology and design. While most absorption bands overlap, no constituents can be directly interpreted and quantified from the NIR spectrum. The common use involves development of calibration models (transfer functions) between the NIR spectra and constituents measured by conventional methods on the same samples. The calibration functions are then used to predict the constituents from NIR spectra of new samples. This approach utilises the simplicity and speed of NIR analysis, making quantification by NIR predictions inexpensive compared to other methods.

Karl Norris is often acknowledged as the "inventor" of the NIR technology. Together with co-workers, Norris started using wavelengths in the NIR region to quantify components of grain in the 1970s (McClure, 1994) and was thereby the first to use MRS for analysis of chemically complex samples. Since then, NIRS has become widely used for quantification of certain constituents in the food and feed industry (Osborne & Fearn, 1988), for product identification in, for example, the pharmaceutical industry, and in the process industry for process monitoring (Davies & Williams, 1997). More recently NIRS has found some environmental applications, including palaeolimnological applications (Nilsson et al., 1992; Malley & Nilsson, 1995; Foley et al., 1998; Dåbakk, 1999). Since 1997 there have been sessions on environmental applications at the international meetings organised by The International Committee for Near Infrared Spectroscopy (Davies, 1997).

Theory

NIRS is based on absorption of radiation between polar bonds in molecules, and in particular the bonds between light atoms, such as those in the first period of the periodic table. The molecular bonds vibrate in a manner similar to a diatomic oscillator, and the simplest model explaining these absorptions is that of the harmonic oscillator. However, the harmonic oscillator does not explain overtone transitions, and the model of the anharmonic oscillator is more precise (Fig. 1; Bokobza, 1998).

The NIR spectrum contains overtones and combination bands that are derived from fundamental absorptions known from infrared (IR) spectroscopy. The overtone transitions are absorptions from the ground level to vibrational energy level 2 or higher (Fig. 1). Combination bands arise from combinations of fundamental C-H, O-H, N-H and S-H vibrations. The absorbtion spectra for some typical molecular bonds are shown in Figure 2.

The number of combinations and overtones in a NIR spectrum is large, resulting in overlapping bands that are rather smooth. Bonds that vibrate at high energy and with large amplitude carry the most intensity and are those involving hydrogen, the lightest element. The overtones and combination bands are much weaker (usually by a factor of 10 or more) than the fundamental absorption bands. This allows analysis of samples that are several millimetres thick (Bokobza, 1998).

The interpretation of NIR spectra is not as straightforward as that of IR spectra. The NIR spectra are smoother and the peaks broader. In NIR spectra, bonds with high dipole moments give the strongest overtone absorptions. A basis for quantification in absorption spectroscopy is the Beer-Lambert equation, which relates concentration directly to the absorption

$$A = \varepsilon C l, \tag{1}$$

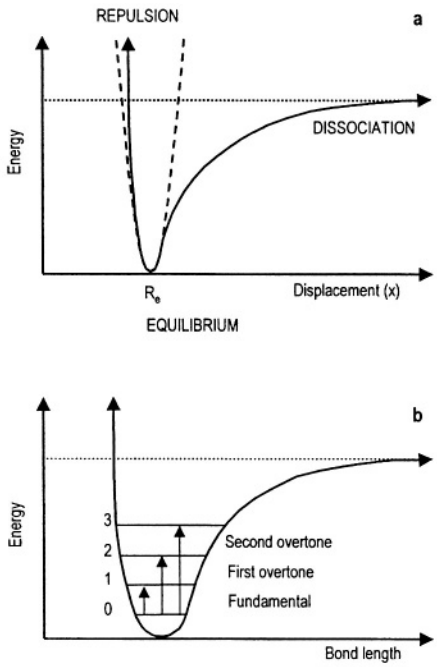


Figure 1. a) Oscillation models for NIR absorptions. The solid line represents energy as a function of atomic bond distances in the anharmonic model. The dashed line shows the corresponding function for the harmonic oscillator b) Graphical representation of the overtone absorptions used in NIR spectrometry. The fundamental absorptions form the basis of IR spectroscopy.

where ε is the molecular absorptivity, C is the concentration and l is the path length. Absorbance is calculated from transmission using

$$A = \log(1/T) \tag{2}$$

or

$$A = \log\left(T_0/T\right), \tag{3}$$

where T_0 is the 100% transmission (Skoog & Leary, 1992). In reflectance spectrometry, one measures the reflectance (R) and not transmittance (T). The theory on diffuse reflectance is not as extensive as that on absorption, although there are some good references in the literature (Kubelka & Munk, 1931; Williams, 1987; Burger et al., 1998).

Several equations are used in diffuse reflectance spectrometry to relate the measured reflectance to absorbance so that quantification can be achieved. All equations are based on the assumptions in Beer-Lambert's equation. It is found that the simple transform of

$$A = \log(1/R), \tag{4}$$

where R is the measured reflectance, is a reasonable approximation. However, in reflectance spectroscopy, the Beer-Lambert model ceases to be valid because of changes in effective

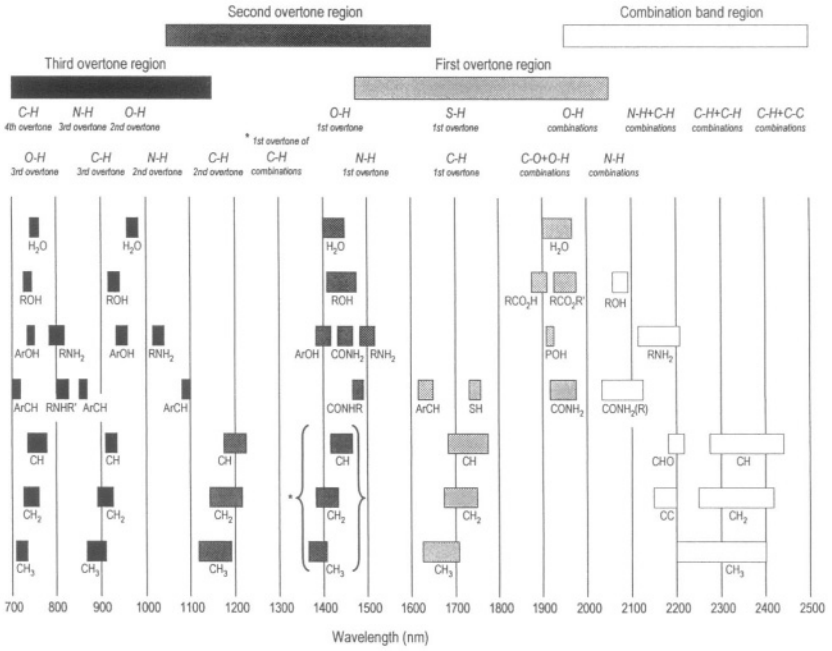


Figure 2. Absorptions in the near-infrared region for some common organic chemical bonds. The figure shows the major analytical bands and their relative peak positions. Reproduced with permission from FOSS NIRSystems Inc.

pathlength that are caused by light scattering. These changes in pathlength can be corrected for, and there are quite a few data pre-treatments to choose from. The pre-treatments are also referred to as spectral filters.

The interaction between NIR radiation and the sample changes as a function of wavelength, making different parts of the NIR spectrum useful for different purposes. Since the spectral information is largely derived from overtones of fundamental absorptions, chemical information is repeated along the spectrum. For instance, water peaks are found at approximately 1940, 1410 and 920 nm, corresponding to absorptions of the first, second and third overtones, respectively. The properties of NIR spectra as a function of wavelength are summarized in Figure 3.

Currently NIR spectrometry is most commonly used to predict or monitor macroconstituents, i.e. >0.1–1% of the sample weight. Common constituents are carbohydrates, cellulose and hemicellulose, proteins and lipids (Osborne & Fearn, 1986; Davies & Williams, 1996). Constituents other than those containing organic, hydrogen bonds have also been monitored by NIR, e.g. heavy metals (Malley et al., 1996). Such NIR applications are based on "indirect or correlative" modelling, i.e. the concentration of the constituent of interest (e.g. a heavy metal) correlates with some organic constituent occurring at levels detectable by NIR.

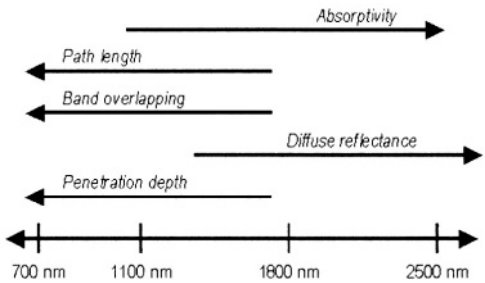


Figure 3. Summary of sample interaction properties of NIR radiation. In general, the properties change as a function of wavelength.

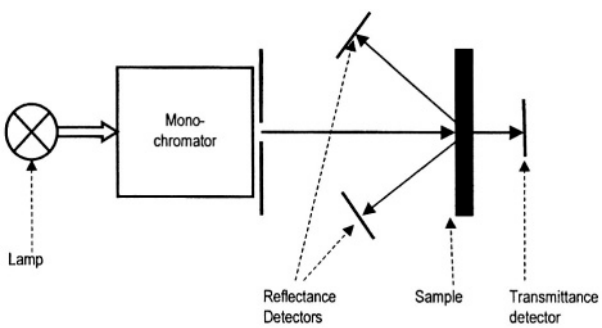


Figure 4. Schematic illustration of a scanning NIR spectrophotometer. The light energy comes from a tungsten-halogen lamp and is often divided into separate wavelengths before interaction with the sample (pre-dispersive). Instruments can also be post-dispersive. The way that wavelength selection is done is what differentiates most types of instruments (e.g., grating, FT, AOTF and Diode Arrays).

Instrumentation

There are four basically different instrument designs, based on how incident energy is selected (McClure, 1994). These are grating instruments (monochromators), Fourier transform instruments, filter instruments and Diode Array-based instruments. Figure 4 illustrates the basic design of a scanning NIR spectrophotometer.

Instruments used for palaeolimnological research should preferably have a scanning region that covers the entire NIR region (780 to 2500 nm). The instruments should also have rather high signal-to-noise ratios (S/N) or low RMS noise. If, in research, one starts using an instrument with high noise, possible applications may not be discovered because of signals being drowned in instrument noise. Resolution is of less interest (Norris, 1998), since, for all practical use of NIRS on complex biological samples, wavelengths close to each other have very high correlations. If the S/N is poor, high resolution can partly compensate for this (Norris, 1998).

Grating instruments

Tungsten halogen lamps are usually used as the energy source for NIR instruments. Holographic gratings are manufactured through a photoetching process, have fewer defects and better throughput along the entire NIR spectrum than mechanically grooved gratings, and they have therefore, to a large extent, replaced the old mechanically grooved gratings. Use of otherwise proper instrument designs allows very low instrument noise, i.e., root mean square (RMS) noise, and good wavelength accuracy for grating instruments (in some cases specified RMS noise is less than 20 microabsorbances). The major drawback of grating instruments is their lack of speed when it comes to monitoring of fast chemical processes or products moving quickly, such as on a hopper. For most laboratory use, the speed is of little interest, since data are usually obtained in less than a minute.

Fourier-transform instruments

Although the Fourier transform (FT) technology is rather new, A. A. Michelson presented the interferometer principle already in 1881 in his search for the aether. There are several different intereferometer techniques on the market. The use of FT-IR is mature and many manufacturers of FT-IR instruments have extended the wavelength interval from the mid-IR to the NIR wavelength region based on the same instrument optical bench as used for IR measurements. However, the noise increases when going from mid-IR to near-IR, because the moving part (e.g., wishbone, crystal) has to move quicker on account of the higher frequency. An advantage of many FT-NIR instruments is that the spectral resolution is superior to grating NIR instruments.

Filter instruments

Filter instruments use several narrow band filters that are usually mounted on a rotating filter wheel to acquire data at several different wavelengths. Fixed filters are also used. A drawback is that filters have to be selected specifically for each application and that rather few variables are obtained. A rather interesting break-through in near infrared spectroscopy came along with the acousto-optical tuneable filter (AOTF), supposed to consist of a monochromator with no-moving-parts. It relies on a crystal (for NIR it is TeO_2) in which optical and acoustical waves move at different angles. The acoustic waves are used to tune the filter and obtain monochromatic beams. The scanning speed is large as compared to grating and FT instruments. The major drawback is that the crystals themselves appear to be difficult to manufacture in a reproducible way, making transfer calibrations between instruments difficult. The crystals also change over time.

Diode Array-based instruments

A problem with grating instruments, as well as FT-instruments, is both the scanning speed as well as the moving parts that make them unsuitable in certain industrial environments. These problems are largely overcome by using diode array (DA) detector spectrophotometers that have no moving parts, and where the grating can also be fixed. Although there

are commercially available DA spectrophotometers, the search for improvements in this technology is extensive because of high noise.

NIR analysis of sediment samples

Sample preparation

Two important properties in NIRS should be considered in analysis of sediment samples. These are the influence of the particle sizes and the water content on the spectral signal. Differences in particle sizes and sample cup packaging may result in light-scattering effects that are not necessarily of interest for the specific constituent that is to be analysed. NIR analysis of samples with a high water content results in broad peaks with high absorptivity that may hide spectral information from other constituents than water. These problems have to be dealt with in sample preparation and by spectral pre-treatments (see next section). The basic rule is that the samples should be both dried and as homogenous as possible, before the spectral information is collected.

Freeze-drying is probably the most appropriate way of drying sediment samples prior to NIR-analysis. To avoid destruction of important organic structures, the samples should preferably be dried at low temperature. The NIR signal in samples dried at 90 °C differs significantly from samples dried at lower temperature (Fig. 5), which might be explained, for instance, by the destruction of protein structures at temperatures above 60 °C. However, there are also differences between samples dried at low temperature in an oven, and freeze-dried samples. A probable explanation for this could be that drying of very wet sediment samples at low temperature takes a long time, which allows considerable bacterial activity to take place before the sample is completely dry. Furthermore, from a practical point of view, a freeze-dried sample usually has a structure that facilitates the following homogenisation, while mechanical processing of samples dried in an oven is more difficult.

The further handling of samples involves grinding using a simple mortar or an analytical mill. We propose the following sample handling and preparation scheme for NIR-analysis of sediment samples:

1. Freeze the samples in the field, directly after sampling (e.g., on dry ice), and store the samples frozen until further processing to avoid biochemical degradation.

2. Freeze-dry the samples.

3. Grind the sample in a mortar, and homogenise the sample before transferring the powdered sediment into the sample cup.

This sample handling and preparation scheme has been subjected to various tests, and proved to result in reproducible spectral signals (see e.g., Dåbakk et al., 1999). As suggested by Malley & Williams (1997), the sample could be sieved prior to NIR analysis in case the sediment contains coarse grained particles (>2 mm). Apart from the possible effects of grinding, the sample preparation and the subsequent NIR-analysis is non-destructive. This means that the sample can be used for further physical, chemical or biological analyses using “conventional” analytical techniques.

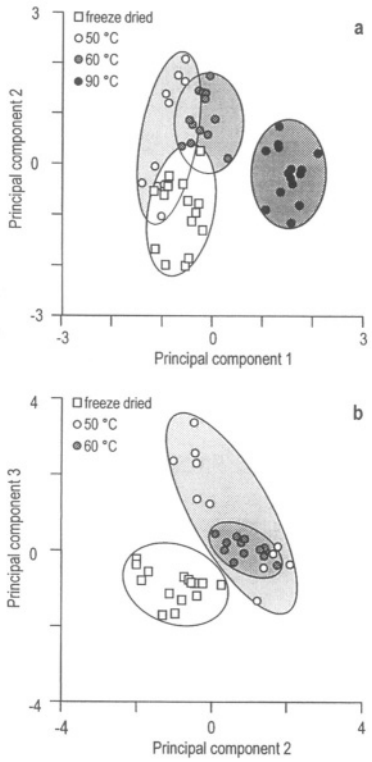


Figure 5. Differences in NIR spectra due to drying of samples. A short sediment core (ca 30 cm) was homogenized, and subsamples were dried at different temperatures (90, 60, 50 °C, and freeze drying). Before NIR analysis, the sediment samples were ground in a mortar. NIR spectra from the powdered sediment samples were obtained using a Technicon InfraAnalyzer 400 DR (Day & Fearn, 1982). The absorbance was measured as log 1/reflectance for 19 wavelengths between 1445 and 2348 nm. The first principal component scores for samples dried at 90 °C differed significantly from samples dried at low temperature (a), while a difference between freeze-dried samples and samples dried at 60 or 50 °C was seen for the second and third component (b).

A suitable amount of dried sediments for NIRS analysis is 2 cm^3 or more. The sediment should, after being ground, be transferred to sample cups suitable for reflectance analysis. It is advantageous if the spectrometer has a spinning cup module so that the samples are rotated during NIR measurement. This allows a bigger portion of the sample to be measured and, to some extent, it also compensates for sample heterogeneity. Fiber-optic sample modules can also be used to measure the dried sediment if the fiber optic is suitable for reflectance analysis. This will usually require a bundle of smaller fibers in order to transfer sufficient light to the sample; such bundles are commercially available.

Spectral filters and pretreatments

An obstacle with NIR spectra is that they often carry unwanted physical information about the sample, e.g. particle size, that are usually expressed in the first few components in

the multivariate data analysis. There are many means of filtering the unwanted signals in the spectra. Multiplicative signal correction (MSC; Geladi et al., 1985), derivation, and standard normal variate (Barnes et al., 1989), are all frequently applied for these purposes. When spectral signals are interpreted as such, i.e. without creating calibrations by some mean of multivariate regression techniques, the spectral data need to be scatter-corrected. However, the scatter effects may be overcome by using, for example, partial least squares (PLS) regression to create calibrations. Prediction using scatter-corrected data generally do not improve the modeling results.

MSC is a way of removing spectral effects that arise from different effective path lengths in reflectance spectrometry caused by different particle sizes (Geladi et al., 1985). By assuming that each sample spectrum has an offset and a slope that is caused by some unwanted physical effects, one can correct for this if the variability is systematic. The correction is done against a reference spectrum, which is usually the mean spectrum of all sample spectra. However, outliers (i.e. samples that do not belong to the sample population of the sediment NIR spectra) should be removed before the MSC. For further discussion on outlier detection, see Martens & Næs (1989), Geladi & Dåbakk (1995) and Birks (1998). Each spectrum is plotted against the reference spectrum, and the slope and offset is then calculated using least squares. The sample spectrum is then corrected by subtracting the offset and dividing by the slope. There are a few modifications on the MSC algorithm, amongst them the piece-wise MSC. In piece-wise MSC, one does not assume that the varying offset and slope is constant over the spectral range, but uses windows of different samples to adjust offset and slope locally.

Derivatives are intuitive ways of treating NIR spectra and, generally, the first and second derivative spectra achieve roughly the same result as MSC. The first derivative gets rid of the baseline (offset), while the second derivative removes the slope. A problem with derivatives is that they amplify spectral curvature. This is often desired, but it may also increase the random noise, which becomes an important aspect as soon as the detection limit for the spectrophotometer is approached. To reduce the effect of increasing random noise, one can smooth the spectra prior to differentiation.

Recently, orthogonal signal correction (OSC) was developed (Wold et al., 1998). OSC works in a similar manner as MSC, but differs in one important aspect. The filtering matrix is orthogonalised with respect to the dependent variable, which then assures that no information, which carries information on the dependent variable in the calibration step, is removed.

Calibration

The purpose of measuring NIR spectra of sediment samples is to relate spectral variability to attributes of the samples or their origin, e.g., for analysis of a specific organic constituent in lake sediments or for inferring lake-water pH from sediment samples. This modelling is usually done multivariately since there are many correlated variables in the NIR spectra. Valuable guidance on multivariate analyses in NIRS is found in Martens & Næs (1989) and in Geladi & Dåbakk (1995). The concepts of multivariate modelling are further described in Volume 3 of this book series (Birks et al., in preparation).

To obtain a proper NIR calibration, experimental-design aspects also need to be considered, i.e. both the spectral variability as well as the whole concentration gradient of the

constituents to be measured should be covered within the calibration data-set. A practical way of setting up a proper NIR calibration is to measure all the samples on the NIR instrument and then to select a subset of samples that are as different as possible for further analysis. An optimal selection of such a calibration set can be made by means of, for example a PCA (Jackson, 1991) or a D-optimal design (Carlsson, 1992). The transfer function obtained from the calibration can then be used to predict the sediment constituent of interest for the samples that were not included in the calibration.

Uses of NIRS in palaeolimnology

The initial exploration of near-infrared reflectance spectrometry in palaeolimnology has shown that NIRS has the potential to become a valuable complement to conventional chemical and biological analyses. Several properties make NIRS a suitable technique for routine analysis in palaeolimnology. It is sensitive to all types of organic molecules, it is easy to use without advanced training and, furthermore, it is a rapid, and thereby a cost-effective tool. However, it is important to remember that what is actually measured by NIR in a sample is the organic constituents. Some studies also show that hydrogen or water bound to mineral particles may influence the NIR spectra. It is important to remember that constituents at the per mille level or lower are probably not directly reflected in the NIR spectra. These components can, in some cases, be quantified through correlation to other constituents present at higher concentrations. Since the beginning of the 1990s the NIR technique has started to take its first steps into palaeolimnology, and currently NIRS is used in three major types of applications:

1. In combination with conventional analytical techniques, NIR spectra can be calibrated for direct analysis of a specific sediment constituent or environmental variable of interest, thereby allowing analysis to be made at a higher temporal or spatial (e.g. whole basin studies) resolution. This approach is in line with the application of NIR spectroscopy in the agricultural and food industries.

2. The NIR spectra can be used for reconstruction of water chemistry, or other environmental parameters, from lake sediments. This approach requires establishment of transfer functions by calibration of NIR spectra from surface sediment samples against measured parameters of the water, such as pH, total phosphorus (TP) or total organic carbon (TOC). These transfer functions can then be applied down-core for inference of past water quality. A similar application is in contemporary lake monitoring programs. Surface sediment samples could be taken, for example, each 5th year for NIR measurements and subsequent inference of several water chemistry parameters, or other environmental parameters, for which transfer functions are available. In this approach effects of diagenetic processes on NIRS, which may be a problem in down-core studies, are circumvented.

3. The NIR spectra *per se* can be used as a "fingerprint" to detect temporal or spatial changes in the chemical and biological composition of the sediment samples. The NIR spectra can then be used for optimal selection of samples for further detailed analysis by other chemical or biological means. This is in line with the approach in which NIR

spectroscopy is applied today in many industrial processes, e.g., for quality assurance and on-line process control in the wood and pulp industry.

These current uses of NIRS in palaeolimnology will be briefly described below. For a more extensive review of sediment constituents and properties analysed by NIRS, see Malley (1998). In her article, she also discusses further research needed to prepare for NIRS to become a routine analysis of sediments.

NIR calibration for direct analysis of sediment sample composition

One use of NIRS on sediments is to replace more expensive and slower classical chemical analyses. Successful NIR calibrations for carbon, carbonate, nitrogen, and phosphorus concentrations in a sediment core were recently reported by Malley et al. (1999), which demonstrates that a rapid, non-destructive, simultaneous analysis of these elements can be achieved by the use of NIRS. In this study on the eutrophication history of the lake Arendsee, Germany, an initial attempt was also made to develop calibrations for total diatoms, as well as the relative frequencies of three dominant diatom species. A similar study was also conducted on sediment cores from four Canadian lakes. In this study, the explained variance between results from conventional chemical analysis and NIR-predicted concentrations ranged between 97 and 99% for total C, organic C, and N (Malley et al., 2000).

The NIR approach has also been used for direct prediction of chemical constituents in marine sediment. Balsam & Deaton (1996) determined the carbonate, organic carbon, and opal content in marine sediments from spectral data. Besides near-infrared spectral data, reflectance spectra from the near ultra-violet and the visible region were also included in their study.

Further support for the use of NIRS in palaeolimnology can be found from NIR analyses of peat and soil samples. For instance, McTiernan et al. (1998) utilised the different organic chemical compositions in peat forming plant species to predict the degree of humification and the botanical composition in peat cores from NIR spectra of the peat samples. Successful quantification of the energy content, carbohydrates, lignin and amino acids in peat has also been achieved by NIR analysis of peat samples (Johansson et al., 1987; Albano et al., 1988). In studies of forest floor litter decomposition, McLellan et al. (1991a; 1991b) replaced the classical wet chemical methods with NIR predictions of nitrogen, carbohydrates and lignin. Based on the successful calibrations (e.g., R^2 for the N calibration was 0.94), the authors concluded that NIR determination could be the future analysis of organic-matter carbon chemistry, because the NIR-analyses are more easily standardised than traditional wet chemistry procedures.

In addition to quantification of organic constituents directly reflected in the NIR absorbance spectra, constituents not directly observed from the NIR spectra have been quantified. The success of these calibrations probably depends on correlation between the particular constituents (e.g., heavy metals), and organic components reflected in the NIR spectra. Malley & Williams (1997) modelled the metal composition in the sediments of Lake 382 in the Experimental Lakes Area in north-western Ontario, Canada. The predictive power of the calibration models was generally very good. For instance, the R^2 between NIR-predicted metal concentrations and metal concentrations analysed by conventional chemical methods were 0.93 for Zn and Mn, 0.91 for Cu, 0.88 for Ni, 0.86 for Fe, and 0.81 for Pb,

while the poorest calibration was achieved for Cd (0.63). The authors interpreted that the NIR information primarily described the metal concentrations by the metal association with sediment organic matter. The wavelengths associated with most of the variance in heavy metal concentrations were attributed to protein, cellulose, and oil. The poorer performance of the Cd-model was attributed to its greater association with inorganic ligands as compared with the other metals.

Reconstruction of water chemistry, or other environmental parameters, using NIRS

In palaeolimnology it is also common to develop "indirect" calibrations, e.g., models (transfer functions) aimed at predicting the water-chemistry from biological indicators in the sediment. These transfer functions developed from data sets on surface sediment and water chemistry for corresponding time periods can then be used to reconstruct water quality changes (e.g., changes in pH or total phosphorus) by applying the surface sediment model to fossil data (stratigraphic data) of the biological indicators. The conceptual approach for water chemistry reconstruction using NIRS on surface sediment samples is presented in Figure 6. This is how NIRS was introduced in palaeolimnology (Korsman et al., 1992), and the basic assumptions for this approach are that:

1. the organic material in lakes, which settles and forms the sediment, is either influenced by the water chemistry conditions and the biota living in the lake, or influences the lake-water chemistry (e.g., catchment-derived humic compounds);

2. properties of this sediment material can be recorded by measuring the NIR spectra; and

3. the NIR spectra can be multivariately modelled to obtain transfer functions between the NIR spectra of the surface sediments and the water chemistry.

Korsman et al. (1992) and Nilsson et al. (1996) evaluated the possibility to establish transfer functions for lake-water pH, total phosphorus (TP), and total organic carbon (TOC) of the lake water. The top 1-cm of sediment was sampled from a series of lakes with different pH, TP and TOC, and NIR spectra from the samples were obtained. The spectra were calibrated against average values for the lake-water chemistry for a time period corresponding to the time period represented by the surface sediment sample. The results have been encouraging and suggest that intense lake-water sampling programmes can partly be replaced by surface sediment samples collected at well-spaced intervals (such as every 2–5 years), and analysed by NIR spectroscopy. The NIR spectra of surface sediment samples can then be used to monitor temporal trends in lake-water chemistry.

Malley et al. (1993, 1996) also analysed N, P and C content in lake-water seston. The seston was captured on a glass fibre filter, dried and scanned on a NIR reflectance instrument. A sub-set of the samples was used to develop calibration functions, while the remaining samples were used to test the prediction performance. The r^2-values between NIR predictions of C, N and P, and the wet chemical determinations, ranged between 0.88 and 0.97. The authors concluded that the prediction performance was as good as for the wet-chemistry techniques used.

Similar results were achieved in a study of Swedish lakes, although with a somewhat lower predictive performance (Dåbakk et al., 2000). In this study, the ability to estimate

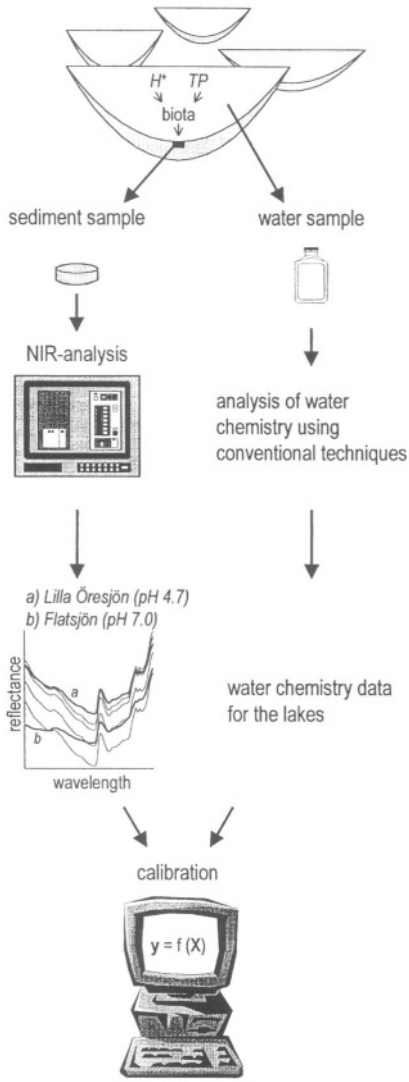


Figure 6. A conceptual model for development of water-chemistry calibrations using NIRS on surface sediment samples. The spectral data shown in the figure (bottom left) are NIR-signals from surface sediments used for development of pH, TP and TOC calibrations (Nilsson et al., 1996).

some water chemistry variables (i.e., total nitrogen, TP and TOC) from NIR spectra of paniculate organic matter (POM) captured on filters, was also investigated. A clear relationship between NIR spectra of the filters and lake-water chemistry was obtained, however, the standard error of prediction was too large to suggest that NIR spectroscopy could replace the current methods. The unexplained variance was also much larger then when modelling lake water chemistry from surface sediments. One major reason for the limited correlation

between MR spectra of particulate organic material and lake-water chemistry is probably that the two entities represent different time periods. The lake water chemistry represent the conditions at the sampling date, while POM represents an extended time period. To achieve a better correlation between the two entities, water chemistry data averaged over the time period during which the particulate organic material was formed are needed.

Another novel approach for NIRS in a palaeolimnological context was the climate reconstruction in a northern Swedish lake by Rosén et al. (2000). The northern Swedish mountain area is characterised by a distinct zonation in vegetation; from a mountain-birch forest (*Betula pubescens* ssp. *tortuosa* Led.) at low altitude, through a *Salix*-dominated shrub zone, up to an alpine heath zone at higher altitude. In this study, the NIR-signal from surface sediments from 76 lakes significantly differentiated between lakes situated in these three vegetation zones. A model between NIR spectra of surface sediments and lake altitude was also established. This model captured 86% of the variance in altitude among the training-set lakes and the cross-validated error was 78 m, representing 8.3% of the altitude gradient. Previous studies from northern Fennoscandia have shown a significant relationship between temperature change and altitude (Laaksonen, 1976). Thus, the altitude model was used to reconstruct temperature change in a small headwater lake situated about 100 m above the present treeline in the northern Swedish mountains. The temperature record derived from this NIRS-altitude model showed similar trends to inferred temperature based on other proxy data (diatoms, pollen and chironomids).

NIK spectra as a "fingerprint" for temporal and spatial changes of sediment properties

The use of NIR spectra on sediment samples to predict certain constituents from calibration models is, by itself, one important development taking advantage of the speed and low cost of the method. This approach, though, only utilises a small proportion of the information on the organic chemical composition contained in the MR spectra. One alternative, then, is to use the whole NIR spectra as a "fingerprint", which can be used to evaluate the variation in sediment composition both in time and space. The total variation represented by several hundred absorbance values can normally be compressed to less then 10 "latent variables", components, by different multivariate statistical methods. Similar approaches are used in the process industry where hundred or thousand of signals, used to monitor the performance of some production process, are compressed to a "finger print" and followed over time.

The close link between lakes and their catchments was evident in a study of spatial variability in surface sediment composition in a small northern Swedish lake (Korsman et al., 1999). In this study, the information in the near-infrared spectra of surface sediment samples was used to determine how sediment composition varied over the lake bottom. The study showed that the NIR spectra *per se* provide information that can be used to study sediment characteristics as well as sediment focusing in a qualitative way. The variance in the NIR spectra (Fig. 7) was only to a minor extent explained by the variation in water depth or sediment organic content. More importantly, the spatial evaluation of the spectral data suggested that NIR analysis of lake sediments mainly reflects sediment properties that cannot be simply explained by water depth or amount of organic matter. Principal component modelling of NIR spectra from 165 coring sites, established along a 50m x 50m

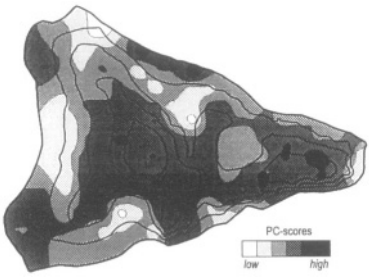


Figure 7. Near-infrared spectral variation in surface sediments of Stor-Skärträsket. The figure shows the spectral variance in the first principal component from a PCA-analysis based on 165 surface sediment samples. The bottom topography is presented as depth curves with a 2-m interval. Modified from Korsman et al. (1999).

grid, revealed that the influence of land-use and inlets on sediment characteristics was more pronounced in the spectral data than what would be expected from loss-on-ignition analysis.

In palaeolimnological studies, the possibility to use the NIR spectra *per se* has not been used for optimal stratigraphic sample selection. However, successful results from the use of NIRS in soil science suggest that such an approach would be fruitful in palaeolimnology. Stenberg et al. (1995) proposed an excellent strategy for sample selection based on NIR spectra. Using principal component score plots of the NIR spectra, 20 of the originally 146 samples were selected. These 20 samples represented all variations in clay content, soil organic matter, cation exchange capacity and base saturation that occurred in the total set of samples. All further classical chemical analyses or experiments could then be performed on the reduced data set, which included the full variation in the variables of interest. Using this reduced data set, transfer functions between NIR spectra and soil variables were developed and further used to predict these same variables in all other samples. Using this approach for the actual sample set, the analysis costs would have been reduced by 70%. The same strategy could easily be used on sediment cores or surface sediment samples.

Future perspectives

The successful use of NIRS in different industrial applications (e.g., Davies & Williams, 1996), and the promising results from various environmental applications including the previously described sediment studies, suggests that NIRS can become a valuable tool in palaeolimnology. A potential limitation for the use of NIRS in palaeolimnology could be the effects of diagenetic processes on the NIR signals. A test, comprising a comparison of NIR spectra from the top 0–1 and 1–2 cm from 56 mountain lakes in northern Sweden (Rosén et al., 2000), indicated that the decomposition of organic material, which inevitably occurs at the sediment/water interface, was not a significant problem. However, these results can not be used for general conclusions about sediment-ageing effects on NIR signals, and this needs further investigation.

If diagenetic processes prove to cause problems for some sediment-NIR applications, calibration data-sets using consolidated (sub-surface) samples rather than surface sediment samples might be a solution. For example, a transfer function between sediment-NIR and

lake-water pH could be established using sediment samples from cores and pH values inferred using diatom analysis (cf. Korsman et al., 1992). For analyses of sediment chemistry using NIRS, such as of organic sediment constituents that normally require expensive analyses, a lake specific data-set consisting of a limited number of samples of consolidated sediments can be used to construct transfer function. The NIR spectra could then easily be collected at any interval and the sediment constituent of interest could be predicted using the transfer function. In such a case, the simplicity and the rapidness of NIRS would allow a temporal resolution solely based on the aim of the study and the limitations set by the sediment, e.g., accumulation rate or bioturbation.

Summary

Near-infrared spectrometry (NIRS), which is a rapid, non-destructive spectroscopic technique, is commonly used for process control and quality assurance in food, pharmaceutical, and pulp and paper industries. However, until recently there has been limited use of NIRS in a palaeolimnological context.

Several properties make near-infrared spectrometry (NIRS) a suitable technique for analysis of lake sediments. It is sensitive to all types of organic molecules, it is easy to use without advanced training, and it is a rapid, and thereby a cost-effective tool. NIRS utilises absorbance within the near-infrared region (780–2500 nm) resulting from bending and stretching vibrations in molecular bonds, and in particular the bonds between light atoms (e.g., C-H, O-H, N-H or S-H). Absorptions in the near-infrared region for some common organic chemical bonds are presented in the chapter.

A spectrum obtained for a sediment sample is rich in chemical information. However, the information is found in several overlapping combination bands and spectral overtones, rather than in distinct absorption peaks. The development of a reliable calibration model is therefore one of the most important steps to gain quantitative information on chemical compounds from the spectral response of a sample. This involves a thorough consideration of experimental design and multivariate calibration.

The influence of, e.g., the particle sizes and the water content on the spectral signal also need consideration in the analysis of sediment samples. For instance, differences in particle sizes may result in light-scattering effects, while analysis of samples with high water content results in broad peaks with high absorptivity that may hide spectral information from other constituents. These problems have to be dealt with in sample preparation and by spectral pre-treatments. A sample handling and preparation scheme involving freeze-drying and grinding of the sediment samples, and different spectral filters and pretreatments are presented and discussed in the chapter.

Since the beginning of the 1990s the NIR technique has started to take its first steps into palaeolimnology, and currently NIRS is used in three major types of applications: 1) the calibration of NIR spectra for direct analysis of a specific sediment constituent or environmental variable; 2) the use of NIR spectra for reconstruction of water chemistry, or other environmental parameters, from lake sediments; and 3) the use of NIR spectra as a “fingerprint” to detect temporal or spatial changes in the chemical and biological composition of the sediment samples. These palaeolimnological applications of NIRS, which are briefly presented in the chapter, show that NIRS has the potential to become a valuable complementary or alternative tool for chemical and biological analyses of lake sediments.

References

Albano, C., Å. Albano, E. Bohlin, M. Hämäläinen, C. Röckner & T. Sundén, 1988. Néar infrared spectroscopy and peat characterization. Proc. VIII Intern. Peat Congress IV: 241-246.

Balsam, W. L. & B. C. Deaton, 1996. Determining the composition of late Quaternary marine sediments from NUV, VIS, and NIR diffuse reflectance spectra. Marine Geol. 134: 31-55.

Barnes, R. J., M. S. Dhanoa & S. J. Lister, 1989. Standard normal variate transformation and de-trending of near-infrared diffuse reflectance spectra. Appl. Spectrosc. 43: 772-777.

Birks, H. J. B., 1998. D. G. Frey & E. S. Deevey review #1 — Numerical tools in palaeolimnology: progress, potentialities, and problems. J. Palcolim. 20: 307–332.

Birks, H. J. B., S. Juggins, A. Lotter & J. P. Smol, in preparation. Tracking Environmental Change Using Lake Sediments: Data Handling and Statistical Techniques. Kluwer Academic Publishers, Dordrecht, The Netherlands.

Bokobza, L., 1998. Near infrared spectroscopy. J. Near Infrared Spectrosc. 6: 3–17.

Burger, T., J. Fricke & J. Kuhn, 1998. NIR radiative transfer investigations to characterise pharmaceutical powders and their mixtures. J. Near Infrared Spectrosc. 6: 33–40.

Carlson, R., 1992. Design and Optimization in Organic Synthesis. Elsevier, Amsterdam.

Davies, A. M. C., 1997. The continuing progress of NIR spectroscopy: highlights from NIR-97. Spectroscopy Europe 9: 16–18.

Davies, A. M. C. & P. Williams (eds.), 1996. Near Infrared Spectroscopy: The Future Waves. NIR Publications, Chichester, xx pp.

Day, M. S. & F. R. B. Fearn, 1982. Near infra-red reflectance as an analytical technique. Part 2. Design and development of practical NIR instruments. Laboratory Practice 31: 439–443.

Dåbakk, E., 1999. Near Infrared Spectrometry: A Potential Tool for Environmental Monitoring of Aquatic Systems. PhD thesis. Umeå University, Sweden.

Dåbakk, E., M. Nilsson, P. Geladi, S. Wold & I. Renberg, 1999. Sampling reproducibility and error estimation in near infrared calibration of lake sediments for water quality monitoring. J. Near Infrared Spectrosc. 7: 241–250.

Dåbakk, E., M. Nilsson, P. Geladi, S. Wold & I. Renberg, 2000. Inferring lake water chemistry from filtered seston using NIR spectrometry. Water Research 34: 1666–1672.

Foley, W. J., A. McIlwee, I. Lawler, L. Aragones, A. P. Woolnough & N. Berding, 1998. Ecological applications of near infrared reflectance spectroscopy: a tool for rapid, cost-effective prediction of the composition of plant and animal tissues and aspects of animal performance. Oecologia 116: 293–305.

Geladi, P. & E. Dåbakk, 1995. An overview of chemometrics applications in NIR spectroscopy. J. Near Infrared Spectrosc. 3: 119–132.

Geladi, P., D. MacDougall & H. Martens, 1985. Linearization and scatter-correction for near-infrared reflectance spectra of meat. Appl. Spectrosc. 39: 491–500.

Herschel, W., 2000. Herschel's paper [reprint]. J. Near Infrared Spectrosc. 8: 75–86.

Jackson, J. E., 1991. A User's Guide to Principal Components. John Wiley & Sons, New York, 569 pp.

Johansson, E., J. Å. Persson & C. Albano, 1987. Determination of water content and calorific value of peat by n.i.r. spectroscopy. Fuel 58: 1173–1178.

Korsman, T., M. Nilsson, J. Öhman & I. Renberg, 1992. Near-infrared reflectance spectroscopy of sediments: a potential method to infer the past pH of lakes. Environ. Sci. Technol. 26: 2122–2126.

Korsman, T., M. B. Nilsson, K. Landgren & I. Renberg, 1999. Spatial variability in surface sediment composition characterised by near-infrared (NIR) reflectance spectroscopy. J. Paleolim. 21: 61–71.

Laaksonen, K., 1976. The dependence of mean air temperatures upon latitude and altitude in Fennoscandia (1921–1950). Ann. Acad. Sci. Fennicae 119: 5–19.

Kubelka, P. & F. Munk, 1931. Ein Beitrag zur Optik der Farbanstriche. Zeithschrift für Technische Physik 12: 593–604.

Malley, D. F., 1998. Near-infrared spectroscopy as a potential method for routine sediment analysis to improve rapidity and efficiency. Water Sci & Technol. 37: 181–188.

Malley, D. F., P. C. Williams, M. P. Stainton & B. W. Hauser, 1993. Application of near-infrared reflectance spectroscopy in the measurement of carbon, nitrogen, and phosphorus in seston from oligotrophic lakes. Can. J. Fish. Aquat. Sci. 50: 1779–1785.

Malley, D. F. & M. Nilsson, 1995. Environmental applications of near infrared spectroscopy: seeing the environment in a different light. Spectroscopy Europe 7: 8–16.

Malley, D. F, P. C. Williams & M. P. Stainton, 1996. Rapid measurement of suspended C, N, and P from Precambrian shield lakes using near-infrared reflectance spectroscopy. Water Research. 30: 1325–1332.

Malley, D. F. & P. C. Williams, 1997. Use of near-infrared reflectance spectroscopy in prediction of heavy metals in freshwater sediment by their association with organic matter. Environ. Sci. Technol. 31: 3461–3467.

Malley, D. F., H. Rönicke, D. L. Findlay & B. Zippel, 1999. Feasibility of using near-infrared reflectance spectroscopy for the analysis of C, N, P, and diatoms in lake sediments. J. Paleolim. 21: 295–306.

Malley, D. F., L. Lockhart, P. Wilkinson & B. Hauser, 2000. Determination of carbon, carbonate, nitrogen, and phosphorus in freshwater sediments by near-infrared reflectance spectroscopy: rapid analysis and a check on conventional analytical methods. J. Paleolim. 24: 415–425.

Martens, H. & T. Nass, 1989. Multivariate Calibration. John Wiley & Sons, New York, 419 pp.

McClure, W. F, 1994. NIR spectrosopy: the giant is running strong. Analytical Chemistry 66: 43A–52A.

McLellan, T. M., J. D. Aber, M. E. Martin, J. M. Melillo & K. J. Nadelhoffer, 1991a. Determination of nitrogen, lignin and cellulose content of decomposing leaf material by near infrared reflectance spectroscopy. Can. J. Forest. Res. 21: 1684–1688.

McLellan, T. M., M. E. Martin, J. D. Aber, J. M. Melillo, K. J. Nadelhoffer & B. Deway, 1991b. Comparison of wet chemistry and near-infrared reflectance measurements of carbon fraction chemistry and nitrogen concentration of forest foliage. Can. J. Forest. Res. 21: 1689-1693.

McTiernan, K. B., M. H. Garnett, D. Mauquoy, P. Ineson & M. M. Coûteaux, 1998. Use of near infrared reflectance spectroscopy (N1RS) in palaeoecological studies of peat. Holocene 8: 729–740.

Nilsson, M.,T. Korsman, A. Nordgren, C. Palmborg, I. Renberg & J. Öhman, 1992. NIR spectroscopy used in the microbiological and environmental sciences. In Hildrum, K. I., T. Isaksson, T. Næs & A. Tandberg (eds.) Near Infra-red Spectroscopy: Bridging the Gap Between Data Analysis and NIR Applications. Ellis Horwood, New York: 229–234.

Nilsson, M. B., E. Dåbakk, T. Korsman & I. Renberg, 1996. Quantifying relationships between near-infrared reflectance spectra of lake sediments and water chemistry. Environ. Sci. Technol. 30: 2586–2590.

Norris, K. 1998. Interaction among instrument bandpass, instrument noise, sample absorber bandwidth and calibration error. NIR News 9: 3-5.

Osborne, B. G. & T. Fearn, 1986. Near Infrared Spectroscopy in Food Analysis. John Wiley & Sons, New York, 200 pp.

Rosén, P., E. Dåbakk, I. Renberg, M. Nilsson & R. Hall, 2000. Near-infrared spectrometry (NIRS): a new tool to infer past climatic changes from lake sediments. Holocene 10: 161–166.

Skoog, D. A. & J. J. Leary, 1992. Principles of Instrumental Analysis. Saunders College Publishing, Forth Worth, 879 pp.

Stenberg, B. O., E. Nordkvist & L. Salomonsson, 1995. Use of near-infrared reflectance spectra of soils for objective selection of samples. Soil Sci. 159: 109–114.

Williams, P., 1987. Variables affecting near-infrared reflectance spectroscopic analysis. In Williams, P. & K. Norris (eds.) Near-infrared Technology in the Agricultural and Food Industries. American Association of Cereal Chemists, St. Paul, Minnesota, USA: 143–167.

Wold, S., H. Antti, F. Lindgren & J. Öhman, 1998. Orthogonal signal correction of NIR spectra. Chemometrics Intellig. Lab. Systems 44: 175–185.

12. FLY-ASH PARTICLES

NEIL ROSE (nrose@geog.ucl.ac.uk)
Environmental Change Research Centre
University College London
26 Bedford Way
London WC1H 0AP
United Kingdom

Keywords: atmospheric deposition; combustion products; industrial pollutants; inorganic ash spheres; sediment dating; spheroidal carbonaceous particles

Introduction

What is fly-ash?

Fossil-fuels are burned at high temperatures to produce heat and power for electricity generation and other industries. At temperatures of up to 1750 °C (Commission on Energy and the Environment, 1981) and at a rate of heating of approaching 10^4 °C s^{-1} (Lightman & Street, 1983), the droplets, or pulverised grains of fuel, are efficiently burned even though they only remain in the furnace for a matter of seconds. The products of this combustion are porous spheroids of mainly elemental carbon (Goldberg, 1985) and fused inorganic spheres formed from the mineral component of the original fuel (Raask, 1984). These spheroidal carbonaceous particles (SCPs) (Fig. 1) and inorganic ash spheres (IASs) (Fig. 2) are collectively known as fly-ash, the term used to describe the particulate matter within emitted flue-gases.

There are, in fact, three components of fly-ash and they are formed in different ways. First, non-combustible material (IASs), second, combustible matter that was not burned (SCPs) and third, matter which was formed during the combustion process. These processes of formation determine the morphology of these particles and, as this is the main means of identification in paleolimnological studies, it is worthwhile to briefly describe them. They also control the relative abundances of the different particle types in the various fuel fly-ashes and this information can be used in source apportionment studies.

The non-combustible material when heated rapidly undergoes some volatilisation, giving rise to sub-micron particles termed 'fume', whilst the non-volatile component coalesces to form hollow ash spheres termed 'cenospheres' (Raask, 1984) with a variety of internal structures (Lightman & Street, 1968). Less frequently, solid spheres (Lightman & Street, 1968) and plerospheres (cenospheres containing encapsulated smaller spheres formed by inconsistent heating through the mineral grain, Fig. 3) are formed. Up to 25%



W.M. Last & J. P. Smol (eds.), 2001. *Tracking Environmental Change Using Lake Sediments. Volume 2: Physical and Geochemical Methods.* Kluwer Academic Publishers, Dordrecht, The Netherlands.

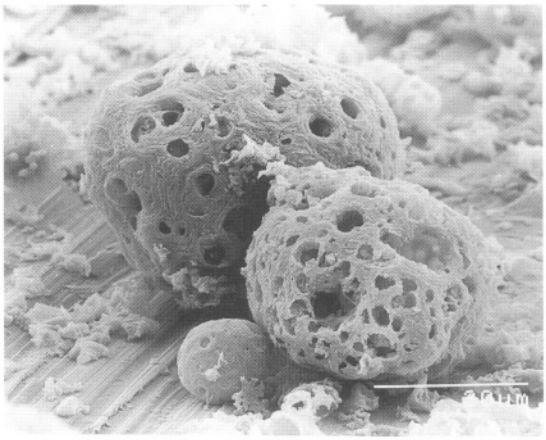


Figure 1. SEM photograph of spheroidal carbonaceous particles (SCPs) from oil combustion.

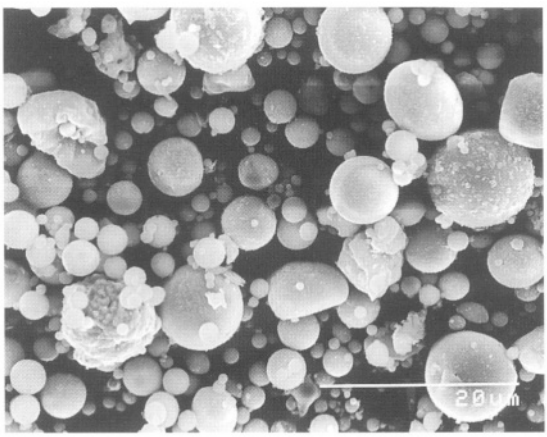


Figure 2. SEM photograph of inorganic ash spheres (IASs) from the combustion of coal (From Rose, 1996; reprinted with permission from Elsevier).

(typically 15–17%) of coal is non-combustible and approximately 0.1% of fuel-oil (Goldstein & Siegmund, 1976). Hence IASs comprise 95–98% of coal fly-ash (Raask, 1984) and less than 20% of oil fly-ash (Mamane et al., 1986).

When pulverised coal particles are heated rapidly, they change from angular non-porous coal fragments to porous and often partitioned spheroids having a molten appearance (Lightman & Street, 1968). These particles are fragile and will fragment if they remain in the combustion chamber. In oil-droplet combustion, volatiles are produced as the droplet heats and it is in this expelled cloud of hydrocarbons that ignition first occurs. Then, as heat is given back to the droplet, burning of the volatiles on the particle surface takes place. As emission of volatiles decreases, the droplet collapses and becomes rigid forming the final SCP (Lightman & Street, 1983). Oil SCPs are spheroidal, often more porous than coal

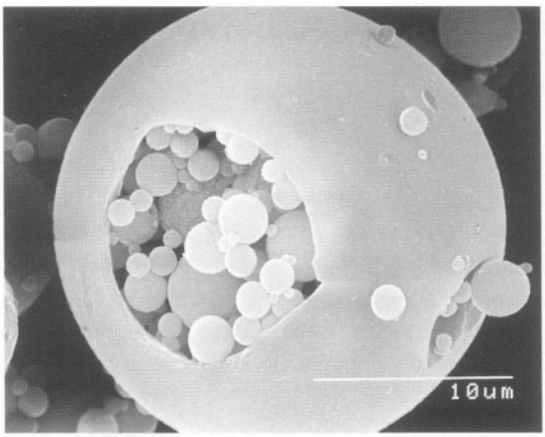


Figure 3. SEM photograph of a plerosphere, a hollow cenosphere containing encapsulated smaller spheres. (From Rose, 1996; reprinted with permission from Elsevier)

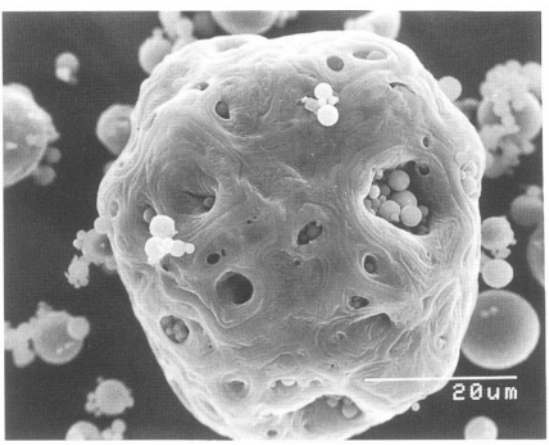


Figure 4. SEM photograph of a spheroidal carbonaceous particle from the combustion of coal, showing a convoluted surface texture, previously thought typical of oil combustion and used in fuel-type apportionment of SCPs.

SCPs due to the greater emission of hydrocarbons, and have a complex internal structure. On some particles a contour effect around the pores is seen, which some authors have suggested is characteristic of this fuel-type (Lightman & Street, 1983; Kothari & Wahlen, 1984; Griffin & Goldberg, 1981). However, this contouring has also been observed on the surfaces of coal particles (Rose, 1991) (Fig. 4).

The component formed during the combustion process is termed soot (Chigier, 1975; Nettleton, 1979) and although carbonaceous, is usually sub-micron in size and bears no morphological resemblance to SCPs. It is for this reason that it is important from the outset

to define the terms and hence the particulates, under study. This chapter will deal only with the SCP and IAS components. The combustion of wood does not give rise to SCPs and charcoal particles will be dealt with in a separate chapter in Volume 3 of this book series.

Definition of terms

Although SCPs and IASs are produced by the alteration of original particles passing through the furnace, and soot is produced during combustion processes, there has been some confusion in the literature, especially in earlier works. However, it is important to realise that these studies are referring to the same particle types. For example, SCPs have been variously referred to as soot (Charles et al. 1990), soot balls (Punning et al., 1994), (Tolonen et al., 1990), soot particles (Renberg & Wik, 1984; 1985a), soot spheres (Renberg & Wik, 1985a), soot spherules (Hilgers et al., 1993) carbon particles/elemental carbon particles (Griffin & Goldberg, 1975; 1979), carbonaceous particles (Guilizzoni et al., 1992; Rose, 1990a), charcoal particles (Kothari & Wahlen, 1984) and spheroidal fly-ash particles (SFP) (Punning et al., 1997a), although this latter may also include black IASs. Wik et al. (1986) identified the potential mis-interpretation problem of using the term 'soot' and changed to 'coarse carbonaceous spheres'. Recently, however, the term spheroidal carbonaceous particle or spheroidal carbonaceous fly-ash particle (both abbreviated to SCP) has become the usual term and is now widely used (e.g., Korhola et al., 1996; Korhola & Blom, 1996; Lan & Breslin, 1999; Odgaard, 1993, Renberg & Hultberg, 1992; Rose et al., 1994; 1998a; 1999a; Rose, 1995; Virkenan et al., 1997; Wik & Renberg, 1991a; 1991b; 1996). However, in a more comprehensive description of many combustion-related particles, classified using morphological features, Doubleday (1999) refers to SCPs as 'SPCBK', an abbreviation of 'spheroidal carbonaceous black'.

The nature of their formation and their porosity means that both oil and coal SCPs are never spherical. However, they do have some degree of sphericity to their morphology and for this reason they are termed spheroidal. IASs are spherical and come in a variety of colours from colourless through yellow, red, brown and black, depending on their elemental, and in particular iron, content. Therefore, the counting of black 'spheres' and terming them SCPs (e.g., Larsen et al., 1996) may lead to further confusion as to the exact nature of the particle types included in the enumeration. Here, spherical fly-ash particles of any colour are deemed IASs and are precluded from being identified as SCPs for that reason.

Why use fly-ash in paleolimnology?

SCPs are not produced from wood, biomass or charcoal combustion, and hence have no natural sources. Therefore, they are unambiguous indicators of deposition from industrial combustion of fossil-fuels. Their use as markers in sediments and other depositional sinks is enhanced by their easily identifiable morphology and, because of their elemental carbon composition, by their relatively simple extraction from the sediment matrix. IASs, on the other hand, or rather particles morphologically identical to them, do have natural sources from volcanic emissions (LeFèvre et al., 1986) and micro-meteorites (Handy & Davidson, 1953; Hodge & Wright, 1964). In addition, their aluminosilicate composition makes them less able to withstand chemical attack and, compositionally, similar to many of the sediment

Table I. Examples of the use of combined sediment metal and SCP data with catchment moss metal data to suggest sources of contaminants (abbreviated from Rose et al., 1998b).

Sediment metal	Moss metal	Sediment SCP	Suggested source
High	High	High	Atmospheric deposition from an industrial source including a significant fossil-fuel component
High	High	Low	Atmospheric deposition from an industrial source with no significant fossil-fuel component
High	Low	Low	Catchment source of metal

minerals from which they are being extracted. This results in a less efficient extraction technique (Rose, 1990b). Finally, the chemical composition of IASs is dependent on that of the original mineral, whereas the elemental composition of SCPs can give clues as to their source fuel-type (Rose et al., 1996). In consequence, most paleolimnological studies involving fly-ash have focused on SCPs whilst IASs have been the subject of only a few (e.g., Rose, 1990b;1996; O. Nagafuchi, pers. commun.).

Historically, SCPs have been used in two main ways. First, as supporting evidence for the acid deposition hypothesis in the surface water acidification debate of the 1980s, and second as a cheap and simple means of adding a few recent dates to sediment cores. In the former, the sediment record of SCPs, along with other indicators of atmospheric deposition (e.g. metals, magnetics), were seen to correspond with unprecedented acidification as reconstructed from fossil diatom assemblages. This work was undertaken on both sides of the Atlantic as part of SWAP (Surface Water Acidification Project) in Europe (e.g. Battarbee & Renberg, 1990) and PIRLA (Paleoecological Investigation of Recent Lake Acidification) in North America (e.g., Charles & Whitehead, 1986; Charles et al., 1990). The use of SCPs for sediment dating was developed by Renberg & Wik (1984; 1985a) in Sweden and has latterly been employed throughout Europe, especially in the UK and Ireland (Rose et al., 1995). This is discussed in more detail later.

More recently, the spatial distribution of atmospheric deposition has been studied using SCP concentrations in a number of surface sediments across a region (e.g., Wik & Renberg, 1991a; Rose & Juggins, 1994; Alliksaar & Punning, 1998; Bowman & Harlock, 1998; Fott et al., 1998; Rose & Harlock, 1998) or within a lake (e.g., Lake Baikal, Rose et al., 1998a). Patterns have been shown to be similar to those of other deposited pollutants such as metals and sulphur. Similarly, full core SCP inventories have been seen to show good agreements with sources across wide regions e.g. Europe (Rose et al., 1999c) whilst within-lake inventories of multiple cores show good agreement with inventories of deposited metals such as Hg and Pb. SCP concentrations in surface sediments have also been used in combination with metal concentrations in sediments and catchment mosses to give indications as to sources of deposition (Rose et al., 1998b). Some examples are given in Table I.

Finally, as mentioned above, the chemistry of SCPs has been used to determine the fuel-type of individual particles. This has been employed to trace both changes in deposition sources through time at an individual site (Rose et al., 1996) and to map deposition from different fuel sources across a region using SCPs from surface sediments (e.g., Rose et al., 1999b). Again, this is discussed more fully later.

A brief history

Wik and Renberg's (1996) review of environmental records of SCPs included a synopsis of the historical development of their use, so only a brief outline will be given here.

Griffin & Goldberg (1975) were the first to describe the presence of spheroids of elemental carbon, in coastal marine sediments off the California and British Columbia coasts. In 1979 they extracted elemental carbon from a box-core taken from Lake Michigan and suggested that the change in morphology of particles up the core towards a greater degree of sphericity was due to changes in fuel-use from wood to coal and oil combustion (Griffin & Goldberg, 1979). They therefore became the first to extract and identify SCPs from a lake sediment core. They used this approach to produce a simple fuel-type classification based on particle morphology and surface texture (Griffin & Goldberg, 1981) whilst Goldberg et al. (1981) showed a comparison between the sediment profile of elemental carbon concentration and profiles of a number of trace metals thereby implying the impact of fossil-fuel combustion on the sediment metal record of Lake Michigan. After briefly returning to the subject of black carbon in Lake Michigan, although this time the sub-micron component (Griffin & Goldberg, 1983), and expanding on these works in a book (Goldberg, 1985), these pioneers appear to have stopped working in the field.

The method employed by Griffin & Goldberg, developed by Smith et al. (1975), used approximately 10 g of dry sediment and an infra-red technique to determine elemental carbon concentrations. For most paleolimnological studies, this is an impractical amount of sediment to obtain and work with and therefore the technique developed in Sweden by Renberg & Wik (1984; 1985a) using much smaller amounts of sediment, chemically treated and directly counted by microscopy, was a great step forward towards using SCP analysis routinely in paleolimnological studies. Renberg & Wik were also the first to use SCP profiles as a lake sediment dating tool (Renberg & Wik, 1984; 1985a), the first to look at SCPs in soils (Wik & Renberg, 1987), and sediment traps (Wik & Renberg, 1991b), and the first to publish a regional distribution of SCPs using surface sediments and compare this to excess sulphate in deposition and Pb in moss (Wik & Renberg, 1991a), although similar work was being undertaken concurrently in Scotland (Rose, 1991; Rose & Juggins, 1994). The Renberg & Wik technique was employed in SWAP so that the first sediment profiles for the UK (Darley, 1985; Wik et al., 1986) and Norway (Wik & Natkanski, 1990) were produced.

In the UK, Rose (1990a; 1994) developed the chemical extraction of SCPs further so that more of the unwanted sediment fractions were removed, whilst larger numbers of sediment samples could be treated simultaneously. In addition, a technique was also developed which, for the first time, extracted IASs from lake sediments (Rose, 1990b). Rose et al (1996) also developed a technique whereby SCPs from coal, oil and peat could be allocated to their fuel-type by means of their elemental chemistry and this technique was applied to SCPs extracted from both surface sediments across a region and from a single site down a core. This was later expanded to include all the major fuel-types of Europe (Rose et al., 1999b).

In North America, for PIRLA, "soot" particles were counted on slides made for charcoal and pollen analysis (Charles & Whitehead, 1986) and profiles of coal and oil "soot" were produced using the morphological parameters described by Griffin & Goldberg (1981). In recent years, SCP analysis has been undertaken by many workers on sediments from all continents in the world, although much of the work to date has been focused within Europe (Table II).

Table II. Currently available dates for features of SCP profiles from around the world.

Country	Region	Start of record	Rapid increase	SCP peak	Reference
EUROPE					
Austria	South	1850s	1940s	1960s	Wathne, 1999 (MOLAR)
Czech Republic	Bohemia	?	1950s/1960s	1970s?	Schmidt et al., 1993
Denmark	All	c. 1900	1950s	c. 1970	Odgaard, 1993
Estonia (IAS&SCP)	North-east	?	1950s	?	Alliksaar et al., 1998
					Punning et al., 1997b
Finland	South	c. 1850	c. 1955	1973 & 1990	Korhola et al., 1996
	South	c. 1850	1950s	late 1970s/early 1980s	Tolonen et al., 1990
	North	c. 1860	1940s	1985 ± 2	Korhola et al., unpubl.
France	Alps	1890s	1950s	1970 ± 2	Rose et al., 1999c
	Pyrenees	1930s	1980s?	1985?	Rose et al., 1999c
	Vosges	1860s	1960s	c. 1980	Krieser et al., 1995
Germany	Black Forest	?	1950s	early 1970s	Hilgers et al., 1993
Ireland	North	1880s	1960s	1981 ± 2	Rose et al., 1995
Italy	Alps	1930s	1950s	mid-1980s?	Rose et al, 1999c
	Tyrol	1910s	1950s	1980s	Rose et al, 1999c
Norway	South	c. 1850	c. 1930	1972±?	Wik & Natkanski, 1990
	South	1860s	1950s	1985 ± 1	Rose et al., 1999c
	Mid-	?	?	c. 1970	Wik & Natkanski, 1990
	Mid-	1920s	1960s	1991 (surface)	Rose et al., 1999c
Poland	Tatra Mountains	?	1960s	1992 ± 2 & 1993 (surface)	Rose et al., 1999c
Portugal	Sierra Estrela	1920s	early 1970s	1984 ± 2	Rose et al., 1999c
Slovakia	Tatra Mountains	1930s	?	1976 ± 2 & 1990 ± 2	Rose et al., 1999c
Slovenia	North-west	1850–1875	1950s	1987 ± 2 & 1962 ± 2	Brancelj et al., unpubl.
					Rose et al., 1999c
	Pohorje (north, central)	?	?	mid-1980s	Brancelj et al., 1999
Spain	Gredos	c. 1880	1960s	1986 ± 2	Toro et al., 1993
	Sierra Nevada	1950s*	1980s	1989 ± 2	Rose et al., 1999c
	Pyrenees	1840s/1850s	1950s	1960*s*&1989 ± 2	Rose et al., 1999c

Table II. Currently available dates for features of SCP profiles from around the world (cont.)

Country	Region	Start of record	Rapid increase	SCP peak	Reference
Europe (cont.)					
Svalbard	West Coast	1860s*	1960s–1980s*	mid-late 1970s†	Rose et al, unpubl.
Sweden	All	c. 1850	1950s	c. 1970	Renberg & Wik, 1984; 1985a
	North	18th century	1950s	c. 1970	Renberg & Wik, 1985b
Switzerland	All	early 1800s–1880	mid-1940s–1950s	late-1970s	Lotter et al., unpubl.
UK	N. Scotland	1850s	1960s	1976 ± 2	Rose et al., 1995
	S.Scotland/N.England/N.Wales	1850s	1950s	1978 ± 2	Rose et al., 1995
	S.England	?	1950s	1969 ± 2	Rose et al., 1995
NORTH AMERICA					
USA	Adirondacks	1860s/1870s	1950s	c. 1970	Charles et al., 1990
	Great Lakes	1820s–1840s	c. 1900	late 1960s	Goldberg et al., 1981
					Lan & Breslin, 1999
Canada	Arctic	Late 19th century	?	1991 (surface)	Doubleday, 1999**
ASIA					
China	Jianghan Plain	1950s*	1960s/1970s	surface	Boyle et al., 1999
Japan	West	c. 1900	1950s	1972 ± 2	Nagafuchi, unpubl.
Russia	Siberia (Baikal)	1860s*	1970s	1990 ± 2	Rose et al., 1998
					Flower et al., 1997
AFRICA					
Morocco	North	1920s	1970s	1990 (surface)	Flower et al., 1992
	North	1930s–1960s*	1950s–1970s	1982–1984 ± 2	Rose et al. unpubl.
Egypt	North	1900–c. 1950*	?	1989–1997 (surface)	Rose et al. unpubl.
Tunisia	North	1920s–c. 1980*	?	1997 (surface)	Rose et al. unpubl.
AUSTRALIA					
Australia	Tasmania	?	1940s	1991 (surface)	Cameron et al., 1993

* May depend on detection limit
** Peak of SCPs as a percentage of total combustion particles
† Not always present

Methods of extraction and enumeration

As mentioned above, SCPs are composed of elemental carbon and, although physically fragile, this makes them resistant to chemical attack. Strong reagents can therefore be used to remove unwanted fractions of sediment without doing the SCPs any physical damage.

Smith et al. (1975) used basic peroxide (a mixture of hydrogen peroxide (H_2O_2) and potassium hydroxide (KOH)) to remove organic material followed by hydrochloric (HCl) and hydrofluoric acid (HF) stages to remove carbonate and silicate fractions respectively. An infra-red technique was then employed to determine elemental carbon levels. This approach reduced their original 10 g of marine sediment to 10–30 mg.

However, the two currently most frequently used techniques are those devised by Renberg & Wik (1984) and that described by Rose (1994). The former of these is the simpler, using an H_2O_2-only digestion to remove the organic material. The residue is then poured onto a petri-dish and the SCPs counted under a binocular microscope at 100x magnification. In this way SCPs down to 5 μm diameter can be identified. In the technique described by Rose (1994), the digestion is performed in polytetrafluoroethylene (PTFE) tubes in a water-bath rather than in beakers and hence a larger number of samples can be prepared at a time. In a modification of the Smith et al. (1975) procedure, unwanted sediment fractions are removed by sequential chemical attack, with nitric acid (HNO_3), HF and HCl used to remove organic, siliceous and carbonate material respectively. A starting sediment mass of 0.15 g is reduced to less than 0.001 g using this technique, thus removing more than 99.3% of the sediment (Rose, 1994). A weighed sub-sample of the final residue, consisting of carbonaceous material and a few persistent minerals, is then evaporated onto a coverslip, mounted on a microscope slide and counted at 400x magnification. SCPs down to c. 2 μm can be identified in this way.

The method for extracting IASs from sediments is less vigorous as the particles are less chemically robust. Being composed mainly of aluminosilicate precludes the use of HF whilst the use of concentrated HCl would severely erode if not dissolve entirely the iron-rich spheres. In addition, many of the surrounding sediment minerals are themselves composed primarily of aluminosilicate minerals and thus a chemical extraction is by necessity both subtler and less complete. Consequently, the final residue contains more material and hence enumeration of the IASs is also more difficult than for SCPs. The procedure is similar to that of the SCP extraction in that sequential chemical digestion is used to remove unwanted fractions (Rose 1990b). However, using this method, H_2O_2 is used to remove organic material, 0.3 M sodium hydroxide (NaOH) to remove biogenic silica, and dilute HCl to remove the more readily dissolvable carbonates. The final residue is treated in the same way as for SCPs, and the slide counted at the same magnification. Finally, in a technique to enumerate a combination of both particle types (as "spheroidal fly-ash particles"), Punning et al., (1997a) used 2 M NaOH and 10% $Na_4P_2O_7$ to remove organic matter before mounting the samples in glycerine and counting at 420x magnification.

Safety note

The removal of sediment fractions by selective digestion, particularly using the SCP method, involves the use of a number of hazardous chemicals. It is important to stress that these procedures should always be undertaken in fume cupboards employing all the necessary

laboratory protocols for the use of these substances. This includes protection of the analyst, by wearing appropriate eye protection, laboratory gloves and protective clothing, and other laboratory users by the correct use of chemicals and the disposal of digestion residues. In particular, HF should be used with the upmost caution. Additional safety procedures for the use of this chemical are in place wherever it is employed and these should be followed at all times. These include additional protection for face, hands and clothing as well as procedures for the disposal of residues and dealing with any spillages or burns. It is strongly recommended that training in the use of this chemical and these associated procedures is undertaken before using it for the first time.

Temporal distribution

Most paleolimnological research studies involving fly-ash particles have been down-core profiles of particle concentrations. There have been three main underlying reasons for doing this. First, in order to correlate with some other temporal trend and thus attribute an atmospheric deposition cause (e.g. biological change such as a move towards a more acidic sediment diatom assemblage; increases in metal concentration). Second, to allocate dates to a core, and third, in order to determine the trends in particle concentrations through time *per se,* i.e., as indicators of impacts from atmospheric deposition or as surrogates for other pollutants.

Given certain criteria, such as a sediment accumulation rate which allows a reasonable temporal resolution, and an undisturbed record, temporal trends in SCP concentration (e.g., numbers of particles per gram dry mass - gDM^{-1}), or accumulation rate (e.g., numbers of particles $cm^{-2}\ yr^{-1}$) are remarkably consistent wherever they have been analysed. The reasons for this are that there have been such major changes in the development of global fossil-fuel combustion at certain times, that although there are local depositional influences, these only tend to modify the underlying patterns rather than causing radical differences from one region to another. Thus, there are similar temporal patterns in the SCP records in lakes across Europe, in China, Siberia, the USA, and in circum-polar Arctic regions. These major features are the start of the particle record, the rapid increase in particle concentration and a particle concentration peak.

The start of the particle record

As SCPs are not produced by any natural means, the first major change in the sediment record was the start of the record or the move from the absence to the presence of particles. This is the most regionally variable feature of the SCP profile and depends both upon the strength of the initial source and the detection limit of the analysis (this latter criterion is further influenced by the sediment accumulation rate, the amount of sediment available for analysis and so on). In the UK, the start of the SCP record begins in c. 1850/1860 (Rose et al., 1995) as a result of the combustion of coal at high temperatures following developments in the Industrial Revolution. At this time, emissions were vented to the atmosphere via low chimneys and hence distribution was more spatially limited with highest concentrations close to the source. However, as the sources were small and local, they were more abundant with each town having at least one small coal-fired station. The spread in this technology was

rapid and hence it was only a matter of a decade or so from the first power station generating electricity for public heating and lighting (Holborn Viaduct, London on 12th January 1882) to thousands of stations creating particulate emissions right across the country. The start of the SCP record in lake sediments thus predates the first electricity generating station and therefore probably reflects the earlier use of coal in industrial processes as a whole (Rose et al., 1995). In addition, this early industrial coal combustion was both less efficient than today and lacking in any emission controls. Thus each town became a significant point source for the surrounding district.

A simple calculation demonstrates this. A modern 2000 MW coal-fired power station consumes about 22,000 tonnes of coal a day if it operates continually for 24 hours. Depending on the mineral content of the coal there may up to 6000 tonnes of ash to remove per day (Hart & Lawn, 1977). In a modern station most of this ash is removed by efficient electrostatic precipitators and only 10–15 tonnes a day is emitted to the atmosphere (Hart & Lawn, 1977). Values of c. 12 tonnes a day have also been suggested for both coal and oil-fired power stations (1000 MW) fitted with "appropriate emission controls" (Laxen, 1996). Given that the masses of a 20 μm SCP and a 10 μm IAS are in the region of 4.2×10^{-9} g and 5.3×10^{-10} g respectively, then 10 tonnes of ash consisting of 95% IAS and 5% SCP will emit to the atmosphere c. 1.8×10^{16} IASs and c. 1.2×10^{14} SCPs, each day of operation. The small early power stations may have been 100 or even 1000 times smaller than this, and their lack of efficiency also probably increased the number of larger particles removed as bottom ash or travelling only very small distances from the source, thus having minimal impact beyond the immediate vicinity. However, they would not have included any emission controls to efficiently reduce the number of particles emitted to the atmosphere. Consequently, even the most conservative estimates suggest that from early on millions of SCPs and IASs were being emitted every day from hundreds of sources across the UK. It only takes a small proportion of these to be transported away from the local area for lake sediments across the country to store fly-ash particles in detectable numbers.

The start of the record throughout the UK therefore occurs at a reasonably uniform time. However, the UK is not an isolated case and similar situations will have occurred in every industrialised country as this new form of power generation was developed. The start of the SCP record therefore occurs within a few decades (1850–1900) in most industrial countries, although in northern Sweden records of SCPs in the 18th century have been reported (Renberg & Wik, 1985b). Although a few other sites may show pre-1850 records, this has been attributed to core smearing (i.e. the movement of high concentration sediment to lower levels during the process of coring or extrusion) and currently, there is little other convincing evidence for these very early particles.

Meteorological phenomena will transport airborne contaminants many thousands of kilometres to relatively clean areas. Industrial spherules have been recorded in the middle of the Atlantic Ocean (Folger, 1970) and in Greenland (Hodge et al., 1964) and Antarctic (Fredriksson & Martin, 1963; Hodge et al., 1967) ice deposits. Therefore, particles may also be detected in the lake sediments of areas prior to the time of the first local or regional emissions. In these situations, the detection limit of the technique may influence the date at which the presence of fly-ash in the lake sediment record is first observed rather than the date of first deposition (e.g. Rose et al., 1998a). Therefore, in sediments where SCP concentrations are very low, dates for the start of the record should be treated with caution.

As far as IASs are concerned, there is no start of the record as a natural background of volcanic and possibly micrometeoritic particles are present (Rose, 1990b). However, this background appears to be approximately uniform and removing this tends to give an 'industrial signal' starting at a similar time as the SCP record (Rose, 1990b; 1996).

The rapid increase in particle concentration

The second major change in fossil-fuel combustion, reflected in the lake sediment fly-ash particle record, followed the end of the Second World War. At this time there were two significant developments. First, a major expansion in the consumption of fossil-fuels at power stations rapidly increasing in size (Laxen, 1996) as a result of a dramatic demand for electricity, and second, the availability, for the first time, of cheap fuel oil leading to the development of the first large-scale oil-fired power stations. In lake sediment profiles this is observed as a rapid increase in particle concentration following almost a century of slow, but steady increase. This is observed throughout Europe (e.g., Wik et al., 1986; Rose et al., 1995) and in some areas of North America (e.g., the Adirondacks, Charles et al., 1990) although in other areas such as the Great Lakes a rapid increase has been observed since the early years of the 20th century (Griffin & Goldberg, 1981; Lan & Breslin, 1999) with no significant changes during or after the Second World War. This undoubtedly reflects the differences between the industrial developments of Europe and the USA and the impact that the Second World War had upon them. For example, a great deal more restructuring and rebuilding was required in Europe following this period leading to a sudden increase in demand for electricity, whereas development in the USA was a more continuous process.

In terms of its use as a dating feature, the rapid increase in SCP concentration is therefore probably more useful in Europe than in North America, although further studies are required to determine the geographical extent of the contrasting patterns in the Great Lakes and the Adirondacks. As a dating point on a profile, it has been defined as the depth at which the intercept of the extrapolated gradients of the slow, steady increase (pre-feature) and the rapid increase (post-feature) occurs (Fig. 5) (Rose et al., 1995).

Where both fly-ash particle analyses have been undertaken (e.g. UK, Japan) the rapid-increase in concentration occurs simultaneously in both SCP and IAS profiles showing the major influence of coal combustion. However, in other areas such as Sweden (Wik et al., 1986) and Norway (Wik & Natkanski, 1990), the increase in fossil-fuel consumption is almost entirely attributable to an increase in oil use and therefore, although the SCP profile shows a rapid increase at this time, it is uncertain whether an IAS profile would also do so.

The particle concentration peak

In many countries, as combustion technology has developed, so there has been a move away from a large number of small, local power stations providing electricity to a limited area, to a smaller number of large power stations located outside urban areas feeding into a national grid of electricity supply. Alongside this trend has been an increase in combustion efficiency, as well as an increased awareness of environmental concerns, both urban and non-urban. This has led to the introduction of tall stacks which dilute and distribute emissions more effectively, but perhaps more importantly has led to the introduction of

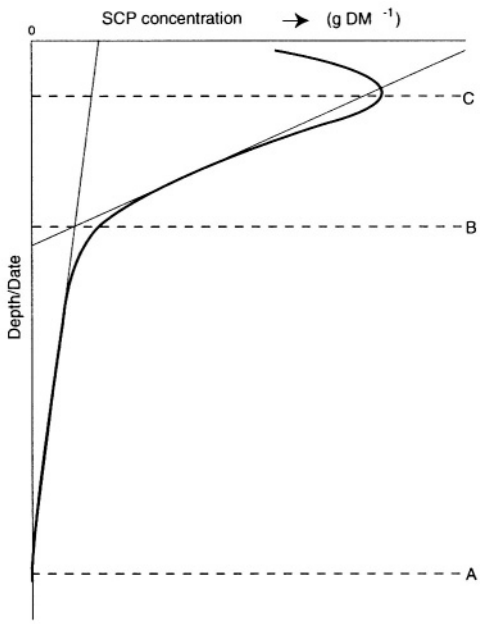


Figure 5. Schematic figure of a typical SCP profile showing the three current features used in sediment core dating. A - the start of the record; B - the start of the rapid increase in SCP concentration; C - the concentration peak. (From Rose et al., 1995; reprinted with permission from Edward Arnold)

emission control legislation and hence particle control technologies, such as electrostatic precipitators, cyclones and 'baghouses'.

This increase in combustion efficiency and the introduction of particle arrestors at source, in addition to the implementation of successively more rigorous control legislation, has meant that despite the continued increase in fuel consumption, in many industrialised areas, particulate emissions have started to decline. In addition, in some countries, such as the UK, changes in policy have led to a decline in heavy industry, reducing emissions both directly and indirectly via a reduced demand for electricity, as well as a move away from the use of traditional fuels such as coal and fuel-oil to natural gas.

In the lake sediment record, the above changes are recorded as a move away from the rapid increase in concentration of the 1950s and 1960s to a particle concentration peak and subsequent decline to the sediment surface. In many areas, such as Sweden, Norway (Wik & Natkanski, 1990), Finland (Korhola & Blom, 1996), Germany (Hilgers et al., 1993), North America (Charles et al., 1990; Lan & Breslin, 1999) and southern UK (Rose et al., 1995), this occurs in the late-1960s to early-1970s. Whereas in other areas, such as northern UK (Rose et al., 1995), Ireland (Flower et al., 1994; Rose et al., 1995) and Slovenia (Brancelj et al., 1999) this occurs in the late-1970s or early-1980s.

Such variability is probably due to national and regional changes in the processes described above. Despite tall stacks, particle sources still impact areas nearer to them rather than those more remote, and hence the gradual retro-fitting of particle controls, the tactical switching to alternative fuels to reduce sulphur emissions to agreed levels, and

the reduction of industrial processes will all affect local and regional areas more greatly than the national picture. Therefore, despite the particle concentration peak being the least ambiguous and most clearly definable SCP profile feature, it is probably also the one most open to local variability.

It is also a feature which, depending on local sources, has only recently become apparent in some areas. Although even early works of Griffin & Goldberg (1981) and Renberg & Wik (1984; 1985a) showed peaks and surface declines in their profiles, the rather later appearance of this feature in the north of the UK meant that in early studies (e.g., Darley, 1985; Wik et al., 1986) the surface decline was absent and the particle concentration maximum was at the surface. The first published work showing a surface decline for a UK site is thus Wik & Natkanski's (1990) paper where Loch Doilet and Lochan Uaine in Scotland show this sub-surface peak, although no date is ascribed to it. Four other sites from Scotland also included in this paper show no surface decline. The reason for this simultaneous presence and absence of the feature in UK cores is probably a combination of differences in sediment averaging processes between sites (physical mixing due to water currents, bioturbation, etc.) and differences in sediment accumulation rate leading to variability in sampling resolution. Despite this, post-1985, almost all UK cores now appear to show a sub-surface peak except in exceptional circumstances where sediment accumulation rate is very slow (e.g., Lochan Uaine, Scotland; Barber et al., 1999). The same is seen to be true across Europe where most sediment profiles show surface declines except for some mountain lakes (Rose et al., 1999c) or arctic lakes (Rose et al., unpubl.) where slow sediment accumulation rates are the controlling factor.

In other areas of the world, where coal consumption is increasing rapidly and where particle control technologies are less widespread, for example in China, SCP concentrations continue to show surface concentration maxima despite the lakes having more rapid sediment accumulation rates (Table II) (Boyle et al., 1999).

Dating

Allocating the features described above to an undated sediment profile is usually quite straightforward, although only rarely do profiles approach that of the schematic profile shown in Figure 5. Renberg & Wik (1985a) described this method of SCP dating as "indirect" as it relies upon other means in order to calibrate the profile within a region before it can be used on an undated core. Consequently, several SCP profiles must be dated by independent techniques, such as varve counting or ^{210}Pb chronology, before one can be confident about using these dates. However, once this has been done, confidence in allocated SCP dates can be high and where this has been done "blind" i.e. SCP dates allocated prior to obtaining independent dates, this author at least can report an often surprisingly good agreement.

To date, it is only rarely that more than one independently dated sediment core has been analysed for SCPs within a region such that a regional dating consensus can be determined. This is something that will need to be done in the future, as the ability of ^{210}Pb to date the 19th century becomes less reliable. However, where independently dated SCP profiles are available in the literature, Table II summarises this information.

Apart from these three features, other techniques have been employed in order to allocate SCP dates to undated cores. Matching cumulative SCP percentiles between dated and

undated cores has been undertaken on cores taken simultaneously from adjacent lakes (Renberg & Wik, 1984) and multiple cores from within a lake basin (Rose et al., 1999a) in order to allocate up to nine dates in addition (but related) to the dating features described above. However, this approach has so far been limited to cores taken at the same time, although a development, in order to make this approach more widely applicable, might be to use the concentration peak of an independently dated profile as 100% and relate the percentiles of the undated core to this.

Another more complicated approach to obtaining further dates on SCP profiles is to use particles characterised to their fuel-type, and then use documentary evidence for major changes in fuel-use to allocate dates to those changes. Particle characterisation and other methods of determining changes in fuel-use are described later.

A complication in using SCP profiles in order to allocate dates to sediment cores is that of profile variability, and this occurs on two scales, within-lake and regional. Rose et al. (1999a) showed ten profiles taken from within the deep basin of Loch Coire nan Arr, a site in the north-west of Scotland, and showed the variability that occurred between them in terms of both concentration (peak and surface) and historical patterns. Although the profiles showed quite significant variability, the major dating features were identifiable in each and the cumulative profiles showed good agreement. This suggests that, although SCP concentrations may vary at a sediment depth between cores, over time the cores were receiving similar SCP deposition. This was highlighted by the calculation of full SCP inventories for each core which also showed good agreement. Thus a SCP inventory is a better way of comparing the depositional impact at a number of sites. However, SCP inventories may still contain some variability due to, for example, the inwash of particles from catchment sources (e.g., Rose et al., 1999c). In dated cores, this can be compensated for by normalising the SCP inventories to the inventories of ^{210}Pb. The resulting SCP/^{210}Pb ratio is therefore a 'pollution index' for the total deposition period and is probably the best inter-site comparison available for SCP data.

An additional conclusion from the Loch Coire nan Arr study is that, although within-lake processes may alter SCP deposition to the sediment, even over very small distances, the three major features used for dating were still present and readily identifiable. Subsequent studies (Rose, unpublished data) have shown that within lake variability in the SCP profile, and also in full inventory, increase when the full lake basin is considered, as might be expected. This work, which builds on that described by Wik & Renberg (1991b), is beginning to identify the processes involved in SCP movement within a lake and factors that are important in SCP focusing. Such work will be important in further interpreting the sediment record.

Inter-site comparisons on a regional basis cannot practically also include multiple cores from within each lake and hence there is a reliance on a single core from the deep area of a lake providing a reasonable record of atmospheric deposition through time. However, some studies have shown that SCP dates vary between regions within a country (Rose et al., 1995) and therefore the extent of coherent dating regions, and the within-region and between region variability, must be fully understood before SCP dates from one area of a country can be allocated to another. To date, the work of Rose et al (1995) is the only attempt to explore this, although individual sites in northern and southern Sweden (Renberg & Wik, 1984) appear to show similar dates for profile features whilst those in southern and mid-Norway (Wik & Natkanski, 1990) may differ by a few years. This approach is currently being developed in the UK (Rose, 2000).

Spatial distribution

Spatial distribution data on SCP and IAS in lake sediments has been produced on a variety of scales from within-lake to national and international. Within a lake, information can be obtained on recent sediment distribution and the extent of sediment focusing (e.g., Wik & Renberg, 1991b; Wathne, 1999) such that the processes involved in sediment deposition, movement and storage within a lake can be further understood. On a larger scale, but still within a lake, 26 surface sediments and six full sediment cores were analysed for SCP within Lake Baikal, Siberia c. 500 km apart (Rose et al., 1998a) to show atmospheric deposition from different sources in the catchment.

On a national scale surface sediment SCP concentrations have been shown to have a good spatial agreement with atmospheric lead deposition (as recorded in moss samples) and excess sulphate in wet deposition in Sweden (Wik & Renberg, 1991a), total sulphur deposition in Scotland (Rose & Juggins, 1994) and atmospheric deposition of trace metals as recorded by catchment mosses in the UK (Rose & Harlock, 1998), Estonia (Alliksaar & Punning, 1998), Ireland (Bowman & Harlock, 1998) and the Czech Republic (Fott et al., 1998). In these latter studies, particle concentrations where also shown to have a good agreement with known emission sources. IAS concentrations in surface sediments in Scotland were also found to have a positive correlation with sulphur deposition (total, dry, wet; measured and modelled) of a similar order to those of SCP (Rose, 1996). Surface sediment SCP concentrations have also been shown to have a good spatial correlation with distance from source in areas where single point sources provide the only significant inputs to a region. In such cases, for example Svalbard (Rose et al., unpubl.), and the Jianghan Plain of central China (Boyle et al., 1999), impacts from the source are observable above a background level up to 60–80 km from the source. The use of lake sediments as a series of spatially-arrayed depositional archives rather than pollutant sinks *per se* allows regional patterns of deposited contaminants to be identified. Hence the data can be used to assess the impacts not only on the freshwater bodies included in the study, but also on the wider environment, such that there are implications from these studies to both human and environmental health (Rose et al., 1998c).

One of the major problems in using particle data in the above way is determining exactly what a surface sediment concentration represents. As discussed above, sediment accumulation rates can significantly alter particle concentrations and whilst a 0.5 cm sediment slice in one lake may represent one year, in another it may represent ten or more years. Whilst acknowledging this limiting dimension to the data, this has not and should not preclude the use of SCP concentration data in a spatial way. In the studies described above, the association with SCP and IAS concentrations with other deposited pollutants (sulphur, metals) and with known source areas suggests that spatial patterns are dependant on atmospheric deposition rather than on variation in sediment accumulation rate. The variability of sediment accumulation rate between lakes can never be fully overcome without independent dating but the selection of similar lakes through adherence to pre-determined criteria goes some way to avoiding gross differences (Rose et al, 1998b). Within any of the countries where such studies have been undertaken, particle concentrations varied by at least 100 times (>4000 times in Wik & Renberg, 1991a). For sediment accumulation rates to vary by the same amount would mean a range of, for example, between 0.01 and $1.0\,g\,cm^{-2}\,yr^{-1}$, which although not impossible is unlikely in similar lakes. Therefore, although variation

in sediment accumulation rate will without doubt modify surface sediment concentrations it is still possible to identify high and low deposition areas. Indeed, the chance that the patterns observed are the product of physical processes rather than depositional patterns mustbeinfinitesimal.

On a still broader geographical scale, 33 ^{210}Pb dated sediment cores from mountain lakes across Europe were analysed for SCP as part of the EU funded AL : PE (I & II) projects (Rose et al, 1999c). Sites ranged from the north-west of Svalbard to the Sierra Nevada in southern Spain, and from the Sierra Estrela in Portugal in the west to the Tatra Mountains of Slovakia and Poland in the east. At this scale it is not possible to say anything about national trends as only one or two sites were taken from within a small mountainous area of each country. However, the sites were deliberately selected to adhere to strict criteria and were thus as comparable as any set of lakes across such a wide area could be. There were four main conclusions of this work. First, the temporal trends in the SCP profiles were similar throughout the continent. Second, the distribution of SCP surface concentrations, but especially SCP surface accumulation rates and SCP/^{210}Pb inventory ratios, showed a latitudinal pattern, with most contamination in a band between 48–52 °N decreasing towards the north (Svalbard; 89 °N) and the south (Sierra Nevada; 37 °N) in good agreement with the latitudinal pattern of emissions. Third, only a few of the profiles could be interpreted using combustion statistics from a single (the host) country. Although many of these sites are located close to national boundaries, this result emphasises the transboundary nature of SCP movement and airborne pollutant transport within Europe generally. Fourth, that despite the remote nature of these sites, in particular Arresjøen in north-west Svalbard, there were no sites at which contemporary sediments gave a zero concentration of SCPs. By contrast with some other pollutants, in particular some persistent organics, there is no distillation effect for SCPs, by which they can move to these remote latitudes and altitudes and, consequently, their presence in these remote sites is due to a simple emission, transport and deposition process. This latter point highlights two key concepts. First, that particles can travel thousands of kilometres from their emission source and second, that even relatively large fly-ash particles have reached the most remote areas of, at least, the northern hemisphere.

Studies in the remotest areas throughout the northern hemisphere appear to show similar SCP concentrations in the surface sediments. Sites in northern Sweden (Wik & Renberg, 1991a), Svalbard (Rose, 1995; Rose et al., 1999c), mid- to northern Norway (Wik & Natkanski, 1990; Rose et al., 1999c), northern Finland (Korhola et al., unpubl.), Arctic Canada (Doubleday et al., 1995), Arctic Russia, Iceland and Greenland (Rose, unpublished data) show concentrations of between 100–1000 gDM^{-1} suggesting a possible hemispherical background of SCPs upon which local and regional influences are superimposed closer to sources. Doubleday (1999) found SCPs to be the most common 'combustion-type' particle in both Self Pond and Kirk Lake in the eastern Canadian Arctic although data were presented in percentage form preventing direct comparison with published particle concentration data from elsewhere.

Currently, there is little SCP and IAS data for the southern hemisphere. Cameron et al. (1993) showed a SCP profile for Lake Nicholls in Tasmania which had a surface concentration just above the level suggested as a northern hemispherical background and an improbably long historical record. Chenhall et al. (1994; 1995) presented 'ash' profiles for Lake Illawarra in New South Wales, Australia. Here, the ash, extracted by flotation of

the $>63\,\mu m$ fraction, included siliceous ash (IASs), carbonaceous ash (including charcoal, coke, graphite, soot and presumably SCPs), sulfide particles and iron oxide particles and reached up to 35% (by dry weight) in some sediment levels. However, as this includes many particle types such measurements are difficult to compare with other literature data, although significant contamination of the site is suggested. Some, currently unpublished, SCP work has been undertaken in south-eastern Australia (S. Mooney, pers. commun.) and New Zealand (F. Davies, pers. commun.) whilst one or two isolated samples have been analysed from Chile, Peru and the maritime Antarctic (Rose, unpublished). Of these, the Peruvian (Lake Titicaca) and the Antarctic (Signy Island, South Orkneys) samples produced SCP concentrations of zero suggesting a southern hemisphere background, if it exists, may be significantly lower than the north and that truly pristine areas (in the absence of SCP sense) may exist in remote areas of the southern hemisphere. However, this may be due to the detection limit of the technique and further work is needed to determine whether these areas are truly pristine and if so, their geographical extent.

Source apportionment

Information on the historical and spatial distributions of SCP, IAS and associated pollutants (trace metals, sulphur, PAHs, etc.) can be obtained or inferred from interpreting particle concentration data or transforming these data into particle accumulation rate, or inventory form. However, further information is available from fly-ash particles, extracted from lake sediments, when they are allocated to their fuel-type such that the total concentration is sub-divided into fuel-classes.

Particle characterisation can be applied to both core samples and surface sediments to obtain information on the impacts of changes through time at a site or the impacts of contemporary emissions across a region, respectively. Such information is useful for policy formulation and in terms of targeted emission reductions, whether to protect a sensitive environment or the health of a population, source identification for airborne pollutants is vital. Supporting evidence can also be provided for long-range transport models as particulate sources may be identified from external sources (e.g. Davies et al., 1984).

Such studies are really only of use for SCPs rather than IASs. The vast majority of IASs come from solid fossil-fuels (coals, oil shale) but there is no morphological means by which to separate them, coming as they do from the fused minerals present within the fuel. Similarly, there is no certain way of identifying sources chemically, as the chemical composition of the IAS particle is dependent upon the original mineral rather than the fuel-type and hence the particle compositions are also potentially very similar between fuel-types (i.e., mainly aluminosilicate). However, Alliksaar et al. (1998) suggest that oil shale IASs contain higher Ca and K and lower Al than their coal-derived counterparts.

In regions where there is only one fuel-type producing IASs, the IAS/SCP ratio can provide information on the relative impacts of deposition from these fuel-types (Rose, 1996). For example, in the UK, coal combustion produces SCPs and IASs whilst oil combustion produces only SCPs. Consequently, an IAS/SCP ratio can provide some information on the relative distributions (both spatial and historical) of these fuel-types. Similarly in Estonia, the main fuel-source is oil shale which produces a very high IAS/SCP ratio. Consequently, the relative impacts from this and other fuel-types can be obtained by determining the

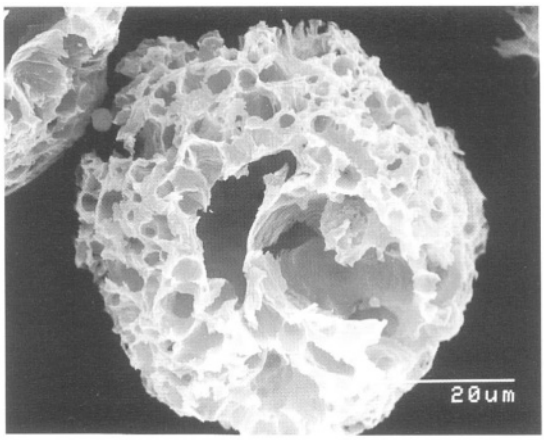


Figure 6. SEM photograph of a SCP with little surface area, described as 'lacy'. Produced by both coal and oil combustion and characteristic of SCPs which have remained longer in the furnace.

IAS/SCP ratio. Here, additional information is produced on the various impacts of sources from within and outside Estonia (Alliksaar & Punning, 1998).

Fuel-type apportionment by morphology

Fisher et al (1978) used light microscopy to differentiate between 11 morphological types of coal fly-ash (including SCP and IAS), but the first attempt at a fuel-type allocation for SCPs was by Griffin & Goldberg (1981) who used a combination of scanning-electron microscope (SEM) derived shape and surface texture to allocate particles into coal, oil, wood or wood/coal categories. The shape categories were 'porous spheres', 'elongate prismatic' and 'irregular fragments'. Here, we are concerned only with SCPs and hence the 'porous sphere' class. In this class, coal and oil were distinguished by their surface textures; coal having a 'smooth' or 'rough, irregular, pitted or cellular' texture whilst that of oil was described as 'etched, convoluted or layered'. Such a simple classification is undoubtedly useful, although coal SCPs have also been observed which show these surface features (Fig. 4). Many particles of both oil and coal origin have very little surface area, being highly porous or 'lacy' (Fig. 6) (Lightman & Street, 1968). This limits the use of surface features in a fuel-type classification, and this group of particles, which will become more abundant as combustion efficiency increases, were not included in the Griffin & Goldberg (1981) classification.

A morphological approach has been used to differentiate between coal and oil SCP types in North American studies (e.g. Kothari & Wahlen, 1984), including PIRLA (Charles et al., 1990). However, in this latter study, fuel-type determinations were difficult in many cases (D. Charles, pers. commun.) and although it was still possible to produce individual profiles of coal and oil, these were found to contain more "variation" than some metal and PAH profiles (Charles et al., 1990) and this may be as a result of these difficulties.

In a more all encompassing classification, Doubleday (1999) produced a morphologically based description for all combustion derived particles collected in the eastern Canadian Arctic (including those from waste incineration, aircraft emission and domestic burning), where the fly-ash particles considered in this chapter formed classes. However, this was only used as a classification tool and not for fuel-type apportionment of the fly-ash particles. When applied to sediment material from the same area the results were expressed in terms of percentages of total particles or as percentages of total combustion particles.

Size distribution studies (Shen et al., 1976) indicate that particulates emitted from coal-fired boiler stacks generally have a higher mean diameter than those from oil-fired boilers, but there is a large overlap, especially as particles from different coal combustion techniques also appear to show morphological and size differences due to differing furnace temperatures (McCrone & Delly, 1973; Falster & Jacobsen, 1982). Particles cannot therefore be classified to fuel-type on size criteria alone.

When embedded in resin and thin-sectioned, oil carbonaceous particles appear roughly circular with extensive and regular cross partitioning (Raask & Street, 1978), and are anisotropic in cross-polarised light (i.e., they give incomplete extinction upon rotation). Lightman & Street (1968) identified four different types of coal-derived particle using this approach: (1) solid particles produced from the fusain maceral; (2) 'balloons' with thin walls and a single large cavity; (3) 'C' shaped particles with thick walls and a single large pore opening to the surface; and (4) 'lacy' particles with many internal partitions similar to those from oil combustion. The relative numbers of these particles produced during coal combustion depends on the type of coal and burning conditions (size of flame, furnace type, etc.), and hence will change through time. However, the 'C' shaped particles were generally found to be the most common (Lightman & Street, 1968). In cross-polarised light, the ash particles from low rank coals are isotropic (i.e. give complete extinction upon rotation) and mid- to high-rank coals are anisotropic (Griest & Harris, 1985).

Fuel-type classification by optical microscopy has been used with a high degree of success (80–90%) with power station ash (P. Street, pers. commun.). However, it is not convenient with particles extracted from lake sediments, because the number of particles available to embed in the resin is many orders of magnitude lower and the 'lacy' particles would remain unclassified. Thus it would appear that there is currently no morphological approach which both effectively separates the fuel-types and is applicable to particles extracted from lake sediments. We must therefore turn to particle chemistry.

Chemical apportionment

Elemental analysis has been performed on particulates from many different combustion sources including car emissions, incinerators and cigarettes, as well as from coal and oil-fired power stations (McCrone & Delly, 1973). The results from McCrone & Delly and other studies (Shen et al., 1976; Cheng et al., 1976) show that the major elements present in power station emission particulates are, for oil: V, Fe, Si, S, and Ca; and for coal: Fe, Ti, Si, S, K, and Ca. Titanium and vanadium have, therefore, been used in the past as indicative of coal and oil particles, respectively (e.g. Ganor et al., 1988). However, both oil and coal are heterogeneous materials, and vanadium is present in some coals and titanium in some oils. Consequently, these elements do not allow consistent discrimination between fuel

types for all particles. Since particles from different fuel-types cannot be accurately and consistently differentiated on the basis of individual chemical parameters, multi-element characterisation must be used.

Multi-element approaches to SCP characterisation

Rose et al. (1996) described the development of a SCP characterisation for oil and coal fuel-types, using particle chemistries determined by energy dispersive X-ray spectroscopy (EDS). This technique is described as semi-quantitative as the results are expressed as a percentage of the total of elements selected for analysis. Additionally, the EDS detector used was unable to determine elements lighter than sodium, and thus carbon and oxygen, most probably the major constituents in SCPs (c.f. traffic-derived soot; Fruhstorfer & Niessner, 1994), were not measurable and do not appear in the total. However, rather than being a drawback, this had a positive effect as the 17 trace elements analysed consequently appeared to be much more important to the particle composition than in reality, and it was these, rather than the carbon content, which were used in differentiating between the fuel-types.

Individual particle chemistry data were acquired by computer controlled SEM, and thus it was possible to analyse many thousands of particles relatively quickly (Rose et al., 1996). A reference dataset of almost 6000 coal and oil particles was produced using fly-ashes obtained from ten power stations in the UK and Ireland. After data screening to remove outliers, linear discriminant function analysis produced a discrimination rule which allocated over 95% of the particles to the correct fuel-type under cross-validation. The technique was then applied to SCPs extracted from a ^{210}Pb-dated sediment core taken from a lake on Hampstead Heath in north London, UK. The results showed good agreement with known combustion history of coal and oil in the region, with 100% coal until the early 1950s when the first major oil-fired power station in the UK was commissioned at Bankside on the River Thames in 1952. Although coal particles dominate throughout the core, the proportion of oil SCPs increased from the 1950s through to the mid-1970s when the record first declined and then became more erratic. This coincides with the period of the oil crisis caused by the embargo of 1974 and the subsequent increased uncertainty over the future of fuel-oil. There is a general decline in oil particles after this point except for a small peak at c. 1984 which may correspond to the increase in oil use during the national coal-miners strike of 1984/85. If this is not an over-interpretation of these trends, then SCP characterisation data could be used to add these additional dates to a sediment profile.

The spatial distribution of characterised particles was also studied using surface sediments from lakes in Scotland, northern England and Northern Ireland (Rose et al., 1996). Above average concentrations of oil particles occurred around Glasgow, the east coast near Aberdeen, and Galloway in the south-west. These agreed with the location of known oil-combustion sources and suggests that the acidification of lochs in the Galloway area (e.g., Battarbee et al., 1989) may partly relate to pollutants originating from oil-fired power stations in Northern Ireland.

An attempt was also made to extend the characterisation to identify individual power station sources, but this was only partially successful (Rose et al., 1996). However, even these allocations were probably over-estimated as the dataset was unlikely to include the

full range of chemistries produced from each individual power station. This is because the fuels burned at each station vary through time and hence the overlap between stations using the same fuel-types was unlikely to be fully observed. This situation has become exacerbated since the introduction of multi-fuel stations.

The Rose et al. (1996) study also showed that particles from peat combustion were distinguishable from coal and oil suggesting that the technique could be extended to include other fuel-types. As part of the EU COPERNICUS funded project 'FLAME' (Fly-ash and metals in Europe - 1994–1996, Rose et al., 1998c) a particle characterisation was developed which included all the non-gaseous fossil-fuels used for power generation in Europe, i.e. coal, oil, peat, brown coal and oil shale. This is described in Rose et al (1999b). The approach was similar to that described above. 33 reference ashes were obtained from six fuel-types (Czech and UK coal were treated as separate fuels to determine any within-fuel variability) in the four participating countries (UK, Ireland, Estonia, Czech Republic) and over 48,600 particles were analysed for 21 elements. After removal of univariate and multivariate outliers, 1000 particles were randomly selected from each fuel-type to produce a 6000 particle dataset from which to develop the discrimination.

The final classification involved a hierarchy of quadratic discriminant functions (QDFs). The first hierarchical level separated the six fuels into three 'fuel-groups' (oil; coal series; oil shale/Czech black coal), whilst the second hierarchical level used separate QDFs to separate each fuel group into its component fuel-types. Some fuel separations proved to be very good with oil, oil shale, Czech black coal and brown coal being 94.1%, 89.3%, 86.0% and 84.1% correctly allocated to their fuel-types, respectively. The coal-series and, in particular peat and coal, showed considerable overlap and were less effectively separated. In total, of those particles allocated to a fuel-type, over 80% were allocated correctly.

This discrimination was then applied to particles extracted from 196 lake surface sediments across the four countries (Alliksaar & Punning, 1998; Fott et al., 1998; Bowman & Harlock, 1998; Rose & Harlock, 1998). Spatial trends in most key fuel-types in each country (oil shale in Estonia, brown coal in the Czech Republic, peat and oil in Ireland, coal and oil in the UK) showed good agreement with emission sources, increasing confidence in the technique. However, in all countries, absolute percentages were low due to high allocations to the coal fuel-type even in areas where coal-use was known to be low. It is thought that these high coal values were due to mineral particles surviving the chemical pre-treatment and being allocated to the coal fuel-type due to the similarity in both the major elements comprising these minerals and those elements important in the allocation of particles to coal (e.g., Si, Al, K). A critical assessment of the techniques employed in the chemical analysis of carbonaceous particles together with possible future directions for this work is discussed in Watt (1998).

Although primarily paleolimnologically based in its development, the above approach to SCP source apportionment is applicable to particles extracted from any depositional sink including atmospheric collectors, building stone crusts, soils and leaves.

Comparisons between source apportionment techniques

Although no direct comparisons between morphological fuel-type apportionments and multi-element chemical apportionments have yet been made, Rose (1996) compared the results obtained from the EDS-derived fuel-type trends at the Hampstead Heath site

(described above) with those derived from interpreting trends in the IAS/SCP ratio. As IASs, in the UK, are almost solely derived from the combustion of coal, an increase in the IAS/SCP ratio should correspond to a higher proportion of SCP allocated to coal by the EDS technique, whilst a lower ratio should indicate more oil.

The results from Hampstead Heath did show similar trends (Rose, 1996). At the base of the core where SCP characterisation showed 100% coal, the IAS/SCP ratio was at a maximum (1.5), and as oil SCPs were seen to increase between the 1950s and the mid-1970s, so the ratio also declined. However, in more recent years, in the mid-to-late 1970s, where there is a dramatic increase in IAS/SCP, there is only a slight corresponding increase in coal SCP%. From the late 1970s or early 1980s there is a general decrease in both profiles followed by an increase just below the sediment surface. There is no definite trend during this period probably reflecting the uncertain fuel policies in the UK at this time.

An alternative way of using IAS to follow temporal fuel-use changes is to compare IAS concentration directly rather than using the IAS/SCP ratio. Here, the suggestion is that so few IASs are produced from oil combustion that they can be used as a surrogate for coal consumption directly. In the Hampstead Heath core the trends are once again comparable showing an increase between the base of the core and the early-1970s, a decrease in the mid-1970s followed by another increase from the late-1970s to the early-1980s and a subsequent decline.

IAS/SCP is therefore a useful means of detecting trends in fuel-type changes and influences at lake sites, but is probably not as reliable as that of SCP characterisation. It was beneficial to conduct this study in the UK where coal and oil are the main fossil-fuels used in industrial combustion and where coal is almost solely the source of the IAS particle type. In countries where there are influences from other fuel-types (e.g. brown coal, peat), the IAS/SCP relationship as an indicator of fuel-type may not be as clear. Both approaches can therefore yield useful information on trends in fuel use through time and the changes in deposition from these sources at a site. However, although the trends appear to compare quite well, there is probably less quantitative value in either an IAS concentration or an IAS/SCP profile and they should be interpreted with caution.

The future

It is likely that fly-ash particles, especially SCPs, will continue to be used in paleolimnological studies for many years to come, fulfilling the roles that they have up until now. In particular, their use as a means of dating recent sediments may become more important as the half-life of ^{210}Pb gradually precludes it from effectively dating the late-19th century and progressively successive periods. Eventually, it may be that SCP dating becomes one of the few reliable ways of dating the late-19th and 20th centuries. However, in order to do this, reliable, independently dated SCP chronologies need to be established before ^{210}Pb becomes too unreliable for this period. Currently, there are few parts of the world where such work has been undertaken and hence this is a global challenge which needs to be addressed over the next few years. However work has now started in this area (Rose, 2000).

In terms of the use of SCP chronologies to date future periods, this remains unclear. In some areas of the world (e.g. China and India) industrial combustion of fossil-fuels is still expanding and hence the SCP record is assured. Indeed, it has recently been predicted that there will be a doubling in the global amount of coal used for electricity production by 2020 and most of this will be in China and India (ENDS, 1999). In Europe and North America, as alternative energy sources are sought, clean combustion technologies improve and the major switch from traditional fuels to natural gas and nuclear energies is pursued, SCP and IAS concentrations in sediment records may continue to decline and possibly even fall back to zero. This would be the final particle dating feature for paleolimnological studies in these areas concluding a discrete stratigraphic period which, as there is currently no evidence for particle decay in the sediment archive, may remain of use to paleolimnologists for hundreds of years. However, as long as coal and oil are burned at industrial temperatures, and it appears this will continue well into the 21st century at least, then there will be a fly-ash sediment record for paleolimnologists to use.

SCP characterisation may become more problematic. As combustion technology develops, so industrial sources are making use of multiple fuels such that an individual furnace can now use a combination of coal, oil and natural gas, or even domestic refuse. The problems faced in the past, and discussed above, whereby the use of single fuels from different sources (cf. using, for example, coal from a single source as in the case of pit-head power stations) caused significant overlap within particles derived from that fuel, will become exacerbated to such an extent that source apportionment may become impossible. It will still be possible to differentiate a coal SCP from an oil SCP for example, and this may be improved by developing techniques (e.g. individual particle PAH analysis), but they may be being produced from the same point source. This may still be of use in high resolution air sampling research programmes, but in paleolimnological terms it may prove too complicated to be of practical use. However, as with SCP dating, the historical sediment record will remain such that fuel-type changes through time at a site or historical regional patterns can still be determined, but these will be restricted to a discrete historical period.

In parts of the world where single fuels are used extensively, however, particle characterisation may remain useful in, for example, transboundary studies. An example of this is in eastern Asia where coal combustion from China may influence areas such as Japan where mainly oil is used. In such cases, identification of coal SCPs may still provide evidence of long-range transport from external sources (Nagafuchi pers. commun.).

An area which may develop further is the use of SCPs as surrogates for reconstructing trends in deposition of other pollutants. In the past, the spatial distribution of SCPs has been shown to be well correlated with Pb (Wik & Renberg, 1991a; Boyle et al., 1999), polycyclic aromatic hydrocarbons (PAHs - Broman et al., 1990; Wathne et al., 1997) and sulphur (Wik & Renberg, 199la; Rose & Juggins, 1994), whilst the spatial record of IASs has also been shown to agree well with sulphur (Rose, 1996) and the temporal trends of SCP have been shown to agree at least qualitatively with the interpolated historical record of sulphur deposition (Rose, 1991) and PAHs (Wathne et al., 1997). Further work is required to explore the changes in the relationships between these various pollutants though time, but with some development it maybe that fly-ash can provide a reliable way of reconstructing historical, site-specific sulphur deposition and this would have implications for providing input data for freshwater acidification and recovery models.

Summary

The combustion of non-gaseous fossil-fuels at industrial temperatures gives rise to emissions of SCPs and IASs, together termed fly-ash. When these are deposited from the atmosphere onto a lake and its catchment, the lake sediment record preserves the patterns of deposition and these can be interpreted by paleolimnologists. Most paleolimnological work has been undertaken using SCPs. The temporal patterns of SCP deposition are similar in many areas of the world and are used in three main ways: (i) to correlate with some other temporal change, such as a shift in pH, and attribute this to an atmospheric deposition source; (ii) to allocate dates to cores; and (iii) to determine trends in particles as indicators of deposition or as surrogates for other pollutants.

There are currently three main features employed in SCP sediment dating. These are the start of the particle record, the rapid increase in concentration, and the concentration peak. Some regional variability occurs and these features must be calibrated to independently-derived dates (e.g. annual varves; ^{210}Pb chronologies) before application to sediment profiles from other lakes. In lakes with very slow sediment accumulation, the maximum concentration may be at the surface. Other dates may be attributable by using cumulative percentage profiles, or possibly by SCP fuel-type characterisation.

The spatial distribution of SCP concentrations, accumulation rates, inventories and SCP/^{210}Pb inventory ratios have been undertaken at a range of scales from within-lake to continental. Within a lake, profile variability can occur to a significant degree, although the main profile shape is almost always present allowing core cross-correlation. At large scales, regional, national and international trends reflect emission sources and show good agreement with atmospherically deposited sulphur, lead and PAHs. The transboundary nature of particle movement has also been highlighted by these studies.

Particle source apportionment allows further information to be obtained from SCPs. Morphologically, this has been done by thin-sectioning and by size, but multi-element chemical apportionment is probably the most reliable for SCPs extracted from sediments. This has now been undertaken for the major fuels of Europe and, when applied to almost 200 lakes in four countries, showed good agreement with the distribution of major fuel use. IAS/SCP ratios have also been used to determine trends in both spatial and temporal fuel-use and where this has been compared with SCP characterisation results reasonable agreement has been found.

For the future, SCP dating may become important, especially for the 19th century, as the half-life of ^{210}Pb progressively precludes its use for this period. Coal consumption for electricity generation is currently predicted to double by 2020 and hence the use of fly-ash particles in paleolimnological studies is assured for at least the short term. However, interpretation of particle characterisation data may become more problematic as industrial sources move towards the use of multiple fuels.

Acknowledgements

I would like to thank all those who have aided the compilation of this chapter. These are all the people who have extracted fly-ash particles from lake sediments and then sat for many patient hours at the microscope. In particular, I would like to thank Tiiu Alliksaar, Nancy Doubleday and Don Charles for searching for and providing requested information at short

notice. Finally, I am indebted to all my colleagues at the ECRC who have helped with all the sediment coring, preparation and analysis that allowed me to be in a position to be able to write this chapter.

References

Alliksaar, T. & J.-M. Punning, 1998. The spatial distribution of characterised fly-ash particles and trace metals in lake sediments and catchment mosses: Estonia. Wat. Air. Soil Pollut. 106: 219–239.

Alliksaar,T., P. Horstedt& I. Renberg, 1998. Characteristic fly-ash panicles from oil-shale combustion found in lake sediments. Wat. Air Soil Pollut. 104: 149–160.

Barber, K. E., R. W. Battarbee, S. J. Brooks, G. Eglinton, E. Y. Haworth, F. Oldfield, A. C. Stevenson, R. Thompson, P. G. Appleby, W. E. N. Austin, N. G. Cameron, K. J. Ficken, P. Golding, D. D. Harkness, J. A. Holmes, R. Hutchinson, J. P. Lishman, D. Maddy, L. C. V. Pinder, N. L. Rose & R. E. Stoneman, 1999. Proxy records of climate change in the UK over the last two millenia: documented change and sedimentary records from lakes and bogs. J. Geological Society, London 156: 369–380.

Battarbee, R. W. & I. Renberg, 1990. The Surface Water Acidification Project (SWAP) paleolimnology programme. Phil. Trans. R. Soc. Lond. B327: 227–232.

Battarbee, R. W., A. C. Stevenson, B. Rippey, C. Fletcher, J. Natkanski, M. Wik & R. J. Flower, 1989. Causes of lake acidification in Galloway, south-west Scotland: A palaeoecological evaluation of the relative roles of atmospheric contamination and catchment change for two acidified sites with non-afforested catchments. J. Ecol. 77: 651–672.

Bowman, J. J. & S. Harlock, 1998. The spatial distribution of characterised fly-ash particles and trace metals in lake sediments and catchment mosses: Ireland. Wat. Air. Soil Pollut. 106: 263–286.

Boyle, J. F., N. L. Rose, H. Bennion, H. Yang & P. G. Appleby, 1999. Environmental impacts in the Jianghan Plain: Evidence from lake sediments. Wat. Air Soil Pollut. 112: 21–40.

Brancelj, A., N. Gorjanc, R. Jacimovic, Z. Jeran, M. Šiško & O. Urbanc-Bercic, 1999. Analysis of sediment from Lovrenška Jezera (lakes) in Pohorje. Geografski Zbornik 39: 7–28.

Broman, D.,C. Näf, M. Wik & I. Renberg, 1990. The importance of spheroidal carbonaceous particles for the distribution of paniculate polycyclic aromatic hydrocarbons in an estuarine-like urban coastal water area. Chemosphere 21: 69–77.

Cameron, N. G., P. A. Tyler, N. L. Rose, S. Hutchinson & P. G. Appleby, 1993. The recent palaeolimnology of Lake Nicholls, Mount Field National Park, Tasmania. Hydrobiologia. 269/270: 361–370.

Charles, D. F. & D. R. Whitehead (eds.), 1986. Paleoeological Investigation of Recent Lake Acidification. Methods and project description. Report EA-4609 Electric Power Research Institute, Palo Alto, CA., 228pp.

Charles, D. F., M. W. Binford, E. T. Furlong, R. A. Hites, M. J. Mitchell, S. A. Norton, F. Oldfield, M. J. Paterson, J. P. Smol, A. J. Uutala, J. R. White, D. R. Whitehead & R. J. Wise, 1990. Paleoecological investigation of recent lake acidification in the Adirondack Mountains, N.Y. J. Paleolim. 3: 195–241.

Cheng, R. J., V. A. Mohnen, T. T. Shen, M. Current & J. B. Hudson, 1976. Characterisation of particles from power plants. J. Air Poll. Cont. Assoc. 26: 787–783.

Chenhall, B. E., G. E. Batley, I. Yassini. A. M. Depers & B. G. Jones, 1994. Ash distribution and metal contents of Lake Illawarra bottom sediments. Aust. J. Mar. Freshwater Res. 45: 977–992.

Chenhall, B. E., I. Yassini, A. M. Depers, G. Caitcheon, B. G. Jones, G. E. Batley & G. S. Ohmsen, 1995. Anthropogenic marker evidence for accelerated sedimentation in Lake Illawarra, New South Wales, Australia. Envir. Geology 26: 124–135.

Chigier, N. A., 1975. Pollution formation and destruction in flames — Introduction. Prog. Energy Combust. Sci. 1: 3–15.

Commission on Energy and the Enviroment, 1981. Coal and the Environment. HMSO, London, 257pp.

Darley, J., 1985. Particulate Soot in Galloway Lake Sediments. Its application as an indicator of environmental change and as a technique for dating recent sediments. Department of Geography. University College London. B301 Project, 94pp.

Davies, T. D., P. W. Abrahams, M. Tranter, I. Blackwood, P. Brimblecombe & C. E. Vincent, 1984. Black acidic snow in the remote Scottish Highlands. Nature 312: 58–61.

Doubleday, N. C., 1999. A Paleolimnological Survey of Combustion Particles from Lakes and Ponds in the Eastern Arctic, Nunavut, Canada. An Exploratory Classification, Inventory and Interpretation at Selected Sites. Unpublished PhD thesis. Queen's University, Kingston, Ontario, 408pp.

Doubleday, N. C., M. S. V. Douglas & J. P. Smol, 1995. Paleoenvironmental studies of black carbon deposition in the High Arctic: a case study from Northern Ellesmere Island. Sci. Tot. Envir. 160/161:661–668.

ENDS, 1999. ENDS Daily, April 23, 1999. Environmental Data Services Ltd., London.

Falster, H. & L. Jacobsen, 1982. Dust Emission, its Quantity and Composition, Depending on Dust Collecter; Coal Quality etc. Proceedings of the International Conference on coal-fired power plants and the aquatic environment, August 1982. Copenhagen, Denmark: 16–18.

Fisher, G. L., B. A. Prentice, D. Silberman, J. M. Ondov, A. H. Biermann, R. C. Ragaini & R. McFarland, 1978. Physical and morphological studies of size classified coal fly-ash. Envir. Sci.Technol. 12:447–451.

Flower, R. J., J. D. Dearing, N. L. Rose & S. T. Patrick, 1992. A palaeoecological assessment of recent environmental change in Moroccan wetlands. Würzb. Geogr. Arb. 84: 17–44.

Flower, R. J., B. Rippey, N. L. Rose, P. G. Appleby & R. W. Battarbee, 1994. Palaeolimnological evidence for the acidification and contamination of lakes by atmospheric pollution in western Ireland. J.Ecol. 82:581–596.

Flower, R. J., S. V. Politov, B. Rippey, N. L. Rose, P. G. Appleby & A. C. Stevenson, 1997. Sedimentary records of the extent and impact of atmospheric contamination from a remote Siberian highland lake. Holocene 7: 161–173.

Folger, D. W., 1970. Wind transport of land derived mineral, biogenic and industrial matter over the North Atlantic. Deep Sea Res. 17: 337–352.

Fott, J., J. Vukic & N. L. Rose, 1998. The spatial distribution of characterised fly-ash particles and trace metals in lake sediments and catchment mosses: Czech Republic. Wat. Air Soil Pollut. 106: 241–261.

Fredriksson, K. & L. R. Martin, 1963. The origin of black spherules found in Pacific Islands, deep-sea sediments and Antarctic ice. Geoch. Cosmoch. Acta. 27: 245–248.

Fruhstorfer, P. & R. Niessner, 1994. Identification and classification of airborne soot particles using an automated SEM/EDX. Mikrochim. Acta. 113: 239–250.

Ganor, E., S. Altshuller, H. A. Foner, S. Brenner & J. Gabbay, 1988. Vanadium and nickel in dustfall as indicators of power plant pollution. Wat. Air Soil Pollut. 42: 241–252.

Goldberg, E. D., 1985. Black Carbon in the Environment: Properties and Distribution. Wiley Interscience Publication, New York, 198pp.

Goldberg, E. D., V. F. Hodge, J. J. Griffin & M. Koide, 1981. Impact of fossil-fuel combustion on the sediments of Lake Michigan. Envir. Sci. Technol. 15: 466–470.

Goldstein, H. L. & C. W. Siegmund, 1976. Influence of heavy oil composition and boiler combustion conditions on particulate emissions. Envir. Sci. Technol. 10: 1109–1114.

Griest, W. H. & L. A. Harris, 1985. Microscopic identification of carbonaceous particles in stack ash from pulverised-coal combustion. Fuel. 64: 821–826.

Griffin, J. J. & E. D. Goldberg, 1975. The fluxes of elemental carbon in coastal marine sediments. Limnol. Oceanogr. 20: 256–263.

Griffin, J. J. & E. D. Goldberg, 1979. Morphologies and origin of elemental carbon in the environment. Science 206: 563–565.

Griffin, J. J. & E. D. Goldberg, 1981. Sphericity as a characteristic of solids from fossil-fuel burning in a Lake Michigan sediment. Geoch. Cosmoch. Acta. 45: 763–769.

Griffin, J. J. & E. D. Goldberg, 1983. Impact of fossil fuel combustion on the sediments of Lake Michigan: A reprise. Envir. Sci. Technol. 17: 244–245.

Guilizzoni, P., A. Lami & A. Marchetto, 1992. Plant pigment ratios from lake sediments as indicators of recent acidification in alpine lakes. Limnol. Oceanogr. 37: 1565–1569.

Handy, R. L. & D. T. Davidson, 1953. On the curious resemblance between fly-ash and meteoritic dust. Iowa Acadamy of Sci. 60: 373–379.

Hart, A. B. & C. J. Lawn, 1977. Combustion of coal and oil in power station boilers. CEGB Research. August 1977:4–17.

Hilgers, E., H. Thies & W. Kalbfus, 1993. A lead-210 dated sediment record on heavy metals, polycyclic aromatic hydrocarbons and soot spherules for a dystrophic mountain lake. Verh. Internat. Verein. Limnol. 25: 1091–1094.

Hodge, P. W. & F. W. Wright, 1964. Studies of particles for extra-terrestrial origin, 2. A comparison of microscopic spherules of meteoritic and volcanic origin. J.Geophys. Res. 69: 2449–2454.

Hodge, P. W., F. W. Wright & C. C. Langway, 1964. Studies of particles for extra-terrestrial origin. 3. Analyses of dust particles from polar ice deposits. J. Geophys. Res. 69: 2919–2931.

Hodge, P. W., F. W. Wright & C. C. Langway, 1967. Studies of particles for extra-terrestrial origin. 5. Compositions of the interiors of spherules from Arctic and Antarctic ice deposits. J. Geophys. Res. 72: 1404–1406.

Korhola, A. & T. Blom, 1996. Marked early 20^{th} century pollution and the subsequent recovery of Töölö Bay, central Helsinki, as indicated by sub-fossil diatom assemblage changes. Hydrobiologia 341: 169–179.

Korhola, A., J. Virkanen, M. Tikkanen & T. Blom., 1996. Fire-induced pH rise in a naturally acid hill-top lake, southern Finland: a palaeoecological survey. J. Ecol. 84: 257–265.

Kothari, B. K. & M. Wahlen, 1984. Concentration and surface morphology of charcoal particles in sediments of Green Lake, New York. Implications regarding the use of energy in the past. Northeastern Env. Sci. 3: 24–29.

Kreiser.A., N. L. Rose, A. Probst & J.-C. Massabuau, 1995. Relationship between lake-water acidification in the Vosges mountains and SO_2-NO_x emissions in western Europe. In Landmann, G. & M. Bonneau (eds.) Forest Decline and Atmospheric Deposition Effects in the French Mountains. Springer, Berlin: 363–370.

Lan, Y. & V. T. Breslin, 1999. Sedimentary records of spheroidal carbonaceous particles from fossil-fuel combustion in western Lake Ontario. J. Great Lakes. Res. 25: 443–454.

Larsen, J., J. F. Boyle & H. J. B. Birks, 1996. Variation in the geochemistry of recent lake sediments along a west-east pollution gradient in the Bergen area, Norway. Wat. Air Soil Pollut. 88: 47–81.

Laxen, D., 1996. Generating emissions? Studies of the local impact of gaseous power-station emissions. A National Power publication, 74 pp.

LeFèvre, R., A. Gaudichet & M. A. Billon-Galland, 1986. Silicate microspherules intercepted in the plume of the Etna volcano. Nature 322: 817–820.

Lightman, P. & P. J. Street, 1968. Microscopical examination of heat treated pulverised coal particles. Fuel 47: 7–28.

Lightman, P. & P. J. Street, 1983. Single drop behaviour of heavy fuel oils and fuel oil fractions. J. Inst. Energy 56: 3–11.

Mamane, Y., J. L. Miller & T. G. Dzubay, 1986. Characterisation of individual fly ash particles from coal and oil-fired power plants. Atmos. Env. 20: 2125–2135.

McCrone, W. C. & J. G. Delly, 1973. The Particle Atlas. An Encyclopedia of Techniques for Small Particle Identification. 2nd Edition. Ann Arbor Science Publishers, Michigan, USA.

Nettleton, M. A., 1979. Particulate formation in power station boiler furnaces. Prog. Energy Combust. Sci. 5: 223–243.

Odgaard, B. V., 1993. The sedimentary record of spheroidal carbonaceous fly-ash particles in shallow Danish lakes. J. Paleolim. 8: 171–187.

Punning, J.-M., T. Koff, M. Varvas, T. Martma, R. Rajamäe, K. Tolonen, M. Verta, O. Sandman, P. Uimonen-Simola, K. Eskonen, E. Grönlund & T. Mikkola, 1994. Impact of natural and man-made processes on the development of Lake Linajärv, NE Estonia. Proc. Estonian Acad. Sci. Ecol. 4: 156–174.

Punning, J.-M., J. F. Boyle, T. Alliksaar, R. Tann & M. Varvas, 1997a. Human impact on the history of Lake Nômmejärv, NE Estonia, a geochemical and palaeobotanical study. Holocene 7: 91–99.

Punning, J.-M., V. Liblik & T. Alliksaar, 1997b. History of fly-ash emission and palacorecords of atmospheric deposition in the oil shale combustion area. Oil Shale 14: 347–362.

Raask, E., 1984. Creation, capture and coalescence of mineral species in coal flames. J. Inst. Energy 57: 231–239.

Raask, E. & P. J. Street, 1978. Appearance and pozzolanic activity of pulverised fuel ash. Unpublished proceedings of a Conference on Ash Technology and Marketing. London: 22–27, October 1978.

Renberg, I. & H. Hultberg, 1992. A paleolimnological assessment of acidification and liming effects on diatom assemblages in a Swedish Lake. Can. J. Fish. Aquat. Sci. 49: 65–72.

Renberg, I. & M. Wik, 1984. Dating of recent lake sediments by soot particle counting. Verh. Internat. Ver. Limnol. 22: 712–718.

Renberg, I. & M. Wik, 1985a. Soot particle counting in recent lake sediments. An indirect counting method. Ecol. Bull. 37: 53–57.

Renberg, I. & M. Wik, 1985b. Carbonaceous particles in lake sediments-pollutants from fossil-fuel combustion. Ambio. 14: 161–163.

Rose, N. L., 1990a. A method for the extraction of carbonaceous particles from lake sediment. J. Paleolim. 3: 45–53.

Rose, N. L., 1990b. A method for the selective removal of inorganic ash particles from lake sediments. J. Paleolim. 4: 61–68.

Rose. N. L., 1991. Fly-ash Particles in Lake Sediments: Extraction, Characterisation and Distribution. Unpublished PhD thesis. University of London, 290pp.

Rose, N. L., 1994. A note on further refinements to a procedure for the extraction of carbonaceous fly-ash particles from sediments. J. Paleolim. 11: 201–204.

Rose, N. L., 1995. The carbonaceous particle record in lake sediments from the Arctic and other remote areas of the northern hemisphere. Sci. Tot. Env. 160/161: 487–496.

Rose, N. L.. 1996. Inorganic fly-ash spheres as pollution tracers. Envir. Pollut. 91: 245–252.

Rose, N. L., 2000. Carbynet. On-line sediment dating information. http://www.geog.ucl.ac.uk/ecrc/carbynet/

Rose, N. L. & S. Harlock, 1998. The spatial distribution of characterised fly-ash particles and trace metals in lake sediments and catchment mosses in the United Kingdom. Wat. Air Soil Pollut. 106: 287–308.

Rose, N. L. & S. Juggins, 1994. A spatial relationship between carbonaceous particles in lake sediments and sulphur deposition. Atmos. Env. 28: 177–183.

Rose, N. L., S. Juggins, J. Watt & R. W. Battarbee, 1994. Fuel-type characterization of spheroidal carbonaceous particles using surface chemistry. Ambio. 23: 296–299.

Rose, N. L., S. Harlock, P. G. Appleby & R. W. Battarbee, 1995. The dating of recent lake sediments in the United Kingdom and Ireland using spheroidal carbonaceous particle concentration profiles. Holocene 5: 328–335.

Rose, N. L., S. Juggins & J. Watt, 1996. Fuel-type characterisation of carbonaceous fly-ash parti-

cles using EDS-derived surface chemistries and its application to particles extracted from lake sediments. Proc. Roy. Soc. London (Series A) 452: 881–907.

Rose, N. L., P. G. Appleby, J. F. Boyle, A. W. Mackay & R. J. Flower, 1998a. The spatial and temporal distribution of fossil-fuel derived pollutants in the sediment record of Lake Baikal, eastern Siberia. J. Paleolim. 20: 151–162.

Rose, N. L., T. Alliksaar, J. J. Bowman, J. Fott, S. Harlock, J.-M. Punning, K. St. Clair-Gribble, J. Vukic & J. Watt, 1998b. The FLAME project: General discussion and overall conclusions. Wat. Air Soil Pollut. 106: 329–351.

Rose, N. L., T. Alliksaar, J. J. Bowman, J. Fott, S. Harlock, S. Juggins, J.-M. Punning, K. St. Clair-Gribble, J. Vukic, J. Watt & J. Boyle, 1998c. The FLAME research project: Introduction and methods. Wat Air Soil Pollut. 106: 205–218.

Rose, N. L., S. Harlock & P. G. Appleby, 1999a. Within-basin profile variability and cross-correlation of sediment cores using the spheroidal carbonaceous particle record. J. Paleolim. 21: 85–96.

Rose, N. L., S. Juggins & J. Watt, 1999b. The characterisation of carbonaceous fly-ash particles from major European fossil-fuel types and applications to environmental samples. Atmos. Envir. 33: 699–2713.

Rose, N. L., S. Harlock & P. G. Appleby, 1999c. The spatial and temporal distributions of spheroidal carbonaceous fly-ash particles (SCP) in the sediment records of European mountain lakes. Wat. Air Soil Pollut. 113: 1–32.

Schmidt, R., K. Arzet, E. Facher, J. Fott, K. Irlweck, Z. Rehakova, N. L. Rose, V. Straskrabova & J. Vesely, 1993. Acidification of Bohemian Lakes. Recent trends and historical development. A report to the State Ministry for Science and Research and the Austrian Academy of Science, 86pp.

Shen, T. T., R. J. Cheng, V. A. Mohnen, M. Current & J. B. Hudson, 1976. Characterisation of Differences between Oil-fired and Coal-fired Power Plant Emissions. Proceedings of the 4th International Clean Air Congress: 386–391.

Smith, D. W., J. J. Griffin & E. D. Goldberg, 1975. A spectroscopic method for the quantitative determination of elemental carbon. Anal. Chem. 47: 233–238.

Tolonen, K., R. Haapalahti & J. Suksi, 1990. Comparison of varve dated soot ball chronology and lead-210 dating in Finland. In Saarnisto, M. & A. Kahra (eds.) Laminated Sediments. Geological Survey of Finland, Special Paper 14: 65–75.

Toro, M., R. J. Flower, N. L. Rose & A. C. Stevenson, 1993. The sedimentary record of the recent history in a high mountain lake in central Spain. Verh. Internat. Verein. Limnol. 25: 1108–1112.

Virkenan, J., A. Korhola, M. Tikkanen & T. Blom., 1997. Recent environmental changes in a naturally acidic rocky lake in southern Finland, as reflected in its sediment geochemistry and biostratigraphy. J. Paleolim. 17: 191–213.

Wathne, B., S. Patrick & N. Cameron (eds.), 1997. AL : PE — Acidification of Mountain Lakes: Palaeolimnology and Ecology. Part 2 - Remote mountain lakes as indicators of air pollution and climate change. Final Report to the Commission of the European Communities. NIVA, Oslo, 525 pp.

Wathne, B. W. (ed.), 1999. MOLAR. Progress Report 3/1999. Measuring and modelling the dynamic response of remote mountain lake ecosystems to environmental change: A programme of Mountain Lake Research. NIVA-report SNO: 4070–99, 124 pp.

Watt, J., 1998. Automated characterisation of individual carbonaceous fly-ash particles by computer controlled scanning electron microscopy: Analytical methods and critical review of alternative techniques. Wat. Air Soil Pollut. 106: 309–327.

Wik, M. & J. Natkanski, 1990. British and Scandinavian lake sediment records of carbonaceous particles from fossil-fuel combustion. Phil. Trans. R. Soc. Lond. B327: 319–323.

Wik, M. & I. Renberg, 1987. Distribution in forest soils of carbonaceous particles from fossil-fuel combustion. Water, Air Soil Poll. 33: 127–129.

Wik, M. & I. Renberg, 1991a. Recent atmospheric deposition in Sweden of carbonaceous particles from fossil-fuel combustion surveyed using lake sediments. Ambio 20: 289–292.

Wik, M. & I. Renberg, 1991b. Spheroidal carbonaceous particles as a marker for recent sediment distribution. Hydrobiologia 214: 85–90.

Wik, M. & I. Renberg, 1996. Environmental records of carbonaceous fly-ash particles from fossil-fuel combustion. A summary. J. Paleolim. 15: 193–206.

Wik, M., I. Renberg & J. Darley, 1986. Sedimentary records of carbonaceous particles from fossil-fuel combustion. Hydrobiologia 143: 387–394.

13. APPLICATION OF STABLE ISOTOPE TECHNIQUES TO INORGANIC AND BIOGENIC CARBONATES

EMI ITO (eito@umn.edu)
Department of Geology and Geophysics
and Limnological Research Center
University of Minnesota
310 Pillsbury Drive, SE
Minneapolis, MN 55455
USA

Keywords: lake water, sediment, stable isotope, trace element, paleoenvironmental reconstruction, carbonates, ostracode, *Phacotus, Chara*

Introduction

The application of stable isotopes of oxygen and carbon to the study of sedimentary carbonates has become commonplace since it was first proposed by Urey (1947) and since pioneer studies by Emiliani (1955), Epstein and colleagues (1951, 1953) and McCrea (1950). Coupled with the study of polar ice-cores (e.g., Dansgarrd et al., 1982; Jouzel et al., 1987), the study of marine carbonates has given us a wealth of information about past climates and sea-level changes. The study of non-marine sedimentary carbonates, be they endogenic (i.e., forming in the water column) carbonate or biogenic shell material, has become more common since the early studies by Fritz and colleagues (1974, 1975) and Stuiver and colleagues (1968, 1970).

Nevertheless, the isotopic study of lacustrine carbonates for the purpose of paleoenvironmental reconstruction is far from a quick and simple routine for two reasons: (1) bulk carbonates in lake sediments are composed of several components, each having a different source and thus containing different information; and (2) a lake may be supported by variable amounts of groundwater and surface water, and range from ephemeral or permanent and small to large and thus tends to be a more complex system than the ocean, demanding a full accounting of the factors that affect its stable-isotope values and hydrochemistry (e.g., Gat, 1995; Hostetler, 1995; Winter, 1995).

Thus bulk carbonates should not *a priori* be assumed to be a single endogenic phase, but instead they require full characterization, for they are typically composed of inorganic and biogenic fractions, and one or both fractions may include detrital components that are likely to be out of isotopic equilibrium with the (paleo)water and other carbonate fractions in the sediment. Various carbonate fractions must first be identified through x-ray diffraction and



W. M. Last & J. P. Smol (eds.), 2001. *Tracking Environmental Change Using Lake Sediments. Volume 2: Physical and Geochemical Methods.* Kluwer Academic Publishers. Dordrecht, The Netherlands.

petrographic means, may need to be separated from one another depending on their identity and quantity, and must be prepared differently prior to analysis.

The isotopic study of lacustrine carbonate cannot be undertaken without supporting evidence. It needs the context, the framework, or the constraints provided by other proxy records (such as pollen, diatom, and ostracode assemblages) before it can be made to tell an intelligent story. The complexity of a lacustrine system means that any isotopic study of carbonates requires some knowledge of processes operating in the modern lake system and a thorough characterization of the core and the bulk sediment *before* any carbonate analysis is undertaken. The physical and chemical characteristics of the modern lake and the relation of the modern lake water to modern lacustrine carbonates are needed to understand how the lake might have responded to environmental change, and, in turn, how its archive, the carbonates, might have recorded this change. The whole-core as well as the bulk-sediment studies provide the additional framework within which to interpret the carbonate data.

The main purpose of this chapter is to provide a guide for the isotopic analysis of lacustrine carbonates, pointing out potential pitfalls and how to avoid them. A full discussion of the complex relationships among lake morphometry, hydrologic budget, and the hydrochemical response to climatic change is outside the scope of this chapter (simple treatments can be found in Siegenthaler & Eicher, 1986; Hosteller & Benson, 1994; Gat, 1995; Winter, 1995). However, a brief discussion of the relationship between carbonate $\delta^{18}O$ and lake-water $\delta^{18}O$ and between lake-water $\delta^{18}O$ and climate is included.

Nomenclature and systematics

Delta (δ) notation, fractionation factor, and standards

Stable isotope geochemistry uses a relative scale rather than absolute ratio of isotopes. The delta (δ) notation, defined as

$$\delta(‰ = \text{per mil}) = \left(\frac{R_{\text{sample}}}{R_{\text{std}}} - 1\right) \cdot 10^3, \quad (1)$$

where R is the isotope ratio and is equal to $^{18}O/^{16}O$, $^{13}C/^{12}C$, $^{2}H/H$, etc., requires an internationally agreed-upon standard against which the isotope ratios of any sample are compared. The δ notation for different isotope pairs is written such that the mass of the less abundant isotope is placed after the symbol δ and is written, for example, as $\delta^{18}O$ for oxygen.

The current standard for carbon isotopes is VPDB (Vienna Pee Dee Belemnite $\equiv 0.000\ldots00‰$), which has replaced PDB (Pee Dee Belemnite from Pee Dee Formation, South Carolina). PDB was consumed long ago, necessitating this change. VPDB, unlike PDB, is not an actual material and is defined relative to isotopic reference material NBS-19, TS-limestone: $\delta^{13}C$ of NBS-19 relative to VPDB is +1.95‰. NBS-19 is quite homogeneous as long as at least 3 grains are analyzed together and is isotopically stable during long-term storage in a desiccator.

There are two standards for oxygen, VSMOW (Vienna Standard Mean Ocean Water) and VPDB. Conventionally, VPDB is used for carbonates and paleotemperature work and

VSMOW for silicates and water. As for PDB, the original SMOW (Standard Mean Ocean Water) material is no longer available. SMOW was defined as

$$\left({}^{18}O/{}^{16}O\right)_{SMOW} \equiv 1.008\left({}^{18}O/{}^{16}O\right)_{NBS\text{-}1} \tag{2}$$

by Craig (1961) and has been accepted internationally. The $\delta^{18}O$ of VPDB is defined relative to NBS-19: $\delta^{18}O$ of NBS-19 relative to VPDB is –2.20‰.

Additional terms that may be of some use are the isotope fractionation factor α, defined as

$$\alpha_{xy} = \frac{R_x}{R_y}, \tag{3}$$

where R_x = the isotope ratio of substance x, and R_y = the isotope ratio of substance y. Chemists tend to use α only in situations where thermodynamic equilibrium can be demonstrated; geologists tend to use α to designate any observed isotope ratio differences. The thermodynamic fractionation factor α, as a function of temperature is generally given in the form of the isotopic distribution coefficient

$$10^3 \ln \alpha_{xy} = B10^6 T^{-2} \pm A, \tag{4}$$

where A and B are experimentally determined or calculated constants, and T is temperature in Kelvins.

Isotopic analysis of carbonates typically is carried out to investigate environmental or climatic conditions that prevailed in the past. However, the above equation makes it clear that, in order to calculate the temperature of carbonate formation, the $\delta^{18}O$ of water and the constants A and B must be known for that carbonate mineral, and to find out the $\delta^{18}O$ of water, the constants A and B as well as the temperature of carbonate formation must be known. As we shall see, there are situations in which the knowledge of temperature or even of $\delta^{18}O$ of water matters little. And there are other situations in which multiple proxies must be used to estimate one or the other.

The relationship between climate and $\delta^{18}O$ of meteoric precipitation (Fig. 1)

The stable-isotopic composition of meteoric precipitation is a natural tracer of airstreams that bring moisture inland from its predominantly marine sources. The progressive condensation of water vapor from the airmass as it travels inland causes the remaining vapor to become increasingly depleted in ^{18}O, making the resulting precipitation lower in $\delta^{18}O$. The $\delta^{18}O$ of the precipitation at any one location depends on the airmass trajectory (which determines the rate of temperature-change with time or dT/dt) as well as the source of the moisture. In most of the mid- to high-latitude regions of the world, the $\delta^{18}O$ and δD of precipitation vary seasonally because of the changes in the north-south temperature gradient (Siegenthaler & Eicher, 1986; Rozanski et al., 1993). Monthly isotopic measurements of precipitation collected over a given time period, say 10 years, are needed to determine how closely the shifts in isotopic values mimic temperature changes. The long-term mean of precipitation falling at any one place (with the exceptions of ocean islands and maritime tropics) fits the relationship

$$\delta^{18}O \propto 0.58‰°C^{-1} \tag{5}$$

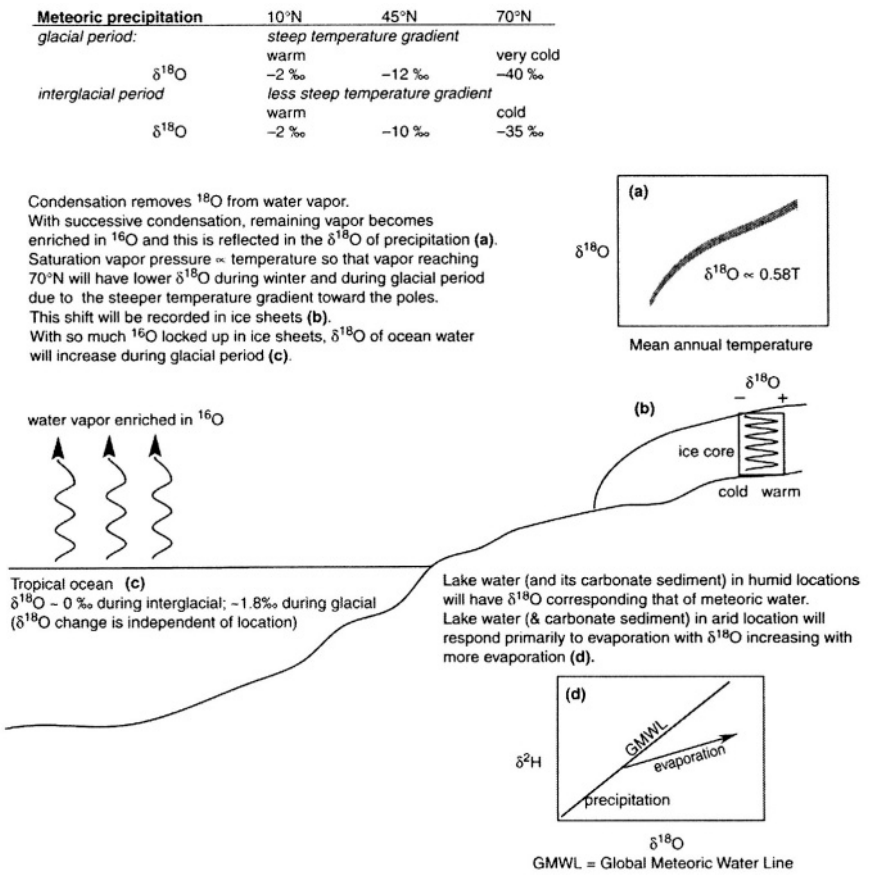


Figure 1. Schematic illustration of the hydrologic cycle. The relationship between climate, seasons, temperature, latitude, and $\delta^{18}O$ of meteoric precipitation (**a** and **c**) are shown. The figure also shows the $\delta^{18}O$ evolution of lake water due to evaporation (**d**).

(Rozanski et al., 1993), or

$$\delta^{18}O \propto 0.7T(°C) - 13.6‰ \tag{6}$$

(Siegenthaler & Eicher, 1986), and most of the precipitation falls on the line

$$\delta^{2}H = 8\delta^{18}O + 10 \tag{7}$$

known as the Global Meteoric Water Line.

The relationship between carbonate $\delta^{18}O$ and lake-water $\delta^{18}O$

If endogenic or biogenic lacustrine carbonate forms in thermodynamic equilibrium with lake water, and if the carbonate is low-Mg calcite, there is a well established temperature

dependence on oxygen-isotope fractionation between water oxygen and carbonate oxygen:

$$T(°C) = 16.9 - 4.2(\delta_c - \delta_w) + 0.13(\delta_c - \delta_w)^2, \quad (8)$$

where $\delta_c = \delta$ of CO_2 liberated from $CaCO_3$ at 25 °C in the laboratory and $\delta_w = \delta$ of CO_2 in isotopic equilibrium at 25 °C with water from which calcite precipitated (Craig, 1965). The $\delta^{18}O$ of aragonite is higher than that of coexisting calcite within the temperature range of interest (Tarutani et al., 1969; Horibe & Oba, 1972; Grossman & Ku, 1986). Depending on the climatic setting of the lake, this difference in the $\delta^{18}O$ of aragonite and calcite will need to be taken into consideration. For example, given that the $\delta^{18}O$ of $CaCO_3$ varies by about –0.23‰/°C, a simple shift in $CaCO_3$ mineralogy or in the proportion of aragonite to calcite, can give the false signal of temperature shift of 2 °C.

$\delta^{18}O$ and trace-element ratios of lake-water as indicators of P-ET and groundwater contribution

A lake is a water body that temporarily stores surface water and/or groundwater. Groundwater is normally recharged from surface water, but it may be considerably older than modern surface water. Shallow, regional, or localized aquifers (such as glacial outwash or tunnel valleys) should be recharged by local precipitation and may be nearly contemporaneous with surface water. Confined aquifers with recharge zones in far-away places and aquifers with episodic recharge events, such as only during extremely wet periods, will have water with $\delta^{18}O$ and $\delta^{2}H$ of precipitation that reflect the climate of the time and place of recharge. In all cases, the ionic composition of groundwater is determined partly by biological activities in the soil zone and partly by aquifer lithology.

$\delta^{18}O$ of lake-water

The $\delta^{18}O$ of lake water is rarely that of contemporaneous meteoric precipitation except for short-residence-time lakes in humid environments. Evaporation removes ^{16}O, with the rate of removal dependent on surface wind speed, relative humidity (RH), and temperature (saturation vapor pressure is a function of temperature, hence RH is also a function of temperature). Calm wind and high RH mimic a closed-system equilibrium condition (free energy change becomes more important), and windy and/or arid conditions result in large observed fractionation. The fractionation depends on the translational velocity of different isotopes of water molecules. The overall isotopic fractionation during evaporation is the net result of the kinetic fractionation during the liquid-to-vapor phase transition and the kinetic fractionation during the vapor-to-liquid phase transition. Light isotopes undergo phase transition more readily whether it be liquid-to-vapor or vice versa. The near absence of reverse phase-change under the condition of low RH and/or high wind speed can be thought of as contributing to large observed isotope fractionation. Detailed treatment of evaporation can be found elsewhere (Craig & Gordon, 1965; Gonfiantini, 1986; Hostetler & Benson, 1994; Gat, 1995).

Closed-basin lakes are cut off from surface outflow and some may have no stream inflow, but many can be regarded as windows to the shallow (and in some cases deep) groundwater

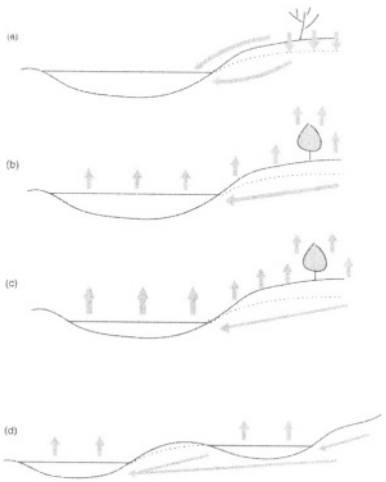


Figure 2. Schematic illustration of seasonal changes in inflow of water to a lake in a topographically closed-basin. (a) Spring or before active growth of plants have started. Without active evapotranspiration by plants, water from melting snow or rain will be transported more effectively as slope wash directly into the lake or seep into shallow aquifer system. (b) Once plants start to actively grow and leaf out, much of precipitation may not get past the root zone and recharge of shallow aquifers may cease. (c) Evaporative evolution of lake water $\delta^{18}O$ may be offset to various degrees depending on the amount and $\delta^{18}O$ of the water that enters the lake. (d) Closed basin lakes that are in the same groundwater flowpath are hydrologically connected. The lake located lower in the flowpath may receive water that has been evolved isotopically by evaporation from lakes located higher in the groundwater flowpath.

system. Neighboring closed basin lakes may be connected by a groundwater system. The $\delta^{18}O$ of water in such lakes can have unexpected values (Fig. 2): (1) both the groundwater recharge and the direct runoff into the lakes may occur preferentially in early spring before plants have leafed out; (2) during the growing season active evapotranspiration by plants may preclude any significant recharge of the shallow groundwater system; (3) evaporation during summers from such lakes and unconfined aquifers will evolve the $\delta^{18}O$ toward higher values, but the effect of the previous summer's evaporation may be partially (or greatly) offset by the runoff from snowmelt, and by continued input from the groundwater system (Ito et al., 1998); and (4) groundwater recharged from evaporated lakes will then discharge isotopically evolved water into those lakes lower in the groundwater flow path (Smith et al., 1997). Hence $\delta^{18}O$ and $\delta^{2}H$ of groundwater discharging into lakes may be very different from those of local precipitation.

Mg/Ca and Sr/Ca ratios of lake-water

Meteoric precipitation has little to contribute to lake water's major and minor element chemistry, except for dissolved CO_2 and O_2 (except near marine coasts), but groundwater discharging into a lake contains dissolved cations and anions reflecting its previous history. Groundwater contains cations such as Ca, Mg, Si, and Sr, anion such as Cl and anion complexes such as $SO_4^{=}$ and HCO_3^{-}, and organic compounds depending on the lithology

of the aquifers and the biological activity in the soil zone. The concentration of each ionic species will depend on several factors, such as the chemical reactivity of the water recharging the aquifer (e.g., the concentration of H_2CO_3), the lithology and mineralogy of the aquifer, the residence time of water in the aquifer, as well as the climate and whether the groundwater was recharged from a highly evaporative surface-water body.

Not all lakes are supersaturated with respect to (low-Mg) calcite, but in lakes that do exceed calcite saturation, Ca, HCO_3^- and minor amounts of Mg and Sr are removed from the water. Hence low-Mg calcite precipitation removes Ca from solution and leaves Mg and Sr in solution. If low-Mg calcite precipitation or saline groundwater discharge keeps pace with the evaporative concentration, both the salinity and Mg/Ca ratio in water will increase, and aragonite rather than low-Mg calcite becomes a stable phase (Müller et al., 1972; Eugster & Jones, 1979). Aragonite has a high distribution coefficient for Sr/Ca (Veizer, 1983) so that its formation removes Sr from lake water, lowering water's Sr/Ca even though the salinity of water may be increasing. Mg continues to be excluded from aragonite, so that with continued evaporation the salinity and the Mg/Ca of water increases (Eugster & Jones, 1979; Haskell et al., 1996; Xia et al., 1997c) until some Mg-bearing mineral starts to precipitate. Under some conditions, monohydrocalcite (Hull & Turnbull, 1973; Spencer, 1977) or magnesian (i.e., high-Mg) calcite (Last, 1982) forms rather than aragonite. The formation of high-Mg calcite is common in seawater and should occur in waters with similar or higher Mg/Ca ratios as in seawater, but its occurrence in lacustrine settings has not been widely reported, possibly because the carbonate phases are not routinely fully characterized. One caveat in relating Mg/Ca to salinity is that, under some circumstances, a change in the physical structure of a lake alone will enable calcite to precipitate, leading to an increase in Mg/Ca independent of salinity (LaBaugh & Swanson, 1992).

Mg/Ca and Sr/Ca ratios thus generally can be used to track the evolution of salinity in closed-basin lakes (Eugster & Jones, 1979) until Mg becomes a major element in some evaporite mineral that forms in hypersaline water. However, the $\delta^{18}O$ of water does not necessarily keep increasing with increased residence time or continued drought. The small volume of water remaining at the end of the dry period can be overwhelmed by the addition of water either from snowmelt or sudden rain. The salts may redissolve and the salinity remain high, but the $\delta^{18}O$ of the added water may reset the isotope value, erasing the isotopic memory of the dry period.

$\delta^{13}C$ of dissolved inorganic carbon (DIC)

The $\delta^{13}C$ of DIC can change seasonally as a result of (1) annual turnovers which mix low $\delta^{13}C$ DIC from oxidized or respired organics from the lake bottom throughout the water column; (2) the extraction of low $\delta^{13}C$ CO_2 by photosynthesis, atmosphere-water exchange, or evasion of CO_2 from water (Cole et al., 1994); and (3) input of DIC or dissolved organic carbon (DOC) into the lake from surface runoff and groundwater inflow. In addition, the $\delta^{13}C$ of epilimnion and hypolimnion DIC will differ always in meromictic lakes, or seasonally if there is annual turnover. Even within the epilimnion, the DIC $\delta^{13}C$ of water adjacent to actively photosynthesizing plants and algae may differ from the DIC $\delta^{13}C$ elsewhere.

Carbonates in lake-sediments

Carbonate minerals contained in lake sediments consist of inorganic and biogenic components. One or both components may include detrital (formed outside the catchment) and/or terrestrial (formed in catchment) fractions. Whether these non-lacustrine fractions must be removed depends on the amount and the delta values of these "foreign" fractions compared to lacustrine fractions. Inorganic and biogenic carbonates may also need to be separated from each other for the very same reasons.

Inorganic carbonates

Inorganic carbonates found in lake sediments can have multiple origins: endogenic fraction precipitated in the water column, authigenic (but non-endogenic) fraction formed from pore water, detrital fraction, and a fraction formed by alteration (diagenesis) within the sediment. Under ideal conditions, endogenic carbonates are formed in thermodynamic equilibrium with lake-water, typically in the epilimnion, due to photosynthetic uptake of dissolved CO_2, or due to evaporation of water and evasion of CO_2. Hence, if the information we want is that of lake-water when carbonate mineral(s) formed, then the endogenic carbonate fraction is what we need to separate and analyze.

However, inorganic detrital components may be very difficult to identify and remove. Smear-slide examination is helpful, and SEM analysis can reveal the presence or absence of good crystal forms. Oxygen and carbon isotopic values, Mg/Ca and Sr/Ca ratios, or even $^{87}Sr/^{86}Sr$ ratios of any carbonates in the surrounding regions can be measured and compared with the measured values of carbonate sediment. While this does not prove conclusively that there is no detrital fraction, it can tell whether the detrital fraction occurs in enough abundance to affect the values of the non-detrital component.

Pore-water carbonates and altered carbonates, if they are found together with the endogenic component, may be difficult to identify. Pore-water carbonates may occur as overgrowths on the endogenic and detrital component, and if any alteration of endogenic carbonates occurs due to reaction with pore waters, the admixture would be nearly impossible to separate.

Biogenic carbonates

Biogenic carbonates may be derived from ostracode and aquatic mollusk shells, or terrestrial mollusk shells. Terrestrial mollusks obviously do not carry any record of lake water and must be removed. The $\delta^{18}O$ of biogenic fractions is typically offset from thermodynamic equilibrium values because of vital effects. The organisms form the shells at a significant metabolic cost to themselves. For example, ostracodes are found in waters that are undersaturated with respect to calcite and in waters that are forming endogenic aragonite or high-Mg calcite. Without significant expenditure of energy on their part, low-Mg calcite could not be forming in such waters. Whenever energies are expended, the assumption of chemical or isotopic equilibrium must be questioned, and the deviation from the expected thermodynamic equilibrium value is called the vital effect.

Some of the biogenic fractions are remains of planktonic organisms and others of nektic or benthic species. Yet others are partial to groundwater seepage sites and may not have been living in the lake. Some species are stream dwellers and they or their remains are washed in during floods. So in most cases the fossil material needs to be separated from the inorganic fraction, and fossil material must be identified and non-lacustrine species removed. In general, good practice calls for identification and separation of species.

Mollusks

Aquatic snails and clams can be a good source of stable-isotope information. Most mollusks precipitate aragonite, others calcite (typically low-Mg). Their habitat influences the $\delta^{13}C$ values — those living on aquatic plants will likely show the effect of photosynthetic uptake of low-$\delta^{13}C$ CO_2 by plants (McConnaughey, 1991). Snails and clams keep adding new carbonate as they grow, and unless the shells are subsampled, the analysis yields some sort of averaged information. The value obtained is not a strict average over the lifespan of the mollusk: the early years have less carbonate than later years, unfavorable years have less carbonate than favorable years, and new shell material is not added continuously in all seasons. The vital effect on isotope fractionation is known to exist for some mollusks (Fritz & Poplawski, 1974; Barrera et al., 1994), but the effect has not been quantitatively investigated. A new study on aragonitic shells of certain species of clams indicates that this species has little if any vital effect on oxygen-isotope fractionation (Dettman et al., 1999). With the myriad factors that can affect the magnitude of isotope fractionation by living organisms, more such studies on a few common species with wide environmental tolerance are needed.

Ostracodes

Ostracodes are nearly ubiquitous minute crustaceans with a pair of low-Mg calcite shells enclosing the soft body (Fig. 3). The shape of the shells vary from kidney-shaped, spherical, to lenticular, and are species specific with local variations (e.g., van Morkhoven, 1962). Some species exceed 1 mm in length (anterior to posterior) while others are about 0.2 mm in the largest dimension. The proper identification of ostracodes and fossil ostracode shells requires some training and readers are encouraged to refer to specific publications (e.g., Delorme, 1970a, 1970b, 1970c, 1970d, 1971).

Ostracodes moult 8 times before becoming adults, each time creating new shell from the dissolved Ca^{2+} and HCO_3^- in the water (Chivas et al., 1983). There are nektic (swimmers) and benthic (crawlers) species of ostracodes, with some of the latter species being infaunal. The nektic species in lacustrine settings are typically not open-water swimmers but live on aquatic plants in near-shore settings. Some benthic species are found in groundwater discharge sites in wetlands, springs, and in lakes. They may not really live in the lake so much as live in the groundwater.

The seasonality of ostracode hatches and moults is still being worked out for many species, and this information is critical for the interpretation of isotopic data (Xia et al., 1997a; von Grafenstein et al., 1999). Species reaching adult stage in spring will naturally carry information different from those doing the same in summer or fall. The vital effect on

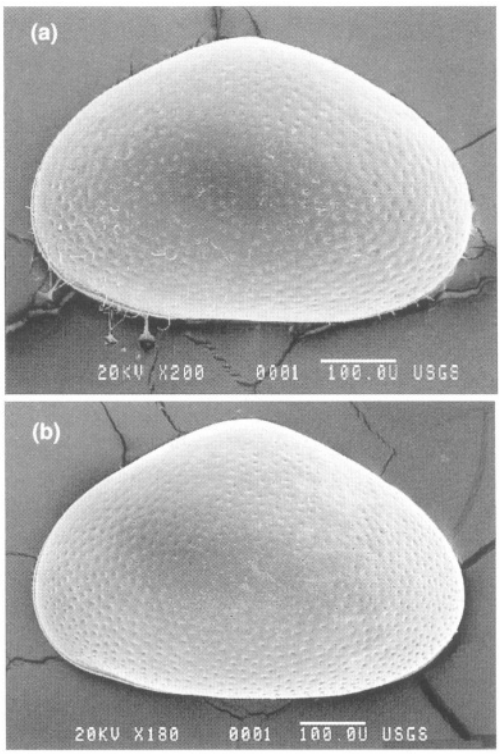


Figure 3. SEM photographs of modern and fossil ostracode, *Cypridopsis vidua*, a common species in temperate dilute water. Magnification is 200x for both photographs. (a) Modern C. vidua was harvested live in 1987 from Point of Rocks Spring, a pond in Nevada, by E.D. Gutentag. The photo shows the left valve of a female. (b) Fossil C. vidua is from a sediment core retrieved from Indian Springs Valley, Nevada. The photo shows the left valve of a female. The fossil is ca. 12,000 years old (J. Quade, pers. commun.) and was picked by S. Lundstrom. Both photographs are courtesy of K. Conrad, USGS.

oxygen-isotope fractionation is known in many ostracode species, contrary to early studies in which several species had to be bulked (Fritz et al., 1975; Durazzi, 1977). For example, the candonids for which some data exist, the $\delta^{18}O$ is about 1.5‰ higher than expected for equilibrium inorganic calcite (Dettman et al., 1995; Xia et al., 1997c; von Grafenstein et al., 1999). The vital effects on isotope fractionation are said to be genera-specific. However, the different timing of moults or microhabitat preference of different species within a genus make it inadvisable to randomly mix species for analysis. The rate of calcification, which is faster for early instars and slower for late instars, may also affect oxygen-isotope fractionation. This effect has been observed for trace-element uptake (Chivas et al., 1983).

Bio-induced carbonates

Bio-induced carbonates might be termed those that form as an extra-cellular by-product. However, the rigid classification of biogenic, bio-induced, or even inorganic carbonates is

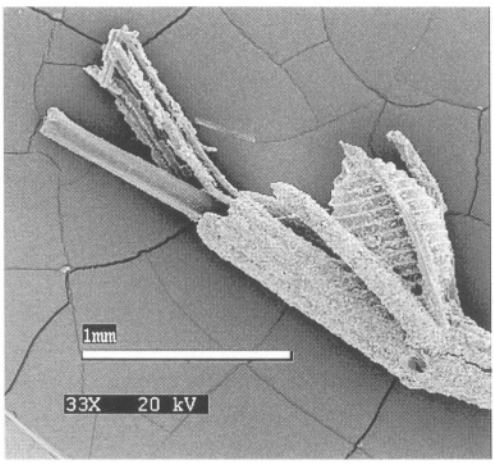


Figure 4. A SEM photograph of modern *Chara* stem and calcite coating with gyrogonite, a calcite casing surrounding an oogonia. A more "mature" plant may have calcite coating with a smooth exterior. The *Chara* was collected in 1991 from Alta Lake, Washington, by D. Carter and others of USGS.

difficult. The minute calcite or aragonite crystals that form as summer whiting observed on many lake surfaces as a result of algal bloom are generally considered inorganic but perhaps should be called bio-induced. Extracellular calcite on stoneworts or characean algae and calcite loricae of phacotacean algae, which I include here as an examples of bio-induced carbonate, perhaps could be called biogenic in the sense that calcification is the immediate result of bicarbonate assimilation for photosynthesis.

Charaphytes

Chara is a well-known green alga (Chlorophyta) of the class Chraphyceae, order Charales (Fig. 4). Because of its appearance, it is commonly mistaken by non-specialists for a vascular plant. It can reach about 0.5 m in length, is anchored to the lake or pond bottom in shallow water by rhizoids, and appears as though it has leaves (the determinate laterals) and seeds (oogonia). Chara generates the proton necessary to convert dissolved HCO_3^- into CO_2 by an exchange withintracellular Ca^{2+} involving active Ca^{2+} transport (McConnaughey, 1991; McConnaughey & Falk, 1991). Calcification appears to be stoichiometric to photosynthesis in moderately alkaline solution so long as sufficient Ca^{2+} is present (McConnaughey & Falk, 1991). The $\delta^{18}O$ of $CaCO_3$ thus formed appears to be in isotopic equilibrium with that of water, but the $\delta^{13}C$ is elevated by about 5‰ compared to the $\delta^{13}C$ of benthic ostracodes living among the *Chara* (R.M. Forester, pers. commun.). This is likely a result of the local depletion of ^{12}C in HCO_3^- due to photosynthetic uptake of ^{12}C. The systematics of the stable isotope fractionation of photosynthetically-induced *Chara* $CaCO_3$ await proper study.

The intact stem casts of *Chara* are sometimes found in lake sediments. When these stem casts are found, then we need to be concerned whether much of the fine-grained

carbonate is actually composed of crushed *Chara* stem casts. The $\delta^{18}O$ of the stem cast may be in isotopic equilibrium with the water from which it formed, just as we assume or hope is the case for all endogenic carbonates. The $\delta^{13}C$, however, is not, and will skew the reconstructed $\delta^{13}C$ value of the paleo DIC toward a higher value.

Phacotus

Phacotus is a nearly ubiquitous (e.g., Naef & Martin, 1987; Schlegel et al., 1998) but a not well known unicellular flagellated green algal nannoplankton (Chlorophyta) belonging to the class Chlorophyceae, order Chlamydomonadales (Fig. 5). Phacotaceae are characterized by bivalved "loricae" or shells composed of an outer layer of rings of staggered calcite crystals in an organic meshwork and an underlying organic layer (Dunlap & Walne, 1993; Hepperle & Krienitz, 1996). *P. lenticularis* and *P. sphaericus* the two commonly studied species, are about 15 to 20 μm in diameter (but half as thick) with a lorica thickness of about 1.0 to 1.8 μm (Hepperle & Krienitz, 1996). In order to form the calcite lorica, *P. lenticularis* appears to require water supersaturated with calcium carbonate (Hepperle & Krienitz, 1997). Hepperle & Krienitz, op. cit., suggest that when the pH of water reaches 8.6 and the availability of free CO_2 for photosynthesis becomes limited, extracellular carbonic anhydrase catalyzes the transformation of HCO_3^- to molecular CO_2 and OH^-. This makes free CO_2 available for photosynthesis, while locally increasing the pH, which promotes calcification. Apart from the requirement of $CaCO_3$ supersaturation, *P. lenticularis* and *P. sphaericus* occur in oligotrophic to hypertrophic waters with temperatures of 15 to 25 °C, and during summer months they can occur in concentrations exceeding 5 million individuals per liter of water (Koschel et al., 1987; Schlegel et al., 1998). Koschel et al., op. cit., have also reported concentrations of about a million shells per liter or the equivalent of 380 μg of $CaCO_3$ per liter in Lake Tollense, Germany.

Unfortunately, little if anything is known about the $\delta^{18}O$ values of the *Phacotus* loricae. Kelts & Hsu (1978) called attention to this green alga as a possibly significant source of carbonate sediment in lakes, but no studies have appeared in the last 20 years. As early as 1902, an occurrence was reported of Eemian carbonate lake sediment (near Hollerup, Denmark) that consisted almost entirely of fossil loricae (Lagerheim, 1902). Such great abundance suggests that fossil loricae may constitute a significant fraction of the fine-grained carbonate found in lake sediments. Because, unlike ostracodes and mollusks, *Phacotus* does not form calcite lorica in undersaturated water, it is possible that the $\delta^{18}O$ of lorica calcite is in thermodynamic equilibrium with the $\delta^{18}O$ of water. However, by analogy with *Chara,* the $\delta^{13}C$ of lorica calcite is likely to be elevated. The systematics of stable isotope fractionation during lorica calcification await verification either through empirical observation or through laboratory culture.

Post-deposition alteration

The alteration of endogenic and biogenic carbonates within the sediment due to reactions with pore-water can be a serious problem. The decay of organic sediments produces CO_2 which may lead to partial to complete dissolution of calcite and aragonite (Dean, 1999). Partial dissolution is the more difficult problem, for the remaining carbonate may contain

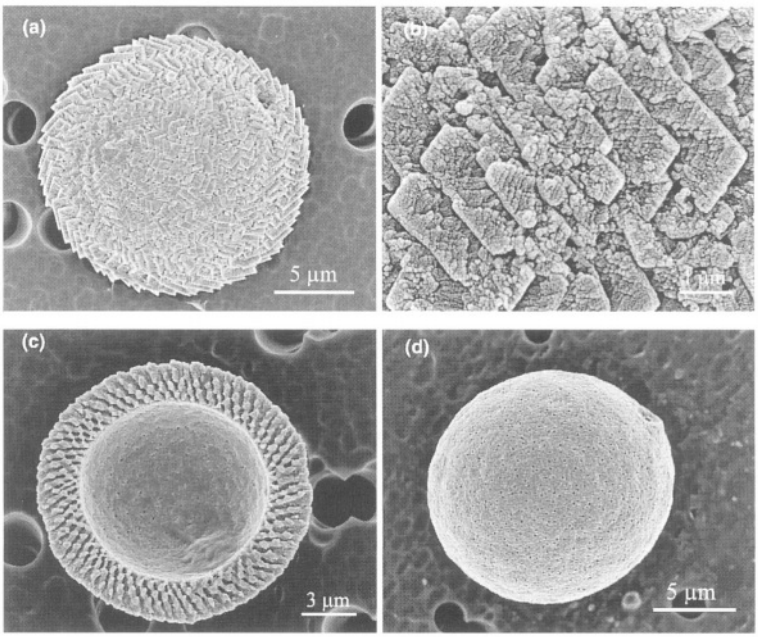


Figure 5. SEM photographs of of *Phacotus* loricae from natural samples. (a) *Phacotus lenticularis*. Lorica with a ring-like arrangement of rhombohedral calcite crystals, typical for young cells. (b) Fine structure of a *Phacotus-lenticularis* lorica. (c) View into a lorica. Calcite crystals are arranged with negative declination angles (d) *Phacotus sphaericus* with a spherical calcite-lorica. All photographs are courtesy of Ines Schlegel, Institute of Freshwater Ecology and Inland Fisheries, Germany.

a skewed record. Recognition of partial dissolution of fine-grained endogenic carbonates probably requires careful SEM investigation. Mollusk and ostracode fossils can be checked for the disappearance of surface features. The ornamentation and muscle-attachment scars on the surfaces of ostracode shells and the fine growth lines of mollusk shells are the first to dissolve. There is strong evidence that the $\delta^{18}O$ and $\delta^{13}C$ values as well as trace-element concentrations within an ostracode shell are not uniform. Poorly calcified ostracode shells have a high concentration of Mg (Chivas et al., 1983) and a low $\delta^{18}O$ (Xia et al., 1997c), and by inference the early calcified part of any shell may have higher Mg/Ca and lower $\delta^{18}O$ and be the first to be removed during partial dissolution.

Another problematic alteration is that of carbonate overgrowth. Such overgrowth is impossible to remove since anything that will chemically dissolve the overgrowth will also dissolve the original carbonate, and mechanical means will likely destroy the delicate fossil shells of ostracodes and mollusks. Attempts to remove the overgrowth in an adjustable power ultrasonic bath or with an ultrasonic probe have proved unsuccessful in my laboratory.

Isotope analysis

The isotopic analysis of calcite and aragonite can be accomplished by liberating CO_2 in a reaction with 104% phosphoric acid in the classic method described by McCrea (1950).

Studies have shown that the use of acids of concentrations other than 104 ~ 105% can cause shifts in $\delta^{18}O$ (Wachter & Hays, 1985). Automated preparation devices such as the common acid bath or the drip method systems used with modern mass spectrometers have, in some sense, taken the CO_2 preparation methods out of our direct control. The automated systems typically react carbonate samples as little as a few tens of micrograms at elevated temperatures (e.g., 70 °C) for a short time. Swart et al. (1991) report that different reaction methods result in different carbonate-CO_2 fractionation values. Be that as it may, the key is to include enough standards in the day's run to insure reproducibility and to normalize all values with respect to VPDB.

Fine-grained carbonates containing dolomite or siderite require a different strategy. If isotopic value of the bulk carbonate material is desired, the prepared sample can simply be reacted at a high temperature (Rosenbaum & Sheppard, 1986) since the reaction rate of dolomite and siderite in phosphoric acid is very slow at 25 or even 70 °C. If isotopic values of individual carbonate minerals are desired, then this can at least be accomplished partially. The prepared material can first be reacted at 25 °C for just 1 hour, which should leave intact resistant fractions such as dolomite and siderite. The residue is then washed and dried and reacted at the requisite high temperature. In my laboratory, when this method is employed, we spot-check some samples by subjecting them to XRD-analysis both before and after the 25 °C reaction.

In some laboratories, the remaining acid residue is used to obtain trace-element chemistry. The samples destined for tandem trace-element analysis must then be reacted in ultra-pure phosphoric acid with very low concentrations of metals such as Mg and Sr. The reaction with the acid should also be carried out preferably in a quartz vessel. If a Pyrex vessel is used, it should have been acid-leached for a sufficiently long time to insure that leachable metals have been removed.

Preparation of carbonate samples for isotope analysis (Fig. 6)

Best material for stable-isotope analysis is a pure carbonate phase. However, even what appears to be pure marl is probably not all carbonate and silt but contains small amount of organics. Biogenic carbonates are never pure and contain chitin and other organic material that hold the shell together. Some material can be left and will not affect the isotopic analysis; other materials must be removed or the obtained $\delta^{18}O$ and $\delta^{13}C$ values will not be accurate.

Bulk sediments

Fine-grained carbonates contained in lacustrine sediment are typically analyzed "as is" after freeze-drying. However, organic components and sulfides in the sediment do react with phosphoric acid. Organics cause a shift in $\delta^{13}C$ to a lower value, and sulfides cause a shift in $\delta^{18}O$. Some laboratories clean the sediment in hydrogen peroxide solution to remove labile organic compounds. The experience in my laboratory, which is heavily skewed toward sulfate- and sulfide-rich sediments of the northern Great Plains of North America, is that hydrogen peroxide does little to remove organics. The treatment creates some organic acids that in turn attack the carbonates but leave sulfide minerals intact. One of the present routines

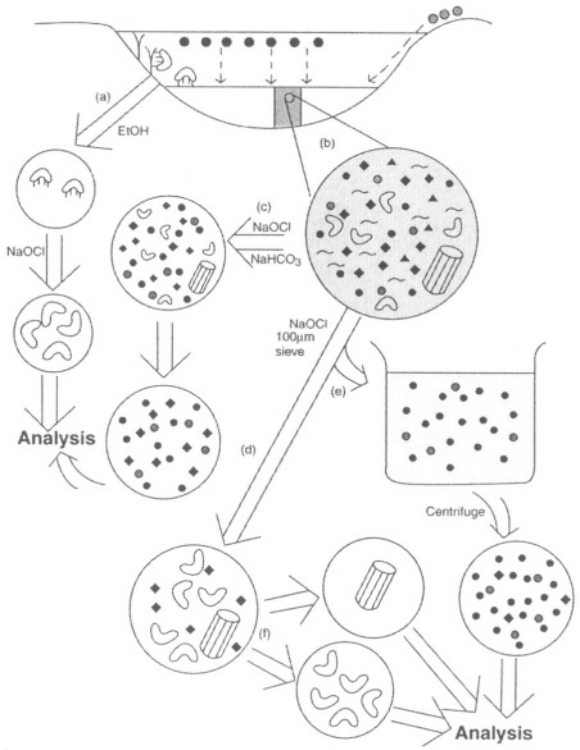


Figure 6. A schematic of sediment sample preparation for the stable isotope analysis. (a) Live or modern ostracodes (and other biogenic or bio-induced carbonates) are harvested and stored in absolute ethanol. Ethanol softens the soft body and the chitin layer so that they can be removed. If the valves are not going to be analyzed for trace elements, the valves can be dried and are ready for analysis. If the valves are to be analyzed for trace elements, they need to be cleaned with NaOCl solution (see text) to destroy organic material. (b) Sediment containing biogenic and inorganic carbonates, organic material, silicates, and sulfides are subsampled. (c) The bulk sediment may be treated with NaOCl solution whose pH has been adjusted with $NaHCO_3$ to destroy all organics and sulfides. Coarse carbonates are hand-picked and the fine fraction is analyzed for oxygen and carbon isotopes. (d) Alternatively, in order to more effectively concentrate coarse fractions, the sediment may first be treated with NaOCl solution and then passed through 100 μm sieve. The coarse material can be rinsed, freeze-dried and ostracodes, mollusks, and *chara* stem casts hand-picked. Ostracodes and mollusks are separated by species for analysis. (e) The fine fraction that passes through the 100 μm sieve can be collected, centrifuged to concentrate the fine carbonates and silicates, rinsed and dried for analysis. Symbols used in the schematic are: • = endogenic carbonate grains, • = detrital carbonate, ▲ = sulfides, ♦ = silicates, ~ = organics, boomerang shape = ostracode, tubular shape = *chara* stem cast.

at my laboratory is to treat the bulk-sediment samples with lab-grade 2.5% NaOCl solution (Fig. 6c). Coarse carbonate matter such as ostracodes and mollusks is then hand-picked from the treated sediment. If the sediment contains detrital carbonate and it is sufficiently coarse, the grains can be picked out at this stage (we should be so lucky!). An alternative method we use is to pass the treated sediment through a 100-μm sieve and catch the fine fraction (Fig. 6e). This suspension of fine-grained endogenic carbonates is then centrifuged and freeze-dried. We have also started to experiment with a differential settling technique in

which treated bulk sediment is made into a thin slurry and subjected to sequential centrifuge treatments for different time-duration at different speeds (K. Conrad, pers. commun.).

Some very organic-rich samples have required multiple treatments with NaOCl of up to 24 hours each. Comparative tests with other cleaning methods have shown that while the NaOCl treatment does cause some shifts, especially in Mg/Ca and Sr/Ca ratios in ostracode shells, its effect may be the smallest AND it results in complete removal of organics and sulfides (Forester et al., 1971; Gaffey et al., 1991; Love & Woronow, 1991; Gaffey & Bonninmann, 1993; Keatings et al., 1999). One other key point in bulk-carbonate sample preparation is the need to modify the pH of any solution that is used for cleaning and rinsing. Deionized or distilled water has a pH well below the bicarbonate stability field, so that prolonged contact of sediment with such water will result in a loss of carbonate. Addition of some $NaHCO_3$ to bring up the pH to the range of the bicarbonate stability field seems advisable. Prolonged contact with tap water, especially at elevated temperatures (ca. >50 °C), should be avoided to minimize isotope exchange and trace-element contamination.

Removal of fine-grained detrital carbonate is a difficult problem with no clear-cut solution. In some sediment, the detrital component is dolomitic, and its dissolution along with the endogenic calcite or aragonite can be prevented by reacting the prepared sediment with 104% phosphoric acid for just 1 hour at 25 °C. If the detrital component has the same mineralogy as the endogenic component, some indirect and much less satisfactory methods can be tried. One method assumes that the proportion of some detrital silicate fraction such as feldspar and detrital carbonate is constant with time. Then some likely sources of detrital carbonate phase are investigated and appropriate samples are collected. The averaged (or some other) isotopic value of these carbonates is subtracted on mass-normalized basis (such as based on the abundance of feldspars) from the measured isotopic value of the prepared sediment. Such attempts are time-consuming but can place some limits on the likely contribution of the detrital carbonate component(s).

Separated fossils

The separation of biogenic carbonates from bulk sediment is typically accomplished by soaking the sediment in a pH-stabilized deionized water containing a solution of commercial Calgon or Triton-X 100 to help disaggregate the sediment (Colman et al., 1994; Xia et al., 1997b). The sediment is then wet-sieved through a 100-μm filter and the residue is dried either in the air or in a freeze-dryer (Xia et al., 1997b; Wansard et al., 1998) (Fig. 6d). Fossils should be separated by species, and in the case of ostracodes by instars as well (Fig. 6f). The seasonality of moults as well as habitat preference are different for different species of ostracodes and for different instars (von Grafenstein et al., 1992, 1999; Xia et al., 1997a). The best bivalves and ostracode shells are those that are still articulated with all surface features clearly visible. Unfortunately, such fossils are not necessarily available. Nevertheless, those shells with signs of corrosion or overgrowth should be avoided. Trapped or adhered clays may have little effect on isotopic analysis, but will have a large effect on trace-element analysis. The degree to which the samples must be cleaned will vary depending on whether the samples are to be subjected to tandem isotope and trace-element analysis. Chitin in ostracode shells apparently contains a measurable concentration of Mg (A. Chivas, pers. commun.) so it is important that the shells be treated with NaOCl solution. Fossil samples destined for isotope analysis alone or that appear to

be clean under the microscope may need nothing more than cleaning in deionized water (amended with $NaHCO_3$), followed by a rinse in absolute ethanol (von Grafenstein et al., 1992; Yu & Ito, 1999).

Modern or live specimens

Live ostracode specimens can be drowned in ethanol, resulting in open shells (U. von Grafenstein, pers. commun.). Subsequent storage in absolute ethanol also results in the separation of the soft body and the main chitin layer from modern ostracode shells (e.g., Wansard et al., 1998). U. Von Grafenstein (pers. commun.) does not subject the shells to any further aggressive treatments, for his samples are analyzed only for their stable isotopes. In my laboratory, where most samples are also analyzed for Mg/Ca and Sr/Ca, the samples stored in ethanol are subjected to NaOCl treatment to remove all organic components. Some bivalve specimens are large enough to sample individual growth bands separated by hibernation periods (Dettman et al., 1999). The micro-drilled samples are then cleaned to remove the organic components.

Conclusions

Useful information on paleohydrology and paleoclimate can be obtained from lacustrine carbonates through stable-isotope and Mg/Ca- and Sr/Ca-ratio analysis. In order to maximize the quality of data, thorough characterization, separation, and the cleaning of samples are necessary. Invaluable constraints on the interpretation of sediment data can be obtained by the analysis of modern water and live calcareous organisms or core-top or sediment-trap endogenic carbonates. Where groundwater is important, samples of domestic and agricultural well water as well as samples taken by mini-piezometers are useful. The final key to getting the most out of carbonate isotope analysis is to use other proxy data to constrain all possible interpretations.

Summary

The oxygen- and carbon-isotope analysis of lacustrine sedimentary carbonates can yield useful paleoclimatologic and paleohydrologic information. However, because lacustrine carbonates are composed of several components, each having a different source and thus containing different information, and because a lake may be supported by variable amounts of groundwater and surface water, and range from ephemeral or permanent and small to large, a full accounting of the factors that affect its stable-isotope values and hydrochemistry is needed. Specifically, (1) carbonate phases must be well-characterized and separated according to their origin; (2) the isotopic relationship among today's climate, lake water, and modern carbonates must be investigated, and (3) constraints from whole-core and bulk-sediment studies and other proxy records are taken into consideration. From analytical point of view, care must be taken to ensure that the carbonate phases are pure and free of organics and sulfides.

Acknowledgments

I thank Rick Forester, Alison Smith, Zicheng Yu, Dan Engstrom, Bill Last, Jim LaBaugh, Patrick DeDeckker, Kelly Conrad, and Kevin Keatings for discussions on myriad aspects of lacustrine carbonates. Rick Forester, Jim LaBaugh, Don Palmer, Don Rosenberry, Herb Wright, Bill Last, John Smol, and an anonymous reviewer read a draft version of which there has been several. I owe special thanks to Herb Wright, Dan Engstrom, and Sheri Fritz who nudged me into Quaternary studies. The preparation of this paper was assisted by NSF grant EAR-9725033. This is Contribution #547 of the Limnological Research Center.

References

Barrera, E., M. J. S. Tevesz, J. G. Carter & P. L. McCall, 1994. Oxygen and carbon isotopic composition and shell microstructure of the bivalve *Laternula-elliptica* from Antarctica. Palaios 9: 275–287.

Chivas, A. R., P. De Deckker & J. M. G. Shelley, 1983. Magnesium, strontium, and barium partitioning in nonmarine ostracode shells and their use in paleoenvironmental reconstructions — a preliminary study. In Maddocks, R. F. (ed.) Applications of Ostracoda. University of Houston, Geosciences Department, Houston: 238–249.

Cole, J. J.. N. F. Caraco, G. W. Kling & T. K. Kratz, 1994. Carbon dioxide supersaturation in the surface waters of lakes. Science 265: 1568–1570.

Colman, S. M., R. M. Forester, R. L. Reynolds, D. S. Sweetkind, J. W. Kling, P. Gangemi, G. A. Jones, L. D. Keigwin & D. S. Foster, 1994. Lake-level history of Lake Michigan for the past 12,000 Years: The record from deep lacustrine sediments. J. Great Lakes Res. 20: 73–92.

Craig, H., 1965. The measurement of oxygen isotope peleotemperatures. In Tongiorgi, E. (ed.) Stable Isotopes in Oceanographic Studies and Paleotemperatures, Spoleto 1965. Conoglio Nazionale delle Ricerche, Pisa: 161–182.

Craig, H. & L. Gordon, 1965. Deuterium and oxygen-18 isotope variations in the ocean and marine atmosphere. In Tongiorgi, E. (ed.) Stable Isotopes in Oceanographic Studies and Paleotemperatures, Spoleto 1965. Conoglio Nazionale delle Ricerche, Pisa, Italy: 9–130.

Dansgaard, W., H. B. Clausen, N. Gundestrup, C. U. Hammer, S. F. Johnsen, P. M. Kristinsdottir & N. Reeh, 1982. A new Greenland deep ice core. Science 218: 1273–1277.

Dean, W. E., 1999. The carbon cycle and biogeochemical dynamics in lake sediments. J. Paleolim. 21: 375–393.

Delorme, L. D., 1970a. Freshwater ostarcodes of Canada. Part II. Subfamily Cypridopsinae and Herpetocypridinae, and family Cyclocypridinae. Can. J. Zool. 48: 253–266.

Delorme. L. D., 1970b. Freshwater ostracodes of Canada. Part I. Subfamily Cypridinae. Can. J. Zool. 48: 153–168.

Delorme, L. D., 1970c. Freshwater ostracodes of Canada. Part III. Family Candonidae. Can. J. Zool. 48: 1099–1127.

Delorme, L. D., 1970d. Freshwater ostracodes of Canada. Part IV. Families Ilyocyprididae, Notodromadidae,Darwinulidae,Cytherideidae, and Entocytheridae.Can. J. Zool. 48: 1251–1259.

Delorme, L. D., 1971. Freshwater ostracodes of Canada. Part V. Families Limnocytheridae, Loxoconchidae. Can. J. Zool. 49: 43–64.

Dettman, D. L., A. K. Reische & K. C. Lohmann, 1999. Controls on the stable isotope composition of seasonal growth bands in aragonitic fresh-water bivalves (unionidae). Geochim. Cosmochim. Acta 63: 1049–1057.

Dettman, D. L., A. J. Smith, D. K. Rea, T. C. Moore & K. C. Lohmann, 1995. Glacial meltwater in Lake Huron during early postglacial time as inferred from single-valve analysis of oxygen isotopes in ostracodes. Quat. Res. 43: 297–310.

Dunlap, J. R. & P. L. Walne, 1993. Microarchitecture and mineralization in loricae of phacotacean flagellates. Acta Protozoologica 32: 237–243.

Durazzi, J. T., 1977. Stable isotopes in the ostracod shell: a preliminary study. Geochim. Cosmochim. Acta 41: 1168–1170.

Emiliani, C., 1955. Pleistocene temperatures. J. Geol. 63: 538–578.

Epstein, S., R. Buchsbaum, H. A. Lowenstam & H. C. Urey, 1951. Carbonate-water isotopic temperature scale. Geol. Soc. Amer. Bull. 63: 417–426.

Epstein, S., R. Buchsbaum, H. A. Lowenstam & H. C. Urey, 1953. Revised carbonate-water isotopic temperature scale. Geol. Soc. Amer. Bull. 64: 1315.

Eugster, H. P. & B. F. Jones, 1979. Behavior of major solutes during closed-basin brine evolution. Amer. J. Sci. 279: 609–631.

Findlay, D. L., H. J. Kling, H. Römick & W. J. Findlay, 1998. A paleolimnological study of eutrophied Lake Arendsee (Germany). J. Paleolim. 19: 41-54.

Forester, R. M., P. A. Sandberg & T. F. Anderson, 1971. Isotopic variability of cheilostome bryozoan skeletons. In Larwood, G. P. (ed.) Living and Fossil Bryozoa. Academic Press, New York: 79–94.

Fritz, P., T. W. Anderson & C. F. M. Lewis, 1975. Late Quaternary climatic trends and history of Lake Erie from stable isotope studies. Science 190: 267–269.

Fritz, P. & S. Poplawski, 1974. ^{18}O and ^{13}C in the shells of freshwater molluscs and their environments. Earth Planet. Sci. Lett. 24: 91–98.

Gaffey, S. J. & C. E. Bronnimann, 1993. Effects of bleaching on organic and mineral phases in biogenic carbonates. J. Sed. Petrol. 63: 752–754.

Gaffey, S. J., J. J. Kolak & C. E. Bronnimann, 1991. Effects of drying, heating, annealing, and roasting on carbonate skeletal material, with geochemical and diagenetic implications. Geochim. Cosmochim. Acta 55: 1627–1640.

Gat, J. R., 1995. Stable isotopes of fresh and saline lakes. In Lerman, A., D. Imboden & J. R. Gat (eds.) Physics and Chemistry of Lakes. Springer-Verlag, Berlin: 139–165.

Gonfiantini, R., 1986. Environmental isotopes in lake studies. In Fritz, P. & J. C. Fontes (eds.) Handbook of Environmental Isotope Geochemistry, 2. Terrestrial Environment, B. Elsevier, Amsterdam: 113–168.

Grossman, E. L. & T.-L. Ku, 1986. Oxygen and carbon isotope fractionation in biogenic aragonite: temperature effects. Chem. Geol. (Isot. Geosci. Sect.) 59: 59–74.

Haskell, B. J., D. R. Engstrom & S. C. Fritz, 1996. Late Quaternary paleohydrology in the North American Great Plains interred from the geochemistry of endogenic carbonate and fossil ostracodes from Devils Lake, North Dakota, USA. Palaeogeogr., Palaeoclimatol., Palaeoecol. 124: 179–193.

Hepperle, D. & L. Krienitz, 1996. The extracellular calcification of zoospores of *Phacotus lenticularis* (Chlorophyta, Chlamydomonadales). European J. Phycology 31: 11–21.

Hepperle, D. & L. Krienitz, 1997. *Phacotus lenticularis* (Chlamydomonadales, Phacotaceae) zoospores require external supersaturation of calcium carbonate for calcification in culture. J. Phycology 33: 415–424.

Horibe, Y. & T. Oba, 1972. Temperature scales of aragonite-water and calcite-water systems (in Japanese). Fossils 23/24: 69–79.

Hostetler, S. W., 1995. Hydrological and thermal response of lakes to climate: description and modeling. In Lerman, A., D. M. Imboden & J. R. Gat (eds.) Physics and Chemistry of Lakes. Springer-Verlag, Berlin: 63–82.

Hostetler, S. W. & L. V. Benson, 1994. Stable isotopes of oxygen and hydrogen in the Truckee River-Pyramid Lake surface-water system. 2. A predictive model of $\delta^{18}O$ and $\delta^{2}H$ in Pyramid Lake. Limnol. Oceanogr. 39: 356–364.

Hull, H. & A. G. Turnbull, 1973. A thermalchecmial study of monohydrocalcite. Geochim. Cosmochim. Acta 37: 685–694.

Ito, E., Z. Yu, D. R. Engstrom & S. C. Fritz, 1998. Is paleoclimatic interpretation of oxygen-isotope records from glaciated Great Plains possible? American Quaternary Association Program & Abstracts of the 15th Biennial Meeting 119.

Jouzel, J., C. Lorius, J. R. Petit, C. Genthon, N.I. Barkov, V. M. Kotlyakov & V. M. Petrov, 1987. Vostok ice core: a continuous isotope temperature record over the last climatic cycle (160,000 years). Nature 329: 403–408.

Keatings, K. W., E. Ito, D. R. Engstrom, Z. C. Yu, T. H. E. Heaton & B. J. Haskell, 1999. An investigation into the effect on ostracod shell chemistry of some chemical and physical cleaning techniques. EOS, Supplement 80: S 176.

Koschel, R., G. Proft & H. Raidt, 1987. *Phacotus* Massenentwicklungen eine Quelle des authochthonen Kalkeintrages in Seen. Limnologica 18: 457–160.

LaBaugh, J. W. & G. A. Swanson, 1992. Changes in the chemical characteristics of water in selected wetlands in the Cottonwood Lake area, North Dakota, USA, 1967–1989. In Robarts, R. D. & M. L. Bothwell (eds.) Aquatic Ecosystems in Semi-Arid Regions: Implications for Resource Management. Environment Canada, Saskatoon, Saskatchewan.: 149–162.

Lagerheim, G., 1902. Untersuchungen über fossile Algen, I & II. Geol. För. Stockh. Förh. 24:475–500.

Last.W. M., 1982. Holocene carbonate sedimentation in Lake Manitoba. Sedimentology 29: 691–704.

Love, K. M. & A. Woronow, 1991. Chemical changes induced in aragonite using treatments for destruction of organic material. Chem. Geol. 93: 291–301.

McConnaughey, T., 1991. Calcification in *Chara corallina:* CO_2 hydroxylation generates protons for bicarbonate assimilation. Limnol. Oceanogr. 36: 619–628.

McConnaughey, T. A. & R. F. Falk, 1991. Calcium-proton exchange during algal calcification. Biol. Bull. 180: 185–195.

McCrea, J. M., 1950. On the isotopic chemistry of carbonates and a paleotemperature scale. J. Chem. Physics 18: 849–857.

Müller, G., G. Irion & U. Förstner, 1972. Formation and diagenesis of inorganic CaMg carbonates in the lacustrine environment. Naturwissenschaften 59: 158–164.

Naef, J. & P. Martin, 1987. Plancton du lac Léman (XI) année 1985. Archives des Sciences (Geneva) 40: 23–46.

Rosenbaum, J. & S. M. F. Sheppard, 1986. An isotopic study of siderites, dolomites and ankerites at high temperatures. Geochim. Cosmochim. Acta 50: 1147–1150.

Rozanski, K., L. Araguas-araguas & R. Gonfiantini, 1993. Isotopic Patterns in Modern Global Precipitation. In Swart, P. K., K. C. Lohmann, J. Mckenzie & S. Savin (eds.) Climate Change in Continental Isotopic Records. American Geophysical Union: 1–36.

Schlegel, I., R. Koschel & L. Krienitz, 1998. On the occurrence of *Phacotus lenticularis* (Chlorophyta) in lakes of different trophic state. Hydrobiologia 353: 369–370.

Siegenthaler, U. & U. Eicher, 1986. Stable oxygen and carbon isotope analyses. In Berglund, B. E. (ed.) Handbook of Holocene Palaeoecology and Palaeohydrology. J. Wiley, New York: 407–422.

Smith, A. J., J. Donovan, E. Ito & D. R. Engstrom, 1997. Groundwater processes controlling prairie lake response to mid-Holocene drought. Geology 25: 391–394.

Spencer, R. J., 1977. Silicate and Carbonate Sediment-water Relationships in Walker Lake, Nevada. M.S. thesis. University of Nevada.

Stuiver, M., 1968. Oxygen-18 content of atmospheric precipitation during last 11,000 years in the Great Lakes region. Science 162: 994–997.

Stuiver, M., 1970. Oxygen and carbon isotope ratios of fresh-water carbonates as climatic indicators. J. Geophys. Res. 75: 5247–5257.

Swart, P. K., S. J. Burns & J. J. Leder, 1991. Fractionation of the stable isotopes of oxygen and carbon in carbon dioxide during the reaction of calcite with phosphoric acid as a function of temperature and technique. Chem. Geol. (Isot. Gcosci. Sect.) 86: 89–96.

Tarutani, T., R. N. Clayton & T. Mayeda, 1969. The effect of polymorphism and magensium substitution on oxygen isotope fractionation between calcium carbonate and water. Geochim. Cosmochim. Acta 33: 987–996.

Urey, H. C., 1947. The thermodynamic properties of isotopic substances. J. Chem. Soc. (Lond): 562–581.

van Morkhoven, F. P. C. M., 1962. Post-Palaeozoic Ostracoda, Their Morphology, Taxonomy, and Economic Use. Elsevier, Amsterdam, 204 pp.

Veizer, J., 1983. Trace elements and isotopes in sedimentary carbonates. In Reeder, R. J. (ed.) Carbonates: Mineralogy and Chemistry. Mineralogical Society of America, Washington, D. C.: 265-300.

von Grafenstein, U., H. Erlenkeuser, J. Müller & A. Kleinmann-Eisenmann, 1992. Oxygen isotope records of benthic ostracods in Bavarian lake sediments. Naturwissenschaften 79: 145–152.

von Grafenstein, U., H. Erlernkeuser & P. Trimborn, 1999. Oxygen and carbon isotopes in modern fresh-water ostracod valves: assessing vital offsets and autoecological effects of interest for paleoclimate studies. Palaeogeogr., Palaeoclimatol., Palaeoecol. 148: 133–152.

Wachter, E. A. & J. M. Hayes, 1985. Exchange of oxygen isotopes in carbon-dioxide-phosphoric acid systems. Chem. Geol. (Isot. Geosci. Sect.) 52: 365–374.

Wansard, G., P. DC Deckker & R. Julià, 1998. Variability in ostracod partition coefficients D(Sr) and D(Mg): Implications for lacustrine palaeoenvironmental reconstructions. Chem. Geol. 146: 39–54.

Winter, T. C., 1995. Hydrological Processes and the Water Budget of Lakes. In Lerman, A., D. Imboden & J. Gat (eds.) Physics and Chemistry of Lakes. Springer-Verlag: 37–62.

Xia, J., D. R. Engstrom & E. Ito, 1997a. Geochemistry of ostracode calcite: 2. the effects of water chemistry and seasonal temperature variation on *Candona rawsoni*. Geochim. Cosmochim. Acta 61: 383–391.

Xia, J., B. J. Haskell, D. R. Engstrom & E. Ito, 1997b. Holocene climate reconstructed from tandem trace-element and stable-isotope composition of ostracodes from Coldwater Lake, North Dakota, USA. J. Paleolim. 17: 85–100.

Xia, J., E. Ito & D. R. Engstrom, 1997c. Geochemistry of ostracode calcite: 1. an experimental determination of oxygen isotope fractionation. Geochim. Cosmochim. Acta 61: 377–382.

Yu, Z. & E. Ito, 1999. Possible solar forcing of century-scale drought frequency in the northern Great Plains. Geology 27: 263–266.

14. CARBON AND OXYGEN ISOTOPE ANALYSIS OF LAKE SEDIMENT CELLULOSE: METHODS AND APPLICATIONS

BRENT B. WOLFE (bwolfe@sciborg.uwaterloo.ca)
THOMAS W. D. EDWARDS
RICHARD J. ELGOOD
Department of Earth Sciences
University of Waterloo
Waterloo, Ontario
Canada N2L 3G1

KRISTINA R. M. BEUNING
Department of Biology
University of Wisconsin - Eau Claire
Eau Claire, WI
USA 54701

Keywords: cellulose, lake sediment, oxygen isotopes, carbon isotopes, paleohydrology, paleoclimate

Introduction

Carbon and oxygen isotope analysis of lake sediment cellulose is a paleolimnological approach that is gaining increasing usage, especially in carbonate-free sedimentary systems. As with carbonate-based paleolimnological investigations (see Ito, this volume), lake sediment cellulose can provide a record of lake paleohydrology. As a result, studies incorporating this technique typically aim to address the following research questions:

1. How has the water balance of the study lake varied during the past?
2. What does the inferred paleohydrologic record suggest about past changes in climatic conditions?
3. What is the relationship between past hydrologic change and lake or watershed carbon cycling?

Lake sediment cellulose has been used as an archive of paleoenvironmental information in diverse geographic and ecoclimatic settings. These include Great Lakes of both North America (Ontario; Duthie et al., 1996; Wolfe & Edwards, 1998; Wolfe et al., 2000c) and East



W. M. Last & J. P. Smol (eds.), 2001. *Tracking Environmental Change Using Lake Sediments. Volume 2: Physical and Geochemical Methods.* Kluwer Academic Publishers, Dordrecht, The Netherlands.

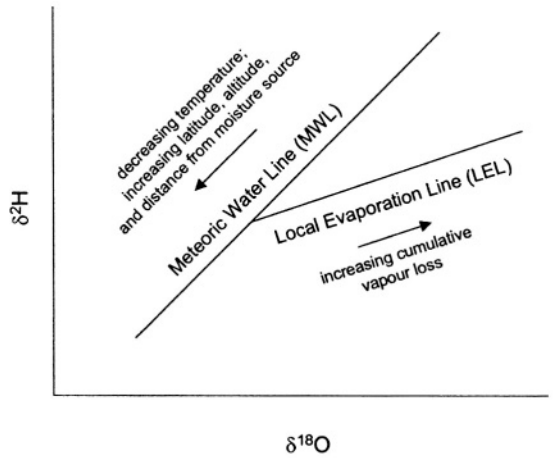


Figure 1. The oxygen and hydrogen isotope compositions of precipitation and surface waters commonly define two linear relations in δ^2H and $\delta^{18}O$ space. Precipitation plots along a meteoric water line (MWL), while surface waters having undergone vapour loss plot on a local evaporation line (LEL).

Africa (Victoria; Beuning et al., 1997), smaller lakes in temperate regions of North America (Edwards & McAndrews, 1989; Padden, 1996; Padden et al., 1996; Wolfe et al., 2000a), in the circumpolar arctic and subarctic (MacDonald et al., 1993; Edwards et al., 1996; Wolfe et al., 1996, 1999, 2000b) and in the subtropical Andes (Abbott et al., 2000), as well as ancient Glacial Lake Agassiz (Buhay & Betcher, 1998). While substantial progress has been made over the last decade in methodological development and interpretation of stable isotope data from lake sediments, various intriguing questions remain to be addressed in future investigations.

This chapter details the technical procedures used to prepare and analyze lake sediment samples for cellulose carbon and oxygen isotope composition, considers important factors in the interpretation of cellulose isotope data, briefly highlights key results from recent applications, and outlines future research needs and directions.

Stable isotope tracers in lake waters — ^{18}O, ^{2}H, ^{13}C

Phase changes during the passage of water through the hydrologic cycle cause variations in the respective abundances of ^{18}O and ^{2}H relative to ^{16}O and ^{1}H, because of slight differences in the volatilities of the different water isotopomers. This isotopic fractionation results in characteristic isotopic labeling of meteoric waters. A key feature of this natural labeling is the existence of strong linear relations ("Meteoric Water Lines", MWLs) commonly observed between $\delta^{18}O$ and $\delta^{2}H$ values in precipitation falling at different times of the year. MWL relationships arise because of isotopic rain-out of atmospheric vapour masses and temperature-dependent fractionation effects in clouds (Fig. 1). As a result, decreasing temperature at the site of condensation and increasing latitude, altitude, and distance from

moisture source (continentality) will generally result in progressively decreasing $\delta^{18}O$ and $\delta^{2}H$ values in precipitation (Dansgaard, 1964; Rozanski et al., 1993).

Preferential loss of molecules containing the common light isotopes, ^{16}O and ^{1}H, during subsequent evaporation from surface waters enriches the remaining water in the heavy isotopes, ^{18}O and ^{2}H, causing displacement from the MWL in $\delta^{18}O$-$\delta^{2}H$ space (Fig. 1). Surface waters within an individual catchment frequently plot along well-defined Local Evaporation Lines (LELs) having slopes generally between 4 and 7, largely depending on the relative humidity, and offset from the MWL in relation to the amount of cumulative vapour loss (Craig & Gordon, 1965; Gonfiantini, 1986).

In contrast to lake water $\delta^{18}O$ and $\delta^{2}H$, which are largely controlled by physical mechanisms, the $\delta^{13}C$ of dissolved inorganic carbon (DIC) in lake water may be strongly mediated by in-lake biological processes, as well as exchange with atmospheric CO_2 (McKenzie, 1985; Quay et al., 1986; Herczeg, 1987; Herczeg & Fairbanks, 1987; Lee et al., 1987). During photosynthesis, phytoplankton preferentially consume $^{12}CO_{2(aq)}$, leaving the remaining $CO_{2(aq)}$ relatively enriched in the heavy carbon isotope, ^{13}C. Recent work suggests that many lakes may act as sources rather than sinks of atmospheric CO_2 (Cole et al., 1994). However, in productive lakes where diffuse influx of atmospheric CO_2 does occur, this input replenishes $CO_{2(aq)}$ withdrawn by phytoplankton and may serve to amplify the biologically-induced ^{13}C-enrichment of the epilimnetic DIC pool.

Decaying plant material that sinks below the photic zone releases ^{13}C-depleted DIC, which may be reincorporated into phytoplankton tissue upon circulation and mixing of lake water. In lakes where the carbon isotope effects of photosynthesis and respiration are not as pronounced, river and groundwater input of DIC may exert a greater influence on lake water DIC $\delta^{13}C$ (Rau, 1978). Catchment-derived DIC $\delta^{13}C$ may potentially span a wide range of values (≈ -30 to 0‰) reflecting influx of dissolved CO_2 from the decomposition of ^{13}C-depleted soil organic matter (in areas devoid of carbonate) and the chemical weathering of ^{13}C-enriched carbonate terrane (Boutton, 1991b).

Close linkage may occur between seasonal cycles of lake water $\delta^{18}O$ and DIC $\delta^{13}C$. For example, lakes may develop progressively increasing values of epilimnion $\delta^{18}O$ and $\delta^{13}C$ during the open-water season due to the combined effects of evaporative ^{18}O-enrichment and ^{18}O-enriched summer precipitation in addition to productivity-driven ^{13}C-enrichment and atmospheric CO_2 drawdown, respectively. Variations through time in the amplitude and pattern of these seasonal cycles may be manifested as long-term trends, recorded in the lake sediments. These variations result from changes in numerous climatic and environmental factors including the carbon and oxygen isotope composition of source waters, relative humidity, residence time, lake nutrient status, and physical characteristics of the catchment such as vegetation, hydrology, geology, and soil development.

Thus, isotope-based paleolimnological and paleoclimatological reconstructions have relied mainly on carbon and oxygen-isotope signals preserved in carbon- and oxygen-bearing inorganic and organic matter produced within the lake water and preserved in bottom sediments. Carbonates of both authigenic and biogenic origin have been used extensively in hard-water lakes, especially at low and mid-latitudes (Ito, this volume), whereas organic matter and cellulose have proven to be useful archives in carbonate-deficient soft-water lakes. Increasing attention is now being focused on nitrogen isotope composition of bulk organic matter (Talbot, this volume) and the hydrogen isotope composition of kerogen (Krishnamurthy et al., 1995; Meyers & Lallier-Vergès, 1999) and aquatic plant lipids

(Sternberg, 1988; Buhay, 1997; Sauer et al., 2001a) as additional isotopic paleo-nutrient and paleohydrologic tracers, respectively.

Historical development

Cellulose is the most abundant bio-molecule in nature, occurring in the cell walls of higher and lower plants primarily in stalks, stems, trunks and all woody components of plant tissues (Ott et al., 1954). Cellulose is also a structural component of the cell walls of some algae, comprising from 1–10% of the dry weight of the organism (Prescott, 1968; De Leeuw & Largeau, 1993). Cellulose in algal cell walls can exist as native cellulose (cellulose I) or as amorphous forms or single chain molecules (Ott et al., 1954; Kreger, 1962). Primary algal groups in which cellulose has been identified in freshwater species are Charophyta, Chlorophyceae, Desmidiales and Zygnematales, including such common genera as *Cladophora, Closterium, Nitella, Oocystis, Pediastrum, Spirogyra, and Botryococcus* (Kreger, 1962; Prescott, 1968; Tsekos, 1999). Although some studies suggest otherwise (Chapman, 1962), there is no conclusive evidence for cellulose in blue-green algal cell walls (Kreger, 1962).

Within lake sediments, cellulose may be preserved as identifiable algal cells (e.g., *Botryococcus* in Lake Victoria (Beuning, unpublished data)), within zooplankton fecal pellets (Edwards, 1993), or as amorphous organic matter. The chemical structure of cellulose contains carbon, hydrogen, and oxygen, each a potential archive of isotopic information. While the ratio of carbon, oxygen and carbon-bound hydrogen isotopes is "locked in" with death of the cellulose-synthesizing organism, oxygen-bound hydrogens are exchangeable (Sternberg, 1989a). As a result, hydrogen isotope analysis of cellulose requires nitration or equilibration preparative procedures to control exchangeable hydrogen. Moreover, strong species-dependent effects on cellulose-water hydrogen isotope fractionation have precluded its use as a paleo-isotopic archive (e.g., Sternberg, 1988).

Carbon and oxygen isotope analysis of cellulose in lake sediments was first conducted by Edwards & McAndrews (1989) to investigate the Holocene paleohydrology of a lake in southern Ontario, Canada. Two important conclusions were drawn from this study. Firstly, the fine-grained cellulose fraction in offshore sediments appeared to be dominantly aquatic in origin. This interpretation was based primarily on coherent isotopic relations between the surface sediment cellulose and the modern lake water as well as overlapping $\delta^{18}O$ records from two widely separated sediment cores. Secondly, lake sediment cellulose $\delta^{18}O$ could be used to trace lake water $\delta^{18}O$ history by applying a similar cellulose-water fractionation factor as had been shown to exist between terrestrial cellulose and leaf water (DeNiro & Epstein, 1981; Sternberg et al., 1984; Edwards et al., 1985). This study, combined with prior isotopic investigations in southern Ontario (Edwards et al., 1985; Edwards & Fritz, 1986, 1988), led to the conceptual development of analogous oxygen isotope relations between terrestrial cellulose, lacustrine inorganic authigenic carbonate and lacustrine aquatic cellulose, and the oxygen isotope composition of the respective source waters (Fig. 2).

For terrestrial cellulose:

$$\delta^{18}O_{cell} = \delta^{18}O_{mw} + \varepsilon_{evap} + \varepsilon_{cell\text{-}leafwater}, \quad (1)$$

where $\delta^{18}O_{cell}$ is the isotopic composition of terrestrial cellulose, $\delta^{18}O_{mw}$ is the isotopic composition of local meteoric water, ε_{evap} is the isotopic enrichment due to combined kinetic

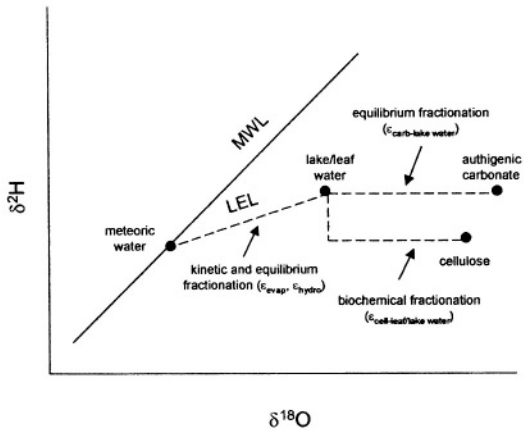


Figure 2. Location of cellulose in δ^2H-$\delta^{18}O$ space and associated fractionation effects. Authigenic carbonate is also shown, although note that position is in relation to δ^{18}O only illustrating the equilibrium fractionation offset from lake water.

and equilibrium effects during evapotranspiration, and $\varepsilon_{\text{cell-leafwater}}$ is the net biochemical enrichment between cellulose and leaf water.

For lacustrine inorganic authigenic carbonate:

$$\delta^{18}O_{\text{carb}} = \delta^{18}O_{\text{mw}} + \varepsilon_{\text{hydro}} + \varepsilon_{\text{carb-lakewater}}, \quad (2)$$

where $\delta^{18}O_{\text{carb}}$ is the isotopic composition of lacustrine inorganic authigenic carbonate, $\delta^{18}O_{\text{mw}}$ as in (1), $\varepsilon_{\text{hydro}}$ is the isotopic enrichment between lake water and meteoric water due to hydrologic factors which are commonly dominated by evaporative enrichment effects, and $\varepsilon_{\text{carb-lakewater}}$ is the temperature-dependent enrichment that occurs between carbonate and lake water.

For lacustrine aquatic cellulose:

$$\delta^{18}O_{\text{cell}} = \delta^{18}O_{\text{mw}} + \varepsilon_{\text{hydro}} + \varepsilon_{\text{cell-lakewater}}, \quad (3)$$

where $\delta^{18}O_{\text{cell}}$ is the isotopic composition of aquatic cellulose, $\delta^{18}O_{\text{mw}}$ as in (1), $\varepsilon_{\text{hydro}}$ as in (2), and $\varepsilon_{\text{cell-lakewater}}$ is the isotopic enrichment that occurs during cellulose synthesis and is identical to $\varepsilon_{\text{cell-leafwater}}$.

Thus it was proposed that, with stratigraphic analysis of lacustrine aquatic cellulose, reconstruction of lake water δ^{18}O could be used to document shifts along a LEL and/or MWL from which paleohydrologic and paleoclimatic information may be derived.

Methods

Sample preparation

Methods for lake sediment sample preparation for cellulose carbon and oxygen isotope analyses have been developed at the University of Waterloo - Environmental Isotope Laboratory (UW-EIL), (Heemskerk & Diebolt, 1994; Edwards et al., 1997; Elgood et al., 1997).

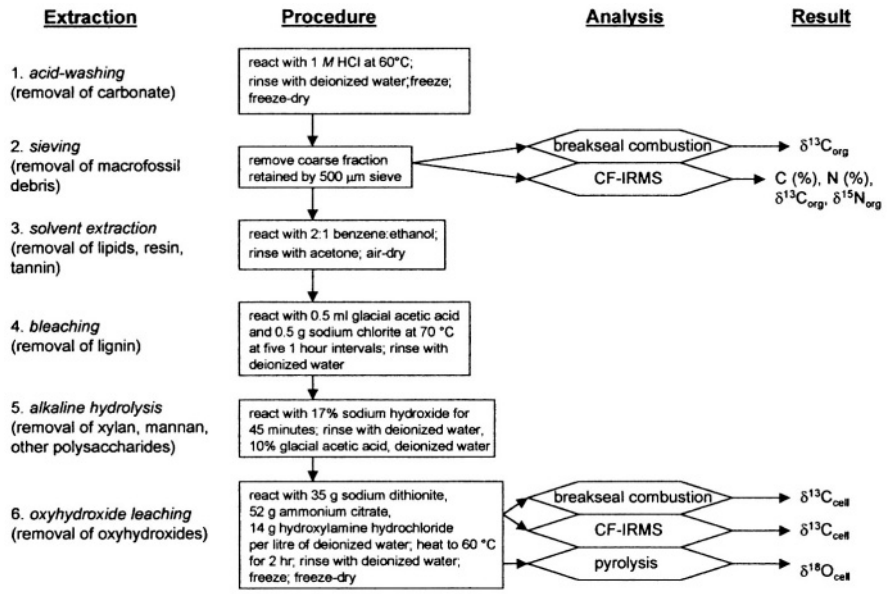


Figure 3. Flow diagram illustrating steps involved in preparing lake sediment for cellulose carbon and oxygen isotope analysis.

These techniques closely follow those of Green (1963) and Sternberg (1989a) for extracting cellulose from wood powder, as indicated in the inaugural study of Edwards & McAndrews (1989). Modifications have been introduced to accommodate the much finer grain size typical of sediments and for removal of other potentially interfering geochemical fractions (Fig. 3). Preliminary sample treatment involves acid-washing to dissolve carbonate material and dry sediment sieving to remove macrofossil debris after which analysis of bulk carbon and nitrogen elemental and isotope composition may be conducted. Sediment cellulose preparation on the acid-washed residue is generally a three-part process involving sequential extraction of non-cellulose organic components. An additional leaching step removes oxyhydroxides. All extractions are performed in a fume hood and normal laboratory safety precautions should be adhered to (e.g. lab coat, gloves, dust mask and safety glasses should be worn). Batches of 10 or more may be processed simultaneously, depending on the size of the bottles used and space restrictions in the fume hood and water bath. Details of methods used at the EIL are provided below.

A) Acid-washing (removal of carbonate)

1. Place sample in a labeled 75 ml test tube and add 1 M (approximately 8% by volume) HC1. Stir and cover with watch glass. Place in water bath for a minimum of two hours at 60 °C.

2. Check the pH to ensure samples are acidic. If not acidic or visible reaction occurs upon agitation, pour/aspirate supernatant and add fresh HC1 and repeat step # 1. If acidic, pour/aspirate supernatant, fill with deionized water and stir.
3. Leave standing until sediment settles or centrifuge and pour/aspirate supernatant. Rinse repeatedly with deionized water until neutral.
4. Pour/aspirate supernatant, freeze, freeze-dry, and store in labeled, clean, dry vial.
5. Following removal of carbonate and freeze-drying, lake sediment samples are sieved to $<500\ \mu m$ to eliminate macrofossil plant debris (which may be of terrestrial origin). Scattered fragments may be removed with tweezers.

B) Solvent extraction (removal of lipids, resins, tannin)

1. Extract 2–5 g of freeze-dried sediment (depending on organic content of the sediment) in a covered 125 ml glass (or Teflon) wide-mouth, screw-top bottle with about 100ml of 2:1 benzene:ethanol, swirling the solution occasionally. Decant/aspirate the solution after 48 hours. If the liquid is deeply coloured (i.e. darker than weak tea), repeat the extraction with fresh solvent for an additional 24 to 48 hours.
2. Add about 100ml of acetone and replace cover. After 24 hours, decant/aspirate and allow samples to air-dry in the fumehood.

C) Bleaching (removal of lignin)

1. Add about 100 ml of deionized water to the air-dried sample and place in a water bath at 70 °C. Add 0.5 ml of glacial acetic acid, followed by 0.5 g of sodium chlorite, stir, and cover.
2. After one hour, add fresh aliquots of acetic acid and sodium chlorite (always adding the acetic acid first), and stir. Repeat 5 times or until sediment residue is a pale grey to yellowish-grey colour.
3. Allow sediment residue to settle, decant/aspirate supernatant liquid, andre-fill with deionized water. Repeat 5–10 times, or until odour of the bleach solution fades, to completely displace bleach solution. Do not test the odour until the solution is thoroughly diluted.
4. After the final dilution, decant/aspirate to within 1 cm of the residue.

D) Alkaline hydrolysis (removes xylan, mannan, other polysaccharides)

1. Add about 100 ml of 17% sodium hydroxide solution to the wet sample. Let stand for 45 minutes, decant/aspirate, and fill with deionized water. Rinse with deionized water 3–4 times or until solution is neutral.
2. After the final dilution, decant the water to within 1 cm of the grey cellulose residue.

E) Oxyhydroxide leaching (removes oxyhydroxides)

1. Oxygen isotope results may be affected (and the nickel pyrolysis tube contaminated) if iron or manganese oxyhydroxides are present (often indicated by distinctive reddish or orange-brown colour of the final cellulose concentrate) and should be removed using the following leach solution:

   Dissolve in 1 L of deionized water:

   35 g sodium dithionite (also called sodium hydrosulfite)

   52 g ammonium citrate

   14 g hydroxylamine hydrochloride

2. Extract oxyhydroxide-contaminated cellulose concentrate with about 75 ml of leach solution in water bath at 60 °C for 2 hours. Remove and let stand at room temperature for 24 hours.
3. For samples with solution that is visibly discoloured, decant/aspirate and replace with fresh dose of leach solution and let stand at room temperature for 24 hours. If no discolouration is visible, decant/aspirate and replace with deionized water. Let stand for 24 hours.
4. If colour remains (or returns to those samples which have been rinsed with deionized water), repeat with fresh dose of leach solution and let stand for 24 hours. For samples in deionized water that continue to show no colour, wash by repeated dilution and decanting/aspirating with deionized water (approximately 5–7 times).
5. After the final dilution, decant the water to within about 1 cm of the grey cellulose residue, freeze, and freeze-dry.
6. After the sample is thoroughly dry, transfer to a clean, dry, labeled vial for subsequent carbon and oxygen isotope analysis.

Analysis

Carbon isotope analysis on lake sediment cellulose may be performed by routine breakseal combustion (Boutton et al., 1983; Boutton, 1991a) or by continuous flow — isotope ratio mass spectrometry (CF-IRMS). Comparison of lake sediment samples analyzed by both methods at the UW-EIL show excellent agreement.

Oxygen isotope analysis of lake sediment cellulose has been performed mainly by Ni-tube pyrolysis in re-sealable nickel vessels, as first described in Edwards et al. (1994), although a $HgCl_2$ technique has also been used (Sternberg, 1989b; Sauer & Sternberg, 1994; Sauer et al., 2001b). Vessels currently in use at the UW-EIL have undergone minor design modifications since those described by Edwards et al., including the use of stainless-steel rather than nickel Cajon VCR® metal gasket face seal fittings (Fig. 4). With the original vessel design, which included a tapered nickel plug fitted to a beveled nickel seat (see Fig. 1 in Edwards et al., 1994), cleaning of the interior of the vessels rapidly wore down the sealing surface, eventually resulting in gas leakage. More recently, changes in vessel design has enabled better sealing and significantly improved the durability of the vessels. While this new design does result in exposure of a small amount of stainless steel to the

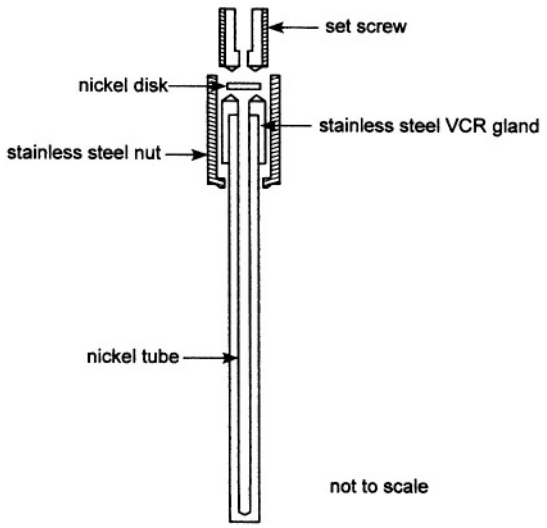


Figure 4. Current vessel design used for pyrolysis at the University of Waterloo.

interior of the vessels, there is no evidence to suggest that this has any apparent effect on $\delta^{18}O$ results.

Vessels are loaded with terrestrial cellulose, lake sediment cellulose, or water and graphite (as a carbon source) and sealed in an argon atmosphere, followed by heating (pyrolysis) at 1050 °C in an evacuated quartz tube. The addition of an encapsulating quartz tube has been incorporated to prevent repeated oxidation of the outer nickel surface and to simplify the cleaning procedure. Heating has been increased from 950 °C used in the original experiments to 1050 °C to account for the insulation of the quartz tube (see Motz et al., 1997).

The pyrolysis reactions can be described by the general (unbalanced) equations:

$$(CH_2O)_n \longrightarrow CO + CO_2 + C + H_2, \tag{4}$$

$$H_2O + C \longrightarrow CO + CO_2 + C + H_2. \tag{5}$$

Hydrogen in the samples forms H_2 gas that diffuses out through the nickel vessel walls and which may be collected and used to determine δ^2H (Motz et al., 1997). Oxygen is incorporated into CO and CO_2 and contained within the vessels. Oxygen isotope analysis is performed on the CO_2 after cryogenic purification on a vacuum extraction line. Quantitative recovery of oxygen from CO is considered unnecessary as the oxygen isotope composition in CO and CO_2 appears to equilibrate at high temperatures with negligible fractionation, which is then retained during cooling to room temperature (Edwards et al., 1994).

The technical procedure for Ni-tube pyrolysis described below is based on equipment designed at the UW-EIL. Modifications may be introduced to adapt to existing laboratory equipment, vacuum extraction lines, etc.

A) Vessel cleaning

Prior to use, pyrolysis vessels must be carefully cleaned to remove all debris remaining from the previous sample.

1. Clean the interior of vessel using a stainless steel brush (1/4" diameter). Gently tap out debris. Care must be taken not to score the raised circular seats at the opening of the vessel as this will result in a poor seal and loss of gas during pyrolysis.
2. Flush interior of vessel with acetone and allow to air-dry.
3. Place clean vessels in oven at 60 °C or keep in a desiccator under vacuum. During periods of prolonged non-use, the pyrolysis vessels should be kept in a desiccator to minimize oxidation of nickel surfaces.

B) Loading vessels (with water or cellulose samples) and pyrolysis

Although samples are vacuum-dried during the process of cellulose extraction (see above), it has been demonstrated that moisture is readily absorbed from the air (Edwards et al., 1994). Furthermore, due to the small sample size, any moisture can have a significant effect on the final analysis. It is therefore important to adhere to the following procedure designed to remove all traces of atmospheric moisture that may cause sample contamination.

1. Place samples in desiccator, attach to freeze dryer or extraction line and evacuate. Leave samples under vacuum for a period of at least 12 hours.
2. Clean and dry vessels as described above.
3. For water samples, load pre-baked, dry carbon (1 mg/1 μlH_2O) into vessels, cover with tinfoil and place in desiccator. Five ml of H_2O typically produces 1.5 to 2 cc of CO_2. For cellulose samples, load into vessels, place in desiccator chamber and cover with tinfoil. Gloves should be worn to prevent contamination of sealing surfaces. For lake sediment samples with very low organic content, it is important not to overload vessels as the pyrolysis reaction will not go to completion. Typically, 3–5 mg are used for pure terrestrial cellulose samples (producing 1.5 to 2 cc of CO_2) and roughly 20 mg are used for lake sediment cellulose (producing roughly 0.5 cc of CO_2). The amount of lake sediment cellulose concentrate required to produce sufficient CO_2 will vary according to the amount of refractory mineral matter.
4. Place vessels in desiccator and attach to freeze dryer or extraction line and evacuate. Leave vessels under vacuum for a period of at least 12 hours.
5. Close desiccator and remove from freeze dryer or extraction line. Place desiccator in glovebox.
6. Flood glovebox with argon. Allow sufficient time for glovebox to be totally flushed with argon.
7. Open desiccator to argon atmosphere.
8. Place nut in holder and transfer vessel from desiccator to holding rack in glovebox. Gloves should be worn to prevent contamination of sealing surfaces.

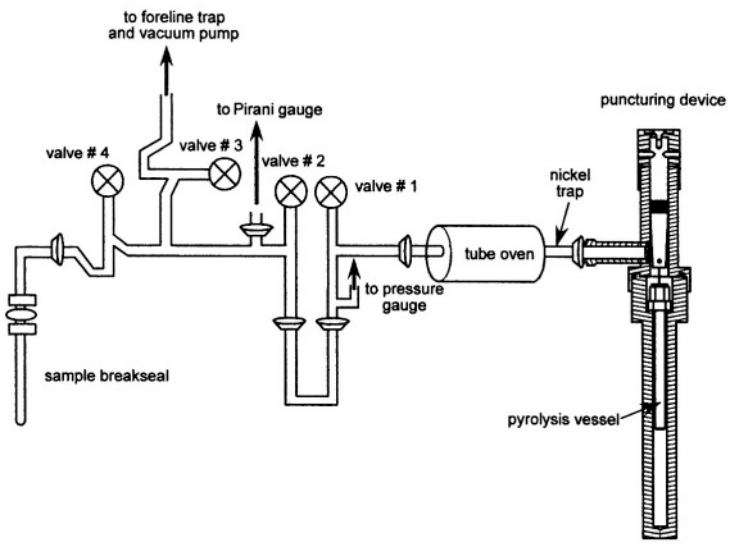


Figure 5. Schematic of CO_2 extraction line used at the University of Waterloo.

9. Flush vessel with thin stream of argon to further ensure that all atmosphere is displaced. Note that pure cellulose is easily blown out of vessel! (For cellulose samples, go to step 11).
10. Lower syringe as far as possible into the vessel and inject water sample.
11. Quickly place nickel disk and setscrew on vessel and tighten.
12. Rinse outside of sealed vessel in acetone and allow to air-dry.
13. Insert sealed vessel into quartz envelope and evacuate on vacuum extraction line.
14. Bake sealed vessel in evacuated quartz envelope at 1050 °C for 50 minutes. After baking, allow quartz envelope and vessel to cool to room temperature (30 minutes).

C) Collection of CO_2 (see Fig. 5)

1. Preheat tube oven to 350 °C (to decompose traces of $Ni(CO)_4$ produced in the vessels; Brenninkmeijer & Mook, 1981) at least one hour in advance to permit thermal stabilization. Note that the Ni-trap should be cleaned in 10% nitric acid routinely to prevent excess build-up of Ni and carbon.
2. Establish a vacuum downstream of valve #1 (i.e. open valves #2, #3, and #4).
3. Place a cooled pyrolysis vessel inside the sample shaft of the puncturing device. Check that the puncturing needle is withdrawn to the correct height and that o-rings are clean. Replace securing head and puncturing hilt and screw tightly to the sample shaft.

4. Attach the puncturing device to the vacuum line; open valve #1 to evacuate the puncturing device. Pump on the entire line for several minutes until vacuum is obtained.
5. Place liquid nitrogen dewar on bottom of u-trap. Close valve #1. Carefully screw down the puncturing hilt (resistance will indicate that the pyrolysis vessel has been pierced). Slowly raise the hilt to remove the needle from the pyrolysis vessel and allow the gases to escape onto the heated portion of the line.
6. Allow the gases to remain in the heated portion of the line for 2 minutes. Close valve #2. Slowly open valve #1 and allow the CO_2 gas to condense in u-trap.
7. Record change in pressure from the presence of non-condensable gases (mainly argon and CO).
8. Raise liquid nitrogen dewar halfway up u-trap; wait several minutes and then raise to about 3 cm from top of u-trap.
9. Bleed off non-condensable gas by opening valve #2 slowly. Pump on the trapped CO_2 to remove non-condensable gases and to ensure complete transfer from punctured sample vessel. When the initial (full vacuum) reading on the pressure gauge is restored, close valves #1 and #2.
10. Replace liquid nitrogen dewar with ethanol/dry ice dewar on u-trap to vaporize the CO_2. Record the new reading on the pressure gauge.
11. Place a liquid nitrogen dewar on the bottom of sample breakseal and close valve #3 to isolate the line from the vacuum pump. Slowly open valve #2 and allow the CO_2 to condense in the sample breakseal. Raise liquid nitrogen dewar over condensed CO_2.
12. After a few minutes, during which the pressure gauge should have returned to near its full-vacuum reading, raise liquid nitrogen dewar. Open valve #3 to pump off any residual non-condensable gases that may have remained in the solid CO_2.
13. Flame off sample breakseal. Ensure that the sample vessel is correctly labeled and remove it for analysis by mass spectrometry.
14. Close valves #1 and #2. Heat for 2–3 minutes and check for an increase in pressure. A change may indicate the presence of water vapour suggesting that the pyrolysis reaction was incomplete. Open valve #2 to check vacuum recovery. A substantial fall in the vacuum also suggests residual water. Replace sample breakseal, change pyrolysis vessel in puncturing device, and re-evacuate line.

New pyrolysis vessels require conditioning before analysis. Standards should be loaded, pyrolysed and the resulting gas released for at least two runs before CO_2 is collected for analysis. Repeated runs with water and cellulose standards should then be undertaken until consistent reproducibility is obtained and until accurate calibration of results can be developed. After extended periods of non-use, standards should be run in each vessel to re-establish the catalytic activity of the nickel. A water or cellulose standard should be routinely run with each sample batch, rotating the vessel in which the standard is loaded to monitor vessel performance. Analytical uncertainties of water, lake sediment and terrestrial cellulose are generally ±0.5 to 1.0‰.

Key criteria for paleohydrologic reconstruction

Two fundamental assumptions in the interpretation of carbon and oxygen isotope data from lake sediment cellulose are 1) the fine-grained cellulose fraction in offshore lake sediments is derived from aquatic plants/algae and 2) the oxygen isotope fractionation between ambient water and aquatic cellulose is known (or constant), allowing for reconstruction of lake water $\delta^{18}O$ history from the sediment record. The validity of these assumptions is briefly discussed below.

Origin of lake sediment cellulose

Incorporation of terrestrial cellulose in fine-grained offshore lake sediment would appear to be a primary complicating factor, yet $\delta^{18}O_{cell}$ records obtained from lakes in many hydrological and ecological settings seem to support a dominantly aquatic origin (Edwards & McAndrews, 1989; Duthie et al., 1996; Edwards et al., 1996; Padden, 1996; Beuning et al., 1997; Buhay & Betcher, 1998; Abbott et al., 2000; Wolfe et al., 2000b). Less favourable sites include lakes characterized by low aquatic productivity relative to allochthonous organic matter input and sediment that undergoes substantial post-depositional loss of organic matter (e.g., Sauer et al., 2001b). Physical removal of coarse organic debris by sieving is evidently a key step in sample preparation, as this fraction may be derived in part from terrestrial sources (e.g., Meyers, 1997). Source interpretation of cellulose may be additionally constrained by supplementary isotopic and elemental data. For instance, low C/N ratios (<10) commonly indicate aquatic-derived organic matter reflective of the higher mean protein content of microplankton (mean ~35%) as compared to terrestrial plants (only 1–8%) (Tyson, 1995; Meyers & Lallier-Vergès, 1999). However, this aquatic-origin "boundary" of C/N <10 is not exclusive (see Tyson, 1995). Even in sediments with C/N ratios ranging from 10 to >15, oxygen isotope analyses of the cellulose fraction appear to predominantly reflect lake water $\delta^{18}O$ based on close correspondence between inferred lake water oxygen isotope composition from surface sediment cellulose and the isotopic composition of the overlying lake water (Duthie et al., 1996; Beuning et al., 1997; Abbott et al., 2000) and other supporting evidence (Wolfe et al., 1999, 2000b). This consistency may perhaps be due to preferential preservation of aquatic cellulose as compared to other organic compounds due to rapid sedimentation and burial (Edwards, 1993). Alternatively, high C/N ratios in aquatic organic matter have been documented for cellulose-producing green algae such as *Botryococcus* ($C/N \approx 36$) (Street-Perron et al., 1997). In other cases, high C/N ratios may result from lake waters that are nitrogen deficient (Talbot & Lærdal, 2000) or may be due to diagenetic effects on organic matter that originally derived from aquatic sources (Meyers & Ishiwatari, 1993; Tyson, 1995). Hydrogen indices can serve as an additional test of an aquatic source for sedimentary organic matter (Talbot & Livingstone, 1989; Talbot & Lærdal, 2000).

Parallel time-series trends between bulk organic carbon isotope ($\delta^{13}C_{org}$) and cellulose carbon isotope ($\delta^{13}C_{cell}$) profiles may indicate carbon uptake from the same source (i.e. DIC) and can provide further indirect support for an aquatic origin of cellulose. Conversely, stratigraphic variation in the isotopic difference between $\delta^{13}C_{org}$ and $\delta^{13}C_{cell}$ may be due to variable terrestrial contribution (Wolfe et al., 1996). However, these empirical relationships can be complicated by the lower sensitivity of bulk organic matter to fluctuations in

DIC $\delta^{13}C$, as well as temporal changes in bulk organic matter preservation (Edwards & McAndrews, 1989).

Cellulose-water oxygen isotope fractionation

Both laboratory and field studies have been conducted to investigate the relationship between the oxygen isotope composition of aquatic cellulose and the oxygen isotope composition of the water in which the plants or algae grew (Epstein et al., 1977; DeNiro & Epstein, 1981; Sternberg et al., 1984, 1986; Edwards et al., 1985; Yakir & DeNiro, 1990; Sauer et al., 2001b; Abbott et al., 2000). Many of these data indicate that the oxygen isotope fractionation between cellulose and water is nearly constant, being independent of the oxygen isotope composition of CO_2, the plant species, the water temperature, and the photosynthetic mode of the organism. Reported cellulose-water oxygen isotope fractionation factors are mostly within the range of 1.025 to 1.029 for most aquatic plant/algae species in which both the water and cellulose have been measured directly (Table I).

Two primary models have been proposed to account for the constant cellulose-water oxygen isotope enrichment factor (see reviews by Sternberg, 1989b and Yakir, 1992). Epstein et al. (1977) suggested that during cellulose synthesis, oxygen is incorporated from dissolved CO_2 and H_2O (which are in isotopic equilibrium) in a 1:1 ratio. As a result, 2/3 of the oxygen in cellulose is derived directly from dissolved CO_2 enriched in ^{18}O relative to the plant water by about 41‰, according to an oxygen isotope fractionation factor of 1.0412 between CO_2 and H_2O at 25 °C (thus $2/3 \times 41 \approx 27$‰). As discussed by Yakir (1992), however, there are several difficulties with this theory including: 1) oxygen incorporated from water is lost during subsequent metabolic reactions, 2) the isotopic relationship is consistent in plants that do not consume CO_2 (heterotrophic metabolism), and 3) the isotopic effect associated with CO_2 equilibration with water is highly sensitive to temperature, yet no clear temperature-dependent isotope effect has been demonstrated between water and cellulose.

The second alternative model favoured by most workers suggests that the oxygen isotope composition of plant cellulose is determined by the carbonyl hydration reaction which occurs during cellulose synthesis (DeNiro & Epstein, 1981). According to this theory, carbonyl oxygen atoms exchange with water in an equilibrium reaction that is apparently insensitive to temperature. Experiments analyzing oxygen isotope exchange between the carbonyl oxygen of acetone and water across a temperature range of 15 to 35 °C resulted in fractionation factors ranging from 1.025 to 1.030, similar to those observed between cellulose and water (Sternberg & DeNiro, 1983).

Prior to 1998, the majority of field studies examining cellulose-water oxygen isotope fractionation were conducted in temperate aquatic environments (Table I). Recent calibration work by Beuning & Anderson (in review) from samples collected in tropical East African lakes (also shown in Table I) suggests a lower mean fractionation factor (1.025 ± 0.003) than samples from temperate freshwater environments (1.027 ± 0.003). This difference could result from sampling of ^{18}O-enriched water at the end of the dry season, but only newly emerged leaves were used in the analyses. In addition, samples from large lake systems with minimal seasonal fluctuations in lake water $\delta^{18}O$ also showed

Table I. Published values for $\alpha_{cell\text{-}water}$. Marine field values from DeNiro & Epstein (1981) represent ranges based on winter and summer $\delta^{18}O$ values for the water. Values from Sternberg et al. (1984) were estimated from Figure 1. Values from Sauer et al. (2001b) are adjusted assuming a constant $\alpha_{cell\text{-}water}$ of 1.028 in aquarium studies of cultured mosses under controlled conditions.

Field (F) or Laboratory (L)		T (°C)	$\alpha_{cell\text{-}water}$	Reference
Freshwater vascular plants				
Ceratopteris sp.	L	20	1.0292	DeNiro & Epstein (1981)
Cryptocoryne sp.	L	25	1.0289	
Hygrophila polysperma	L	20	1.0266	
	L	25	1.0273	
Ludwigia natans	L	15	1.0262	
	L	20	1.0258	
	L	25	1.0265	
Nymphoides aquaticum (roots)	L	20	1.0289	
Nymphoides aquaticum (submerged leaves)	L	20	1.0285	
Nymphoides aquaticum (floating leaves)	L	20	1.0289	
Synnema triflorum	L	15	1.0267	
	L	20	1.0262	
Vallisneria spiralis	L	25	1.0289	
Isoetes howellii	L		1.0290	Sternberg et al. (1984)
Ranunculus aquatilis	L		1.0260	
Chara contraria	L		1.0280	
Vallisneria spiralis	L	25	1.0285	
Ludwigia natans	L	15	1.0255	
	L	25	1.0265	
Ceratopteris sp.	L	20	1.0255	
Hydgrophila polysperma	L	20	1.0290	
		25	1.0255	
Synnema triflorum	L	15	1.0260	
		20	1.0255	
Isoetes bolanderi	F		1.0270	
Chara contraria	F		1.0265	
Chara longipedunculata	F		1.0240	
Fontinalis antipyretica	F		1.0260	
Eleocharis acicularis	L		1.0300	
Ranunculus aquatilis	F		1.0286	
Sphagnum sp.	F		1.0253	Aucour et al. (1993)
Nymphaea sp.	F		1.0250	Aucour et al. (1996)
green algae	F		1.0294	Abbott et al. (2000)
Myriophyllum	F		1.0287	
submerged aquatic moss	F		1.0287	Sauer et al. (2001b)
	F		1.0263	
	F		1.0278	
	F		1.0285	
	F		1.0249	
	F		1.0265	

Table 1. Published values for $\alpha_{cell\text{-}water}$. Marine field values from DeNiro & Epstein (1981) represent ranges based on winter and summer $\delta^{18}O$ values for the water. Values from Sternberg et al. (1984) were estimated from Figure 1. Values from Sauer et al. (2001b) are adjusted assuming a constant $\alpha_{cell\text{-}water}$ of 1.028 in aquarium studies of cultured mosses under controlled conditions (continued).

Field (F) or Laboratory (L)	T (°C)	$\alpha_{cell\text{-}water}$	Reference
	F	1.0277	
	F	1.0290	
	F	1.0236	
	F	1.0280	
	F	1.0250	
	F	1.0293	
	F	1.0274	
	F	1.0276	
	F	1.0292	
	F	1.0286	
	F	1.0292	
	F	1.0261	
	F	1.0253	
	F	1.0287	
	F	1.0269	
	F	1.0276	
	F	1.0334	
	F	1.0238	
	F	1.0284	
	F	1.0287	
	F	1.0297	
	F	1.0298	
	F	1.0299	
	F	1.0313	
	F	1.0319	
	F	1.0300	
	F	1.0312	
	F	1.0316	
	F	1.0306	
	F	1.0301	
Eicchornia	F	1.0260	Beuning & Anderson (in review)
Eicchornia - leaves	F	1.0255	
Ceratophyllum demersum	F	1.0234	
KRB 105 (Unknown)	F	1.0225	
Najas cf. *horrida*	F	1.0268	
KRB 112 (Unknown)	F	1.0247	
Ceratophyllum sp.	F	1.0248	
Lemna trisulca	F	1.0256	
Botryococcus braunii	L	1.0249	
Characeae (cf. *Chara*)	F	1.0246	
Nymphaea-leaves only	F	1.0253	
Nymphaea-flower	F	1.0247	

Table I. Published values for $\alpha_{cell\text{-}water}$. Marine field values from DeNiro & Epstein (1981) represent ranges based on winter and summer $\delta^{18}O$ values for the water. Values from Sternberg et al. (1984) were estimated from Figure 1. Values from Sauer et al. (2001b) are adjusted assuming a constant $\alpha_{cell\text{-}water}$ of 1.028 in aquarium studies of cultured mosses under controlled conditions (continued).

Field (F) or Laboratory (L)	T (°C)	$\alpha_{cell\text{-}water}$	Reference
Nymphaea-stem only	F	1.0251	
Nymphaea-leaves & stem	F	1.0253	
Najas	F	1.0221	
Characeae (cf. *Chara*)	F	1.0270	
KRB 109 - leaves	F	1.0264	
Marine aquatic plants and algae			
Turtle grass	F	1.0272	Epstein et al. (1977)
Phyllospadix	F	1.0280	
Eurasian water milfoil	F	1.0276	
Thalassia testudinum	F	1.0276	DeNiro & Epstein (1981)
Macrocystis sp.	F	1.0293–1.0280	
Laminaria sp.	F	1.0283–1.0272	
Gelidium robustum	F	1.0291–1.0285	
Macrocystis sp.	F	1.0270–1.0264	
Ulva sp.	F	1.0254–1.0248	
Phyllospadix torreyi	F	1.0290–1.0284	
Zostera marina	F	1.0285–1.0279	
Ascophyllum nodosum	F	1.0299–1.0263	
Chondria tenuissima	F	1.0290–1.0254	
Chondrus crispus	F	1.0304–1.0268	
Fucus vesiculosus	F	1.0306–1.0270	
Laminaria agardhii	F	1.0303–1.0267	
Polysiphonia nigrescens	F	1.0304–1.0268	
Ulva lactuca	F	1.0290–1.0254	
Thalassia sp.	F	1.0316–1.0280	

reduced cellulose-water isotopic fractionation. While these results suggest a possible small temperature-dependent effect on the fractionation factor between cellulose and water, clearly, additional field studies, particularly in tropical environments, are required to clarify this discrepancy (Beuning & Anderson, in review).

Assuming a constant oxygen isotope fractionation between cellulose and water, $\delta^{18}O$ analysis of the cellulose component of surface sediment samples may be consistent with contemporary water and plant samples, as has been shown for Lago Taypi Chaka Kkota, Bolivia (e.g. Abbott et al, 2000). This lake is characterized by suppressed seasonal isotopic variability due to perennial through-flowing conditions and thus single-episode sampling of sediments, plants and lake water, which frequently forms the basis for "calibration", produced coherent results. Indeed, caution must be exercised in evaluating water and sediment data of strongly differing temporal representation. For example, lakes near boreal treeline in central Siberia are susceptible to strong seasonal isotopic variation. As a result, single-episode water and surface sediment sampling demonstrated that the hydrologic conditions

inferred from the surface sediments at most sites were systematically offset from those prevailing at the time of sampling due to the influence of snowmelt on lake water isotopic composition (see Wolfe & Edwards, 1997).

Applications

Holocene water and carbon balance record of treeline lakes, central Canada

Reconstruction of lake water $\delta^{18}O$ ($\delta^{18}O_{lw}$) histories from analysis of fine grained cellulose at small treeline lakes in central Canada has provided key insight into shifting water balance and its influence on watershed carbon cycling during the Holocene (MacDonald et al., 1993; Wolfe et al., 1996). In this region, terrestrial vegetation change following local deglaciation around 9000 ^{14}C yr B.P. was characterized by the advance and retreat of boreal treeline, in response to shifts in the mean summer position of the Arctic frontal zone (Dyke & Prest, 1987; MacDonald et al., 1993). Abrupt changes from dwarf shrub tundra to *Picea mariana* forest-tundra occurred at about 5000 ^{14}C yr B.P. (Fig. 6), as the frontal zone moved northward. Minor local fluctuations in treeline position or forest density occurred during the subsequent 2000 years, followed by return to the modern dwarf shrub tundra vegetation after 3000 ^{14}C yr B.P.

Cellulose isotope records from Queen's Lake (MacDonald et al., 1993), located 25 km north of the forest-tundra zone, and Toronto Lake (Wolfe et al., 1996), situated at the transition between forest-tundra and tundra, show shifts to lower $\delta^{18}O_{lw}$ values during the mid-Holocene (Fig. 6), reflecting decreased evaporative ^{18}O-enrichment with a northward shift in the Arctic front. An isotope mass-balance model, based primarily on the Queen's Lake $\delta^{18}O_{lw}$ record, suggests relative humidity may have increased by 10-15% overall during this interval (Edwards et al., 1996). High-resolution analysis of the Toronto Lake sediments indicates century-scale correspondence between increasingly moist conditions and forest expansion (Fig. 6; Wolfe et al., 1996). The hydrologic sensitivity of Toronto Lake may be largely a function of the lake's complex drainage basin. Under present climatic conditions, the two subcatchments providing inflow to Toronto Lake have markedly different hydrological budgets. The larger of the two subcatchments (ca. 2100 ha) yields continuous outflow during the thaw season, whereas the smaller subcatchment (ca. 650 ha) apparently discharges only intermittently following spring melt. Abrupt changes in the size of the contributing drainage basin area, in response to changes in moisture conditions in the past, appear to have strongly influenced lake water residence time and degree of evaporative enrichment at Toronto Lake. In contrast, Queen's Lake drains a considerably smaller catchment than Toronto Lake and thus contains a $\delta^{18}O_{lw}$ record that is largely dependent on the hydrologic sensitivity of this single lake, which has apparently remained closed for most of the Holocene.

The forest-tundra interval at Queen's Lake and Toronto Lake was also marked by changes in carbon balance. Increased organic content (i.e., high loss-on-ignition) and diatom valve concentration clearly indicate that lake productivity increased during this interval (MacDonald et al., 1993; Pienitz et al., 1999). Increasing $\delta^{13}C_{cell}$ values during the mid-Holocene are likely caused by this elevated lake productivity, through photosynthetically-driven ^{13}C-enrichment of dissolved inorganic carbon (DIC) and decreased cellulose-DIC isotope fractionation. However, at various times during the Holocene, contemporaneous

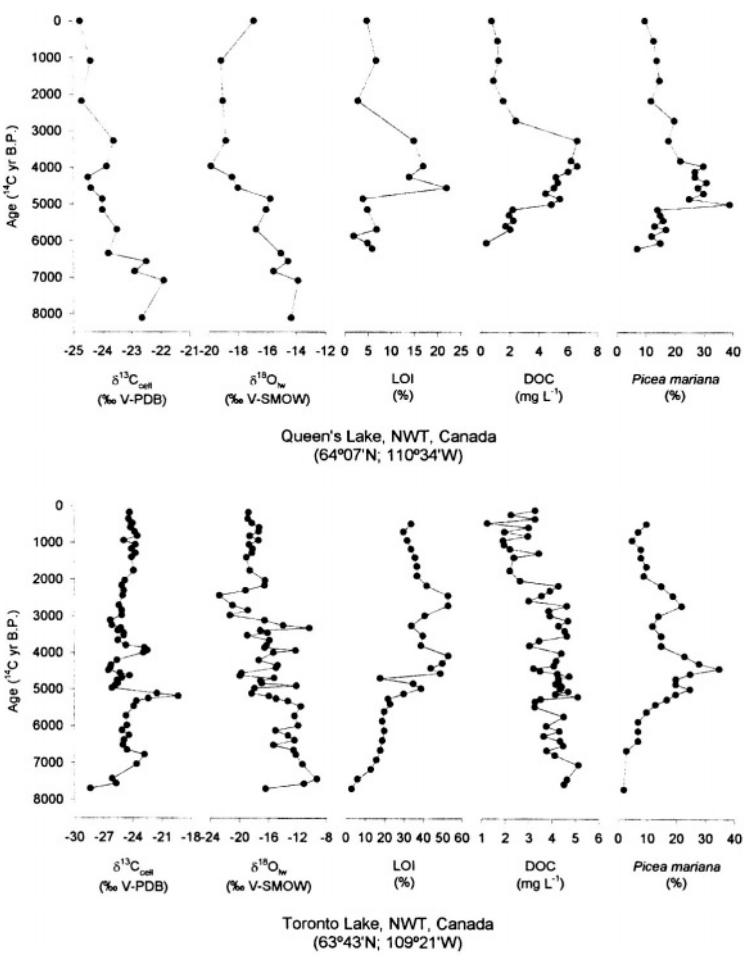


Figure 6. Stratigraphic profiles of cellulose carbon isotope composition ($\delta^{13}C_{cell}$), cellulose-inferred lake water $\delta^{18}O$ composition ($\delta^{18}O_{lw}$) calculated using a cellulose-water fractionation factor of 1.028, loss-on-ignition (LOI), diatom-inferred dissolved organic carbon concentration (DOC), and *Picea mariana* pollen concentration for Queen's Lake and Toronto Lake, Northwest Territories, Canada (from MacDonald et al., 1993; Wolfe et al., 1996; Pienitz et al., 1999).

rapid lake water through-flow and supply of soil-derived ^{13}C-depleted $CO_{2(aq)}$ have probably played an important role in offsetting and, in some cases, completely masking these isotopic enrichment signatures (i.e., compare LOI with $\delta^{13}C_{cell}$ at 3500 ^{14}C yr B.P. at Queen's Lake; at 5100, 4500, 4000, 2700 ^{14}C yr B.P. at Toronto Lake; Fig. 6). Increasingly moist conditions combined with developing soils and forest-tundra vegetation during the mid-Holocene are also reflected by the high diatom-inferred dissolved organic carbon (DOC) concentrations indicating increased humus input (Fig. 6; Pienitz et al., 1999). At Toronto Lake, the "noisier" DOC record is likely related to the hydrologic variabilty at this

site, whereas the apparent high values during the early Holocene are considered unreliable due to a "no-analog" application of the diatom-based transfer function (see Pienitz et al., 1999).

Postglacial record of the isotopic composition of precipitation in the Great Lakes region

In lake basins for which evaporation is a small component of the water balance (and where the primary inputs of water derive from precipitation or inflow that has experienced little evaporative evolution), sediment-inferred lake water $\delta^{18}O$ and $\delta^{2}H$ histories may reflect the mean annual isotope composition of precipitation ($\delta^{18}O_p$; $\delta^{2}H_p$). This parameter is frequently used as a tracer of past temperature change as well as evidence for changes in moisture sources, seasonal distribution of precipitation, and other aspects of air mass circulation.

In the Great Lakes region of North America, recent oxygen and hydrogen isotope studies of lake sediment cellulose and lake sediment kerogen, respectively, in addition to $\delta^{18}O$ and $\delta^{2}H$ analysis of fossil wood cellulose, have resulted in a largely consistent pattern of shifting isotopic composition of post-glacial precipitation. The initial reconstruction was based on isotopic evaluation of fossil wood cellulose preserved in a kettle-fill sequence near Brampton, Ontario (Edwards & Fritz, 1986). A semi-empirical model was used to separate humidity-dependent isotopic enrichment of leaf water during evapotranspiration from the primary isotopic signature of water taken up by the trees, presumably reflecting the local mean annual isotopic composition of precipitation. Calibration of the model using modern trees permitted quantitative reconstruction of both $\delta^{18}O_p$ as well as relative humidity during the growth season for the past 11,500 ^{14}C years (Fig. 7a).

Oxygen isotope analysis of fine-grained cellulose in sediments underlying Hamilton Harbour, a bay at the western end of Lake Ontario, has verified and further supplemented the later pan of the regional $\delta^{18}O_p$ record from about 8000 ^{14}C yr B.P. to present (Duthie et al., 1996). Comparison of the Hamilton Harbour cellulose-inferred lake water $\delta^{18}O$ ($\delta^{18}O_{lw}$) record with the reconstructed precipitation $\delta^{18}O$ history from the Brampton site shows that lake water $\delta^{18}O$ was primarily controlled by the changing isotopic composition of precipitation falling in the region (Fig. 7b). The only strong evidence of local hydrologic overprinting is the marked positive offset of $\delta^{18}O_{lw}$ at the base of the profile, likely due to evaporative enrichment when the harbour was isolated from Lake Ontario. Rising water level in Lake Ontario and confluence of harbour and lake water is reflected by reduced evaporative enrichment and subsequent decrease in Hamilton Harbour $\delta^{18}O_{lw}$ at about 7000 ^{14}C yr B.P. This major hydrologic event is also clearly demarcated in the diatom and cellulose carbon isotope records (Duthie et al., 1996; Wolfe et al., 2000c).

At Austin Lake, southwestern Michigan, $\delta^{2}H$ analysis of sediment kerogen has been used to reconstruct late Glacial and Holocene lake water $\delta^{2}H$ ($\delta^{2}H_{lw}$) history (Fig. 7c; Krishnamurthy et al., 1995). The kerogen-inferred $\delta^{2}H_{lw}$ record was derived from extending the empirical relationship between surface-sediment kerogen $\delta^{2}H$ and lake-recharged groundwater $\delta^{2}H$ down-core. The relationship closely resembles the hydrogen isotope fractionation between non-exchangeable hydrogen in cellulose and ambient water reported by Yapp & Epstein (1982). Notably, groundwater $\delta^{2}H$ in this region is similar to local $\delta^{2}H_p$ so as a first-order approximation, Krishnamurthy et al. (1995) assumed the kerogen-inferred $\delta^{2}H_{lw}$ record was primarily a reflection of the $\delta^{2}H_p$ history. This interpretation

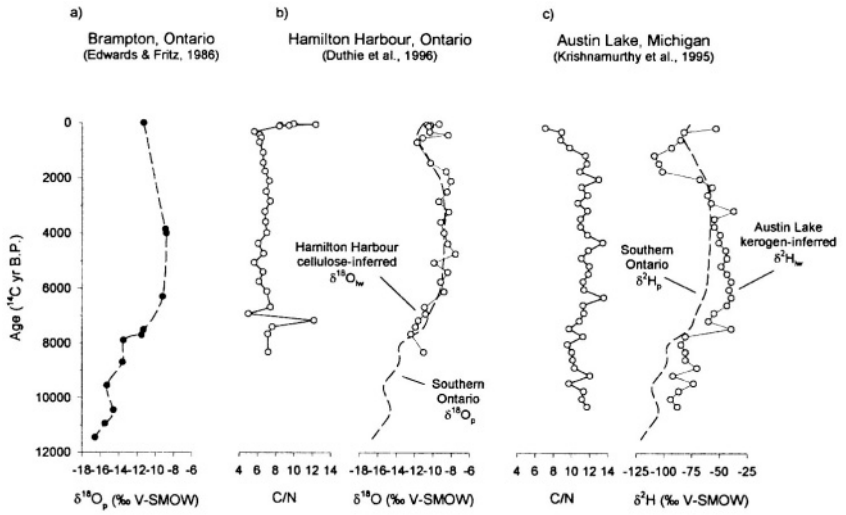


Figure 7. a) Mean annual oxygen isotope composition of precipitation ($\delta^{18}O_p$) history derived from isotope analysis of fossil wood cellulose near Brampton, Ontario. b) Hamilton Harbour bulk organic C/N ratio and cellulose-inferred lake water $\delta^{18}O$ ($\delta^{18}O_{lw}$) profiles. Also shown is the $\delta^{18}O_p$ record for southern Ontario from a) modified slightly during the late Holocene to account for the newer data from Hamilton Harbour. Low C/N ratios indicate that the organic matter is derived predominantly from aquatic sources (cf. Meyers & Lallier-Verges, 1999). The abrupt increase in C/N ratios at the top of the core is likely related to watershed deforestation and increased terrestrial input of organic matter, although this does not seem to have strongly influenced the cellulose $\delta^{18}O$ record. Notably, $\delta^{18}O_{lw}$ (calculated using a cellulose-water fractionation factor of 1.028 ± 0.001) in the uppermost sediment sample (-9.4 ± 1.0‰) is similar to surface water isotope data sampled in May, 1994 (-8.3 to -7.8‰; Harvey et al., 1997). c) Austin Lake bulk organic C/N ratio and kerogen-inferred lake water δ^2H (δ^2H_{lw}) history calculated using a kerogen-water fractionation factor of 0.9725. The southern Ontario δ^2H_p record is also shown, calculated from b) using the local meteoric water line for Simcoe ($\delta^2H = 7.92\ \delta^{18}O + 10.53$) reported in Fritz et al. (1987). The "latitude effect" is likely responsible for the positive offset of Austin Lake δ^2H_{lw} from Brampton δ^2H_p for most of the profile (see Fig. 1; also Rozanski et al., 1993). Further work is needed to evaluate the large δ^2H_{lw} oscillation during the late Holocene.

is strongly supported by correlative trends in the records from Brampton and Hamilton Harbour (Fig. 7a, b).The lower parts of these profiles, in particular, show striking agreement and are characterized by low values during the late-Glacial and early Holocene rising to maximum values in the mid-Holocene.

The record of post-glacial isotopic composition of precipitation in the Great Lakes region is likely a reflection of both changes in temperature and air mass circulation (Edwards & Fritz, 1986; Krishnamurthy et al., 1995; Edwards et al., 1996). Increasing $\delta^{18}O_p$ and δ^2H_p values from the post-Glacial to the mid-Holocene appear to result from progressive post-glacial warming as influence of Arctic air diminished and warm, moist, ^{18}O-enriched air masses from the Gulf of Mexico became increasingly prevalent. Superimposed on this meridional fluctuation in atmospheric circulation is a shorter-term episode of enhanced zonal circulation between 7500 and 6000 ^{14}C yr B.P. that accounts for a lag between rising temperature and humidity (Bryson & Wendland, 1967; Edwards & Fritz, 1986; Dean et al., 1996; Edwards et al., 1996). Increased penetration of warm, dry Pacific air into the

continental interior during the summer months likely resulted in increased lake water evaporation which may partly account for the abrupt ^{2}H-enrichment at about 7000 ^{14}C yr B.P. in the Austin Lake record. The end of the warm mid-Holocene is clearly shown by the shift to lower Austin Lake $\delta^{2}H_{lw}$ and Hamilton Harbour $\delta^{18}O_{lw}$ values at about 2000 ^{14}C yr B.P., reflecting decreased influence of air masses from the Gulf of Mexico, and is consistent with other paleoclimatic records from southern Ontario (see Edwards et al., 1996). A subsequent return to warmer conditions is suggested by increasing Austin Lake $\delta^{2}H_{lw}$ and Hamilton Harbour $\delta^{18}O_{lw}$ values after 1000 ^{14}C yr B.P.

Future research directions

Isotope analysis of lake sediment cellulose has undergone rapid growth over the last decade as a useful approach for paleohydrologic and paleoclimatic reconstruction. The need remains, however, for further research into key areas of analysis and application to refine this technique and to improve upon its contribution to paleolimnology. Specific areas to be addressed are outlined below.

Sample preparation and analytical techniques

Oxygen isotope analysis of lake sediment cellulose is currently a labour-intensive process, requiring off-line CO_2 gas purification prior to mass spectrometric analysis. However, recent development of successful on-line techniques (i.e., CF-IRMS) for $\delta^{18}O$ analysis of organic compounds (e.g., Farquhar et al., 1997; Saurer et al., 1998) suggests that similar methods may be utilized to expedite lake sediment cellulose $\delta^{18}O$ analysis. Preliminary analyses using CF-IRMS at the UW-EIL suggest that development of a viable technique requires the removal of refractory material from the cellulose residue. Modifications to the sample preparation technique are currently in development including flotation with sodium polytungstate to separate cellulose from mineral detritus. Improvements in analytical capabilities will increase the cost-effectiveness of studies and may allow for very small samples to be analyzed including cellulose derived from identifiable aquatic remains in sediment cores. In addition, multiple analysis of several individual samples will warrant more comprehensive evaluation of differences in sample reproducibility (from site to site and also stratigraphically), which may also potentially reveal information characteristic of a lake's hydrologic setting and variability (see Wolfe et al., 2000b).

Investigation of cellulose-water fractionation

Recent work by Beuning & Anderson (in review) clearly points to the need for more studies examining the oxygen isotope relationship between aquatic cellulose and ambient water under varied conditions. While applications of a constant fractionation factor in the past have proven to be a useful first-order approximation, this critical assumption requires further testing. Additional laboratory-based studies are in progress, where the effects of key parameters (e.g. temperature, species) on the oxygen isotope composition of important cellulose-producing aquatic plants may be re-evaluated (Beuning, unpublished data). Greater understanding of the cellulose-water $\delta^{18}O$ relationship in natural settings

would also benefit from comprehensive field surveys involving multiple lake water samples to characterize intra-annual lake water isotopic composition and variability, sediment trap collections to measure aquatic cellulose $\delta^{18}O$ *in situ,* and corresponding surface-sediment samples for lake sediment cellulose $\delta^{18}O$ determination.

Characterization of sediment cellulose origins

Organic petrography needs to be explored as a potentially useful complementary tool for evaluating the significance of terrestrial cellulose contributions to the fine-grained sediment component of lake sediments. This and other sediment identification techniques (e.g., scanning electron microscopy) may also prove useful for determining whether the lake sediment cellulose is derived from varied aquatic sources, with species-specific oxygen isotope fractionation factors.

Quantitative applications using multiple isotopic archives

Interpretation of cellulose-interred lake water $\delta^{18}O$ records would benefit from coupled estimation of lake water $\delta^{2}H$ in order to clearly decipher shifting isotopic composition of precipitation from changes in water balance (see Fig. 1). Exploratory paleolimnological reconstructions at Austin Lake demonstrate that further studies on the hydrogen isotope composition of kerogen and its isotopic relationship with ambient water is an especially promising new research direction (Krishnamurthy et al., 1995; also see Fig. 7). "Mapping" temporal shifts in lake water isotopic composition in two-dimensional $\delta^{18}O$-$\delta^{2}H$ space would also provide a more solid foundation for quantitative reconstructions. For example, stratigraphic changes that occur along a well-defined local evaporation line may be used to determine shifting percentages of lake water evaporative loss, as in contemporary hydrologic investigations (e.g., Gibson et al., 1993).

Coupled carbon and oxygen isotope analyses of carbonate and organic fractions should also be further exploited as a paleolimnological approach as these studies provide strong potential for quantitative reconstruction of past lake water temperature (Padden, 1996; Padden et al., 1996; Wolfe et al., 2000a).

Summary

Systematic variations occur in the isotopic composition of water as it passes through the hydrologic cycle due to fractionation effects that separate the common, light stable isotopomers from the rare, heavy isotopomers. The isotopic composition of lake water captures a time-integrated reflection of these processes, which are strongly influenced by climatic and hydrologic factors. Aquatic cellulose readily incorporates the oxygen isotope composition of lake water and this signature is preserved in lake sediment stratigraphic records. Hydrologic as well as lake nutrient balance information may additionally be contained in profiles of lake sediment cellulose carbon isotope composition. Although case studies presented here focus on qualitative interpretation of the isotope profiles, results from both cellulose carbon and oxygen isotope analyses also offer the potential for quantitative recovery of paleohydrologic and paleoclimatic information that may not necessarily

be readily attainable from other conventional sources of proxy data (e.g., Edwards & McAndrews, 1989; Edwards et al., 1996; Wolfe et al., 2000a, c). We emphasize, however, that interpretation is most effectively constrained within the context of a multidisciplinary approach (e.g., Abbott et al., 2000). High priority is currently focused on simplification of the analytical procedure in order to foster more routine incorporation of cellulose-isotope analyses in paleolimnological investigations.

Acknowledgements

This manuscript was prepared while BBW was supported by a Natural Sciences and Engineering Research Council of Canada postdoctoral fellowship. We thank R. Pienitz for providing Queen's Lake and Toronto Lake diatom-inferred DOC data and R.V. Krishnamurthy for Austin Lake bulk organic C/N and kerogen δ^2H data. Enthusiastic support for isotope paleoenvironmental studies at the University of Waterloo by the staff of the Environmental Isotope Laboratory is greatly appreciated.

References

Abbott, M. B., B. B. Wolfe, R. Aravena, A. P. Wolfe & G. O. Seltzer, 2000. Holocene hydrological reconstructions from stable isotopes and paleolimnology, Cordillera Real, Bolivia. Quat. Sci. Rev. 19: 1801–1820.

Aucour,A. M., C. Hillaire-Marcel & R. Bonnefille, 1993. A 30,000 year record of ^{13}C and ^{18}O changes in organic matter from an equatorial peatbog. In Swart, P. K., K. C. Lohmann, J. McKenzie & S. Savin (eds.) Climate Change in Continental Isotopic Records. Geophysical Monograph 78, American Geophysical Union, Washington: 343–351.

Aucour, A. M., C. Hillaire-Marcel & R. Bonnefille, 1996. Oxygen isotopes in cellulose from modern and Quaternary intertropical peatbogs: implications for palaeohydrology. Chem. Geol. 129: 341–359.

Beuning, K. R. M. & W. T. Anderson, in review. Calibration of the cellulose-water oxygen isotope fractionation factor in aquatic algae and plants of tropical East Africa, in review.

Beuning, K. R. M., K. Kelts, E. Ito & T. C. Johnson, 1997. Paleohydrology of Lake Victoria, East Africa, inferred from $^{18}O/^{16}O$ ratios in sediment cellulose. Geology 25: 1083–1086.

Boutton, T. W., 1991a. Stable carbon isotope ratios of natural materials: I. Sample preparation and mass spectrometric analysis. In Coleman, D. C. & B. Fry (eds.) Carbon Isotope Techniques. Elsevier, New York: 155–171.

Boutton, T. W., 1991b. Stable carbon isotope ratios of natural materials: II. Atmospheric, terrestrial, marine, and freshwater environments. In Coleman, D. C. & B. Fry (eds.) Carbon Isotope Techniques. Elsevier, New York: 173–185.

Boutton, T. W., W. W. Wong, D. L. Hachey, L. S. Lee, M. P. Cabrera & P. D. Klein, 1983. Comparison of quartz and pyrex tubes for combustion of organic samples for stable carbon isotope analysis. Analyt. Chem. 55: 1832–1833.

Bryson, R. A. & W. M. Wendland, 1967. Tentative climatic patterns for some late-glacial and post-glacial episodes in central North America. In Mayer-Oakes, W. J. (ed.) Life, Land and Water. University of Manitoba Press, Winnipeg: 271–298.

Buhay, W. M., 1997. Inferring precipitation isotopic compositions from lake sediment organics and pore water: Workshop on water and climate studies in Canada using isotope tracers: Past, present, future. University of Waterloo, Waterloo.

Buhay, W. M. & R. N. Betcher, 1998. Paleohydrologic implications of ^{18}O enriched Lake Agassiz water. J. Paleolim. 19: 285–296.

Chapman, V. J., 1962. The Algae. Macmillan & Co., London, 472 pp.

Cole, J. J., N. F. Caraco, G. W. Kling & T. K. Kratz, 1994. Carbon dioxide supersaturation in the surface waters of lakes. Science 265: 1568–1570.

Craig, H., 1961. Isotopic variations in meteoric waters. Science 133: 1702–1703.

Craig, H. & L. I. Gordon, 1965. Deuterium and oxygen-18 variations in the ocean and marine atmosphere. In Tongiorgi, E. (ed.) Stable Isotopes in Oceanographic Studies and Paleotemperatures. Cons. Naz. Rich. Lab. Geol. Nucl., Pisa: 9–130.

Dansgaard, W., 1964. Stable isotopes in precipitation. Tellus 16: 436–468.

Dean, W. E., T. S. Ahlbrandt, R. Y. Anderson & J. P. Bradbury, 1996. Regional aridity in North America during the middle Holocene. The Holocene 6: 145–155.

De Leeuw, J. W. & C. Largeau, 1993. A review of macromolecular organic compounds that comprise living organisms and their role in kerogen, coal, and petroleum formation. In Engel, M. H. & S. A. Macko (eds.) Organic Geochemistry: Principles and Applications. Plenum Press, New York: 23–72.

DeNiro, M. J. & S. Epstein, 1981. Isotopic composition of cellulose from aquatic organisms. Geoch. Cosmoch. Acta. 45: 1885–1894.

Duthie, H. C., J.-R. Yang, T. W. D. Edwards, B. B. Wolfe & B. G. Warner, 1996. Hamilton Harbour, Ontario: 8300 years of limnological and environmental change inferred from microfossil and isotopic analyses. J. Paleolim. 15: 79–97.

Edwards, T. W. D., 1993. Interpreting past climate from stable isotopes in continental organic matter. In Swart, P. K , K. C. Lohmann, J. McKenzie & S. Savin (eds.) Climate Change in Continental Isotopic Records. Geophysical Monograph 78, American Geophysical Union, Washington: 333–341.

Edwards, T. W. D., R. O. Aravena, P. Fritz & A. V. Morgan, 1985. Interpreting paleoclimate from ^{18}O and ^{2}H in plant cellulose: comparison with evidence from fossil insects and relict permafrost in southwestern Ontario. Can. J. Earth Sci. 22: 1720–1726.

Edwards, T. W. D., W. M. Buhay, R. J. Elgood & H. B. Jiang, 1994. An improved nickel-tube pyrolysis method for oxygen isotope analysis of organic matter and water. Chem. Geol. (Iso. Geosci. Sect.) 114: 179–183.

Edwards, T. W. D., R. J. Elgood & B. B. Wolfe, 1997. Cellulose Extraction from Lake Sediments for $^{18}O/^{16}O$ and $^{13}C/^{12}C$ Analysis. Technical Procedure 28.0, Environmental Isotope Laboratory, Department of Earth Sciences, University of Waterloo, 4 pp.

Edwards, T. W. D. & P. Fritz, 1986. Assessing meteoric water composition and relative humidity from ^{18}O and ^{2}H in wood cellulose: Paleoclimatic implications for southern Ontario, Canada. Appl. Geochem. 1: 715–723.

Edwards, T. W. D. & P. Fritz, 1988. Stable-isotope paleoclimate records for southern Ontario. Canada: comparison of results from marl and wood. Can. J. Earth Sci. 25: 1397–1406.

Edwards, T. W. D. & J. H. McAndrews, 1989. Paleohydrology of a Canadian Shield lake inferred from ^{18}O in sediment cellulose. Can. J. Earth Sci. 26: 1850–1859.

Edwards, T. W. D., B. B. Wolfe & G. M. MacDonald, 1996. Influence of changing atmospheric circulation on precipitation $\delta^{18}O$-temperature relations in Canada during the Holocene. Quat. Res. 46: 211–218.

Elgood, R. J., B. B. Wolfe, W. M. Buhay & T. W. D. Edwards, 1997. $\delta^{18}O$ in Organic Matter and Water by Nickel-tube Pyrolysis. Technical Procedure 29.0, Environmental Isotope Laboratory, Department of Earth Sciences, University of Waterloo, 8 pp.

Epstein, S., P. Thompson & C. J. Yapp, 1977. Oxygen and hydrogen isotopic ratios in plant cellulose. Science 198: 1209–1215.

Farquhar, G. D., B. K. Henry & J. M. Styles, 1997. A rapid on-line technique for determination of oxygen isotope composition of nitrogen-containing organic matter and water. Rapid Commun. Mass Spectrom. 11: 1554–1560.

Gibson, J. J., T. W. D. Edwards, G. G. Bursey & T. D. Prowse, 1993. Estimating evaporation using stable isotopes: Quantitative results and sensitivity analysis for two catchments in northern Canada. Nord. Hydrol. 24: 79–94.

Gonfiantini, R., 1986. Environmental isotopes in lake studies. In Fritz, P. & J. C. Fontes (eds.) Handbook of Environmental Isotope Geochemistry, Volume 2, The Terrestrial Environment, B. Elsevier, Amsterdam: 113–168.

Green, J. W., 1963. Wood cellulose. In Whistler, R. L. (ed.) Methods in Carbohydrate Chemistry, Vol. III. Academic Press, New York: 9–20.

Harvey, F. E., S. K. Frape & R. J. Drimmie, 1997. Isotopic variations in Hamilton Harbour water as an indicator of Lake Ontario exchange flow. J. Great Lakes Res. 23: 169–176.

Heemskerk, A. R. & P. Dieboldt, 1994. Breakseal Organic Combustion. Technical Procedure 22.0, Environmental Isotope Laboratory, Department of Earth Sciences, University of Waterloo, 11 pp.

Herczeg, A. L. & R. G. Fairbanks, 1987. Anomalous carbon isotope fractionation between atmospheric CO_2 and dissolved inorganic carbon induced by intense photosynthesis. Geoch. Cosmo. Acta. 51: 895–899.

Herczeg, A. L., 1988. Early diagenesis of organic matter in lake sediments: a stable carbon isotope study of pore waters. Chem. Geol. 72: 199–209.

Kreger, D. R., 1962. Cell walls. In Lewin, R. A. (ed.) The Physiology and Biochemistry of Algae. Academic Press, New York: 315–335.

Krishnamurthy, R. V., K. A. Syrup, M. Baskaran & A. Long, 1995. Late glacial climate record of midwestern United States from the hydrogen isotope ratio of lake organic matter. Nature 269: 1565–1567.

Lee, C., J. A. McKenzie & M. Sturm, 1987. Carbon isotope fractionation and changes in the flux and composition of particulate matter resulting from biological activity during a sediment trap experiment in Lake Greifen, Switzerland. Limnol. Oceanogr. 32: 83–96.

MacDonald, G. M., T. W. D. Edwards, K. A. Moser, R. Pienitz & J. P. Smol, 1993. Rapid response of treeline vegetation and lakes to past climate warming. Nature 361: 243–246.

McKenzie, J. A., 1985. Carbon isotopes and productivity in the lacustrine and marine environment. In Stumm, W. (ed.) Chemical Processes in Lakes. Wiley, Toronto: 99–118.

Meyers, P. A., 1997. Organic geochemical proxies of paleoceanographic, paleolimnologic, and paleoclimatic records. Org. Geochem. 27: 213–250.

Meyers, P. A. & R. Ishiwatari, 1993. The early diagenesis of organic matter in lacustrine sediments. In Engel, M. H. & S. A. Macko (eds.) Organic Geochemistry: Principles and Applications. Plenum Press, New York: 185–209.

Meyers, P. A. & E. Lallier-Vergès, 1999. Lacustrine sedimentary organic matter records of late Quaternary paleoclimates. J. Paleolim. 21: 345–372.

Motz, J.E., T. W. D. Edwards & W. M. Buhay, 1997. Use of nickel-tube pyrolysis for hydrogen-isotope analysis of water and other compounds. Chem. Geol. 140: 145–149.

Ott, E., H. M. Spurlin & M. W. Grafflin, 1954. Cellulose and Cellulose Derivatives. Part 1. Interscience, New York, 509 pp.

Padden, M. C., 1996. Holocene Paleohydrology of the Palliser Triangle from Isotope Studies of Lake Sediments. M.Sc. Thesis, University of Waterloo, Waterloo, 108 pp.

Padden, M.,T. W. D. Edwards & R. Vance, 1996. Temperature dependent oxygen and carbon isotope fractionation between carbonate and cellulose in lake sediments: Symposium on isotopes in water resources management. International Atomic Energy Agency, Vienna, 20–24 March 1995: 241–244.

Pienitz, R., J. P. Smol & G. M. MacDonald, 1999. Paleolimnologial reconstruction of Holocene climatic trends from two boreal treeline lakes. Northwest Territories, Canada. Arct. Ant. Alp. Res. 31: 82–93.

Prescott, G. W., 1968. The Algae: A Review. Houghton Mifflin Co., Boston, 436 pp.

Quay, P. D., S. R. Emerson, B. M. Quay & A. H. Devol, 1986. The carbon cycle for Luke Washington — a stable isotope study. Limnol. Oceanogr. 31: 596–611.

Rau, G., 1978. Carbon-13 depletion in a subalpine lake: Carbon flow implications. Science 201: 901–902.

Rozanski, K., L. Araguás-Araguás & R.Gonfiantini, 1993. Isotopic patterns in global precipitation. In Swart, P. K., J. A. McKenzie & K. C. Lohmann (eds.) Continental Isotopic Indicators of Climate. Geophysical Monograph 78, American Geophysical Union, Washington: 1–36.

Sauer, P. E., T. I. Eglinton, J. M. Hayes, A. Schimmelmann & A. L. Sessions, 2001a. Compound-specific D/H ratios of lipid biomarkers from sediments as a proxy for environmental and climatic conditions. Geoch. Cosmoch. Ada. 65: 213–222.

Sauer, P. E., G. H. Miller & J. T. Overpeck, 2001b. Oxygen isotope ratios of organic matter in arctic lakes as a palcoclimate proxy: field and laboratory investigations. J. Paleolim. 25: 43–64.

Sauer, P. E. & L. D. S. L. O. Sternberg, 1994. Improved method for the determination of oxygen isotopic composition of cellulose. Analyt. Chem. 66: 2409–2411.

Saurer. M., I. Robertson, R. Siegwolf & M. Leuenberger, 1998. Oxygen isotope analysis of cellulose: an interlaboratory comparison. Analyt. Chem. 70: 2074–2080.

Sternberg, L. S. L., 1988. D/H ratios of environmental water recorded by D/H ratios of plant lipids. Nature 333: 59–61.

Sternberg, L. S. L., 1989a. Oxygen and hydrogen isotope measurements in plant cellulose analysis. In Linskens, H. F. & J. F. Jackson (eds.) Plant Fibers. Springer-Verlag, New York: 89–99.

Sternberg. L. S. L., 1989b. Oxygen and hydrogen isotope ratios in plant cellulose: Mechanisms and applications. In Rundel, P. W., J. R. Ehleringer & K. A. Nagy (eds.) Stable Isotopes in Ecological Research. Springer-Verlag, New York: 124–141.

Sternberg. L. S. L. & M. J. DeNiro, 1983. Biogeochemical implications of the isotopic equilibrium fractionation factor between the oxygen atoms of acetone and water. Geoch. Cosmo. Acta. 47: 2271–2274.

Sternberg, L., M. J. DeNiro & J. E. Keeley, 1984. Hydrogen, oxygen, and carbon isotope ratios of cellulose from submerged aquatic Crassulacean acid metabolism and non-Crassulacean acid metabolism plants. Pl. Physiol. 76: 68–70.

Sternberg, L. S. L., M. J. DeNiro, M. E. Sloan & C. C. Black, 1986. Compensation point and isotopic characteristics of C_3/C_4 intermediates and hybrids in *Panicum*. Pl. Physiol. 80: 242–245.

Street-Perrott, F. A., Y. Huang, R. A. Perrott, G. Eglinton, P. Barker, L. B. Khelifa, D. D. Harkness & D. O. Olago, 1997. Impact of lower atmospheric carbon dioxide on tropical mountain ecosystems. Science 278: 1422–1426.

Talbot, M. R. & T. Lærdal, 2000. The Late Pleistocene — Holocene palaeolimnology of Lake Victoria, East Africa, based upon elemental and isotopic analyses of sedimentary organic matter. J. Paleolim. 23: 141–164.

Talbot, M. R. & D. Livingstone, 1989. Hydrogen index and carbon isotopes of lacustrine organic matter as lake level indicators. Palaeogeog. Palaeoclim. Palaeoecol. 70: 121–137.

Tsekos, I., 1999. The sites of cellulose synthesis in algae; diversity and evolution of cellulose-synthesizing enzyme complexes. J. Phycol. 35: 935–655.

Tyson, R. V., 1995. Sedimentary Organic Matter. Chapman & Hall, London, 615 pp.

Wolfe, B. B., W. M. Buhay & A. Schwalb, 2000a. A varved lake sediment carbonate and organic isotope record of late Glacial — early Holocene paleohydrology and paleotemperature in the Northern Great Plains, USA. International Paleolimnology Symposium, Queen's University, Kingston.

Wolfe, B. B. & T. W. D. Edwards, 1997. Hydrologic control on the oxygen-isotope relation between sediment cellulose and lake water, western Taimyr Peninsula, Russia: Implications for the use of surface-sediment calibrations in paleolimnology. J. Paleolim. 18: 183–191.

Wolfe, B. B. & T. W. D. Edwards, 1998. Comment on "Stable carbon and oxygen isotope records from Lake Erie sediment cores: Mollusc aragonite 4600 BP–200 BP" (*JGLR* 23: 307–316). J. Great Lakes Res. 24: 736–738.

Wolfe, B. B., T. W. D. Edwards & R. Aravena, 1999. Changes in carbon and nitrogen cycling regimes during tree-line retreat recorded in the isotopic content of lacustrine organic matter, western Taimyr Peninsula, Russia. The Holocene 9: 215–222.

Wolfe, B. B., T. W. D. Edwards, R. Aravena, S. L. Forman, B. G. Warner, A. A. Velichko & G. M. MacDonald, 2000b. Holocene paleohydrology and paleoclimate at treeline, north-central Russia, inferred from oxygen isotope records in lake sediment cellulose. Quat. Res. 53: 319–329.

Wolfe, B. B., T. W. D. Edwards, R. Aravena & G. M. MacDonald, 1996. Rapid Holocene hydrologic change along boreal treeline revealed by $\delta^{13}C$ and $\delta^{18}O$ in organic lake sediments, Northwest Territories, Canada. J. Paleolim. 15: 171–181.

Wolfe, B. B., T. W. D. Edwards & H. C. Duthie, 2000c. A 6000-year record of interaction between Hamilton Harbour and Lake Ontario: Quantitative assessment of recent hydrologic disturbance using ^{13}C in lake sediment cellulose. Aquat. Eco. Sys. Health Manage. 3: 47–54.

Yakir, D., 1992. Variations in the natural abundance of oxygen-18 and deuterium in plant carbohydrates. P1. Cell Environ. 15: 1005–1020.

Yakir, D. & M. J. DeNiro, 1990. Oxygen and hydrogen isotope fractionation during cellulose metabolism in *Lemna gibba* L. P1. Physiol. 93: 325–332.

Yapp, C. J. & S. Epstein, 1982. A reexamination of cellulose carbon-bound hydrogen δD measurements and some factors affecting plant-water D/H relationships. Geoch. Cosmoch. Acta. 46: 955–965.

15. NITROGEN ISOTOPES IN PALAEOLIMNOLOGY

MICHAEL R. TALBOT (michael.talbot@geol.uib.no)
Geological Institute
University of Bergen
Allégt. 41, 5007 Bergen
Norway

Keywords: stable isotopes, nitrogen, organic matter, palaeolimnology, C/N, mass spectrometry

Introduction

Nitrogen is a small but essential constituent of all organisms and as such can be regarded as a key nutrient. Together with phosphorous and silicon, it is commonly viewed as one of the nutrients that ultimately limit organic productivity. Indeed, in many lakes, N is probably *the* limiting nutrient. The fundamental role of nitrogen in organic production means that changes in N sources or cycling commonly have far-reaching consequences for the production, composition and accumulation of sedimentary organic matter (OM) in lakes. Knowledge of past variations in these and other aspects of the N cycle may thus provide unique palaeolimnological information that can be related to regional or global environmental change. A comprehensive overview of the central importance of N to all organic life, and of the N biogeochemical cycle, is given in Schlesinger (1997).

Nitrogen in lacustrine sediments has traditionally been characterised either as weight percent total nitrogen (TN) or by the carbon:nitrogen ratio (C/N). The latter is also commonly regarded as a means of identifying the source of the OM (e.g., Meyers & Ishiwatari, 1993; Tyson, 1995; Meyers & Lallier-Vergès, 1999). In palaeolimnology considerably less use has been made of N-isotope analysis as a method of characterising sedimentary nitrogen, even though the necessary analytical techniques and isotope fractionation effects have been known for over 40 years (Hoering, 1955; Létolle, 1980; Owens, 1987). There are two principal reasons for this, one practical, the other interpretational. Until comparatively recently, very few laboratories were equipped to carry out nitrogen isotope analyses and in those that were, the number of analyses that could be performed was commonly limited, because of the laborious, offline sample preparation. Interpretational problems were related to the fact that measured isotopic values may not necessarily have an unambiguous solution, due to the variety of biogeochemical processes and N sources that can contribute to the production of sedimentary OM. The situation has changed radically over the last decade, thanks to faster and improved analytical techniques and the growing realisation that even apparently ambiguous N-isotopic values may be interpretable when combined with other sorts of geochemical data.



W. M. Last & J. P. Smol (eds.), 2001. *Tracking Environmental Change Using Luke Sediments. Volume 2: Physical and Geochemical Methods*. Kluwer Academic Publishers, Dordrecht, The Netherlands.

A basic understanding of the nitrogen biogeochemical cycle and its impact upon N-isotope distribution in nature is essential for the succesful execution of any N-isotope study. The main goals of this chapter are: (1) to review the nitrogen cycle with particular emphasis on lacustrine and associated environments; (2) give an introduction to nitrogen isotope geochemistry as applied to palaeolimnological problems, (3) to examine briefly some of the practical aspects of N-isotope analysis; and (4) by means of examples show how N-isotope studies can provide unique palaeolimnological information on such fundamental features as OM and nutrient sources, nutrient cycling, mixing regime, water column stability and sediment provenance.

Nitrogen in lakes: forms and distribution

Inorganic nitrogen occurs in a variety of chemical forms and in several oxidation states, a fact which leads to complex cycling of nitrogen through the various inorganic and organic reservoirs. Inventories of the commonest forms of inorganic nitrogen and their principal reservoirs are summarised in Létolle (1980), Kaplan (1983), Blackburn (1983), Jaffe (1992) and Schlesinger (1997). Some of the reservoirs are relatively poorly constrained, estimates of their absolute size varying considerably, but atmospheric nitrogen (N_2, dinitrogen) is generally considered to be by far the largest reservoir of relevance to surface processes, although it has recently been suggested that the importance of N released by rock weathering may have been significantly underestimated (Holloway & Dahlgren, 1999). In aquatic environments, ammonium (NH_4^+), nitrate (NO_3^-) and nitrite (NO_2^-) are important components of the dissolved inorganic nitrogen (DIN) reservoir, as they represent the principle sources of N available for primary production (see below).

One important aspect of today's nitrogen cycle that needs to be borne in mind, especially when using modern lakes as analogues for ancient lacustrine systems, is that it has been profoundly influenced by anthropogenic effects. Fossil fuel combustion and many industrial processes discharge gaseous and particulate nitrogen compounds into the atmosphere; agriculture and urban developments have added copious amounts of dissolved and solid nitrogen to many surface and groundwater drainage networks (Vitousek et al., 1997; Schlesinger, 1997). It might be expected that the impact of these nitrogen sources would be vanishingly small in comparison with the huge reservoir of atmospheric N_2, but in reality many of the anthropogenic products are highly mobile N compounds which readily enter the food chain. Their effects on primary production, and the N-isotopic composition of the OM, may far outweigh their absolute volume. Neither are these influences confined to industrialized regions; few, if any, modern lakes may be entirely free of the effects of atmospheric N fallout. In tropical Africa, for example, it has been shown that one of the last remaining pristine great lakes, Lake Malawi, receives ca. 72% of its annual N input from the atmosphere, mainly *via* slash-and-burn agriculture (Bootsma, et al., 1996).

Nitrogen cycling in lakes

As indicated above, nitrogen occurs in nature in a variety of forms. Figure 1 summarises those of significance to the assimilation and recycling of N in the aquatic environment. The following aspects are of particular importance:

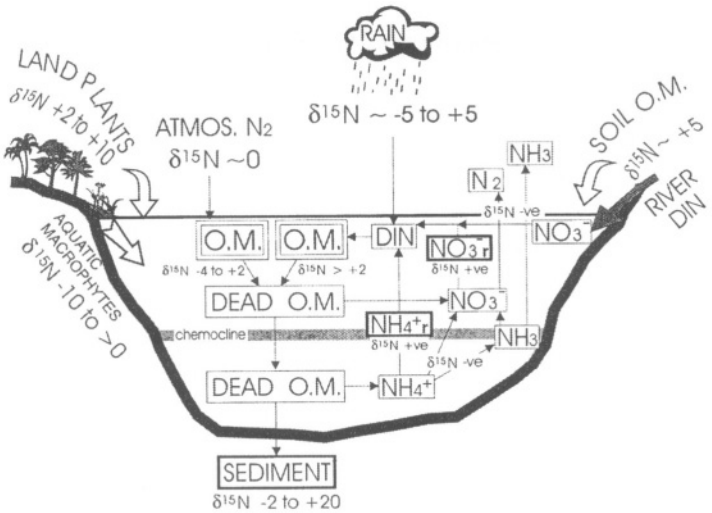


Figure 1. Key features of the nitrogen biogeochemical cycle in an idealised stratified lake with typical (but not unique) $\delta^{15}N$ values for the most important inputs and products. The two heavily lined boxes marked **r** represent the residual pools of ammonium (NH_4^+) and nitrate (NO_3^-) available for phytoplankton assimilation after microbial reworking (nitrification, denitrification) or ammonia volatilisation. In each case the residual pool is enriched in ^{15}N ($\delta^{15}N$ + ve) in comparison with the original pool because of discrimination against the heavier isotope (see text for a detailed explanation). This, in turn, leads to relative isotopic enrichment in phytoplankton that consume these N pools. (Compiled from many sources. $\delta^{15}N$ values for aquatic macrophytes based mainly upon unpublished data provided by Carol Kendall, pers. comm., 2000).

Biological processes

- *Ammonia* and *nitrate assimilation* are the two principle processes by which nitrogen is obtained during primary production. In highly productive lakes exploitation of these reservoirs may be so intense that dissolved NH_4^+ and NO_3^- concentrations are below detection level. Nitrite (NO_2^-) provides an additional, but subsidiary, dissolved N source.

- *Nitrogen fixation* is the process by which N_2 is assimilated and is the principal route for atmospheric nitrogen's entry into the biological cycle. It is, however, a metabolically expensive process due to the large amount of energy required to break the triple bond between the two nitrogen atoms, and is confined to a number of specialised bacteria and algae (diazotrophes), of which the blue-green algae (cyanobacteria) are particularly important in lakes.

- *Ammonification* results from the bacterial reduction of organically bound N to NH_3 or NH_4^+ and is a process that requires anoxic conditions. It plays a major role in the mineralisation of suspended or sedimentary OM; ammonium is the dominant N-bearing product of bacterial OM decomposition in anoxic sediments.

- *Nitrification* is the oxidation of NH_4^+ to nitrate or nitrite by aerobic bacteria.

- *Denitrification* occurs when bacteria reduce NO_3^- to gaseous N_2. Denitrifying organisms require anoxic or dysoxic conditions, so the process commonly takes place within the sediment where its impact is limited by the diffusive supply of the reactants. Supply rates are significantly higher if the oxycline lies within the water column, as is the case in lakes with an anoxic hypolimnion (Hecky et al., 1996). In such circumstances, denitrification can be of major importance to a lake's nitrogen cycle, leading to significant loss of N. Globally, denitrification, and the return of molecular N to the atmosphere, must be the main process responsible for maintaining a balanced N cycle.

Inorganic processes

- N_2 *dissolution* and *ammonia volatilisation* are the only inorganic processes of importance to the lacustrine N cycle. The former makes atmospheric N_2 available for fixation by aquatic diazotrophes. Regrettably, the $[N_2]_{aq}$. (dissolved molecular nitrogen) concentration in lakes is rarely measured, but if the oceans are any guide it may well represent by far the largest aquatic N reservoir (Tyrrell, 1999); the few available data tend to support this view (e.g., Hollander, 1989). Ammonia volatilisation is pH dependent, the proportion of total ammonium present as ammonia rising sharply where the pH exceeds 8.5. In alkaline lakes, significant N loss may occur via ammonia degassing (Collister & Hayes, 1991).

In terms of N utilisation, we can distinguish between two major groups of primary producers, those which exploit the easily assimilated forms NH_4^+, NO_3^- and NO_2^- (combined nitrogen), and "nitrogen fixers", dominated by the cyanobacteria, which utilise N_2. Because N-fixation is energetically expensive, the latter are normally outcompeted by phytoplankton such as diatoms and green algae when supplies of the other dissolved nitrogen species are adequate. However, if sources of nitrate and ammonium are exhausted, and other key nutrients, notably phosphorus and iron, are not limiting, the N-fixers can flourish. The distinction between these two forms of N utilisation is important because of frequent isotopic differences between cell material produced by the two phytoplankton groups. As variations in the availability of the different N sources are often environmentally related, identifying the products of one or the other metabolic pathway may have important palaeolimnological implications. Nitrogen isotopes provide a powerful means of potentially distinguishing between these two sorts of OM.

Nitrogen in lacustrine organic matter

Lake sediments may contain organic matter from several sources, but the dominant are aquatic plants and algae (phytoplankton and macrophyte), terrestrial plants and soil humus. These contain varying amounts of nitrogen. In phytoplankton the mean N content is conventionally given by the Redfield ratio with a C/N of 6–7. Many lake sediments, even those dominated by phytoplankton remains, have C/N values that are higher than this. The cause may in part be due to preferential early diagenetic loss of N (see below), but it is also clear that algal growth under N-limited conditions can result in cell material with a C/N as high as 20 (Healey & Hendzel, 1980; Hecky et al., 1993; Talbot & Lærdal,

2000). Phytoplankton OM is relatively N-rich, due to their high protein (which accounts for much of the N) and lipid content; terrestrial plants, on the other hand, are dominated by cellulose and lignin, both of which are N-poor. Although leaf cuticle is relatively N-rich, C/N values in excess of 200 are common in grasses and woody plants, and the mean C/N for the terrestrial biomass has been estimated at about 160 (Schlesinger, 1997). In soils, the activities of nitrogen-fixing microrganisms can lead to N enrichment, particularly around plant roots. Soil OM may thus have rather high N contents, with C/N values that are similar to or even lower than those in planktonic OM (Tyson, 1995), although the mean for all soils is probably around 15 (Schlesinger, 1997).

These large differences in N content emphasize just one of the several contrasts between carbon and nitrogen isotopic studies of sedimentary OM. While in the former, it can normally be assumed that each component makes a proportional contribution to the bulk C-isotopic composition, this may not be the case with N isotopes. The N-rich fraction can determine the isotopic character of the sediment, even if it does not volumetrically dominate the OM assemblage. Conversely, the degraded, N-poor woody and grass cuticle fragments that occur in many lake sediments will not seriously distort the N-isotopic signature of the waterbody preserved in the autochthonous om (see, for example, Yoshioka, et al., 1989; Talbot & Johannessen, 1992).

Nitrogen isotopes

In the natural environment nitrogen exists as a mixture of two stable isotopes, ^{14}N and ^{15}N. The former is by far the more abundant of the two (ca. 99.634% by atoms), but measurable differences in the relative proportion of the two isotopes in various naturally occuring inorganic and organic substances forms the basis of nitrogen isotope geochemistry. Comprehensive reviews of isotope systematics in general, and the history of N isotope study and measurement, are given in Kaplan (1983), Owens (1987) and Hoefs (1997); Kendall (1998) provides a useful summary of N-isotope theory and applications in catchment and groundwater studies. Only a brief overview of the most essential aspects of N-isotope geochemistry will be given here. Although stable isotope geochemistry has the reputation of being difficult, and can seem daunting to the beginner, many of the perceived complications are in reality easily surmounted.

Isotope systematics, notation and conventions

Isotope effects and isotope fractionation

Various isotope effects are the ultimate cause of natural variations in the distribution of the stable isotopes of nitrogen. There are two types of isotope effect: (i) physical, and (ii) chemical. Physical effects are associated with processes such as freezing/melting, evaporation/condensation, adsorbtion, diffusion, etc; chemical effects occur in both inorganic and biochemical reactions and are the dominant reason for observed N-isotopic variations in living and sedimentary OM. Isotope effects are manifest as differences in the relative distribution of ^{14}N and ^{15}N between reactants and products, the result of such changes is commonly referred to as isotope *fractionation.* Processes like those outlined above typically have a characteristic fractionation associated with the reaction. The fundamental cause of the

isotope effect, and thus fractionation, is the lower bond strength of ^{14}N relative to ^{15}N, the former thus react more rapidly than the latter, and ^{14}N compounds diffuse more rapidly or evaporate at a lower temperature than their ^{15}N colleagues. Fractionation is conventionally expressed as *the fractionation factor,* α. In a reaction between two substances, A and B, or any other process which involves isotopic fractionation, α is defined as the ratio between the relative abundance of two isotopes in A versus those in B. For example, the fractionation factor for the dissolution of N_2 gas in water is given by:

$$\alpha_{(N_{2(gas)} \rightarrow N_{2(aq)})} = \frac{(^{15}N/^{14}N)_{gas}}{(^{15}N/^{14}N)_{aq}}. \quad (1)$$

Chemical isotope effects are divided into two types: *equilibrium* and *kinetic.* The latter are of particular importance in palaeolimnology (and other branches of the sedimentary N cycle) and are typically associated with complex, irreversible, biologically mediated reactions. A characteristic, but not invariable aspect of kinetic isotope fractionation is a marked discrimination against the heavier ^{15}N isotope, such that the product of the reaction is enriched in ^{14}N relative to the substrate.

Notation and conventions

Because absolute amounts of ^{14}N and ^{15}N atoms are difficult to measure, natural isotope abundances are conventionally given as $\delta^{15}N$ values, where:

$$\delta^{15}N = \left[\frac{(^{15}N/^{14}N)_{sample}}{(^{15}N/^{14}N)_{standard}} - 1 \right] \times 1000. \quad (2)$$

δ values are expressed as *permille* (‰) with respect to the standard, which in the case of $\delta^{15}N$ is atmospheric nitrogen, commonly shortened to AIR. By convention this has a value of 0‰. Note that the correct symbol is δ (Greek delta) *not* ∂ (del). The latter is assumed by many to be interchangeable with δ but in fact denotes partial derivative.

Nitrogen isotope fractionation

The isotope fractionation factors associated with reactions of significance to the lacustrine nitrogen cycle are summarised in Table I. Detailed reviews of the physiology of N assimilation, mechanisms of fractionation, their measurement and the range of known fractionations are given in Owens (1987), Handley & Raven (1992), Fogel & Cifuentes (1993) and Goericke et al. (1994).

It will be apparent from Table I that many of the important N assimilation reactions discriminate strongly against the heavier ^{15}N isotope. This is in keeping with other biochemical reactions such as carbon assimilation during photosynthesis and bacterial methane genesis, both of which also involve a marked kinetic fractionation effect. The one notable exception, a fact of major significance in the interpretation of N-isotope data, is N_2 fixation by cyanobacteria, a process which involves little discrimination (Table I). As minimal fractionation also occurs during the dissolution of gaseous N_2 (Table I), cell material produced by diazotrophes has a $\delta^{15}N$ value that typically lies around 0 ± 2‰.

An important consequence of the fractionation associated with DIN assimilation is that as organic production proceeds, preferential incorporation of ^{14}N intophytoplankton

Table I. Equilibrium (a) and kinetic (b) isotopic fractionation factors (α) of importance to nitrogen cycling in lakes (Collister & Hayes, 1991). As a first approximation, an α value of, for example, 1.020 implies a difference in δ of ca. 20‰ between the reactant and product. In the case of N_2 gas dissolution, therefore, δ differs by less than 1‰ between the gaseous and aqueous phases, whereas gaseous ammonia liberated during ammonia volatilisation will be ca. 34‰ lighter than the aqueous ammonia.

PROCESS	FRACTIONATION
(a) Inorganic	α (reactant ⇒ product)
Nitrogen dissolution: $N_{2(gas)} \Rightarrow N_{2(aq.solution)}$	1.00085
Ammonia volatilisation: $NH_4^+{}_{(aq.)} \Rightarrow NH_{3(gas)}$	1.034
(b) Biochemical	
Nitrogen fixation: $N_2 \Rightarrow$ Cell-N	0.996–1.0024
Nitrate assimilation: $NO_3^- \Rightarrow$ Cell-N	1.011–1.023
Ammonium assimilation: $NH_4^+ \Rightarrow$ Cell-N	0.993–1.013
Remineralisation: Cell-N ⇒ NH_4^+	1.001
Nitrification: $NH_4^+ \Rightarrow NO_2^-$	1.02
Denitrification: $NO_3^- \Rightarrow N_2$	1.02

cell material inevitably leads to a corresponding ^{15}N enrichment in the remaining DIN reservoir. This effect, called *Rayleigh distillation orfractionation,* also occurs in inorganic-reactions, and is summarised diagrammatically in Figure 2. Despite the *instantaneous kinetic fractionation* (the difference between the isotopic composition of the substrate and product at any given stage during the reaction), in closed systems, where all the substrate is consumed, the isotopic composition of the bulk product must equal that of the initial substrate (Fig. 2). There is thus no apparent isotopic discrimination, although the isotopic effect in fact occurred throughout the reaction. In such circumstances the composition of the OM should record that of the DIN pool from which it was produced. In reality the situation is rarely as simple as this. For example, the magnitude of the fractionation tends to decrease as the DIN concentration falls (Wada & Hattori, 1991; Fogel & Cifuentes, 1993; François et al., 1996; Pennock et al., 1996; Waser et al., 1998). Fractionation may also be affected by growth rate or other environmentally determined factors (Wada & Hattori, 1978). As a general rule in N-limited systems, however, it can be assumed that where all available DIN is consumed, the fractionation will be small and the composition of the product very close to that of the substrate from which it formed. Very low DIN concentrations or other environmentally related factors may favour a switch from nitrate-, nitrite- and ammonium-assimilating algae to those capable of atmospheric N_2 fixation (Gu et al., 1996; Schlesinger, 1997). As this change can be seasonal (e.g., Hecky & Kling, 1987; Gu et al., 1996). sedimentary OM in some lakes may contain N derived from more than one reservoir with very different isotopic compositions.

Where ammonium is the principal product only limited fractionation effects accompany the microbial reworking (*mineralisation, decomposition*) of bulk organic matter.

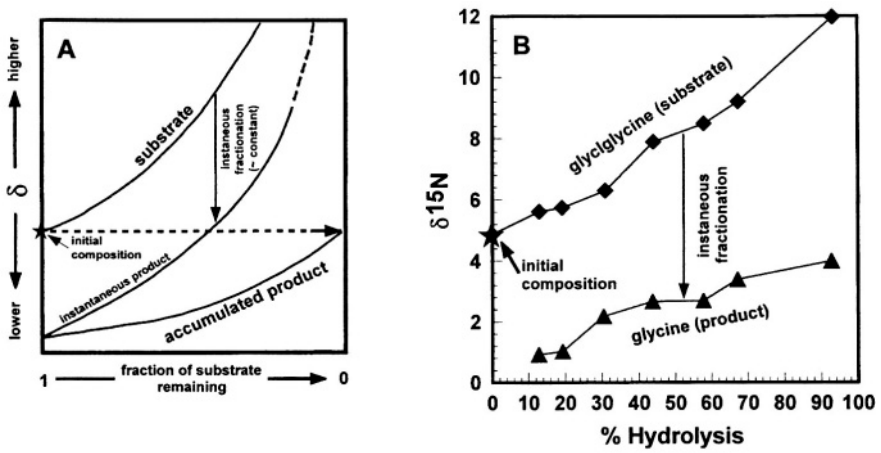


Figure 2. (A) Rayleigh distillation. Progressive change in the relative isotopic compositions of a reactant (the substrate) and its product in a closed system where the fractionation is such that the product is isotopically lighter than the substrate. Note that if the reaction goes to completion (i.e. all the substrate is consumed), the composition of the accumulated product must equal that of the original substrate. Thus no *apparent* fractionation has occurred, although the instantaneous fractionation at any stage in the reaction is always such that the product has a lower δ value than the remaining substrate. (B) An actual example of the Rayleigh distillation process, in this case produced by bond cleavage during the abiogenic hydrolysis of glycylglycine to glycine. The fractionation is 4–5‰ (data replotted from Silfer et al., 1992).

Subsequent nitrification of this ammonium, and denitrification of the resulting nitrate, both discriminate strongly against ^{15}N (Table I). In the last case, selective loss of the resulting $^{14}N_2$ may leave an isotopically enriched residual DIN pool, particularly when denitrification occurs within the water column. An example is provided by Lake Kizaki, Japan, where during the summer stratification period the $\delta^{15}N$ of the residual deepwater NO_3^- was found to be +15.1‰, whereas shallow-water NO_3^- had a $\delta^{15}N$ of –2.2 (Yoshioka et al., 1988).

The only purely inorganic process with a potentially major impact on a lake's N cycle is ammonia volatilisation which imparts the strongest fractionation (ca. 34‰) of all the isotope effects reviewed here (Table I). In alkaline lakes, loss of isotopically light ammonia by degassing may lead to strong isotopic enrichment of the remaining DIN (Collister & Hayes, 1991; Talbot & Johannessen, 1992).

$\delta^{15}N$ *variations in lakes and related environments*

Comprehensive compilations of $\delta^{15}N$ variations in nature can be found in Kaplan, (1983), Owens (1987) and Hoefs (1997); Meyers & Lallier-Vergès, (1999) provide a brief review of variations in lakes. Figure 1 shows typical (but not unique) δ values for the major N pools that may influence an idealised lake. The range of known values is very large, in excess of 100‰ (Owens, 1987; Wada & Hattori, 1991; Kendall, 1998), but generally lies between –5 and +20‰ (Owens, 1987). Values outside these limits tend to occur in unusual circumstances or rather extreme environments such as Antarctic or alkaline lakes (e.g., Wada et al., 1991). One reason for the relatively limited range of common $\delta^{15}N$ values

is, of course, the buffering effect of the atmospheric N_2 reservoir. In addition, there are no major near-surface reservoirs of highly enriched or depleted N, equivalent for example to those provided by biogenic methane or microbially produced sulphide for respectively the sedimentary carbon and sulphur cycles.

As with most other branches of palaeolimnology, we might hope that studies of modern environments and organisms would provide a firm foundation upon which to build our interpretations of ancient N-bearing materials. While this is to some extent also the case for N-isotope studies, current knowledge is very far from complete, and it is universally agreed that we still lack important insights into many aspects of the surface N cycle and its associated isotopic characteristics. This is true at all scales, from N assimilation at the algal cell wall (e.g., Handley & Raven, 1992; Fogel & Cifuentes, 1993) to lake-atmosphere interactions (e.g., Hecky et al., 1996). Some gaps exist simply because the necessary studies have yet to be carried out, but others are inherent to lacustrine systems. Investigating the factors that control phytoplankton composition is bound to be difficult when reliable data on the isotopic composition of the nutrients (i.e., DIN) are hard to obtain. This is largely a result of practical difficulties which will not easily be overcome, in particular because DIN is often present at such low concentrations that isotopic analysis is impossible, or the little that remains has been so altered by the Rayleigh distillation effect outlined above that its composition bears little resemblance to that of the original substrate. Culture studies can go some way towards redressing our current ignorance, but these must be used with caution as the conditions under which cultures are raised and sampled rarely match those found in nature (Fogel & Cifuentes, 1993; Waser et al., 1998).

Studies in modern lakes

Nitrogen isotopic studies of organic matter production and sedimentation in modern lakes are few in number, but those that exist do provide us with some insights into the range of composition among modern phytoplankton assemblages, and in some cases they also allow us to compare the OM composition with that of ambient DIN and some of the major DIN sources.

Sediment trap studies

Monitoring of OM production by means of sediment traps immediately below the epilimnion, and at greater depths, provides information on the N-isotopic composition of the primary photosynthate, and of possible changes that occur because of biological reworking during the OM's passage through the water column. It must be admitted that these studies also demonstrate some of the complications that might confuse our interpretation of ancient deposits!

Trap studies of algal om from arctic to tropical lakes indicate seasonal differences in $\delta^{15}N$ of up to several permille (Fig. 3). In most cases these changes have been explained in terms of DIN composition and concentration variations, particularly in association with the seasonal cycle of production and stratification, but other factors that affect algal growth, notably temperature and light availability, are also thought to play a pan (e.g., Estep & Vigg, 1985; Yoshioka, et al., 1989; Hollander, 1989; Gu & Alexander, 1993; Gu et al., 1996; François et al., 1996; Bernasconi et al., 1997; Hodell & Schelske, 1998). There has

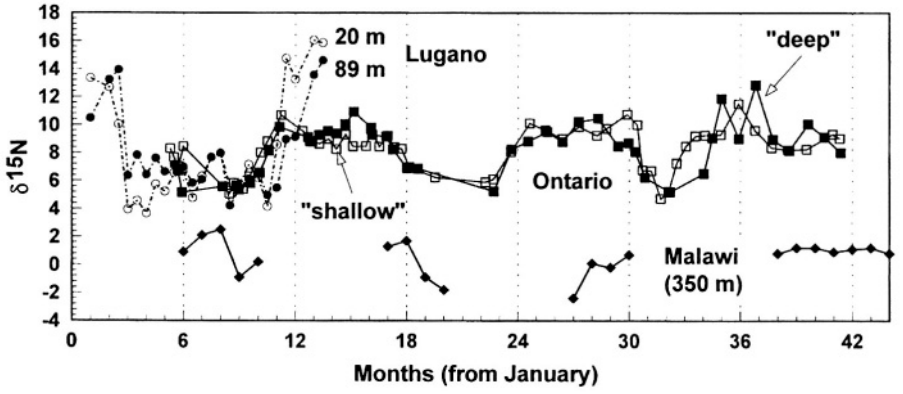


Figure 3. Seasonal variations in the N-isotopic composition of settling organic matter collected by sediment traps in lakes Lugano (circles), Ontario (squares) and Malawi (diamond). Lake Lugano: January 1994 – February 1995 (data replotted from Bernasconi et al., 1997). Lake Ontario: May 1993 – May 1996 ("shallow" and "deep" indicate the relative depths of sets of traps suspended through the water column. Data replotted from Hodell & Schelske, 1998). Malawi: June 1987 – August 1990 (data replotted from François et al., 1996).

been a lesser tendency to explain seasonal variations in terms of changes in the dominant algal group even though these are widely documented, most notably the tendency for N-fixing blue-green algae to predominate during the period of maximum water column stability (e.g., Hecky & Kling, 1981, 1987; Gu et al., 1996). Estep & Vigg (1985) and Gu & Alexander (1993), for example, equate periods of low $\delta^{15}N_{plankton}$ values with the presence of abundant blue-green algae; nevertheless, in a comparative study of Florida lakes, Gu et al. (1996, p. 882) conclude that "... primary productivity is a stronger determinant of $\delta^{15}N$ than changes in species composition ..." Measured modern $\delta^{15}N_{plankton}$ values mainly lie in the range of +2 to +14‰ (Fig. 3), but in a study of particulate organic nitrogen (PON) taken from a trap in northern Lake Malawi, François et al. (1996) record periods when the composition was – 0.2 to – 2.4‰. They explain such low values in terms of abundant DIN supply during upwelling periods, but $\delta^{15}N_{plankton} < 0$ are also typical of blue-green algae. In the absence of DIN concentration data, and given that DIN is probably a limiting nutrient in the lake (Hecky et al., 1996; Bootsma et al., 1999), a seasonally important role for N-fixing algae at the sample site must be considered a distinct possibility.

$\delta^{15}N_{PON}$ *vs.* $\delta^{15}N_{DIN}$ *or* $[DIN]_{aq}$

Studies in some modern lakes allow us to compare the isotopic composition of bulk phytoplankton with that of ambient DIN. The few data that are available provide us with something of a surprise. Whereas theory and culture experiments lead us to expect that the kinetic isotope and Rayleigh distillation effects associated with NO_3^-, NO_2^- and NH_4^+ assimilation should produce OM with a $\delta^{15}N$ value that is lower than or equal to that of the DIN substrate, observations in North American (Pang & Nriagu, 1977; Estep & Vigg, 1985; Ostrom et al, 1998) and Japanese lakes (Yoshioka et al., 1989) reveal the

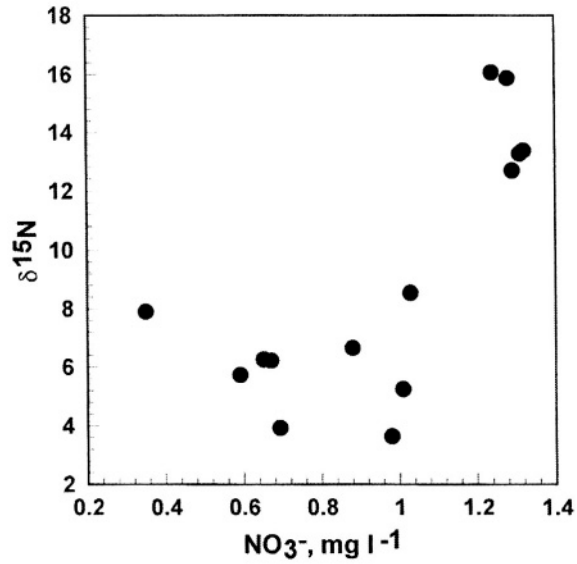


Figure 4. Relationship between dissolved nitrate composition and the N-isotopic composition of near-surface (<20 m) particulate organic matter in Lake Lugano (data replotted from Bernasconi et al., 1997). The apparent positive correlation is the opposite of that predicted by isotopic theory and culture experiments.

opposite relationship, $\delta^{15}N_{PON}$ is in each case higher by up to several permille than $\delta^{15}N_{DIN}$. Theory also predicts fractionation increases with DIN availability. However, Bernasconi et al. (1997) show that although the relationship is not linear, there is a clear tendency in Lake Lugano, Switzerland, for $\delta^{15}N_{PON}$ to increase with nitrate concentration (Fig. 4). In Lake Hoare, Antarctic, on the other hand, where OM is generally isotopically light ($\delta^{15}N$ typically –5 to 0‰), there is circumstantial evidence that the low δ values are related to high DIN concentrations (Wharton et al., 1993).

The reasons for these discrepancies are not known. Various explanations have been offered, including fractionation during partial mineralization of the dead OM (Bernasconi et al., 1997; Ostrom et al., 1998), alternative sources of isotopically heavy N, including recycling of excretory products, and lateral advection of water masses (Estep & Vigg, 1985; François et al., 1996), but it is clear we still have much to learn about N-isotope cycling in modern lakes.

$\delta^{15}N$ *in atmospheric precipitation*

Rain contains significant amounts of dissolved N, principally as NO_3^-, NO_2^- and NH_4^+. Organic N (notably in urea and amino acids; Paerl & Fogel, 1994) may also be present. Precipitation may thus be an important supplier of N to some lakes, particularly large waterbodies where rain falling on the lake surface can be the dominant source of inflow. Data on the isotopic composition of rain N are sparse, but those that exist indicate that both dissolved nitrate and ammonium commonly have relatively low $\delta^{15}N$ values, in the range of –18 to +4‰, with local average values typically <0‰ (Owens, 1987; Heaton, 1987;

Paerl & Fogel, 1994). Precipitation may thus represent a major source of ^{15}N-depleted dissolved N, and is the probable explanation for the low $\delta^{15}N$ values reported for dissolved nitrate in Lake Superior (Ostrom et al., 1998; see above). Once again, a degree of caution must be exercised in applying modern data to ancient lacustrine systems, as both the concentration and compostion of today's atmospheric N gases have undoubtedly been influenced by anthropogenic emissions. Nevertheless, consideration of the fractionation effects (see above) taking place in the dominant natural sources of nitrogen oxide gases (soils - Jaffe, 1992; Schlesinger, 1997) and ammonium (animal excretory products - Jaffe, 1992, with a minor contribution from lakes and swamps) suggests that atmospheric DIN is always likely to have been isotopically depleted.

Historical changes in sedimentary $\delta^{15}N_{om}$

Dated, high-resolution cores of recent sediment accumulation in modern lakes allow the $\delta^{15}N_{om}$ record to be compared with historical records of the waterbody's limnological and catchment evolution. This may allow us to identify some of the factors responsible for observed variations in the isotopic records. Four such records, spanning the last 100–200 years, are shown in Figures 5, 6, 7 and 8. Three, Greifensee (Switzerland; Fig. 5), Lake Ontario (Canada/USA; Fig. 6) and Lake Hollingsworth (Florida; Fig. 7), are from urbanised, industrialized regions with advanced agricultural and sewage disposal practices; the third, Lake Victoria (Uganda, Tanzania, Kenya; Fig. 8), is from an under-developed, non-industrial region that has undergone recent massive population growth. The L. Ontario and Greifensee records show similar historic trends, with rising $\delta^{15}N$ from the 19th through 20th centuries. Isotopic changes are matched by rising sediment TN contents. Similar trends are also apparent in the recent sediments of Lake Arresø, Denmark (Niles-Bo Jensen, personal communication). The record from L. Victoria, in contrast, shows no clear trend until the last decade when $\delta^{15}N$ began to rise.

L. Ontario and Greifensee have both experienced eutrophication, following recent changes in nutrient loading due to urbanisation and modern land-use practices (Hollander et al., 1992; Hodell & Schelske, 1998). The parallel variations in $\delta^{15}N$ and N content are probably primarily the result of intensified utilisation of the DIN reservoir with transfer of organic N to the sediments as productivity rose due to anthropogenic fertilisation. Selective assimilation of ^{14}N, low DIN concentrations, and increased production and burial of phytoplankton OM would all tend to cause $\delta^{15}N$ values to rise (see above). Other factors may have contributed to this trend. Sewage N is relatively enriched in ^{15}N ($\delta^{15}N$ 5–20‰ — Sweeney & Kaplan, 1980; Heaton, 1986; Owens, 1987), so increased effluent discharge, plus release of soil N due to deforestation and agriculture, may have caused some of the observed rise in $\delta^{15}N$. The study by Hodell & Schelske (1998) also demonstrates how additional complications to the interpretation of N-isotopic records may arise when changes in an upstream lake (in this case L. Erie) are passed on to the next waterbody.

In a study of four Floridan lakes, Brenner et al. (1999) detected a rather different $\delta^{15}N$ trend with increasing eutrophication. Cores from these waterbodies record a change to lower $\delta^{15}N_{om}$ during the 20th century, while $\delta^{13}C_{om}$ rose markedly and C/N fell over the same period (Fig. 7). The carbon isotopic change again reflects increased primary productivity with selective removal of ^{12}C from the DIC reservoir, but a similar effect clearly cannot explain the N-isotope change. Brenner et al. (1999) suggest that as productivity rose, drawdown

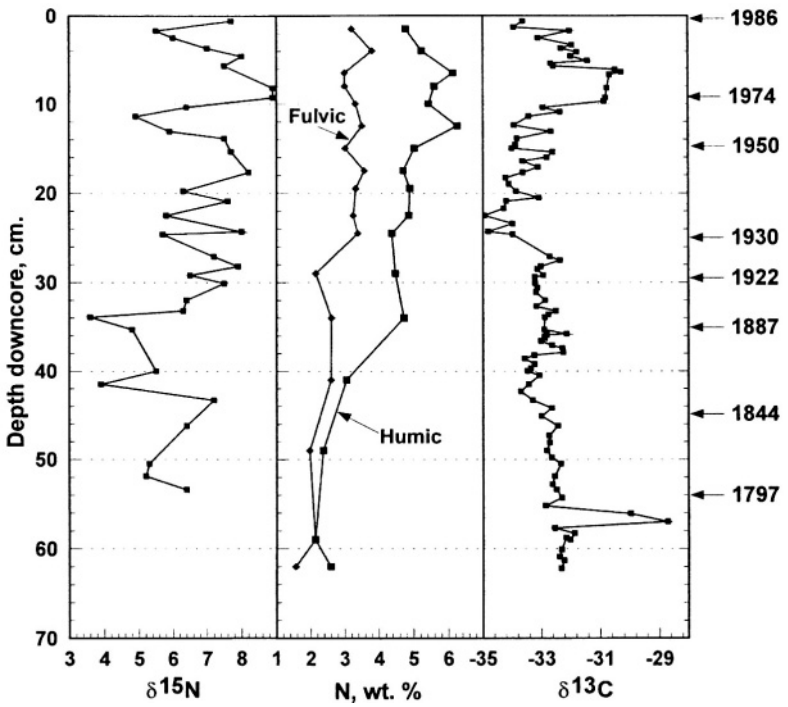


Figure 5. Historical changes in the isotopic composition and N content of sedimentary OM in a core from Greifensee, Switzerland (chronology based on varve counts; data replotted from Hollander, 1989). Note the generally rising $\delta^{15}N$ and N values through much of the past century, and maxima in $\delta^{15}N$ and $\delta^{13}C$ during the 1970's when pollution and eutrophication were at their height. With the introduction of stricter effluent and organic fertiliser controls values have tended to decrease in more recent times.

in the DIN reservoir became sufficiently extreme to favour N-fixing cyanobacteria which have contributed increasing amounts of isotopically light OM to the sediment. However, they also note that while there is a general correlation between N-isotopic composition and other indicators of trophic state, not all fluctuations in $\delta^{15}N$ are matched by changes in these tracers and conclude (Brenner et al., 1999, p. 219) that "... multiple factors may ultimately control the $\delta^{15}N$ of sedimented organic matter."

Major ecological changes have occurred in Lake Victoria over the past 2–3 decades, with dramatic reorganisation of the fish fauna (including mass extinction of many endemic species), primary production and bottom-water oxygenation (Kaufman, 1992; Hecky, 1993; Bootsma & Hecky, 1993). Here, too, there seems to be an important anthropogenic element involved in the changes, but not because of industrialization or waste discharge. The region has experienced dramatic population growth, and increased nutrient loading due to accelerated soil erosion and slash-and-burn agriculture may well have been the principal causes of the limnological changes (Verschuren et al., submitted). The rising trend in $\delta^{15}N$ (Fig. 8) probably reflects the impact that denitrification is having on the lake's isotopic budget, a consequence of a larger and more persistent anoxic hypolimnion (Hecky et al., 1996). Increased supply of isotopically heavy soil N may also have contributed to the change. In

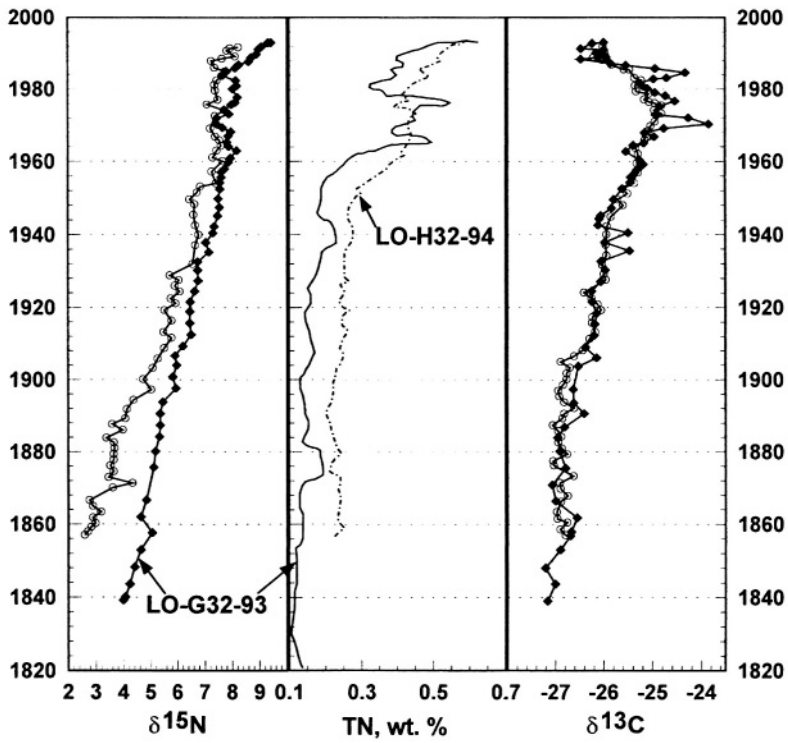


Figure 6. Historical changes in the isotopic composition and N content of sedimentary OM in cores LO-G32-93 and LO-H32-94 from Lake Ontario (chronology from ^{210}Pb and ^{137}Cs dating. Data replotted from Hodell & Schelske, 1998). In common with Greifensee (Fig. 5), the records show that rising values accompanied population growth, and industrialisation of the catchment. Stricter pollution controls since the 1980s are reflected in the δ^{13}C data; the reason why the nitrogen cycle has not responded in similar fashion is not known with certainty.

the case of Lake Victoria, it is also interesting to note that a natural event, the series of very wet years in the early 1960's with ensuing rise of lake level, has also left its mark on the N record (Fig. 8), and may have played a part in triggering the full impact of the anthropogenic effects.

Nitrogen isotope studies in palaeolimnology: sampling and measurement

Modern gas-source mass spectrometers are high precision instruments capable of consistently producing high-quality analytical data. The value of these measurements is nevertheless limited if the samples used have not been chosen and prepared with care. Ideally, sample selection should begin with the choice of sampling location. If nitrogen isotopic analyses are to form a central part of a palaeolimnological study, the sample site should be chosen such that it optimises the chances of obtaining abundant, well-preserved organic matter.

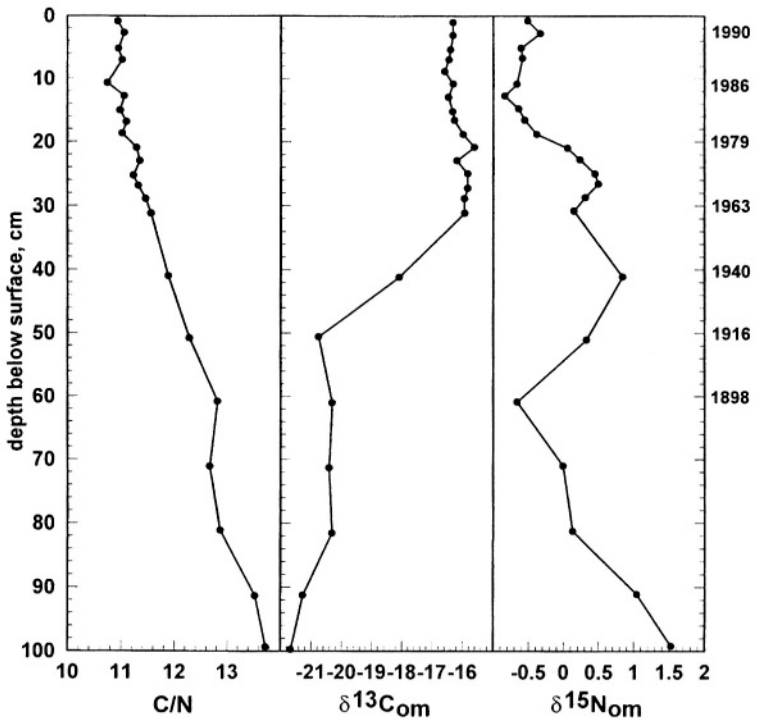


Figure 7. Changes in the isotopic and elemental composition of OM over approximately the last two centuries in core 20-II-92-14 from Lake Hollingsworth, Florida (data replotted from Brenner et al., 2000). Note the sharp increase in $\delta^{13}C$ during the middle of the last century, suggesting a rise in productivity due to eutrophication. $\delta^{15}N$ values also rose initially, but thereafter have gradually declined over the past 60 years, probably due to an increasing contribution of N-fixing cyanobacteria to the sediment (see text for further discussion).

Sample selection

The success of any stable isotopic study is, to a large degree, dependent upon the choice of suitable sample material. Sample selection will obviously depend upon the goals of the study, but assuming that these are palaeolimnological, the aim will be to obtain proxy information on the waterbody by measuring the isotopic composition of one or more types of aquatic organic matter. Almost any type of lake or marsh sediment may be used, providing it contains sufficient nitrogen. At the Geological Institute, University of Bergen (UB) we routinely analyse sediment samples containing less than 0.1% (by weight) total N. In general, the higher the OM content, the better the chances of obtaining a good set of analyses. These requirements will clearly constrain the choice of sample site. If cores are to be used, the best coring sites are typically found offshore, where phytoplankton dominate the OM assemblage, and in deep water where predominantly fine-grained sediments accumulate. Productive lakes tend to provide sediments that are more OM-rich than those in oligotrophic waterbodies. Organic matter preservation is further enhanced by high rates of accumulation and seasonal or permanent bottom water anoxia. Sites where accumulation rates are low and

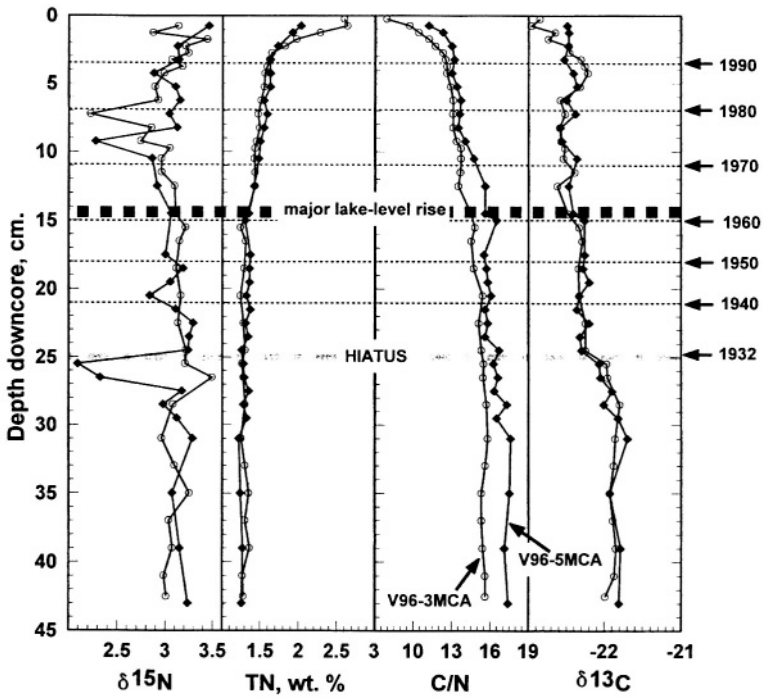


Figure 8. Historical changes in the isotopic and elemental composition of sedimentary OM from cores V96-3MC and 5MC, Lake Victoria (chronology from ^{210}Pb dating; Verschuren et al., submitted). The abrupt fall in TN values in the uppermost 5 cm is probably due to diagenetic loss of labile N compounds (see text). Note the tendency for δ^{15}N to rise since the mid-1980s and the changes in δ^{15}N, δ^{13}C and C/N following the rise in lake level in the early 1960s.

the bottom sediments are oxic may be prone to post-depositional alteration of the OM (see below). Although cores from existing lakes and bogs are probably the commonest means of obtaining samples for isotopic analysis, satisfactory results can also be obtained from trenches and natural exposures of sediments and rocks. The primary concern is that the original organic matter has not been invaded by roots or significantly altered by weathering or, in the case of rocks, severly affected by thermal maturation.

Having collected the samples, it may be possible in some cases to separate or concentrate specific fossil remains for analysis, but in many lake sediments the OM is simply too fine-grained to allow physical separation of individual components. For deposits of this sort a bulk sample must be analysed. Although a dominance of phytoplankton remains is preferred, in many instances the sediments contain mixtures of OM, including terrestrial plant fragments. This may not be a major problem, however. As indicated earlier, the low N content of woody and degraded cuticular material means that they make a very small contribution to the total N; the measured δ^{15}N value of these bulk samples may thus still represent the composition of the aquatic OM fraction. In all cases it is nevertheless desirable to know exactly what has been analysed. Surprisingly many palaeolimnologists and palaeoclimatologists are still happy to submit their samples to the mass spectrometer

without having first determined what sort of OM is actually present in the sediment. This is *not* recommended! Our first step, after having opened and logged a core, for example, is to make a set of smear slides; every one of our isotopic analyses is backed up by at least a smear-slide description of the sediment. This is a cheap, quick and extremely effective means of gaining a semi-quantative overview of the major organic components present in lake sediments (see Kelts, 1999, for information on slide preparation and a guide to grain identification), especially if it includes an examination of the mount under ultraviolet light (Talbot & Livingstone, 1989). Geochemical techniques, notably C/N determination (see above), organic petrography (Tyson, 1995), RockEval pyrolysis (Talbot & Livingstone, 1989; Tyson, 1995)and biomarker determination (Peters & Moldowan, 1993;Tyson, 1995) provide additional, but more time-consuming means of characterising sedimentary OM.

Although I have emphasised the need to have as exact information as possible about what we analyse, it must also be stressed that any palaeolimnological isotopic study should be supported by good core (or section) descriptions and sedimentological interpretations. There are, unfortunately, still all too many cases of cores being extruded and immediately sliced up for analysis, without so much as a simple lithological log being kept as a record of the stratigraphy. Erosional discontinuities, paleosols, turbidites, condensed sections and many other sedimentological features can introduce isotopic anomalies which may not be easily understood without access to an adequate sedimentological framework for the sequence being studied. A recommended succession of steps from core opening to organic matter isotopic analysis is summarised in Figure 9.

Sample preparation

Figure 9 gives a brief overview of the sample preparation procedure used in our laboratory. One point of note is that drying is carried out at 40 °C, instead of the 80–100 °C that is normal in many laboratories. Experience from organic geochemistry indicates that the lower temperature is preferable to ensure that no volatile components are lost before analysis. Splits from the dry, powdered sample are also used for carbon isotopic analysis and RockEval pyrolysis (Talbot & Livingstone, 1989; Talbot & Lærdal, 2000; Fig. 9), in fact it is our practice to perform the $\delta^{13}C$ analysis first, as %N data from the elemental analyser allows us to estimate how much sample needs to be weighed for the N-isotope determination. As little as 100 μg N are required for analysis.

Mass spectrometery

Determining the N-isotopic composition of sedimentary OM requires that N_2 gas be prepared from the sample. The gas is then fed into a mass spectrometer for analysis. An excellent, comprehensive review of mass spectrometry, and the various sample preparation techniques that may be used for N-isotope analysis, is given in Owens (1987). Attention here will be confined to some of the more pertinent practical aspects of isotopic analysis with particular reference to the system used at UB. As indicated in the Introduction, the adoption of nitrogen isotopes as a standard technique in the earth and biological sciences was hindered by the time-consuming, off-line preparation techniques that most studies required. A few labs have stuck to the original, wet-chemistry sample preparation, feeling

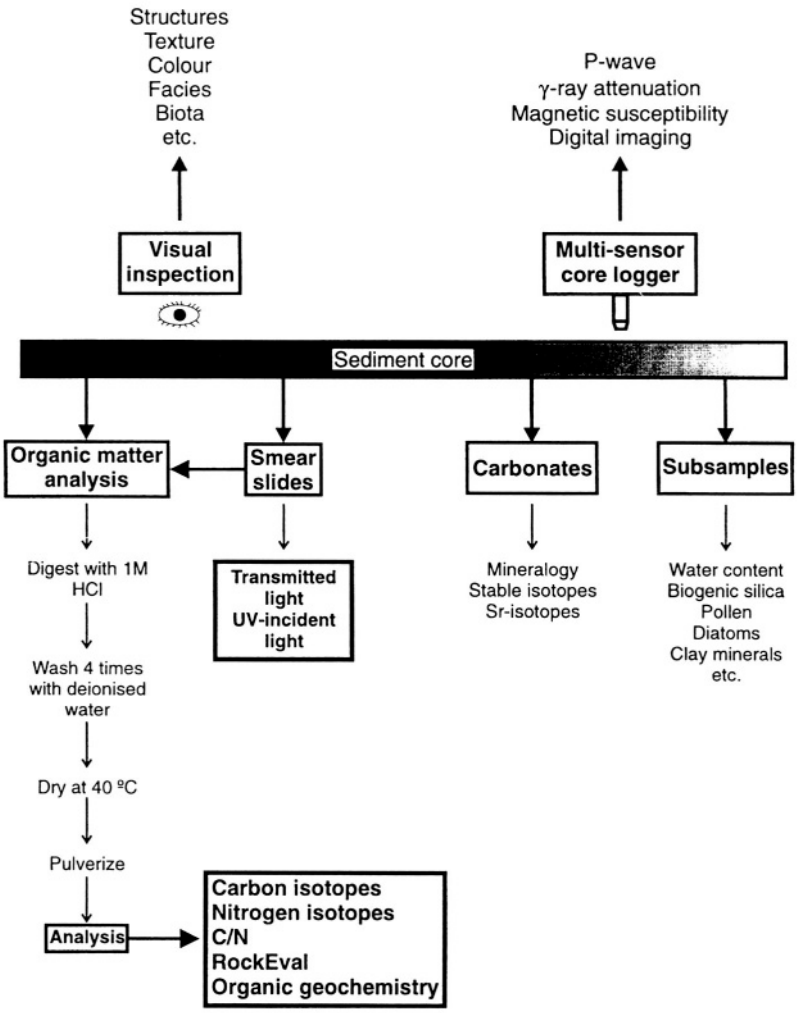


Figure 9. Flow diagram (starting at an idealised sediment core) for the preparation of lacustrine sediment samples for the isotopic analysis of organic matter, emphasising the importance of integrating such studies with a range of other analytical techniques. Based in part on procedures used by the International Decade for the East African Lakes (IDEAL) project (LRC, 1999).

that the offline method provides a more reliable means of monitoring the progress of each sample as it passes through the various stages of preparation and analysis. Most, including the UB lab, have chosen the newer, automated route that takes advantage of the speed and convenience of an online elemental analyser for gas preparation (see below). In doing so it must be stressed that we have not traded expedience for precision. A well-setup elemental analyser-mass spectrometer line yields results that are analytically as good or better than those obtained with offline preparation. It may also avoid some of the undesirable

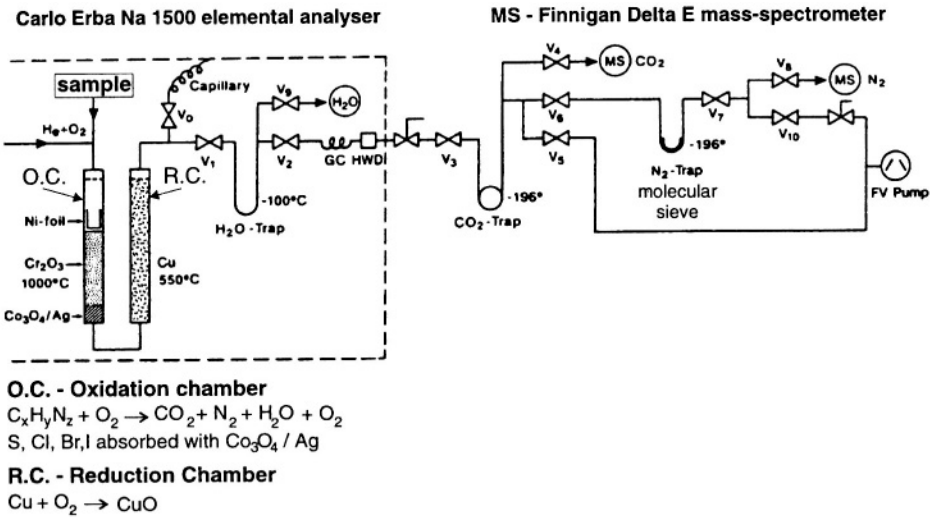


Figure 10. Schematic view of the element analyser — mass spectrometer system used for nitrogen isotopic analyses at the University of Bergen (partially redrawn from Johannessen, 1992).

fractionation effects due to incomplete conversion to N_2 gas that can plague the latter (see Owens, 1987, for details).

The UB system is outlined in Figure 10, and a full description is given in Johannessen (1992). Up to 50 samples are loaded into a carousel which automatically feeds each sample in turn into a Carlo Erba elemental analyser. Here flash combustion takes place at 1700–1800 °C, ensuring quantitative yields of carbon and nitrogen from the OM. As Figure 10 shows, this system is used for producing both CO_2 and N_2 for isotopic analysis, however, for convenience, and to ensure optimum analytical conditions, we have opted to measure only one gas species at a time. Other laboratories have succesfully developed gas separation systems which allow the reliable measurement of $\delta^{13}C$ and $\delta^{15}N$ from the same sample (e.g., Fry et al., 1992). After cleaning, separation of CO_2 and N_2 is performed by an automated trapping device. A critical part of the N line is the molecular sieve, which not only must trap the gas effectively but also release it quantitatively when the N_2 is transferred to the mass spectrometer. If the yield is less than 100%, isotopic fractionation will occur between the released and the retained portions of the gas. The molecular sieve has been a source of trial and frustration for many laboratories. In our case we have settled on a synthetic 5 Å zeolite sieve produced by Alltech Associates, Deerfield, IL, which has proved very reliable. The other major potential source of error is contamination, as any mass spectrometer operator will tell you, there are three problems with N-isotope analysis: "Leaks, leaks and leaks". The apparatus is continually bathed in a N_2-rich atmosphere, so penetration of the system by air can be a major source of error and difficult to detect.

The reproducibility of measurements in our laboratory is typically 0.04–0.08‰ (1σ), depending upon the material used. A variety of international standards are available for interlaboratory comparisons (Nevins, et al., 1985; Böhlke et al., 1993).

Some words of caution

In addition to the inherent complexities of the global nitrogen cycle, and the complications these impose on the interpretation of N-isotope data, there are three aspects of N biogeochemistry which might, in certain circumstances, impact the isotopic record to such a degree that the primary signature becomes distorted. These are: (i) diagenesis, (ii) the presence of inorganic N, and (iii) N released from diatom frustules.

Diagenesis

In common with all other stable isotopic studies, the possibility that the original N-isotope ratios have been altered by diagenetic processes should always be borne in mind. In fact, the potential for diagenetic reworking may be particularly acute in the case of OM N isotopes, because N-rich compounds such as proteins and lipids are among the most labile of the major constituents of living OM and thus tend to decompose relatively rapidly after death. Preferential loss of N is clearly shown by plots of percent nitrogen against depth, which typically show falling N content and rising C/N through the first 5–10 cm below the sediment-water interface (Figs. 8 & 11). It has also been suggested that some loss occurs while OM sinks through the water column, but the interpretation of trap data in this way is often complicated by the presence of zooplankton remains and the effects of interflows and bottom-sediment resuspension (Bernasconi et al., 1997; Ostrom et al., 1998).

If isotope effects are associated with diagenetic N loss, kinetic fractionation considerations suggest that the remaining N ought to be enriched in ^{15}N, i.e. $\delta^{15}N_{om}$ should rise (Macko et al., 1993; Ostrom et al., 1998; see above). Enrichment in ^{15}N has been demonstrated in decomposing marine plankton (Wada, 1980), and similar changes have been recorded in sinking particles (particulate organic nitrogen - PON) collected below the photic zone in the ocean, where in some areas an enrichment of up to 3–7‰ has been measured (e.g., Altabet & François, 1994a, b). Care should be taken in applying oceanic data to lakes, however, due to the longer residence time of marine PON in the water column, a consequence of the more effective turbulent mixing of the surface layer and greater depth of the oceans. The few available limnological data are inconclusive, neither Meyers & Eadie (1993), Hodell & Schelske (1998), nor Ostrom et al. (1998) detected any significant change in the N-isotopic composition of sinking particles from, respectively, Lakes Michigan, Ontario and Superior, and Bernasconi et al. (1997) found a maximum change of only ca. 1‰ over a depth of 69 m in L. Lugano. Neither is there any clear pattern of change within the sediment. No consistent $\delta^{15}N$ trend accompanies the decline in %N below the sediment-water interface. In Lake Victoria (Fig. 8), high $\delta^{15}N$ values occur in the uppermost sediments and decline downcore, probably because of limnological changes (see above), while in L. Superior, Ostrom et al. (1998) record a rise in $\delta^{15}N$ of ca. 1.5‰ downward through the uppermost, oxic part of the sediment column in one core, but another core from a similar setting shows no trend and the data as a whole are inconclusive (Fig. 11). In L. Ontario, however, Hodell & Schelske (op. cit.) suggest that a difference in mean $\delta^{15}N$ of ca. 2‰ between two core sites (Fig. 6) reflects differential loss of ^{14}N from the area with lower sedimentation rate where OM degradation is presumed to be more intense. Rapid burial of sedimented OM, particularly under anoxic conditions, may thus help preserve the composition of the original phytoplankton OM.

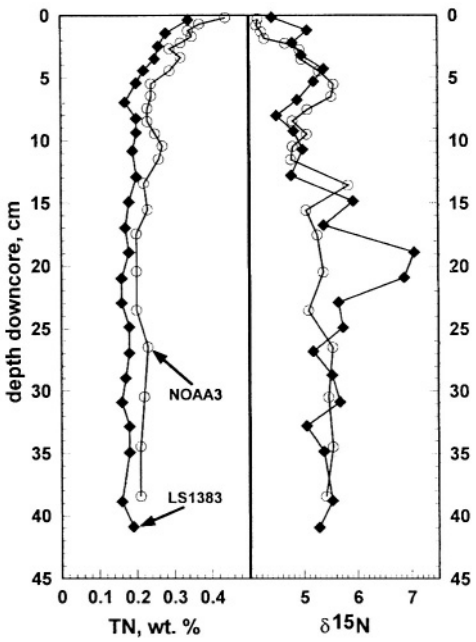


Figure 11. Downcore changes in TN and $\delta^{15}N$ in cores LS1383 and NOAA3 from Lake Superior. TN values fall consistently through the first 6–7 cm below the sediment surface and then stabilise. The tendency for increasing $\delta^{15}N$ values, on the other hand, is reversed at 4–6 cm, suggesting that factors other than diagenesis may contribute to or control the isotopic variations. (Data replotted from Ostrom et al., 1998)

Inorganic nitrogen

Positive ammonium ions are readily adsorbed onto the negatively charged surfaces and interlayers of clay minerals, the affinity with illite being particularly strong, because of the similar cationic radii of ammonium (1.43Å) and potassium (1.33Å) (Bremner, 1965). Thus, ammonium released by the degradation of sediment or soil OM may be retained on the surface of clay minerals, and, as a consequence, some OM-rich lacustrine sediments contain relatively large amounts of inorganically bound N (e.g., Viner, 1975). In pedology it has been normal to distinguish between *exchangeable and fixed* N (Bremner, 1965), but bulk N determination by elemental analyser does not allow the separation of these two. In marine sediments, exchangeable N typically forms only a minor proportion of the total inorganic N (Müller, 1977; Lew, 1981). The presence of inorganic N is easily detected from a plot of %C vs. %N. Figure 12 shows examples where the regression lines for the data do not pass through the origin, but intercept the N axis at a positive value, indicating that N is present in excess of that associated with carbon (i.e. in organic matter). As these C and N analyses were carried out on an elemental analyser from which the liberated N was passed to a mass spectrometer for isotopic analysis, the measured $\delta^{15}N$ value must include a component derived from this inorganically bound N.

The isotopic composition of adsorbed N, and its relationship to the composition of the source OM, have apparently never been investigated. The kinetic fractionation associated

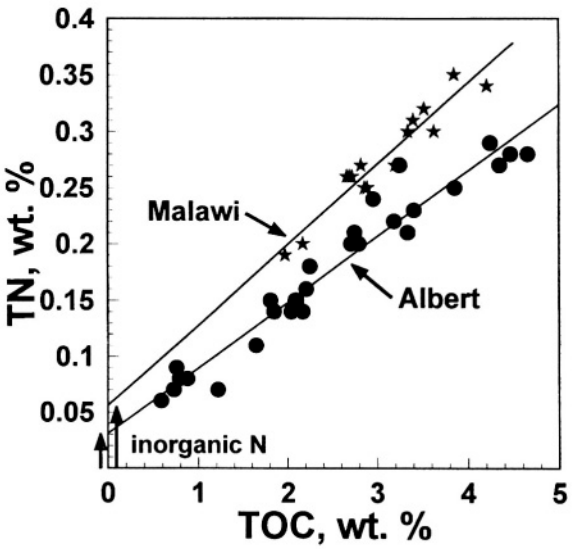


Figure 12. Plots of TOC versus TN for core F from Lake Albert (Beuning et al., 1997) and core M98-2P from Lake Malawi. In both cases the regression lines intercept the TN axis at a positive value, implying that some of the nitrogen is present in a form not associated with organic carbon. This is commonly referred to as *inorganically bound nitrogen*. The value of the N intercept (arrows) can be used to correct the C/N such that it reflects only the organic component of the sediment.

with ammonium formation from decomposing OM is small (Table I); in anoxic marine sediments the $\delta^{15}N$ of porewater ammonia is commonly slightly lower, but within 1-2% *of* the paniculate OM (Fogel & Cifuentes, 1993). Adsorbtion is a physical fractionation effect which discriminates slightly in favour of the heavy isotope (Delwiche & Steyn, 1970), so there may be selective loss of ^{14}N by diffusion of NH_3 out of the sediment, while the clays retain a pool of isotopically heavier nitrogen. However, given the modest fractionations involved, the net effect of inorganic N on measured $\delta^{15}N$ values may be relatively small. Despite these words of cautious optimism, the test for inorganically bound N should be a routine part of any N-isotope study. The mean value of % inorganic N, obtained as shown in Figure 12, can also be used to correct measured C/N values such that they represent only the organic fraction of the sediment. The correction can have significant consequences for our interpretation of the geochemical data (see below).

Diatom nitrogen

Altabet & François (1994a) found that concentrates of cleaned marine diatoms contained sufficient N for isotopic analysis and suggested that this was present as part of the organic template upon which the opaline frustules were constructed. Frustule dissolution during diagenesis could release N into the sediment that differed in composition from cell N. The possible impact of diatom-bound N on the isotopic composition of lacustrine sediments has not been investigated, but as many of these are rich in diatoms, it is an aspect of lacustrine N biogeochemistry that is in urgent need of study.

Some examples

The complexity of the nitrogen biogeochemical cycle, the range of isotope effects and fractionations, and the apparent lack of correlation between theory or culture experiments and the real world, might suggest that N-isotope studies are at best likely to provide ambiguous or even uninterpretable information. While the last-named are certainly possibilities, it also clear that N isotopes may provide unique and important palaeoenvironmental information that could not have been obtained from any other known proxy. There is no doubt in my mind, at least, that N-isotope analyses should be an integral part of any major palaeolimnological study, especially one that involves the analysis of OM-rich sediment. The following section provides some examples of studies of this sort, demonstrating how the isotopic data themselves, or in combination with other sorts of information, can be interpreted.

Lake Bosumtwi, Ghana: the N-isotopic record of a closed, tropical lake

Lake Bosumtwi occupies a ca. 1 m.y. meteorite impact crater in the forest zone of Ghana, West Africa. At present it is a hydrologically closed, moderately alkaline waterbody, but there is evidence of it having been at times both deeper and fresher, and shallower and more saline than it is today (Talbot et al., 1984; Talbot & Johannessen, 1992). The sediments of Lake Bosumtwi are thought to contain one of the best high-resolution archives of the last one million years of tropical environmental change, one reason for this belief being its outstanding OM isotopic record. Figure 13 shows the C- and N-isotopic stratigraphy of a deep and intermediate depth core. The range in δ values is very large — almost 17‰ in the case of $\delta^{15}N$. Some of the variation is due to different mixtures of macrophyte and phytoplanktonic OM, the densely vegetated, steep inner wall of the crater favouring rapid transport of terrestrial plant OM to the lake. The presence of abundant woody and cuticular OM is confirmed by smear-slide and C/N data. However, the high C/N values of modern terrestrial plants and surface sediment particulate OM (26–156, Talbot & Johannessen, 1992) indicates that their contribution to the TON must be modest in comparison to the phytoplankton fraction. Furthermore, as Talbot & Johannessen (1992) emphasise, many of $\delta^{15}N$ values lie outside the range of what can reasonably be expected from land plants, so the observed variations must largely reflect changes in Lake Bosumtwi's N cycle. (The C isotopic record, on the other hand, for the reasons given above, will be more influenced by the terrestrial OM component. Nevertheless, the very high $\delta^{13}C$ values — > -10‰ — must reflect processes within the lake — see Talbot and Johannessen, 1992, for a detailed discussion.)

High $\delta^{15}N$ values (>+ 10‰) characterise much of the late Pleistocene record from 25 to 10 ^{14}C ka BP (Fig. 13). Sedimentological and mineralogical evidence indicate that the lake was shallow and alkaline for much of this period, especially from 18 to 10.5 ^{14}C ka BP. The combination of sediments rich in OM and high pH waters (almost certainly in excess of today's maximum pH of 9.6) would have favoured the production of abundant ammonia and its subsequent loss through volatilisation. The latter involves a strong fractionation effect of ca. 34‰ (Table I) and would lead to the development of lake waters with a very high $\delta^{15}N_{DIN}$. Assimilation of this strongly enriched DIN pool is the likely explanation for the correspondingly high $\delta^{15}N_{om}$ values. An alternative explanation is offered by Meyers & Lallier-Vergès (1999), who suggest that the very high $\delta^{15}N_{om}$ values reflect biological

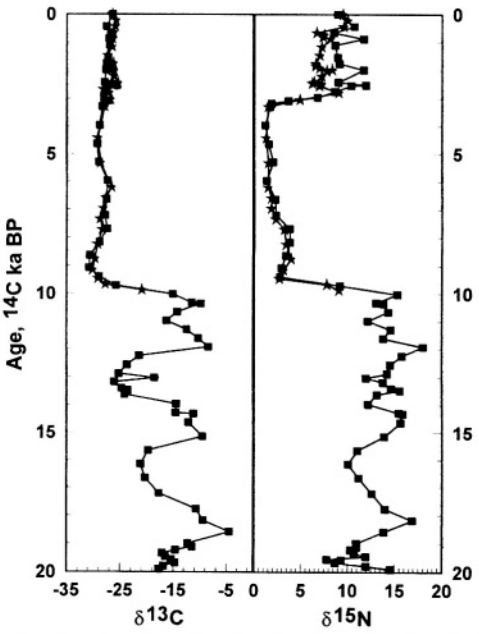


Figure 13. Profiles of $\delta^{13}C$ and $\delta^{15}N$ from cores B-6/B-7 (squares) and B-2 (stars) from Lake Bosumtwi, Ghana (Talbot et al., 1984; Talbot & Johannessen, 1992). The abrupt transition to low $\delta^{15}N$ values at 10 ka reflects the onset of a stable stratification regime which favoured the dominance of the N-fixing cyanobacteria *Anabaena*. This period terminated almost as abruptly at ca. 3.3 ka when deeper mixing increased the availablity of dissolved N, allowing a shift in the phytoplankton flora to those utilising combined N. The absence of any corresponding variation in the $\delta^{13}C$ profile at this time is because there was no significant change in either DIC availabilty or the C_3/C_4 of the terrestrial vegetation.

drawdown of a limited DIN pool, a consequence of reduced flushing of soil N during this period of aridity. However, if soil productivity were of critical importance, it might be expected that a change to lower $\delta^{15}N$ would have accompanied the onset of forest expansion at ca. 14 ^{14}C ka BP (Talbot & Johannessen, 1992).

At around 10 ka, $\delta^{15}N_{om}$ declined abruptly to values of +1 to +3‰ and remained low until ca. 3.3 ka, when there was an almost equally abrupt rise (Fig. 13). The interval of low $\delta^{15}N$ coincides with a unit of dark blue-black, very homogeneous mud. On their own, $\delta^{15}N$ values like these do not have a unique explanation; they might be due to increased N-fixing cyanobacterial remains in the sediment, but they could also be due to phytoplankton that grew in a lake with an abundant supply of DIN. Neither are the carbon isotopic data of much assistance, $\delta^{13}C_{om}$ values of –30 to –25‰, being typical of many aquatic and terrestrial plants. It is here that the smear slides show their worth, for throughout this interval the sedimentary OM fraction is characterised by abundant well-preserved filaments of the cyanobacteria *Anabaena,* a well-known N-fixing member of the phytoplankton flora in many African lakes. It can thus be confidently concluded that the low $\delta^{15}N$ values must be due to a dominance of cyanobacteria in the early to mid-Holocene phytoplankton of Lake Bosumtwi. This, in turn, has important palaeoenvironmental implications. As these

cyanobacteria tend to flourish when water column stability is at a maximum, their dominance at this time must reflect minimal vertical mixing, probably because of a very uniform climate, with little seasonal contrast and low wind stress.

It is also important to note that, while the $\delta^{13}C$ record followed that of the N isotopes at 10 ka, it did not register a corresponding rise at 3.3ka. A return to deeper, probably seasonal mixing at this time had dramatic consequences for the phytoplankton flora, allowing the N-fixers to be replaced by forms adapted to assimilating dissolved nitrate and ammonium, but carbon assimilation by the two groups is similar, hence the lack of change in $\delta^{13}C$.

Middendorf Lake: nitrogen cycling during the mid-Holocene forest-tundra transition in arctic Russia

Middendorf Lake is a very small (ca. 100 x 90m) waterbody in the tundra of northern Russia, ca. 70km northwest of the modern tree-line. Wolfe et al. (1999) have described elemental and carbon and nitrogen isotopic variations in a 2.2 m-long core which spans approximately the last 4.4 ka of the lake's history. Palynological evidence from the same core indicates that a rapid but major vegetation change occurred in the region around ca. 4.0 ^{14}C ka BP. At this time the forest which had covered the area during the mid-Holocene was replaced by treeless tundra similar to that bordering the lake today. The change was primarily a response to climatic cooling and can be expected to have had a significant impact upon the Middendorf Lake's nitrogen cycle, due to its impact upon the rate of N mineralisation in catchment soils, reduced productivity and seasonal fluctuations in N availability (Wolfe et al., 1999). Organic production in the present arctic climate is probably restricted to brief phytoplankton blooms, the lake supporting no macrophyte growth.

Figure 14 shows the core's geochemical stratigraphy. The N-isotopic composition changes only gradually, but is characterised by higher $\delta^{15}N$ in the lower part of the section. The other parameters show more rapid changes at the forest-tundra transition with TOC, TN and C/N values significantly higher and $\delta^{13}C_{om}$ values significantly lower in the forest interval. Wolfe et al. provide no scatter plots of their data (cf., for example, Tyson, 1995; Talbot & Lærdal, 2000), but the utility of the latter in the identification of compositional groupings is well illustrated by Figures 15A-D which indicate that their are two distinct OM populations, one characterising the forest interval, the other the tundra. Figure 15A also suggests that sediments deposited during the forest period contain some inorganically bound nitrogen, presumably because of the presence of clays formed under the relatively mild, humid climatic conditions at that time, and abundant ammonia production in the highly OM-rich sediments. The importance of correcting for the presence of bound N is well-illustrated in Figures 15C & D, where both the uncorrected and corrected C/N values are shown. When the latter are used, much of the apparent scatter in the C/N versus $\delta^{15}N$ plot disappears and a regular trend become apparent. The corrected data also bring out even more clearly the separation between the forest- and tundra-period sediments.

Wolfe et al. (1999) consider a number of alternative scenarios to explain the differences in $\delta^{15}N$ between the forest and tundra intervals, including: (1) varying supply of allochthonous OM, (2) changes in trophic status, (3) changes in DIN cycling within

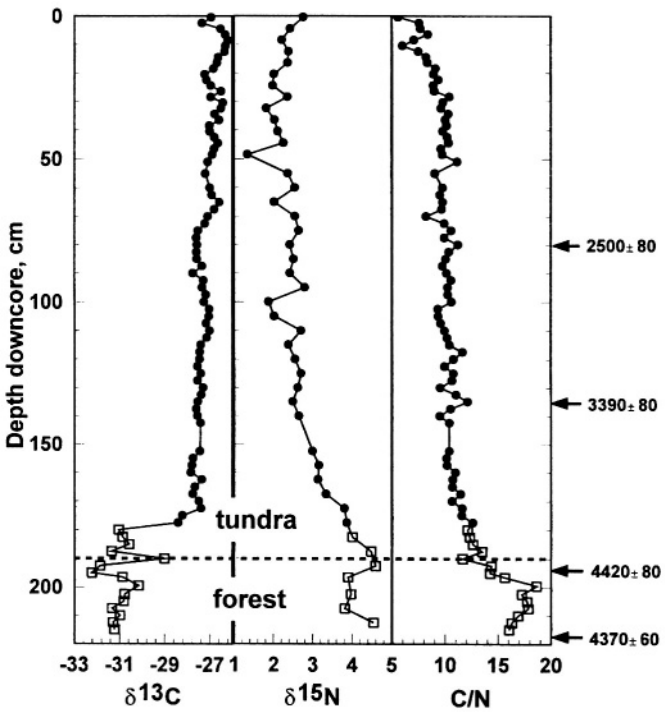


Figure 14. Isotopic and C/N profiles for a core from Middendorf Lake, artic Russia. Dates are AMS ^{14}C age determinations (Wolfe et al., 1999). A major limnological change evidently followed the transition from forest to tundra conditions. The change in symbols indicates the limnological transition as revealed by compositional groupings in the plots of isotopic and elemental data shown in Figure 15. (Data replotted from Wolfe et al., 1999. See text for further discussion).

the lake, and (4) varying rates of soil N production. Terrestrial plant macrofossils are relatively abundant, and the corrected C/N values for sediments deposited during the forest interval (Fig. 15) are certainly consistent with the presence of some higher plant remains, predominantly of cuticular origin. The inverse relationship between $\delta^{15}N$ and C/N (Fig. 15) suggests that the autochthonous OM is the more ^{15}N-enriched of the two components. As an explanation for these relatively high $\delta^{15}N$ values, Wolfe et al. suggest that, when the catchment was forest covered, deeper and more OM-rich soils with relatively higher rates of biogeochemical reworking (due to the moist, mild climate) led to isotopic enrichment of the soil N, a relationship that is also observed in modern forest soils (Nadelhoffer & Fry, 1988). Nitrate leached from these soils and assimilated by lake phytoplankton would lead to elevated $\delta^{15}N_{om}$ values. An abundance of isotopically light, soil-derived DIC may in part explain the very low $\delta^{13}C$ values of this OM (Figs. 14 & 15B). The gradual decline in $\delta^{15}N$ through the tundra period probably reflects a decreasing rate of soil OM decomposition, reduced flux of soil nitrate from the catchment, and an increase in the relative importance of atmospheric N_2 as a source of nitrogen in the lake.

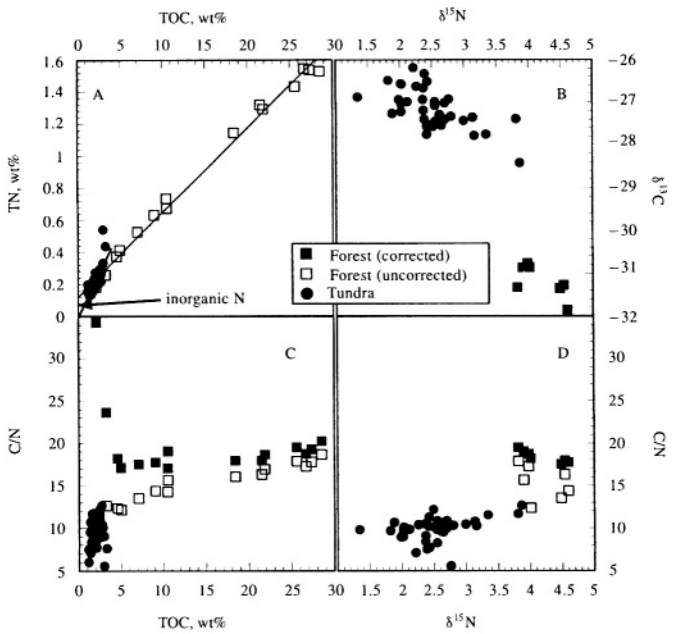


Figure 15. Crossplots of elemental and isotopic data from Middendorf Lake; symbols are the same as those in Figure 14 (data replotted from Wolfe et al., 1999). Note that the regression line (A) for the forest period indicates the presence of inorganically bound N in these sediments, whereas that for the tundra period passes through the origin. The N intercept for the forest data has been used to correct the C/N values plotted in (C) and (D).

Lake Victoria: the filling of a giant lake

Lake Victoria is the largest in area of all the African lakes, but despite its great size has a maximum depth of only 69 m. Around 80% of the total inflow to the lake is by direct precipitation onto the lake surface (Crul, 1995), a hydrology that makes it particularly sensitive to variations in precipitation/evaporation (P/E) balance. Although the lake is known to have responded rapidly to historic changes in rainfall, it nevertheless came as a surprise when sediment cores in combination with the first high-resolution seismic profiles revealed the presence of a basin-wide discontinuity (paleosol) formed when the lake was completely desiccated in the Late Pleistocene (Johnson et al., 1996). Deposits above the paleosol thus record the refilling of the basin and the establishment of the present lake. Sediments from the deepest part of the basin are highly organic-rich and dominated by phytoplankton remains, providing ideal material for a N-isotope study (Talbot & Lærdal, 2000).

Figure 16 shows the TOC, TN, $\delta^{13}C$ and $\delta^{15}N$ profiles for sediments above the paleosol in core V95-2P, from a depth of 68 m in the east-central basin of Lake Victoria. The N-isotopic record can be subdivided into three sections: (i) relatively low values just above the palaeosol surface, followed by a period of rising $\delta^{15}N$ from 15.2-14 cal. ka BP, (ii) an abrupt decline in δ values from 14-13.6ka, and (iii), from 13.6ka to the present, a gradual decline in $\delta^{15}N$.

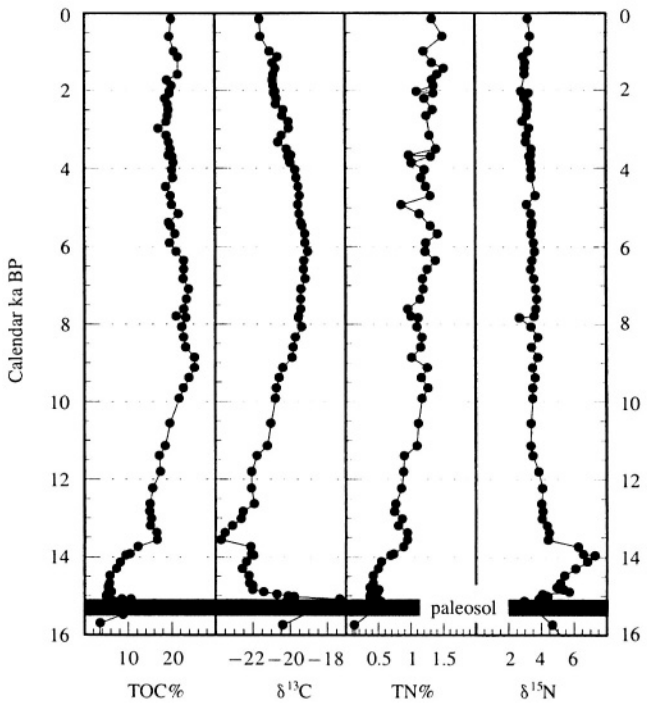


Figure 16. Elemental and isotopic profiles from core V95-2P, Lake Victoria. The paleosol is basin-wide and records complete desiccation of the lake in the Late Pleistocene (Johnson et al., 1996). The main period of basin filling is represented by the sharply rising trend in $\delta^{15}N$ until just after 14 ka. The relatively low and gradually decling $\delta^{15}N$ values from the terminal Pleistocene until today, and their negative correlation with N content, are interpreted as evidence for a dominant role for N-fixation in the lake's N cycle (Talbot & Lærdal, 2000).

Sediments just above the exposure surface are relatively rich in macrophyte remains and the low $\delta^{15}N$ values are thought to reflect the presence of OM from marginal swamp vegetation drowned by the rising lake. Talbot & Lærdal (2000) measured $\delta^{15}N$ down to −1.07‰ in the macrophyte sludge from a modern Lake Victoria swamp, and Kendall (personal communication, 1999) has found δ values as low as – 10‰ in modern Everglades (Florida, USA) macrophytes. Swamps are typically N-rich environments and those around Lake Victoria may be the sites of active N fixation (Gaudet, 1976). Thus the low isotopic values may in part reflect fixation of atmospheric N, but the general abundance of DIN may also allow kinetic isotopic effects to operate close to their maximum during N assimilation by the macrophytes. Rising $\delta^{15}N$ during the subsequent phase of (i) is thought to be a response to the initial flooding and filling of the Lake Victoria basin (Talbot & Lædal, 2000). As the lake transgressed marginal swamps and a vegetated landscape, both would have released large amounts of nutrients to the waterbody, stimulating very high rates of primary productivity. Assimilation and burial of ^{14}N by the flourishing phytoplankton are probably one reason for the rising $\delta^{15}N$ trend. In addition, the large amounts of OM released to the lake from the flooded landscape probably led to seasonal or more prolonged periods of

bottom-water anoxia; similar effects are commonly observed during the early life of many human-made lakes. Under these conditions, denitrification probably had a major impact on the lake's N-isotope budget, selective loss of $^{14}N_2$ to the atmosphere reinforcing the tendency for the DIN to become isotopically enriched. The falling trend in $\delta^{13}C$ supports the inference that the lake at this time was strongly influenced by the land it was transgressing. Flooded soils, and rotting swamp and terrestrial plants, would have provided an abundant supply of ^{13}C-depleted CO_2 to the water column, favouring the production of isotopically light phytoplankton OM.

The abrupt reversal in $\delta^{15}N$, and equally sharp fall in $\delta^{13}C$ values, during period (ii) indicates a dramatic change in N- and C-cycling within the lake. Together they suggest increased availability of DIN and DIC in surface waters, most probably due to a period of deep mixing (Talbot & Lærdal, 2000). More effective recycling of N and C released by om mineralisation would have raised $[DIN]_{aq}$ and $[DIC]_{aq}$ and returned the lighter isotopes preferentially assimilated during primary production to the surface. Both features would favour the production of new OM with low $\delta^{13}C$ and $\delta^{15}N$ values. Deep-mixing was related to a regional climatic event, most probably an intensification in surface wind stress (Talbot & Lærdal, 2000).

Relatively low and gradually declining $\delta^{15}N$ values for the period from 11.6 ka to the present suggest yet another change in the lake's N cycle. The trend is independent of that shown by the $\delta^{13}C$ record (Fig. 16), and is negatively correlated with sediment TN (Talbot & Lærdal, 2000). Furthermore, both the biogenic silica and diatom assemblage profiles show large variations (Stager & Johnson, 2000), none of which are reflected in the $\delta^{15}N$ record. The uniformity of the $\delta^{15}N$ profile, and its lack of correlation with any feature that might be related to N cycling within Lake Victoria, led Talbot & Lærdal (2000) to conclude that the nitrogen reservoir must be infinitely large in comparison to the lake's internal N pools. The only reservoir of this size is the atmosphere, so Talbot & Lærdal (2000) suggest that Lake Victoria's N cycle since the late Pleistocene has been dominated by N-fixation. The reason for this switch was probably also related to basin flooding. Once the main period of transgression was over, the supply of N from drowned soils and vegetation must have declined and eventually become insignificant. With limited recycling of N from OM mineralisation (the very high TOC values indicate effective OM burial and preservation), high rates of primary productivity could only have been maintained by utilisation of the atmospheric nitrogen pool.

Lake Tanganyika: lake level changes and mixing regimes in a tropical rift lake

Lake Tanganyika is the largest and deepest of the East African rift valley lakes. It is meromictic, with a large, anoxic hypolimnion (Coulter, 1991). Unlike Lake Victoria, Tanganyika did not dry out during the Late Pleistocene, but did undergo major changes in water level, the surface being as much as 250 m below present overflow level around the time of the Last Glacial Maximum (Cohen et al., 1997). Although meromictic, some vertical mixing occurs today, mainly driven by wind-induced surface currents, enhanced by evaporative cooling (Coulter & Spigel, 1991). Seasonal upwelling is particularly marked in the southern basin, where the southerly trade winds push surface waters northward during the northern hemisphere summer (Coulter & Spigel, 1991). Upwelling returns nutrients, including DIN, to surface

waters, stimulating high levels of productivity (Hecky et al., 1991). When the southerly trades slacken, the stratification stabilises and is particularly marked during December-May. At this time DIN concentrations become extremely low and the flora is dominated by N-fixing cyanobacteria, instead of the diatoms and chrysophytes which characterise the mixing period (Hecky & Kling, 1981, 1987). It can thus be anticipated that long-term changes in mixing regime in the southern basin, particularly the occurrence of periods of persistent stratification, might be recorded by variations in the N-isotopic composition of the sedimentary OM due to different phytoplankton flora. Such changes would in turn reflect variations in regional climate.

Figure 17 shows the isotopic record from a core taken at a depth of 140 m on the western flank of the southern basin (Tiercelin & Mondeguer, 1991). The Late Pleistocene section is marked by an erosional disconformity, formed when the lake fell below the level of the core site. It was reflooded during the subsequent transgression at ca. 15.2 ^{14}C ka BP. The top of the core was unfortunately lost during recovery, the section terminating at ca. 3.4 ka, but it nevertheless preserves an excellent record of the terminal Pleistocene to mid-Holocene history of the southern basin.

The section above the disconformity shows a gradual rise in δ^{15}N, which culminates in a marked peak at ca. 11.3 ka. Its coincidence with a C/N minimum (Fig. 17) and high Hydrogen Index values (Niels-Bo Jensen, personal communication) suggests that the δ^{15}N peak may, like the maximum in Lake Victoria (Fig. 16), be due to high phytoplankton productivity. Above here the δ^{15}N values remain relatively constant until ca. 7.0 ka, when they begin to decline. The mid-Holocene section also stands out as different from the underlying deposits in a plot of TOC versus C/N (Fig. 17B). δ^{15}N values of less than 0‰ have two possible explanations, either there was an abundance of DIN, allowing the kinetic fractionation involved with nitrate and ammonium assimilation to operate to its full effect, or DIN concentrations were consistently low, favouring a dominance of N-fixing cyanobacteria with low δ^{15}N. These two alternatives have very different implications for the state of the southern end of Lake Tanganyika during the mid-Holocene. Conditions favouring the former would depend upon vertical mixing maintaining a continuous supply of nutrients to the epilimnion, as François et al. (1996) have suggested as an explanation for seasonally low $\delta^{15}N_{om}$ values in Lake Malawi. Low DIN concentrations, on the other hand, would imply prolonged stable stratification with very limited vertical mixing, as happens seasonally in modern Lake Tanganyika. In common with Lake Bosumtwi (see above), the corresponding δ^{13}C data are not definitive, and the smear slides reveal only rare traces of possible filamentous blue-green algae. Decisive supporting evidence is here provided by the elemental data. Figures 17B and C show that samples with a δ^{15}N of >0.5‰ have a positive correlation with C/N, and negative correlation between C/N and TOC, in contrast to the rest of the post-discontinuity samples, and phytoplankton-dominated OM in general (Talbot & Lærdal, 2000; Talbot, unpublished data). Cyanobacteria have a higher N content than other phytoplankton (Gu & Alexander, 1993), the greater the proportion of cyanobacterial remains present, the lower the C/N and δ^{15}N of the bulk sediment. The Tanganyika samples must therefore contain a significant OM fraction derived from these organisms, a conclusion that is also supported by biomarker evidence (Niels-Bo Jensen, pers. comm.). Note that the latter merely demonstrates the presence of compounds characteristic of cyanobacteria, it is the isotopic evidence that confirms these were the dominant component of the phytoplankton. The mid-Holocene in the south basin of Lake Tanganyika thus seems to have been a period of

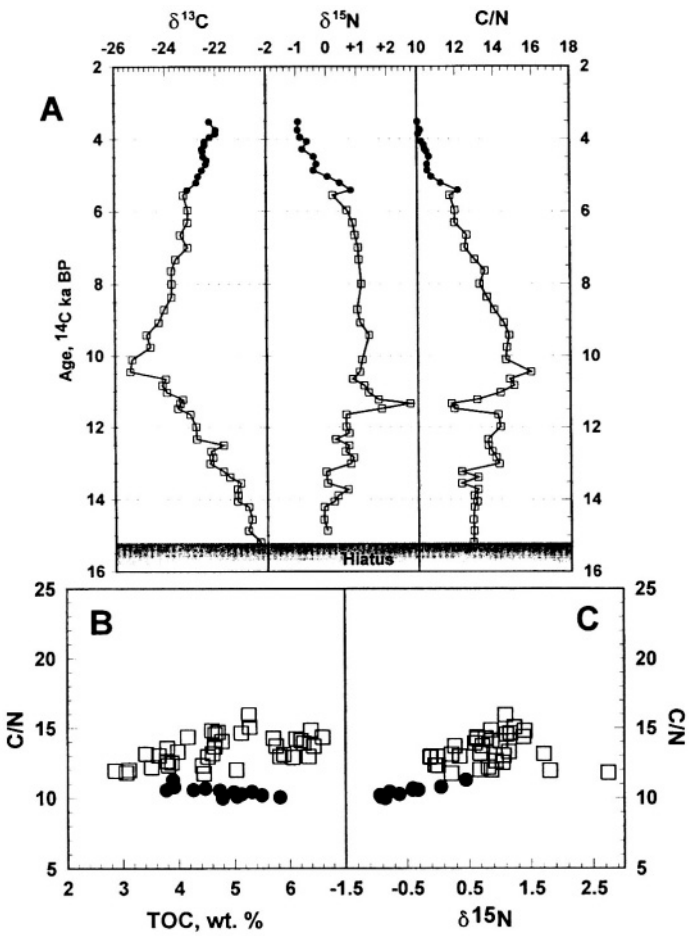


Figure 17. Isotopic and elemental data for core MPU 3 from the southern basin of Lake Tanganyika (Tiercelin & Mondeguer, 1991). The hiatus formed when the lake fell below the level of the core site (140 m) during the Late Pleistocene. Plots (B) and (C) show how samples from the mid-Holocene section (circles) stand out in terms of both their elemental and isotopic composition, probably because of a dominance of N-fixing cyanobacteria. (Data replotted from Jensen, in prep.)

prolonged water column stability, implying greatly reduced southerly trade wind intensities at that time, a finding that is in keeping with other proxy evidence for changes in the regional monsoonal wind systems (Sirocko, 1997; Schulz et al., 1998).

Lake Baikal: differentiating turbidites from other deposits in a mid-latitude rift lake

Lake Baikal is the oldest and deepest lake in the world, with a maximum depth of 1637 m. It is situated in southern Siberia and subject to a mid-latitude continental climate with

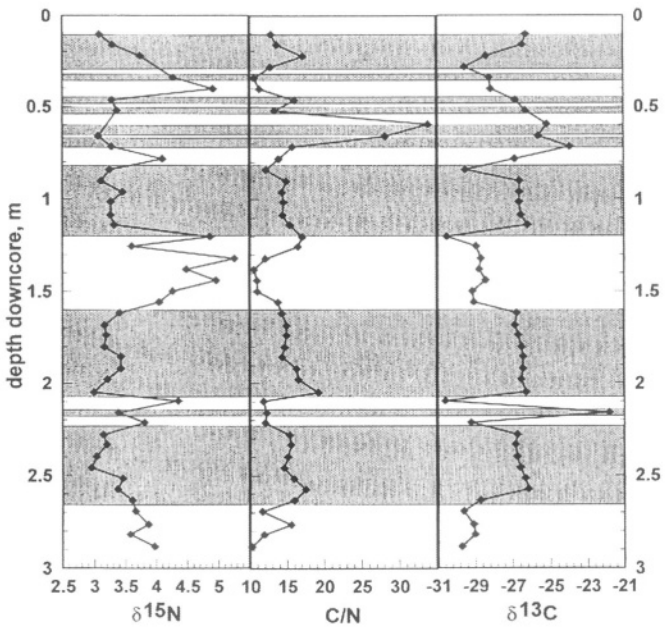


Figure 18. Isotopic and elemental data for core VER92/1-St-10-GC2 from Lake Baikal, the shaded zones are sections dominated by turbidites (data replotted from Yoshii et al., 1997).

strongly contrasting seasons ranging from frigid winters to hot summers. Winter cooling leads to annual overturn of the water column, thus, in contrast to the deep East African rift lakes, Baikal has oxygenated bottom waters even in the deepest basin. Geochemical logs (Fig. 18) of a core taken at a depth of 992m in the central part of the Northern Basin (Yoshii et al., 1997) show that periods with relatively low and invariant $\delta^{15}N$ (+3 to 3.5‰) alternated with intervals when $\delta^{15}N$ vaied significantly and was generally >+3.5‰. Crossplots of some of the geochemical parameters, notably $\delta^{13}C$ versus $\delta^{15}N$ (Fig. 19B), reveal that the data form two separate populations, one having $\delta^{13}C$ values that are mainly less than –27‰ ($\delta^{15}N > 3.5‰$), the other with $\delta^{13}C > -27‰$ ($\delta^{15}N < 3.5‰$). The distribution of the latter group coincides with turbidite units (Fig. 18), so their distinctive composition is presumed to reflect a dominance of allochthonous OM. This may in part be of terrestrial origin (Yoshii et al., 1997), but only the compositional outliers have C/N values which suggest the presence of abundant woody material (confirmed visually in the case of the sample with the highest C/N — Yoshii et al., 1997, p. 280; Fig. 19A & C). The relatively low C/N of the rest of the turbidites (mean 13.4) indicates a dominance of phytoplankton or phytoplankton plus cuticular remains. This, together with their relatively homogeneous isotopic composition, suggests that the turbidites may be derived from the slumping of shallower water lacustrine deposits, rather than deltaic sediments where woody and degraded plant material should be abundant. Smear slides might have provided decisive information on the source of the OM.

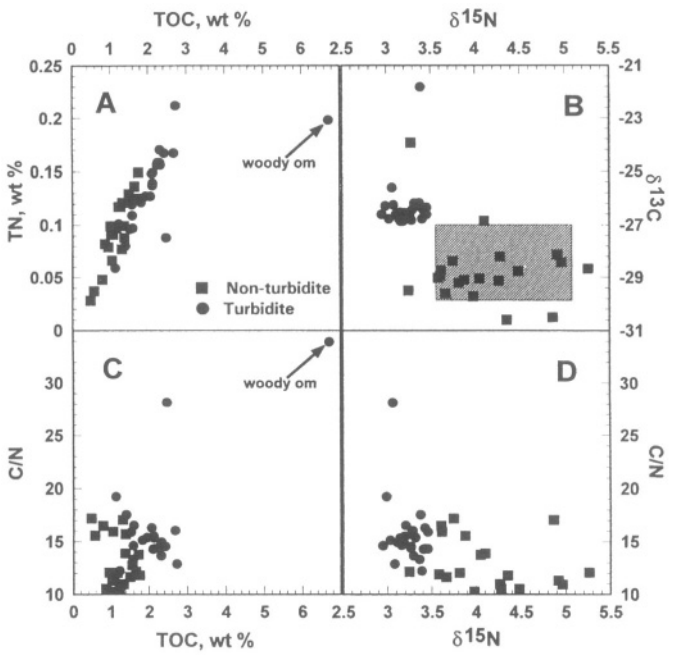


Figure 19. Crossplots of elemental and isotopic data from VER92/1-St-10-GC2, Lake Baikal. The relatively homogeneous composition (A–D) and low C/N (A, C) of most of the turbidite samples suggests that the dominant OM in these is of aquatic origin. The shaded rectangle in (B) shows the range in composition of modern phytoplankton from the lake (data from Yoshii et al., 1999)

The non-turbidite intervals have lower C/N (mean 12) and a larger spread of $\delta^{15}N$ and $\delta^{13}C$ values. However, these fall within the compositional range of modern phytoplankton from the lake (Yoshii et al., 1997, 1999; Fig. 19B), suggesting that the OM is largely of autochthonous origin. Yoshii et al (1997) note that there is an inverse correlation between $\delta^{15}N$ and C/N (Fig. 19D), indicating that the phytoplankton fraction is probably isotopically heavier than the average allochthonous OM. The reason for this may be the impact of denitrification on the N-isotope budget (Yoshii et al., 1997), or other aspects of the lake's N cycle.

Closing remarks

This chapter has hopefully given the reader a summary of what nitrogen isotopic studies have to offer palaeolimnology. It should also have become apparent that, while N-isotope data can provide decisive information on past limnological conditions, their interpretation is in many instances dependent upon supporting evidence provided by carbon isotopes, elemental analyses, petrographic observations or other types of information. Integrated studies of this sort lie at the heart of modern palaeolimnology. Looking to the future, the most exciting developments will probably occur in the growing field of compound-specific isotope studies (Hayes et al., 1990; Macko et al., 1993), where individual organic molecules

are extracted from the sediment for isotopic analysis. As some molecules can be related to specific groups of organisms, for example diatoms or green algae, their analysis can potentially provide very precise information on one part of the water column, eliminating the problems inherent in the interpretation of analyses based on bulk samples of mixed origin. Carbon-isotope molecular-scale studies are already having an impact on palaeolimnology (e.g., Huang et al., 1995, 1999); the writer knows of no corresponding studies based on N isotopes, probably because of the technical difficulties presented by the much lower concentration of N in most sediments, but it is almost certainly only a matter of time before these are overcome.

Summary

Nitrogen is a key nutrient, of fundamental importance to all primary producers. In lacustrine ecosystems its availability is intimately related to limnological, sedimentological and climatic conditions in the lake and its catchment; knowledge of N-cycling in ancient lakes can thus provide unique palaeolimnological information. Studies of the stable N-isotopic composition of sedimentary organic matter provide one of the principal means of gaining insight into past N cycles. In lakes, such cycles are complex, with several potential sources and sinks. Nitrogen is present in a number of forms and in several oxidation states. Isotopic fractionation occurs between the various N compounds, and in the biochemical processes involved in N assimilation by primary producers and other organisms. These isotopic differences are preserved with little or no change in sedimentary OM and are the basis of N-isotope biogeochemistry. Modern mass spectrometers, particularly if on-line to an element analyser, provide a rapid and precise means of determining the isotopic composition of organically bound N and should eventually lead to routine use of the technique in palaeolimnology.

Nitrogen-isotope analysis has a wide range of applications in the study of lacustrine sediments. In particular, it can provide information on N and OM sources, on past mixing regimes, the history of nutrient loading (eutrophication) and other changes in water chemistry. It may also yield insight into catchment changes which impact a lakes N cycle. However, although N-isotope investigations are a powerful tool in their own right, it is also clear that in many instances they are even more effective when carried out as part of a multiproxy study. Other sorts of data may be of critical importance when the isotopic results are ambiguous. Future technical advances should allow the analysis of significantly smaller samples and eventually open the way for the widespread application of compound-specific N-isotope analysis, a field of study with tremendous palaeolimnological potential.

Acknowledgments

This review would not have been possible without the help and inspiration provided by Tine Lærdal, Mizzi Filippi and Niels Bo Jensen. All three are thanked for several years of fruitful collaboration and for valuable comments on earlier versions of this manuscript. Financial support for some of the work presented here has been provided by the Norwegian Research Council, Elf Norge, and NSF, via its support of the IDEAL project. Brent Wolfe

is thanked for providing the raw data from his study of Middendorf Lake. Editors Bill Last and John Smol are gratefully acknowledged for asking me to contribute this chapter, and, together with an anonymous referee, for helpful reviews of the penultimate version.

References

Altabet, M. A. & R. François, 1994a. The use of nitrogen isotopic ratio for reconstruction of past changes in surface ocean nutrient utilization. In Zahn, R., T. F. Pedersen, M. A. Kaminski & L. Labeyrie (eds.) Carbon Cycling in the Glacial Ocean: Constraints on the Ocean's Role in Global Change. Springer-Verlag, Berlin: 281–306.

Altabet, M. A. & R. François, 1994b. Sedimentary nitrogen isotopic ratio as a recorder for surface ocean nitrate utilization. Global Biogeochem. Cycles 8: 103–116.

Arthur, M. A., T. F. Anderson, I. R. Kaplan, J. Veizer & L. S. Land, 1983. Stable Isotopes in Sedimentary Geology. SEPM Short Course 10, 435 pp.

Bernasconi, S. M., A. Barbieri & M. Simona, 1997. Carbon and nitrogen isotope variations in sedimenting organic matter in Lake Lugano. Limnol. Oceanogr. 42: 1755–1765.

Beuning, K. R. M., M. R. Talbot & K. Kelts, 1997. A revised 30,000-year paleoclimatic record and paleohydrologic history of Lake Albert, East Africa. Palaeogeogr. Palaeoclim. Palaeoecol. 136: 259–279.

Blackburn, T. H., 1983. The microbial nitrogen cycle. In Krumbein, W. E. (ed.) Microbial Geochemistry. Blackwell, Oxford: 63–89.

Böhlke, J. K., C. J. Gwinn & T. B. Coplen, 1993. New reference materials for nitrogen-isotope measurements. Geostandards Newsletter 17: 159–164.

Bootsma, H., 1999. Water quality research on Lake Malawi/Nyasa. IDEAL Bulletin, summer: 4–5.

Bootsma. H. A., M. J. Bootsma & R. E. Hecky, 1996. The chemical composition of precipitation and its significance to the nutrient budget of Lake Malawi. In Johnson, T. C. & E. O. Odada (eds.) The Limnology, Climatology and Paleoclimatology of the East African Lakes. Gordon and Breach, Amsterdam: 251–265.

Bootsma, H. A. & R. E. Hecky, 1993. Conservation of the African great lakes: A limnological perspective. Conservation Biol. 7: 644–656.

Bremner, J. M., 1965. Inorganic forms of nitrogen. In Black, C. A. (ed.) Methods of Soil Analysis, Part 2. American Society of Agronomy, Wisconsin: 1238–1255.

Brenner, M..T. J. Whitmore, J.H.Curtis, D. A. Hodell & C. L. Schelske, 1999. Stable isotope ($\delta^{13}C$ and $\delta^{15}N$) signatures of sedimented organic matter as indicators of historic lake trophic state. J. Paleolim. 22:205–221.

Cohen, A. S., K.-E. Lezzar, I. J.Tiercelin & M. Soreghan, 1997. New palaeogeographic and lake-level reconstructions of Lake Tanganyika: implications for tectonic, climatic and biological evolution in a rift lake. Basin Res. 9: 107–132.

Collister, J. W. & J. M. Hayes, 1991. A preliminary study of the carbon and nitrogen isotope biogeochemistry of lacustrine sedimentary rocks from the Green River Formation, Wyoming, Utah and Colorado. U.S.G.S. Bull. 1973-A-G: C1-C16.

Coulter, G. W. & R. H. Spigel, 1991. Hydrodynamics. In Coulter, G. W. (ed.) Lake Tanganyika and its Life. Oxford University Press, Oxford: 49–75.

Crul, R. C. M., 1995. Limnology and Hydrology of Lake Victoria. Studies and Reports in Hydrology — Comprehensive and Comparative Study of Great Lakes. UNESCO/IHP - IV Project M-5.1, UNESCO: 1–79.

Delwiche, C. C. & P. L. Steyn, 1970. Nitrogen isotope fractionation in soils and microbial reactions. Envir. Sci. Technol. 4: 929–935.

Estep, M. L. F. & S. Vigg, 1985. Stable carbon and nitrogen isotope tracers of trophic dynamics in natural populations and fisheries of the Lahontan lake system, Nevada. Can. J. Fish. Aquat. Sci. 42: 1712–1719.

Fogel, M. L. & L. A. Cifuentes, 1993. Isotope fractionation during primary production. In Engel, M. H. & S. A. Macko (eds.) Organic Geochemistry, Principles and Applications. Plenum, New York: 73–98.

François, R., C. H. Pilskaln & M. A. Altabet, 1996. Seasonal variation in the nitrogen isotopic composition of sediment trap materials collected in Lake Malawi. In Johnson, T. C. & E. O. Odada (eds.) The Limnology, Climatology and Paleoclimatology of the East African Lakes. Gordon and Breach, Amsterdam: 241–250.

Fry, B., W. Brand, F. J. Mersch, K. Tholke & R. Garritt, 1992. Automated analysis system for coupled $\delta^{13}C$ and $\delta^{15}N$ measurements. Analyt. Chem. 64: 288–291.

Goericke, R., J. P. Montoya & B. Fry, 1994. Physiology of isotopic fractionation in algae and cyanobacteria. In Lajtha, K. & R. H. Michener (eds.) Stable Isotopes in Ecology and Environmental Science. Blackwell, Oxford: 187–221.

Gu, B. & V. Alexander, 1993. Estimation of N_2 fixation based on differences in the natural abundance of ^{15}N among freshwater N2-fixing and non-N_2-fixing algae. Oecologia 96: 43–18.

Gu, B. & V. Alexander, 1996. Stable carbon isotope evidence for atmospheric CO_2 uptake by cyanobacterial surface scums in a eutrophic lake. Appl. and Envir. Microbiol. 62: 1803–1804.

Gu, B., C. L. Schelske & M. Brenner, 1996. Relationship between sediment and plankton isotope ratios ($\delta^{13}C$ and $\delta^{15}N$) and primary productivity in Florida lakes. Can. J. Fish. Aquat. Sci. 53: 875–883.

Handley, L. L. & J. A. Raven, 1992. The use of natural abundance of nitrogen isotopes in plant physiology and ecology. Plant Cell Environ. 15: 965–985.

Hayes, J. M., K. H. Freeman, B. N. Popp & C. H. Hoham, 1990. Compound-specific isotope analysis: A novel tool for reconstruction of ancient biogeochemical processes. Org. Geochem. 16:1115–1128.

Healey, F. P. & L. L. Hendzel, 1980. Physiological indicators of nutrient deficiency in lake phytoplankton. Can. J. Fish. Aquat. Sci. 37: 442–453.

Heaton, T. H. E., 1986. Isotopic studies of nitrogen pollution in the hydrosphere and atmosphere: a review. Chem. Geol. 59: 87–102.

Heaton, T. H. E., 1987. $^{15}N/^{14}N$ ratios of nitrate and ammonium in rain at Pretoria, South Africa. Atmos. Environ. 21: 843–852.

Hecky, R. E., 1993. The eutrophication of Lake Victoria. Verh. Internat. Verein. Limnol. 25: 39–48.

Hecky, R. E., H. A. Bootsma, R. M. Mugidde & F. W. B. Bugenyi, 1996. Phosphorus pumps, nitrogen sinks, and silicon drains: plumbing nutrients in the African Great Lakes. In Johnson, T. C. & E. O. Odada (eds.) The Limnology, Climatology and Paleoclimatology of the East African Lakes. Gordon and Breach, Amsterdam: 205–224.

Hecky, R. E., P. Campbell & L. L. Hendzel, 1993. The stoichiometry of carbon, nitrogen, and phosphorus in particulate matter of lakes and oceans. Limnol. Oceanogr. 38: 709–724.

Hecky, R. E. & H. J. Kling, 1981. The phytoplankton and protozooplankton of the euphotic zone of Lake Tanganyika: species composition, biomass chlorophyll content, and spatio-temporal distribution. Limnol. Oceanogr. 26: 548–564.

Hecky, R. E. & H. J. Kling, 1987. Phytoplankton ecology of the great lakes in the rift valleys of central Africa. Ergebn. Limnol. 25: 197-228.

Hecky, R. E., R. H. Spigel & G. W. Coulter, 1991. The nutrient regime. In Coulter, G. W. (ed.) Lake Tanganyika and its Life. Oxford University Press, Oxford: 76–89.

Hodell.D. A. & C. L. Schelske, 1998. Production, sedimentation, and isotopic composition of organic matter in Lake Ontario. Limnol. Oceanogr. 43: 200–214.

Hoefs, J., 1997. Stable Isotope Geochemistry. Springer, Berlin, 201 pp.

Hoering, T, 1955. Variations of nitrogen-15 abundance in naturally occurring substances. Science, 122: 1233–1234.

Hollander, D. J., 1989. Carbon and Nitrogen Isotopic Cycling and Organic Geochemistry of Eutrophic Lake Greifen: Implications for Preservation and Accumulation of Ancient Organic Carbon-rich Sediments. ETH, Unpubl. Ph.D. thesis, Zurich, 318 pp.

Hollander, D. J., J. A. McKenzie & H. Lo ten Haven, 1992. A 200 year sedimentary record of progressive eutrophication in Lake Greifen (Switzerland): implications for the origin of organic-carbon-rich sediments. Geology 20: 825–829.

Holloway. J. M. & R. A. Dahlgren, 1999. Geologic nitrogen in terrestrial biogeochemical cycling. Geology 27: 567–570.

Huang, Y, F. A. Street-Perrott, R. A. Perrott & G. Eglington, 1995. Molecular and carbon isotopic stratigraphy of a glacial/interglacial sediment sequence from a tropical freshwater lake: Sacred Lake, Mt. Kenya. In Estornés, I. (ed.) 17th International Meeting on Org. Geochem. CID-CSIC, Donostia: 826–829.

Huang, Y, K. H. Freeman, T. I. Eglington & F. A. Street-Perrott, 1999. $\delta^{13}C$ analyses of individual lignin phenols in Quaternary lake sediments: a novel proxy for deciphering past terrestrial vegetation change. Geology 27: 471–474.

LRC, 1999. Core Studies. http://lrc.geo.umn.edu/Core_Facility/Core_Studies/core_studies.html

Jaffe. D. A., 1992. The nitrogen cycle. In Bulcher, S. S., R. J. Charlson, G. H. Orians & G. V. Wolfe (eds.) Global Biogeochemical Cycles. Academic Press, London: 263–284.

Johannessen.T., 1992. Stable Isotopes as Climatic Indicators in Ocean and Lake Sediments. Unpubl. Ph.D. thesis, Geological Institute, University of Bergen, 209 pp.

Johnson, T. C., C. A. Scholz, M. R. Talbot, K. Kelts, R. D. Ricketts, G. Ngobi, K. Beuning, I. Ssemmanda & J. W. McGill, 1996. Late Pleistocene desiccation of Lake Victoria and rapid evolution of cichlid fishes. Science 273: 1091–1093.

Kaplan. I. R., 1983. Stable isotopes of sulfur, nitrogen and deuterium in recent marine environments. SEPM Short Course 10: 2-1-2-108.

Kaufman. L., 1992. Catastrophic change in species-rich freshwater ecosystems: the lessons of Lake Victoria. BioScience 42: 846–858.

Kelts. K. R., 1999. Smear slide manual. http://lrc.geo.umn.edu/smears/smear.html

Kendall, C., 1998. Tracing nitrogen sources and cycling in catchments. In Kendall, C. & J. J. McDonnell (eds.) Isotope Tracers in Catchment Hydrology. Elsevier, Amsterdam: 519–576.

Lehman, J. T. & D. K. Branstrator, 1993. Effects of nutrients and grazing on the phytoplankton of Lake Victoria. Verh. Internat. Verein. Limnol. 25: 850–855.

Lew, M., 1981. The distribution of some major and trace elements in sediments of the Atlantic Ocean (DSDP samples) 2. The distribution of total, fixed and organic nitrogen. Chem. Geol. 33: 225–235.

Létolle, R., 1980. Nitrogen-15 in the natural environment. In Fritz, P. & J. C. Fontes (eds.) Handbook of Environmental Isotope Geochemistry. Volume I. Elsevier, Amsterdam: 407–434.

Macko, S. A., M. H. Engel & P. L. Parker, 1993. Early diagenesis of organic matter in sediments: Assessment of mechanisms and preservation by the use of isotopic molecular approaches. In Engel, M. H. & S. A. Macko (eds.) Org. Geochem. Principles and Applications. Plenum, New York: 211–224.

Meyers, P. A. & B. J. Eadie, 1993. Sources, degradation and recycling of organic matter associated with sinking particles in Lake Michigan. Org. Geochem. 20: 47–56.

Meyers, P. A. & R. Ishiwatari, 1993. Lacustrine organic geochemistry — an overview of indicators of organic matter sources and diagenesis in lake sediments. Org. Geochem. 20: 867–900.

Meyers, P. A. & E. Lallier-Vergès, 1999. Lacustrine sedimentary organic matter records of Late Quaternary paleoclimates. J. Paleolim. 21: 345–372.

Müller, P. J., 1977. C/N ratios in Pacific deep-sea sediments: Effect of inorganic ammonium and organic nitrogen compounds sorbed by clays. Geoch. Cosmoch. Acta. 41: 765–776.

Nadelhoffer, K. J. & B. Fry, 1988. Controls on natural Nitrogen-15 and Carbon-13 abundances in soil organic matter. Soil Sci. Soc. Am. J. 52: 1633–1640.

Nevins, J. L., M. A. Altabet & J. J. McCarthy, 1985. Nitrogen isotope ratio analysis of small samples: sample preparation and calibration. Analyt. Chem. 57: 2143–2145.

Ostrom, N. E., D. T. Long, E. M. Bell & T. Beals, 1998. The origin and cycling of particulate and sedimentary organic matter and nitrate in Lake Superior. Chem. Geol. 152: 13–28.

Owens, N. J. P., 1987. Natural variations in ^{15}N in the marine environment. Adv. Mar. Biol. 24: 389–451.

Paerl, H. W. & M. L. Fogel, 1994. Isotopic characterization of atmospheric nitrogen inputs as sources of enhanced primary production in coastal Atlantic Ocean waters. Mar. Biol. 119: 635–645.

Pang, P. C. & J. O. Nriagu, 1977. Isotopic variations of the nitrogen in Lake Superior. Geoch. Cosmoch. Acta. 41:811–814.

Pennock, J. R.,D. J. Velinsky, J. M. Ludlam & J. H. Sharp, 1996. Isotopic fractionation of ammonium and nitrate during uptake by Skeletonema costatum: implications for $\delta^{15}N$ dynamics under bloom conditions. Limnol. Oceanogr. 41: 451–159.

Peters, K. E. & J. M. Moldowan, 1993. The Biomarker Guide: Interpreting Molecular Fossils in Petroleum and Ancient Sediments. Prentice-Hall, Englewood Cliffs, NJ, 363 pp.

Schlesinger, W. H., 1997. Biogeochemistry: An Analysis of Global Change. Academic Press, San Diego, 588 pp.

Schulz, H., U. Von Rad & H. Erlenkeuser, 1998. Correlation between Arabian Sea and Greenland climate oscillations of the past 110,000 years. Nature 393: 54–57.

Silfer, J. A., M. H. Engel & S. A. Macko, 1992. Kinetic fractionation of stable carbon and nitrogen isotopes during peptide bond hydrolysis: Experimental evidence and geochemical implications. Chem. Geol. 15:211–222.

Sirocko, F., 1997. The evolution of the monsoon climate over the Arabian Sea during the last 24,000 years. Palaeoecol. Afr. 24: 53–70.

Stager, J. C. & T. C. Johnson, 2000. A 12,400 ^{14}C-year offshore diatom record from east-central lake Victoria, east Africa. J. Paleolim. 23: 373–383.

Sweeney, R. E. & I. R. Kaplan, 1980. Natural abundance of ^{15}N as a source indicator for near-shore marine sedimentary and dissolved nitrogen. Mar. Chem. 9: 81–94.

Talbot, M. R. & T. Johannessen, 1992. A high resolution palaeoclimatic record for the last 27,500 years in tropical West Africa from the carbon and nitrogen isotopic composition of lacustrine organic matter. Earth and Planet. Sci. Let. 110: 23–37.

Talbot, M. R. & T. Lærdal, 2000. The late Pleistocene-Holocene palaeolimnology of Lake Victoria, East Africa, based upon elemental and isotopic analyses of sedimentary organic matter. J. Paleolim. 23: 141–164.

Talbot, M. R. & D. A. Livingstone, 1989. Hydrogen Index and carbon isotopes of lacustrine organic matter as lake level indicators. Palaeogeogr. Palaeoclim. Palaeoecol. 70: 121–137.

Talbot, M. R., D. A. Livingstone, P. G. Palmer, J. Maley, J. M. Melack, G. Delibrias & S. Gulliksen, 1984. Preliminary results from sediment cores from Lake Bosumtwi, Ghana. Palaeoecol. Afr. 16: 173–192.

Tiercelin, J.-J. &A. Mondeguer, 1991. The geology of the Tanganyika Trough. In Coulter, G. W. (ed.) Lake Tanganyika and its Life. Oxford University Press, Oxford: 7–8.

Tyrrell, T, 1999. The relative influences of nitrogen and phosphorus on oceanic primary production. Nature 400: 525–531.

Tyson, R. V, 1995. Sedimentary Organic Matter: Organic Facies and Palynofacies. Chapman & Hall, London, 615 pp.

Verschuren, D.,T. C. Johnson, H. J. Kling, D. N. Edgington, P. R. Leavitt, E. T. Brown, M. R. Talbot & R. E. Hecky, submitted. The chronology of human impact on Lake Victoria. Science.

Viner, A. B., 1975. The sediments of Lake George (Uganda) II: Release of ammonia and phosphate from an undisturbed mud surfaces. Arch. Hydrobiol. 76: 368–373.

Vitousek, P. M., J. D. Aber, R. W. Howarth, G. E. Likens, P. A. Matson, D. W. Schindler, W. H.

Schlesinger & D. G. Tilman, 1997. Human alteration of the global nitrogen cycle: sources and consequences. Ecol. Appl. 7: 737–750.

Wada, E., 1980. Nitrogen isotope fractionation and its significance in biogeochemical processes occurring in marine environments. In Goldberg, E. D. & Y. Horibe (eds.) Isotope Marine Chemistry. Uchida Rokakuho, Tokyo: 375–398.

Wada, E. & A. Hattori, 1978. Nitrogen isotope effects in the assimilation of inorganic nitrogenous compounds by marine diatoms. Geomicrobiol. J. 1: 85–101.

Wada, E. & A. Hattori, 1991. Nitrogen in the Sea: Forms, Abundances, and Rate Processes. CRC Press, Boca Raton, 200 pp.

Wada, E., H. Mizutani & M. Minagawa, 1991. The use of stable isotopes for food web analysis. Critical Reviews in Food Science and Nutrition 30: 361–371.

Waser, N. A. D., P. J. Harrison, B. Nielsen & S. E. Calvert. 1998. Nitrogen isotope fractionation during the uptake and assimilation of nitrate, nitrite, ammonium, and urea by a marine diatom. Limnol. Oceanogr. 43: 215–224.

Wharton, R. A., W. B. Lyons & D. J. Des Marais, 1993. Stable isotope biogeochemistry of carbon and nitrogen in a perenially ice-covered Antarctic lake. Chem. Geol. 107: 159–172.

Wolfe, B. B., T. W. D. Edwards & R. Aravena, 1999. Changes in carbon and nitrogen cycling during tree-line retreat recorded in the isotopic content of lacustrine organic matter, western Taimyr Peninsula, Russia. The Holocene 9: 215–222.

Yoshii, K.. N. G. Melnik, O. A. Timoshkin, N. A. Bondarenko, P. N. Anoshko, T. Yoshioka & E. Wada, 1999. Stable isotope analyses of the pelagic food web in Lake Baikal. Limnol. Oceanogr. 44: 502–511.

Yoshii, K., E. Wada, N. Takamatsu, E. B. Karabanov & T. Kawai, 1997. ^{13}C and ^{15}N abundances in the sediment core (VER 92/l-St-10-GC2) from northern Lake Baikal. Isotopes in Environ. Health Stud. 33: 277–286.

Yoshioka, T, H. Hayashi & E. Wada, 1989. Seasonal variations of carbon and nitrogen isotope ratios of plankton and sinking particles in Lake Kizaki. Japan. J. Limnol. 50: 313–320.

Yoshioka, T, E. Wada & Y. Saijo. 1988. Isotopic characterization of Lake Kizaki and Lake Suwa. Japan. J. Limnol. 49: 119–128.

Glossary, acronyms and abbreviations

α: See fractionation factor.

χ: Mass specific magnetic susceptibility.

χ_{hf}: High-field magnetic susceptibility.

$\delta^{13}C$: Delta notation of stable carbon isotopes, which is used for stable isotopic data, and is equal to $[(R_{sample} - R_{standard})/R_{standard})]1000$, where R is the ratio of ^{13}C to ^{12}C.

$\delta^{13}C_{cell}$: Carbon isotope composition of cellulose.

$\delta^{13}C_{org}$: Carbon isotope composition of bulk organic matter.

δD: Delta notation of stable hydrogen isotopes, which is used for stable isotopic data, and is equal to $[(R_{sample} - R_{standard})/R_{standard})]1000$, where R is the ratio of D (for deuterium, the name given to ^{2}H) to ^{1}H.

$\delta^{18}O$: Delta notation of stable oxygen isotopes, which is used for stable isotopic data, and is equal to $[(R_{sample} - R_{standard})/R_{standard})]1000$, where R is the ratio of ^{18}O to ^{16}O.

$\delta^{18}O_{carb}$: Oxygen isotope composition of carbonate.

$\delta^{18}O_{cell}$: Oxygen isotope composition of cellulose.

$\delta^{18}O_{lw}$: Oxygen isotope composition of lake water.

$\delta^{18}O_{mw}$: Oxygen isotope composition of meteoric water.

$\delta^{18}O_{p}$: Oxygen isotope composition of precipitation.

$\delta^{34}S$: Delta notation of stable sulfur isotopes, which is used for stable isotopic data, and is equal to $[(R_{sample} - R_{standard})/R_{standard})]1000$, where R is the ratio of ^{34}S to ^{32}S.

ε: Molar absorptivity.

$\varepsilon_{carb\text{-}lakewater}$: Isotopic enrichment due to temperature-dependent equilibrium fractionation between carbonate and lake water.

$\varepsilon_{cell\text{-}lakewater}$: Isotopic enrichment due to biochemical fractionation between cellulose and lake water.

$\varepsilon_{cell\text{-}leafwater}$: Isotopic enrichment due to biochemical fractionation between cellulose and leaf water.

ε_{evap}: Isotopic enrichment due to combined kinetic and equilibrium effects during evapotranspiration.

ε_{hydro}: Isotopic enrichment due to combined kinetic and equilibrium effects during evaporation.

γHCH: See lindane.

κ: 1) Loss factor. 2) Volume specific magnetic susceptibility.

λ: 1) Radioactive decay constant. 2) Geographic latitude of a sampling site on the Earth's surface. 3) Wavelength.

μ: 1) Mass attenuation coefficient. 2) X-ray absorption coefficient.

μ_0: Magnetic permeability of free space.

η: Fluid viscosity.

ω: 1) Angular velocity. 2) Frequency in radians.

φ: Fractional porosity or liquid content in completely saturated samples; sediment porosity.

φ^2: A measure of sediment tortuosity (dimensionless).

Φ: The fraction of the total solute concentration on the particle phase (dimensionless).

ϕ: See phi grade scale.

ρ: Density.

ρ_B: Bulk density.

ρ_l: Density of the liquid through which a particle is settling.

ρ_s: Density of the solid particle material in a sample.

P_b: Sediment bulk density.

σ: 1) Standard error or standard deviation. 2) Mineral density.

τ: 1) Intrinsic resolution. 2) ESR or luminescent signal lifetime. 3) Residence time.

θ: The angle between the crystal plane and the diffracted X-ray beam.

a_{H_2O}: Thermodynamic activity of water.

Å: The Ångstrøm, a unit of length principally used to express the wavelength of electromagnetic radiation. 1 Ångstrøm is equal to 0.1 nanometre (10^{-10} m).

A_L, A_C: Areas of a lake and its catchment.

AAS: Atomic absorption spectrometry.

Ad/Al ratio: The ratio of concentrations of the total phenolic acids relative to the total phenolic aldehydes derived from depolymerization of lignin. Larger Ad/Al ratios are indicative of greater oxidation of the lignin fraction of organic matter in a sediment sample.

Absorbance: Absorption of radiation (light) by molecular vibrations.

Accumulation rate: The rate of accumulation of particles or elements on the lake bed. Normally expressed as mass per unit area per unit time (e.g., $mg\ m^{-2}\ yr^{-1}$).

Accuracy: 1) The degree of agreement between an analysis and a standard analysis (also known as quality assurance). 2) The degree of agreement between an analysis and the true value (see also precision).

Acicular: 1) Needle-like in form. 2) A sedimentary particle whose length is more than three times its width.

Acid extractable: That part of the total element concentration that can be extracted using a specified acidic extractant.

Activity: The effective concentration of a component in a fluid, which is determined by adjusting the actual concentration of the component for any affects of nonideality.

AD: 1) *Anno Domino.* 2) The accumulated dose (used in ESR and luminescent dating methods).

Adsorbtion: The process of accumulation of a material, usually a gas or liquid, on the surface of a solid.

Aeolian: Refers to an allogenic particle transported by wind or deposits associated with wind transport.

AES: Atomic emission spectroscopy.

AF: Alternating field.

Air diffusivity: Variable that equates diffusive flux to a concentration gradient in air.

Air side resistance: The partial air side resistance defined as the air side diffusivity divided by the depth of the stagnant air boundary over water ($sec\ cm^{-1}$).

Aliquot: A geochemically identical subsample from a larger solution or other sample (see also subsample).

Allochthonous: 1) Minerogenic and/or organic material transported from its place of origin to form a sediment (or part of a sediment) at another locality. 2) A material (e.g., rock, mineral, fossil) formed elsewhere than its present resting place (cf. autochthonous).

Allogenic: Sediment component(s) formed outside the lake; specifically refers to rock, mineral, and organic particles that were derived form pre-existing materials, eroded and transported to the depositional site.

Alpha (α) particle: A particle emitted during the decay of some nuclei; it consists of 2 protons and 2 neutrons, and thus is the same as the nucleus of a ^4He atom.

Alpha spectrometry: Measurement of alpha particles emitted by radioactive substances.

Aluminosilicates: Rock-forming minerals composed mainly of alumina and silica, including clay minerals and feldspars.

Ambient temperatures: Current average temperatures.

Ammonia assimilation: The metabolic uptake of dissolved ammonia (NH_3) by primary producers.

Ammonia volatilisation: The loss of dissolved ammonia (NH_3) from an aqueous solution by outgassing of gaseous NH_3.

Ammonification: The bacterial reduction of organically bound N to NH_3 or NH_4^+. It is a process that requires anoxic conditions.

Amorphous: Pertaining to a material that lacks crystal structure or whose internal atomic arrangement is so irregular that there is no characteristic external form.

Amphibole: Ferromagnesian silicate mineral.

AMS: 1) Accelerator mass spectrometry. 2) Anisotropy of magnetic susceptibility.

Andesite: A volcanic rock with 52 to 63% SiO_2.

Angiosperms: Advanced plants that produce their seeds within the ovaries of their flowers. Angiosperms are the dominant land flora of today. They consist of woody plants that produce a perennial trunk or stem (trees and shrubs) and herbaceous plants whose stems are annual (grasses and herbs).

Anharmonic oscillator: A simple model used to explain molecular absorption caused by bond vibration. An anharmonic oscillator accounts for overtone transitions.

Anhydrite: An orthorhombic mineral with the formula $CaSO_4$; also called cube spar.

Anhysteretic: Free of hysteresis, does not display hysteresis properties.

Anhysteretic remanent magnetization (ARM): The magnetization that remains in a sample after exposure to a smooth decaying strong alternating field in the presence of a weak direct field.

Anisotropic: 1) Giving incomplete extinction when rotated under cross-polarised light. 2) Opposite of isotropic. That is, a medium in which certain physical properties are different in different directions. Such properties may relate to physical strength, light transmission electrical resistivity, etc.

Anisotropy of magnetic susceptibility (AMS): Measurements of magnetic susceptibility measured along different planes of a sample; a measure of preferred magnetic orientation.

Annually laminated sediments: Sediments with annual layers (usually couplets, i. e., varves) produced by the seasonal delivery of minerogenic material, by seasonal precipitation and/or biological activity. Formed in deep lakes with oxygen-deficient bottom waters and little or no bioturbation; one yearly package is often called a varve.

Anoxic: Strictly speaking, the absence of oxygen. As dissolved oxygen concentrations cannot be measured in ancient sediments, an absence of all evidence for higher life forms (metazoans) has commonly been taken as a strong indication of anoxic conditions. Today such organisms are typically excluded when dissolved oxygen levels fall below ca. 0.01 ml l^{-1}, although some specialized organisms are capable of making "visits" to environments with lower O_2 concentrations.

Anoxia: The complete lack of molecular oxygen. Anoxic waters contain no dissolved oxygen.

Anti-ferromagnetism: Magnetic behavior of substances with equal numbers of unpaired electron sites having perfectly anti parallel sub-lattices resulting in nonferromagnetic behavior.

Anthropogenic: Sediment component(s) derived from human sources.

AOTF: Acousto-Optical Tuneable Filter

AP: Apatite phosphorus.

Apatite phosphorus: That fraction of the total phosphorus concentration that is in the form of apatite.

Aqua regia: A mixture of concentrated nitric and hydrochloric acids (ratio 1:4). This is the most aggressive of the partial extraction procedures.

Aquifer: A saturated permeable layer of rock, gravel, sand, etc., that can transmit appreciable quantities of water.

Aragonite: 1) *Sensu stricto:* An orthorhombic carbonate with the formula $CaCO_3$, which is trimorphous with calcite and vaterite. Also known as Aragon spar; it is a common matrix mineral in invertebrate shells. 2) *Sensu lato:* A group of orthorhombic carbonate minerals, including aragonite, strontianite, cerussite, alstonite, and witherite.

ARM: Anhysteretic remanent magnetization; an artificial magnetization acquired in a strong decaying alternating magnetic field superimposed on a weak static field.

Atomic absorption spectrometry: A method for elemental analysis of solutions based on the photoelectric absorption of characteristic light (produced by a special lamp) by thermally excited of atoms.

Attenuation: 1) Radiation: A reduction in incident radiation energy. Water can significantly attenuate most terrestrially produced radiation. 2) General: A reduction in a signal's amplitude or energy.

Attenuation coefficient: The proportion of the energy in a pulse that is converted into other types of energy (e.g., heat) thus reducing the strength of the signal.

Authigenic: 1) Sediment component(s) formed within the sediment after deposition of the original material. 2) Sometimes used synonymously with endogenic.

Authigenic mineral: Any mineral precipitated within the sediment or rock from geochemical compounds found locally in the rock or sediment.

Autochthonous: 1) Rocks, sediments or deposits formed and deposited at the same place as where they are found today; fossils deposited at the place where the animal lived or the plant grew. 2) A material (e.g., rock, mineral, fossil) formed in the basin or water body where it is found (cf. allochthonous).

Autotrophy: An organism that produces organic matter from mineral nutrients by photosynthesis or chemosynthesis. Plants and many microbes are autotrophs.

$(B_0)_{CR}$: Coercivity of remanence, coercivity of remanent magnetization.

$(B_0)_C$: Coercivity of magnetization.

Backscattering: The reflection and dispersion of ionizing radiation off a mineralogical boundary or surface that reduces the effective radiation transmission into the surface.

Backscatter coefficient: The number of backscattered electrons emitted from a specimen for each incident electron.

Backscattered electron imagery: Incident electrons reflected (elastically) off a material are termed backscattered electrons. The number of backscattered electrons from any given point is related directly to the atomic number of a material. Relatively heavy materials produce a greater number of backscattered electrons (and so produce a brighter image) than relatively light materials. Backscattered electron imaging BSEI) is normally used to examine flat, well-polished surface with contrasting compositional (atomic mass) information. Backscattered imaging of topographic samples may be used to avoid the effects of charging.

Barite: A sulfate mineral with the formula $BaSO_4$; also known as barytes, heavy spar.

Basalt: A volcanic rock with 44 to 52% SiO_2.

Bathymetric map: Map indicating water depth.

BC: Before Christ.

Beer-Lambert equation: A quantitative explanation of how much light is absorbed by a chemical system.

Benthic: Bottom-living.

Bertrand lens: a removable lens in the tube of a petrographic microscope that is used to examine interference figures.

Beta particle (β): A particle emitted during the decay of some nuclei; it is a high-energy electron.

Binary image: A binary image has been transformed by thresholding and is usually displayed in black and white. Numerically, the pixel values are often 0 for black, and either 1 or 255 for white.

Bioconcentration: Chemical uptake and concentration by organisms.

Biogenic: Sediment component(s) formed within the lake, of biological origin.

Biogenic carbonate: Carbonate minerals that are formed by organisms to be an integral part of their body and/or exoskeleton.

Biomagnification: Increased chemical concentrations in tissues of organisms at higher trophic levels. Occurs when rate of assimilation of a chemical is greater than the combined rate of elimination and transformation by the body.

Biophile: Used of elements tending to occur in biogenic particles. Often used synonymously with biogenic.

Bioturbation: 1) Mixing of sediment by biological activity (e.g., burrowing). Occurs in some oxygenated bottom waters, but is typically absent from anoxic bottom waters. Original sedimentary structures are usually destroyed and the stratigraphy is altered in bioturbated sediments. 2) Disturbance of sediment structures, layers or horizons by the activity of borrowing and/or grazing benthic organisms.

Birefringence (birefringent): The ability of a mineral to split a beam of ordinary light into two beams of unequal velocities.

Bloedite: A white or colorless evaporite mineral: $Na_2Mg(SO_4)_2 \cdot 4H_2O$.

Boulder: The term applied to sediment particles coarser than cobble; particles having a diameter of greater than 256 mm.

BP: Literally, before present, but actually before 1950. Defined to be 1950 when ^{14}C dates first began to be published, "present" is used as a calibration point only for ^{14}C dates or ages (see also ky BP).

Bq: SI unit of radioactivity, measured as 1 disintegration per second.

Bragg angle: See Bragg's Law.

Bragg's equation: Bragg's Law

Bragg's Law: A statement that in crystallography, the X-ray diffractions from a crystal lattice may be thought of as reflecting from the lattice planes: $n\lambda = 2d \sin\theta$, in which n is any integer, λ is the wavelength of the X-ray, d is the crystal plane separation and θ is the angle between the crystal plane and the diffracted beam (e.g., Bragg angle).

Breakseal combustion: Procedure where organic compounds are converted to gas by combustion in sealed, evacuated quartz or Pyrex tubes.

Breccia: 1) Geology: A coarsely grained clastic sediment or rock containing angular, and often broken, rock fragments lithified by mineral cements or supported in a more finely grained matrix. 2) Archaeology *sensu stricto*: A well-cemented coarsely grained sedimentary unit, often found in a cave. 3) Archaeology *sensu lato*: Any well-cemented sedimentary unit.

BSE: Backscattered scanning electron microscopy. Backscattered electrons are the result of elastic collisions between energetic beam electrons and atoms within the target, for example a thin-section.

BSEI: Backscattered electron imagery.

BSE-image: Backscattered electron images can be used for porosity and fabric analysis of sediment samples and identification of e.g., microfossils. The production of backscattered electrons varies according to the specimen's atomic number. Objects with a higher atomic number (e.g., mineral grains of quartz) produce more backscatter electrons and are therefore recorded as brighter values within the image.

Buffer: 1) Any pair of solutes that can maintain a solution's pH at an almost constant level despite the addition of moderate quantities of acids or bases. 2) A solution containing such solute pairs.

Buffered solutions: See buffer (2).

Bulk density: Specific weight or density of sediments including their water content; weight per unit volume of a sediment.

Bulk geochemical analysis: Any analytical protocol used for ESR or luminescent dating that involves determining the concentrations for the important radioactive elements using geochemical techniques, such as NAA, XRF, etc.

Bulk sediment: Sediment sample that has not been sub-divided into different fractions.

***C*:** Particle mass concentration.

C1-C5: Operationally defined, sequentially extracted components.

C_3 plants: Plants that employ the Calvin pathway during photosynthesis. C_3 plants are so named because they employ an intermediate compound, phosphoglyceric acid that contains three carbon atoms. Most higher plants and algae use the C_3 pathway. These plants strongly discriminate (20‰) against ^{13}C during carbon incorporation.

C_4 plants: Plants that employ the Hatch-Slack pathway during photosynthesis. C_4 plants are named such because they employ an intermediate compound, oxaloacetic acid that contains four carbon atoms. These plants moderately discriminate (8 to 14‰) against ^{13}C during carbon incorporation. C_4 plants are usually higher land plants that are specially adapted to dry and low-pCO_2 conditions.

C_p: Atmospheric chemical concentration in the particle phase (ng m^{-3}).

C_t: Total atmospheric solute concentration (ng m^{-3}).

C_w: Concentration of a chemical that is dissolved in water.

Cainozoic: see Cenozoic.

Calibration model: A mathematical function developed between one or several independent variables (X-variables; e.g., NIR absorbance values) and a dependent variable (Y-variable; e.g., lake-water pH). This function may later be used to predict values for the Y-variable using X-variables collected on unknown samples.

Caliche: 1) *Sensu lato:* A secondary sedimentary accumulation cemented predominantly by secondary calcitic cements that can include dolomite, aragonite, gypsum, and silica. Formed by groundwater capillary action in regions with high evaporation rates, it is also called hardpan, duricrust, calcrete, kankar, calcareous crust, nari, sabach, and tepetate. 2) *Sensu stricto*: Discrete calcrete nodules that do not form a continuous crust (see also calcrete, silcrete, gypcrete).

CAM plants: Plants that employ crassulacean acid metabolism during photosynthesis. Such plants are able to use either the C_3 or C_4 pathway to survive in harsh environments. Most CAM plants grow in deserts; they rarely contribute organic matter to lake sediments.

Cambrian: The oldest geologic period between 570–510 million years ago with abundant animal fossils and the first period of the Paleozoic Era (570–245 million years ago); also denotes the system of strata deposited during this period.

Carbon/nitrogen ratio (C/N): The ratio between carbon and nitrogen in living or fossil organic matter. It is normally calculated from the concentrations of the two elements measured as weight % of the bulk sample, but may also be expressed as an atomic ratio.

Carbonate carbon: The carbon in sediment that is contributed by carbonate minerals such as calcite, aragonite, dolomite, and siderite.

Catchment: Used synonymously with watershed.

Cathodoluminescence (CL): Luminescence produced by excitation by an incident beam of electrons.

Cation exchange column: A glass column packed with a compound able to adsorb cations to and then desorb cations from its surface. These are often used to desalt solutions before geochemical analysis.

CD ROM: Compact disc read only memory.

Cellulose: 1) A group of polymeric carbohydrates with the empirical formula $C_n(H_2O)_n$ that are major components of the tissue of terrestrial macrophytes. It is the most abundant natural organic compound. 2) A polysaccharide $(C_6H_{10}O_5)$ of linked glucose units and is the principal component of cell walls of higher and lower plants.

Cementation: The diagenetic process whereby clastic sedimentary grains are lithified or consolidated into sedimentary rocks, often by mineral deposition or precipitation on the grain surfaces or in the interstitial spaces.

Cenospheres: Hollow inorganic ash spheres.

Cenozoic (in American English), Cainozoic (in British English): The most recent geological era that began approximately 66.5 Ma (also known as Cainozoic, Kainozoic, the Mammal Age).

CF-IRMS: Continuous flow-isotope ratio mass spectrometry. A procedure that uses an instrument that is capable of repeatedly and rapidly measuring the masses of selected gases (e.g., carbon dioxide, hydrogen, nitrogen) delivered in a continuous gas stream from another instrument, such as an elemental analyzer or a gas chromatograph, to determine their isotopic compositions.

Chemocline: The boundary between the well-mixed upper water mass and the noncirculating lower water mass of a chemically stratified lake.

Chert: A hard dense micro- or cryptocrystalline sedimentary rock with interlocking quartz crystals that displays concoidal fracture, prized by hominids as a material for making tools. Occurring as nodules in limestones or dolomites, it is often considered synonymous with flint. Chert is sometimes considered only to be the varieties with visible colors, the cryptocrystalline types, or varieties lacking visible fossil inclusions (see flint).

Chevrons: (Chevron halite) Halite crystal, which is grown on a basin floor from evaporating brine. It is characterized by enclosed solid, liquid, or vapor inclusions arranged in a chevron pattern.

Chitin: A resistant organic compound similar in structure to cellulose containing repeating N-acetylglucosamine units, which forms the hard skeleton in many invertebrate and foraminiferal inner tests.

Chromatography: A procedure that separates the components of a mixture by partitioning them between two phases. Types of chromatography include gas-solid chromatography, gas-liquid chromatography, column (solvent-solid) chromatography, low- and high-pressure (solvent-solid) chromatography, and thin-layer (solvent-solid) chromatography.

Chronology: 1) A data series or framework referenced with respect to time (i.e., a time series). For lake sediment records, often the chronology describes the sediment depth-age relationship. 2) Time scale, which may be obtained through radiometric dating (e.g., ^{14}C, U/Th) or counting of annual layers.

Chronostratigraphy: 1) Definition and subdivision of the stratigraphic record in terms of time. 2) Nordic: The Nordic chronostratigraphy-chronostratigraphic scheme is based on ^{14}C dated Late Weichselian and Holocene pollen zone boundaries in Scandinavia.

Cinnamyl/vanillyl ratio (C/V): The C/V ratio is calculated as the sum of *p*-coumaric acid plus ferulic acid concentrations divided by the sum of the three vanillyl phenols. It is a measure of the relative contributions of woody and non-woody land-plant tissues to the organic matter in a sediment sample

Clay: 1) Textural: The term applied to sediment particles finer than silt; particles having a diameter of smaller than 3.91 microns or sometimes 1.95 microns. 2) Mineralogical: A poorly defined group of aluminum silicate minerals.

C/N (ratio): See carbon/nitrogen ratio.

C/V ratio: See Cinnamyl/vanillyl ratio.

Cobble: The term applied to sediment particles finer than boulder and coarser than pebble; particles having a diameter of 64–256 mm.

Coercive force (coercivity) $(B_0)_C$: The reverse in-field required to reduce the magnetization from saturation to zero.

Coercivity of remanence $(B_0)_{CR}$: The reverse out-of-field required to reduce the magnetization from saturation to zero.

Coincidence: The phenomenon affecting electrical resistance type of particle sizing equipment caused by more than one particle passing though the sensing zone at once.

Cold-condensation effect: See Grasshopper effect.

Colloid-water partition coefficient: The distribution ratio for chemical substances between colloids and water.

Color reflectance spectroscopy: The measurement of the reflectance of light in separate channels (wavelengths) usually within the visible and near-infrared bands.

Colorimetric methods: Colorimetry, or spectrophotometry, is a chemical analytical method that exploits the link between chemical composition and color intensity for a range of dyes.

Combination band: Arise from combinations of fundamental C-H, N-H and O-H vibrations.

Component: A general term used to denote the separate materials which, when mixed together, make up soils and sediments.

Compton scattering: Scattering of incident photons by electrons resulting in an energy loss of gamma rays passing through sediments. This is the dominant factor controlling gamma ray attenuation.

Compound-specific isotope analysis: Determination of the isotopic ratio of the carbon, nitrogen, hydrogen, sulfur, or oxygen contents of a single compound. The isolation of the single compound is usually achieved by some form of either off-line or on-line preparation in which gas chromatography is an important step.

Computerized tomography: A method of determining X-ray absorption in a series of scanned slides by the use of a narrow X-ray beam. Different sections of a sample are scanned by a rotating X-ray beam allowing complete characterization of X-ray absorption and, by calibration, density.

Congener: A form or a variety of a chemical substance. PCBs have 209 possible forms or congeners due to the different possible positions of chlorine atoms on the biphenyl.

Continuous flow-isotope ratio mass spectrometry: Gas source mass spectrometry where sample and standard gases are transported using helium as a carrier gas into the mass spectrometer for measurement of isotopic ratios.

Cosmogenic: Sediment component(s) derived from outside the Earth system.

Cosmogenic isotope dating: A method using the amount of a cosmogenic isotope accumulated in a rock to determine the length of time the rock has been exposed to the atmosphere.

Coulter Counter: A commonly used particle-sizing instrument employing the principle of electrical resistance.

CPL: Cross-polarized light.

cps: counts per second.

Critical point drying: A method of drying delicate samples for electron microscopy by freeze-drying at the critical point of water. At the critical point of a given substance, the densities and other physical properties of the liquid and gaseous states are identical.

Cryogenic purification: The separation of gases on the basis of their different freezing points using a vacuum-extraction line.

Cryostage: Sample holder that is able to maintain very cold (–160 to –185 °C) temperatures.

Crystal: A homogenous, solid chemical element, compound or isomorphous mixture having a regularly repeating arrangement of atoms; often this atomic arrangement is manifest by a series of plane faces.

Crystalline: Having the nature of a crystal; specifically, having a crystal structure or regular arrangement of atoms in a lattice.

^{137}Cs: Radioactive isotope of cesium with a 30.2 year half-life produced as a fission product of nuclear weapons explosions or in nuclear reactors.

CT (also CT scanning): Computerized tomography.

Cumulates (Cumulate crystals): Saline mineral crystals formed by precipitation at the air-water interface that accumulate when they sink to the bottom of a saline body of water.

Curie temperature or Curie point (T_C): The temperature above which a ferromagnetic or ferromagnetic substance becomes paramagnetic.

***D*:** Distance or depth.

***d*:** Particle or grain diameter.

D_a: See Air diffusivity.

D_{eff}: Effective porous media diffusivity ($cm^2\ sec^{-1}$).

D_{mol}: Aqueous solution molecular diffusivity ($cm^2\ sec^{-1}$)

DA: Diode Array.

DC: Direct current.

DCM: See Dichloromethane.

DDD: Dichlorodiphenyldichloroethane; a metabolite of DDT.

DDE: Dichlorodiphenyldichloroethene; a metabolite of DDT.

DDT: Dichlorodiphenyltrichloroethane; a powerful insecticide.

D/H: Deuterium/hydrogen isotope ratio, or ratio of $^2H/^1H$ in a substance.

Debye-Sherrer method: A method of recording X-ray diffraction patterns on film (i.e., Debye-Sherrer photographs).

Declination: 1) The deviation in degrees of a compass needle or the Earth's magnetic field from geographical or true north in the horizontal plane. 2) A protocol for measuring spectral peak heights or areas in complex peaks. A complex peak is separated mathematically into several theoretical peaks whose peaks are then measured.

Deflation: A form of wind erosion that removes dry finely grained clays and silts from surficial sediment.

Delta notation: A relative measure of the difference, typically in the ratios of molar concentrations of stable isotope of hydrogen, carbon, nitrogen, oxygen, or sulfur, between a substance and an agreed-upon standard material.

Denitrification: The bacterial reduction of dissolved NO_3^- to gaseous N_2. Denitrifying organisms require anoxic or dysoxic conditions. This process typically occurs under the anoxic conditions present in subsurface lake sediments and in the hypolimnions of strongly stratified lakes.

Density slicing: Technique for selecting objects of interest, see thresholding. With density slicing objects within a specific grey-scale range can be identified and selected.

Destructive techniques: A method in which a sample is destroyed in order to obtain an analysis.

Detrital: Pertaining to material derived from detritus (i.e., loose rock, sediment, or other materials that are removed by mechanical means and transported to the depositional site).

Deuterated: A compound that is labelled with deuterium.

Dewar flask: A container designed to prevent heat transfer and used to hold liquified gases, such as liquid nitrogen (–196 °C).

DGT: Diffusive gradient in thin films.

Diagenesis: 1) Sedimentary: All the geochemical, physical, and biological processes that affect sediment after their initial deposition in the sediment, and during and after lithification, except surficial alteration (weathering) and metamorphosis. It can include compaction, cementation, leaching, reworking, authigenesis, replacement, crystallization, recrystallization, biological alteration, concretion formation, and any process at temperatures <100–300°C and pressures <1 kb. Some restrict the term to the period before lithification. 2) Fossil: All the geochemical, physical, and biological processes that affect fossils, during weathering, after their initial deposition in the sediment, and during and after lithification, except metamorphosis.

Diagenetic: Sediment component(s) derived through modification of material after burial of the sediment.

Diagenetic alteration: Any geochemical changes arising from diagenesis.

Diamagnetism: Type of magnetic behaviour exhibited by substances with no unpaired electrons when exposed to a magnetic field. This results in a change in the orbital motion of electrons about the nucleus in the applied field resulting in a very weak negative magnetic susceptibility. Exhibited by e.g., quartz, feldspars, calcite.

Diamict: Term used to denote non-sorted sediments and rocks containing a wide range of particle sizes, regardless of genesis.

Diamicton: Poorly sorted unconsolidated sediment (e.g., till).

Diatom: A microscopic single-celled plant from the class Bacillariophyceae that lives in fresh and marine water and precipitate siliceous tests (frustules).

Diazotrophe: Specialised organisms, notably the cyanobacteria, capable of assimilating ("fixing") molecular nitrogen (N_2).

DIC: See dissolved inorganic carbon.

Dichloromethane: Colorless, volatile liquid. Used as a solvent for extracting POPs from environmental media.

Diffusion: Non-advective flux of material in water.

Differential thermal analysis: A type of incremental thermal analysis in which the difference in temperature between an unknown sample and an inert material is used to identify the mineralogical composition.

Diffraction: 1) The process by which the direction of a wave motion in any medium is modified by bending. 2) The bending of waves in a body of water around an obstacle.

Diffraction spacing: The interplanar spacings in a crystal lattice.

Diffractogram: A record of X-ray diffraction.

Diffractometer: An instrument that records X-ray diffraction patterns.

Diffractometer trace: Diffractogram.

Diffusive gradient in thin films: A technique for measuring trace element availability (a combination of dissolved concentration and diffusive mobility) in sediment using sheets coated with exchange resin.

Digital camera: A camera that directly captures a digital image without the use of a film.

Digital imaging: Acquisition of an image in digital format, usually using a digital camera system.

Digital X-ray imaging system: An X-ray source coupled to a brightness amplifier and digital camera. This allows contrast improvement for fine detail and image enhancement.

DIN: See dissolved inorganic nitrogen.

Diode array detector spectrophotometer: A spectrophotometer that uses a detector system consisting of an array of diodes, where each diode corresponds to a certain wavelength.

Dipole: A magnet that has a concentration of positive charge at one end and negative charge at the other end. A bar magnet is a good example of a dipole.

Dissolved inorganic carbon (DIC): 1) Carbon contained in carbon dioxide, and bicarbonate and carbonate ions dissolved in water. 2) The sum of all dissolved inorganic carbon species ($CO_2 + HCO_3^- + CO_3^{2-} + H_2CO_3$) in an aqueous solution.

Dissolved inorganic nitrogen (DIN): The sum of all dissolved inorganic nitrogen species ($N_2 + NO_3^- + NO_2^- + NH_4^+$) in an aqueous solution. DIN normally excludes dissolved N_2.

Dissolved organic carbon (DOC): 1) Carbon contained in colloidal ($<10\,\mu m$) organic particles and in soluble organic compounds in water. 2) Organic molecules representing decay products of vegetation that pass through a $0.45\,\mu m$ filter.

Distribution coefficient: This is a coefficient quantifying the link between the concentration of a trace substance in solution, and that sorbed to suspended particles. It is typically expressed in the units litres/kilogram. The ratio of an element between two coexisting phases.

DOC: See dissolved organic carbon.

Dolomite: 1) Mineralogy: A common, well-ordered, carbonate mineral with the formula $CaMg(CO_3)_2$; also called magnesian spar. 2) Sedimentology *sensu stricto*: A carbonate rock with more than 90% dolomite mineral, also known as dolostone. 3) Sedimentology *sensu lato*: A carbonate rock with more than 50% dolomite mineral, also known as magnesian limestone.

D-optimal design: Given a limited number of experiments, or samples to collect, the algorithm for D-optimal experimental design are used to select a subset of experiments/samples representing the overall variability of the candidate samples/experiments as accurately as possible. Usually the algorithms used are based on maximisation of the determinant of the variance-covariance matrix of the subset, hence the term D-optimal.

DPI: Dots per inch.

Drag diameter: Diameter of a sphere having the same resistance to motion as the particle in a fluid of the same viscosity and at the same velocity.

Dry bulk density: Dry mass of sediment per unit *in situ* volume.

Dry density: Specific weight or density of all solid sediment components excluding water.

d-spacing: In diffraction of X-rays by a crystal, the distance between successive and identical parallel planes in a crystal lattice.

DTA: Differential thermal analysis.

DVD ROM: Digital versatile disc read only memory.

Dysoxic: The transitional zone between oxic and anoxic environments, where dissolved oxygen concentrations are in the range of $0.01–1.0\,ml\,l^{-1}$. May also be called the dysaerobic zone.

E: Probable error in thin section point counting.

EAAS: Electrothermal atomic absorption.

ECD: See Electron capture detector.

EDS: Energy dispersive spectroscopy or spectrometer.

EDXS: Energy dispersive X-ray spectroscopy or spectrometer.

EIL: Environmental Isotope Laboratory.

Eigen analyis: A mathematical procedure for identifying the principal axes of a multivariate data set.

Electro-osmotic knife: A method of cutting wet sediment that relies on the principal of electro-osmosis. Essentially, a knife is wired as a negative electrode so that it is continuously lubricated by the interstitial water migrating towards it.

Electromagnetic energy (EMR or EM): A form of energy, propagated through space or through a media in the form of an advancing disturbance in electric and magnetic fields. Examples of electromagnetic energy are light and radio signals.

Electron capture detector: A sensitive detector for halogenated compounds when combined with gas chromatography. A steady stream of electrons produced by ^{3}H or ^{63}Ni causes a signal resulting from the capture of electrons by halogen atoms. The result is a detectable change in the electrical current.

Electron microprobe analysis: Analytical technique where samples are exposed to electron beam. Characteristic secondary X-rays are generated and can be converted to concentration.

Electrothermal atomic absorption spectrometry: A form of atomic absorption spectrometry in which an electrically heated graphite tube is used to excite the atoms in a sample.

Elemental analyzer: An instrument that uses high-temperature combustion, typically 800–1000 °C, to convert the carbon, hydrogen, nitrogen, and sulfur constituents of a substance into gases that can be separated and measured. Some instruments can also measure oxygen contents of samples.

Ellipsoidal: Shaped like an ellipsoid (i.e., a geometric form in which all plane sections are either ellipses or circles).

EM: Electromagnetic energy.

EMR: Electromagnetic radiation; see electromagnetic energy.

Emission spectrometry: A method for elemental analysis of solutions based on thermal emission of characteristic photons (mostly within the visible spectrum).

Enantiomers: Stereoisomers whose molecule structures mirror each other at one or more asymmetrical carbon atoms (also called isomers, stereoisomers; see also racimers, epimers).

Endogenic: 1) Sediment component(s) formed within the basin, specifically from within the water column. 2) Sometimes used synonymously with authigenic.

Endogenic carbonate: Carbonate minerals formed in the water column. Typically refers to those formed inorganically.

Endogenic geomorphic processes: Processes originating within the Earth that create relief on the Earth's surface. Tectonism and volcanism are the principal endogenic processes.

Energy dispersive x-ray spectroscopy (EDXS or EDS): A method for elemental analysis based on using a focussed electron beam (in an electron microscope) to cause the fluorescence of secondary x-rays from atoms in a specimen.

Environmental scanning electron microscope (ESEM): A scanning electron microscope in which the sample chamber has a low-pressure gaseous environment, e.g., nitrogen gas, which absorbs excess charge. Coating the sample with a conductive medium is therefore unnecessary.

Eolian transport: Delivery of fine particles (pollen, soot, dust) by winds, often from distant locations.

Epsomite: An evaporitic colorless mineral: $MgSO_4 \cdot 7H_2O$.

Equilibrium isotope effects: The distribution of pairs of stable isotopes between reacting substances in accordance with the principles of chemical equilibria.

Erosion: The general process by which Earth materials are loosened and moved from on place to another.

ESEM-EDS: Environmental scanning electron microscope-energy dispersive spectrometer.

Eucidean distances: Root mean square distances between objects in a numerical matrix.

Euhedral: A mineral grain with edges defined by perfect crystal faces.

Eutectic: A system consisting of two or more solid phases and a liquid that coexist at an invariant point (constant temperature in an isobaric system). This temperature is the minimum melting temperature for the assemblage of solids. Any flux of heat into or out of the system will not affect the temperature until one of the phases is exhausted.

Extractable: That part of the total element concentration that can be extracted using a specified extractant.

Extrusion: Removal of sediment from core barrel by pressure. A technique used when there is no liner.

F: Flux.

FAAS: Flame atomic absorption.

Fabric: The spatial and geometric orientation of elements of a sediment or rock.

Factor analysis: An extension of principal components analysis, in which a small number of axes are considered to represent underlying factors within the data set.

Feldspar: A mineral group comprising silicates of the general formula: XZ_4O_8, where X = Ba, Ca, K, Na, NH_4, Sr; Z = Al, B, Si.

Felsic: Light-colored rocks, rich in feldspar and quartz.

Feret's Diameter: The distance between a pair of parallel lines which are oriented in a given direction (normally parallel to the vertical cross-hair in a microscope field of view) and which touch the extreme points on the perimeter of the projected outline of the particle.

Ferrimagnetism: A type of ferromagnetic behavior with alternating sub-lattices of unequal parallel and anti-parallel alignment giving rise to a net spontaneous magnetization.

Ferromagnetism: Collective term of magnetic behavior in some crystalline substances with unpaired electrons in atoms that are closely and regularly spaced. This results in a strong interaction (coupling) between all unpaired electron spins giving rise to positive and large susceptibilities (ferromagnetism, senso stricto). Exhibited by e.g., iron, nickel, cobalt.

Ferulic acid: One of the cinnamyl degradation products released from the alkaline oxidation of lignin.

F_g: Gravitational force.

Filter instrument: Instruments where filters are used for wavelength selection.

Flame atomic absorption spectrometry: A form of atomic absorption spectrometry in which a flame is used to excite the atoms.

Florisil column: A glass column with an adsorbent that is used for sample cleanup of chlorinated pesticides and PCBs.

Fluid displacive embedding: Displacing one fluid by another, usually water by acetone, and then adding low viscosity epoxy resin, which is then cured to produce a solid resin-embedded sample.

Fluid inclusion: Fluid-filled vacuoles trapped within minerals.

Fluvial: Pertaining to streams.

Flux: The rate of transfer of a substance across a given surface area.

Fly-ash: Particulate matter emitted to the atmosphere with flue gases.

Fossil: 1) *Sensu stricto*: Any evidence for past lifeforms in which the original minerals or tissues have been completely replaced new minerals. 2) *Sensu lato*: Any evidence for past lifeforms in which the original minerals or tissues have experienced some secondary cementation or have suffered some diagenetic alteration. 3) *Sensu lato extremis:* Any dead organism or other evidence for past life.

Fourier analysis: 1) Mathematical operation for calculating the frequency content (i.e., spectrum) of a data set that is a function of time or space. 2) A system in which the frequency spectrum contained within a signal is determined and altered such that certain noise in the data can be filtered out.

Fourier transform instrument: Instruments based on interferometers for wavelength separation. Near infrared light passes through a scanning interferometer and Fourier transformation gives intensity as a function of frequency. When samples are placed in the beam (before or after the interferometer), the sample absorbs at some frequencies, and the intensities are reduced into an interferogram. The mathematical FT function is then used to convert the interferogram to an absorption spectrum of the sample.

Fourier transformation: Mathematical transformation of time domain functions into frequency domain.

Fractal: A geometric pattern that is repeated at ever-smaller scales to produce irregular shapes and surfaces that cannot be represented by classical geometry. Fractals are used especially in computer modeling of irregular patterns and structures in nature.

Fractionation: 1) Selective separation of chemical elements or isotopes through physical, chemical or biochemical processes. For example, the fractionation of carbon isotopes: of the naturally occurring carbon isotopes ~98.9% is ^{12}C, 1.1% is ^{13}C and only 1 part in 10^{10}% is ^{14}C. In nature, however, a fractionation of this ratio occurs (e.g., photosynthesis results in an enrichment of ^{12}C relative to the other isotopes in most plant tissues). Based on thermodynamical laws, which show that the heavier isotope ^{14}C is twice as enriched as ^{13}C, radiocarbon laboratories correct for the probable effects of fractionation. ^{13}C can be measured in a sub-sample of the material to be dated and the ^{13}C : ^{12}C ratio is then compared with a standard (PDB) and published as deviation from this standard. See also normalization. 2) In physical and chemical processes involving the isotopes of a particular element, the relative abundance of the isotopes may change between the initial substance (the "substrate") and its product. In isotope geochemistry, this change is commonly referred to as fractionation. (see also: fractionation factor; isotope effects).

Fractionation factor (α): In any process involving the fractionation of stable isotopes x and y (where y is the heavier isotope), such as the transformation of substance A to substance B, α defines the relative abundance of the isotopes in A and B:

$$\alpha_{(A\text{-}B)} = \frac{(y/x)_A}{(y/x)_B}.$$

Free-falling diameter: Diameter of a sphere having the same density and the same free-falling speed as the particle in a fluid of the same density and viscosity.

Freeze drying: A technique for drying biological or sediment samples that relies on freezing sufficiently fast to inhibit the formation of ice crystals. This is then followed by vacuum dehydration.

Frequency dependent magnetic susceptibility (χ_{fd}): Calculated from the measurements of initial magnetic susceptibility at two or more AF frequencies.

Friable lithology: A sediment or rock type that crumbles easily.

FT: Fourier transform

Fume: Sub-micron particles produced from the condensation of volatilized non-combustible material.

Fundamental absorption: Molecular vibrational absorption from ground level to level one.

Fusion methods: As an alternative to total digestion using acids, a sample may be brought completely into solution by first fusing it with an alkaline carbonate or borate, and dissolving the alkaline residue.

F_{sed}: Loss rate of chemicals by sedimentation (yr^{-1}).

F_v: Viscous drag force.

Galai CIS Particle Size Analyzer: A sizing instrument based on the amount of time a finely focused rotating laser beam is intersected by a particle in suspension.

Gamma rays (γ): A high-energy photon. Photons emitted during nuclear decay are referred to as gamma rays.

Gamma rays (natural): Energy emitted by natural radioactive substances corresponding to X-rays and visible light but with much shorter wavelengths.

Gamma ray attenuation: Absorption of gamma rays passing through the sediment is caused by Compton attenuation (scattering), pair production, and by photoelectric absorption. The amount of gamma ray attenuation is a measure of bulk density, from which water content and porosity can be calculated.

Gamma ray attenuation porosity evaluator (GRAPE): Instrument that measures gamma ray attenuation through unsplit cores and provides an estimate for bulk density, water content, and porosity.

Gamma spectrometry: Measurement of gamma particles emitted by radioactive substances.

Gar (fish, pike): Any ganoid fish of the genus *Lepisosteus* or several closely related extinct genera, with elongated bodies, long snouts, and enameloid scales, found in fresh and brackish waters in North America.

Gas chromatography (GC): A process for separating and analyzing mixed gases or vapors in which a carrier gas (e.g., helium, argon, nitrogen, hydrogen) carrying the dissolved gaseous or vaporous mixture is passed over a nonvolatile liquid (gas-liquid chromatography) or solid (gas-solid chromatography) coating an inert porous solid.

The analytes are resolved by the differential mobility rates of the constituents as they repeatedly adsorb to, and then desorb from, the inert solid surfaces.

GC: Gas chromatograph or gas chromatography.

GC-MS: Gas chromatography-mass spectrometry. An analytical procedure that combines a gas chromatograph, which separates mixtures of compounds into individual components, with a mass spectrometer, which breaks the compounds into fragments that indicate the molecular weight and structure of each component. This procedure is one of few that can provide reliable identifications of organic compounds.

Genetic classification: A scheme for classifying sediments, or sedimentary components, based on their origins.

Geochemical fossil: A distinctive organic compound that can be isolated from a sedimentary deposit and that can provide evidence of a specific organism or group of organisms that lived in the past.

Geochemical palaeolimnology: The study of past environments using the geochemical properties of lake sediments.

Geochemistry: A broad research field aiming both to understand the chemistry of the natural environment, and to use chemistry as a tool in describing the natural environment.

Geomagnetic field: The magnetic field produced by the motion of the inner and outer cores of Earth.

GFF: Glass fiber filter.

GFZ: GeoForschungsZentrum, Potsdam in Germany.

Glagolev-Chayes Method: A method of point counting thin sections using a superposed grid.

Global Meteoric Water Line: A "line" on the $\delta^{18}O$-$\delta^{2}H$ plane formed when the $\delta^{18}O$ and the $\delta^{2}H$ values of meteoric precipitation from all parts of the globe are plotted together. For precipitation collected at any one locality, the slope or the intercept may deviate from this line.

Glycolation: In clay mineralogy, the process of saturating the prepared specimen with ethylene glycol in order to expand the smectite and other expandable lattice clay minerals.

Glycolator: Any sealed container into which a prepared clay mineral slide can be placed in order to achieve glycolation.

Goniometer: 1) An instrument that measures X-ray diffractions. 2) An instrument used in optical crystallography for measuring the angles between crystal faces.

Grade scale: A systematic, arbitrary division of the essentially continuous range of particle sizes of a sediment or rock into a series of classes (grades) for the purpose of terminology and statistical analysis.

Grain size: Size of particles that make up a rock or sediment.

GRAPE: Gamma ray attenuation porosity evaluator.

Graphite: An opaque, lustrous black to steel gray hexagonal mineral composed of C.

Grasshopper effect: Progressive evaporation of chemicals from warmer environments toward colder environments in high latitudes and high altitudes.

Grating instrument: Instruments based on gratings for wavelength separation.

Gray (Gy): 1) The S.I. unit of radiation dose. 1 Gy = 1 J of radiation energy absorbed per kg of matter. 2) A unit of ionizing radiation or absorbed dose, equivalent to 0.1 rads: 1 Gray = 1 J/kg = 1 m^2/s^2.

Greigite: An iron sulfide (Fe_3S_4) that forms under anoxic conditions. It is ferrimagnetic and can form a stable magnetic signal in sediments.

Grey-scale: The different shades of grey present in a black and white image, e.g., 256 tones where 0 is black and 255 is white.

Gymnosperms: Primitive plants that produce their seeds in cones or cone-like bodies. Most modern gymnosperms are trees that are adapted to dry climates, although ferns are also gymnosperms.

Gypcrete: A conglomeratic surficial sedimentary crust cemented by secondary gypsum or anhydrite. Often formed under strongly evaporative conditions, it is common in playa lake beachrock (see also caliche, calcrete, silcrete, ferricrete).

Gypsum: A common hydrated mineral with the formula $CaSO_4 \cdot 2H_2O$, frequently associated with anhydrite and halite. Also called gypsite, plaster of Paris, gyp.

Gyro remanent magnetization (GRM): The magnetization acquired by an anisotropic sample during AF demagnetization in a plane perpendicular to the applied AF (see also rotational remanent magnetization, RRM).

Gyttja: 1) Low density organic mud found at the bottom of lakes. 2) A Swedish term, introduced by H. von Post, denoting organic lake sediments, which are formed mainly under anaerobic conditions and have an organic content of >30%. It consists of a mixture of allochthonous and autochthonous material. Coarse detritus gyttja is rich in macro- and microfossils and occurs in shallow water, while homogenous fine detritus gyttja is deposited in deeper water. Drift gyttja with larger, rounded plant fragments and sand is found in the littoral zone. Algae gyttja is mainly composed of autochthonous algae detritus and to a minor extent of minerogenic particles and often forms in shallow, high-productive lakes. Calcareous gyttja, which is usually rich in fragments from

carbonate algae and shells, has a $CaCO_3$ content of 20–80% and forms in shallow water. Shell-gyttja is mainly composed of shell fragments, but may have a matrix of algae or fine detritus. Gyttja clay has an organic carbon content of 3–6% and clay gyttja of 6–30%. 3) A dark anaerobic mud, rich in organic matter, formed primarily in well-oxygenated lakes and marshes rich in nutrients.

H: 1) Magnetic field, measured in Am^{-1}. 2) Henry; SI unit of magnetic inductance.

Halite: A common evaporitic mineral having the chemical formula NaCl; also known as rock salt.

Harmonic oscillator: A simple model used to explain molecular absorption caused by bond vibration. A harmonic oscillator does not account for overtone transitions.

HCB: Acronym for hexachlorobenzene.

Heavy metal: This term is applied in a number of different ways. Usually, it refers to metallic elements with an atomic number greater than 20. Frequently, it is used to imply toxicity, and sometimes erroneously is used to include non-metallic elements such as As and Se.

Henry's Law constant: The air-water distribution ratio for chemical substances.

Heterotroph: An organism that metabolizes organic matter. Animals and many microbes are heterotrophs.

HI: Hydrogen index.

High-field magnetic susceptibility (χ_{hf}): Magnetic susceptibility measured at a higher frequency.

High performance liquid chromatography: Technique for separating chemicals in solution by passing an inert solvent over a sorbent.

High-resolution sampling: Contiguous or close-interval sub-samples with decadal or finer resolution.

Holocene (Recent): 1) Time: The last epoch within the Quaternary Period and the Cenozoic Era, equivalent to Oxygen Isotope Stage 2. Traditionally defined to have begun at 10 ka, some now place the boundary at approximately 10.8 ka, at the end of the Younger Dryas event. 2) Rocks: The rocks or sediment formed during the Holocene Epoch, also known as the Flandrian in Britain.

Homogenization temperature: The temperature at which a multi-phase fluid inclusion becomes a single, homogenous phase.

HPLC: High performance (or precision) liquid chromatography.

HRMS: High resolution mass spectrometer.

Humus: Mixtures of complex, high-molecular weight organic compounds produced in soils from the remains of microbially reworked primary soil organic matter.

Hydrogenic: Sediment component(s) of inorganic origin formed within the lake.

Hydrogen index (HI): An expression of the relative abundance of hydrogen with respect to carbon derived from RockEval pyrolysis of sedimentary organic matter. The hydrogen index is derived from measurement of the amount of hydrocarbon-rich material released by Rock-Eval pyrolysis of organic matter, divided by the TOC concentration of the sediment sample. It is a proxy for the atomic H/C ratio of organic matter.

Hydrolysis: The process whereby peptide or other organic bonds are broken by adding OH^- and H^+ from a water molecule to complete the charge differentials on the two cleaved bond ends.

Hydrophobicity: The tendency for nonpolar substances to avoid water.

Hypersaline: 1) *Sensu lato*: Having a total dissolved solid content of great than about 40 ppt. 2) *Sensu stricto*: Having salinity above the lowest salinity needed to precipitate halite.

Hz: Hertz, a unit for frequency, $1\ Hz = 1\ s^{-1}$.

I_o: Gamma ray beam intensity at its origin.

IA: Image analysis.

IAS: 1) Inorganic ash spheres. 2) Image analysis system.

IC: Ion chromatograph.

ICP-AES: Inductively coupled plasma atomic emission spectrometry.

ICP-MS: Inductively coupled plasma-mass spectrometer.

Illite: A group of mica-like clay minerals having the general formula: $(K, H_3O)(Al, Mg, Fe)_2(Si, Al)_4O_{10}[(OH)_2, H_2O]$.

Image analysis: The methodology of extracting data from images instead of counting or measuring directly on the samples.

INAA: Instrumental neutron activation analysis.

Inductively coupled plasma (ICP): An emission spectrometric method where excitation is achieved using a plasma. Detection can be photometric or mass spectrophotometric.

Inductively Coupled Plasma Mass Spectrometry (ICP-MS): Analytical technique where samples are injected into a plasma as solution. Ion are generated and focused into a mass spectrometer for detection.

Indurated sediment: Sediment that has become hardened.

Infaunal: An adjective meaning "living in the soft sediment near the sediment-water interface". Can refer to any substrate; not necessarily restricted to sediment.

In-field magnetization: Refers to the magnetization of a sample placed within a magnetic field.

Initial (low field) magnetic susceptibility (χ): A measure of how easily a material can be magnetized, i.e., reflecting how much iron-bearing minerals there is in a sample.

Inorganic ash spheres (IAS): Microscopic spheres of inorganic material formed by the fusing of mineral components during fossil-fuel combustion. A component of fly-ash.

Inorganic geochemistry: Geochemistry of inorganic elements, or geochemical analysis based on inorganic chemical species.

Instantaneous isotope fractionation: The difference between the isotopic composition of substrate and product at any given stage during a reaction involving isotopic exchange.

Instar: A stage of arthropod between moults.

Instrumental Neutron Activation Analysis (INAA): Analytical technique where samples are irradiated, generating new, short-lived radioactive isotopes, which emit characteristic gamma radiations.

Intensity of magnetization (M): The magnitude of magnetic remanence.

Interferometer: A device used to make precise measurements of wavelengths of light by utilising the phenomenon of interference of light waves, i.e., the effect that occurs when two or more light waves overlap or intersect.

Interflow: A continuous or discontinuous current of water or water/sediment mix that flows at an intermediate depth in a lake, typically along a density interface (cf. underflow).

Interlaboratory calibration (tests): Any series of standardized analyses using a single or a series of unknown samples used to determine the collective reliability for an analytical method used by many laboratories.

Intrinsic resolution: Temporal resolution within a stratigraphy, i.e., the amount of time represented in a stratigraphy that is obscured by mixing processes.

INV_w: Inventory of total suspended sediment in the water column on an areal basis ($mg\ cm^{-2}$).

Ion chromatograph: Analytical device that determines the concentration of both cations and anions in solution.

Ionizing radiation: Any electromagnetic or particulate radiation that displaces electrons from atoms. It includes α, β, γ, χ and cosmic radiation.

IR: Infrared or InfraRed.

IRM: Isothermal remanent magnetization.

IRMS: See Isotope ratio mass spectrometry.

Isomers: Chemical compounds having the same formula, but different three-dimensional structures.

Isopleth: 1) Geochemistry *sensu stricto*: A line or surface on a map or chart representing a constant physical or geochemical quantity, such as concentration, temperature, etc. 2) Geochemistry *sensu lato*: An "isocompositional" line or surface, i.e., a line depicting a constant concentration, or concentration ratio. 3) General *sensu lato*: Any line or surface representing a constant physical or geochemical quantity, including isograds, isolats, isohyets, isopachs, and isorithms.

Isostatic rebound: 1) The unloading effect of melting and retreating ice sheets on the Earth's mantle and crust, resulting in local/regional land uplift. 2) A regional increase in Earth surface elevation due to removal of a large load of ice, rock, sediments, or ocean or lake water.

Isothermal remanent magnetization (IRM): The magnetization that remains in a sample after the sample has been removed from an applied magnetic field.

Isotope effects: These arise from differences in the atomic mass of the isotopes of an element and their compounds, causing each isotope to have differing physical, chemical or biochemical properties.

Isotopic fractionation: Processes that result in a change in the isotopic ratio of a compound.

Isotope fractionation factor: The ratio of the ratios of isotopes of a given element in two phases.

Isotope ratio mass spectrometry (IRMS): An analytical procedure that measures the isotopic ratios of elements in a substance.

Isotopic rain-out: Continued preferential removal of water containing the heavy isotopes, ^{18}O and ^{2}H, from a moist air mass.

Isotropic: 1) Giving complete extinction when rotated under cross-polarised light. 2) Denoting a medium in which a particular physical property is independent of direction.

J: Joule, the S.I. unit of energy.

JCPDS: Joint Committee on Powder Diffraction.

JPEG: Joint photographic expert group.

K: Absolute temperature in degrees Kelvin.

K_c: Colloid-water partition coefficient.

K_d: Distribution coefficient.

K_{oc}: Organic carbon-water partition coefficient.

K_{ol}: Overall mass transfer coefficient ($cm\ sec^{-1}$).

K_{ow}: Octanol-water partition coefficient.

K_p: Particle adsorption coefficient ($cm^3\ g^{-1}$).

ka: Literally, thousand years ago. This time unit is used to delineate dates or ages, and is calibrated (or linked) to the present (i.e., "10 ka" implies "10 thousand years ago"; see also ky, ky BP). It is used for dates for most radiometric and many chemical methods, except for ^{14}C ages.

Kaolinite: 1) A non-expandable clay mineral in the kaolin group with the formula $Al_2Si_2O_5(OH)_4$, which does not exchange iron or magnesium. 2) Any kaolin clay mineral.

Kinetic isotope effects: These are typically associated with complex, irreversible, and, in many cases, biologically mediated reactions. A characteristic, but not invariable aspect of kinetic isotope fractionation is a marked discrimination against the heavier isotope, such that the product of the reaction is significantly enriched in the lighter isotope relative to the substrate.

Kerogen: The least reactive form of organic matter. In the context of δ^2H studies, this is the organic matter residue following hydrofluoric and hydrochloric digestions.

KeV: Kilo electron volts.

kHz: Kilo Hertz.

Krumbein's diameter: The length of the longest line in a given direction (normally parallel to the horizontal cross-hair in a microscope field of view) that is bounded by the projected outline of the particle.

Kurtosis: The state or condition of peakedness or flatness of a graphic representation of a statistical distribution.

kW: Kilowatt, a unit of power.

ky: Literally, thousand years. This time unit is used to delineate time spans, and is not calibrated to any particular time (i.e.,"10 ky" implies "10 thousand years"; see also ka, ky BP).

ky BP: Literally, thousand years before present. This time unit is used to delineate ^{14}C dates or ages, and is calibrated (or linked) to 1950 (i.e., "10 ky BP" implies "10 thousand years before 1950"; see also ka, ky).

L* a* b* color space: A method of depicting color that is uniform and recommended by the Comission Internationale d'Eclairage for standard color description. L* - psychometric lightness (0 = black; 100 = white); a* psychometric red (+ve values), green (–ve values); b* psychometric yellow (+ve values), blue (– ve values).

Labile: Used synonymously with extractable.

Laminae: Sedimentary beds or layers that are less than 10 mm in thickness.

Lapilli: Pyroclastic material 2–64 mm.

Laser ablation: Involves the use of a laser to cut a tunnel into a host mineral in order to breach an inclusion wall, and expel the inclusion fluids into an analytical device (typically an ICP-MS).

Laser diffraction technique: The technique of evaluating the size of grains in a sediment mixture by evaluating the amount of diffraction of light by the particles.

Laser raman microspectroscopy: Involves the use of a laser, which excites the covalent bonds of complexes. Can be used to identify various covalently bonded ionic complexes in fluid inclusions.

Latitude effect: With increasing latitude, the isotopic composition of precipitation generally becomes more depleted in heavy isotopes because of the rain-out process and reduction in temperature.

Lattice: Crystal lattice.

Lattice spacing: d-spacing.

LCD: Liquid crystal display.

Least-squares determination: Any statistical method for fitting lines, curves, or surfaces to a data set that minimizes the sum of the squared distances between each data point and the line, curve, or surface.

LEL: Local evaporation line.

Leptokurtic: Refers to a particle size distribution that is excessively peaked (cf. Platykurtic).

Lignin: The substance that binds together cellulose fibers in higher plants to stiffen their structures. Wood may contain as much as 50% lignin. It is a high-molecular-weight polyphenolic compound that varies in composition with different plant types.

Lindane: γ isomer of hexachlorocyclohexane (γHCH). Used as an insecticide.

Liquefaction: The temporary transformation of a stable granular material into a fluid by application of shock forces or vibration in association with a liquid.

Lithology: Composition of rock or sediment.

Lithogenic: Used synonymously with minerogenic.

Lithostratigraphy: The description and subdivision of stratified rock and sediment units based on a unit's lithologic characteristics, such as mineralogical composition, grain size, sorting, fossil content, and sedimentary structures.

Lithostatic pressure: The pressure imposed by the weight of lithologic material deposited on top of the sample, sometimes referred to as overburden pressure.

Local evaporation line: The isotopic composition of surface waters within catchments or within the same climatic region commonly plot on lines with slopes ranging from about 4 to 7 in $\delta^{18}O$-$\delta^{2}H$ space, due to equilibrium and kinetic fractionation effects associated with evaporation.

Loess: Aeolian sediment, usually predominantly silt-sized grains, but possibly including clays and fine sands, produced by glacial activity, deposited up to thousands of kilometres away from the glacier. A common sediment in Quaternary and late Pliocene stratigraphic sequences in China, Eastern Europe, and the US, it may be interstratified with paleosols, tufa travertines, glacial and periglacial sediment packages.

Logging: 1) Systematic (generally equidistant) measurement of a physical property along the axis of a core or a borehole. 2) Non-destructive measurements of physical sediment properties down a borehole or along a sediment core at frequent intervals or on a continuous basis.

LOI: Loss-on-ignition.

Long diameter: The distance between the two most distant points on the particle.

Loss-on-ignition (LOI): Procedure in which the organic matter content of a sample is estimated by the percent weight difference between the dry sample and the sample after combustion at usually 550 °– 600 °C.

Low vacuum scanning electron microscope (LVSEM): Low vacuum, or variable pressure, scanning electron microscopes are used to examine samples at air pressures considerably greater than those utilized by a standard SEM (> 122 Pa as opposed to 10^{-2} Pa). The presence of a partial atmosphere in the SEM specimen precludes secondary electron imaging so that backscatter electron imaging (BSEI) is employed. This facilitates examination of material susceptible to charging effects, and wet and/or uncoated specimens. Sediments examined in this manner may also be resampled for analysis using other techniques, such as micropaleontological slide counts and geochemistry.

Luminescence: The light emitted by something in response to a stimulus. Specific names are used for different stimuli, e.g., thermoluminescence, optically-stimulated luminescence, photoluminescence, triboluminescence etc.

Luminescence petrographic techniques (also luminescence microscopy): Thin section petrographic techniques utilizing luminescence or the light emitted from a solid that is excited by an incident beam of some form of energy.

LVSEM: Low vacuum scanning electron microscope.

m_{Mg}: Moles of magnesium per kilogram of water.

M: Depth in sediment core measured as cumulative dry mass.

M: Magnetization, either induced and/or permanent, measured in Am^{-1}.

Ma: One million years ago.

Macromolecules: High-molecular-weight organic molecules. Cellulose, lignin, and proteins are biological macromolecules. Humic substances are geological macromolecules.

Mafic: Dark-colored, iron and magnesian-rich minerals found in basic, igneous rocks.

Magnetic hysteresis: The lagging effect of magnetization at increasing and decreasing magnetic fields.

Magnetic resonance: The interaction between the magnetic motion, electron spin and nuclear spin of certain atoms within an external magnetic field.

Magnetic susceptibility: 1) the proportionality factor between an induced magnetization and the inducing magnetic field. 2) The property of a material that determines the size of an applied magnetic field required to generate a certain level of magnetism in the material.

Magnetite: An iron oxide (Fe_3O_4) that is most important magnetic mineral. It is strongly ferrimagnetic, and fine-grained magnetite ($<2\,\mu m$) forms a very stable magnetic signal. Can undergo diagenesis under anoxic conditions.

Magnetometer: Instrument that measures magnetic intensities.

Marker bed: A distinctive sedimentary unit that is recognizable throughout the depositional basin.

MAR: Mass accumulation rate.

Martin's diameter: The length of a line that divides the projected outline of the particle into two equal areas and is parallel to a given direction (normally the horizontal cross-hair in a microscope field of view).

Mass accumulation rate (MAR): The accumulation rate of either total sediment or of any sediment component that is calculated from the linear sedimentation rate and the sediment dry bulk density.

Mass spectrometer: 1) An instrument for measuring the relative abundance of isotopes. 2) An apparatus used to separate a stream of ions according to their mass to charge ratio.

Mass susceptibility: magnetic susceptibility related to the mass of a test sample, measured in $m^3\ kg^{-1}$.

Matrix flushing method: A method of quantitative evaluation of the mineral suite in a sample from XRD data using the relationship: $W_i = [((I_i/I_c)/I_i)(\Sigma I_x/(I_x/I_c))]^{-1}$; where W_i is the mineral concentration in the sample mixture, I_i is the intensity of diffracted X-rays of that mineral in the mixture, I_c is the intensity of synthetic corundum, I_x is the intensity of each mineral in the mixture.

MDL: See method detection limit.

Metal enrichment: A metal concentration above that which is expected. Typically expressed as a ratio to the expected concentration.

Meteoric water: Generally refers to snow and rain.

Meteoric water line: Linear relationship between $\delta^{18}O$ and $\delta^{2}H$ in precipitation that occurs due to equilibrium fractionation effects during the condensation of moisture. This is generally described by the equation $\delta^{2}H = 8\,\delta^{18}O + 10$, known as the Global Meteoric Water Line.

Meromictic: A lake in which annual or other mixing events do not stir the entire water column. This commonly results in the development of a deep anoxic water mass.

Method detection limit: The minimum concentration of a substance that is detectable using a specified analytical method.

MHz: Megahertz.

Mica: A mineral group with sheet-like structure, comprising polymerized sheets of silicate terahedra having the general formula:
$(K, Na, Ca)(Mg, Fe, Li, Al)_2(Al, Si)_4O_{10}(OH, F)_2$.

Microprobe: An instrument for elemental analysis of particles using a focussed electron beam to cause x-rays fluorescence from atoms in a specimen. It differs from EDS (which is attached to an electron microscope) in being optimised for chemical analysis, and therefore more accurate and precise.

Microthermometry: Fluid inclusion analysis that involves the heating and cooling of samples to determine the temperature of phase changes.

Microwave extraction: A method for isolating hydrocarbons and hydrocarbon-like organic matter components from samples of sediment or biota by using microwave energy to heat an organic solvent and the sample and mix them together.

Middle diameter: The smallest possible distance between two points on the particle, between which the projection of the particle can pass.

Mie theory: The theory dealing with the quantification of light scattering caused by particulate matter.

MilliTesla (mT): See Tesla.

Mineral: A naturally occurring inorganic element or compound having an orderly internal structure and characteristic chemical composition, crystal form, and physical properties.

Mineral matrix: 1) A general term for the inorganic material in a sedimentary deposit. 2) The interlinked mineral structure that forms the hard structure in complex biologically produced hard parts, including hydroxyapatite in bones and teeth, calcite or aragonite in shells and corals, apatite minerals in chitin, etc.

Mineralisation: As used in organic geochemistry, and studies of carbon and nutrient cycling, the term implies breakdown of organic matter to simple dissolved carbon, nitrogen, etc. species (e.g., CO_2, NO_3^{2-}, NH_3, etc.).

Mineralogy: The study of the formation, occurrence, properties, composition, and classification of minerals.

Minerogenic: Sediment component(s) comprising minerals.

Mirabilite: A soluble, white or yellow, hydrated sodium sulfate evaporitic mineral: $Na_2SO_4 \cdot 10H_2O$.

MIS: Marine oxygen isotope stage.

Mixolimnion: The upper, low-density, well-mixed layer of a meromictic lake.

Molecular sieve: A substance capable of absorbing large volumes of a certain compound while excluding others, hence their value in the cleaning and separation of gases for analysis in a mass spectrometer.

Moment measures: A weighted measure of central tendency of a distribution. The first moment measure is the mean; the second is the standard deviation; the third is the skewness; the fourth is the kurtosis.

Monimolimnion: The deep, dense, usually salty layer of a meromictic lake.

Monochromator: The part of the spectrophotometer that disperse the light into separate wavelengths or groups of wavelengths.

Monohydrocalcite: A hydrated carbonate mineral with the formula $CaCO_3 \cdot H_2O$, also known as hydrocalcite.

Montmorillonite: 1) A group of expandable clay minerals with the general formula $R_{0.33}Al_2Si_4O_{10}(OH)_2 \cdot nH_2O$, where R can be Na^+, K^+, Mg^{2+}, Ca^{2+}, among others. Also known as smectite. May also have Mg or Fe substituting for Al and Al for Si. 2) The clay mineral with the formula $Na_{0.33}Al_{1.67}Mg_{0.33}Si_4O_{10}(OH)_2 \cdot nH_2O$; also known as beidellite. 3) Any member of the montmorillonite group of expandable clay minerals.

MS: 1) Mass spectrometer. 2) Magnetic susceptibility.

MSC: Multiplicative Signal Correction.

mT: (MilliTesla): See Tesla.

Multiplicative signal correction (MSC): A mathematical treatment of spectra used prior to regression to correct for baseline and offset shifts caused by e.g., a difference in particle size or in colour between samples. Based on a standard spectrum (usually a mean of several good spectra) every sample is corrected for a slope and an offset calculated by least squares regression on the standard spectrum.

Munsell charts: Standard color reference charts taken from the Munsell soil color scheme where the hue and chroma of a color are given.

MWL: Meteoric water line.

NAI-P: Non-apatite inorganic phosphorus.

***n*-alkane:** A normal alkane, which is a straight-chain hydrocarbon in which all the carbon-carbon bonds are saturated, i.e., they exist as single bonds.

Nannoplankton: Very small plankton.

Natural remanent magnetization (NRM): the magnetization of a sample that has not been subject an external magnetic field.

NBS-19: Carbon and oxygen isotopic standard comprised of TS-limestone.

Near infrared: The region of the electromagnetic spectrum between 780 and 2500 nm.

Near-infrared spectrometry: The study of sample properties as a function of absorptions by near-infrared radiation. Sometimes the term spectroscopy is used, but spectroscopy is restricted to the study of the spectra.

Neél temperature: See Curie temperature.

Neogene: The last ~23 million years of the Geologic Time Scale.

Neotectonism: Geologically recent movement or deformation of the lithosphere caused by processes originating within the Earth.

NIR: Near InfraRed.

NIRS: Near-Infrared spectrometry.

NIST: National Institute of Standards and Technology.

Nitrate assimilation: The utilisation by aquatic organisms of nitrate (NO_3^-) as a source of dissolved nitrogen.

Nitrification: The oxidation of ammonium (NH_4^+) to nitrate or nitrite by aerobic bacteria.

Nitrogen fixation: 1) the process by which molecular dinitrogen (N_2) is assimilated by primary producers. N fixation is metabolically expensive and restricted to a number of specialised bacteria and algae (diazotrophes), notably the blue-green algae (cyanobacteria). 2) Conversion of N_2 to NH_4^- and incorporation into living biological matter. This process is commonly done by prokaryotes such as cyanobacteria, phototrophic bacteria, and symbiotic nitrogen-fixing bacteria. Eukaryotes do not typically perform nitrogen-fixation.

Nodular: Having the shape of a nodule, or occurring in the form of nodules.

Nodule: A small, irregularly shaped mineral or mineral aggregate, normally having an uneven surface and no internal structure, and is typically distinct in mineralogy and appearance compared to the host lithology.

Non-apatite inorganic phosphorus: That fraction of the total phosphorus concentration that is not organically bound, or in the form of apatite.

Non-combustible material: Matter that cannot be burned (e.g., mineral components within fossil-fuels).

Non-vascular plant: Any simple plant that lacks the fluid-transport systems that is common to most higher plants. Algae, molds, and lichens are non-vascular plants.

Normative calculations: A procedure for determining the concentration of hypothetical ideal (normative) minerals in a specimen, determined by calculation from the total elemental composition.

NRM: Natural remanent magnetization.

OC: 1) Organochlorine. 2) Organic carbon.

Octanol-water partition coefficient: The distribution ratio for chemical substances between octanol and water. Generally used as a measure of a chemical's hydrophobicity.

OI: Oxygen index. The oxygen index is derived from measurement of the amount of CO_2 released by Rock-Eval pyrolysis of organic matter, divided by the TOC concentration of the sediment sample. It is a proxy for the atomic O/C ratio of organic matter.

Off-line preparation: A method that prepares a sample for isotopic analysis that uses a vacuum system in which the gaseous forms of the elements of interest are produced, purified, and put into vials for subsequent analysis in an isotope ratio mass spectrometer.

OM: Organic matter.

On-line preparation: A method that prepares a sample for isotopic analysis that uses a high-temperature system in which the gaseous forms of the elements of interest are produced, separated, and introduced directly into an isotope ratio mass spectrometer.

OP: Organic phosphorus.

Optical isomers: See Enantiomer.

Optical mineralogy: The branch of geoscience dealing with the optical properties of minerals.

Optical microscopy: The utilization of a visible light microscope to study the optical properties of material.

Organic carbon-water partition coefficient: The distribution ratio for chemical substances between organic carbon and water.

Organic matrix: The interlinked organic molecular structure that forms the "soft" structure in complex biologically produced hard parts, including the collagenous and non-collagenous matrices in bones and dentine.

Organic matter (OM): Complex substances consisting mainly of C, H and O, with subordinate quantities of N, S, and other elements, produced by the growth of organisms. OM is present in trace amounts in virtually all sediments, is particularly abundant in some muds and silts, and is the dominant component of gyttja, peat and coal.

Organic phosphorus: That fraction of the total phosphorus concentration that is bound up in organic substances.

Organochlorine: Any organic molecule containing one or more covalently-bound chlorine atoms.

Orthogonal signal correction: A mathematical technique used to filter unwanted information from spectral data containing information of the sample of interest. OSC ensures that information relevant for the dependent variable (Y-variable) is not removed by orthogonalisation of the filter matrix with respect to the dependent variable.

Orthogonal solutions to factor analysis: Any solution in which all axes are mutually perpendicular, and therefore mathematically independent of each other.

OSC: Orthogonal signal correction.

Ostracode (also Ostracod): A millimetre-sized crustacean with the soft body enclosed in a carapace comprised of a pair of kidney-shaped, spherical or lenticular shells made of chitin and low-Mg calcite.

Out-of-field magnetisation: The magnetisation of a sample measured when the sample has been removed from the magnetic field (i.e., having a remanent magnetisation).

Overall mass transfer coefficient (K_{ol}): Variable that relates air-water flux rate of a chemical to the gradient between water concentration and air concentration divided by Henry's Law constant. Also called the transfer velocity and the 'piston' velocity because in the case where air concentration is zero, the rate of outgassing would be equal to the flux that would result if a hypothetical piston were to move vertically through the water column at the speed of K_{ol}.

Overtone transition: Molecular vibrational absorption from ground level to level two or higher.

Oxic: An environment having normal oxygen concentrations. In lakes this commonly implies dissolved O_2 concentrations in the range of 2.0–7.0 ml l^{-1} (cf. anoxic, dysoxic).

Oxidation: The process whereby an atom or ion loses electrons, causing its oxidation number to increase.

Oxide: The oxide component of a sediment is usually dominated by oxides (and related hydrated oxides) of Mn and Fe.

Oxidizable: That part of the total element concentration that can be extracted using a specified oxidizing agent as an extractant.

Oxycline: A zone within the water column where the dissolved oxygen content declines steeply. Waters above the oxycline are commonly oxic, those below anoxic; the lower part of the oxycline itself may dysoxic. It is a permanent feature of meromictic lakes and in other water bodies may appear during the period of seasonal stratification.

Oxygen index (OI): The oxygen index is derived from measurement of the amount of CO_2 released by Rock-Eval pyrolysis of organic matter, divided by the TOC concentration of the sediment sample. It is a proxy for the atomic O/C ratio of organic matter.

Oxygen Isotope Stages: A sequence of sedimentation events recognized in deep oceanic cores by the oxygen isotope ($^{18}O/^{16}O$) ratios in the benthic and planktonic foraminifera therein.

***P*:** 1) Percentage error. 2) Mean annual flux of fallout ^{210}Pb from the atmosphere and to the sediment record.

***p*CO_2:** Partial pressure of carbon dioxide in the atmosphere, which was approximately 200 ppm during the last glacial maximum (about 18 ka), 280 ppm prior to the growth of industry in the mid-1800's, 365 ppm at the end of the twentieth century, and continues to rise as coal and oil are burned.

***p*-coumaric acid:** One of the cinnamyl degradation products released from the alkaline oxidation of lignin.

Pa: Pascal.

PAH: See Polyaromatic hydrocarbon.

Paleomagnetic: Records that indicate past variations in the Earth's magnetic field.

Palaeomagnetic Secular Variation (PSV): Regional, short lasting fluctuations (10^1 to 10^4 years), of the geomagnetic field of smaller amplitude than those involved in complete reversals of the Earth's geomagnetic field.

Paleosol: A buried soil dating from some previous period of subaerial exposure.

Paramagnetism: A type of magnetic behavior occurring in substances with unpaired electrons when exposed to a magnetic field. This results in a small positive susceptibility due to the alignment of the magnetic moment of individual atoms in the applied field. Paramagnetic behavior is displayed e.g., by substances with rare earth transition members, e.g., clays, pyroxenes, amphiboles.

Partial least squares regression: A multivariate regression method that uses an algorithm that maximises the covariance between a number of independent variables (X-variables; e.g., NIR absorbance values) and one or several dependent variables (Y-variables; e.g., lake-water pH). This regression method summarises all X-variables containing the same information into latent variables, partial least square components (similar to principal components).

Particulate organic carbon (POC): Carbon contained in smaller organic particles.

Particulate organic nitrogen (PON): That portion of the total nitrogen present in the water column as an integral part of suspended, solid organic matter.

Partition coefficient: Synonym for distribution coefficient.

Pascal: SI unit of pressure equal to 1 newton/m^2.

PCA: Principal components analysis.

PCB: Polychlorinated biphenyl. A toxic substance used in plastics and electrical equipment.

PCDD/F: Polychlorinated dibenzo-p-dioxins and polychlorinated dibenzofurans.

PDB: Pee Dee Belemnite, a belemnite fossil from Pee Dee Formation, South Carolina, USA.

PDF: JCPDS Powder Diffraction File.

P/E: See precipitation/evaporation ratio.

Peat: An unconsolidated combustible deposit of partially carbonized plant remains, common in bogs, fens, and lakes in tundra or periglacial regions.

Pebble: The term applied to sediment particles finer than cobble and coarser than sand; particles having a diameter of 2–32 mm.

PeeDee Belemnite (PDB): Oxygen and carbon isotope ratios are measured as relative deviations (δ^{18}O per mil; δ^{13}C per mil) from a laboratory standard value. The standard normally employed for the analysis of carbonates is a PDB limestone (belemnite shell from the Cretaceous Peedee Formation of South Carolina).

Penecontemporaneous: formed or existing at about the same time; contemporaneous.

Perimeter diameter: Diameter of a circle having the same perimeter as the projected outline of the particle.

Permeability: The capacity of a porous sediment or rock for transmitting a fluid.

Permille (also per mil and permil): Literally parts per thousand, the conventional unit for expressing isotopic delta (δ) values.

Persistent organic pollutant (POP): A group of chemicals defined as being highly toxic and persistent.

P-ET: Precipitation minus evapotranspiration.

Petrography: The branch of geoscience that deals with the description and classification of rocks (cf. petrology).

Petrology: The branch of geoscience that deals with the origin, occurrence, structure, and history of a sedimentary deposit or rock (cf. petrography).

PFE: Pressurized fluid extraction.

Phenol: Hydroxy benzene biopolymers built with phenol-based compounds that have oxygen-containing groups attached to the central aromatic ring are common in higher plants (lignins and tannins), but they are rare in algae and animals.

Phenolic aldehyde: One of the degradation products released from the alkaline oxidation of lignin. Aldehydes represent a level of oxidation of the building blocks of the lignin macromolecule that is intermediate to ketones and acids.

Phenolic ketone: One of the degradation products released from the alkaline oxidation of lignin. Ketones represent a level of oxidation of the building blocks of the lignin macromolecule that is less than that of aldehydes and acids.

Phenolic acid: One of the degradation products released from the alkaline oxidation of lignin. Acids represent a level of oxidation of the building blocks of the lignin macromolecule that is greater than that of aldehydes and ketones.

Phi grade scale (also phi scale; phi unit): A logarithmic transformation of the Wentworth grade scale in which the particle diameter becomes the negative logarithm to the base 2 of the diameter measured in millimeters.

Photoluminescence (PL): The photons of light emitted in response to an incident beam of photons, the emitted photons usually having lower energies (longer wavelengths) than those of the incident photons. If the emitted photons have higher energies the term optically-stimulated luminescence is normally used.

Photon: A quantum (particle) of electromagnetic radiation. The energy of a photon is equal to hc/λ, where h is Planck's constant, c is the speed of light, and λ is the wavelength of the light. The light emitted by an ordinary light bulb, light-emitting diode, the sun etc. can be thought of as a stream of photons. Radio waves, microwaves, X-rays, and gamma rays can also be thought of as photons, although they are not visible to the eye.

Photosedimentometer: Particle sizing equipment employing the technique of measuring the attenuation and extinction of multiple beams of light as the sediment settles through an aqueous solution.

Phthalates: Forms as colorless crystals. Used as plasticizers.

Phytodetritus: Fragments of plant tissue that typically contribute to the total organic matter present in lake sediments.

Phytolith: 1) Paleontology: A microscopic biologically precipitated silica or calcium oxalate nodule found in the stems and other tissues in plants. 2) Sedimentology: A rock or partially cemented sediment formed by plant activity.

Piece-wise MSC: Piece-wise Multiplicative Signal Correction is a mathematical treatment of spectra used prior to regression to correct for baseline and offset shifts caused by e.g. difference in particle size or in colour between samples. While in ordinary MSC the varying offset and slope is assumed to be constant over the spectral range, piece-wise MSC uses windows for different spectral regions to adjust offset and slope locally.

Pisolite: 1) A coarsely grained oolitic limestone deposit. 2) A small round or ellipsoidal accretionary body in a sedimentary deposit. A grain in a pisolitic deposit; the term is synonymous with pisolith.

Pixel: The picture element in an image.

Plagioclase: A variety of feldspar; a group of triclinic silicates with the general formula: $(Na, Ca)Al(Al, Si)Si_2O_8$.

Plasticizers: Compounds used to make plastics more flexible.

Platy: Refers to a particle or shape in which the length dimension is more than three times the thickness dimension.

Platykurtic: Refers to a particle size distribution that is deficiently peaked (cf. leptokurtic).

Playa lake: A lake, typically shallow, that exists on an intermittent basis, such as in wet seasons or in especially wet years.

Plerospheres: Hollow inorganic ash spheres (cenospheres) containing encapsulated smaller spheres.

Pliocene: 1) Time: The last epoch in the Tertiary Period. The Pliocene is estimated to have begun at roughly 5.3 Ma, but its end is currently controversial, either having lasted until the Gauss-Matuyama at approximately 2.48 Ma (assuming the long Quaternary chronology) or until about 1.78 Ma (according to the short and traditionally defined Quaternary chronology; see also Quaternary). 2) Rocks: The sediment and rocks formed during the Pliocene Epoch.

PLS: Partial least squares.

Pollen: Grains formed by seed-producing plants. They are widely spread by a variety of means (wind, water, insects, birds, animals) and are usually well preserved in lake sediments and peat bogs. Such deposits have extensively been investigated by palynologists. Changing pollen assemblages in superimposed layers are analyzed to interpret temporal changes in vegetation cover, environment and climate.

Polyaromatic hydrocarbon: Group of chemicals with two or more adjacent aromatic rings.

POM: Particulate organic matter.

PON: See paniculate organic nitrogen.

Pond: 1) A natural or artificial standing freshwater body occupying a small surface depression, often synonymous with lake or pool. 2) A water body formed by stream ponding.

POP: See persistent organic pollutant.

Porosity: The proportion or percentage of the bulk volume of a sediment or rock that is void space.

ppb: Part per billion, a unit of concentration.

PPL: Plane-polarized light.

ppm: Part per million, a unit of concentration.

Precipitation/Evaporation ratio (P/E): The ratio between water supplied by precipitation (rainfall) and that lost by evaporation. In lakes, the P term is normally taken to be all inputs to the waterbody (i.e., runoff, groundwater flow and direct precipitation on the lake surface), E is water lost by evaporation from the lake surface.

Precision: 1) The degree of uniformity between repeated successive measurements for a quantity or an operational performance (also known as quality control; see also accuracy). 2) The deviation of several measurements about their mean.

Primary mineral: A mineral formed at the same time as the material enclosing it.

Primary fluid inclusion: Fluid inclusion trapped during the growth of a crystal. Unaltered primary inclusions contain the fluid responsible for precipitation of the host crystal.

Principal components analysis: A numerical method (based on eigen analysis) for simplifying the expression of multivariate relationships between objects.

Projected area diameter: Diameter of a circle having the same area as the projected areas of the particle resting in a stable position or in a random position.

Provenance: The area or geological unit from which a sediment or fossil originates.

Proxy: A measurement that provides indirect evidence of some process or of some participant in a process. Various proxies exist for paleoenvironmental reconstructions. They range from fossil remains to distinctive organic molecules that provide evidence of former biota.

Proxy data: Data obtained by analytical techniques used to reconstruct past conditions (usually environmental) that are used as surrogates (proxies) for other variables, such as climate. The word has the same root as "approximation".

Proxy records: Materials that accumulate and retain information about past environments or environmental processes (e.g., water chemistry, climate).

Pyrite: An iron sulfide mineral (FeS_2) that is formed in sediments under strongly anoxic conditions. It is non-magnetic and cannot form a stable magnetic signal.

Pyrolysis: A procedure that uses high temperatures to break apart macromolecular organic matter, which is difficult to analyze, to produce smaller molecules that can be analyzed.

Pyroxene: Silicate rock-forming mineral.

Pyrrhotite: An iron sulfide ($Fe_{1-x}S$) that may be formed in sediments as ferrimagnetic (Fe_7S_8) under anoxic conditions. Not usually an important part of the magnetic signal

PSV : Palaeomagnetic secular variation.

Pyrolysis: Heating of organic compounds to very high temperatures.

Q/A: Quantity of a substance diffused per unit area.

Quaternary: 1) Time: The second and last period in the Cenozoic Era. Normally, it is subdivided into the Holocene (Recent) and Pleistocene Epochs. The short chronology places its beginning at the traditionally defined boundary at roughly 1.78 Ma, while the long chronology places it at the start of the Matuyama Magnetochron at approximately 2.48 Ma. 2) Rocks: The sediment and rocks formed during the Quaternary Period.

Q-mode factor analysis: A factor analysis method based on eigen analysis of the cross-product matrix.

***R*:** 1) Reflection coefficient. 2) Reflectance.

R_a**:** Air-side resistance.

R_w**:** Water-side resistance.

R_x**:** Stable isotope ratio of substance x.

Radiography: Usually used in reference to X-ray radiography: a technique based on the differential passage of X-rays through a sample to reveal the structure.

Radiolysis: The process in which ionizing radiation cleaves chemical bonds within organic molecules.

Rayleigh distillation: Fractional separation of isotopes in accordance with the Rayleigh equation for fractional distillation or condensation. For any condensation process

$$\frac{R_v}{R_{vo}} = f^{(\alpha-1)},$$

where R_{vo} is the initial bulk isotope ratio, R_v is the instantaneous isotope ratio of the remaining fraction, f, of the residual vapour and a is the vapour v liquid fractionation factor.

Recent: See Holocene.

Re-deposition: Deposition of reworked or eroded minerogenic and/or organic material.

Redfield ratio: The typical elemental ratio of marine phytoplankton: 106C : 16N : 1P.

Redox potential: The ability of the natural environment to bring about any oxidation or reduction process. Is measured as the potential difference between a platinum electrode and an electrode of known potential (in millivolts).

Reducible: That part of the total element concentration that can be extracted using a specified reducing agent as an extractant.

Reductive diagenesis: The process by which magnetite, and iron oxide, is reduced to iron sulfides under anoxic conditions.

Regression analysis: A statistical technique used to determine the degree of mutual association between an independent variable and one or more dependent variables in a paired data set.

Reflectance: Diffusely reflected light from a sample. (Diffuse reflectance as opposed to specular reflectance).

Reflectance spectrometry: The use of IR reflectance spectra from a sample to predict sample properties.

Refractive index: A number that expresses the ratio of the velocity of light *in vacuo* to the velocity of light within the crystal.

Remanent magnetization or remanence: The magnetization remaining (in a sample) after exposure to an external magnetic field.

Remineralization: Recycling of biological or organic forms of elements into their mineral forms, usually by oxidation or metabolism.

Residual fraction: That part of a sediment or soil not brought into solution by a specified chemical extraction procedure.

RGB: Red-green-blue.

RH: Relative humidity.

Rift lake: Lake formed in a basin produced by continental rifting. Typical modern examples are Lake Baikal and most of the large East African lakes.

RMS: Root mean square

RockEval (also Rock-Eval, RockEval analysis): A rapid analytical method that utilizes pyrolysis to provide a semi-quantitative measure of the relative proportions of hydrogen, carbon and oxygen in bulk sedimentary organic matter. The instrument heats sediment samples to measure the amounts of hydrocarbons and hydrocarbon-like substances that escape at different temperatures from the organic matter contained in the sediment. The unit also calculates the amount of CO_2 created during thermal decomposition of the organic matter. The results of Rock-Eval pyrolysis can help to identify the biotic sources of sediment organic matter.

Root mean square noise: Measurement of spectrophotometric noise of NIR instruments by measuring a reference (usually a ceramic or spectralon) repeatedly and calculate the root mean square error.

Rotational remanent magnetization (RRM): See gyro remanent magnetization.

RR: Sediment recycling ratio (dimensionless).

RRM: Rotational remanent magnetization.

Sand: The term applied to sediment particles finer than gravel and coarser than silt; particles having a diameter of 62.5–2000 microns.

Saturated hydrocarbon: A hydrocarbon having only carbon-carbon single bonds. Its structure may be straight or branched.

Saturation isothermal remanent magnetization (SIRM): The maximum remanence that can be attained in a sample after exposure to a strong magnetic field, generally 1 T.

SCP: See spheroidal carbonaceous particle.

Scanning electron microscope (SEM): An electron microscope from which an image of a sample is produced by scanning an electron beam in a television-like raster over the sample and displaying the resultant signal from an electron detector on a screen.

Secondary electron imagery: Secondary electrons are produced as a result of collisions between electrons from the incident electron beam and atoms within the specimen. Secondary electrons are captured by a phtotomultiplier and converted to a visible image using a CRT or monitor. Imaging using secondary electrons is often used to analyze topographic features.

Secondary fluid inclusion: Fluid inclusion trapped within a crystal after growth of the crystal has ceased.

Secondary mineral: a mineral formed later than the material enclosing it.

Secondary mineralization: A common form of diagenetic alteration in which original minerals in fossils and sediment are replaced by or their interstices are infilled by a new (suite of) mineral(s) that may be identical to the original minerals.

Sediment grade scale: See grade scale.

Sedimentation rate: The amount of sediment deposited during a certain time span.

Sedimentology: The physical and chemical study of sediments, which includes clastic particles and chemical precipitates; particle composition, size, shape, sorting, orientation, and sedimentary structures reveal details regarding the environment in which the sediments were deposited.

Segmentation: The process of identification and selection of objects of interest within an image on the bases of their gray-scale values.

SEI: Secondary electron imagery.

Selenite: The clear colorless variety of gypsum, which typically forms large euhedral crystals.

Self-absorption: Absorption of gamma photons within the sample before they can interact with the detector.

SEM: Scanning electron microscope or microscopy.

SEM-EDS: Scanning electron microscope-energy dispersive spectrometer.

Sequential extraction: A multistage chemical extraction in which the residual fraction of early stages, becomes the extractable fraction for later stages.

SFP: Spheroidal fly-ash particles.

Sheet flood (also sheetflood): l)A broad expanse of moving, often storm-generated, water that spreads as a shallow, continuous uniform film over a large area. 2) A flow or the process of water movement in which the fluid is not concentrated in a discrete channel or defined river banks.

Sieve diameter: The width of the minimum square aperture through which the particle will pass.

Silt: The term applied to sediment particles finer than sand and coarser than clay; particles having a diameter of 3.91–62.5 microns or sometimes 1.95–62.5 microns.

Skirt effect: Beam scattering effect often encountered when using an ESEM. As the electron beam travels through the sample chamber, the electrons interact with the gas in the chamber. The interaction of the molecules and electrons cause some of the electrons to stray from the beam. The straying electrons form a conical shape around the beam, which resembles a “skirt”.

SMOW: Standard Mean Ocean Water.

S/N: Signal-to-noise ratio.

Soot: Sub-micron carbonaceous particles formed during the process of combustion.

Soot balls; particles: Term used in early literature to describe spheroidal carbonaceous particles (SCPs).

Soot spheres; spherules: Term used in early literature to describe spheroidal carbonaceous particles (SCPs).

Sorption: Term for general binding of a soluble substance to particle surfaces. No specific binding mechanism is implied.

Soxhlet: Glass apparatus used to reflux samples repeatedly with solvent to extract analytes.

Soxhlet extraction: A method for isolating hydrocarbons and hydrocarbon-like organic matter components from samples of sediment or biota by repeatedly cycling an organic solvent through the sample.

SPCBK: Abbreviation of 'spheroidal carbonaceous black'; another term for spheroidal carbonaceous particle used in a classification of combustion particles.

Spectral filters: The mathematical treatments of NIR spectra prior to regression used to remove variance that only adds to the error term in the calibration model, (i.e., variance not containing systematic information on the sample). Common spectral filters are multiplicative signal correction (MSC), derivatives and smoothing algorithms.

Spectral reflectometer: An instrument for measuring color reflectance.

Spectroscopy: The production and analysis of a spectrum.

Spheroidal carbonaceous particles: Microscopic spheroids of elemental carbon produced from the incomplete combustion of fossil fuels at industrial temperatures. A component of fly-ash.

Spheroidal fly-ash particles (SFP): Term occasionally used to describe a combination of spheroidal carbonaceous particles and inorganic ash spheres.

Spinning cup module: A device used to rotate the sample during recording of the NIR spectrum. Reduces the within sample variance emanating from heterogeneity in e.g., particle size and chemical composition.

Stable isotope: Atoms with nuclei that contain the same number of protons but different numbers of neutrons and are radioactively stable (i.e., do not undergo radioactive decay) within the limits of available detection methods.

Standard error: Uncertainty in a measured quantity, usually measured by standard deviation of repeated determinations.

Stokes diameter: The free-falling diameter of a particle in a fluid with laminar flow.

Stokes Law: A formula that expresses the rate of settling of spherical particles in a fluid.

Stratigraphy: The study of stratified rocks and sediments especially for the purpose of correlation. Important considerations include each unit's physical, biological, and chemical characteristics, boundary conditions, spatial distribution, relative position with respect to other strata, and age.

Subsample: A portion of a larger solution or other sample that need not be geochemically identical (see also aliquot).

Substrate (as used in stable isotope geochemistry): The initial starting substance for a process involving isotope exchange (see fractionation).

Superconduction quantum interference device (SQUID): Type of magnetometer working at liquid helium temperature (–296 °C) to reduce background noise and increase sensitivity.

Surface diameter: Diameter of a sphere having the same surface area as the particle.

Surface volume diameter: Diameter of a sphere having the same external surface area to volume ratio as the particle.

S/V ratio: Syringyl/vanillyl ratio.

Syringyl phenols: A group of degradation products released from the alkaline oxidation of lignin that includes syringaldehyde, acetosyringone, and syringic acid. The syringyl components are diagnostic of organic matter from angiosperm plants.

Syringyl/vanillyl ratio (S/V ratio): The S/V ratio is calculated as the concentrations of syringyl phenols divided by the sum of vanillyl phenols. It is a measure of the relative contributions of gymnosperm residues and angiosperm residues to sediment organic matter.

T: 1) Temperature. 2) Tesla, a unit of magnetic flux density: $1\ T = 1\ kg/(s^2\ A) = 1\ Vs/m^2$. 3) a ton or 1000 kilograms; 4) Transmittance; 5) Relative transmittance of X-rays.

T_C: Curie temperature.

Technogenic: Used synonymously with anthropogenic.

TEM: Transmission electron microscopy.

Temperature dependent magnetic susceptibility: The variation of magnetic susceptibility with increasing and decreasing temperatures.

Ternary plot (or diagram): A graphical data representation in which three axes are used to show the relationships between three interdependent variables, often three compositional components or trace elements.

Terrigenous: Used synonymously with minerogenic.

Tesla (T): Unit of magnetic induction.

Texture: 1) The general physical appearance of a rock or sediment. 2) The size, shape, and arrangement of component particles in a sediment or rock. 3) The relative proportions of various size groups of grains (e.g., sand, silt, clay) in a sediment or rock.

Th: Homogenization temperature.

Thermal analysis systems: A group of analytical methods that evaluate the mineralogy of a sample by measuring the change in some physical or chemical property or reaction product as a function of change in temperature.

Thermal maturation: The alteration of sedimentary organic matter by the effects of heating. Maturation implies that the altered OM reaches a stage where its thermal breakdown will produce liquid or gaseous hydrocarbons.

Thermal vacuum cell: Sample holder chamber for laser ablation ICP-MS, in which the chamber is under a high vacuum, and the holder has the ability to heat the sample, in order to increase the internal pressure of fluid inclusions.

Thermocline: A marked thermal gradient, which separates warm surface waters from deeper, cooler water in lakes and in the ocean.

Thermogravimetric analytical techniques: A group of thermal analytical techniques in which the change in mass of a sample undergoing incremental heating is used to identify the mineralogical composition.

Thin section: Sample that is mounted on a glass slide and ground to near-transparency. In practice, most samples will be 30 to 100 μm thick. Soft materials found in recent sediments can be hardened by embedding the samples with a hard material like epoxy resin or wax.

Thresholding: Technique for selecting objects of interest. A threshold grey-scale value is chosen from the histogram representing the grey-scale range of the image, e.g., a value that separates mineral-grains from the background. The values over the threshold becomes black (or white) and the values below the threshold becomes white (or black) producing a binary image where the objects of interest are clearly visible.

TIFF: Tagged image file format.

Till: Term to denote poorly sorted sediment deposited by an active glacier or ice sheet or in connection with melting of stagnant ice from a decaying glacier or ice sheet.

TN: Total nitrogen.

TOC: Total organic carbon. TOC is commonly used to represent the amount of organic matter in sediment, inasmuch as organic matter is about 50% carbon.

Tomographic images: Non-destructive 3-dimensional examinations of the internal structures of sediments using X-ray computed tomography.

Torr: Equal to one millibar or 10^2 pascals (or 1 mm Hg).

Tortuosity: The extent of irregularity in a path through a porous medium.

Total carbon: The sum of inorganic and organic carbon in sediment that can be measured by combustion at 800–1000 °C with an elemental analyzer.

Total digestion: A chemical attack that brings the specimen entirely into solution.

Total nitrogen (TN): Bulk nitrogen content of a sediment sample, commonly expressed as weight % and typically determined by means of an element analyzer.

Total organic carbon (TOC): Bulk content of organically bound carbon in a sediment sample, commonly expressed as weight %. "Organic" distinguishes this carbon from that present in inorganic substances, most commonly carbonate minerals.

TP: Total phosphorus.

Trace element: An element that normally has a sufficiently low concentration that variation in its concentration does not significantly alter other element concentrations by dilution. This includes all elements except the major rock forming elements (Si, Al, Ti, Fe, Mn, Ca, Mg, K, Na) and some elements associated with organic matter (C, P and S).

Trace metal: As trace element, but referring only to elements that are metallic in character.

Transfer function: A mathematical function describing the numerical relationship between one/several independent variables and one (several) dependent variable(s). Commonly used to infer past values of an environmental variable (e.g., pH, salinity) from the composition of fossil assemblages (e.g., diatom abundances).

Transmission electron microscopy (TEM): An optical-electron microscope that uses an assembly of magnetic lenses and a beam of high-energy electrons that are transmitted through a thin sample.

Transmittance: The number resulting from division of the intensity of light passing through a sample by the intensity of the light emitted onto the sample.

Travertine: 1) Any finely crystalline massive concretionary limestone formed by surface or groundwater evaporation. 2) Any flowstone deposit, hence the usage travertine implying stalagmitic flowstone. 3) Any carbonate deposit formed within a cave or karst system by secondary precipitation. 4) Massive, hard, dense carbonate deposits formed in association with open-air springs, streams, lakes, or marshes that precipitate carbonate.

Trona: A white or yellow-white monoclinic mineral: $Na_3(CO_3)(CO_2OH) \cdot 2H_2O$.

Tufa: 1) A chemical sedimentary rock composed of calcium carbonate, which form in non-marine settings. 2) Any subaerial travertine deposit formed near a spring mouth, along a stream, in a marsh or lake. The term often refers to thin, porous, or soft deposits, as opposed to travertine used for massive, hard, dense deposits.

Turbidite: A deposit produced from a turbulent, sediment-charged density underflow.

U_{10}: Wind speed ($m\ sec^{-1}$) at a height of 10 meters.

U_z: Wind speed ($m\ sec^{-1}$) at height z (m).

UCM: Unresolved complex mixture of hydrocarbons that is a result of the gradual thermal alteration of the initial biological organic matter during formation of petroleum and that can also sometimes be created by microbial alteration of sediment organic matter. The presence of a UCM in sediment is generally considered to be diagnostic of petroleum hydrocarbons.

Ultrasonication: A method for isolating solvent-extractable components of organic matter from samples of sediment or biota that uses high-frequency sound waves to agitate the sample in an organic solvent.

UNECE: United Nations Economic Commission for Europe.

Unmixing: The term unmixing can be applied to any method used to determine the composition and proportions of components in a mixture.

Underflow: A continuous or discontinuous current of water or water/sediment mix that flows along the bottom of a lake or the ocean. In lakes many underflows originate through the inflow of cooler and/or sediment-charged river water (cf. interflow).

Unrolled diameter: The mean chord length through the center of gravity of the particle.

USEPA: United States Environmental Protection Agency.

USGS: United States Geological Survey.

UV (light or radiation): Ultraviolet light (or radiation).

V_d: Deposition velocity ($m\ day^{-1}$).

Vacuum drying: A method of drying by evacuating the sample.

Van der Waal's forces or bonds: Weak attractive forces (bonding) between neutral atoms or molecules having a negative or positive charge concentration at one end.

Van Krevelen plot: A graphical representation of the carbon, hydrogen, and oxygen elemental composition of organic matter that is used to identify its biotic origins and diagenetic alterations. The cross-plot of the atomic ratios of H/C and O/C separates waxy and algal organic matter rich in hydrocarbons and similar hydrogen-rich compounds from woody organic matter rich in cellulose and other carbohydrate compounds.

Van Krevelen-type plot: A cross-plot that employs Rock-Eval hydrogen index and oxygen index values instead of atomic H/C and O/C ratios to identify the biotic origins and diagenetic alterations of sediment organic matter.

Vanillyl phenols: A group of degradation products released from the alkaline oxidation of lignin that includes vanillin, acetovanillone, and vanillic acid. The vanillyl components are diagnostic of vascular-plant organic matter.

Varimax rotation: A numerical technique applied to factor analysis, yielding an orthogonal solution in which variable loadings on each factor are maximized or minimized. This has the effect of making factors more easily interpretable.

Varve: A sedimentary structure (couplet) representing a single year of deposition. Generally found in environments with strong seasonal changes in environmental conditions.

Vascular plants: Plants that have systems that provide movement of fluids within, to, and between advanced structures such as roots, stems, leaves, and reproductive organs. Most land plants are vascular plants; algae are not.

Vital effect: The deviation from chemical thermodynamic equilibrium in elemental or isotopic composition caused by the input of energy by the organism that formed the compound under consideration.

Volatilization: To cause to evaporate.

Volume diameter: Diameter of a sphere having the same volume as the particle.

VPDB: Vienna Pee Dee Belemnite.

VSMOW: Vienna Standard Mean Ocean Water.

W_i: Concentration of mineral I in a mixture as determined by the matrix flushing technique.

W_g: The gas phase scavenging efficiency (dimensionless).

W_p: The particle phase scavenging efficiency (dimensionless).

W_{sed}: Mass sedimentation rate ($mg\ cm^{-2}\ yr^{-1}$).

W: Watt, a unit of power, $1\ W = m^2 kg/s^3 = 1\ J/s$.

Water diffusivity: Variable that equates diffusive flux to a concentration gradient in water.

Water side resistance: The partial water side resistance defined as the water side diffusivity divided by the depth of the stagnant water boundary at the water's surface ($sec\ cm^{-1}$).

Wavelength dispersive spectrometry (WDS): Electron microprobe-type, generating sequential elemental acquisition.

wt %: Weight percent, which is equal to: (weight of component/total weight) 100.

Xenobiotic: Any substance that is foreign to living organisms.

X-radiograph: An image produced by exposure of a sample material and photographic paper to an x-ray source. Samples with higher density will attenuate the x-ray more than lower density samples, thus decrease the exposure of the photographic paper.

X-radiography: X-rays that pass through heterogeneous media such as sediments are absorbed by certain components. Passing X-rays are captured on an X-ray sensitive film where they produce radiographs of the sediment structure.

X-rays: Electromagnetic radiation with a wavelength shorter than UV and longer than gamma radiation.

X-ray diffractometry (X-ray diffraction; XRD): The diffraction of a beam of X-rays by the three-dimensional array of atoms in a crystal.

X-ray fluorescence (XRF): 1) Method for quantitative determination of the geochemical composition (major and minor elements) of sediments. 2) Analytical technique in which samples are exposed to an X-ray beam. The beam generates secondary X-rays (fluorescence) that have wavelengths characteristic of elements in the sample.

X-ray fluorescence analysis: An elemental analysis method based on x-ray fluorescence.

X-ray images: Comparable to X-radiographs, X-ray images capture the sediment structure by sediment-penetrating X-rays. They differ because the X-ray source is coupled with a digital camera providing digital images that allow a direct image processing.

XRD: X-ray diffraction, diffractometer, or diffractometry.

XRF: X-ray fluorescence.

XRF-ED: X-ray fluorescence analysis using energy dispersive detection.

XRF-scanner: Automated sediment-profiling instrument for qualitative determination of major elements such as K, Sr, Ca, Mg, Mn, Fe, Ti.

XRF-WD: X-ray fluorescence analysis using wavelength dispersive detection.

INDEX

$\delta^{13}C$ 4, 210, 242–244, 246–249, 251, 253, 259–261, 351–367, 373–394, 417, 419, 423–427, 429–430, 432–433
  $\delta^{13}C_{cell}$ 385,390–391
  $\delta^{13}C_{org}$ 239, 242,385
$\delta^{18}O$ 4, 207–208, 210, 212–253, 351–367, 373–396
  $\delta^{18}O_{carb}$ 377
  $\delta^{18}O_{cell}$ 376–377, 385
  $\delta^{18}O_{w}$ 390–394
  $\delta^{18}O_{mw}$ 376–377
  $\delta^{18}O_{p}$ 392–393
$\delta^{34}S$ 210
^{210}Pb 85, 107, 114, 257, 287–289, 332–333, 335, 339,341,343,414,416
AAS (atomic absorption spectrometry) 92–93, 152
absorbance 59, 299, 301, 306, 309, 312, 314
accelerator mass spectrometry (AMS) 231, 426
accumulation rate(s) 24–25, 107–111, 119, 124, 243, 246, 314, 328, 332, 334–336, 343, 415
accuracy 48, 91, 93, 95–96, 161–163, 173, 212, 229, 304
acicular 70–72
acid extractable 87, 104
acidification 89, 114, 120–123, 241, 323, 339, 342
acid-washing 251–252, 378
acousto-optical tuneable filter (AOTF) 303–304
adsorbtion 405, 422
aeolian 87, 107, 126–127, 143, 146
AES (atomic emission spectroscopy) 92–93, 95, 152
AF (alternating field) 224, 232–233
Africa (African lakes) 190, 201, 230, 244–245, 252–253, 326, 374, 402, 423–424, 427
Ag (silver) 94, 118, 156
air side resistance 282
Al (aluminum) 159
algae 243–250, 254, 256, 261, 263–264, 357, 361, 376, 385–387, 389, 403–404, 407, 410, 430, 434
Alizarin red S 171
alkaline hydrolysis 379
alkaline lake(s) 404, 408
allochthonous 219, 243, 385, 425, 432–433
allogenic 87–88, 107, 121, 143–144, 146
allophane 146
aluminosilicate 88, 95, 107, 130, 322, 327, 336
aluminum (Al) 159
ambient temperatures 253, 272, 283
ammonia 422–423, 425
  ammonia volatilisation 403–404, 407–408
  ammonification 403
amorphous 146, 153, 158–159, 164, 167–168, 176, 376
amphiboles 151
AMS (accelerator mass spectrometry) 231, 426
angiosperm(s) 256, 258
anharmonic 300–301
anhydrite 148
anhysteretic 224, 232
  anhysteretic remanent magnetization (ARM) 224, 227, 232
anisotropic 171, 338
anisotropy of magnetic susceptibility 231
anoxic (anoxia) 116, 119, 243, 250, 252, 288, 403–404, 413, 415, 420, 422, 429
Antarctic 329, 336, 408, 411
anthropogenic 85, 87–88, 104, 124, 218, 248, 252, 402, 412–414
anti-ferromagnetism 222
Antonelli Pond, USA 104–105
AOTF (acousto-optical tuneable filter) 303–304
AP (apatite phosphorus) 119
apatite 119, 147, 253
apatite phosphorus (AP) 119
aqua regia 95
aquifer 355–357
aragonite 70–74, 144, 146, 147, 171, 192, 197, 355, 357–359, 361–363, 366
arctic 289, 290, 293, 326, 328, 332, 335, 338, 374, 390, 393, 409, 425
ARM (anhysteretic remanent magnetization) 224, 227, 232
arsenic (As) 95, 116, 118
Asia 190, 326, 342
atmospheric pollution 85, 106, 123
atomic absorption spectrometry (AAS) 92–93, 152
atomic emission spectroscopy (AES) 92–93, 95, 152
attapulgite 165
attenuation 41, 58–60
  attenuation coefficient 169
Austin Lake, USA 254, 392–395
Australia 62, 70, 190, 260, 326, 335, 336
Austria 325

authigenic 42, 87–88, 104, 107, 119, 126–127, 129, 143–144, 146, 151, 219, 358, 375–377
  authigenic minerals 68, 144
autochthonous 117, 243, 405, 426, 433
Aydat Lake, France 245

B (boron) 118
Ba (barium) 94, 118, 147, 150
backscattered electron imagery (BSEI) 11, 16, 31–32, 34
Baja, Mexico 192–193
Baldeggersee, Switzerland 244, 251–252
barite 148
barium (Ba) 94, 118, 147, 150
Basin and Range Province, USA 190
bedding 2, 7–11, 13, 15, 17, 19, 41–42, 73
Beer-Lambert equation 300–301
benthic 281, 359, 361
Bermuda 245
Bertrand lens 170, 171
Betula 312
biaxial 171
binary image 31, 33–34
bioconcentration 272
biogenic 16, 25, 87, 111, 119–120, 126–127, 327, 354, 358–362, 364–366, 375, 409, 429
  biogenic carbonates 107, 351, 358, 362, 364, 366
biomagnification 271–272
biophile 87
bioturbation 8, 10, 16, 69, 281, 314, 332
bio-induced 360–361, 365
birefringence 170–171, 204
bladed 197
blanks 96, 130
bleaching 378–379
bloedite 148, 190–191
borate minerals 149–150
boron (B) 118
Botryococcus 376, 385, 388
boulder 46
Br (bromine) 118, 128
brackish 144, 197
Bragg's Law 154, 156
bromine (Br) 118, 128
brushite 147
BSE (backscattered scanning electron microscopy) 31–34
  BSE-image 11, 16, 31–32, 34
bubble 20, 195, 203–205
bulk density 33, 41, 287
bulk sediment 168, 229, 276, 352, 364–365, 366, 430

C/N 242–246, 385, 393, 401, 404–405, 412, 416–417, 420, 422–423, 425–427, 430, 432–433
C/V (cinnamyl/vanillyl ratio) 258
C3 plants, algae 246, 248, 253, 261
C4 plants 248, 253, 260
Ca (calcium) 24–25, 91, 111, 118, 120, 362
cadmium (Cd) 29, 93–94, 104, 109, 112, 117–118, 122–124, 130, 310
calcite 57, 103, 127, 144, 146–147, 159–160, 170–171, 190, 197–198, 210, 220, 251, 253–354, 355, 357–363, 366
calcium (Ca) 24–25, 91, 111, 118, 120, 362
calibration 32–33, 168–170, 176, 233, 299–300, 307–310, 312, 314, 384, 386, 389, 392
  calibration model 299–300, 314
CAM plants 260
Canada 43, 69, 70, 73, 167, 190, 201, 244, 276, 291, 310, 326, 335, 376, 390–391, 412
  Canadian High Arctic 289
carbonate carbon 241, 245, 247
carbon dioxide (CO_2) 12, 103, 120, 208, 241, 243, 247–248, 251, 253, 259–262, 355–359, 361–364, 375, 381–384, 386, 391, 394, 419, 429
carbon isotope(s) 4, 210, 242–244, 246–249, 251, 253, 259–261, 351–367, 373–394, 417, 419, 423–427, 429–430, 432–433
catchment 3, 33, 83–85, 87–89, 104, 106–109, 120–122, 124–130, 218, 226, 258, 264, 310, 323, 333–334, 343, 358, 375, 390, 405, 414, 425–426, 434
  catchment acidification 122
  catchment evolution 125, 412
cathodoluminescence 152, 172
cation exchange 313
Cd (cadmium) 29, 93–94, 104, 109, 112, 117–118, 122–124, 130, 310
cellulose 4, 240, 243, 253, 302, 310, 373–386, 389–396, 405
cement 172
cenospheres 319
centrifugation 159, 162, 166, 275
centrifuge-on-ceramic tile method 163
CF-IRMS (continuous flow-isotope ratio mass spectrometry) 248, 251, 380, 394
chalcophile 118
Chara 351, 361–362, 365, 387–389
charaphytes 361
Charophyta 376
chemical stains 171
chemocline 70–72, 74
chevron(s) 191, 193–194, 196, 201, 206
China 97, 124, 126–127, 201, 205, 207–209, 326, 328, 332, 334, 342
chitin 364–367
chlorine (Cl) 94, 118, 128, 146, 149, 152, 172–173, 207, 210, 271, 279, 288, 356
chlorite 60, 98, 102–103, 126, 151, 165, 167–168, 379
chromatography 209, 241, 255–257, 259, 276–277

chromium (Cr) 94–95, 116, 118, 121, 124, 156, 224, 284
chronology 3, 332, 413–414, 416
cinnamyl/vanillyl ratio (C/V) 258
citrate-bicarbonate-dithionite 159
Cl (chlorine) 94, 118, 128, 146, 149, 152, 172–173, 207, 210, 271, 279, 288, 356
classification 41, 44, 47–48, 66–67, 86–87, 100, 129–130, 143, 324, 337–338, 340, 360
clastic (& clastic sediment) 8, 26, 33, 84, 102, 125, 126, 164, 220, 242
clay 11, 13, 15–16, 18, 24, 42, 44, 46, 51, 60, 66, 86, 91, 119, 126, 146, 151, 155–168, 173–174, 176, 194, 218, 229, 254, 276, 313, 366, 421–422, 425
  clay minerals 15, 66, 86, 145, 156–168, 176, 254, 421
  clay mineral analysis 158, 160, 166
  clay mineral material 164
  clay mineralogy 42, 163–164
  clay sized material 164
  clay slurry 161–162
cleavage 171, 194–195, 199, 206, 211, 288, 408
climate 3, 69, 207–209, 217, 239, 252–254, 263–264, 312, 352–355, 357, 367, 425–426, 430–431
  climate change 127, 233, 253, 261, 264
CO_2 12, 103, 120, 208, 241, 243, 247–248, 251, 253, 259–262, 355–359, 361–364, 375, 381–384, 386, 391, 394, 419, 429
coal 97, 320–322, 324, 328–332, 336–343
cobble(s) 46, 54
coercivity of remanence 224
coincidence 53, 113, 430
colour (color) 23–24, 26–27, 29, 33, 36, 42, 93, 171, 322, 379–380
  colour reflectance 8
  colour space 8
colorimetric methods 93
composition 3, 24, 36–37, 41, 43, 59–61, 84–89, 91, 99–102, 110–111, 113, 115, 117, 122, 125, 130, 143–152, 160, 163, 167, 170, 174, 191, 202, 205, 207–209, 212, 217, 245–250, 252, 255, 261, 272, 285, 309, 312, 314, 322–323, 336, 339, 353, 355, 374–378, 381, 385–386, 390–393, 395, 401–402, 405, 407–411, 413–417, 420–422, 425, 430–434
compound microscope 170
computerized tomography (CT) 12, 281, 284, 373
congener 280, 285, 289, 291, 293
copper (Cu) 93–94, 104, 112–118, 122–124, 130, 156, 310
core 4, 7–10, 12, 14, 18, 23, 26–27, 26–37, 70–74, 84–85, 95–96, 104, 106–108, 110, 115, 118–119, 123–124, 127, 129, 171, 192–193, 196, 198, 200–201, 203, 206–209, 218–219, 225, 227, 229–230, 233, 243, 246, 248, 251, 257–259, 261, 273–274, 276, 280, 284–285, 287, 289, 292–293, 306, 308–309, 313–314, 323–324, 328–329, 331–333, 336, 339, 341, 343, 351–352, 360, 367, 376, 392–394, 412–418, 420–423, 425–428, 430–432
corer 27, 225
continuous flow-isotope ratio mass spectrometry (CF-IRMS) 248, 251, 380, 394
corundum 150, 169
cosmogenic 87
Coulter counter 49, 51–53
CPL (crossed-polarized light) 170–171
Cr (chromium) 94–95, 116, 118, 121, 124, 156, 224, 284
critical point drying 12
crossed-polarized light (CPL) 170–171
crust 192, 193, 201–202
cryogenic purification 381
cryostage 211
crystal 3, 12, 28, 41, 70–74, 90, 146, 153–154, 160, 163, 169, 174, 189–195, 197–199, 201, 203–206, 208–209, 221–222, 304, 358, 361–363
  crystal habit 171
  crystal size 71, 73–74, 190
crystalline 146, 152–154, 156, 158, 164, 168, 174, 191, 193–194, 197, 277
CT (computerized tomography) 12, 281, 284, 373
Cu (copper) 93–94, 104, 112–118, 122–124, 130, 156, 310
cumulates (cumulate crystals) 191–194
Curie temperature (point) 221–222, 231, 271
Cypridopsis 360
Czech Republic 325, 334, 340

d-optimal design 308
D/H (deuterium/hydrogen isotope ratio) 253–254, 259–261, 352
DCM (dichlormethane) 273–274, 276–277
DDD (dichlorodiphenyldichloroethane) 274, 279, 283, 289
DDE (dichlordiphnyldichloroethene) 271, 279
DDT (dichlorodiphenytrichloroethane) 272, 274, 277, 279, 283, 289–291
Dead Sea 192, 201
Death Valley, USA 193, 196, 199–203, 208
declination 363
deep lakes 110–111, 130
denitrification 245, 249, 252, 403–404, 407–408, 413, 429, 433
Denmark 325, 362, 412
density slicing 31
detection limits 90, 91, 93–94, 211, 278–279
detrital 42, 69, 117, 143, 151, 172, 174, 191,218–219, 233–234, 252, 351, 358, 365–366
deuterated 276, 278

deuterium/hydrogen isotope ratio (D/H ratio) 253–254, 259–261, 352
DGT (diffusive gradient) 114, 129
diagenesis 85, 105, 112, 122–124, 174–175, 219, 243, 245, 248, 251, 257–259, 358, 420–422
dichlormethane (DCM) 273–274, 276–277
dichlorodiphenyldichloroethane (DDD) 274, 279, 283, 289
dichlordiphynldichloroethene (DDE) 271, 279
dichlorodiphenyltrichloroethane (DDT) 272, 274, 277, 279, 283, 289–291
diagenetic 68–69, 87–88, 115, 119, 153, 175, 191, 197, 210, 218, 248, 255–256, 308, 313–314, 385, 404, 416, 420
  diagenetic alteration 143
diamagnetism 220
diameter 43–47, 50–52, 54–59, 66–67, 210, 225, 277, 327, 338, 362, 382
diatom 11–13, 16, 18, 86, 113, 117, 119–120, 125, 263, 309, 312, 314, 323, 328, 352, 390–392, 404, 420, 422, 429–430, 434
DIC (dissolved inorganic carbon) 246–248, 357, 362, 375, 385–386, 390, 412, 424, 426, 429
dichloromethane 255, 273, 276
differential thermal analysis (DTA) 152
diffraction 41, 49, 60–61, 143, 153–156, 159–160, 163–164, 168–169, 175–176, 351
diffractogram 156, 159, 166
diffractometer 155–156, 169
diffusion 86, 108–109, 112–115, 123–124, 128–129, 170, 286, 289, 292, 405, 422
diffusive gradient (DGT) 114, 129
digital camera 27–29, 37
digital imaging 8–9, 16, 26
digital x-ray imaging system 10
dimethylaminoethanol 19
DIN (dissolved inorganic nitrogen) 250, 252, 402, 406–413, 423–425, 428–430
dipole 220, 300
direct measurement of particle size 50–51
dissolved inorganic carbon (DIC) 246–248, 357, 362, 375, 385–386, 390, 412, 424, 426, 429
dissolved inorganic nitrogen (DIN) 250, 252, 402, 406–413, 423–425, 428–430
dissolved organic carbon (DOC) 247, 281–282, 357, 391
distribution coefficient 108, 115, 353, 357
DOC (dissolved organic carbon) 247, 281–282, 357, 391
dolomite 57, 144, 147, 160, 170–171, 173, 198, 364
drag diameter 45
DTA (differential thermal analysis) 152
dysoxic 404

EAAS (electrothermal atomic absorption) 93
ECD (electron capture dectector) 277–280
EDS (energy dispersive spectroscopy) 7, 23, 41, 83, 90–91, 143, 189, 209, 211–212, 217, 239, 271, 299, 319, 339, 341, 351, 373, 401
Egypt 195, 203, 206, 326
eigen analysis 99–100
electrical resistance particle counter 52
electromagnetic radiation (EMR) 154, 156
electron capture detector (ECD) 277–280
electronic particle sizing 51
electro-osmotic knife 8
electrothermal atomic absorption (EAAS) 93
elemental analyzer 241, 243, 248, 251
ellipsoidal 70–71
embedding 12, 14–15, 18–19, 159, 170, 227
emission spectrometry 92, 152
EMR (electromagnetic radiation) 154, 156
enantiomers 272
endogenic 42, 69–70, 87, 143–144, 146, 151, 351, 354, 358, 362–363, 365–367
  endogenic carbonates 144, 358, 362–363, 365, 367
energy dispersive x-ray spectroscopy (EDS) 7, 23, 41, 83, 90–91, 143, 189, 209, 211–212, 217, 239, 271, 299, 319, 339, 341, 351, 373, 401
environmental change 1–2, 7, 23, 41, 83–84, 127, 143, 189, 217–218, 234, 239, 245, 249, 271, 299, 319, 351–352, 373, 401, 423
environmental scanning electron microscope (ESEM) 189, 209, 211–212
eolian transport 258
ephemeral lake 192
epsomite 148, 190–191
equant 43, 61, 68–69, 73, 173
erosion 32–33, 65, 84, 88, 100, 125, 128, 143, 145, 218, 230, 248, 413
  erosion and dilation 32
ESEM (environmental scanning electron microscope) 189, 209, 211–212
Estonia 229, 325, 334, 336–337, 340
Euclidean distances 99–100
euhedral 70, 194, 197, 205
eutectic 203–204
evaporites 189, 212
exotic sediment 125
expandable layer clay minerals 167
Experimental Lakes Area, Canada 285, 287, 310
extinction 171, 338, 413
extractable 87, 95, 97, 99, 104–106, 119, 128, 255, 257, 289
extraction procedures 95, 119, 130, 255
extrusion 274, 329

FAAS (flame atomic absorption) 93
fabric 7, 10, 12, 14–16, 18, 20, 41–43, 66, 68, 152, 153, 171, 174, 191, 194, 231
fades 16, 200
factor analysis 65, 100–101

Fe (iron) 84–85, 87, 94, 98–99, 102–104, 107, 112, 115–123, 126–127, 129, 147–148, 151, 156, 158–159, 310, 338
feldspar 57, 103, 126, 151, 171, 220, 366
Feret's diameter 45, 50
ferrimagnetism 222
ferromagnetism 221–222
ferulic acid 258
F_g (gravitational force) 57, 281–282
filter peel technique 162–163
filter(s) 30–32, 156, 162, 255, 299, 302, 304, 306, 312, 314
Finland 23, 27–29, 32, 34–35, 123, 220, 325, 331, 335
fish 413
flame atomic absorption spectrometry (FAAS) 93
fluid displacive embedding 12
fluid inclusion(s) 3, 189–212
fluorite 150, 169
fluvial 146, 258, 281
flux 36,68, 107–108, 110, 113–117, 119, 121, 123, 125, 127, 129–130, 281–282, 284–286, 288, 426
fly-ash (& particles) 4, 319–343
Folk's graphic mean 63
form 7–8, 28, 42, 53, 66, 68–70, 94, 100, 108, 110, 125, 146, 152–153, 156, 172, 189–192, 219, 247, 249–250, 301, 319, 329, 335–336, 353, 358, 360–362, 414, 422, 432
fossil(s) 4, 218, 239, 310, 319, 322–324, 328, 330, 336, 340–343, 359–360, 362–363, 366, 392–393, 402, 416
Fourier analysis 66
Fourier transform (FT) 31, 304
fourth moment 65
fractal(s) 66
fractionation 85–86, 89, 105, 117, 130, 208, 253, 260, 272, 289, 352–353, 355, 359–362, 364, 374, 376–377, 381, 385–386, 389–395, 401, 405–408, 411–412, 419–423, 430, 434
  fractionation factor 352–353, 376, 386, 389, 391, 393–394, 406
fracture(s) 171
France 245, 325
freeze drying (dryer) 12, 275, 306, 366
free-falling diameter 45
frequency dependent magnetic susceptibility 230–231
FT (Fourier transform) 31, 304
full-pattern fitting 175
fume 14, 89, 95, 164, 327, 378
fundamental absorption 300
fusion method 95

Galai 49, 53–54, 60, 72
gamma (rays) 90, 154
gas chromatography (GC) 255, 257, 259–260, 272, 277–280
GC-MS (gas chromatography-mass spectrometry) 277–280
genetic classification 87
geochemical palaeolimnology 83–84, 112, 129
geomagnetic field 217–218
geothite 150
Germany 18, 264, 309, 325, 331, 362–363
GFF (glass fiber filter) 281
Ghana 244–245, 423–424
Glagolev-Chayes method 173
glass fiber filter (GFF) 281
Global Distillation Model 289–291, 293
glycolated trace 167
glycolation 165, 167
glycolator 166
goniometer 155
grade scale 44
grain size 3, 23, 33–34, 37, 41, 46, 51, 65, 224, 226, 232, 242, 378
graphic skewness 63
graphite 93, 262, 336, 381
grasshopper effect 289
gravel(s) 41, 46, 50, 66
gravitational force (F_g) 57, 281–282
Great Lakes, USA/Canada 69, 254, 283, 286, 291, 326, 330, 373, 392–393, 402
Great Plains, USA/Canada 69–70, 364
green algae 385, 387, 403–404, 410, 430, 434
Greenland 105–106, 329, 335
Greifensee, Switzerland 113, 412–414
greigite 222, 233
grey-scale 23–27, 29, 31, 33, 35–36
growth-zone 197
Gulf of Suez 195, 203, 206
gymnosperm(s) 256, 258
gypsum 70, 148, 171, 189–195, 197, 203–206
gyttja 227

H_2O_2 (hydrogen peroxide) 95, 159, 164, 166, 226, 327, 364
halite 145, 149, 189–194, 196–203, 205–206, 208–212
Hamilton Harbour, Canada 392–394
Hampstead Heath, UK 339, 341
harmonic oscillator 300
HCB (hexachlorobenzene) 283, 290–291
heated trace 167
heavy metal 302
Henry's law 272, 282–284
hexachlorobenzene (HCB) 283, 290–291
hexahydrite 145, 148
Hg(mercury) 93–95, 104, 117–118, 123–124, 128, 130, 276, 323
HI (hydrogen index) 262–263, 430
high-field magnetic susceptibility 234

high performance liquid chromatography (HPLC) 277, 280
high-Mg calcite 357–358
high resolution mass spectrometer (HRMS) 278
Holocene 84, 126–128, 155, 164, 207, 212, 227, 234, 253–254, 261, 376, 390–394, 424–425, 430–431
homogenization temperature 197, 199, 201, 203
HPLC (high performance liquid chromatography) 277, 280
HRMS (high resolution mass spectrometer) 278
human impact 83, 85–86, 122
humus 391, 404
huntite 147
hydrogen index (HI) 262–263, 430
hydrogen perxode (H_2O_2) 95, 159, 164, 166, 226, 327, 364
hydrogenic 87
hydrolysis 378–379, 408
hydromagnesite 70, 147
hydrophobicity 272
hypersaline 69–70, 144, 146, 207, 357

IA (image analysis) 2, 23–27, 29, 31–33, 35–37, 49–51, 66, 173, 174–175
IAS (image analysis system) 51, 66
IAS (inorganic ash spheres) 4, 319–320, 322, 325, 329–330, 334–337, 341–343
IC (ion chromatograph) 169, 209, 212
ICP-AES (inductively coupled plasma atomic emission spectrometry) 92–93, 95, 152, 209
ICP-MS (inductively coupled plasma mass spectrometry) 91, 93, 189, 209–210, 212
illite 102, 103, 151, 165, 167–168, 171, 421
image analysis (IA) 2, 23–27, 29, 31–33, 35–37, 49–51, 66, 173, 174–175
  image analysis system (IAS) 51, 66
impregnation 12–13, 15, 18, 170
incident radiation 154–155, 169
inclusion(s) 3, 171, 189–212
inclusive graphic skewness 63
inductively coupled plasma atomic emission spectrometry (ICP-AES) 92–93, 95, 152, 209
inductively coupled plasma mass spectrometry (ICP-MS) 91, 93, 189, 209–210, 212
infaunal 359
infrared (IR) 4, 36, 154, 299–305, 307–309, 311–314
Inman mean 63
inorganic ash spheres (IAS) 4, 319–320, 322, 325, 329–330, 334–337, 341–343
inorganic carbonate(s) 144, 247, 358, 360, 365
instar(s) 360, 366
instrumental neutron activation analysis 90
interference colour(s) 171
interferometer 304
intergrowth(s) 171
internal standard(s) 168–169, 278
intrinsic resolution 287–288
ion chromatograph (IC) 169, 209–210, 212
IR (infrared) 4, 36, 154, 299–305, 307–309, 311–314
Ireland 218, 323, 325, 331, 334, 339–340
IRM (isothermal remanent magnetization) 232
IRMS (isotope ratio mass spectrometry) 208, 248, 250–251, 259–260, 380, 394
iron(Fe) 84–85, 87, 94, 98–99, 102–104, 107, 112, 115–123, 126–127, 129, 147–148, 151, 156, 158–159, 310, 338
isomer 272, 288
isothermal remanent magnetization (IRM) 232
isotope effect(s) 375, 386, 405–406, 408, 420, 423
isotope fractionation factor(s) 353, 386, 395, 406
isotope ratio mass spectrometry (IRMS) 208, 248, 250–251, 259–260, 380, 394
isotope systematics 405
isotopic fractionation 260, 355, 374, 389, 406–407, 419
isotopic rain-out 374
isotropic 69, 171, 338
Israel 192, 201
Italy 96–97, 263, 325

Japan 97, 244, 326, 330, 342, 408
JCPDS (Joint Committee on Powder Diffraction) 156, 169–170
Johnstone River, Australia 260
Joint Committee on Powder Diffraction (JCPDS) 156, 169–170
JPEG 29

K (potassium) 118, 148, 327, 421
kaolinite 103, 151, 165, 167–168, 171
Kenya 261, 412
kerogen 375, 392–393, 395
Krumbein's diameter 45, 50
kurtosis 63–65
K-feldspar(s) 103, 151, 171

L* a* b* color space 8
labile 99, 104, 116, 123, 125, 364, 416, 420
Lake 227, Canada 286–287
Lake 382, Canada 310
Lake Albert, Africa 422
Lake Baikal, Russia 51, 104, 110, 112–113, 115, 124, 127, 244, 261, 323, 326, 334, 431–433
Lake Biwa, Japan 244
Lake Bosumtwi, Ghana 244–245, 423–424, 430
Lake Estancia, USA 25
Lake Haubi, Tanzania 230
Lake Hollingsworth, USA 412, 415
Lake Illawarra, Australia 335
Lake Jaatilanjarvi, Finland 408

Lake Kizaki, Japan 408
Lake Lehmilampi, Finland 28
Lake Lugano 410–411
Lake Malawi, Africa 422, 430
Lake Michigan, USA 244–245, 284, 324
Lake Nicholls, Australia 335
Lake Ontario, USA/Canada 123, 243–244, 248, 252, 288–289, 392, 410, 412, 414
Lake Pleasant, USA 245
Lake Quinalt (also Quinault), USA 256–257
Lake Superior, USA/Canada 283, 285, 412, 421
Lake Tanganyika, Africa 429–431
Lake Tollense, Germany 362
Lake Victoria, Africa 242, 245, 253, 376, 413–414, 420, 427–428, 430
Lake Washington, USA 256–258
laminae 8–9, 16, 33, 51, 60, 70–74
laminated sediment 8, 11, 16, 29, 33, 41, 70, 193
Laplacian filter 31
laser 41, 49, 53–54, 60–61, 91, 209–210, 212
laser ablation 209–210, 212
laser raman microspectroscopy 209, 212
latitude effect 393
lattice 87, 95, 104, 107, 154–156, 163–164, 166–167, 221–222
layered silicate minerals 151
lead (Pb) 93–94, 104–106, 111–118, 122–124, 130, 287, 310, 323–324, 342
lead–210 (see ^{210}Pb)
LEL (local evaporation line) 374, 377, 395
leptokurtic 64
light microscopy 50, 152, 170, 172, 337
lignin 239–240, 256–258, 260–261, 263, 309, 379, 405
lindane 283, 288
liquefaction 68
lithogenic 16, 87
lithology 355–357
lithophile 118
local evaporation line (LEL) 374, 377, 395
LOI (loss-on-ignition) 91–92, 102–103, 152, 164, 240–241, 313, 390–391
long diameter 45
loss-on-ignition (LOI) 91–92, 102–103, 152, 164, 240–241, 313, 390–391
Lough Neagh, UK 218
low field 228, 230–231
low vacuum scanning electron microscope (LVSEM) 17
low-Mg calcite 354, 357–359
luminescence 172, 176
  luminescence petrographic techniques 152
LVSEM (low vacuum scanning electron microscope) 17

mackinawite 151
macromolecules 261
magnesian calcite 147, 160
magnesite 70, 103, 144, 147, 160, 170–171
magnesium (Mg) 60, 70, 118
magnetic 3, 42, 54, 60, 155, 217–235
  magnetic hysteresis 222–223, 227, 233–234
  magnetic resonance 155
  magnetic susceptibility 217–219, 222, 225, 227–231, 233–234
magnetite 150, 218–222, 232–234
magnetometer 226, 232–233
manganese 118, 152, 221, 380
Mangrove Lake, Bermuda 245
MAR (mass accumulation rate) 109, 242–243
marine oxygen isotope state (MIS) 322
Martin's diameter 45, 50
mass accumulation rate (MAR) 109, 242–243
mass spectrometer 208, 248, 250–251, 277–278, 416–419, 421
Mastersizer 61
matrix 41, 93, 95, 97–98, 100, 169–170, 176, 211, 223, 227, 229, 231, 307, 322
  matrix flushing method 169, 176
MDL (method detection limit) 278–279
median 31–32, 63
  median filter 31
mercury (Hg) 93–95, 104, 117–118, 123–124, 128, 130, 276, 323
meromictic (meromixis) 69, 357, 429
mesokurtic 64
meteoric water 208–209, 374, 377, 393
  meteroric water line (MWL) 208–209, 374–375, 377, 393
method detection limit (MDL) 278–279
Mexico 25, 192–193, 196, 208, 254, 393–394
Mg (magnesium) 60, 70, 118
Mg/Ca 70, 144, 356–358, 363, 366–367
Mg-calcite 144
mica 57, 103, 151
nucroprobe 90–91, 210, 212
microthermometry 202–203, 205
microwave extraction 255
Middendorf Lake, Russia 425–427
middle diameter 45, 50
Mie theory 61
mineralisation 403, 407, 425, 429
mineralogy 42, 52, 59, 102, 126, 143–146, 152–153, 155, 157–158, 163–164, 168, 171, 173, 175–176, 217, 225, 227, 355, 357, 366
minerogenic 24, 36, 87–88, 125, 127, 230
Miocene 193, 195, 203, 205–206, 211
mirabilite 70, 148, 190–191
MIS (marine oxygen isotope state) 322
mixed-layer clay mineral(s) 151, 159, 167
mixolimnion 70–71
Mo (molybdenum) 94, 118, 121, 156
mode 63, 100–101, 278–279, 386
model 24, 52–53, 83–84, 98, 104, 107–110, 112, 114–116, 121, 125, 128, 205, 281, 289–

291, 293, 299–301, 310–312, 314, 336, 342, 386, 390, 392
molecular sieve 419
mollusk(s) 358–359, 362–363, 365
molybdenum (Mo) 94, 118, 121, 156
moment measures 64–65
monimolimnion 70–72
monochromator 304
monohydrocalcite 146–147, 357
montmorillonite 163
Morocco 326
multiplicative signal correction (MSC) 307
Multisizer 52
Munsell colour chart 8
MWL (meteroric water line) 208–209, 374–375, 377

N cycle 401, 404, 406, 408–409, 423, 428–429, 433–434
Na (sodium) 70, 92, 94, 102–103, 118, 125–126, 128, 145, 149–151, 159, 166, 207, 210–212, 275, 277, 327, 339, 379–380, 394
NAI-P (non-apatite inorganic phosphorus) 119
nannoplankton 362
NaOCl 159, 365–367
National Institute of Standards and Technology (NIST) 97, 276
natural remanent magnetization (NRM) 218, 225
NBS-19 352–353
near infrared (NIR) 4, 36, 299–314
  near-infrared spectrometry (NIRS) 4, 299–314
Neél temperature 221
Neogene 211
Ni (nickle) 94, 104, 109, 114, 116, 118, 122–124, 164, 221–222, 253, 310, 380–384
NIR (near infrared) 4, 36, 299–314
NIRS (near infrared spectrometry) 4, 299–314
NIST (National Institute of Standards and Technology) 97, 276
nitrate assimilation 403, 407
nitrification 403, 407–408
nitrogen cycle 401, 404, 406, 408–409, 423, 428–429, 433–434
  nitrogen cycling 252, 402, 425
nitrogen biogeochemical cycle 402–403, 423
nitrogen fixation 249, 253, 403, 407
nitrogen isotope(s) 4, 249, 260, 264, 375, 401–434
nodule(s) 194
nonenyl succinic anhydride 19
non-apatite inorganic phosphorus (NAI-P) 119
non-clay silicate minerals 151
non-combustible material 319
normative calculations 102, 146
North America 54, 69, 85, 124, 244, 254, 289, 291–292, 323–324, 326, 330, 342, 364, 374
Northern Ireland 218, 339
Norway 122, 324–325, 330–331, 333, 335, 401
NRM (natural remanent magnetization) 218, 225
Nunatak Lake, Greenland 105–106
n-alkane 254–256, 259–261

OC (organic carbon) 91–92, 117, 218, 240–243, 246–247, 251, 262, 274, 276–281, 309–310, 357, 385, 391, 422
octanol-water partition coefficient 282
off-line preparation 241, 417
OI (oxygen index) 262–263
OM (organic matter) 4, 16, 36, 84, 87, 91–92, 102, 104, 107, 113, 116–117, 125, 128, 158–159, 164, 172, 194, 220, 222, 227, 239–264, 310, 312–313, 327, 375–376, 385–386, 393, 401–405, 407, 409–411, 413–426, 428–430, 432–434
OP (organic phosphorus) 119, 362, 420
opacity 171
optical 16–17, 33, 58, 153–154, 170–172, 174–176, 304
  optical isomers 272
  optical microscopy 17, 20, 143, 174–175, 338
  optical mineralogy 145, 153, 175–176
optic axial angle 171
optic sign 171
organic carbon 91–92, 117, 218, 240–243, 246–247, 251, 262, 274, 276–281, 309–310, 357, 385, 391, 422
organic carbon-water partition coefficient 281
organic matter (OM) 4, 16, 36, 84, 87, 91–92, 102, 104, 107, 113, 116–117, 125, 128, 158–159, 164, 172, 194, 220, 222, 227, 239–264, 310, 312–313, 327, 375–376, 385–386, 393, 401–405, 407, 409–411, 413–426, 428–430, 432–434
organic phosphorus (OP) 119, 362, 420
organochlorine 271, 274, 279, 290–291
oriented mount 157, 161–162, 165–166
OSC (orthogonal signal correction) 307
ostracode (ostracod) 127, 351–352, 358–363, 365–367
overall mass transfer coefficient 282
Owens Lake, USA 201
oxic 243, 416, 420
oxidation 92, 116–117, 146, 152, 225, 227, 240–241, 247, 250, 256–258, 260, 262–263, 381–382, 402–403, 434
oxide(s) 87–88, 102–103, 115–117, 150, 158–159, 217, 222, 225–226, 250, 257, 336, 412
oxycline 404
oxygen index (OI) 262–263
oxygen isotope(s) 4, 207–208, 210, 212–253, 351–367, 373–396

P (phosphorus) 4, 95, 117–119, 250, 252, 286, 308–310, 404

packing 42, 68
PAH (polycyclic aromatic hydrocarbon) 271–274, 337, 342
palaeomagnetic secular variation (PSV) 218
Paleoecological Investigation of Recent Lake Acidification (PIRLA) 323–324, 337
paleosol 417, 427–428
palygorskite 151, 165
paramagnetism 221
partial extraction 95
partial least squares (PLS) 307
particle counting 53
paniculate organic matter (POM) 312
particulate organic nitrogen (PON) 410, 420
partings 171
partition coefficient 281–282
Pb (lead) 93–94, 104–106, 111–118, 122–124, 130, 287, 310, 323–324, 342
PCA (principal components analysis) 99–101, 125–127, 290, 308, 313
PCB (polychlorinated biphenyl) 271, 273, 276, 278–279, 285–289, 291–293
PCDD/F (polychlorinated dibenzo-p-dioxins and polychlorinated dibenzofurans) 272, 277–278
PDB (Pee Dee Belemnite) 244, 352–353
PDF (powder diffraction file) 156, 169–170
peakedness 63
peat 97, 128, 218, 225, 244, 253, 309, 324, 340–341
pebble(s) 46, 54
Pee Dee Belemnite 244, 352–353
  Pee Dee Formation 352
peel technique 162–163, 166
percussion scar(s) 68
perennial saline lake (s) 192, 203
perimeter diameter 45
permeability 41–42, 68, 170
Permian 192, 196, 199, 210, 212
persistent organic pollutants (POPs) 4, 271–293
petrography 70, 143, 145, 153, 173, 175, 212, 395, 417
petrology 24–25, 50, 54, 102, 172
PFE (pressurized fluid extraction) 275
Phacotus 351, 362–363
phenol 280, 293
phi 44–47, 63
  phi quartile skewness 63
  phi scale 44
  phi unit 46
phosphorus (P) 4, 95, 117–119, 250, 252, 286, 308–310, 404
photoluminescence 152
photons 90
photosedimentometer 49, 58–59
phthalales 274
phytodetritus 252
piece-wise MSC 307
pike 7–8, 10, 12–14, 16–18, 20, 50, 171
pinhole 51–52
pipette method 58
pipette-on-slide method 161, 163
PIRLA (Paleoecological Investigation of Recent Lake Acidification) 323–324, 337
pitting 171
pixel 26, 29–33, 35
plagioclase 145, 151, 171
plane-polarized light 171
plasticizers 274
platy 160, 163
platykurtic 64
playa 69
plerosphere 321
plerospheres 319
PLS (partial least squares) 307
Poland 325, 335
pollen 85–86, 253, 258–260, 312, 324, 352, 391
polychlorinated biphenyl (PCB) 271, 273, 276, 278–279, 285–289, 291–293
polychlorinated dibenzo-p-dioxins and polychlorinated dibenzofurans (PCDD/F) 272, 277–278
polycyclic aromatic hydrocarbon (PAH) 271–274, 337, 342
POM (particulate organic matter) 312
PON (particulate organic nitrogen) 410, 420
pond 97–99, 104–105, 335, 360–361
POPs (persistent organic pollutants) 4, 271–293
pore water 42, 114, 116, 143, 254, 287, 358
porosity 16, 41–42, 51, 68, 287, 322
Portugal 325, 335
post-burial 87, 191, 194, 243, 248, 251
post-depositional 42, 191, 218–219, 233, 288, 385, 416
potassium (K) 118, 148, 327, 421
powder diffraction file (PDF) 156, 169–170
powder mount 176
powder-press 162
precision 54, 91, 93, 96, 107, 160–162, 173, 211, 233, 248, 251, 414, 418
pressurized fluid extraction (PFE) 275
pretreatment 50, 157–158, 164, 176
primary mineral 194
principal components analysis (PCA) 99–101, 125–127, 290, 308, 313
probable error 173
projected area diameter 45, 52
protodolomite 70, 147, 160
provenance 41, 68, 144, 172, 402
proxy 23, 25, 116, 144, 212, 218, 233, 249, 352, 415, 423, 431
  proxy data 312, 367, 396
  proxy records 367
PSV (palaeomagnetic secular variation) 218
Pyramid Lake, USA 242, 244
pyrite 16, 151

pyrolysis 4, 239, 253, 260–263, 380–384, 417
pyroxene(s) 151, 221
pyrrhotite 151

Qaidam Basin, China 201, 205–209
Qinghai Province, China 201, 207, 209
quality control 96, 274
quantification 8, 61, 145, 155–156, 164, 168–169, 173–176, 233, 300–301, 309
quantification techniques 175–176
quartz 16, 51, 57, 68, 145, 151, 167–169, 197, 210, 220, 226, 247, 250, 364, 381, 383
Queen's Lake, Canada 390–391
Q-mode factor analysis 100–101

radiation 59, 92, 152–157, 164–165, 169, 300, 302–303
radiography 8, 10, 16, 26, 33
Rayleigh distillation 408–410
Rb (rubidium) 94, 118
reagent(s) 19–20, 89, 96, 119, 276, 327
recycling ratio (RR) 284
Redfield ratio 404
redox 85, 120, 127
reducible 87–88
reference materials 48, 91, 93, 96–97, 106, 119, 128, 130
reflectance 8, 301, 306–310
  reflectance spectrometry 301, 307–308
reflected light 50, 172
refractive index 61, 170–171
regression analysis 98
relative humidity (RH) 11, 355
remanence 217, 224–225, 227, 231–233
remineralization 241
residual 87–88, 91, 98–99, 104, 130, 241, 245, 247, 250, 262, 276, 384, 403, 408
  residual fraction 85, 88, 107
resin 12–16, 18–20, 170–171, 225, 227, 231, 338
RH (relative humidity) 11, 355
rice-grained morphology 71
rift lake 429, 431–432
RMS (root mean square) 304
Rock-Eval (also RockEval) 239, 261–263, 417
root mean square (RMS) 304
rotational remanent magnetization (RRM) 233
roundness 33, 42, 66–67
RR (recycling ratio) 284
RRM (rotational remanent magnetization) 233
rubidium (Rb) 94, 118
Russia 244, 326, 335, 425–426

S (sulfur) 95, 118, 122, 148, 222, 276, 323, 331, 334, 336, 342–343, 409
S/V (syringyl/vanillyl ratio) 258
Saanich Inlet, Canada 11
Sacred Lake, Africa 261
Salado Formation 192
Salina Omotepec, Mexico 192–193
saline 54, 69–70, 144, 146, 164, 191–194, 197, 199–201, 203, 205–206, 208, 423
  saline groundwater 194, 357
  saline pan 192–193, 201
salinity 53, 70, 128, 144, 202, 204–207, 212, 357
Salix 312
salt 51, 69, 159, 164, 194, 204–205, 209, 244, 357
  salt pan 200–201
Salton Sea, USA 201
sand 41, 44, 46, 50, 54, 59–60, 145, 172, 226
saturated hydrocarbons 254, 277
saturation isothermal remanent magnetisation (SIRM) 227, 232
scanning electron microscope (SEM) 15–18, 20, 27, 68, 152–153, 209, 211–212, 227, 320–321, 337, 339, 358, 360–361, 363
second moment 65
secondary electron imagery (SEI) 16–17
secondary fluid inclusions 189, 196–197
secondary minerals 143
SCP (spheroidal carbonaceous particle) 4, 91, 319, 320–321
SediGraph 49, 59–60
sediment cellulose 4, 373, 376, 378, 380–382, 385, 392, 394–395
sediment grade scale 44
sediment model 310
sediment trap(s) 60, 71, 192, 324, 395, 409, 409–410
sedimentation rate(s) 108, 112–113, 123–124, 246, 284, 286, 420
sedimentology 24, 46, 54, 58, 64–66, 73, 155
segmentation 31
SEI (secondary electron imagery) 16–17
selenite 191, 193, 195, 206
SEM (scanning electron microscope) 15–18, 20, 27, 68, 152–153, 209, 211–212, 227, 320–321, 337, 339, 358, 360–361, 363
Seneca Lake, USA 246, 248
sepiolite 151, 165
sequential extraction 87, 95, 105–107, 119
settling column 58
SFP (spheroidal fly-ash particle) 322, 327
shadow filter(s) 31–32
sheet flood 143
Si (SiO_2, silicon, silica) 63–64, 86, 94–95, 102, 118–119, 126, 145, 151, 169, 338, 340, 356
Sicily, Italy 193
siderite 147, 364
siderophile 118
sieve 44–45, 54–56, 64–65, 164, 365, 419
  sieve diameter 45, 54
  sieving 54, 65, 96, 159, 226, 276, 378, 385
signal preservation 112, 124

silicon (silica, Si, SiO_2) 63-64, 86, 94-95, 102, 118–119, 126, 145, 151, 169, 338, 340, 356, 401
silt 11, 16, 41, 44, 46, 50–51, 54, 173–174, 276, 364
silver (Ag) 94, 118, 156
single particle counters 51, 73
SIRM (saturation isothermal remanent magnetisation) 227, 232
skewed 63–64, 284, 363–364
skewness 63–65
skin effect 211
Slovakia 325, 335
Slovenia 325, 331
smear 161, 163, 358, 417, 423–424, 430, 432
smectite 151, 163, 165, 167, 171
SMOW (standard mean ocean water) 353
Sn (tin) 118, 241
sodium (Na) 70, 92, 94, 102–103, 118, 125–126, 128, 145, 149–151, 159, 166, 207, 210–212, 275, 277, 327, 339, 379–380, 394
sodium pyrophosphate 159
soil organic matter 244, 375
soil redox 127
Solfifera Series 193
solvent extraction 255, 379
soot 321–322, 324, 336, 339
  soot balls 322
  soot particles 322
  soot spheres 322
  soot spherules 322
sorbed 87, 107, 110
sorption 108, 122, 281, 287
sorting 42, 63–64, 68, 70–71, 104, 106, 126, 158, 173, 242
soxhlet 273, 255, 275–276
Spain 325, 335
specific gravity 172
spectral filters 299, 302, 306, 314
spectral retlectometer 9
spectroscopy 91,94, 152, 155, 300–301, 304, 308–310, 312, 339
sphericity 42, 66–67, 322, 324
spheroidal 4, 91, 319–322, 327
  spheroidal carbonaceous particle (SCP) 4, 91, 319–321
  spheroidal fly-ash particle (SFP) 322, 327
spherules 322, 329
spinning cup module 306
Sr (strontium) 94, 118, 127, 147, 210, 356–358, 364, 366–367
Sr/Ca 127, 356–358, 366–367
stable isotope 4, 189, 207–209, 264, 351–353, 355, 357, 359, 361–363, 365, 367, 374, 395, 401, 405
standard deviation 49, 63, 65, 278
standard error 312
standard mean ocean water (SMOW) 353
Stokes Law 54, 57, 226
stratified lake 247, 249, 403
stratigraphy 46, 74, 84–85, 227, 417, 423, 425
striations 68
strontium (Sr) 94, 118, 127, 147, 210, 356–358, 364, 366–367
struvite 148
subsample(s) 52, 54, 60, 241, 251, 306
substrate 191, 247, 406–410
suction-on-ceramic tile method 163
sulfate mineral(s) 148–149, 159, 170, 190
sulfide(s) 151–152, 159, 364–367
sulphur (also sulfur) 95, 118, 122, 148, 222, 276, 323, 331, 334, 336, 342–343, 409
surface diameter 44–45
surface texture 42, 68, 321, 324, 337
surface volume diameter 45
Surface Water Acidification Project (SWAP) 323
Svalbard 326, 334–335
SWAP (Surface Water Acidification Project) 323
Sweden 11, 23, 36, 122, 217, 220, 227, 234, 299, 313, 323–324, 326, 329–331, 333–335
Switzerland 113, 244, 251–252, 264, 326, 411–413
sylvite 149, 190
symmetry 63, 66
syndepositional 191–194
syringyl phenols 258
syringyl/vanillyl ratio (S/V) 258

tagged image file format (TIFF) 30
Tanzania 230, 412
technogenic 87
TEM (transmission electron microscopy) 152, 227
temperature dependent magnetic susceptibility 227, 231
terrigenous 11, 87, 127
test(s) 125, 201, 261, 280, 305, 310, 313, 366, 378–379, 385, 422
texture 2, 41–44, 51, 68–69, 72, 143, 171, 175, 191, 194, 204, 206, 211, 321, 324, 337
thenardite 149
thermal 92, 197–198, 201, 221, 262–263, 383, 416
  thermal analysis 152
  thermal maturation 263, 416
  thermal vacuum cell 210
Ti (titanium) 60, 118, 338
thin section (TS) 8, 12, 14–18, 20, 24, 27, 29, 33–34, 36, 50–51, 67, 153, 170–176, 191–196, 198, 352
third moment 65
thresholding 31, 34
TIFF (tagged image file format) 30
time-series 385
tin(Sn) 118, 241
titanium (Ti) 60, 118, 338
TOC (total organic carbon) 240–243, 245, 261–263, 308, 310–311, 422, 425, 427–430

tomographic images 12
Toronto Lake, Canada 390–391
tortuosity 287
total digestion 95
total nitrogen (TN) 311, 401, 412, 421–422, 425, 427–429
total organic carbon (TOC) 240–243, 245, 261–263, 308, 310–311, 422, 425, 427–430
total phosphorus (TP) 308, 310–311
TN (total nitrogen) 311, 401, 412, 421–422, 425, 427–429
TP (total phosphorus) 308, 310–311
trace element(s) 42, 83, 85–86, 96–98, 103–105, 107–117, 123–125, 127–130, 351, 339, 365
trace metal(s) 122–123, 212, 324, 334, 336
transfer functions 117, 300, 308, 310, 313–314, 392
translucency 171
transmission electron microscopy (TEM) 152, 227
transmittance 59, 301
transmitted light 171
transparency 171, 204
Trask's sorting coefficient 63
trona 147, 191
trophic status 117, 120, 285–286, 293, 425
tropical lakes 409, 423
TS (thin section) 8, 12, 14–18, 20, 24, 27, 29, 33–34, 36, 50–51, 67, 153, 170–176, 191–196, 198, 352
  TS petrography 175
tufa 197
Tunisia 326
turbidite(s) 417, 431–433
two-phase fluid 197, 204, 206

Uganda 412
UK 7, 16, 18, 83, 319, 323–324, 326, 328–334, 336, 339–341
ultrasonic disaggregation 166
ultrasonication 255, 275
ultraviolet (UV) 172, 210
uniaxial 171
unmixing 98–101
unrolled diameter 45
USA 127, 189, 191, 239, 244, 326, 328, 330, 351, 373, 412, 428
USGS 360–361
UV (ultraviolet) 172, 210

vacuum drying 13
vacuum filtration 166
Van Krevelen plot (diagram) 262
vanadium 118, 338
vanillyl phenols 258
variance 65, 309–310, 312–313
varimax rotation 100
varve 9, 11, 16, 23–26, 29, 33, 35–37, 218, 220, 229, 343, 413
  varve counting 23–24, 26, 33, 35–37, 332
vascular plants 240, 243–245, 254, 256, 258, 361, 387
vaterite 146–147
vermiculite 151, 165, 167
video cameras 26
Vienna Pee Dee Belemnite (VPDB) 352–353, 364
Vienna standard mean ocean water (VSMOW) 352–353
vinyl cyclohexene dioxide 19
vital effect(s) 358–360
vivianite 148
volatilization 208, 283, 286
volume diameter 44–45
VPDB (Vienna Pee Dee Belemnite) 352–353, 364
VSMOW (Vienna standard mean ocean water) 352–353

Waldsea Lake, Canada 69–72
Walker Lake, USA 244
water side resistance 282
weighting factors 169
West Basin Lake, Australia 62

XRD (X-ray diffraction) 143, 152–153, 155–164, 166, 168–170, 175–176, 351, 364
XRF (X-ray fluorescence & spectrometry) 89–91, 93–94
X-radiography 10–11, 16
X-ray 10, 12, 16, 26–29, 31, 33, 35, 37, 41, 59, 60, 89–91, 143, 145, 153–156, 158–160, 163, 168, 175, 176, 339, 351
  X-ray attenuation 41, 59–60
  X-ray beam 12, 59, 153–154, 156
  X-ray diffraction (XRD) 143, 152–153, 155–164, 166, 168–170, 175–176, 351, 364
  X-ray diffractometry 153, 155
  X-ray fluorescence (& spectrometry; XRF) 89–91, 93–94
  X-ray image 31, 35

zinc (Zn) 93–94, 98–99, 104–105, 109, 112–118, 122–124, 130, 310
zirconium (Zr) 94, 118